The University Of Sheffield.

Field Investigation of Discolouration Material Accumulation Rates in Live Drinking Water Distribution Systems

By

Dominic Cook

MSc BSc (Hons) ARSM

This thesis is submitted in part fulfilment of the degree of
Doctor of Philosophy in the Faculty of Engineering

The University of Sheffield
Department of Civil and Structural Engineering
November 2007

To My Father

Abstract

Discolouration is the biggest cause of aesthetic customer contacts in the water industry. This project was designed to develop new insight and understanding into discolouration, by investigating the impact of different factors on discolouration material accumulation rates and the effectiveness of traditionally used mains cleaning and rehabilitation methods, through detailed studies of live distribution systems.

Analysis of discolouration customer contacts and burst incidents covering a five year period for two water companies and pipe asset data base for a water company's entire region, at the District Meter Area (DMA) level, shows little correlation between the number of discolouration events and pipe properties, indicating complex inter relationships between a number of factors.

Discolouration accumulation rates were investigated through repeat full zonal flushing in two DMAs. Discolouration material was seen to accumulate at the same rate in all areas of the networks, as a factor of water quality, until equilibrium was reached between accumulation and erosion rates. This equilibrium was as a factor of daily conditioning shear stress, whereby pipes affected by a low daily conditioning shear stress continued to accumulate material longer than pipes with a higher daily conditioning shear stress and thicker layers of discolouration material were formed.

Long term turbidity monitoring in five DMAs has showed that the amplitude of a daily turbidity cycle, based on re-suspension and corrosion processes, can be used to assess the effectiveness of network rehabilitation. A greater improvement in the reduction of discolouration potential was seen in the full zonal flush DMAs, than in DMAs that were rehabilitated under the Distribution Operation and Maintenance Strategy (DOMS), at far greater cost. A significant proportion of recorded discolouration events were attributed to events occurring outside the DMA highlighting the necessity for trunk main cleaning.

Using the principles of change in shear the methodology for a simple modelling tool was designed and field tested to predict the discolouration response to valve movements, to enable valve operations to be managed to reduce discolouration risk.

Acknowledgments

Many thanks have to go to the EPSRC and Yorkshire Water Services for providing the funding for this project.

I would also like to thank all the Yorkshire Water employees who have helped in this project, particularly Marjorie Powell for being a mine of information and helping me considerably with attaining data and navigating round the corporate database systems, and to Steve Hall for being a great help and a very approachable industrial liaison. The biggest praise has to go to Garry Howden who never grumbled despite how cold, wet and tired we got and without whom the flushing would simply not been possible.

Many thanks have to go to my supervisor Dr Joby Boxall for brainwashing me into doing the PhD and introducing me to a new career path. Thank you for always having an open door and enthusiasm to share new ideas.

Lastly I would like to thank Sara for being there through difficult times and putting up with me when I turned into a hermit and only came down from the study when I wanted feeding!

Garry Howden, Yorkshire Water Services.

Table of contents

List of figures

List of tables

Symbols

V	=	velocity
g	=	gravity
r	=	Particle density
d	=	Particle diameter
γ	=	Kinematic viscosity of water.
TSS	=	Total suspended solids
τ	=	Boundary shear stress
ρ	=	Density
R_h	=	Hydraulic radius
S_0	=	Hydraulic gradient
τ_s	=	Corrosion layer yield strength
C	=	Stored turbidity volume of layer
k	=	Gradient of the potential as a function of layer strength.
Cmax	=	Maximum turbidity volume
b	=	Power term to set for first order relationship.
R	=	Rate of supply
As	=	Surface area
Q	=	Flow rate
Po	=	Observed pressure
Pc	=	Computed pressure
Cs	=	Daily conditioning maximum shear stress
N	=	Turbidity
t	=	Time
Dm	=	Depth material eroded
D	=	Date
Di	=	Pipe diameter
R	=	Regeneration rate
SdN	=	Standard deviation of daily turbidity

1 Introduction

Despite high compliance rates for drinking water standards, water companies continue to receive customer contacts relating to water quality. Figure 1 shows a breakdown of customer contacts received by a UK water company over a five year period (Cook et al. 2005) highlighting that over a third of these contacts relate to discoloured water.

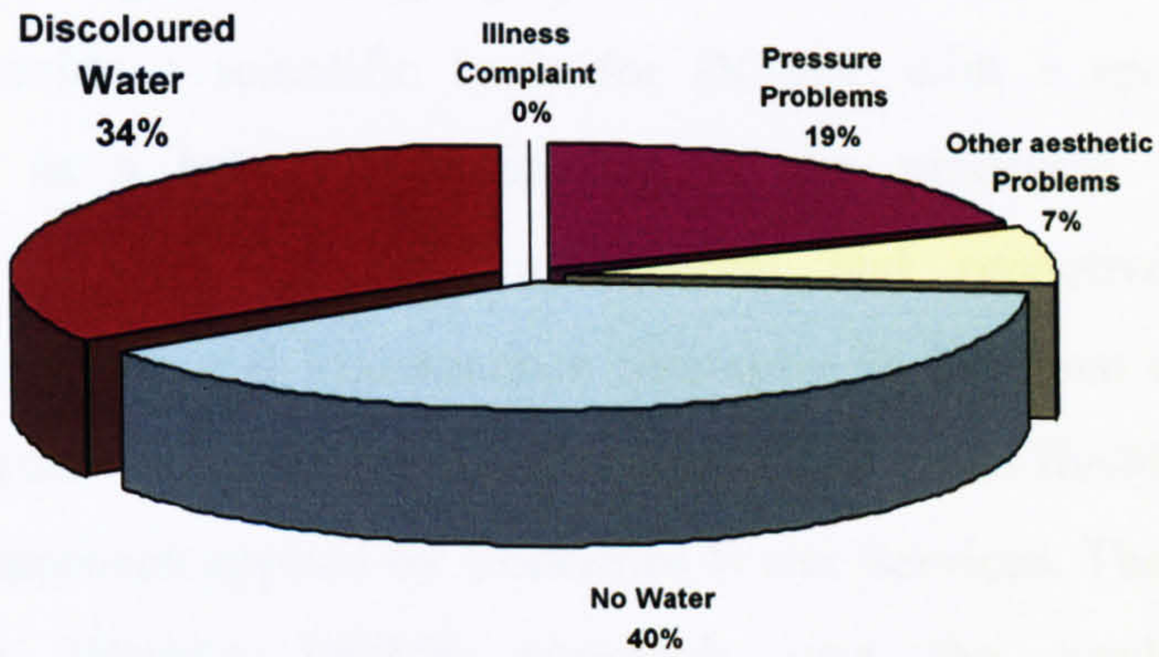

Figure 1 Customer contact groups.

Currently discoloured water is viewed as essentially an aesthetic problem; however the possibility of a high content of metals, organic and inorganic compounds, and viable organisms could potentially pose a health risk. The occurrence of discoloured water greatly affects the customer's confidence in drinking water quality which can lead to poor customer satisfaction and resulting reduction in willingness to pay (Water UK 2003).

Much of the UK water distribution system is of considerable age and water companies have employed a blanket approach to rehabilitating existing mains, referred to as 'Section 19' program, with the aim to improve water quality and structural integrity of the network. As Section 19 draws to a close, maintenance and rehabilitation needs to continue with a more focused and targeted approach in order to maintain the current high standards in water quality. Hence in response to Drinking Water Inspectorate (DWI) information letter 15/2002 (DWI 2002) UK water companies submitted Distribution Operation and Maintenance Strategies (DOMS) to the DWI. Essentially this ensured that water companies had in place a program of strategic investigations in water quality which would lead to timely programmes of planned maintenance work. The strategy is designed to account for the risks to water quality based

upon the likelihood of failure and the consequence of failure on the quality of water received by customers. Under DOMS operational activities such as valve movements and re zoning and their risk on serviceability must also be taken in to consideration. The UK water industry is still developing DOMS and it is continually being updated. Although DOMS is a UK specific strategy, the same issues regarding targeted mains rehabilitation to maintain water quality affect all water companies regardless of geographical location. This research project is intended to provide a scientific basis for DOMS, with a specific focus on discolouration, as a better understanding of the processes which lead to discolouration is vital for the improvement and proactive targeting of Distribution Operation and Maintenance Strategies in the most appropriate and economical manner. In particular effectiveness of full zonal flushing is compared to the DOMS approach applied by Yorkshire Water Services. The cornerstone of the Yorkshire Water's DOMS approach was the implementation of Discolouration Risk Modelling (DRM) to target rehabilitation on a risk vs. cost benefit approach.

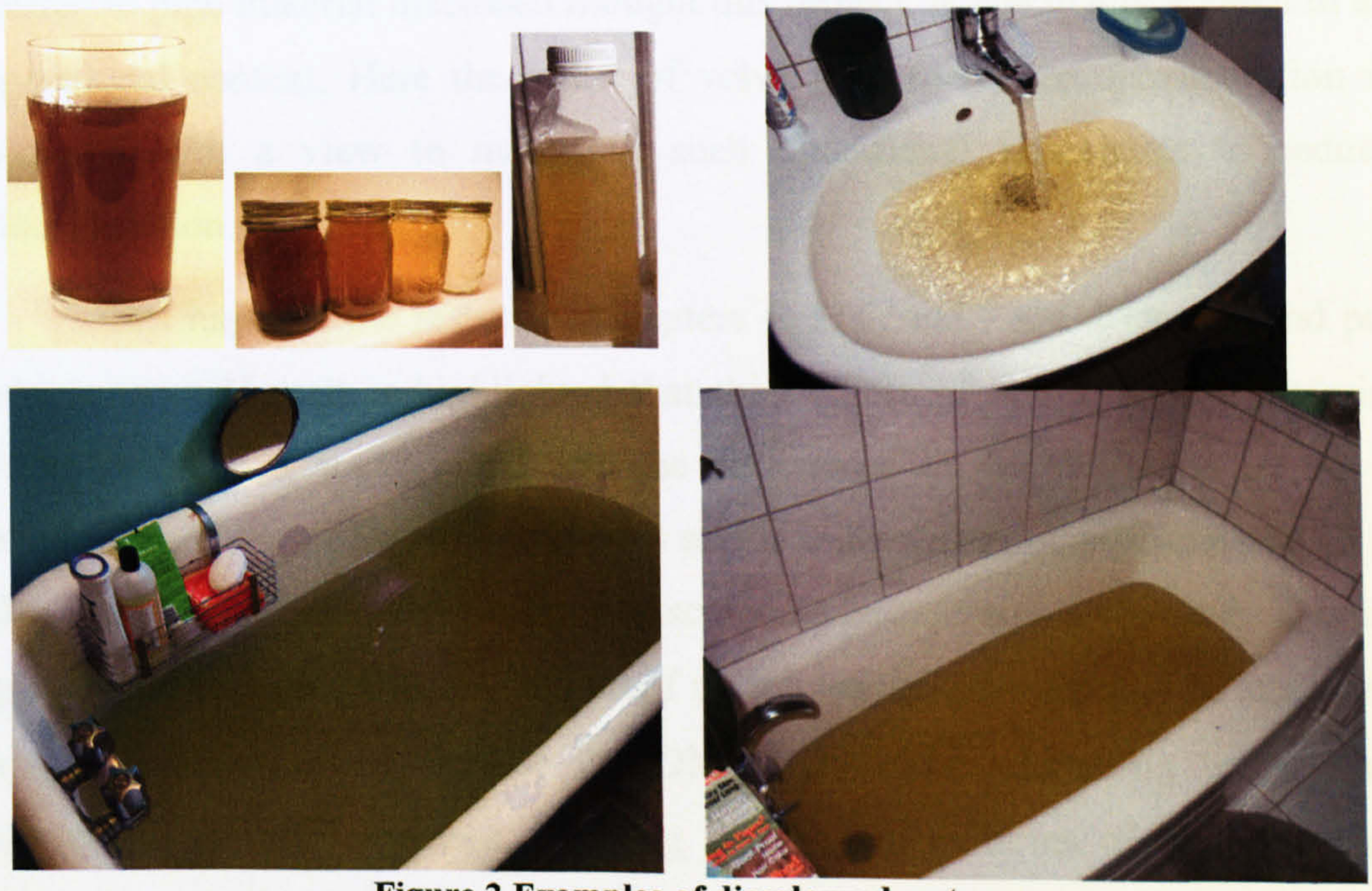

Figure 2 Examples of discoloured water.

The nature of discolouration processes and a review of current research is presented in Chapter 2. The Aims of the project are discussed in Chapter 3.

Chapter 4 addresses the data analysis phase of this project designed to discover any links between discoloured water customer contacts, burst events, and pipe properties at the District Meter Area (DMA) level by analysis of commonly maintained customer contact, asset data bases, and maintenance records.

In Chapter 5 flushing operations are reported to develop an understanding of the rate at which discolouration material builds up within a water distribution network, and whether this rate is affected by differing conditions within the network such as the hydraulic regime, pipe material, diameter and age.

In Chapter 6 long term turbidity monitoring methods are employed to develop an understanding of the effectiveness of existing DOMS rehabilitation strategies and comparing its value to the simple flushing approach applied in Chapter 5.

In Chapter 7 the principles of shear stress mobilising discolouration material, and that the volume of discolouration material found in mains is not related to pipe material discussed thought this project, is practically applied in an operational context. Here the effect of valve movements on discolouration is assessed with a view to managing such operational procedures to reduce discolouration risk.

In Chapter 8 the results of Chapters 4, 5, 6, and 7 are discussed and put into context. Here it is highlighted that the volume of discolouration material found in drinking water mains and the occurrence of discolouration events is primarily a factor of system hydraulics and is independent of pipe material. It is also shown that the regeneration of discolouration material is a factor of water quality and that a significant volume of discolouration material can be attributed to processes occurring outside the DMA. Therefore addressing trunk main cleaning is highly important. Flushing was shown in terms of both cost and reduction of discolouration potential to be more effective than the DOMS approach applied by Yorkshire Water.

The conclusions are presented in Chapter 9 and the need for further research is addressed in Chapter 10.

2 Literature Review

2.1 Introduction

Customer complaints are often used as a key performance indicator by water authorities and their regulators, (Polychronopolous et al. 2003). Cook et al. (2005) highlights that the most common aesthetic customer contacts received by water companies in the UK are due to discoloured water concerns. However the reliability of customer contacts is often questioned as the level of discolouration at which a customer will complain is highly subjective and is dependent on the customer's water quality expectations and their historical experience, (Prince et al. 2000; Prince et al. 2003) and the level of age and education of the customer, (Thurman et al. 1999). There are also inherent difficulties in relating customer contacts to their source, for example a particular pipe, which could be anywhere upstream of the contact (Unwin et al).

Discolouration is caused by the presence of fine particles in the water, measured as turbidity, or by discolouration of the water, measured as true or apparent colour, (Gaultier et al. 1996; Marshall 2001; Polychronopolous et al. 2003; Ryan et al. 2003). Turbidity is a measure of the amount of incident light scattered in a particular direction, typically at an angle of 90° from the source. It is often described as a measure of the cloudiness or clarity of the water, (Twort et al. 2000).

Boxall et al (2003, 2005) states that by definition, colour is absorbed in the chemical composition of water, but customer contacts due to the colour of the water are in fact caused by turbidity. This is because if a sample of discoloured water is left for greater than 24 hours the water clears as fine grained sediment settles out.

Discoloured water is generally seen as an aesthetic problem and an inconvenience to customers. However when considering the elevated concentrations of some metals and other compounds in discoloured water material the health risk, although low, must be considered. Raised levels of turbidity can also be associated with more detrimental problems such as loss of disinfectant residual which can result in increased biological activity within the system, (LeChevallier et al. 1981; McCoy et al. 1986).

The current UK regulations set a maximum standard of 4 Formazine Turbidity Units (FTU) at the customers tap (DWI 2000). However for adequate disinfection World Health Organisation (WHO 2006) guidelines suggest an average level of 0.1 Nephelometric Turbidity Units (NTU) at the treatment works. Slaats (2002) states that, customers will begin to notice discoloured water in a white two litre vessel at a level of 5 NTU.

Discolouration can be conceptualised as essentially a three-phase process: There must be a material source, an accumulation of material, and a process of material mobilisation by which material is brought into suspension (Boxall et al. 2005).

2.2 What is discolouration material and where does it come from?

Flushing is generally accepted by the water industry as a process of removing discoloured water material where hydrants are systematically opened to generate the forces required to remove the material.

Flushing experiments carried out by Boxall et al. (2003), Polychronopolous et al. (2003), Prince et al. (2003) and Seth et al. (2003) indicate there is a strong correlation between turbidity of water and its iron and manganese content. These experiments have also deduced that the size of the material is very small, in the region of 10μm and has a specific gravity of between 1 and 1.3.

This small size and composition of the discolouration material indicates several possibilities as to the nature of its source.

2.2.1 A product of the water treatment process.

Discolouration material may be present in the raw water entering the water treatment works in organic and inorganic forms, (Lin et al. 1997). Soluble Manganese (Mn^{2+}) and Iron (Fe^{2+}) are present in fresh water sources due to electron exchange reactions (anaerobic respiration) that take place in the presence of metal reducing bacteria under anoxic conditions at the water sediment interface (Chandy et al. 2001). It is possible that this material is not fully removed by the water treatment process.

At the treatment works, water filtration or coagulation processes may release material, (Polychronopolous et al. 2003; Prince et al. 2003) such as powdered activated carbon particles (Brazos et al. 1991), or aluminium microflocks. Slaats (2002) states that excessive amounts of coagulant such as iron or aluminium is the main cause of poor treatment practice which can contribute to discolouration.

Currently in England and Wales, treatment works produce very high quality water and hence observable discoloured water rarely originates directly from source treatment or holding works, as these sources are deemed to be at such a low level they are unlikely to directly result in discolouration events (Boxall et al. 2003). However some treatments works employ newer technologies and the role of treatment works must not be completely ruled out when considering the long term chronic effects of very small amounts of discoloured water material building up over a long time.

If source water and treatment process are discounted, Seth et al. (2003) states that discolouration has to be attributed to in-system processes such as precipitation of materials and corrosion of iron mains.

2.2.2 The oxidation of cast iron mains.

Figure 3 Iron corrosion in a 6' cast iron water main. (www.corrosion-doctors.org)

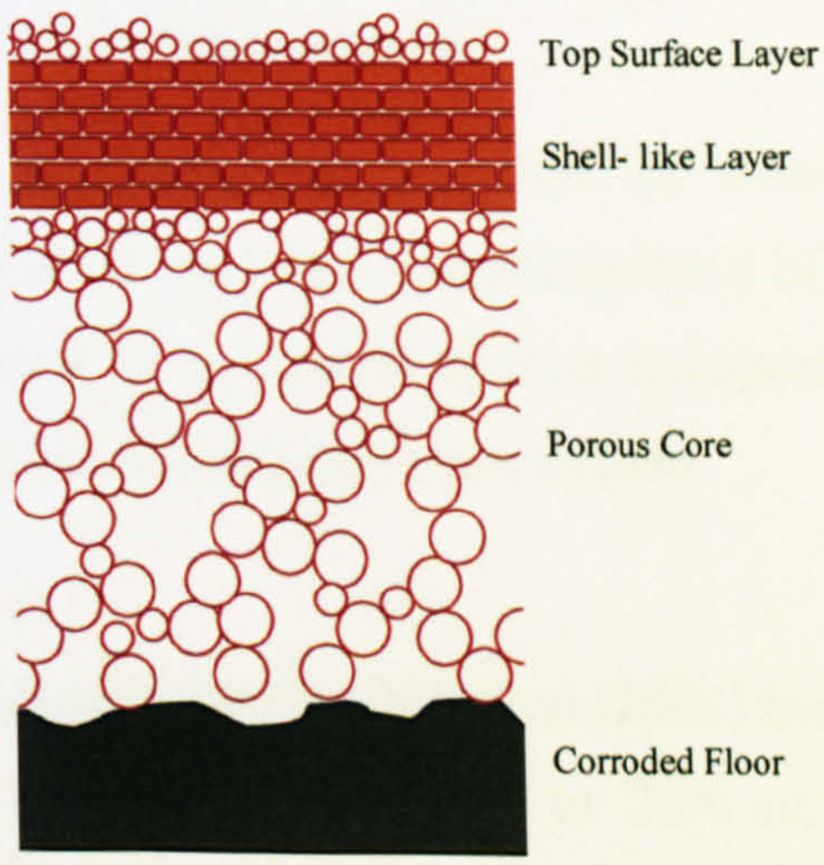

Figure 4 Schematic of corrosion scale found in iron water pipes. (Sarin et al. 2004)

As water travels through the distribution network, water quality changes occur. This may be a result of water interactions with the pipe wall or due to chemical processes such as flocculation and precipitation (Seth et al. 2003). Manganese precipitates have often been found in pipe samples (Sly et al. 1990). Of importance are particles that result from the corrosion of iron pipes. Figure 3 shows typical corrosion tubercles found in unlined cast iron water mains in the UK which can lead to reduced hydraulic capacity. Sarin et al. (2004) characterises typical corrosion and tubercle formation seen in Figure 3 with the schematic depicted in Figure 4.

Sarin et al. (2004) highlights the importance of iron corrosion stating that it can lead to serious water quality degradation and metal deformation. They state that discolouration occurs due to iron release when iron, in soluble or particulate form is transported from the corroding pipe to the bulk water. Sarin et al. (2004) suggests that anoxic conditions are likely to develop in the water distribution network during low flow and that this lack of dissolved oxygen has the effect of increasing the rate at which ferrous iron can diffuse out of the corrosion scale into the bulk water.

McNeil et al. (2001) describes how turbidity in water distribution systems rises during the night as a result of the iron corrosion process occurring on the pipe walls during periods of low flow or stagnation and Fe II changes to insoluble Fe III in the bulk water, irrespective of pipe material.

It was concluded by Boxall et al. (2003) that iron was the dominant material mobilised in UK flushing experiments and this was irrespective of pipe material or age, indicating that there must be a method of iron transport and cohesion occurring during transit through the water distribution system.

2.2.3 Organic matter

Studies in two Canadian water networks by Gauthier et al (2001) indicate that under normal conditions organic matter represents 40 to 76% of total suspended solids, and due to their low density have the potential to be transported far into the water distribution system providing they are not absorbed onto the pipe walls during transit.

Studies of drinking water networks have highlighted that the major part of biomass is attached to pipe surfaces as a biofilm, which can affect water quality, (Van der Wende et al. 1990). The term biofilm is used to describe colonies of surface adherent micro organisms and their associated excreted extra cellular polymers, (Donlan et al. 1994). Biofilms have been attributed to causing taste, odour and discolouration problems, (Gray 1994). Servais et al. (1995) suggests that bacterial growth may affect the turbidity, taste, odour and colour of distributed drinking water, and it is suggested by Lee et al. (1980) that corrosion of pipe materials may be affected by bacterial growth.

Kerneis et al. (1995) suggests that in most drinking water distribution systems, the density of suspended cultivable bacteria increases between the plant and the customers tap as a function of disinfectant decay, substrate uptake and the presence of corrosion deposits.

2.2.4 System maintenance

Slaats et al. (2002) highlights the possibility that foreign material, such as sands and soil can be introduced into a system as a product of poor maintenance practices. McCoy et al. (1986) states that discolouration can be 'a product of line repair within a system.'

2.2.5 Summary of discolouration sources

It can be concluded that the sources of discolouration material could be:

- Oxidation of cast iron mains.
- Reduction of soluble Fe II to insoluble Fe III in the bulk water under anoxic conditions.
- Biological activity.
- Addition of iron or aluminium compounds as part of flocculation processes during water treatment.
- Poor system maintenance practices.
- Breakthrough from treatment process.

2.3 How does material accumulate?

As can be seen in Section 2.2 there is a slow chronic source of discoloration material, but for a discolouration event to occur at a sufficient concentration to be seen, there must be a build up of material in the system. Polychronopolous et al. (2003) suggests that material is accumulated on the bottom of pipes, or it can adhere to the pipe walls. This highlights that two schools of thought exist as to how this accumulation takes place, the first being a sedimentary processes and secondly the cohesive layer theory.

2.3.1 Sedimentation process.

To support the theories of sedimentation, Barbeau et al. (2000) suggests that the build of up of discolouration material inside pipes is a long-term process and accumulates in certain regions of the distribution system, particularly dead ends.

The velocity at which an identified single particle suspended in quiescent water will fall and thus settle under gravity is represented in equation 1, and depends upon a number of factors: the properties of the water- its flow regime and viscosity, and the properties of the particle itself- size, shape, and density (Twort et al. 2000).

$$V = \frac{g}{1.8*10^4}(r-1)\frac{d^2}{\gamma} \qquad \textbf{Equation 1}$$

Where:

V= velocity (mm/s)
g = gravity (m/s)
r = particle density
d= particle diameter (mm)
γ = kinematic viscosity of water.

This equation is only appropriate for particle Reynolds numbers of less than 0.5.

The viscosity of water is temperature dependant, some derived values are seen in table 1 (Twort et al. 2000).

Table 1 Kinematic viscosity of water

Temperature (°C)	0	5	10	15	20	25
γ (m2/s) *10^{-6}	1.79	1.52	1.31	1.15	1.01	0.90

Theoretical analysis of material collected during flushing operations using this particle settling equation by Boxall et al. (2001) concluded that due to the very small particle size of discolouration material (0.01mm), the time to settle 100mm in total quiescent conditions would be in excess of two hours and that, once the materials were remobilised into suspension, the smallest amount of hydraulic activity was sufficient enough to maintain the samples in suspension and that the low flow velocities occurring in distribution networks from leakage meant that this material would never settle out.

Vreeburg (2007) describes that during online recording of turbidity in drinking water distribution systems, turbidity is seen to decrease during low flow periods at night and rise during the day as demand increases indicating that some degree of settling and re-suspension may be occurring. This does not however necessarily suggest settling, but rather a flow dependant change in what ever force is holding the material.

2.3.2 A build up of cohesive layers.

As it seems unlikely that a sedimentation process is occurring within the distribution system Boxall et al. (2003) hypothesized that the materials causing discolouration originate from pipe walls where they exist as cohesive layers held by forces in addition to gravity. This is enforced by work done in Australia (Ryan et al. 2003) on a laboratory pipe loop indicating that the velocity that particles will settle from solution is very small, 10^{-6} m/s. This suggests that a sedimentation process is not dominant within the network.

Pipe samples taken in a study of the effect of different pipe materials (PVC and iron) on manganese deposition in an Honduras drinking water system (Cerrato et al. 2006) showed distinct layering of material with differing colour and chemical composition when analysed with a scanning electron microscope. These layers also varied according to the pipe material. Results showed that more

manganese was found in the water samples taken from PVC pipes than iron pipes due to the smooth surface of the pipe. Iron pipes had a much rougher surface due to corrosion and tuberculation 'the iron pipe surface was not readily scraped by water motion shear stress for continuous flow conditions and there was not a significant release of either Iron or Manganese (Cerrato et al. 2006) thus further supporting the cohesive layer theory.

2.4 What causes discoloured water material to be mobilised?

Much work is covered in scientific literature regarding the suspension and re-suspension of materials in flowing water, particularly relating to sands and gravels in open channel flows (Ackers & White 1973). Here it is generally agreed that boundary generated turbulence holds particles in suspension against the gravitational fall velocity.

Much work has also been done to understand the processes by which discoloured water material is mobilised into the water causing a discolouration event to occur, and these have a common theme of a change in hydraulic conditions disturbing the material, for example an increase in flow (Marshall 2001, Ackers et al. 2001).

During high flow events, Polychronopolous et al. (2003) states that previously accumulated material can be released into the water and if flow is sufficient and sustained, this material can reach the customer's tap creating unacceptable water quality. Prince et al. (2003) states that the particulate material is collected on the pipe walls via sedimentation and electrochemical interactions at antecedent events of low water velocities and is then entrained into the water stream at a concentration that customers can see when a critical velocity, related to shear stress on the pipe wall, has been exceeded, Figure 5.

Powell (2004) also theorises that the acute remobilisation of sediment can take place during flow reversal, Figure 6, and that the frequency of any discolouration event is controlled by the frequency that the critical velocity or flow reversal event occurs and the severity of the incident is a factor of the amount of material that has accumulated.

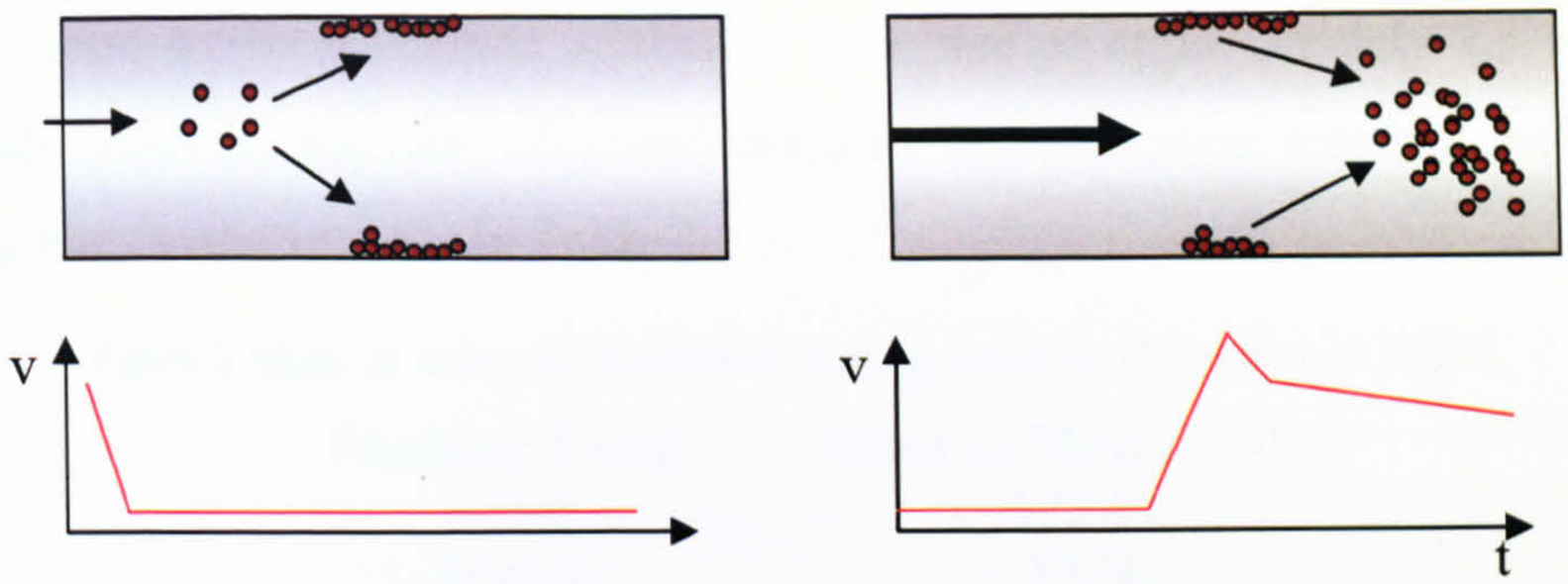

Figure 5 Formation of discoloured water, (Prince et al 2003)

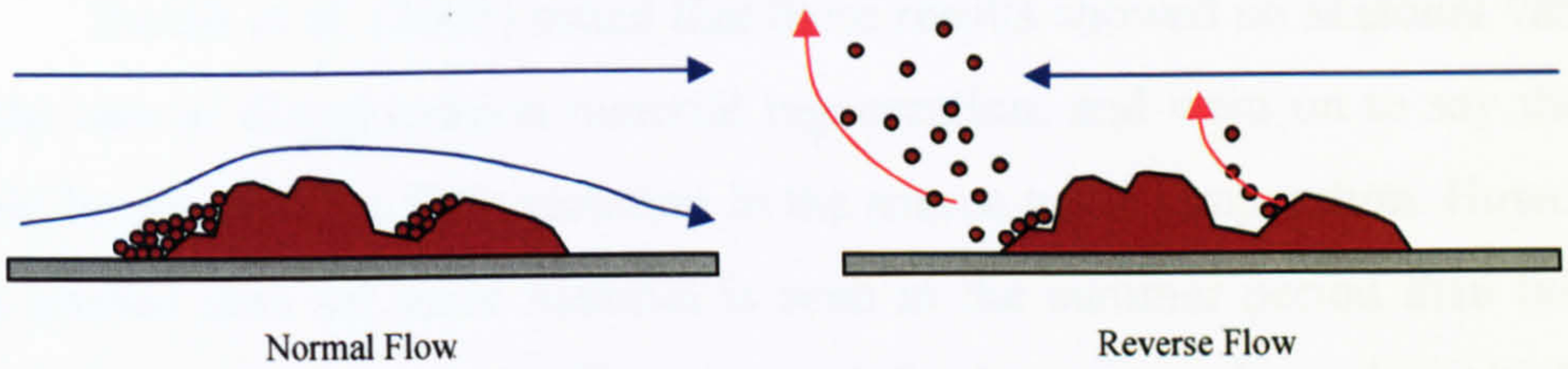

Figure 6 Flow reversal, from (Powell 2004).

The flow reversal theory presented by Powell (Figure 6) is likely to be inaccurate and over simplified, the material shown accumulating on the upstream side of an obstruction contradicts with classical sediment transport and sand dune migration theories where by material is more likely to accumulate on the downstream side of the obstruction due to eddy currents and decrease in velocity.

These theories add to the confusion as to how discolouration material accumulates in the first place; the flow reversal theory would indicate that a process of sedimentation is occurring rather than a build up of cohesive layers where as the change in shear model could support both theories.

2.5 Seasonality in discolouration

During experiments on a pipe rig consisting of sections of cast iron and MDPE pipe Holden et al. (1995) concluded that temperature played an important role in the development of biofilm and corrosion rates thought the distribution network. Work using removable coupons in a live distribution network by Hallam et al. (2001) indicated that biofilm activity fell with lower water temperatures; biofilm activity was approximately 50% lower at a temperature of 7° than 17° C.

Seasonality in discolouration material generation was addressed during repeat flushing operations by Boxall et al. (2003). A section of cast iron main

was flushed at the maximum attainable flow rate of approximately 2.3 l/s at 3 monthly intervals and the calculated mass of discolouration material mobilised during each event is show in Table 2.

Table 2 Mass of material mobilised during flushing (Boxall et al. 2003).

Flushing Event	Mass of Material (kg)
Initial	122.97
Winter	10.66
Spring	9.77
Summer	11.01
Autumn	8.3

Boxall et al. (2003) stated that these results showed no seasonal variation in the rate of discolouration material regeneration, and went on to say that this could be attributed to little variation in the source water temperature. However in this limited data set more material is seen in the summer period than both the autumn and spring periods. Experimental field errors such as the initial flush being slightly less aggressive and the winter flush being slightly more aggressive could easily attribute to the higher winter value seen here and seasonality in discolouration material regeneration must not be discounted.

In addition to increases in corrosion and biological activity during warmer periods, changes in system hydraulics during summer periods can increase the number of discolouration events. During a particularly hot summer in the Netherlands Blokker et al. (2007) documented a strong correlation between the volume of water flowing through a pumping station and the maximum daily temperature.

Vreeburg et al. (2007) demonstrates that in hot summer periods increases in demand can occur in networks often peaking in the evening in domestic areas, where householders return form work and water the garden. This increase in demand can create forces sufficient to mobilise previously accumulated discolouration material.

2.6 Discolouration development.

Work in Australia, (Prince et al. 2000; Polychronopolous et al. 2003; Prince et al. 2003) has been started to assess, characterise and model discolouration events. These are investigating relationships between customer contacts and turbidity with online testing and have investigated the classification

of discolouration particles and relationships between hot weather and discolouration events. However, the results from Prince et al. (2000) show that the main element in discolouration particles is clay and hence these results are not expected to be indicative of a UK environment. This is because the Australian water distribution system is much newer than the UK's and is not generally composed of cast iron pipes. Also Australia relies on a lot of surface water with long storage times to allow for gravitational settling of suspended particles, rather that the addition and subsequent filtration of iron flocks indicative of UK surface water treatment.

2.6.1 Conversion from NTU to total suspended solids

Turbidity can be readily recorded during flushing operations. However to attain a useful figure, independent of flushing volume and flow rate, investigations into converting turbidity to total suspended solids have been carried out.

Turbidity measurement is a function of many optical factors, including obscuration, reflection, refraction, diffraction and scatter. Turbidity is related to particle size, as obscuration is directly proportional to cross-sectional area. WRc (1994) stated that peak scattering occurs with a particle size of around half a micron with rapid fall off either side of this size. However work by Boxall et al. (2003) indicated that the size range and distribution of particles from flushing samples in the UK were fairly constant therefore a conversion to total suspended solids was viable. Using published data on turbidity and material measurements from Gauthier et al. (2001) and Mc Coy and Olsen (1986) and additional flushing data from two UK water companies, Boxall et al. (2003) found a linear relationship between turbidity and total suspended solids with an R^2 of 0.78, Figure 7.

Vreeburg (2007) also carried out two separate turbidity to total suspended solids conversions. Results from two areas were not the same and Vreeburg (2007) states that sediment from the two areas tested had differing light scattering characteristics and could be of different composition.

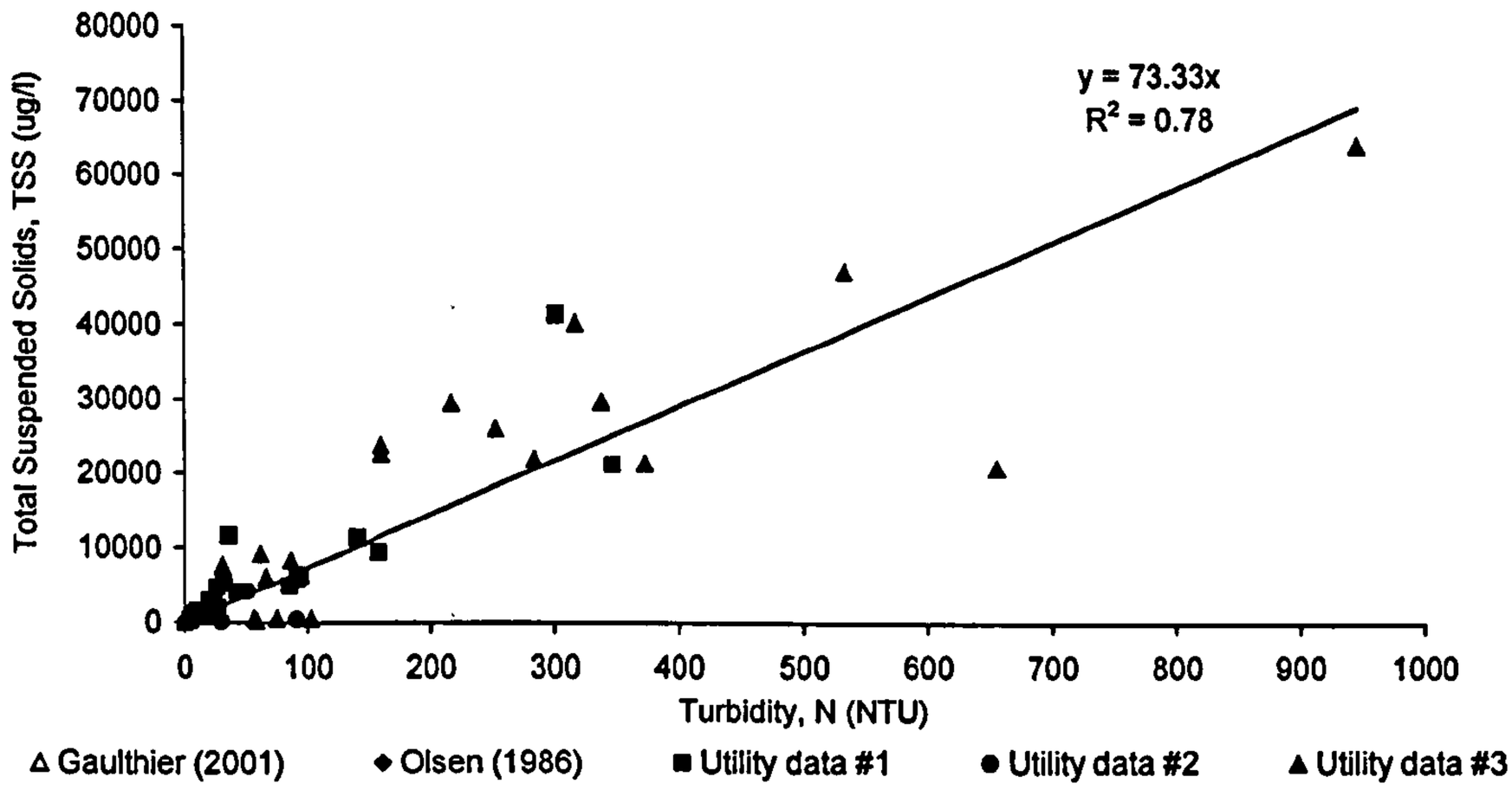

Figure 7 Conversion from turbidity to total suspended solids (Boxall et al. 2003)

There is an order of magnitude difference between Vreeburg (2007) and Boxall et al. (2003). However Vreeburg's conversion did not force the regression line through zero and it would be logical to assume that water with zero turbidity would have no suspended solids. Vreeburg's data also relates to Dutch drinking water systems which are very different in terms of pipe age, composition and chlorine treatment to the UK. Hence discolouration particle size and light scattering characteristics might be different to the UK. This highlights the transferability problems of light scattering methods to measure turbidity.

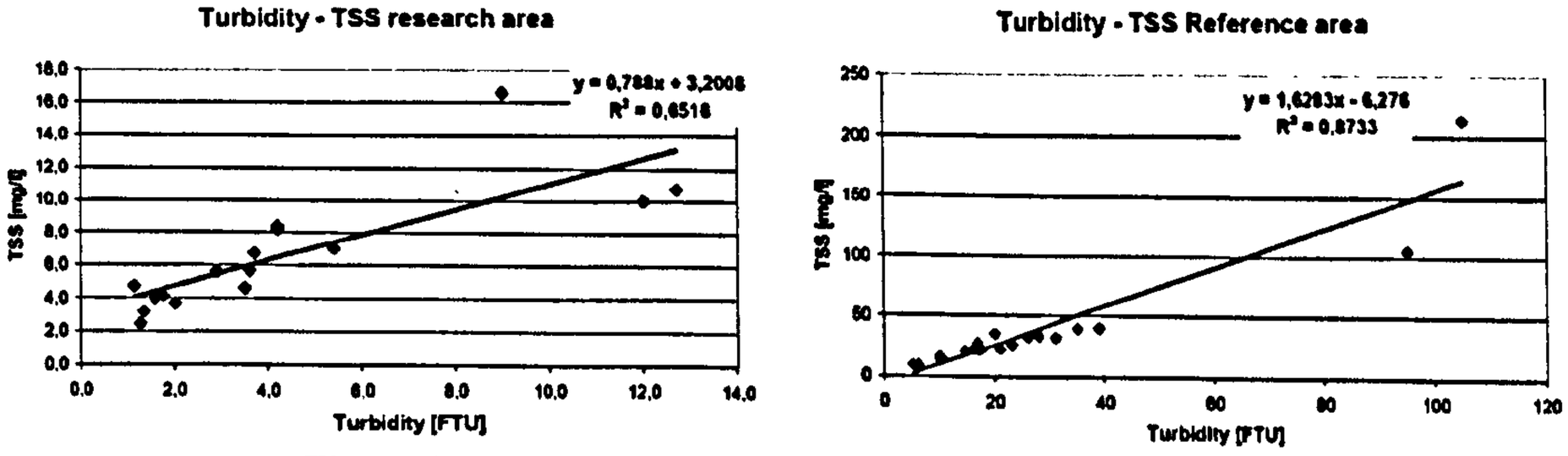

Figure 8 Turbidity to TSS conversion, Vreeburg (2007)

2.6.2 The PODDS Model.

Extensive work by the University of Sheffield, (Boxall et al. 2001; Boxall et al. 2003; Seth et al. 2003) has looked into discolouration events and carried out extensive flushing experiments to characterise discolouration particles and re-mobilisation processes. This has lead to the development of a Prediction of Discolouration in Distribution Systems (PODDS) model (Boxall et al. 2001).

The PODDS model works on the theory that pipe walls within a distribution system are subjected to a daily conditioning shear cycle as a product of the network demand cycle. This daily conditioning shear governs the strength of the cohesive layers.

Shear Stress in pipes is described as the force acting on an area of pipe wall perpendicular to the direction of flow, quantified using equation 2:

$$\tau = \rho g R_h S_0 \qquad \textbf{Equation 2}$$

Where :
τ = boundary shear stress (N/m^2)
ρ = density (kg/m^3)
g = gravity (m/s)
R_h = hydraulic radius (m)
S_0 = hydraulic gradient (unit less)

Discolouration only occurs at atypical times where the equilibrium between layer strength and mobilising forces is unbalanced and higher shear stresses are generated, such as increased demand, re-zoning or a burst. The layers exposed to higher shear stresses will mobilise until new equilibrium conditions are reached or until the layer is exhausted (Boxall et al. 2001).

The relationship between the strength of the layer and the stored turbidity volume (layer thickness) is expressed as (equation 3):

$$\tau_s' = \frac{C^b - C_{max}}{k} \qquad \textbf{Equation 3}$$

τ_s = corrosion layer yield strength (N/m^2)
C = stored turbidity volume of layer - ($NTUm^3$)
k = gradient of the potential as a function of layer strength.
C_{max} = Maximum turbidity volume- fully developed layer with zero strength (impossible to reach)
^{b} = power term to set for first order relationship.

This relationship between stored turbidity and layer strength is represented in figure 3, which demonstrates the influence of the gradient k and the power term b.

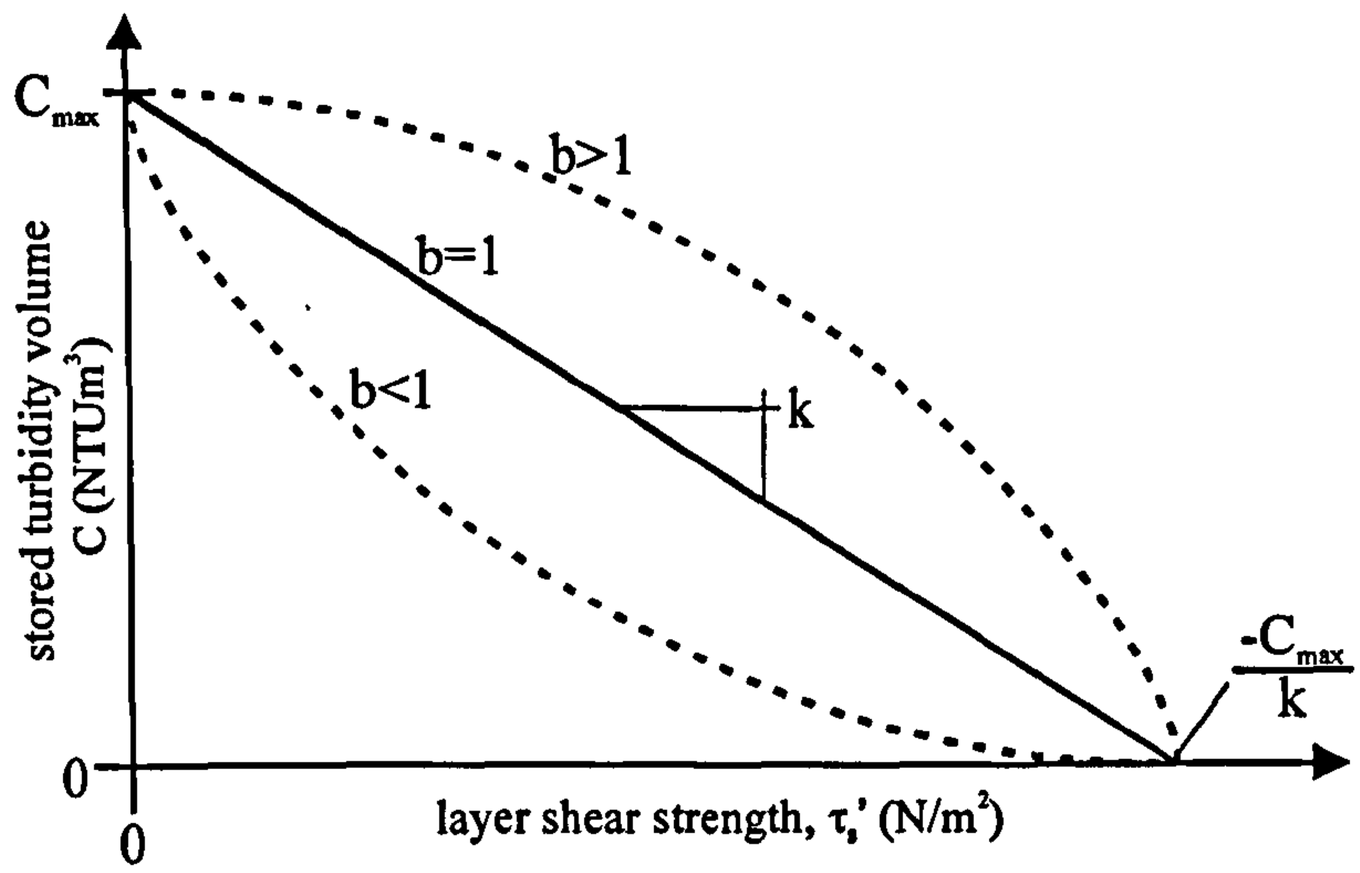

Figure 9 Representation of layer strength versus stored turbidity volume (Boxall et al. 2001).

Thus layers with a low daily conditioning shear stress will have a higher stored turbidity volume and therefore higher discolouration potential. However for discolouration to occur there must also be a mobilising or disturbing hydraulic force. In the PODDS model this is expressed in equation 4:

$$R = P\left(\tau_a - \tau_s^{'}\right)^n \qquad \textbf{Equation 4}$$

Where:

R = Rate of supply

$\left(\tau_a - \tau_s^{'}\right)$ is the change in shear stress.

The gradient term P and the power term n are used to describe the effect of the eroding force.

The incremental change in turbidity resulting from this erosion can be evaluated by the multiplication of the rate of supply by the pipe surface affected and dividing by the flow rate, as seen in equation 5:

$$\Delta N = \frac{RA_s}{Q} \qquad \textbf{Equation 5}$$

Where:

ΔN = change in turbidity

As = surface area
Q = flow rate

The full PODDS model described above can predict the discolouration in a pipe in response to an applied shear stress; however accurate calibration is required. A simplified PODDS model which is essentially an add-on code to EPANET predicts the discolouration response of distribution networks to changes in hydraulic conditions. A demand can be assigned to every node in an EPANET network model, the increase in shear stress above the daily conditioning shear stress is used to model the discolouration potential.

2.6.3 Discolouration risk modelling

An alternative modelling approach to the simple PODDS model is Mouchel's Discolouration Risk Model (DRM), and estimates the propensity of a pipe to cause discolouration based upon a combination of both likelihood and consequence, (Dewis et al. 2005). Here the consequence of a discolouration event is similar to the simple PODDS model where an increased demand is applied systematically to each pipe in a network. However a change in velocity criteria is used to assess the discolouration potential rather than the shear criteria as used in the PODDS model. As a velocity criteria would imply a sedimentation process is occurring, which was discredited in Section 2.3.2, and a velocity in a small diameter rough pipe would have a much higher shear stress than the same velocity through a larger diameter smooth pipe. Hence it can be argued that an increase in shear stress is a more accurate method to describe a hydraulic event capable of causing discolouration.

Discolouration Risk modelling goes a step further than the PODDS model as it incorporates a likelihood function of a burst occurring based on a risk tree approach. However this risk approach uses 'expert judgments' in its weighting system and little science.

2.6.4 Measuring discolouration potential in the field.

As it can be seen two models exist, PODDS and DRM, to assess the discolouration potential of areas in a network based on desk top hydraulic modelling approach. In the Netherlands, Vreeburg et al. (2004) developed the Re-suspension Potential Method (RPM) based on measuring the mobility of discolouration material within a network. Here a section of pipe is isolated and an extra demand of 0.35m/s is applied on top of the actual velocity via a hydrant

for 15 minutes. The discolouration potential is based on a ranking of the maximum and average turbidity in the first 5 minutes and the last 10 minutes of the disturbance and the time to clear, Figure 10.

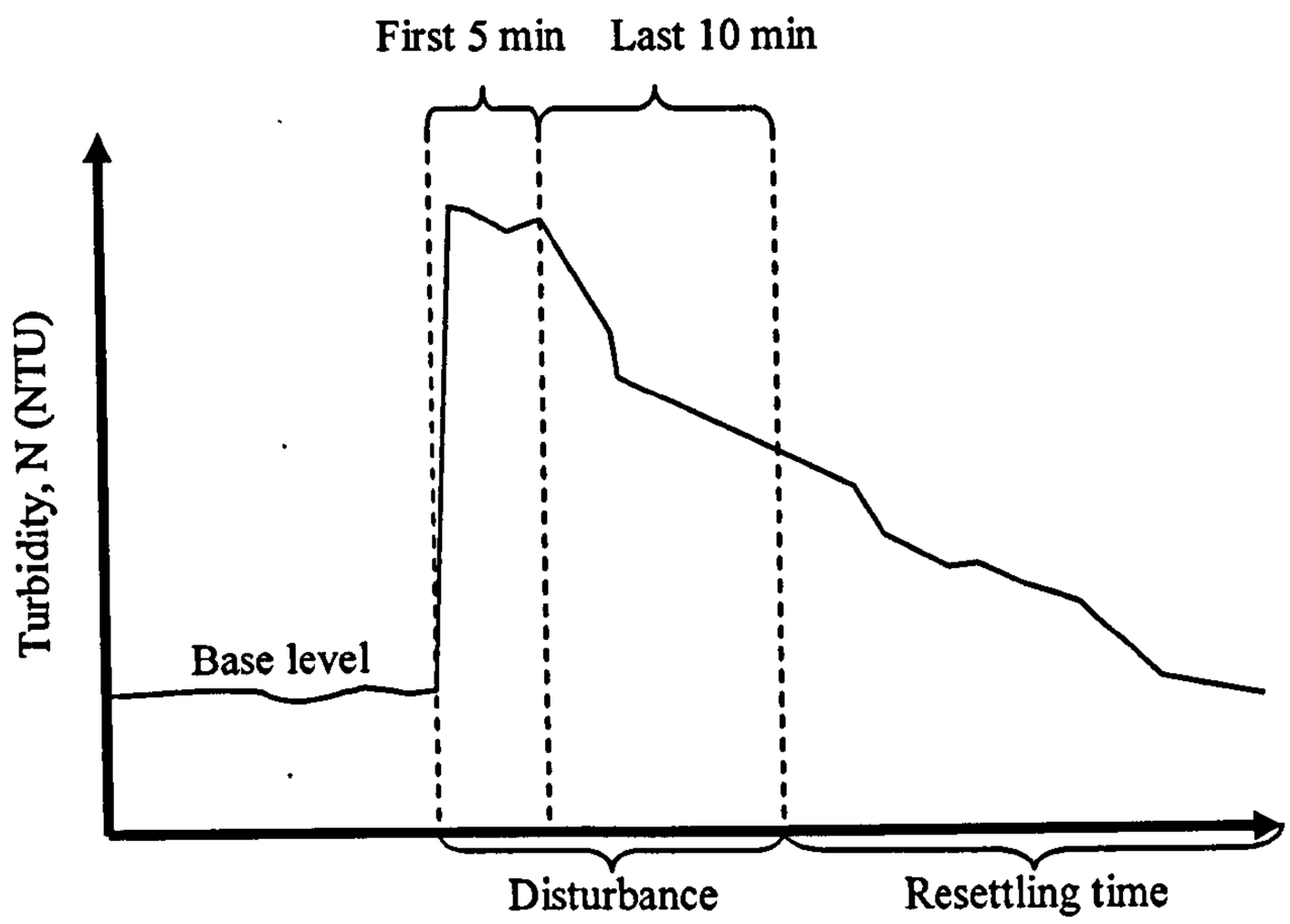

Figure 10 Typical turbidity response during RPM test (Vreeburg et al. 2004)

Although the re-suspension potential method has been implemented by Dutch water companies for more than ten years it does have a significant draw back and limitation when trying to assess changes in turbidity potential for a pipe over time. This is because by its very nature the RPM method must have to some extent its own cleaning effect thus repeating the RPM method is likely to produce an overestimation of reduction in discolouration potential.

Also the RPM method disturbs discolouration material with in the system, and then measures the time this material takes to clear without getting rid of it. The characteristics of distribution systems in the UK are likely to have a higher discolouration potential than the Netherlands and such disturbances in the UK systems are not likely to be sanctioned.

2.6.5 Self cleaning networks

The phenomena that discolouration material will accumulate in areas subjected to low hydraulic forces such as dead ends, and oversized pipes was discussed in section 2.3.2. Slaats (2002) developed the theory of self cleansing networks. Here 0.4 m/s is determined as a velocity above which discolouration material cannot accumulate on the pipe walls. This value appears to work,

however there is no indication of where this value originates from or how it was calculated. The self cleansing velocity is maintained by engineering principles by laying dendritic networks with decreasing pipe diameter with distance. As previously discussed, basing this principal on velocity criteria, rather than shear stress would seem to limit its effectiveness. However a newly engineered self cleansing network was put to the test alongside a looped network and a traditional dendritic network by Blokker et al.(2007). Here, from flushing results and monitoring particles entering and leaving the networks, the self cleansing network seemed to be 'self cleansing'.

Whether these self cleansing principals would be applicable in a UK situation is debatable, as Dutch networks are very different and have a much higher percentage of plastic pipes and chlorination is not used in the water treatment process. Self cleansing networks do have a cost benefit of about 20% compared to looped networks due to shorter lengths of thinner pipes being laid however the cost of retrofitting a self cleansing network in existing UK distribution systems would be prohibitive, (Blokker et al. 2007). It also has to be noted that UK water companies have an obligation to supply flows with sufficient fire fighting capabilities and it is debatable whether pipes of such small diameters would fulfil this requirement; and indeed Dutch regulations had to be changed to allow the implementation of such networks.

Heavily regulated water companies strive to attain the goal of zero supply interruptions. Dendritic distribution networks by their design have inherent problems with security of supply when compared to looped networks. A burst occurring in a dendritic network has the potential of depriving customers downstream of the burst of water and maintaining supply during repair works is further complicated. This gives rise to the scale at which self cleaning networks are applied. The self cleansing network design can however be applied on a scale at which security of supply is not adversely affected in large areas by keeping dendritic areas relatively small and connected by larger looped sections.

Although there is an onus on water companies to reduce discolouration customer contacts, this essentially aesthetic problem must be secondary to maintaining security of supply.

2.7 The knowledge gap

As can be seen, there is some understanding as to the hydraulic processes which cause discolouration events, what discolouration material comprises of and where it comes from. There are also modelling tools available to assess the discolouration potential and risk in distribution networks, and methods to measure discolouration potential in the field. There is however very little understanding of the processes contributing to and controlling the regeneration rates of discolouration material within drinking water distribution networks.

Factors which affect the regeneration rates of discolouration material could include:

- Pipe material.
    - Un-lined cast iron pipes are affected by corrosion releasing iron in to the bulk water
- Pipe diameter
    - Larger diameter pipes have a greater surface area for reactions to take place between the pipe wall / water interface.
- Hydraulic conditions
    - Pipes subjected to higher daily conditioning shear stresses could have less discolouration material accumulated or could even be experiencing 'self cleaning' conditions.
- Source water quality.
    - Surface water sources where iron flocculation is used in water treatment could have a higher discolouration potential.

In order to proactively manage mains rehabilitation and maintenance operations, and to assess the effectiveness of such work, a greater understanding of discolouration material generation rates is essential.

3 Aims

The literature review has highlighted that little is known about discolouration material generation rates which is essential for water companies to effectively plan Distribution Operation and Maintenance Strategies in an efficient cost effective manner. Thus the main aims in this project are designed to address this issue:

Aim 1: Investigate associations between discoloured water customer contacts and information commonly maintained by UK water companies: maintenance records (burst repairs) and asset databases (mains properties).

Aim 2: Using information gained from the desk study data analysis phase, employ field techniques to further develop an understanding of the rate at which discolouration material builds up with in a water distribution network, and whether this rate is affected by differing conditions within the network such as the hydraulic regime, pipe material, diameter and age. This could allow the addition of discolouration material regeneration rates into current discolouration risk models to improve return rate planning.

Aim 3: Develop an understanding of the effectiveness of Yorkshire Water DOMS rehabilitation strategies and the full zonal flushing approach explored in Aim 2, using long term turbidity monitoring and comparing relative values in terms of reduction in discolouration potential and cost effectiveness.

Aim 4: Combining the theories developed in aims 1, 2 and 3, determine the effects of valve movements on discolouration and how such operational procedures can be managed to reduce discolouration risk.

4 Data Analysis

4.1 Introduction

Since it is well known that bursts can cause hydraulic forces capable of eroding previously accumulated discolouration material, this section tries to discover any relationships between burst events and discolouration customer contact frequencies. It is thought that DMAs with a high burst frequency could also experience elevated discoloured water customer contact frequencies. Secondly possible links between discolouration customer contact frequencies and mains properties are investigated at the DMA level. This will include variations between mains material, diameter and age. As the dominant material found in discoloured water samples is iron, it is expected that a positive correlation between occurrence of cast iron mains and discolouration customer contacts will be found.

4.2 Method

Customer contact and burst incident databases along with water into supply figures were available for a five year period for two water companies in the North of England. Pipe information in the form of GIS databases was also available. This was for a sample of 11 DMAs from Water Company A and the entire region from Water Company B.

Limitations regarding the reliability of customer contact data are described in the literature review section 2.1.

4.2.1 Company scale analysis

Burst records, discoloured water customer contacts and water into supply data for the entire regions of the two water company's over the five year period were investigated to study the effects of bursts on water quality. This data was summed at a monthly interval and plotted with respect to time. To correlate this with seasonality trends, average monthly air temperature data was obtained from Met Office weather stations central to each region.

4.2.2 DMA level analysis

Analysis was also carried out at a DMA scale comparing burst and discolouration customer contact rates. For Water Company A, a sample of 11

DMAs were analysed and for Water Company B the full GIS pipe network database was analysed. Small DMAs which represented commercial operations such as a single large factory or hospital were removed from Water Company B's data set resulting in analysis of a total of 2128 DMAs.

4.2.2.1 Burst and contact relationships

Using GIS software, burst incidents and discoloured water customer contacts were plotted, and the total number of contacts and burst incidents associated with each DMA calculated. To account for variations in DMA size and customer populations, burst data was normalised by total pipe length and discoloured water customer contacts by total number of billing addresses within each DMA.

4.2.2.2 Contact and pipe material relationships

In order to investigate relationships between pipe materials within a DMA and discoloured water customer contacts the DMA level data were also analysed for pipe characteristics and customer contact rates. This included analysis of pipe material and diameter by percentage length. GIS software was again used to facilitate this, allowing calculation of the total lengths of the various pipe materials and diameter within each DMA. Graphs were then plotted to compare these with the number of discolouration contacts to highlight any trends visible in the data.

4.3 Results

Due to the sensitive nature of the data and to preserve confidentiality scales have been omitted from the following graphs.

4.3.1 Company scale results

Figure 11 presents the results of the temporal analysis of burst frequencies, customer contacts, water into supply and average air temperature data for both water companies over the five year period.

Blue and red dotted lines on the graphs highlight the winter and summer periods respectively. These have been inserted by eye, since the maximum and minimum temperatures do not fall in exactly the same period each year.

It should be noted that the temperatures shown in Figure 11 do not fall below zero. This is because only average monthly temperature was available and as 'frost heave' is an effect of ground temperature, some degree of time lag is to be expected between air and ground temperatures.

The same patterns in the data were observed for both water companies. Discoloured water customer contacts clearly show a seasonal trend, with highest values being recorded in the summer months. Burst frequencies also show a strong seasonal trend in the data; however the highest number of bursts is seen in the winter months. This seasonality was confirmed by reference to air temperature information supplied from a local Met Office weather station. Water into supply frequencies show a six month cycle in the data, with peaks occurring in both the winter periods due to bursts and summer periods due to increase in demand.

Interestingly in the data for Water Company A, the last winter during the period of study had far fewer recorded burst events (Figure 11) than the trend of the previous years. In the summer immediately after this an abnormally high number of discolouration customer contacts were recorded. Similarly, the two winters of 2000 and 2002 have higher burst frequencies than other years which lead to a decrease in discolouration customer contacts in the subsequent summers.

In the last summer period for Water Company A, a significant event occurred in the trunk main which contributed partly to the abnormal high number of discolouration customer contacts seen in the last summer period. However with contacts relating to this event removed approximately twice the discolouration contacts from the same period in the preceding year remained.

Also of note is that, with contacts relating to the event removed from water company A there is a clear decreasing trend in discolouration customer contacts over the five year period for both water companies.

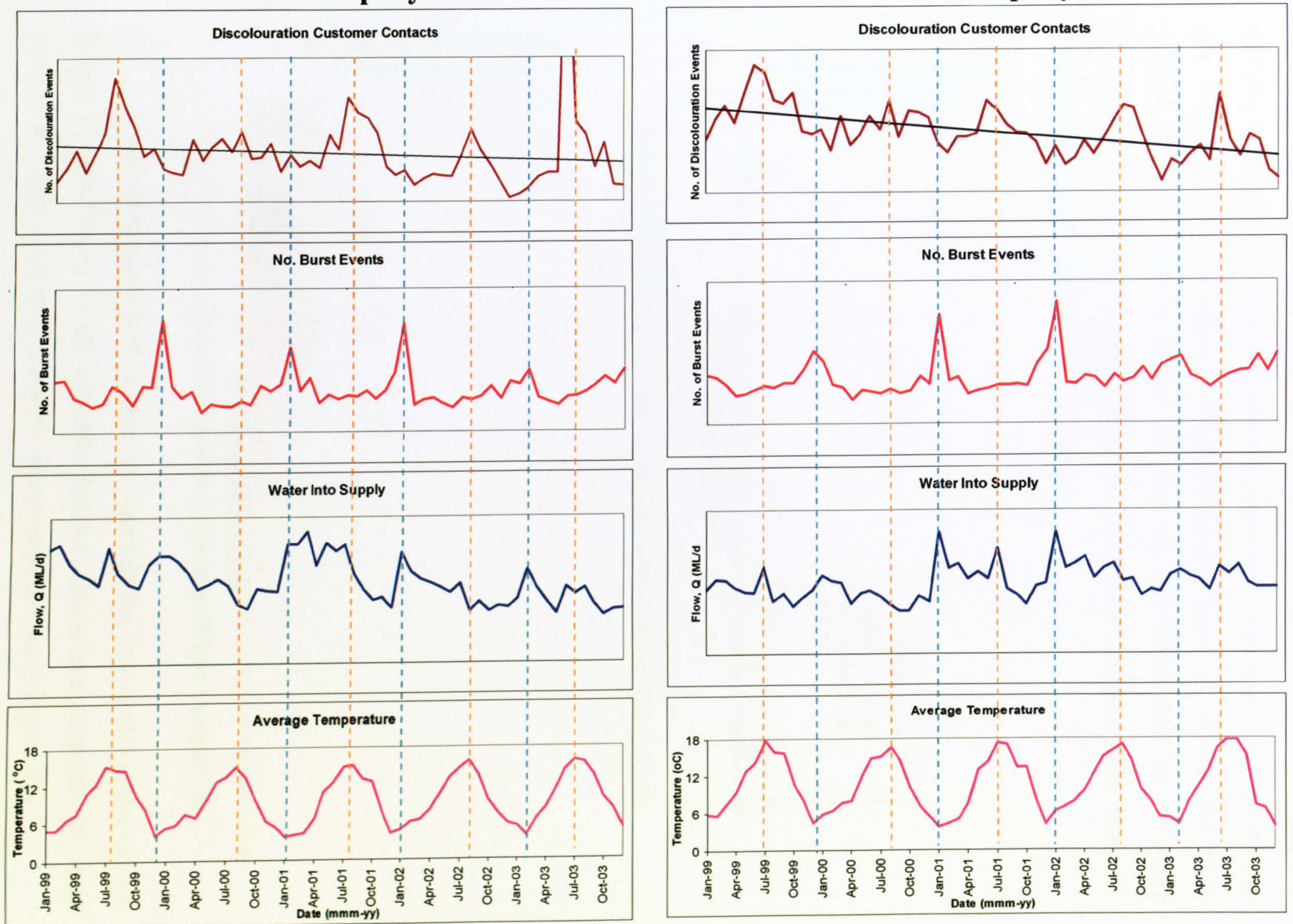

Figure 11 Temporal analysis of data

4.3.2 DMA scale results.

Analysis of the 11 sample DMAs of Water Company A for number of bursts per Km of pipe compared to the number of discolouration contacts per property is presented in Figure 12 showing a possible reduction in scatter as burst rate increases, and a tentative overall downward trend. A similar but more definite picture is seen in Figure 13 from the full DMA data set of Water Company B, areas with high burst rates have low discolouration contacts, however the inverse is not necessarily true.

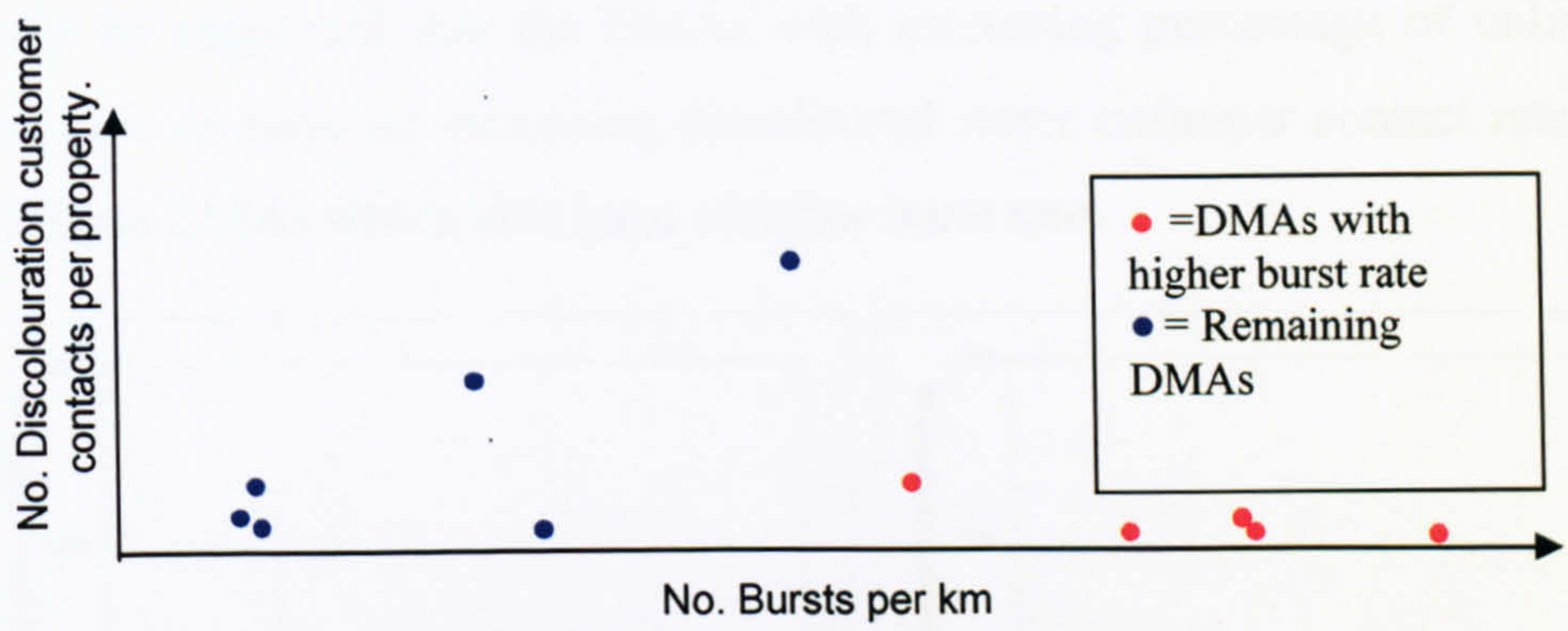

Figure 12 Burst versus discolouration frequencies (Water Company A)

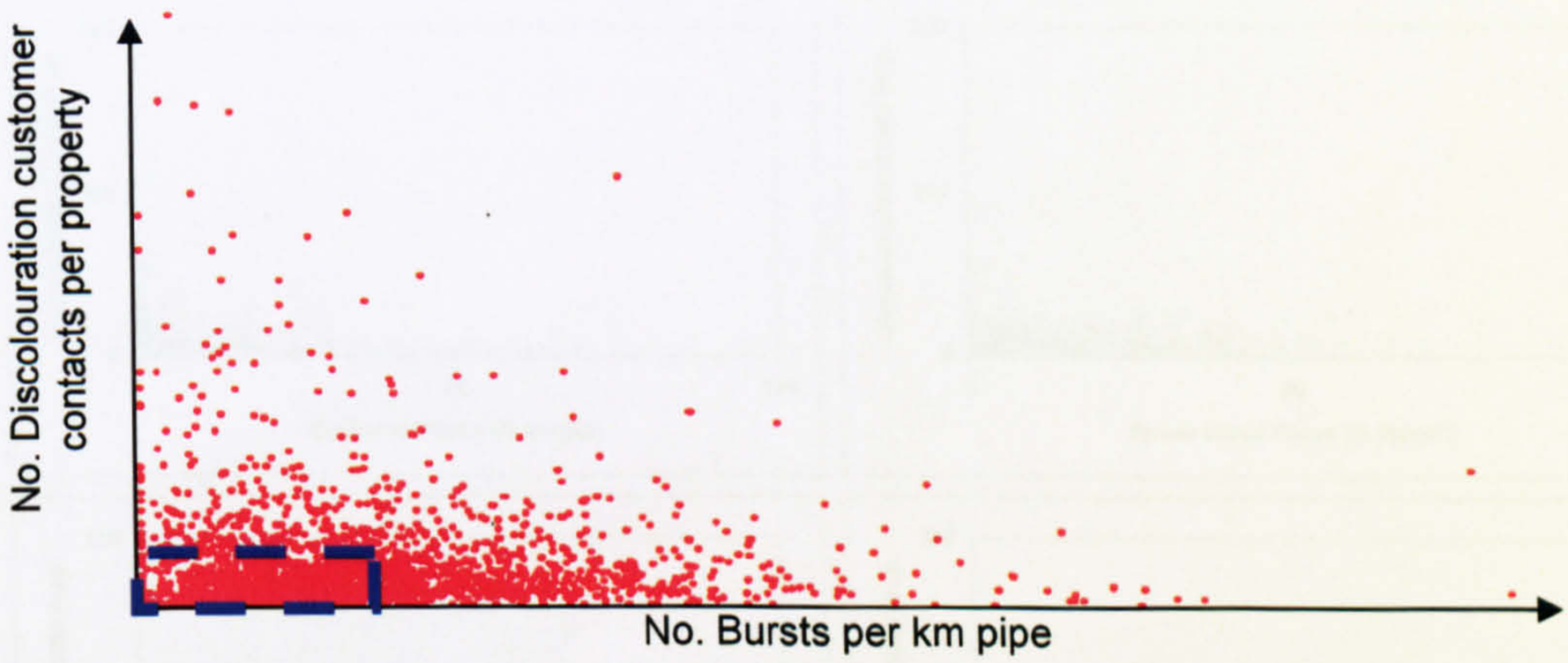

Figure 13 Burst versus discolouration frequencies (Water Company B)

It should be noted that in order to represent the data clearly scales used in Figure 12 and Figure 13 are different, but for comparison purposes the range covered in Figure 12 is approximately represented in blue in Figure 13.

Figure 14 presents results of an analysis to investigate the relationships between the percentage of pipe material and customer contact rates for Water

Company B's entire region. Specific trends in the data are not clearly seen. In particular there is no apparent trend between the percentage of unlined cast iron pipes and customer contacts to support industry perceptions and the theory that iron is the dominant source of material for discolouration as a product of the oxidation of cast iron mains (Section 2.2.2). Figure 15 presents customer contact frequencies compared to the percentage of unlined cast iron pipe for the sample data set supplied by Water Company A. Initially this also appears to show a lack of correlation. However, following further manual investigation including consideration of burst behaviour (Figure 12), possible with this limited data set, it could be suggested that the DMAs with increasing percentage of unlined cast iron pipe do have an increasing discoloured water customer contact rate, except for those DMAs which also have a higher burst rate.

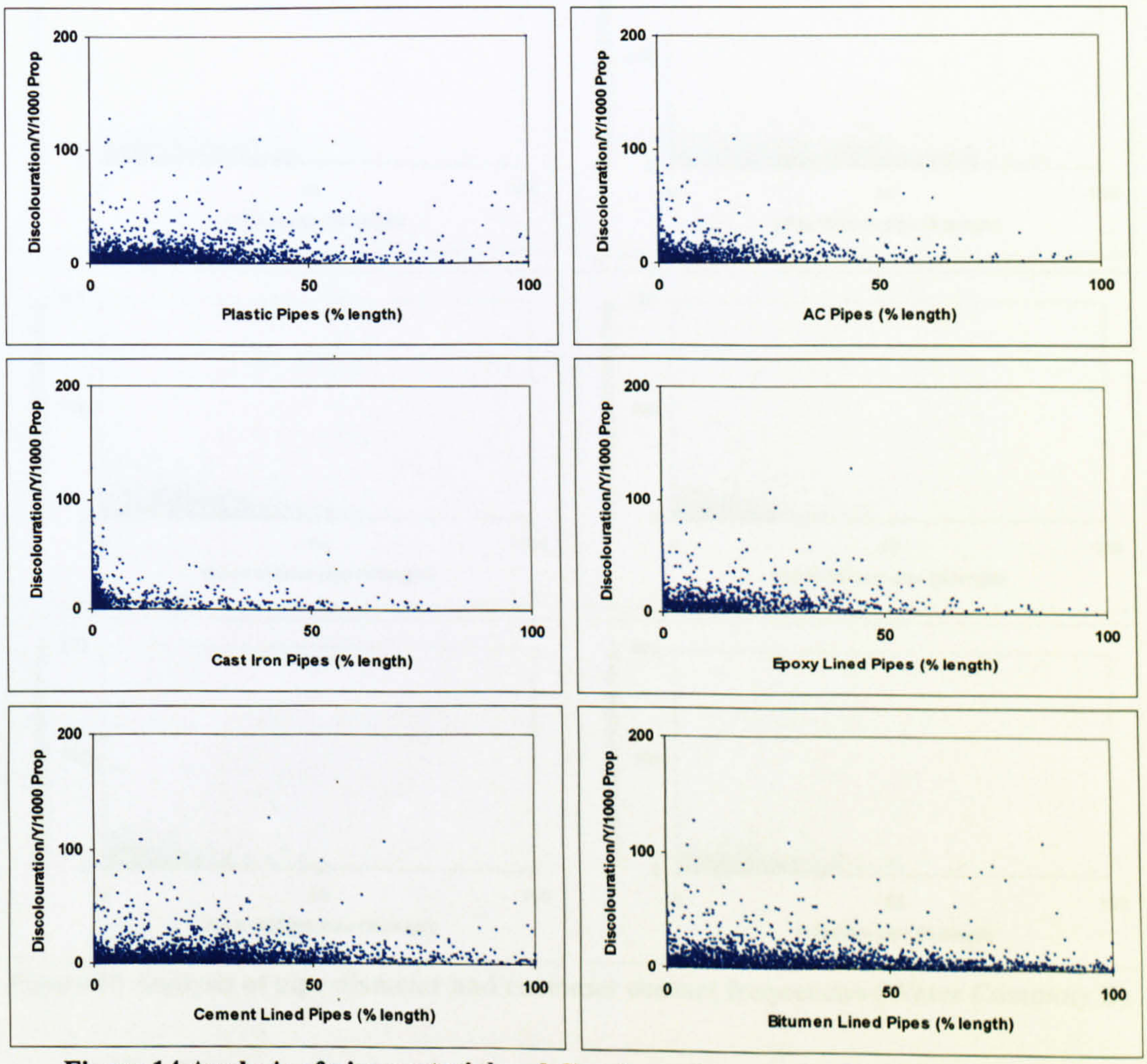

Figure 14 Analysis of pipe material and discolouration contact frequencies (Water Company B)

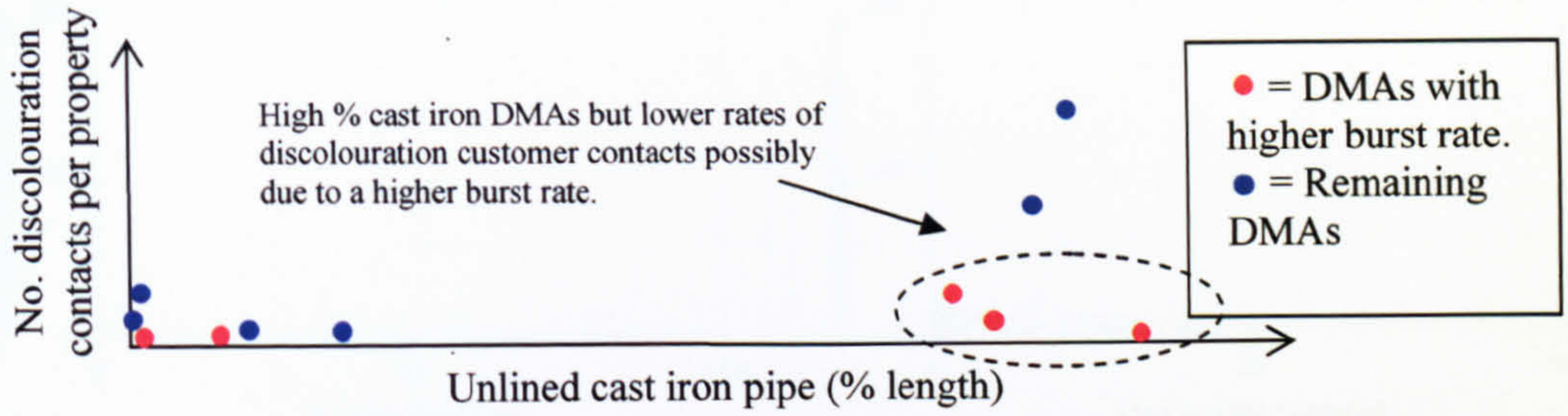

Figure 15 Discolouration frequencies compared to % cast iron pipe.

The full data set of company B was analysed for pipe diameter by percentage length compared to customer contact frequencies. No correlation between pipe diameter and contact rates was seen (Figure 16).

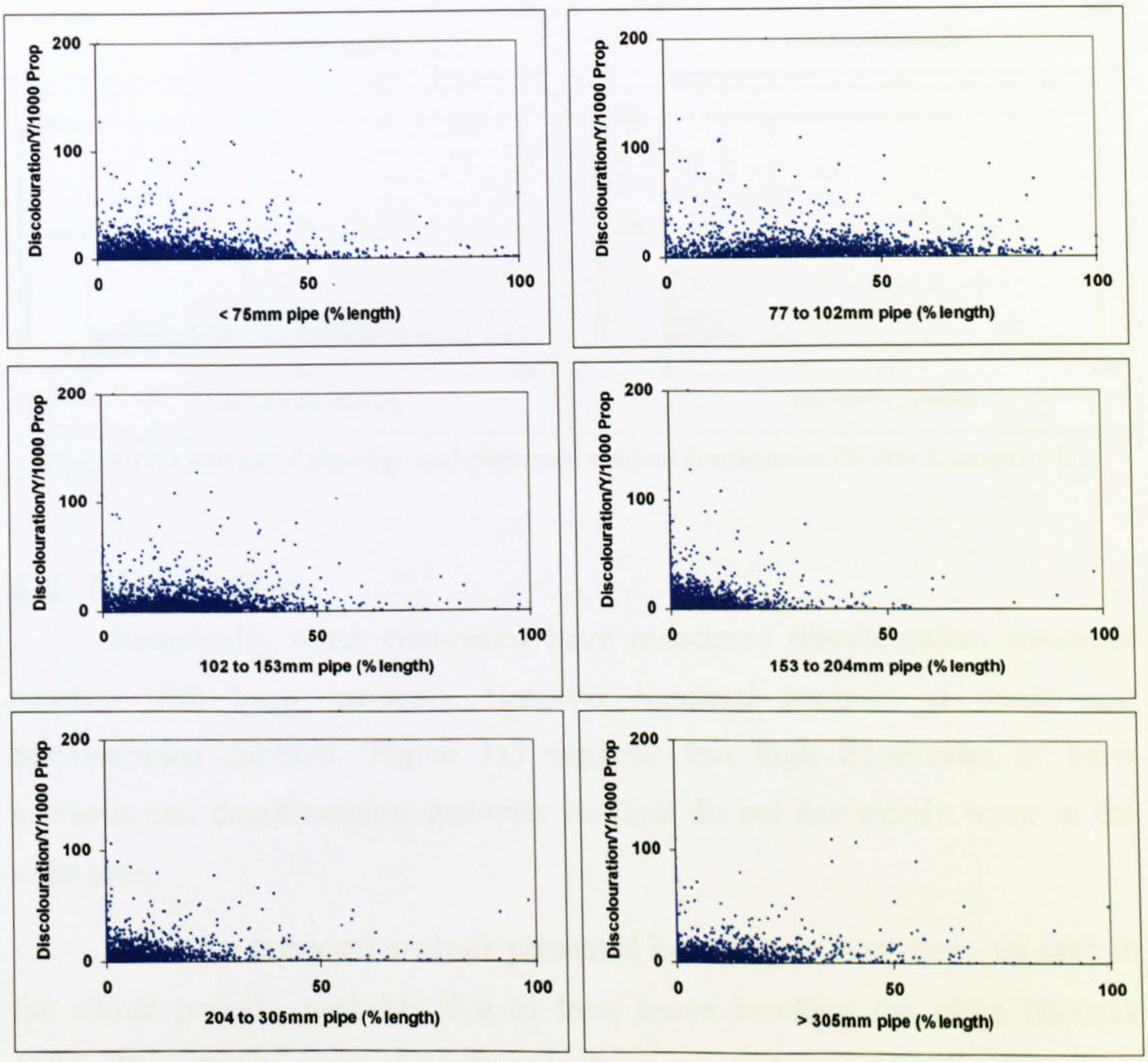

Figure 16 Analysis of pipe diameter and customer contact frequencies (Water Company B).

The full data set of company B was analysed for pipe age by percentage length compared to customer contact frequencies. No correlation between pipe age and contact rates was seen (Figure 17).

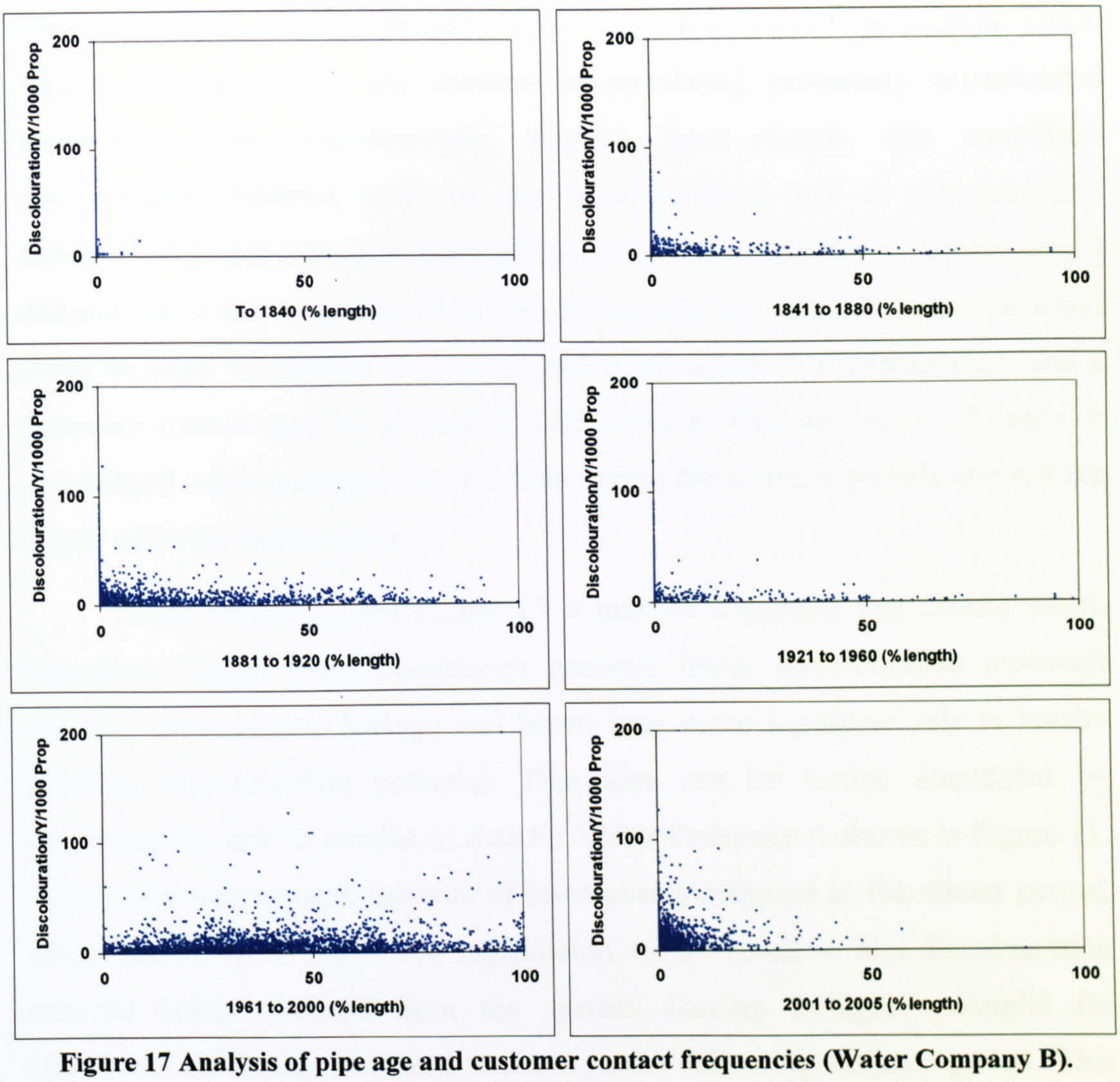

Figure 17 Analysis of pipe age and customer contact frequencies (Water Company B).

4.4 Discussion

Historically water companies have associated discolouration customer contacts with burst incidents. However temporal analysis of bursts and discolouration contacts (Figure 11) suggests that high frequencies of burst incidents and discolouration customer contacts do not necessarily occur at the same time.

From the temporal analysis presented here, higher burst rates are seen in the winter periods, probably due to frost heave breaking the pipes (Bocock 1997). These bursts cause an increase in the amount of water into supply and are reflected in winter peaks in the water into supply data. However an increase in water into supply is also often seen in the summer periods, which can be attributed to increased use of the water by the customer in warmer weather (Prince et al. 2003). Hence hydraulic forces higher than the normal equilibrium

state are likely to exist in the distribution network at both of these times. These abnormally high forces are capable of mobilising previously accumulated material causing discolouration. During burst events this mobilised discolouration material exits at the burst location and is not generally experienced by the customer. During the summer periods however, the increased demand for water is generated at the customer's tap. Discolouration material therefore exits the system at the customer's tap where it is experienced, and a customer contact may be generated. This could explain the observed peaks in discoloured water customer contact rates during the summer periods and not the winter when the bursts occur.

From Figure 12 and Figure 13 it may be suggested that DMAs which experience higher burst frequencies generate fewer discolouration customer contacts, consequently leakage and bursts may serve a positive role in locally reducing discolouration potential. This idea can be further elucidated by examining the last 12 months of data for Water Company A shown in Figure 11. Here lower than typical numbers of burst events occurred in the winter period, which according to the above explanation would result in less discolouration material being removed from the system, leaving a higher potential for discolouration during increased demand in the following summer period. This results in increased summer discolouration contacts, as seen in the data.

It could be argued from the seasonal analysis of discolouration data (Figure 11) that higher discolouration customer contacts are a function of higher temperature, and that more discoloured water material is produced in the system in warmer water. However, analysis of regulatory sampling data taken from the 11 sample DMAs of water company A (Figure 18) showed no correlation between increases in quantity of pH, Fe, Mn, Al, Pb, conductivity and coliforms and increases in the temperature of the water samples, suggesting that there is no physical effect of air temperature on discoloured water material generation.

Regulatory sampling is however a limited method of measuring discolouration performance. The data shown in Figure 18 represents all the samples taken in 11 DMAs over a five year period from 1999 until 2003. The few sampling points shown highlight the low possibility of sampling at the precise time and location to capture a discolouration event.

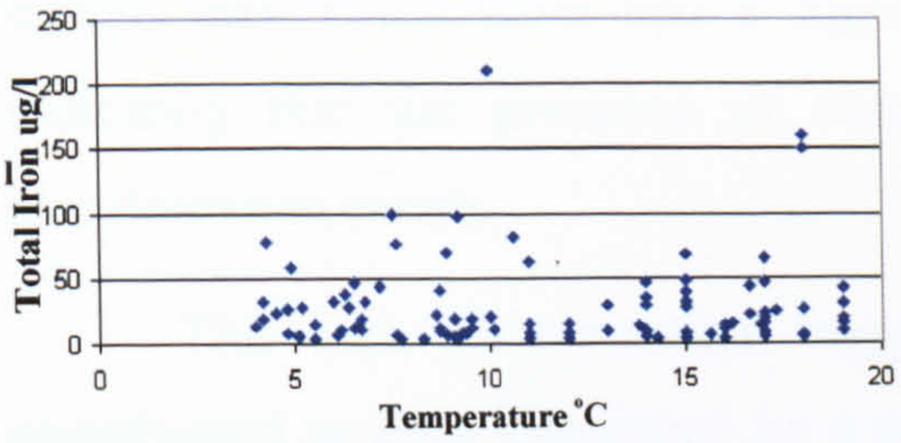

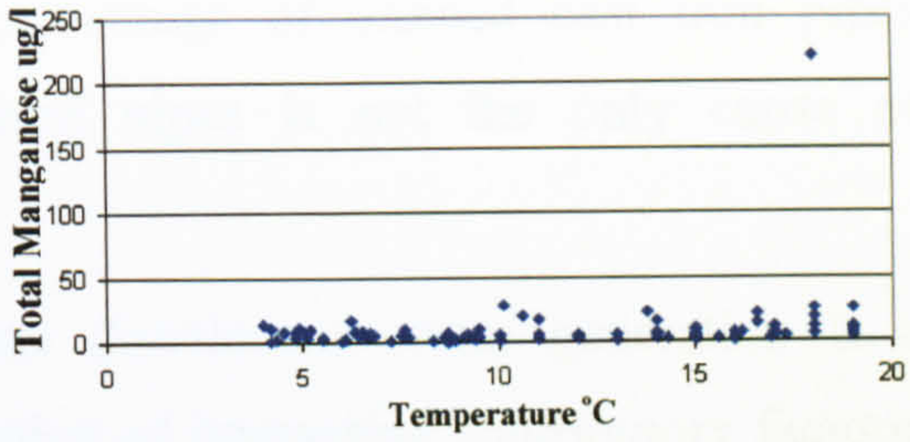

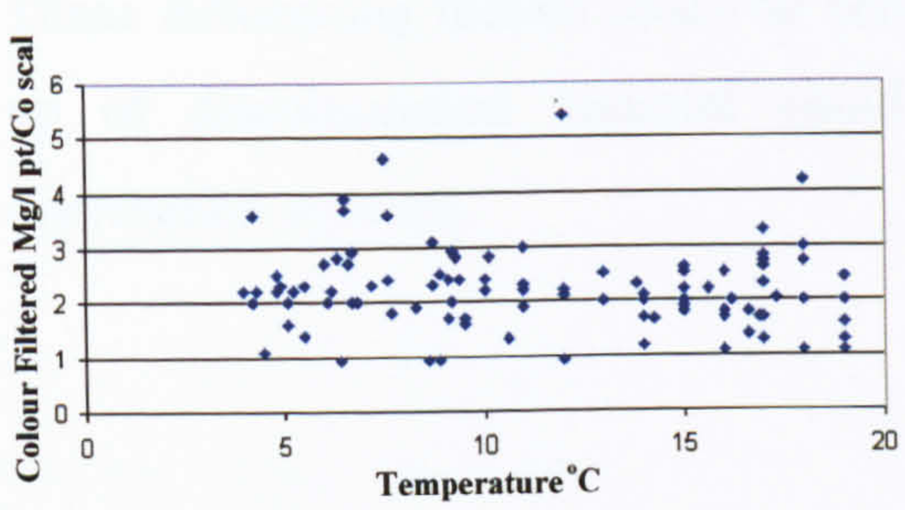

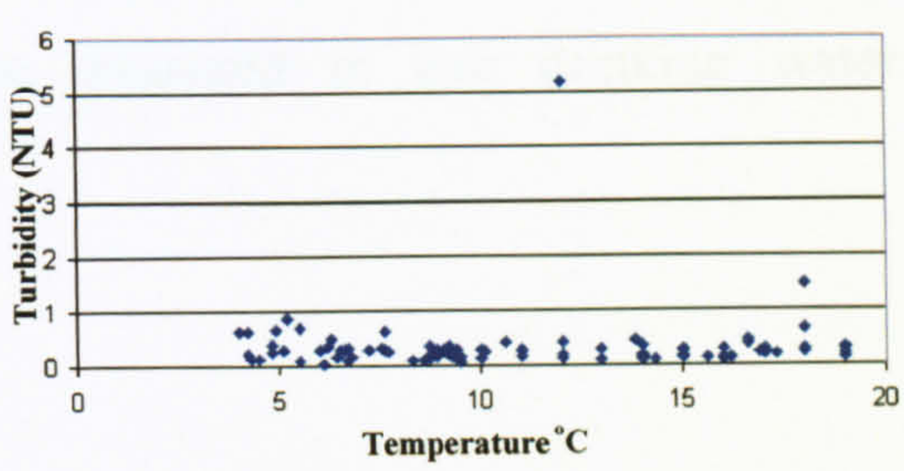

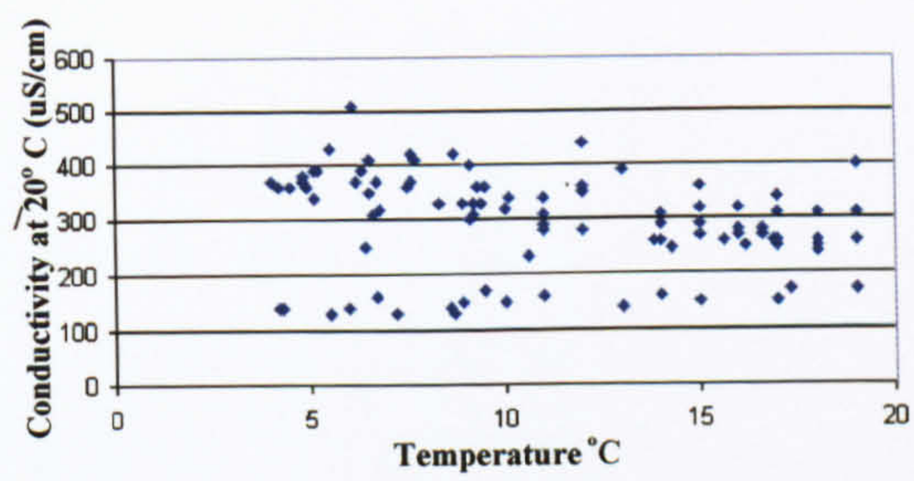

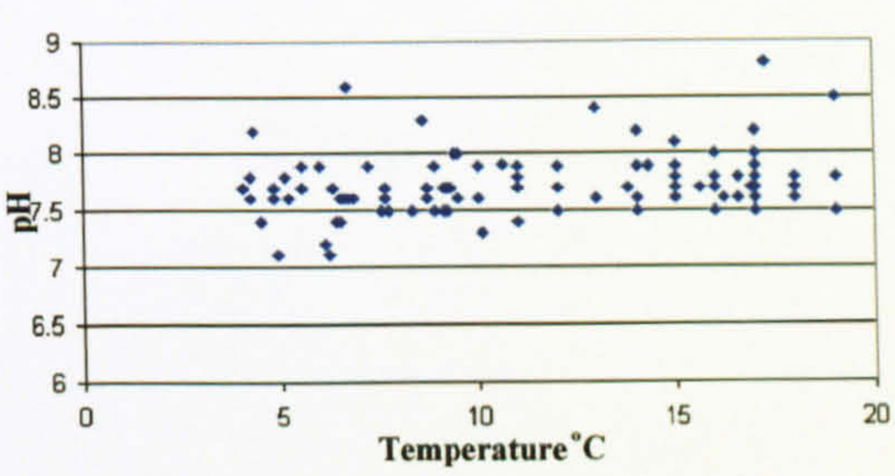

Figure 18 Regulatory sample determinants compared to water temperature.

The suggestion that winter bursts may provide beneficial cleaning is controversial, but should not be considered significant in the drive to reduce leakage and water loss. However, as leakage is reduced this potential benefit will also decrease and discolouration contacts may become more frequent. Thus it is important to gain an understanding of the processes influencing material accumulation and release, so that systems can be proactively managed to efficiently implement operation and maintenance strategies to reduce discolouration contacts by controlled cleaning methods.

The data analysis presented here suggests that there is no simple, direct correlation between the quantity of cast iron pipes, other pipe material or diameter and the frequency of discolouration contacts. The lack of correlation to cast iron pipes is particularly surprising. This however could be a factor of the Section 19 Program. Poorly performing DMAs were targeted for scraping and

lining and mains replacement programs. High performing DMAs were left, even though they could have had a high percentage of unlined cast iron pipes indicating that the presence of cast iron pipes is not the only cause of discolouration events.

This lack of correlation suggests discoloured water generation is a complicated process influenced by a number of interacting contributory factors. These influencing factors could be better assessed in field trials where the build up of discolouration material could be measured in live drinking water distribution systems.

5 Flushing Field Trials

5.1 Introduction

Results from the data analysis in Chapter 4 showed that there was no simple correlation between commonly available information such as pipe material, diameter or age and the number of discolouration customer contacts. In order to gain a greater understanding of discolouration material accumulation, further investigation into the possible contributing factors such pipe age, material, diameter, hydraulic factors and bulk water quality field work was undertaken within live drinking water networks.

Systematic flushing of entire DMAs whilst measuring the turbidity of the flushed water was chosen to assess discolouration material accumulation, as the method is reasonably simple, inexpensive and above all repeatable.

It is suggested that initially flushing an undisturbed pipe whilst recording the turbidity would give an insight as to the maximum discolouration potential of the pipe. As the pipe is flushed until no more discolouration material can be removed, a benchmark is attained where the pipe is considered 'clean'. By repeating the flushing operation after a 3, 6 and 12 month time periods increasingly larger volumes of discolouration material could be expected to be mobilised as there were longer periods of time to accumulate on the pipe walls, Figure 19.

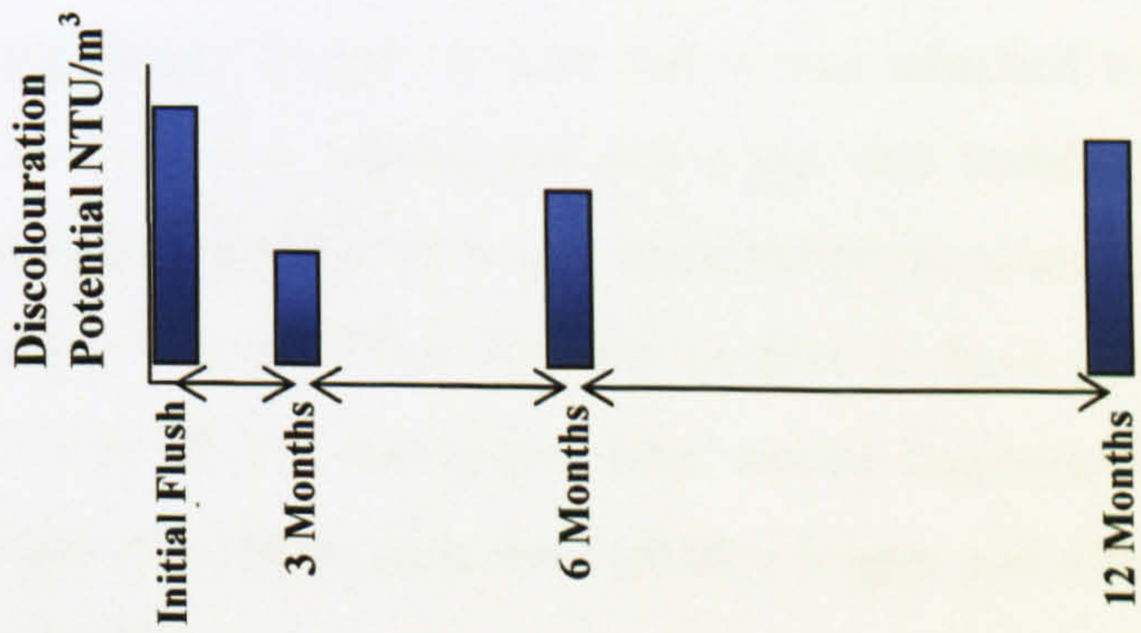

Figure 19 Theoretical relationship of discolouration material volume with time.

By flushing all the pipes within in a DMA, whilst ensuring a clean water front, the amount of material mobilised from each individual pipe could indicate

how material accumulates under different conditions: material, diameter, hydraulic conditioning. This could allow for calculation of the time until the maximum amount of discolouration material (attained from the initial flush) is reached, Figure 20.

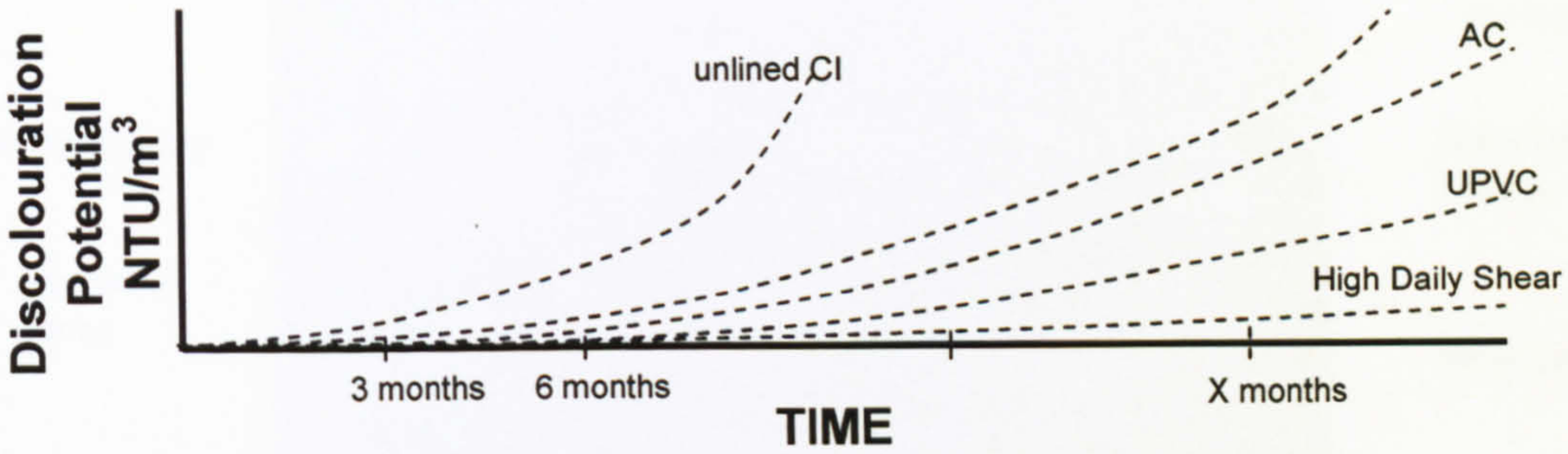

Figure 20 Theoretical discolouration accumulation rates under various conditions.

By flushing at stepped flow rates, further insight into possible changes in cohesive layer strength, thickness and composition over time could be made.

5.2 Apparatus

CT-Cense colour and turbidity sensors were used to measure turbidity. They utilise infrared light at a wavelength between 840 – 920 nm and measure light scatter at 90^0. These probes are stated by the manufacturer to have a range of 0.1 to 200 NTU with a resolution of <0.1 NTU.

Flushing equipment was initially developed by the University of Sheffield for the PODDS project (Boxall et al. 2003) and included a specially adapted flushing standpipe with a Burket flow meter and a pressure fitting for attachment of a pressure logger. A gate valve was attached to the end of the hydrant to enable fine flow adjustment and a tap was installed which allowed turbidity to be monitored via a flow cell installed in an aluminium case, Figure 21. This apparatus was modified for this project to have the turbidity meter installed on the riser of the standpipe. This would improve data accuracy by reducing likelihood of bubbles near the turbidity logger and allow real time data monitoring via a laptop.

Contractor's standpipes are also utilised on hydrants to measure turbidity at non flushing locations at the beginning of the pipe being flushed or at an intermediate location where there is a change in material along the pipe being flushed. A hose is attached to the standpipe's brass tap and run into an

aluminium case. The turbidity probe is located in a flow cell allowing continuous monitoring of turbidity. The case also incorporates a laptop and battery packs for portability and long running time. This equipment was designed for previous flushing research by the University of Sheffield.

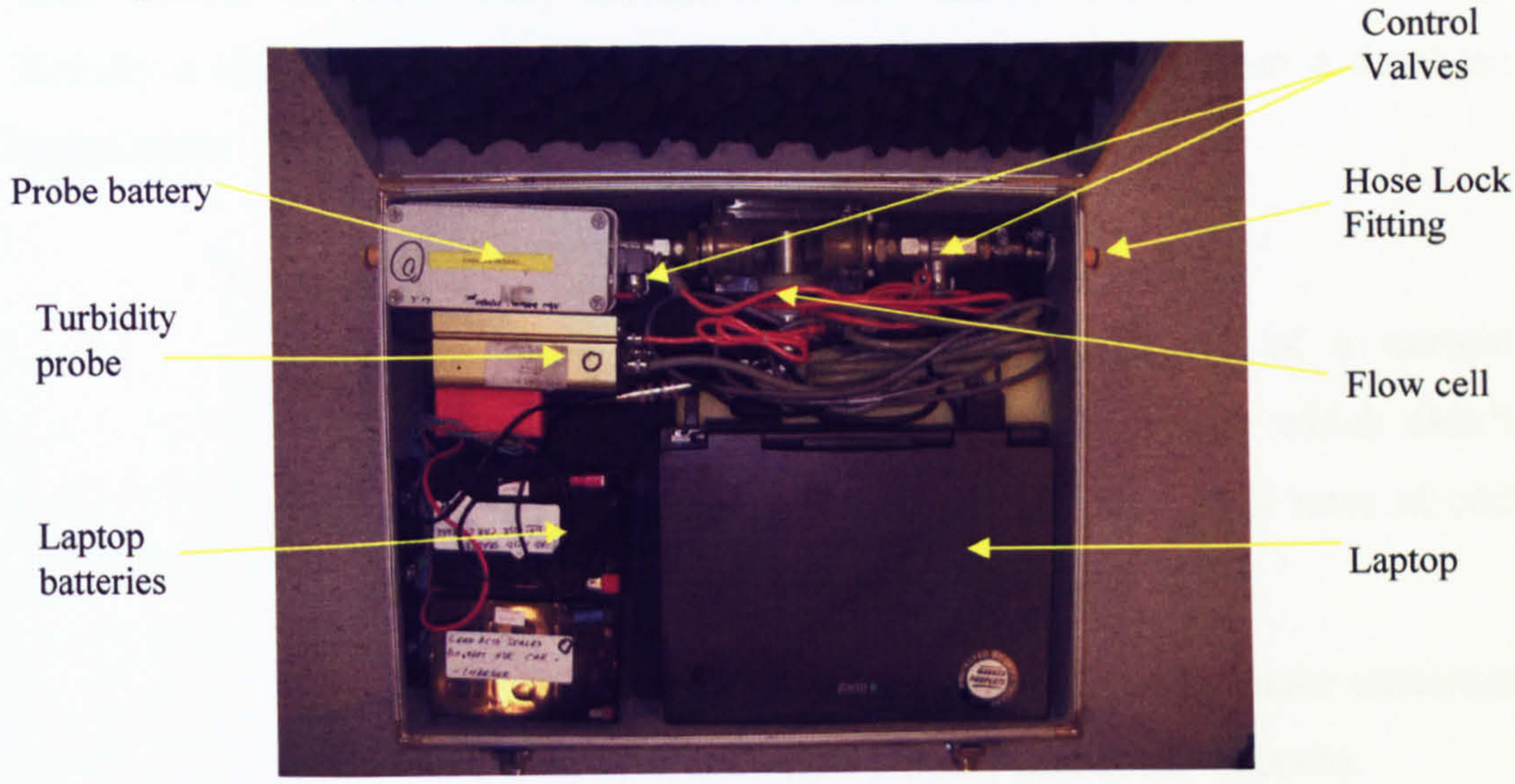

Figure 21 Aluminium case set up

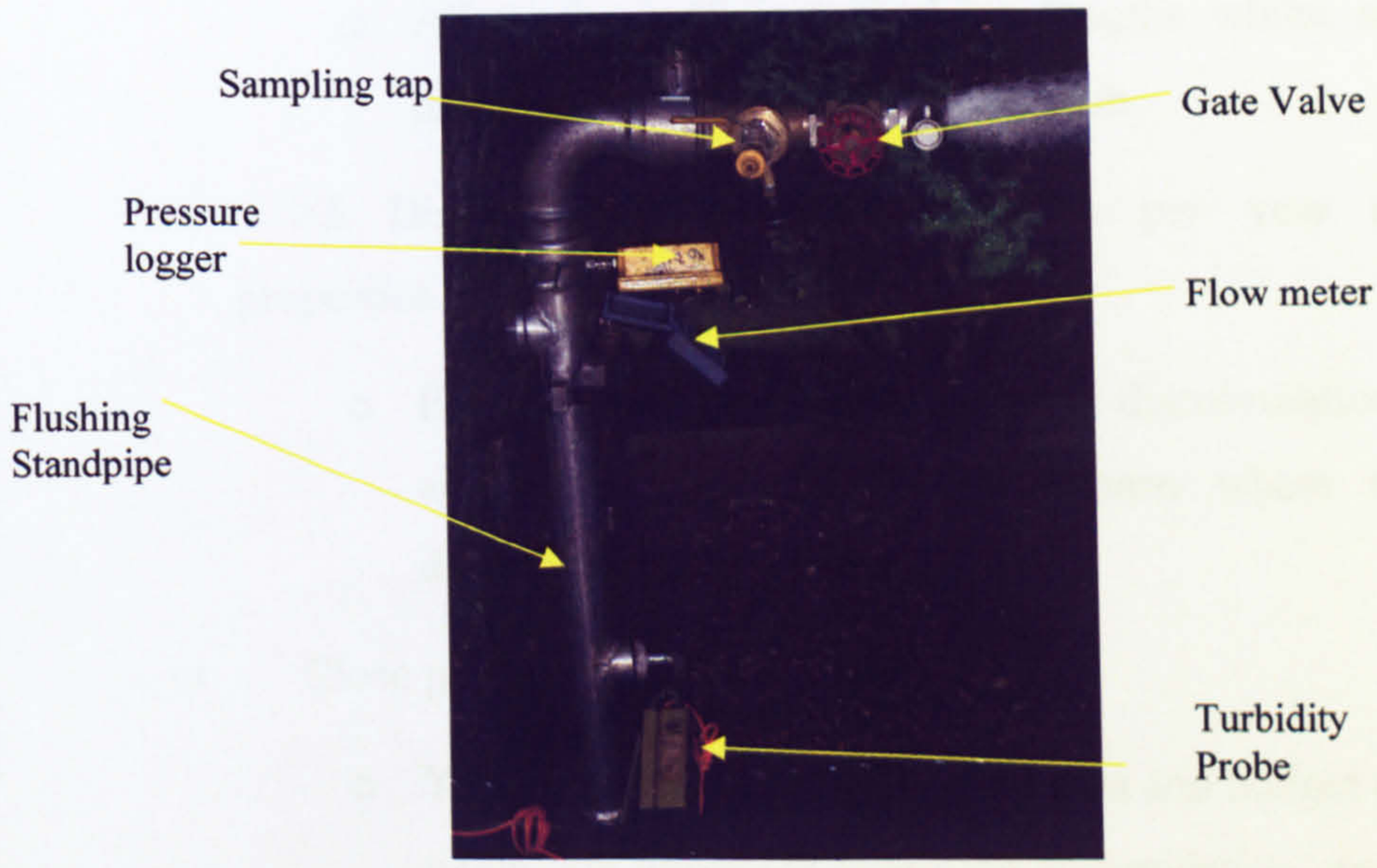

Figure 22 Modified flushing standpipe

A Hach pocket turbidity meter was used to obtain independent turbidity readings. These utilise an infra red light source of 880 nm and has a manufactures stated range of 0.1 to 400 NTU with a resolution of 0.1 NTU.

5.3 Method

5.3.1 Site selection

Selection criteria for the flushing trials were critical and were based upon size, number of customers, accessibility and known discolouration history. Initially a short list of candidates was automatically selected from a database based upon:

- 200-600 Domestic Properties.
  - A DMA which would be representative of a normal domestic profile. I.e. a diurnal flow pattern which didn't include large industrial users with high flow rates at odd times of the day.
  - Not such a large number of customers as to make customer warning notifications a lengthy and costly process.
- 2 -3 km mains length.
  - Allow for sufficient flushing lengths whilst not taking more than a couple of nights to flush.
- >5 Discolouration customer contacts per year per 1000 properties.
  - Essential that in order to measure discolouration material accumulation, a DMA was chosen where there was discolouration occurring.
- Close proximity to Sheffield.
  - Yorkshire Water covers a wide area and budget constraints would not allow for overnight accomidation, necessary for distant DMAs.

From the short list, the DMA was then chosen based on a manual investigation of:

- Variations in pipe material and diameter.
  - Ideally to attain as many variables as possible

- However Yorkshire Water dictated that no areas of unlined cast iron pipes were to be flushed.

- A DMA with a simple structure.
  - In order to simplify flushing by not choosing a highly dendritic network with an excessive number of short lengths.

- No planned work in the DMA.
  - Any work carried out in the DMA would inevitably disturb or remove discolouration material.

Yorkshire Water took the final decision on the chosen DMA based on internal influences and the resultant DMA chosen was J722.

Initially one site was chosen for the flushing program however more resources were made available half way through the project enabling the possibility to flush a second zone. The selection of the second site had to have similarities with the initial zone to allow for sufficient overlap and therefore comparison between the two areas, but it also had to have significant differences to the initial site to allow for further variation in pipe characteristics. During the selection process, several zones were selected which had to be later discarded as they entered in to other maintenance schemes which would disturb the networks. The selection criteria of having a significant discolouration history seemed to be most problematic, as it were these very zones that had been marked for rehabilitation. In the end the discolouration history criteria was abandoned and it was deemed more important that the two DMAs had the same source water. This overlap would allow for the influence of source water to be confirmed, or ruled out. J730 was chosen as it was supplied by the same water treatment works as J722 and would receive water with the same chemical properties. This new zone also included different pipe materials not seen in J722.

5.3.1.1 DMA Characteristics

J722 and J730 are both quiet residential areas in South Yorkshire. J722 consists of 324 properties and has a total mains length of 2.81 km. J730 is a much larger DMA with 1082 domestic properties and 45 commercial users and

would require far too much flushing effort for this trial. Thus only the dendritic North East portion of this DMA with a total of 2.3 km of pipe was chosen, highlighted in red, Figure 23. J730 was ideal for this study since this was an isolated portion of the DMA very close to the inlet with no exports to the rest of the DMA and could be considered as a DMA in its own right. All references to this DMA hereafter only refer to this North East portion.

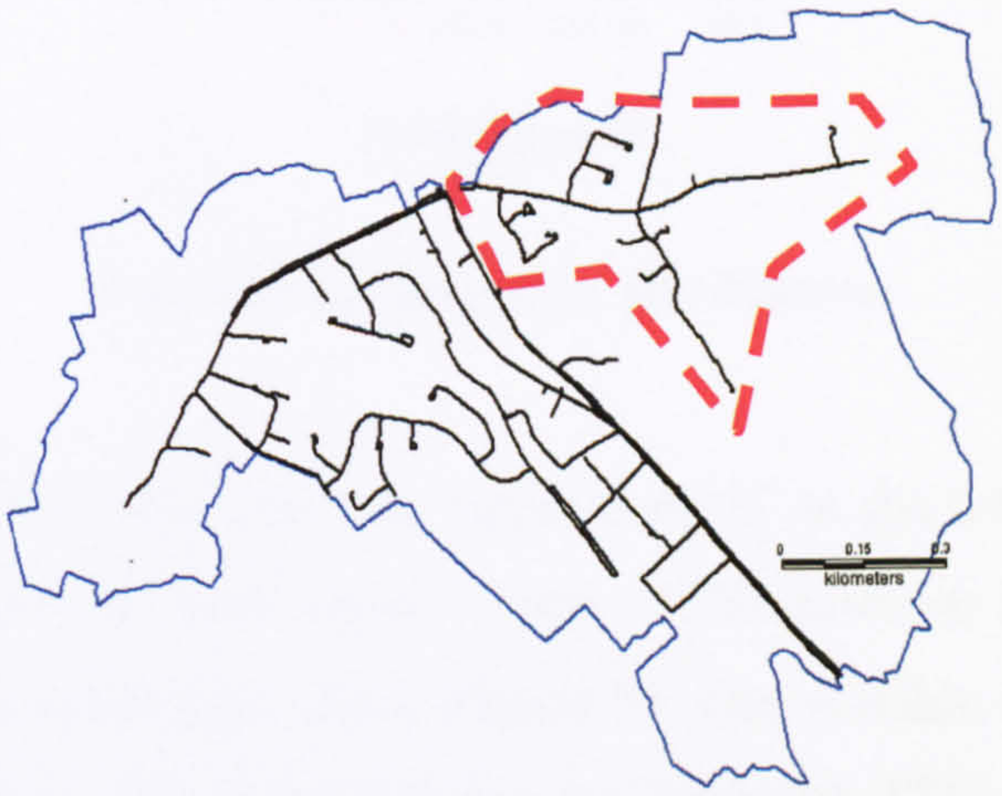

Figure 23 J730 Flushing area.

The majority of pipe material in J722 is Asbestos Cement (65%) the remainder being cement lined Cast Iron pipe (34.5%) and a very small percentage of bitumen lined cast iron pipe (0.5%). J730 has similar pipe material characteristics, the majority of which is cement lined cast and ductile iron (65%). The other pipe materials are Asbestos Cement (6%) and bitumen lined cast iron (1%). J730 also has the addition of plastic pipes (26%) which were not present in J722, Figure 24.

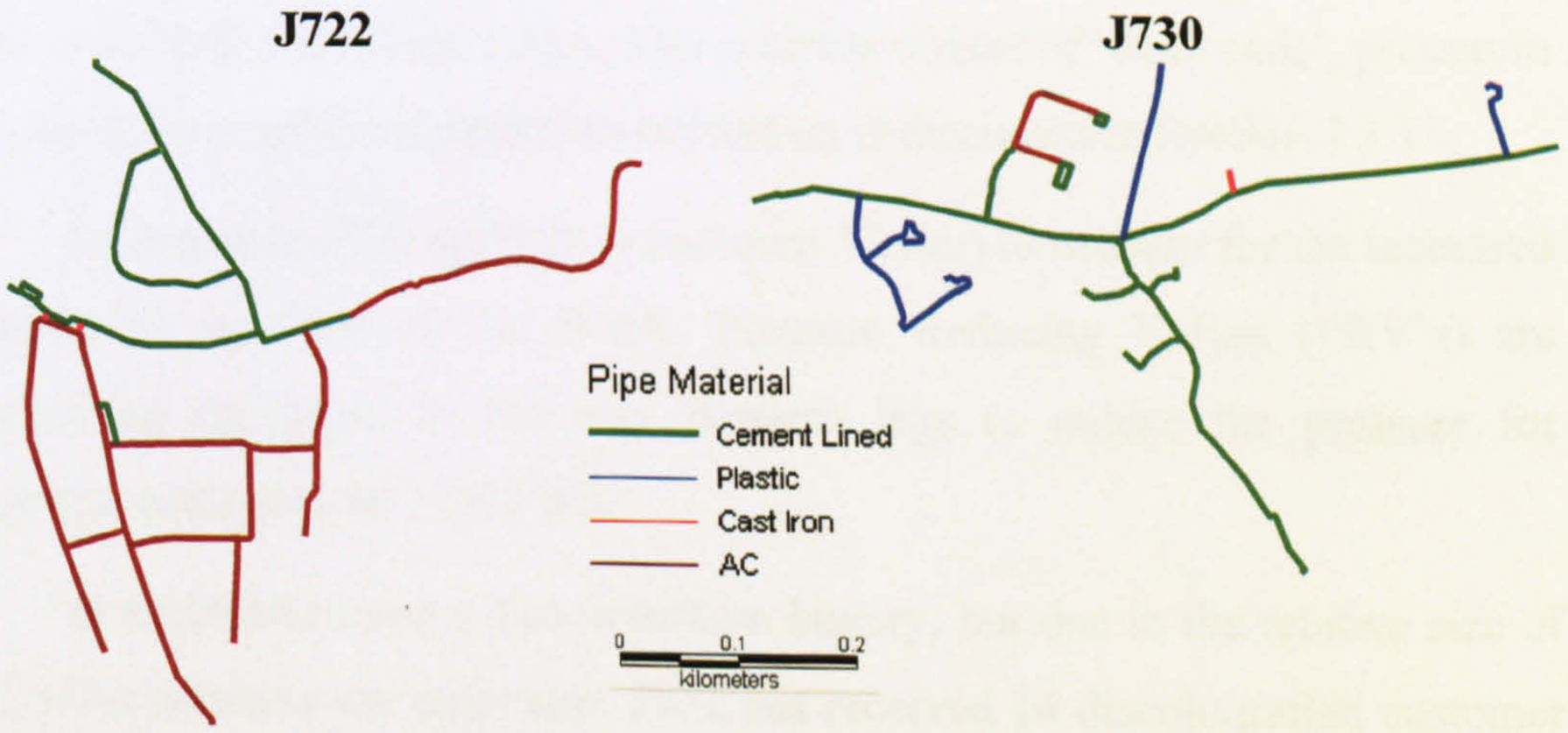

Figure 24 Flushing DMA pipe materials.

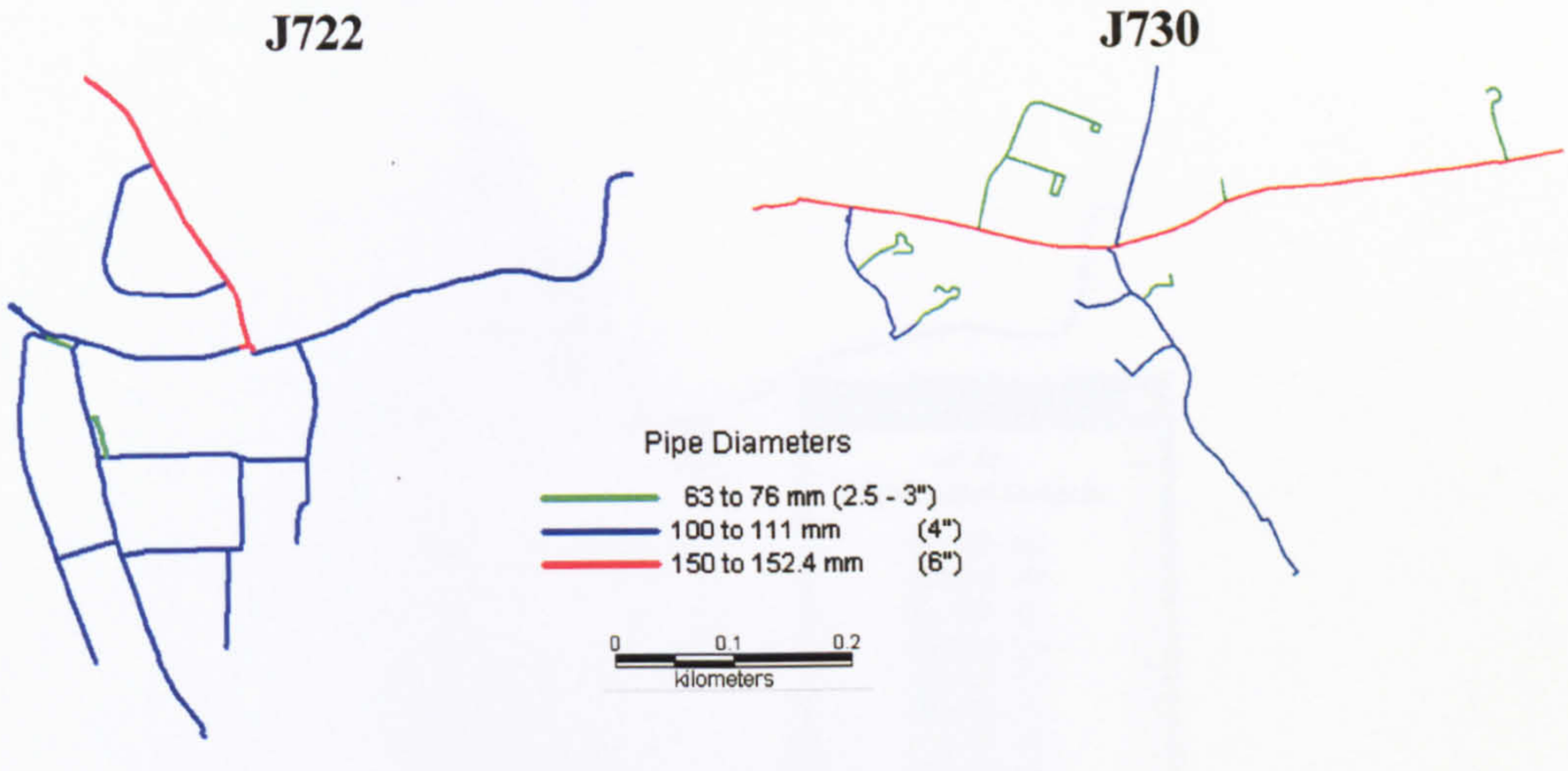

Figure 25 Flushing DMA pipe diameter.

In both DMAs pipe diameter varies from 6" at the inlet to 4" across the majority of the network, with some 3" pipe. J730 however has a much higher proportion of the smaller pipe sizes, Figure 25. One notable difference between the two areas is of the age of the housing development; J722 consists of 2 house styles predominantly built in the 1930's and 1960's, thus 30% of the water distribution network was laid between 1930 and 1940, and 70% of the network was laid between 1950 and 1960. Contrastingly J730 has experienced much more recent housing development and 45% of the pipes were laid between 1970 and 1980 and 51% was laid in the 1990's. Both networks have been rehabilitated, and were largely swabbed between the end of 1999 and beginning of 2000.

Both DMAs significantly differ in terms of their structure which in turn affects the system hydraulics. J722 possesses several loops in its pipe layout where as J730 is a dendritic DMA. The possible effects of 'dead ends', present in J730, on discolouration material accumulation is discussed in Section 2.3.1.

Pressures in J730 are high (maximum 12 Bar) to account for the increased elevation to the East of the DMA. Pressure Reducing Valves (PRV's) are installed on the pipes in the two Western legs to reduce the pressure for customers at the bottom of the hill.

Both DMAs have a discolouration history, but due to the relative size of the DMAs numbers are quite low. J722 has received 14 discolouration customer contacts between 1999 and 2006, Figure 26 and J730 has received 12, Figure 27.

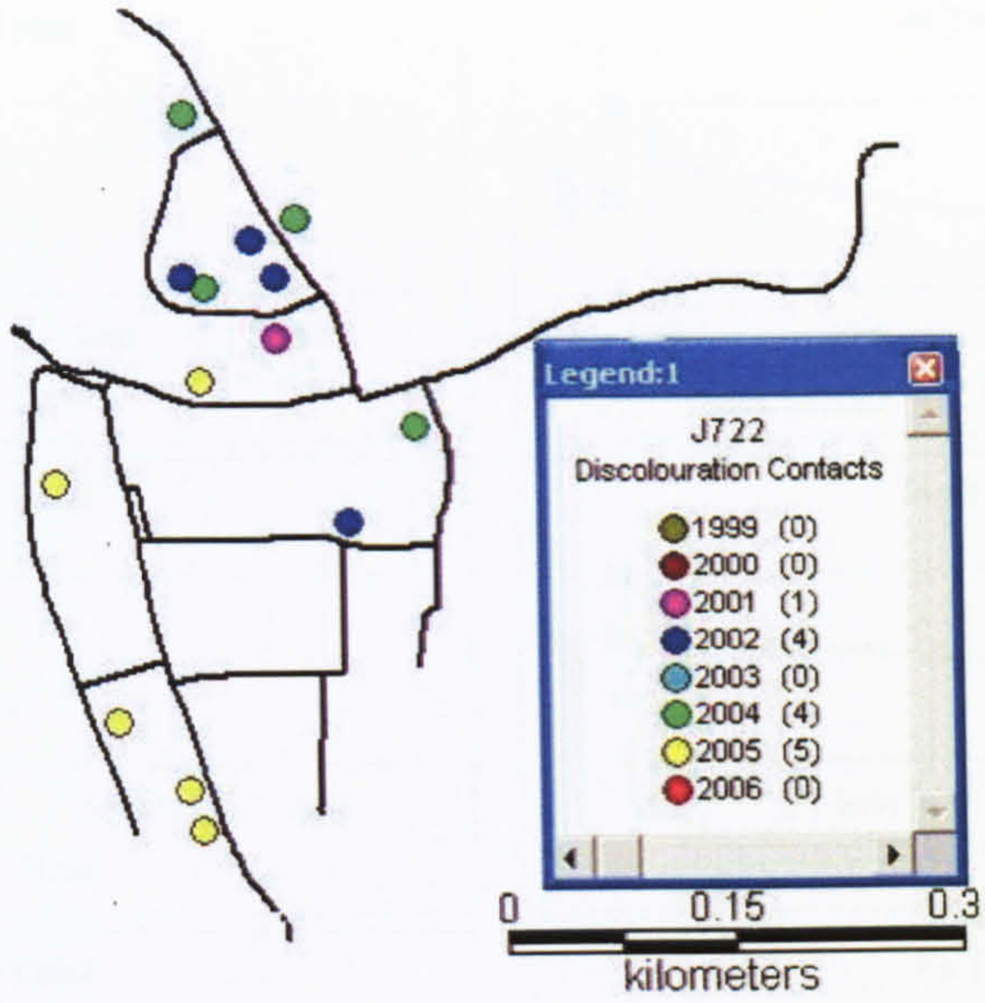

Figure 26 J722 discolouration contact history

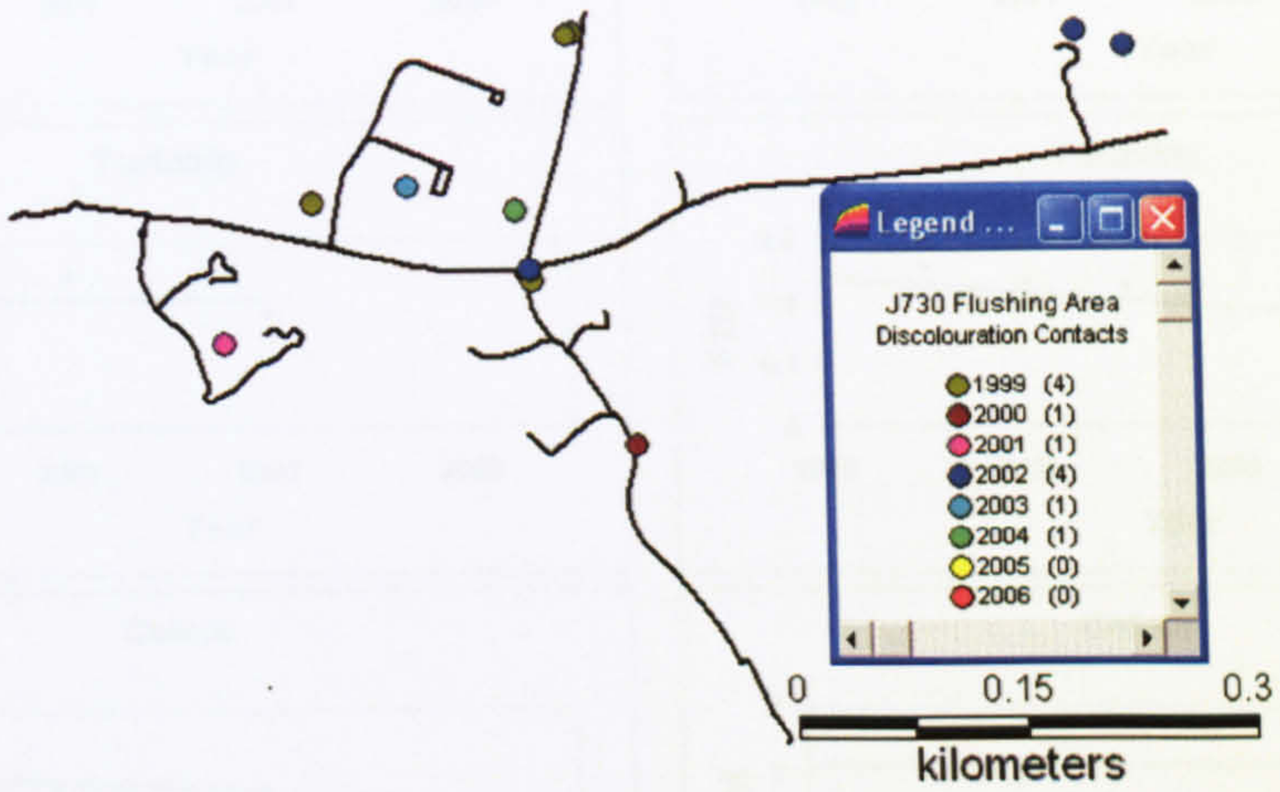

Figure 27 J730 discolouration contact history.

Regulatory sample data for both the DMAs are limited, approximately 30 samples were taken in J722 and there are no records available after September 2003. Only 14 regulatory samples were taken in the cut down area of J730. Figure 28 shows the average sample values each year taken in both DMAs. A decreasing trend in iron, manganese and aluminium concentrations between 1999 and 2003 can be seen.

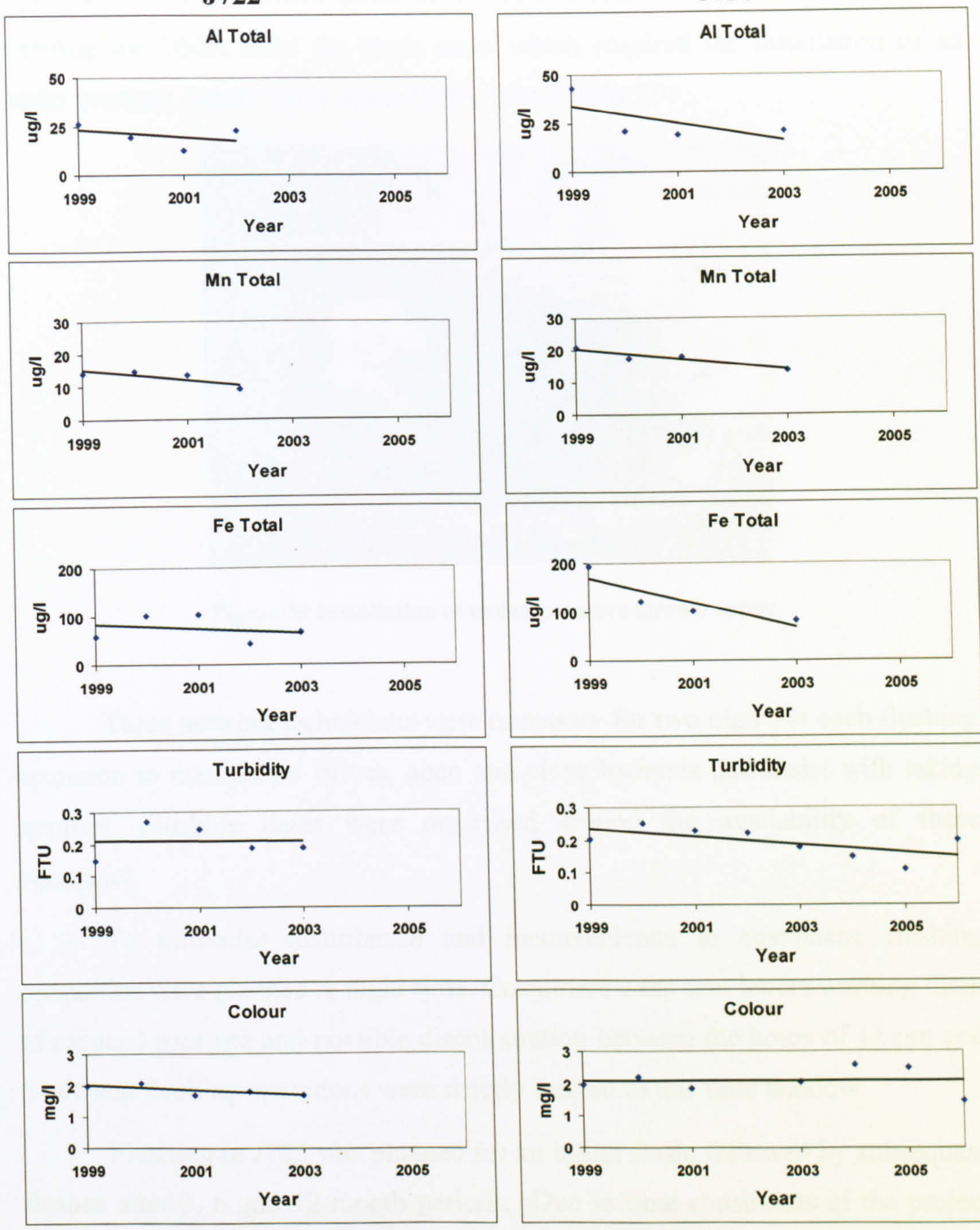

Figure 28 Regulatory sampling data 1999-2006

5.3.2 Planning

Detailed meticulous planning is the key to successful field work, especially with flushing operations as several people have to be involved from different departments within the water company and contractors alike. Firstly any enabling works have to be raised with the contractors as fittings have to be ordered and all works were prioritised and could take several weeks for completion. Flushing operations employed here only utilised existing valves and

hydrants to minimise costs, however it was desirable to monitor turbidity levels entering the DMA from the trunk main which required the installation of an under pressure ferrule valve at the DMA inlet, Figure 29.

Figure 29 Installation of under pressure ferrule valve.

Three network technicians were necessary for two nights at each flushing operation to manipulate valves, open and close hydrants and assist with taking samples. Flushing dates were organised around the availability of these personnel.

To minimise disturbance and inconvenience to customers, flushing operations were planned at night time. Customers were sent letters warning them of reduced pressure and possible discolouration between the hours of 11 pm and 6 am, and flushing operations were strictly limited to this time window.

Flushing in J722 was planned for an initial flush, followed by subsequent flushes after 3, 6 and 12 month periods. Due to time constraints of the project the second zone was planned for only an initial and 6 month flush. During scheduling of these flushes weather had to be taken into account. Flushing by its nature expels large volumes of water through the hydrant onto the public highway. Flushing for 1 hour at 20 l/s expels 72000 l of water, which had to be disposed of down culverts to the sewers. Planning flushing in winter periods was avoided if possible as the water could not be allowed to freeze on the road surface.

5.3.2.1 Hydraulic modelling

Hydraulic models were commissioned and build for the DMAs. This facilitated the design of the flushing sequence, and possible theoretical maximum flow rates that could be obtained. Model calibration was verified using average pressure data from loggers deployed in the DMAs over a seven day period. Figure 30 and Figure 31 show that the model calibration was reasonable with J722 and J730 having a mean RMS error of 0.065 and 1.572 respectively.

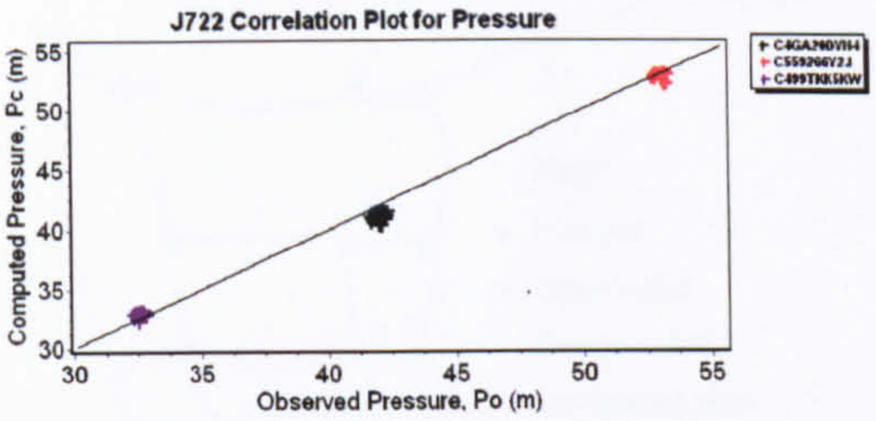

Figure 30 J722 model calibration results

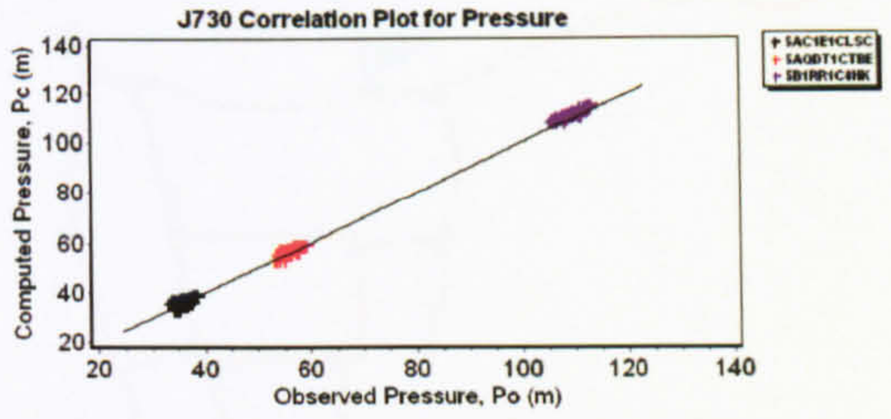

Figure 31 J730 model calibration results

The models used here met with standard industry practices, however in the DMAs the flow rates and therefore headloss in the pipes were low and there fore the shear stress in the pipes was uncertain. This would be particularly evident in dead ends, minor pipes and loops, where a small change in the flow would lead to larger differences in the shear stress. The design specification of these models requires a pressure based calibration. However as pressure is proportional to velocity squared, a small pressure increase can lead to a large velocity increase. Thus a velocity based calibration is more accurate than pressure, but cost often limits such applications in industry.

5.3.2.2 Flushing Sequence

The Flushing sequence was designed to facilitate the full flushing of the entire DMA and ensuring a clean water front for each flush, whilst using the minimum number of flushes and valve movements. This was constrained by utilising existing valves and hydrants to minimise costs of new installations. The program was designed so that where possible a section of pipe being flushed was of the same characteristic with a hydrant at the start of pipe for monitoring any turbidity in the water entering the pipe and a hydrant at the end of the pipe to generate the flushing and record the turbidity created. In situations where a pipe did change in diameter or material along its length, an intermediate monitoring location was added where possible to distinguish which section of pipe any

discolouration material disturbed originated from. In looped sections of the network valve closures were planned to constrain the flow through the section of pipe being flushed. Figure 32 depicts the 11 flushes required for J722 along with the required valve movements.

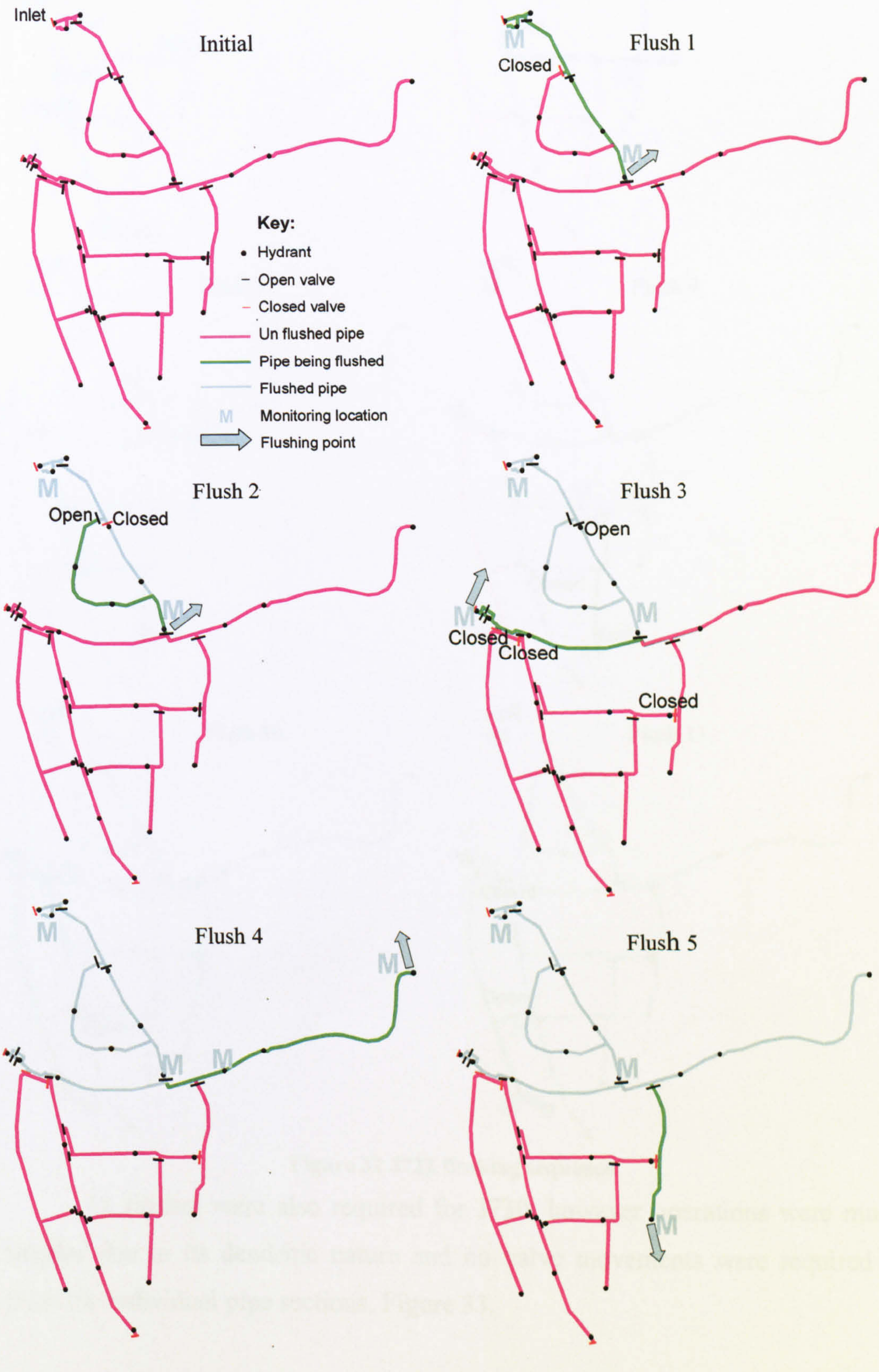

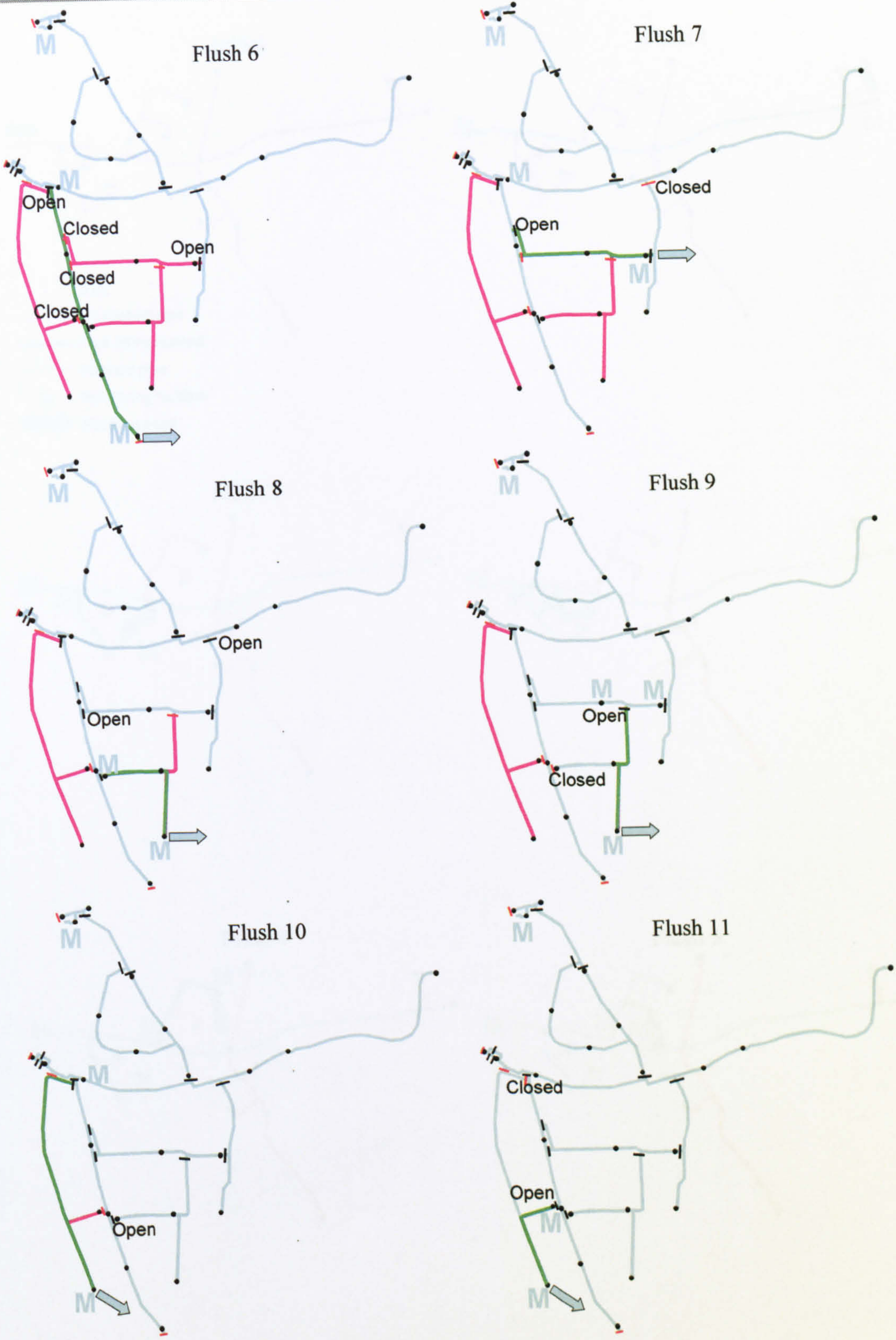

Figure 32 J722 flushing sequence

11 flushes were also required for J730, however operations were much simpler due to its dendritic nature and no valve movements were required to flush the individual pipe sections, Figure 33.

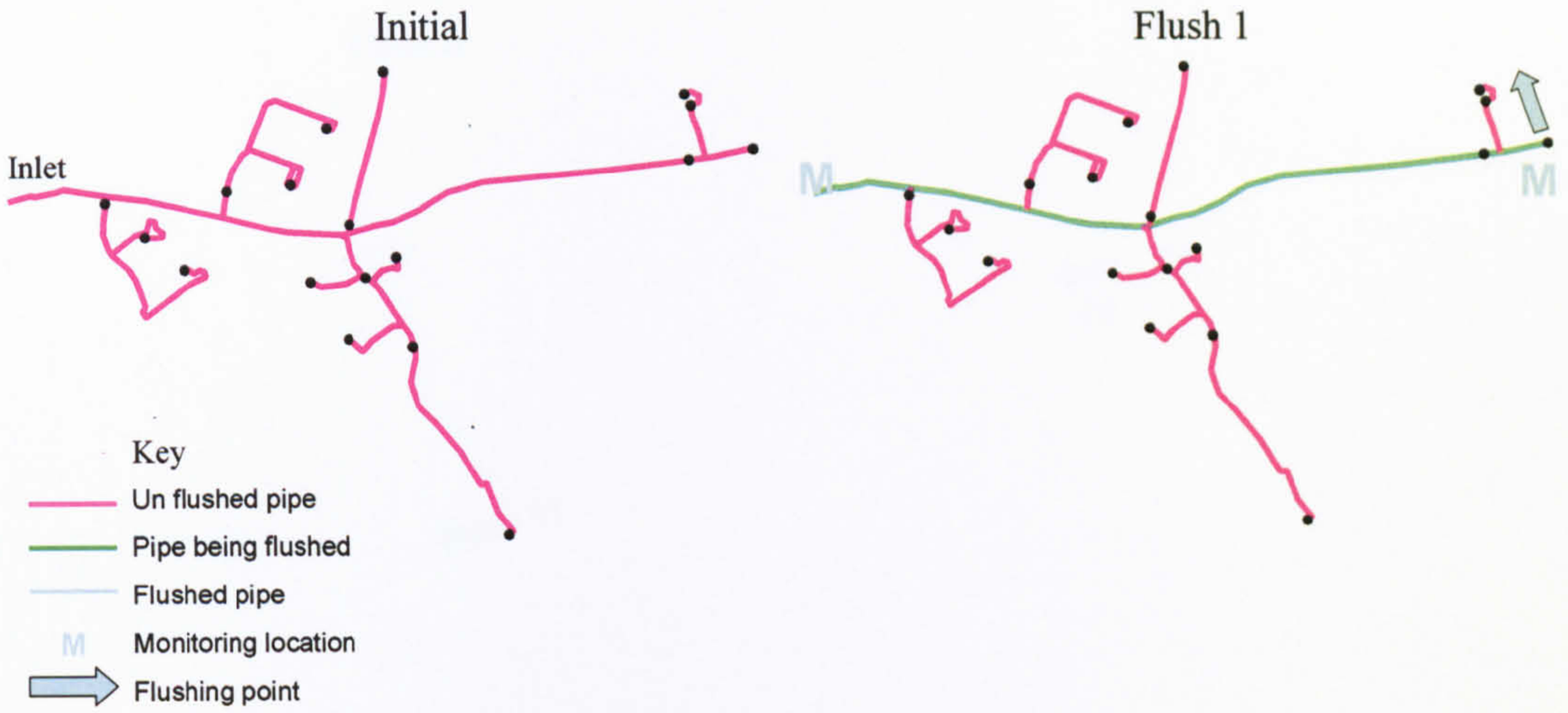
Initial
Inlet
Flush 1
M
M
Key
Un flushed pipe
Pipe being flushed
Flushed pipe
Monitoring location
Flushing point

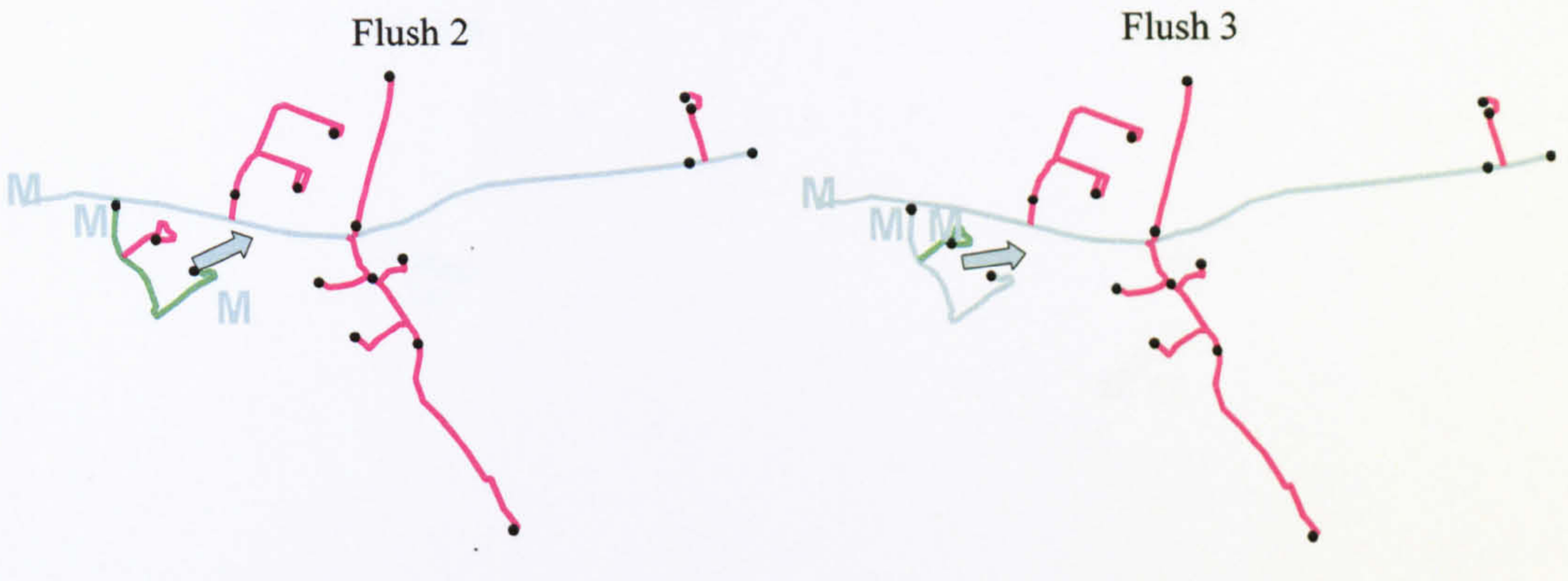
Flush 2
M
M
M
Flush 3
M
M
M

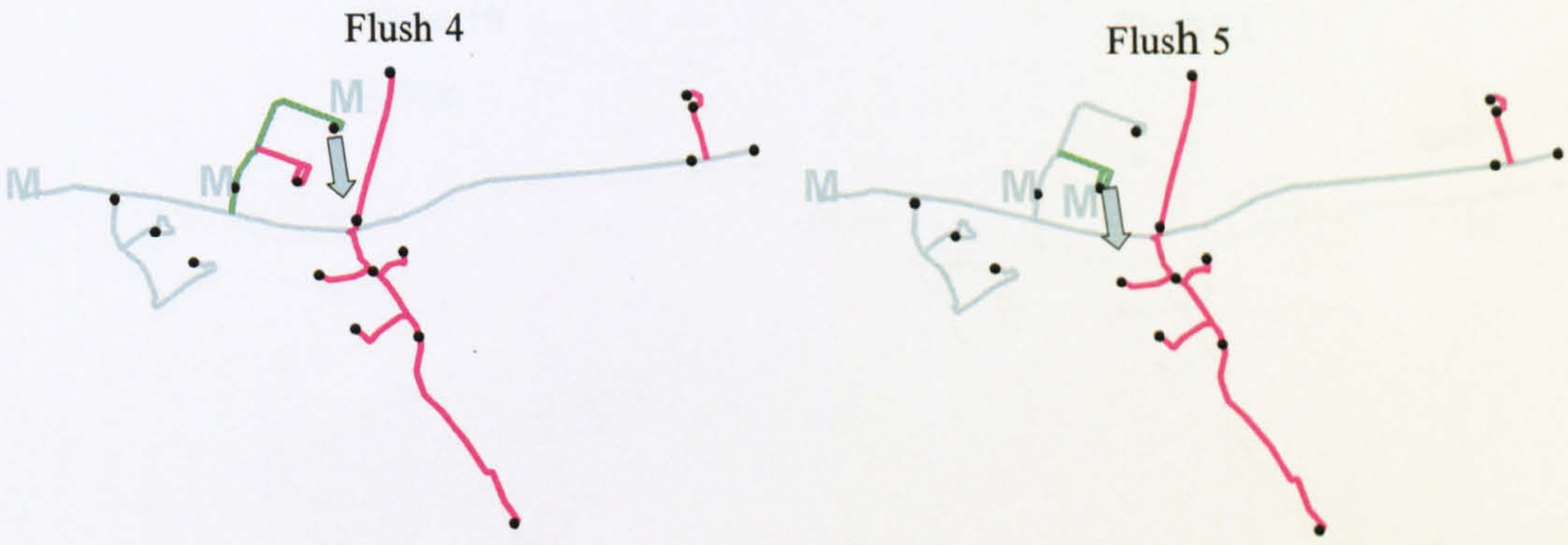
Flush 4
M
M
M
Flush 5
M
M
M

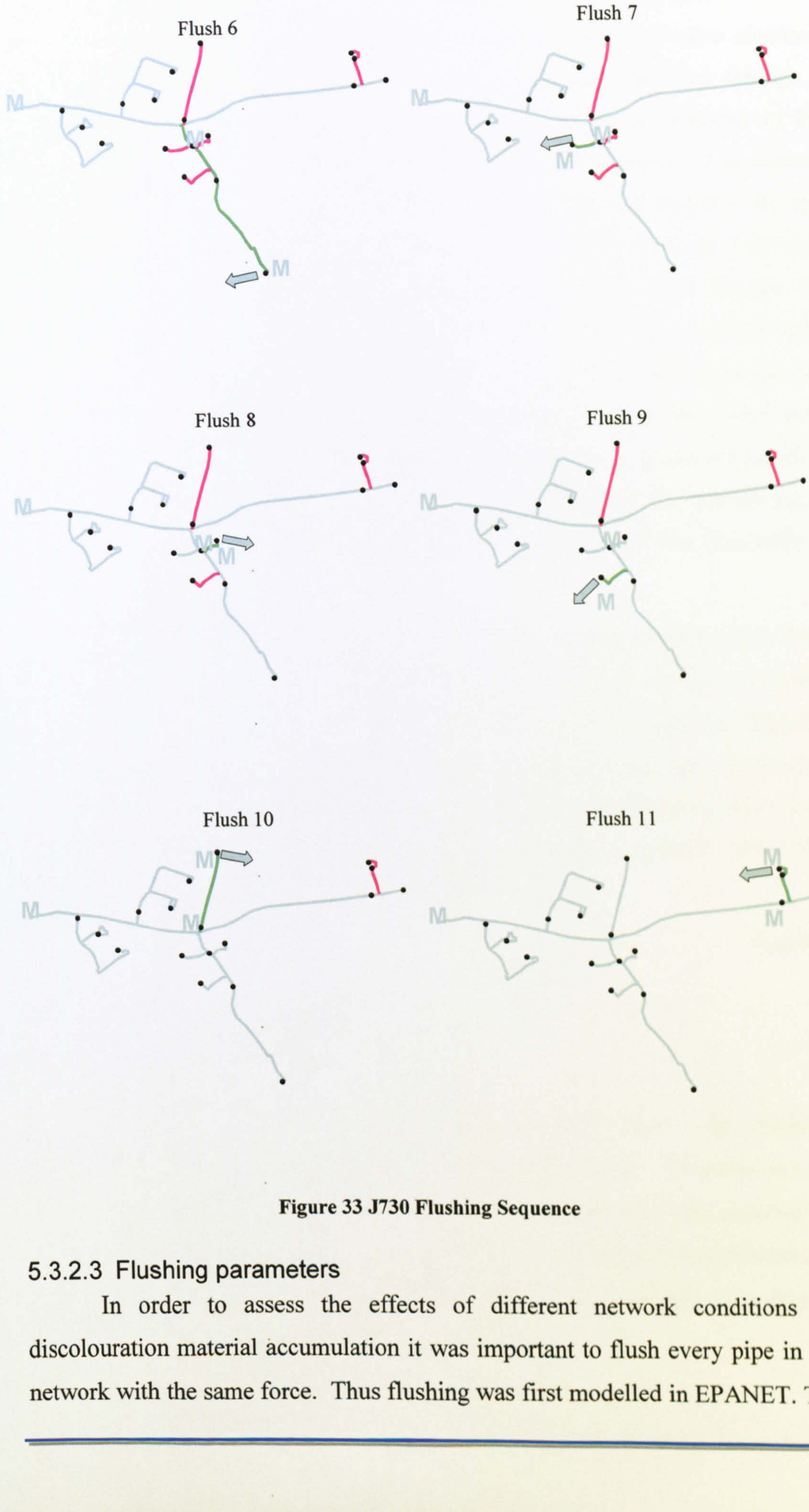

Figure 33 J730 Flushing Sequence

5.3.2.3 Flushing parameters

In order to assess the effects of different network conditions on discolouration material accumulation it was important to flush every pipe in the network with the same force. Thus flushing was first modelled in EPANET. The

maximum flow rates attainable were calculated by adding an emitter at each flushing location and closing the appropriate pipes to simulate valve closures. Emitters are model devices attached to nodes that model the flow through a nozzle or orifice. The diameter of the emitter was set to the diameter of the flushing hydrant with a roughness of 140 and a loss coefficient of 2.7 to account for short radius elbow (0.9) and a Standard tee- flow through branch (1.8), and the model run for each flush. When analysing the modelled results Yorkshire Water requested that no negative pressures were experienced thought the network as this could cause ground water to enter the distribution system through leaks, or cause the pipe to collapse. However hydraulic models generally use steady state simulations where the demands are fixed. Therefore when large extra demands are applied to the model, negative pressures can be generated purely as a result of a poor mathematical solution. In reality demands in the network would change as some areas would receive no water and it would be impossible to achieve negative pressures.

Previous research by Boxall et al (2001), explained in Section 2.6.2, suggested the volume of discolouration material released during a hydraulic event could be proportional to the amount of shear stress applied. Therefore shear stress was of primary importance in designing flow rates for each flushing operation. In this project shear stress in pipes was calculated by rearranging Equation 2 in Section 2.6.2, assuming that the pipes are completely full of fluid and the density of water is 1 kg/l, Equation 6.

Equation 6

$$\tau = \frac{d}{4} * 9.81 * Headloss$$

Where d is the diameter of the pipe (mm).

In order to have the same cleaning effect in all pipes in the network, it was necessary to flush each pipe at the same shear stress. Therefore for each flush the shear stress was calculated for the maximum flow rate possible. The lowest shear stress found across all flushes was then deemed the maximum shear stress to flush at. Reducing this figure slightly for a margin of safety, the maximum flushing shear stress was set at 8 N/m^2.

In order to mobilise discolouration material it is of importance that the flushing shear stress is considerably larger than the daily conditioning shear stress in the system. This was checked by calculating the shear stress for each pipe at daily peak flow conditions.

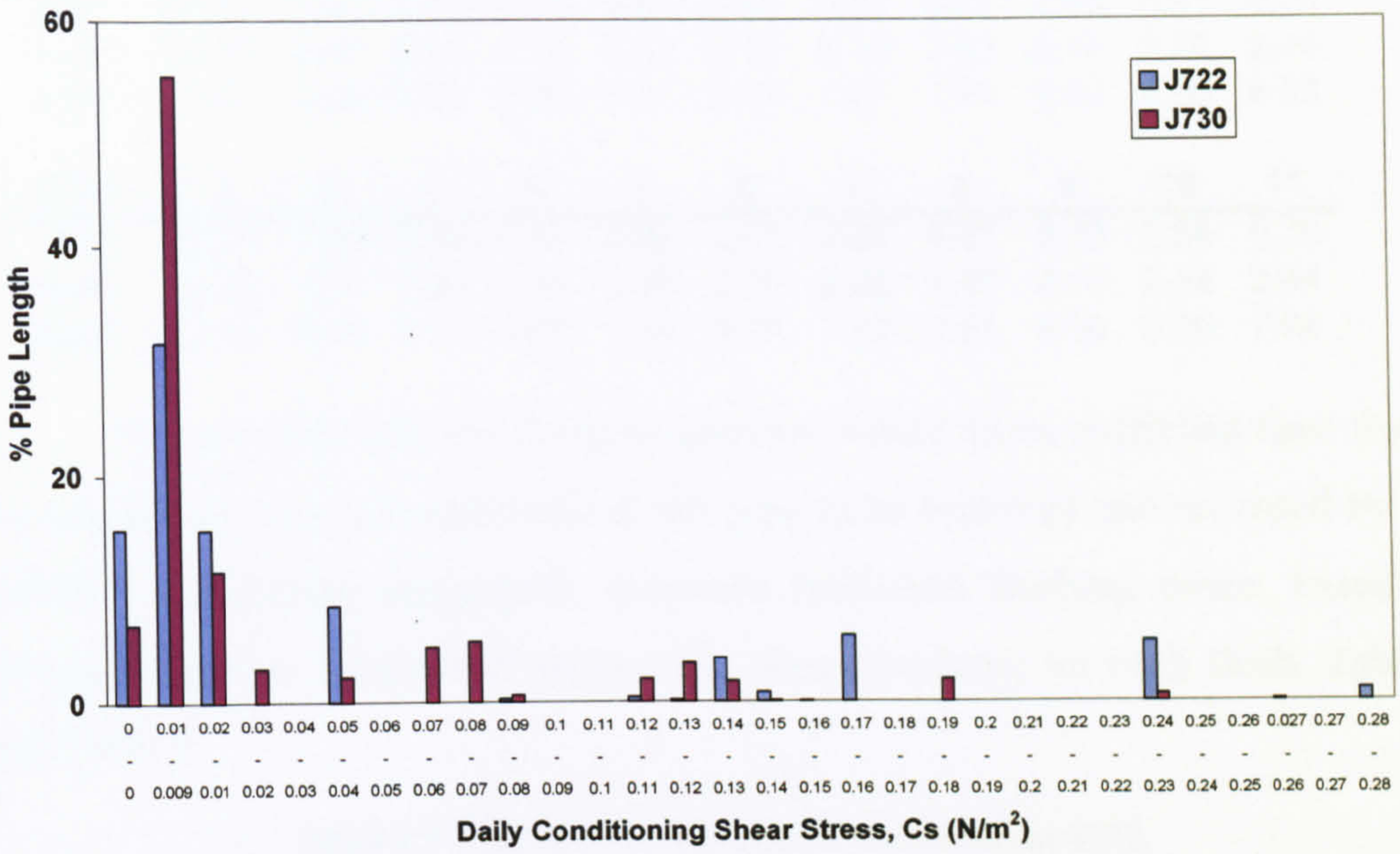

Figure 34 Peak daily Shear Stress

Figure 34 depicts the daily conditioning shear stresses at peak flow rates by percentage pipe length for J722 and J730. Here it can be seen that in over 30% of the pipes in the DMAs the maximum daily shear stress experienced is only 0.009 to 0.01 N/m^2, thus the highest flushing shear stress (8 N/m^2) is 800 times the daily conditioning shear stress.

In order to explore the possibilities or varying composition and accumulation rates with differing layer strengths of discolouration material, step flushing was considered the best method for cleaning the pipes. This is because flushing facilitates ease in recording the resultant turbidity and allows for specific eroding forces to be applied. For ease of field work, the 3 flushing steps were calculated based on the flow rate necessary to the nearest l/s to achieve 8N/m^2 shear stress and then halving this flow rate and halving it again. The flow rate was halved each time as halving the shear stress produced relatively small changes in flow which would be difficult to control in the field. This gave

approximate shear stresses of 0.7, 2.3 and 8 N/m^2 for every pipe. Exact shear stresses modelled for each flush are show in Table 3:

Table 3 Modelled flushing Shear stresses (N/m^2)

	Flush Number										
J730	1	2	3	4	5	6	7	8	9	10	11
low	0.64	0.62	0.70	0.61	0.61	0.60	0.60	0.67	0.60	0.61	0.70
med	2.25	2.20	2.40	2.12	2.12	2.13	2.13	2.43	2.14	2.20	2.44
high	7.95	8.00	8.00	8.00	8.00	8.04	7.97	7.91	8.02	8.00	8.03

J722	1	2	3	4	5	6	7	8	9	10	11
low	0.70	1.06	0.56	0.67	0.66	0.67	0.66	0.67	0.70	0.66	0.70
med	2.29	2.77	1.94	2.34	2.38	2.39	2.38	2.40	2.45	2.38	2.44
high	7.91	8.50	8.03	8.08	7.98	8.04	7.99	7.91	8.10	8.00	7.98

It is essential that the flushing duration would allow sufficient time for all discolouration material mobilised in the pipe to be removed and recorded by the turbidity monitoring equipment, therefore minimum flushing times, based on purging two pipe volumes of water were then calculated for each flush, Table 4 and Table 5.

Table 4 Flushing rates and minimum durations J722.

		Approximate Sheer Stress						
		0.7		2.3		8		
Flush no	Pipe Dia	Approx Flushing rate @Hydrant l/sec	Duration for 2 pipe volumes (mins)	Approx Flushing rate @Hydrant l/sec	Duration for 2 pipe volumes (mins)	Approx Flushing rate @Hydrant l/sec	Duration for 2 pipe volumes (mins)	Total minimum Time (mins)
1	140	5	34.1	10	17.0	20	8.5	59.7
2	80	1.5	27.6	3	13.8	6	6.9	48.3
3	80	1.5	31.5	3	15.8	6	7.9	55.1
4	97	2.5	41.6	5	20.8	10	10.4	72.8
5	97	2.5	19.5	5	9.7	10	4.9	34.1
6	97	2.5	39.5	5	19.8	10	9.9	69.2
7	97	2.5	20.4	5	10.2	10	5.1	35.8
8	97	2.5	18.9	5	9.4	10	4.7	33.0
9	97	2.5	18.9	5	9.5	10	4.7	33.2
10	97	2.5	34.9	5	17.5	10	8.7	61.2
11	97	2.5	16.2	5	8.1	10	4.0	28.3
							total hours	8.8

Table 5 Flushing rates and minimum durations J730.

		Approximate Sheer Stress						
		0.7		2.3		8		
Flush no	Pipe Dia	Approx Flushing rate @Hydrant l/sec	Duration for 2 pipe volumes (mins)	Approx Flushing rate @Hydrant l/sec	Duration for 2 pipe volumes (mins)	Approx Flushing rate @Hydrant l/sec	Duration for 2 pipe volumes (mins)	Total Time (mins)
1	150	6	80.2	12	40.1	24	20.0	140.3
2	99/50	3.25	15.4	6.5	7.7	13	3.8	26.9
3	50	0.875	7.4	1.75	3.7	3.5	1.8	12.9
4	76	1.25	27.0	2.5	13.5	5	6.8	47.3
5	76	1.25	12.6	2.5	6.3	5	3.2	22.1
6	100	2.5	41.7	5	20.9	10	10.4	73.0
7	100	2.5	6.1	5	3.1	10	1.5	10.7
8	80	1.5	5.1	3	2.5	6	1.3	8.9
9	100	2.5	7.4	5	3.7	10	1.8	12.9
10	99	3.25	13.8	6.5	6.9	13	3.4	24.1
11	50	0.875	6.4	1.75	3.2	3.5	1.6	11.2
							total hours	6.5

5.3.3 Equipment calibration

Flow gauges and turbidity loggers were calibrated in the lab prior to commencing fieldwork to ensure they were working properly and accurately. Pressure loggers were used in line with Yorkshire Water's tolerances and specifications and not recalibrated here.

5.3.3.1 Flow meter testing

Manufactures state that ideally flow meters should be installed in sections of straight pipe with a length of at least ten times the pipe diameter. The Burket flow meter used here was installed on a flushing standpipe only a short distance away from the turbidity logger head and the bend in the top of the standpipe. Therefore the flow meter had to be tested in the lab to ensure possible turbulence created by the turbidity logger head and the standpipe did not affect flow meter accuracy. The calibration of a Yorkshire Water Vernon Morris flow meter was also checked. The flow meter calibration rig is shown in Figure 35. Various flow rates were set using the gate valve installed on the flushing hydrant and flow readings taken from both the flow meters. The valve on the measuring tank was then closed and the period of time taken for the water level to rise a measured distance was recorded. Knowing the volume of the measuring tank, the flow rate could be calculated. Care was taken after measuring to reopen the valve to avoid flooding the lab.

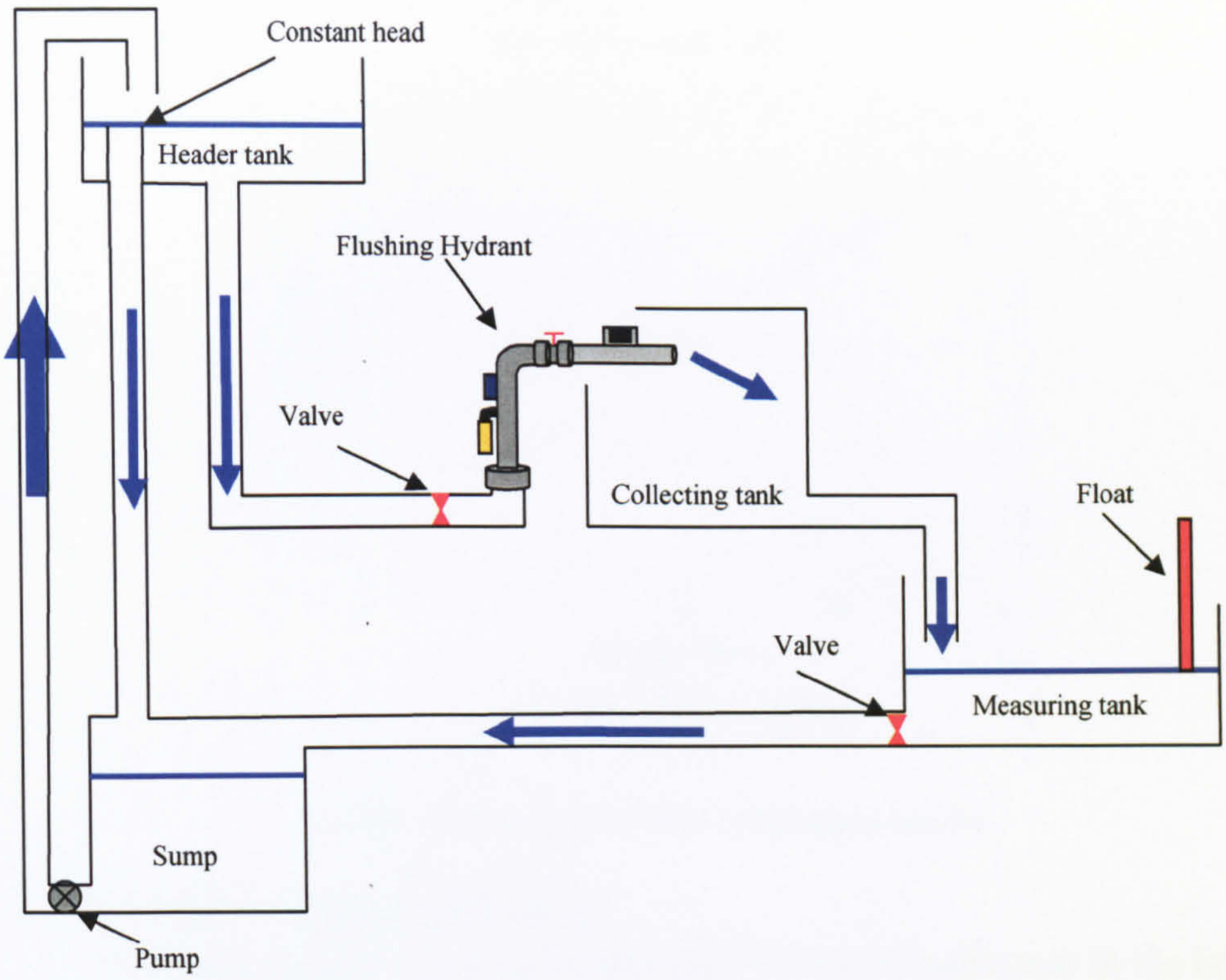

Figure 35 Flow measuring rig set up

Calculated flow and measured flow were then plotted for comparison. Results for both the flow meters were very accurate and no further adjustment for the calibration was required. It was noted however that the rig could only deliver flow rates up to 8/ls so the meters could not be tested higher than this. As the Vernon Morris flow meter was installed on the horizontal, flow readings could not be recorded unless the pipe was completely full of water, thus readings below 3 l/s were not possible. As the Burket meter was installed in the vertical and the pipe was always full of water, much lower flow rates could be recorded down to 0.5 l/s.

An example of calibration results for the Vernon Morris flow meter, and the Burket flow meter with the turbidity logger installed on the riser is shown in Figure 36, indicating accurate readings were obtained even though the Burket flow meter was used against manufacture's recommendations.

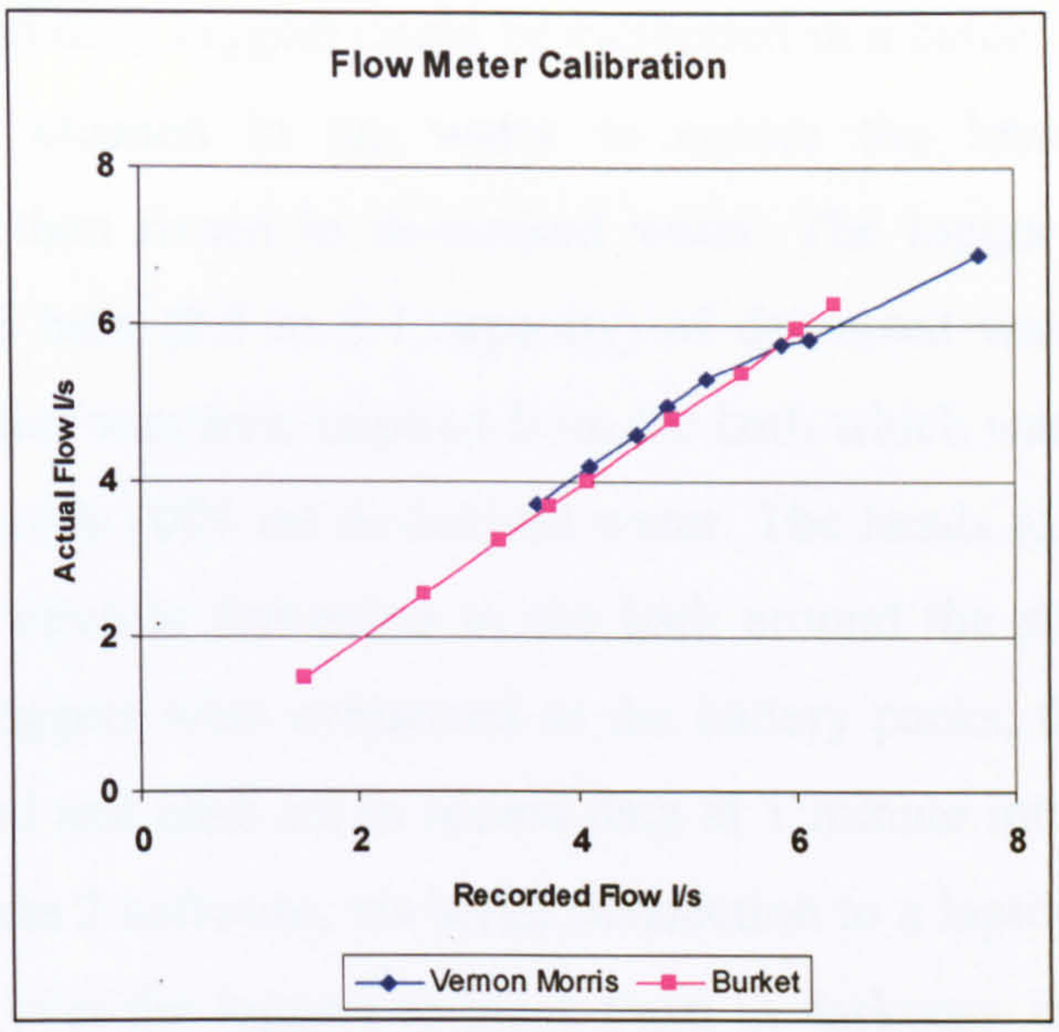

Figure 36 Example of flow calibration results

5.3.3.2 Turbidity logger calibration.

Turbidity loggers were calibrated for FTU with Formazine in the lab prior to deployment in the field. Since NTU is a more widely understood unit of turbidity than FTU, all references to turbidity units in this project will be in NTU, even though the calibration was performed using formazine, as the units are essentially the same.

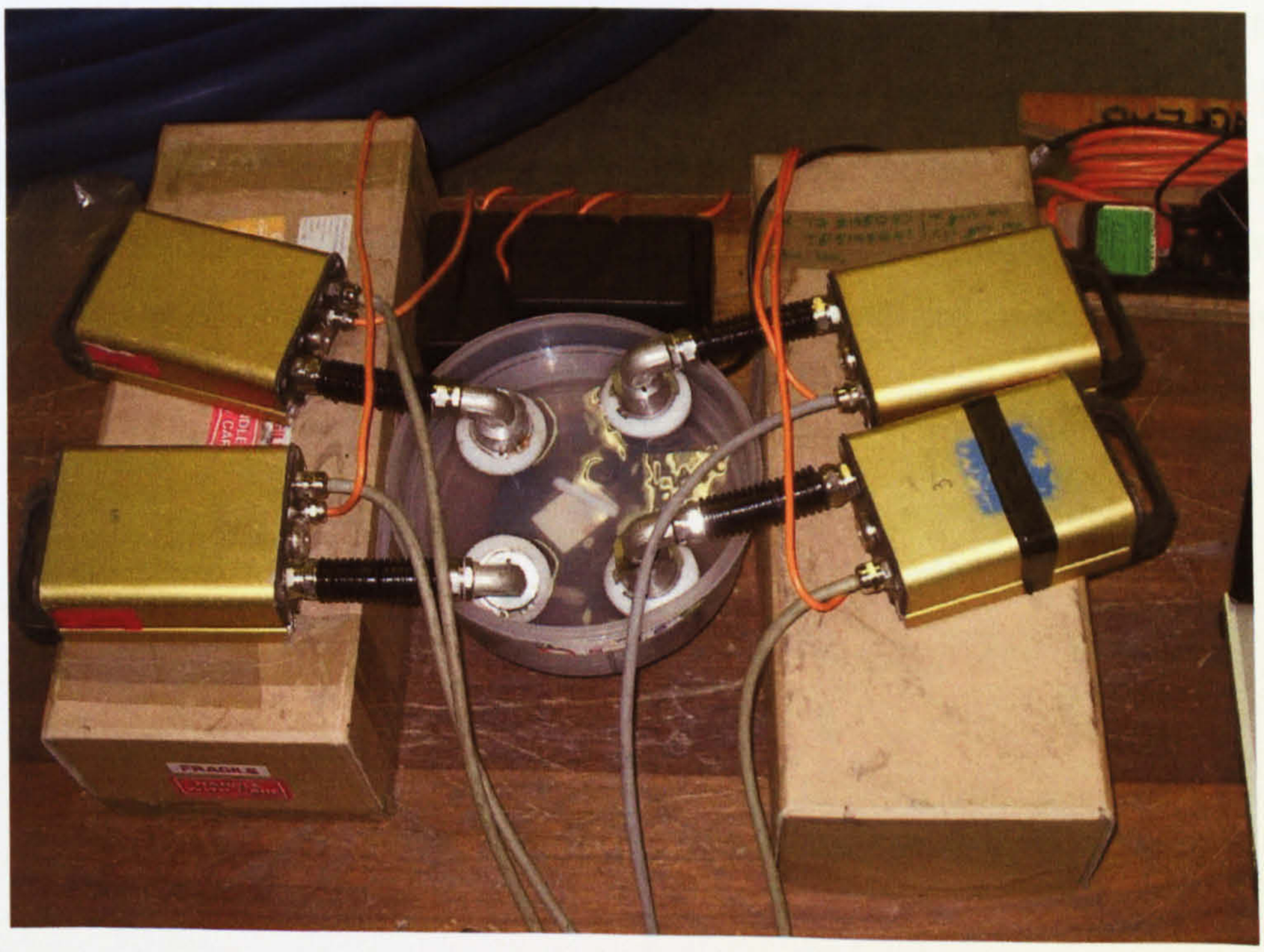

Figure 37 Turbidity Logger calibration set up.

Up to 6 turbidity loggers could be calibrated in a batch. Turbidity loggers were thoroughly cleaned in tap water to ensure the lenses were free of accumulates and then rinsed in de-ionised water. The logger heads were then placed in a small bath (2.5 to 3 l capacity) of deionised water for 2 hours to 'hydrate'. The water was then emptied from the bath which was then placed on a stirrer and filled with 2000 ml de-ionised water. The heads of the loggers were then placed in a circular formation in the bath around the stirrer as shown in Figure 37. The loggers were connected to the battery packs, the internal clocks were synchronised and each set to record data at 1 minute intervals using 'Talk Sense' logging beta 2 software, via serial connection to a laptop. Black-out cloth was then draped over the loggers to place them in darkness, and the time noted for the start of the experiment.

At approximately 15 minute intervals the turbidity in the bath of water was increased by 5 NTU steps with the addition of 2.5ml of 4000 NTU formazine standard. Times were noted for each 5 NTU increase, and the calibration was stopped approximately 15 minutes after a total of 20 NTU was added. Data from each logger was then plotted and an average NTU value was calculated for the stable period of each turbidity step; after 'settling' when all the formazine had mixed. The average recorded NTU for each logger was then plotted against the actual NTU, and the equation describing the straight line through the points was used to adjust the gain and offset to the logger data, providing that the R^2 value was close to 1, Figure 38. The original data recorded from each logger was then adjusted for gain and offset and re plotted to ensure that all loggers were performing similarly, Figure 39.

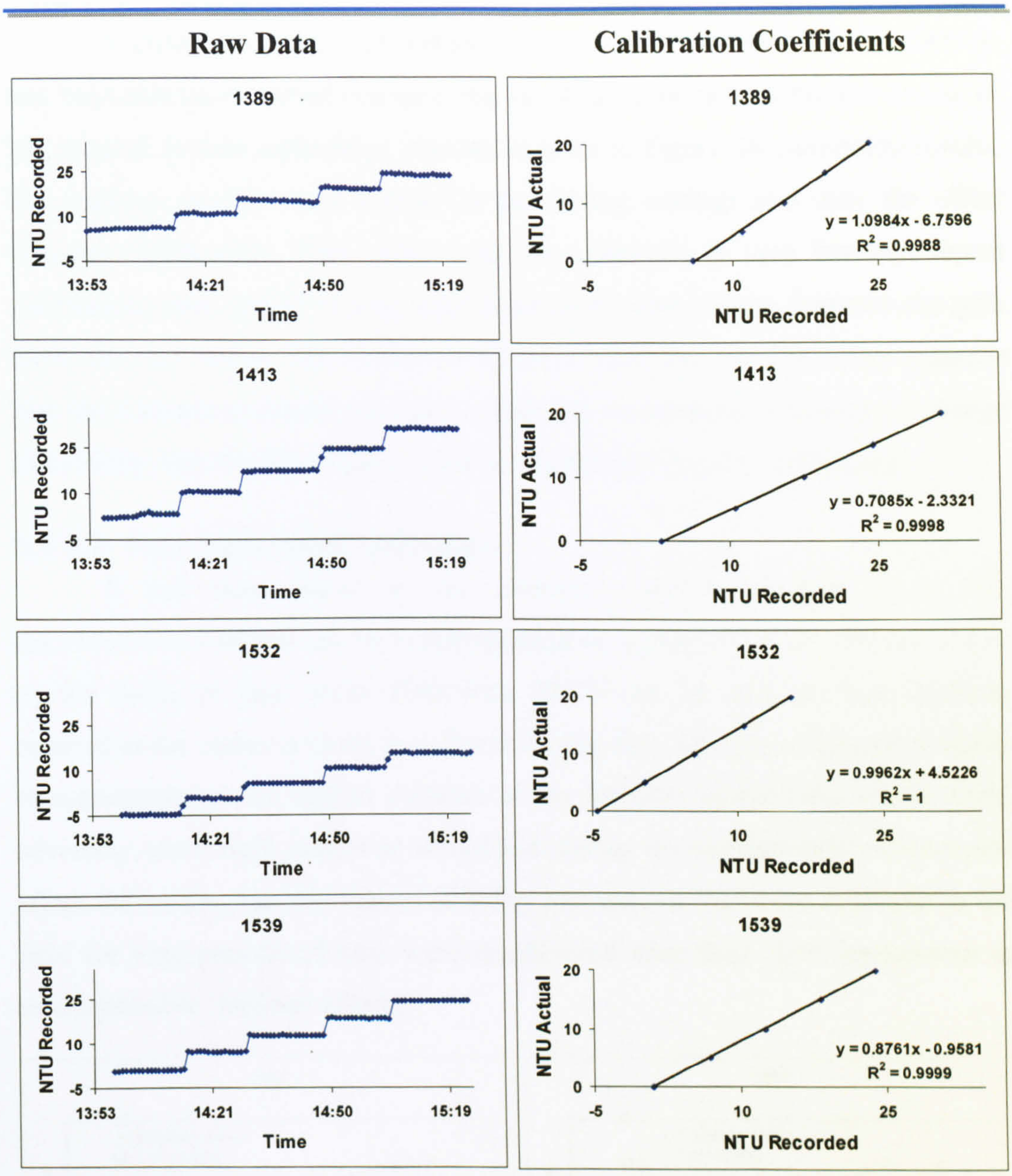

Figure 38 Example graphs of turbidity logger calibration process.

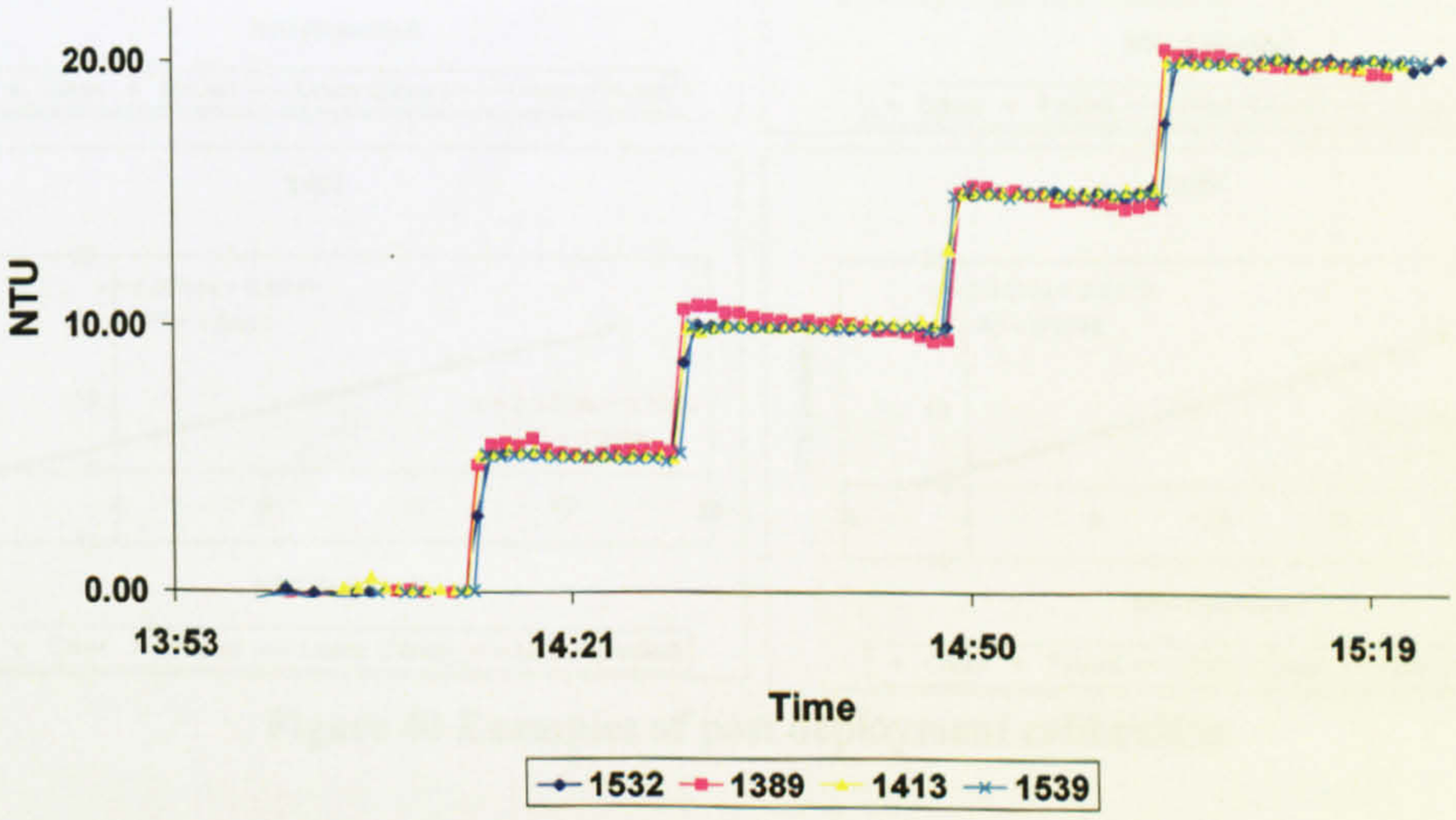

Figure 39 Example of calibrated turbidity logger data.

It should be noted that turbidity loggers were calibrated in the factory, and the calibration carried out here was in effect a second calibration on top of the original factory calibration. As can be seen in Figure 38 calibration results, the gradient remains very similar to the factory settings and only the offset changes significantly. This offset was also observed to vary between repeat calibrations after period of long field deployment and storage, however the gain term was very stable. This behaviour of stable gain and variable offset suggests that the instrument should provide a good and comparable indication of change in turbidity, but absolute values could be suspect and require verification.

5.3.3.3 Post deployment calibration

It has been noted in the literature review (Section 2.3.2) that discolouration material can be conceptualised as accumulating in cohesive layers on the inside of pipe walls. Following this it can be assumed that anything inserted in the mains is likely to suffer the same fate. Therefore material is likely to accumulate on the optical surfaces of the turbidity instruments which could adversely cause light scatter or absorption during the measurement process and affect the results. For this reason turbidity instruments that were deployed in the field for long periods of time were recalibrated after their field deployment to assess possible 'fouling' effects.

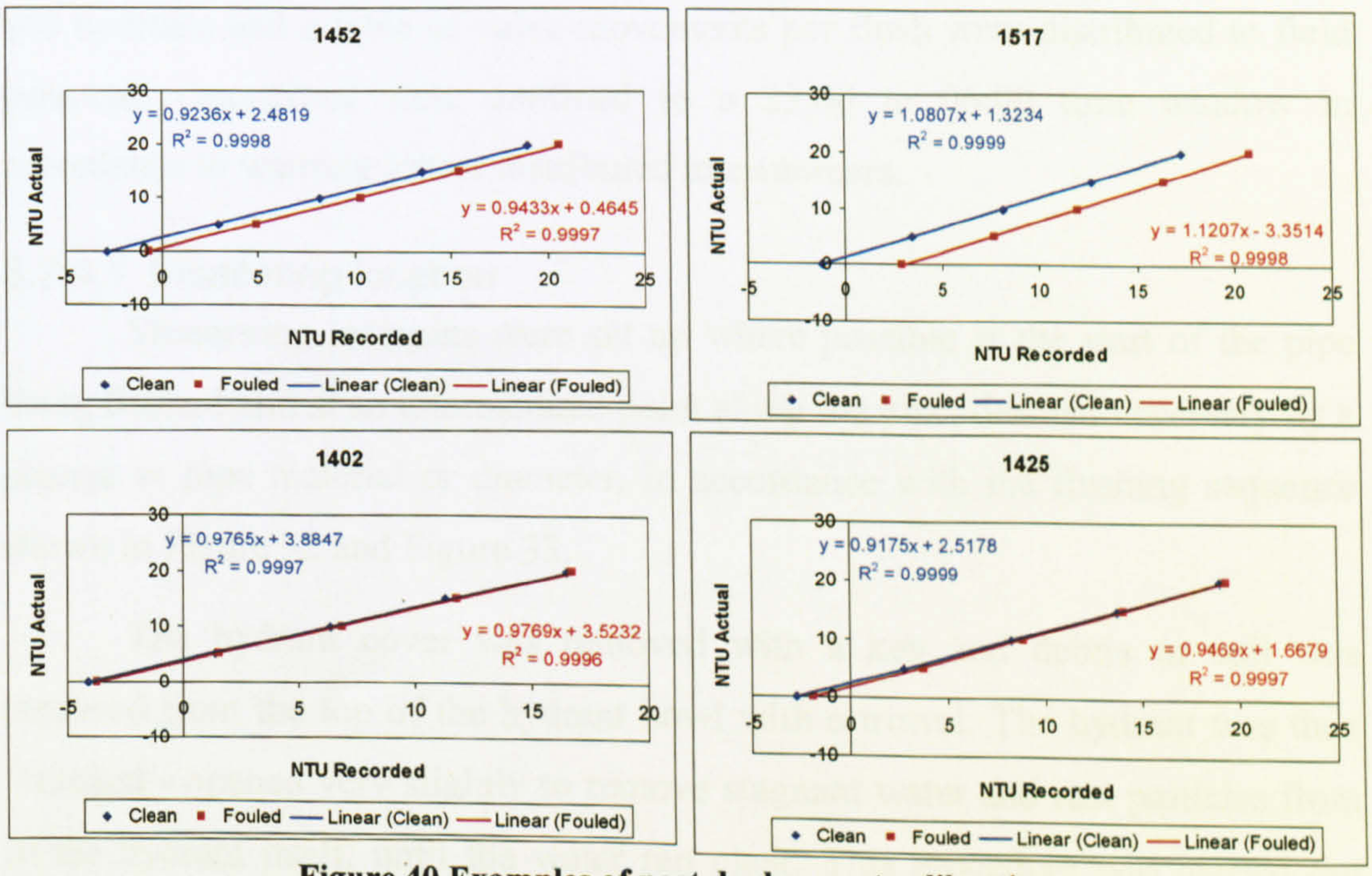

Figure 40 Examples of post deployment calibration.

Long term monitoring turbidity loggers were carefully removed from the field and brought back to the lab with their heads covered in protective caps filled with water with as little disturbance as possible. The loggers were then calibrated following the procedures previously described in section 5.3.3.2. The optical surfaces were then thoroughly cleaned and the calibration procedure repeated. Brown material was observed on the swab used during cleaning; indicating that a film of material had been removed from the optical surfaces of the logger head and some degree of fouling had occurred. Examples of post logger deployment 'fouled' and 'clean' calibration results are shown in Figure 40. Here it can be seen that the calibration results plot in parallel indicating that the gain is very similar and the fouling of the instrument only affected the instrument's offset. Thus Periodically verifying turbidity logger results by taking an independent turbidity reading using a Hach meter would be a suitable method for correcting offset.

5.3.4 Field procedures

Several days before flushing pressure loggers were installed, according to Yorkshire waters standard procedures, at hydrants around the network and set to record at 1 minute intervals.

On the night of flushing, detailed flushing plans with locations of valves and hydrants and a table of valve movements per flush were distributed to field personal. Operations were confined to a 23:00 to 06:00 time window in accordance to warning letters distributed to customers.

5.3.4.1 Monitoring location

Monitoring locations were set up where possible at the start of the pipe being flushed and at an intermediate point along the pipe, deemed necessary by a change in pipe material or diameter, in accordance with the flushing sequence shown in Figure 32 and Figure 33.

The hydrant cover was removed with a key and debris or soil was removed from the top of the hydrant bowl with a trowel. The hydrant was then 'cracked'- opened very slightly to remove stagnant water and rust particles from in the hydrant itself, until the water ran clear. This procedure was carried out very carefully to ensure that only material from inside the hydrant was removed,

and the main was not flushed. Any water that collected in the hydrant was then allowed to drain away and the standpipe was then screwed onto the hydrant. A pressure logger recording at 1 minute intervals was connected to the nipple at the base of the standpipe. Hoses were then connected from the standpipe to the inlet of the aluminium case and the outlet to drain. Ensuring that the valves around the flow cell and the brass tap were closed the hydrant was then opened by a few turns. The brass tap was then opened slightly. In order to reduce air bubbles in the flow cell the upstream valve was fully opened before the downstream valve. The downstream side of the box could also be elevated on the kerb or hydrant lid to allow the bubbles to escape. Increasing the flow through the cell and opening and closing the downstream cell valve was effective in removing any persistent bubbles. Flow was adjusted with the brass tap to ensure that there would be water constantly flowing through the cell, even when the pressure dropped during flushing. The laptop was then turned on and the logger set to record calibration mode using 'Talk Sense' which enabled 11 second sampling. The screen on the laptop was then turned off to preserve battery life and the aluminium case was closed. Cones were then placed around the equipment to warn pedestrians and vehicles, Figure 41.

Figure 41 Intermediate monitoring location setup.

5.3.4.2 Flushing Location

Flushing locations were set up on hydrants in a similar way to the monitoring location. The hydrant bowl was cleaned and 'flushed', the same way as with the monitoring location, before the flushing standpipe was screwed onto the hydrant. In some cases the position of the hydrant was too close to the edge

of the chamber, or was particularly deep and caused the turbidity logger to foul the sides of the chamber. In this situation a standard standpipe was used, and turbidity was recorded using the aluminium case set up and a Vernon Morris was used to measure flow, Figure 43.

Figure 42 Flushing setup normal operation.

The gate valve was checked that it was in the closed position and then fitted to the standpipe, pointing in a direction accounting for the disposal of water. In some cases where a drain was not in an immediately accessible location or the flow of water could cause potential damage, 'bagging' was connected to the gate valve assembly, Figure 44.

A pressure logger was installed on the fitting on the flushing stand pipe and set to record at 1 minute intervals. The turbidity logger was connected to a laptop via a long serial cable. The logger was then set to record in calibration mode and the 'view trend graph' feature of Talk Sense software enabled real-time monitoring of the turbidity response. The valve on the hydrant was opened fully and flushing commenced upon confirmation from the field technicians that the appropriate valves had been opened or closed in accordance with the flushing plan.

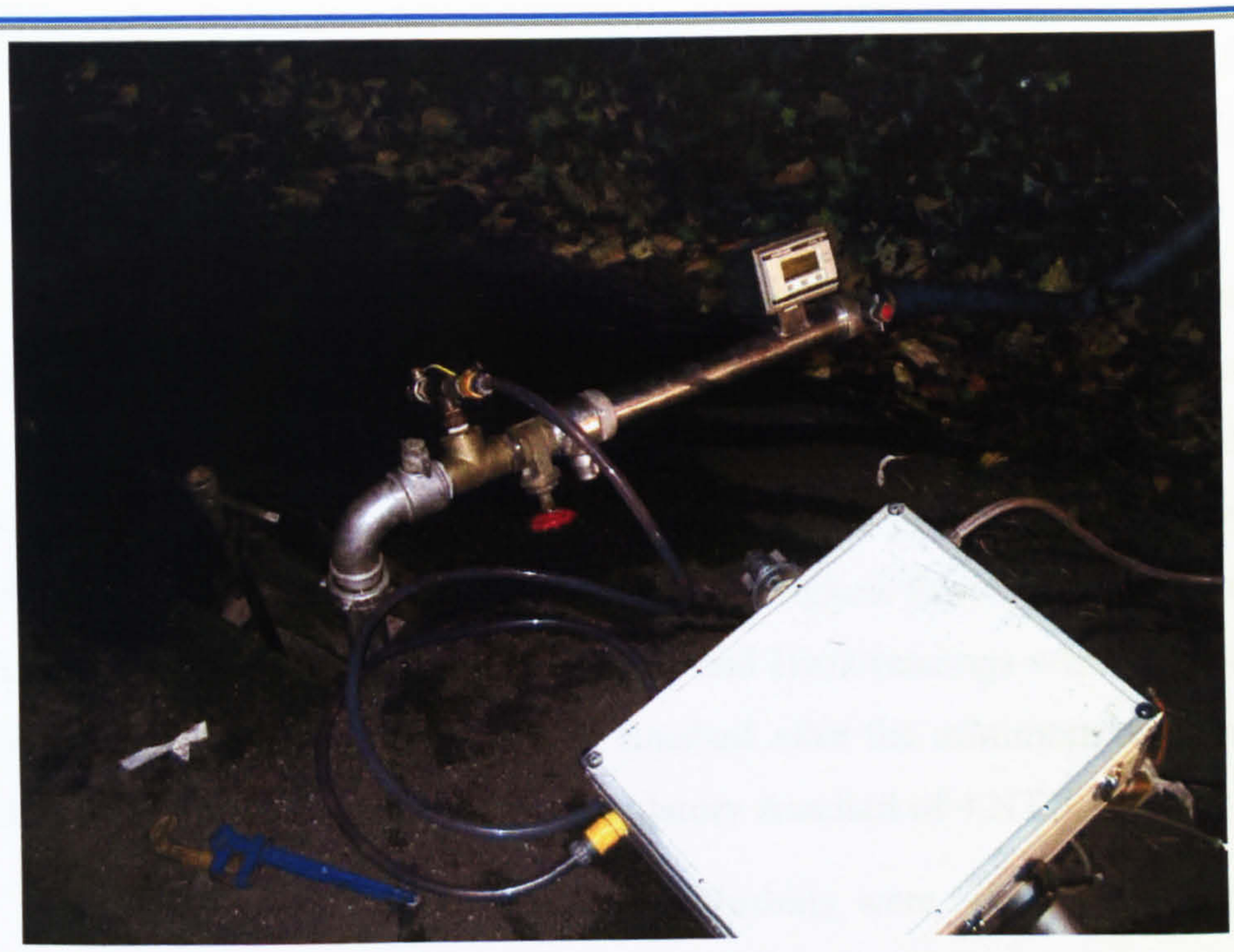

Figure 43 Flushing setup on restrictive hydrants.

Figure 44 Use of bagging for disposal of water.

The gate valve on the flushing hydrant was opened until the appropriate flow rate for the first flushing step (0.7 N/m^2) was achieved according to the flushing plan. After 1 minute a physicals and a metals sample were taken for lab analysis following Yorkshire Water's procedures (YWS 2005). This would enable to analyse how the composition of discolouration material changes with respect to pipe material, layer strength and time. Independent turbidity readings were taken with a hand held Hach meter following manufactures instructions as

often as possible to verify the turbidity logger's results. Flushing continued for at least minimum duration of two pipe volumes or until the turbidity had fallen to below 4 NTU (which ever was longer).

The gate valve was then opened further until the appropriate flow rate for the next flushing step (2.3 N/m^2) was achieved, in accordance to the flushing plan. Sampling and Hach readings were again taken as previously. After a minimum duration of two pipe volumes was achieved or until the turbidity fell below 4 NTU the flow rate was increased to the highest flushing step ($8N/m^2$) in accordance with the flushing plan. Samples and Hach readings were again taken as before and flushing at the location finished after the minimum duration, or until the turbidity fell well below the regulatory standard of 4 NTU.

Timings for every action during the flushing were noted in a field table. All equipment was then moved to the next systematic location in accordance to the flushing plan and the flushing method repeated. Flushing operations had to cease and the network returned to its normal operational condition before the warning letter window closed at 06:00 the following morning. On the last day of flushing, pressure loggers were removed and downloaded in accordance with Yorkshire Water's procedures.

5.3.5 Post flushing model calibration

After flushing operations, pressure and flow information recorded during flushing was used to further verify the hydraulic model calibration and substantiate the flushing flow rates which were estimated in the field.

The hydraulic models used here had pattern time steps of one hour, and every node had a separate demand pattern. This caused problems in calibrating the model with field data, as the flushing location, flow rates and therefore system pressures would change several times within an hour period. Therefore separate 1 hour simulation models were built for each flushing step at each location.

For each flush, where necessary, the valve closures were simulated by closing the appropriate pipe in the model. The correct boundary conditions were achieved by adjusting the appropriate hour of the inlet reservoir pattern to equal the average pressure recorded during the flushing step at the DMA inlet. The

flushing hydrant was then modelled by adding a 1 metre pipe of diameter 63mm, roughness 140 (Hazen-Williams units) and loss coefficient of 2.7 similar to Section 5.3.2.1. However in order to model the pressure recorded during flushing, the emitter was attached to a further 0.1 m length of pipe. The diameter of this 0.1m length of pipe was adjusted and the model run repetitively until the flushing flow rate was achieved. The average pressures recoded in the field at each flushing step were then checked against the modelled results.

Figure 45 shows the calibration of the 1 year flush performed in J722. Results from flush 7, highlighted with red circles calibrate poorly between field and modelled results. The modelled pressures for this flush were shown to more closely match the recorded field pressures after swapping round the open and closed valves at the beginning of the pipe in flush 6, Figure 32, and it was concluded that that these valves were incorrectly closed during flush 7 by the field technicians.

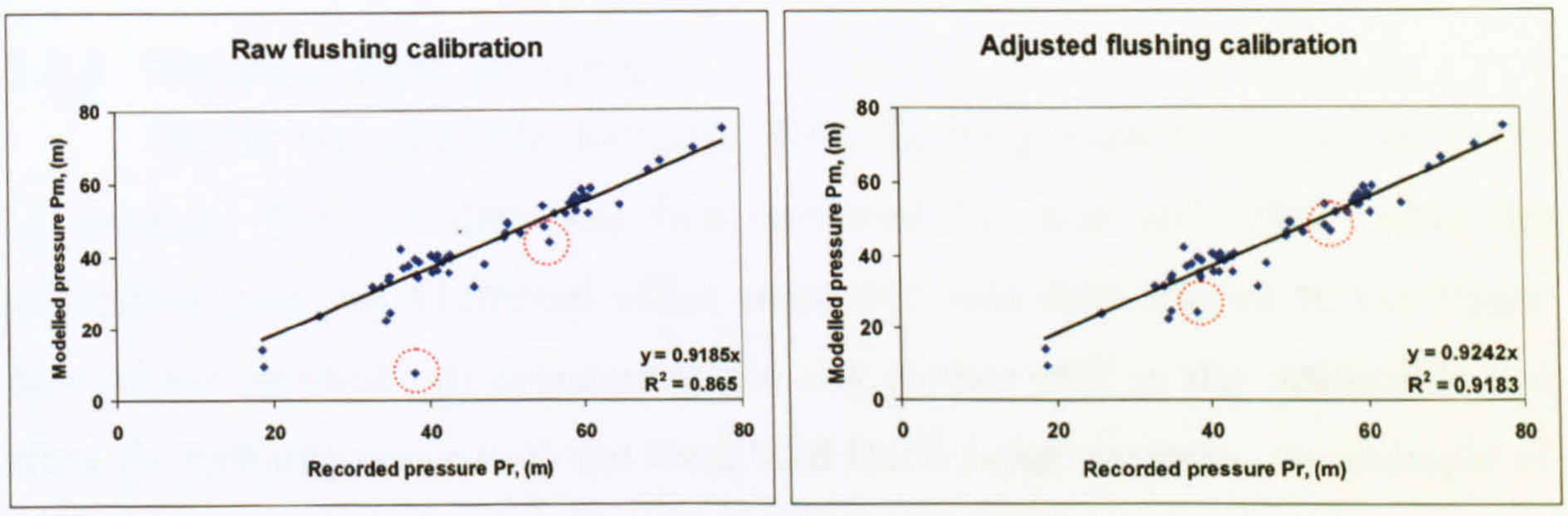

Figure 45 J722 post flushing calibration.

Figure 46 shows the calibration of the initial flush performed in J730. Results from flush 1, highlighted with red circles show that pressures recorded in the field were much lower than the model predictions. Since recorded and modelled pressures were similar for flushes 2- 11 which all branch from the flush 1 pipe, it was thought that there was a restriction in the section of pipe after the junction of the flush 11 pipe and before flush 1 hydrant, Figure 33. Closer inspection of the GIS database revealed a 50m length of cast iron pipe which was 50 years older than the majority cement lined 150mm ductile iron pipe. It was therefore assumed that this section of ductile iron pipe was unlined and could be heavily tuberclated. Pressures for this flush were therefore reduced in the model

to closely match recorded pressures by decreasing the diameter of the last section of pipe in flush 1 to 100mm and increasing the roughness to 20.

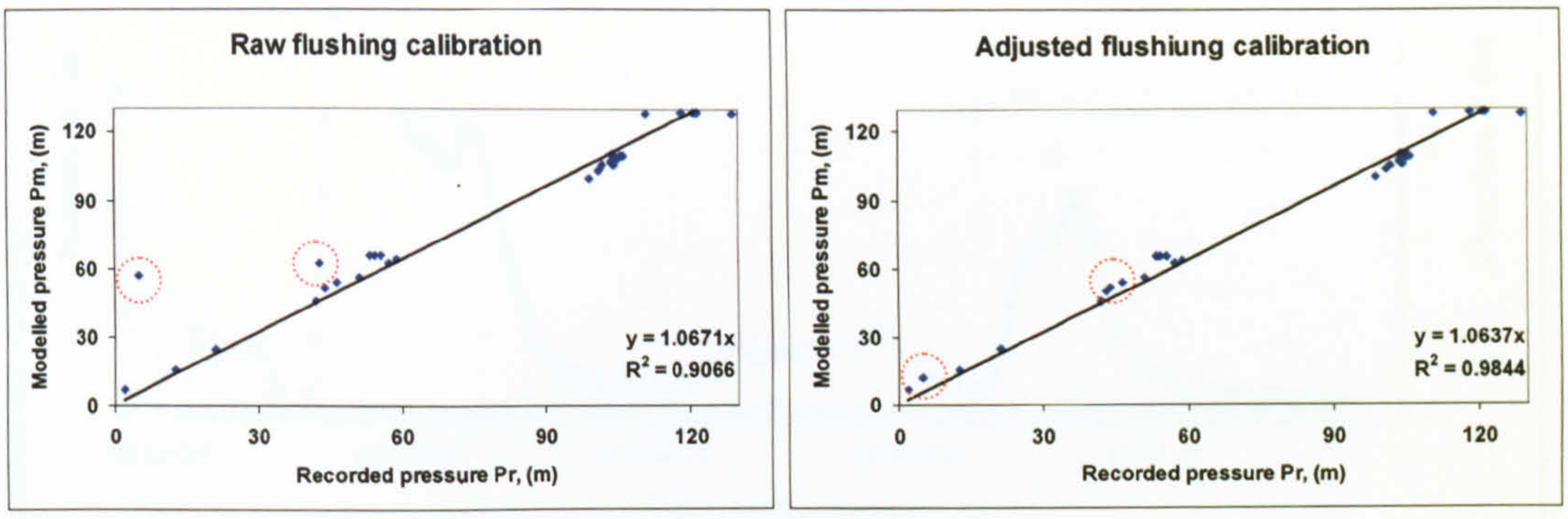

Figure 46 J730 post flushing calibration.

Following the minor adjustments described above the hydraulic models were shown to calibrate well with R^2 values of 0.92 and 0.98 in J722 and J730 respectively. Therefore good confidence is seen in the headlosses and consequent shear stresses during flushing.

5.3.6 Flushing data analysis

During each flush the turbidity of the flushing water was recorded every 11 seconds. The raw data was first corrected for gain and offset using the calibration data. An additional offset correction was then applied to the logger data where necessary to compensate for any further drift in the instrument and align the turbidity curve with the hand held Hach meter readings. An example of the turbidity response verses time for a typical flush is shown in Figure 47. As Turbidity is a measure of the light scatter from small particles suspended in the water, it can be assumed that the higher the turbidity the greater the number of small particles (if they are all the same size, and composition as discussed in section 2.6.1). However it is not as simple to conclude that a higher peak NTU recorded during flushing equates to more discolouration material in one pipe or another.

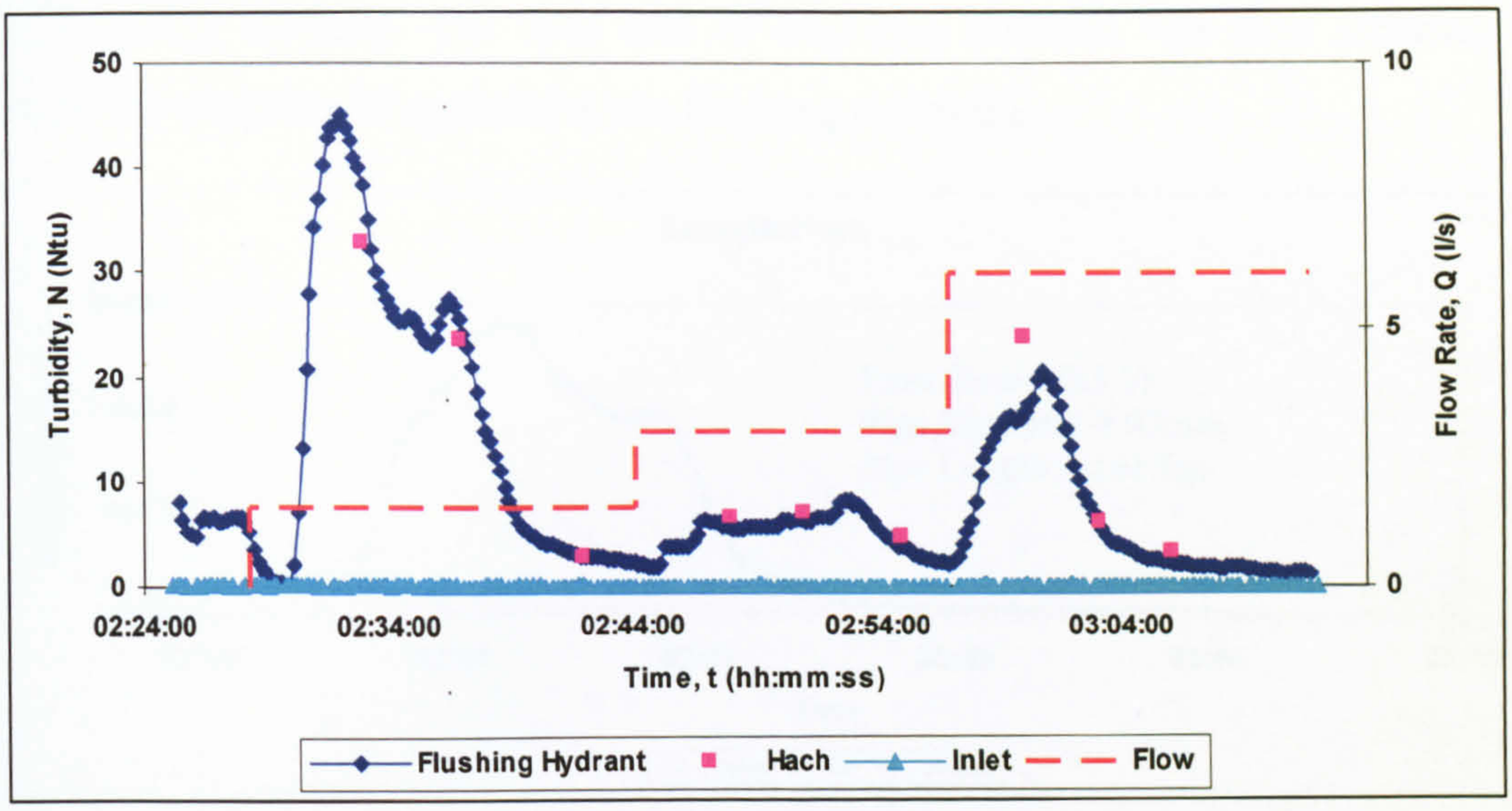

Figure 47 Typical flush example

The turbidity response shown in Figure 47 is a factor of both the flow rate and the amount of discolouration material. For example if exactly the same turbidity response was seen in a pipe flushed at 5 l/s and a similar pipe at 10/ls more turbidity material must have been present in the 10 l/s pipe. This is because during the same time period, more water containing the same concentration of suspended particles will have passed by the turbidity meter in the 10 l/s pipe. Therefore in order to compare discolouration potential between different flushes it would be more practical to calculate the amount of discolouration material mobilised during each flush. This figure would then have to be normalised for pipe length and diameter, because if the same amount of discolouration material was mobilised from a short small diameter pipe and a longer pipe of larger diameter the shorter pipe must have a higher discolouration potential. Thus assuming that discolouration material is held in cohesive layers over the entire internal surface of the pipe it would be sensible to convert the amount of discolouration material to a thickness on the pipe walls.

5.3.6.1 Calculations in data analysis

Figure 48 shows an example of data recorded during one flushing step. The area under the graph is first calculated to give total NTU.seconds for the flush (Equation 7). If a turbidity response was seen at the monitoring location located at the inlet to the pipe being flushed, then material was imported into the

pipe during flushing. The total area of imported material was then subtracted from the total area of material at the flushing standpipe.

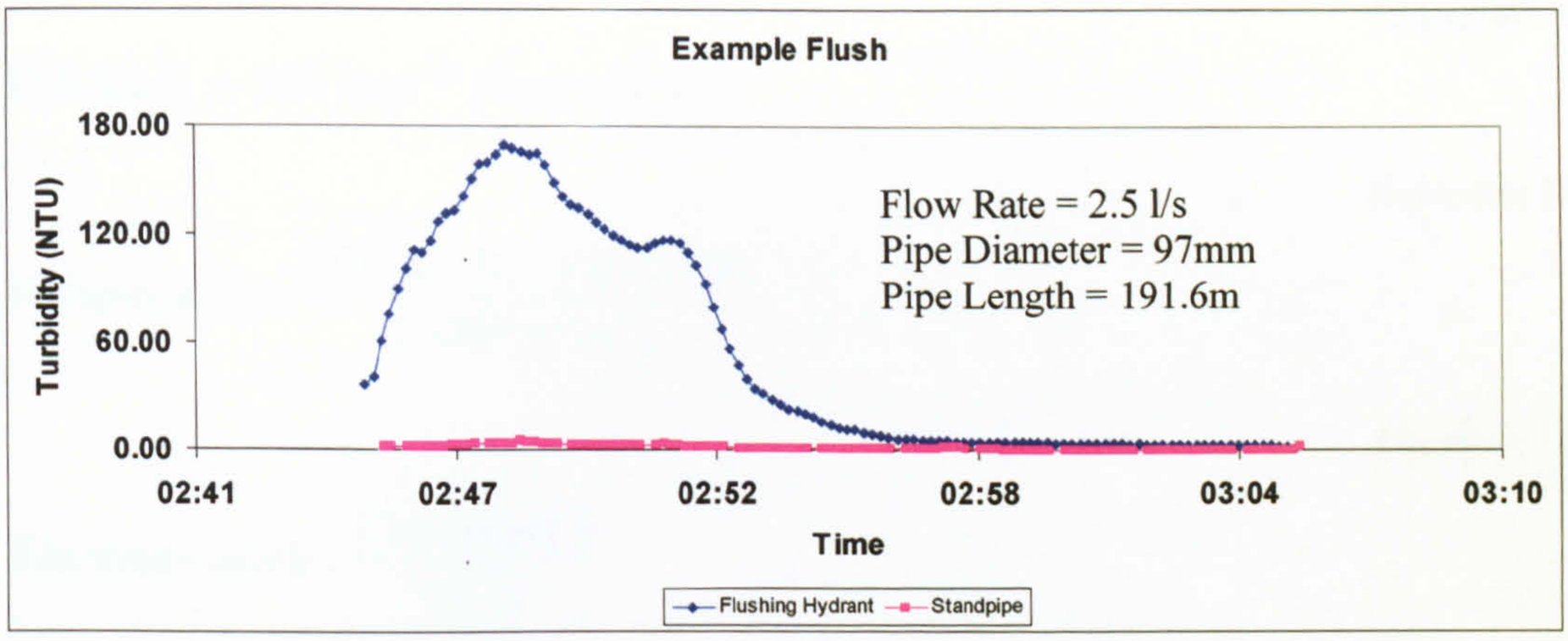

Figure 48 Example data from one flushing step.

This area was then converted to total suspended solid (TSS) seconds using a conversion factor from Boxall et al. (2003), Equation 8, represented in the graph previously shown in Figure 7. Limitations to the accuracy of this conversion based on differing particle light scattering properties were discussed in Section 2.6.1. The expression of Boxall et al (2003) was used rather than those of Vreeburg (2007) since the work of Boxall was indicative of UK systems. Also given the expectation of consistent discolouration particles from different flushes, the absolute conversion value does not necessarily matter for relative comparison.

Time was then removed from the data by multiplying TSS.time (ug/l.s) by the flow rate (l/s) to give total solids (ug/l) (Equation 9). Assuming that discolouration material has a density of 1300kg/m^3 (Boxall et al. 2003) TSS was then converted to volume (Equation 10). Lastly as pipe diameters and lengths are normalised by assuming that discolouration material accumulates uniformly on the full pipe surface in cohesive layers, and the volume of discolouration material is converted to thickness of material mobilised (Equation 11).

Equation 7

$$NTU.s = \sum_{n=1}^{\infty} t * \frac{NTU(n) + NTU(n+1)}{2}$$

Where t = time interval between readings.

Equation 8

$$TSS.time\ (ug/l.s) = NTU.s * 73.33 + 0$$

Equation 9

$$TSS\ (ug/l) = TSS.time * Flow\ rate\ (l/s)$$

Equation 10

$$Volume(m^3) = \frac{TSS(ug/l)/1000/1000}{1300(kg/m^3)}$$

Equation 11

$$Thickness(mm) = \frac{Volume(m^3)}{\pi d * l}$$

Where d is the diameter (mm) and l is length (m) of pipe being flushed.

Using the example data depicted in Figure 48 a worked example of the calculations follows:

Area under the graph = 63919.32 NTU.s

TSS.time = 63919.32 * 73.33

= **4687416 ug/l.s**

TSS = 4687416 ug/l.s * 2.5 l/s

= **$1.17 * 10^7$ ug/l**

Volume = $1.17 * 10^7$ ug/l / 1000000 / 1300 kg/m3

= **$9.01 * 10^{-3}$ m^3**

Thickness = $9.01 * 10^{-3}$ m^3 / (π 97mm/1000 * 191.6m)

= **0.15mm**

The thickness of discolouration material on the pipe walls is the parameter used in all the flushing results.

5.4 Flushing results

5.4.1 Raw data

Examples of typical flush results are shown in Figure 49 to Figure 51. The light blue line is the turbidity recorded at the beginning of the pipe being flushed. Independent Hach readings taken during flushing are displayed in pink and correlate well with the turbidity recorded at the flushing hydrant depicted in dark blue. The flow rates of the three flushing steps are depicted with the red dotted line on the secondary Y axis.

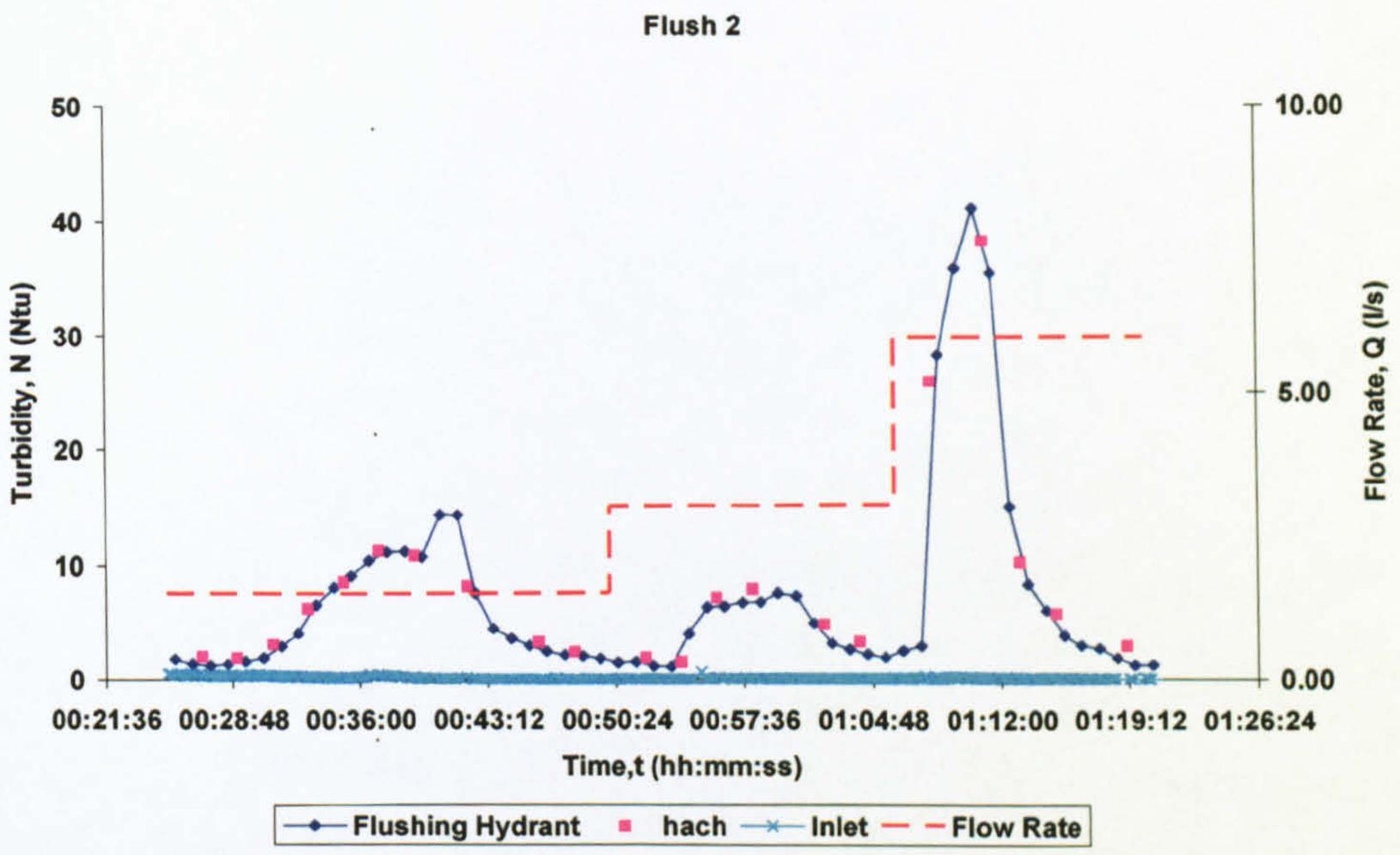

Figure 49 Typical flush results (J722 3 month flush 2).

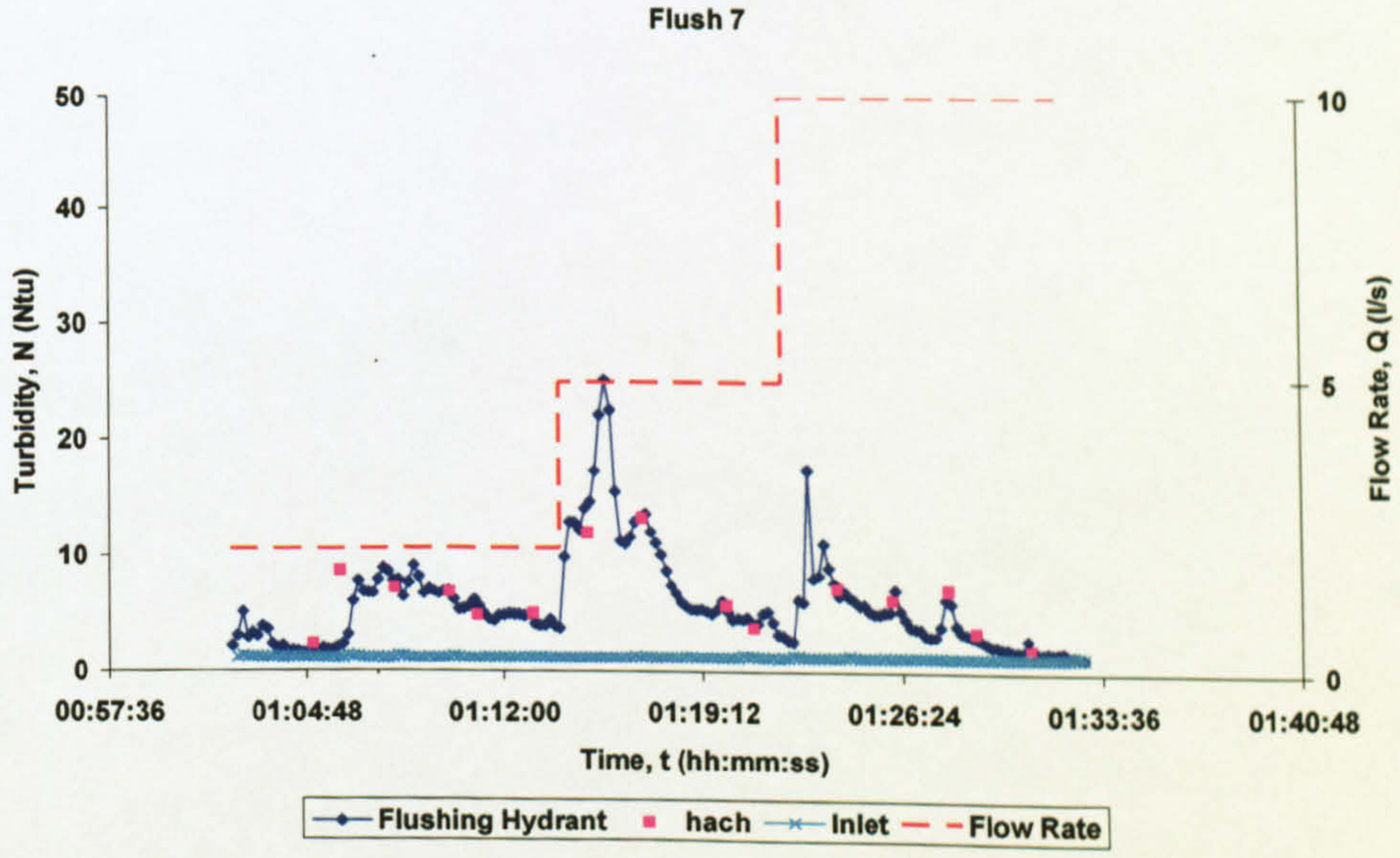

Figure 50 Typical flush results (J722 3 month flush 7).

There is an increase in turbidity recorded at the inlet of the pipe being flushed seen in Figure 51. Since this turbidity was not generated in the pipe being flushed, these values were taken away from the overall turbidity values recorded at the flushing hydrant.

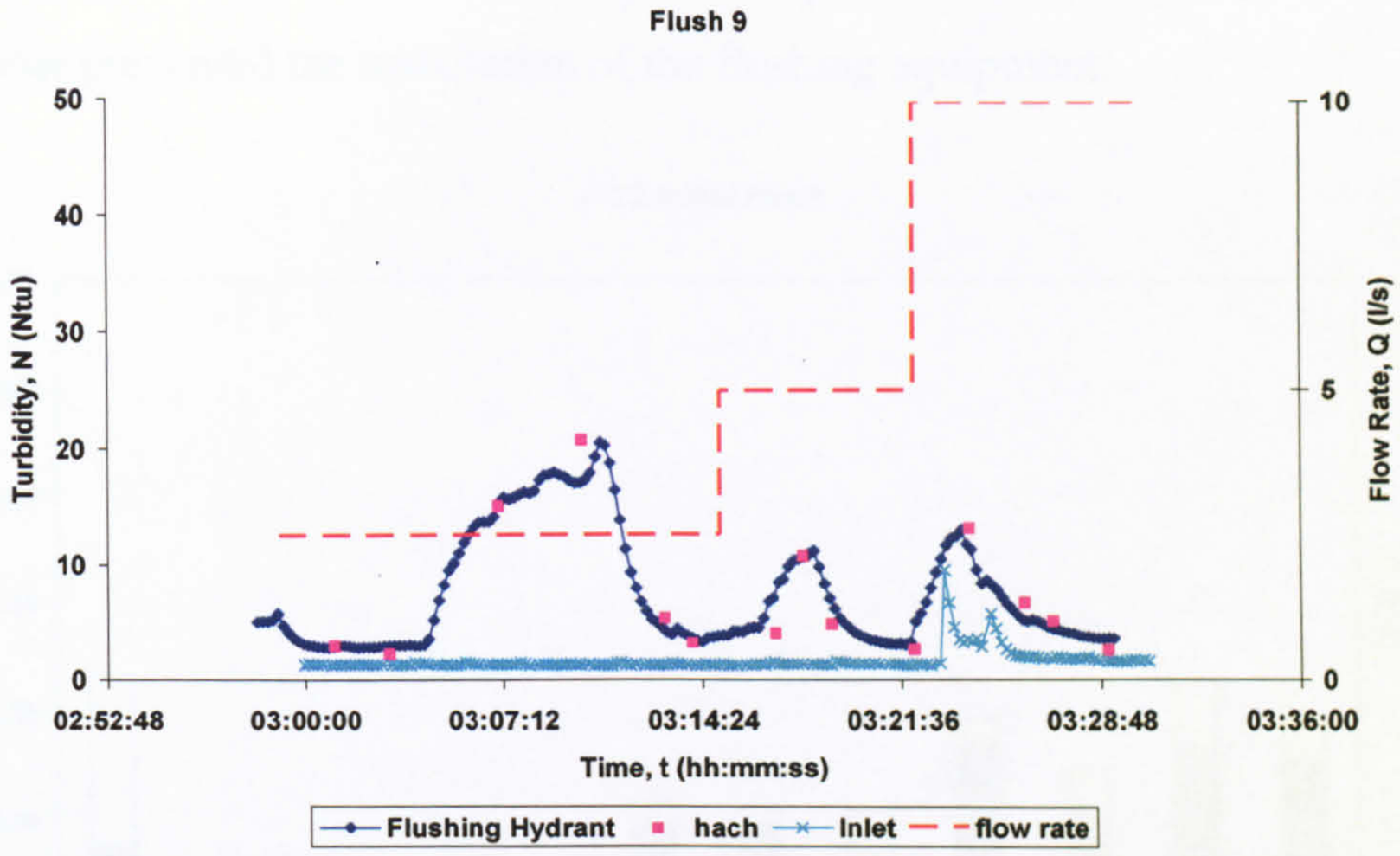

Figure 51 Typical flush results (J722 3 month flush 9).

The flushing examples shown here were chosen to highlight that the highest levels of turbidity attained during flushing were not necessarily always reached during the highest flushing flow rate, as seen in Figure 49. Figure 50 shows that the highest turbidity (27 NTU) reached during this flush, was generated at the 2.3 N/m^2 shear stress flushing step at 5 l/s. In Figure 51 the highest levels of turbidity (25 NTU) were generated during the 0.7 N/m^2 flushing step at 2.5 l/s.

5.4.2 Thickness of material mobilised

For each flush, the area under the turbidity graph was calculated, and this was converted into thickness of discolouration material mobilised using the calculations previously described in Section 5.3.6. Summary results showing the thickness of discolouration material mobilised during each flush in J722 at the initial, 3 month, 7 month and one year flushes are shown in Figure 52, Figure 53, Figure 54, and Figure 55 respectively. The results for the initial and six month flush in J730 are shown in Figure 56 and Figure 57. In the graphs the thickness of material removed during the first flushing step (0.7 N/m^2) is shown in light

blue, the middle flushing step (2.3 N/m^2) is shown in maroon and the highest flushing step (8 N/m^2) is shown in cream. Characteristics of each pipe being flushed (daily conditioning shear stress, diameter and pipe material) are shown on the x axis of each graph (ordered in flushing sequence). No values are recorded for flush 5 in J730 DMA, as the position of the hydrant within the chamber prevented the installation of the flushing equipment.

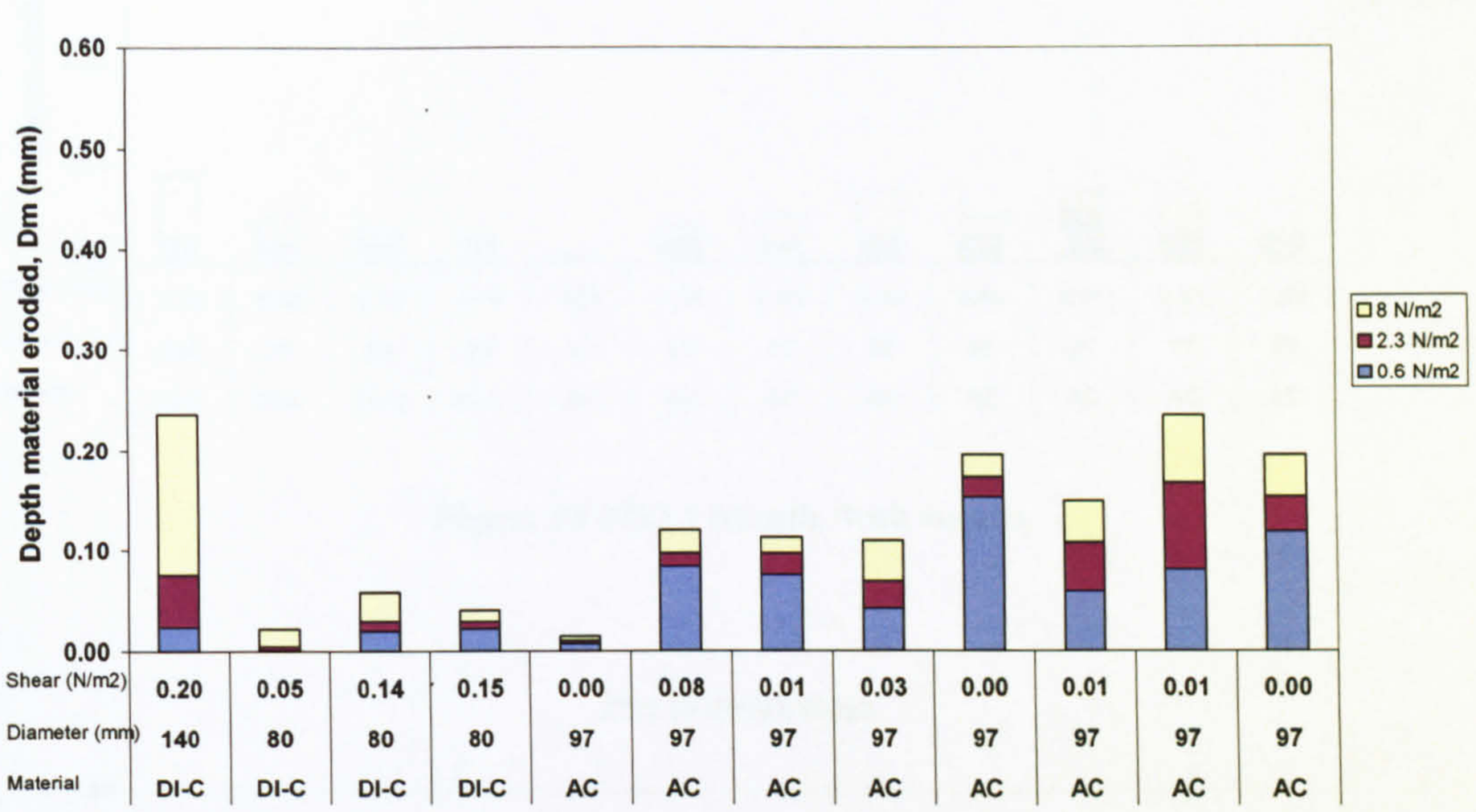

Figure 52 J722 initial flush results.

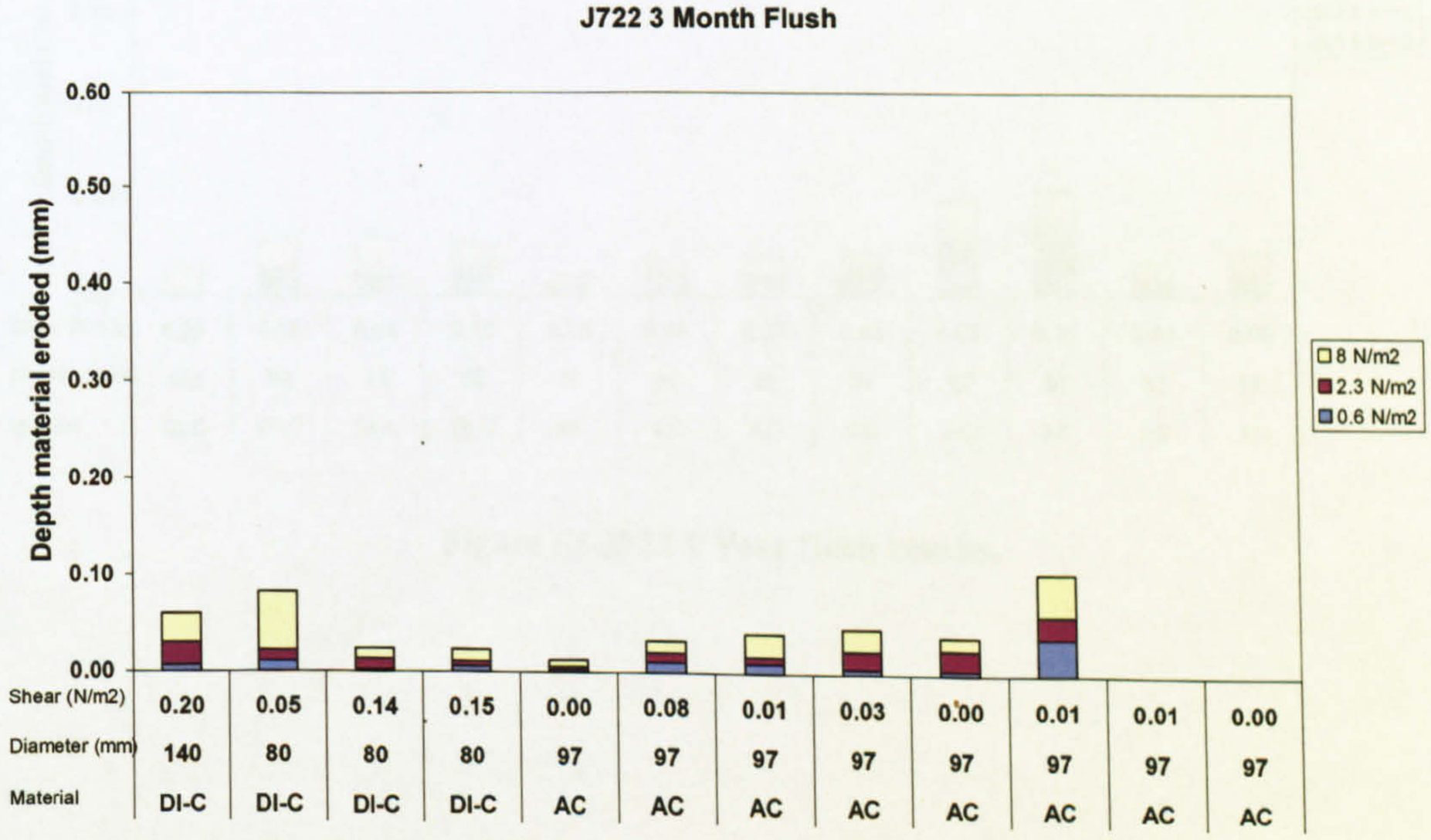

Figure 53 J722 3 Month flush results.

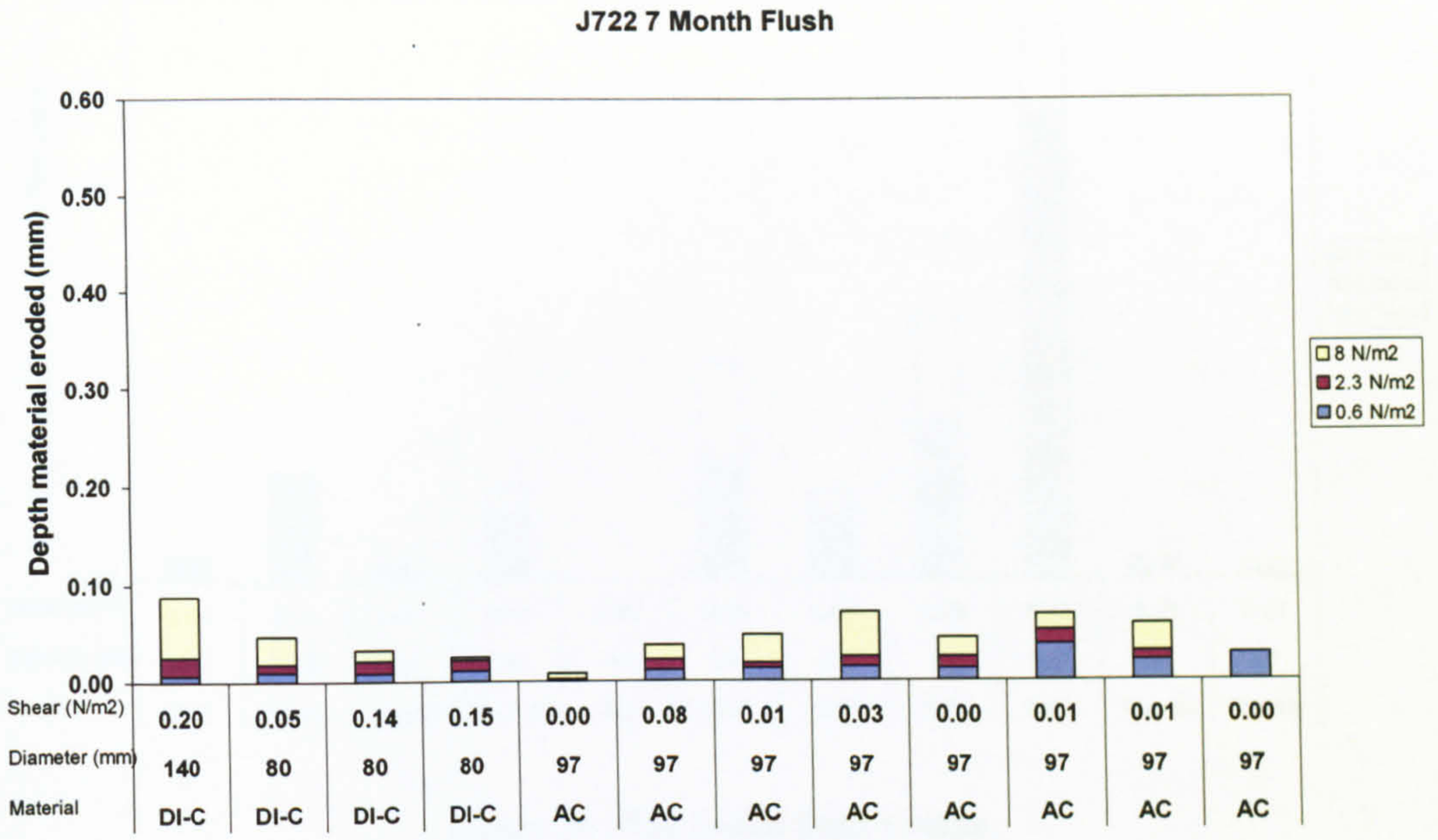

Figure 54 J722 7 Month flush results.

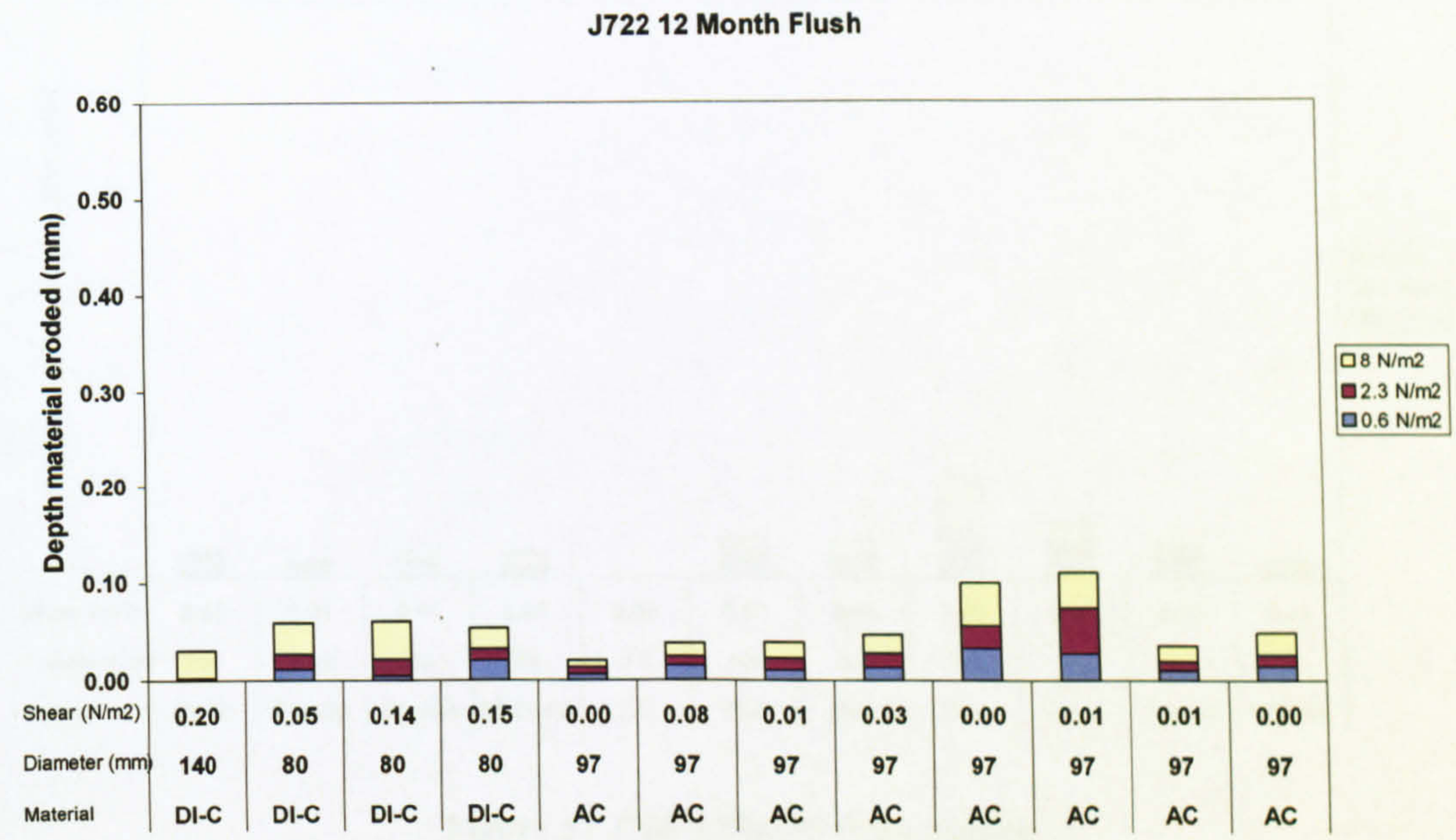

Figure 55 J722 1 Year flush results.

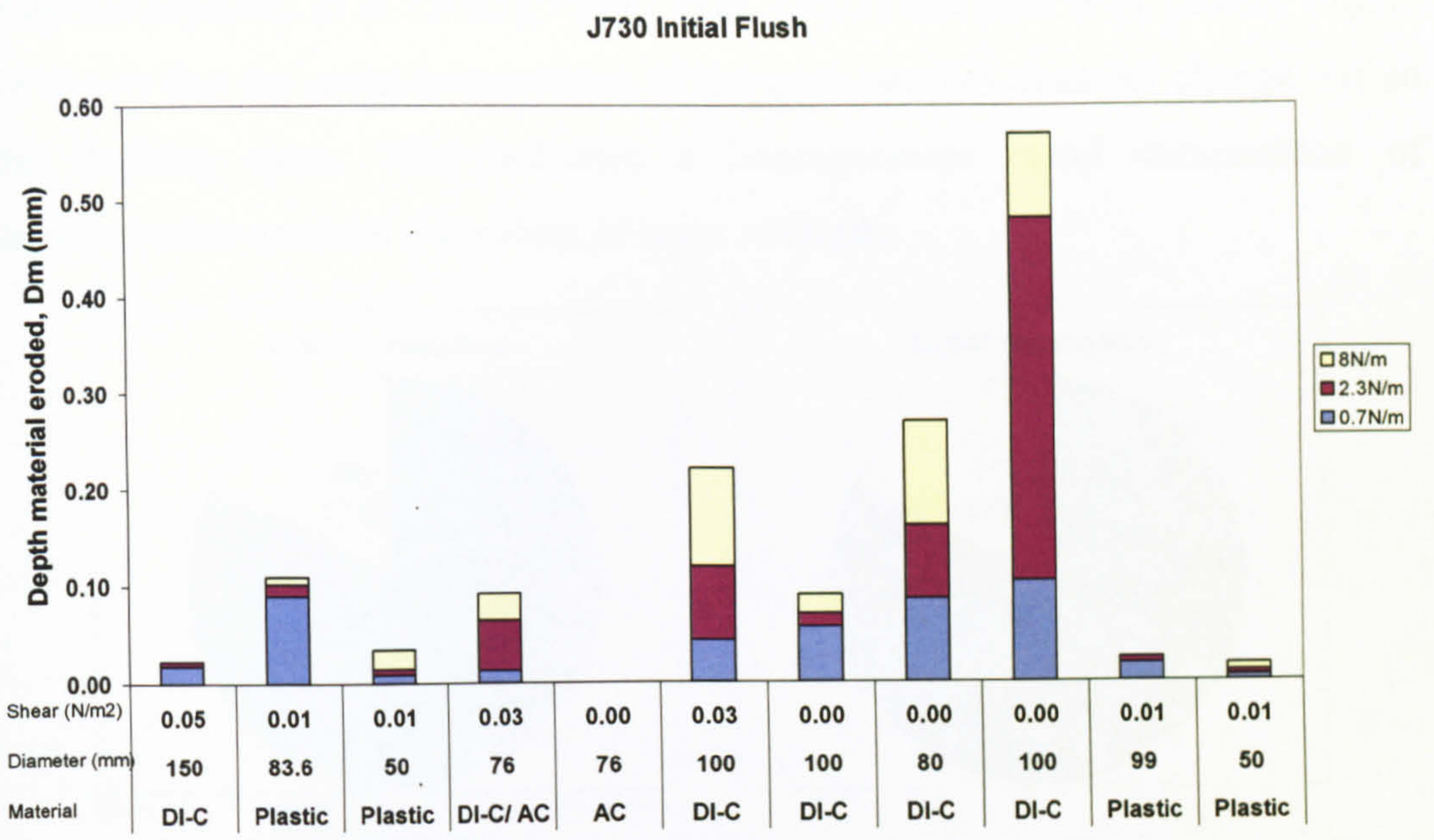

Figure 56 J730 Initial flush results.

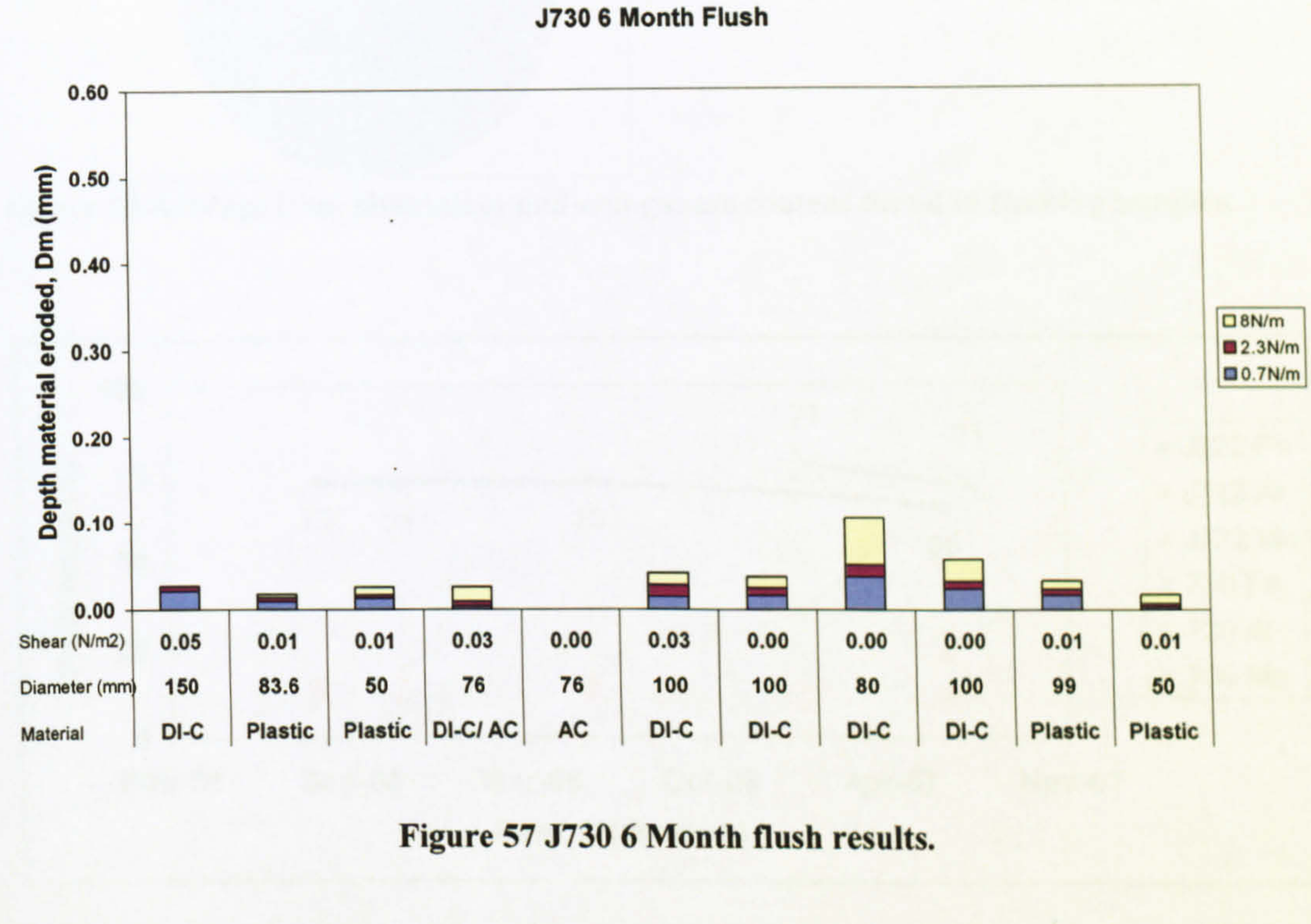

Figure 57 J730 6 Month flush results.

5.4.3 Sample analysis

Analysis of grab samples taken in both zones during flushing shows that the total metal content comprised on average 72% Iron, 17% Manganese and 11%Aluminiumm, and remained fairly consistent, irrespective of pipe material or diameter. This concurs with previous work by Boxall et al. (2003),

Polychronopolous et al. (2003), Prince et al. (2003) and Seth et al, (2003). Figure 58 shows that the metal composition of the grab samples does not change within the flushing steps. This indicates a homogeneous metal composition of discolouration material regardless of layer strengths.

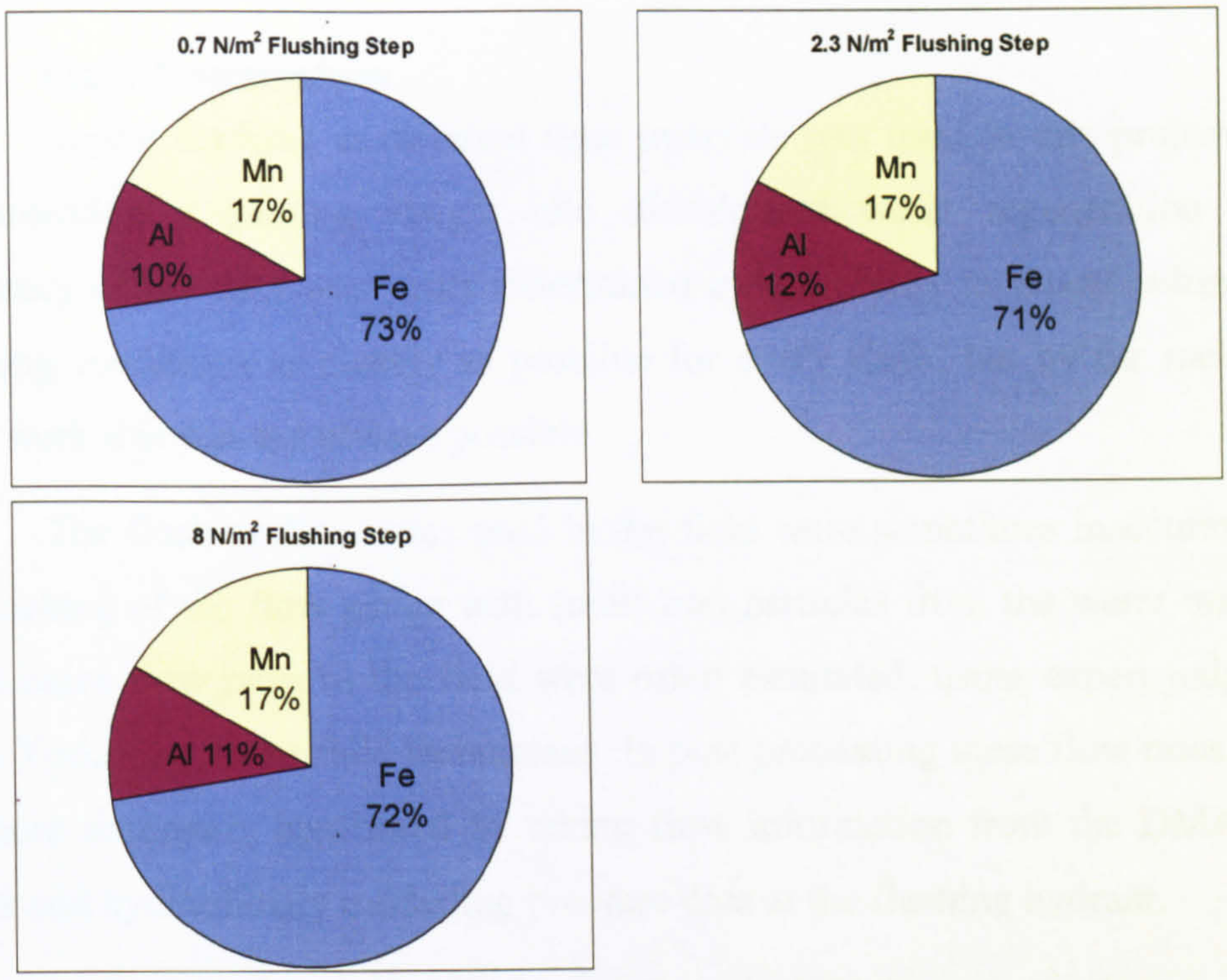

Figure 58 Average iron, aluminium and manganese content found in flushing samples.

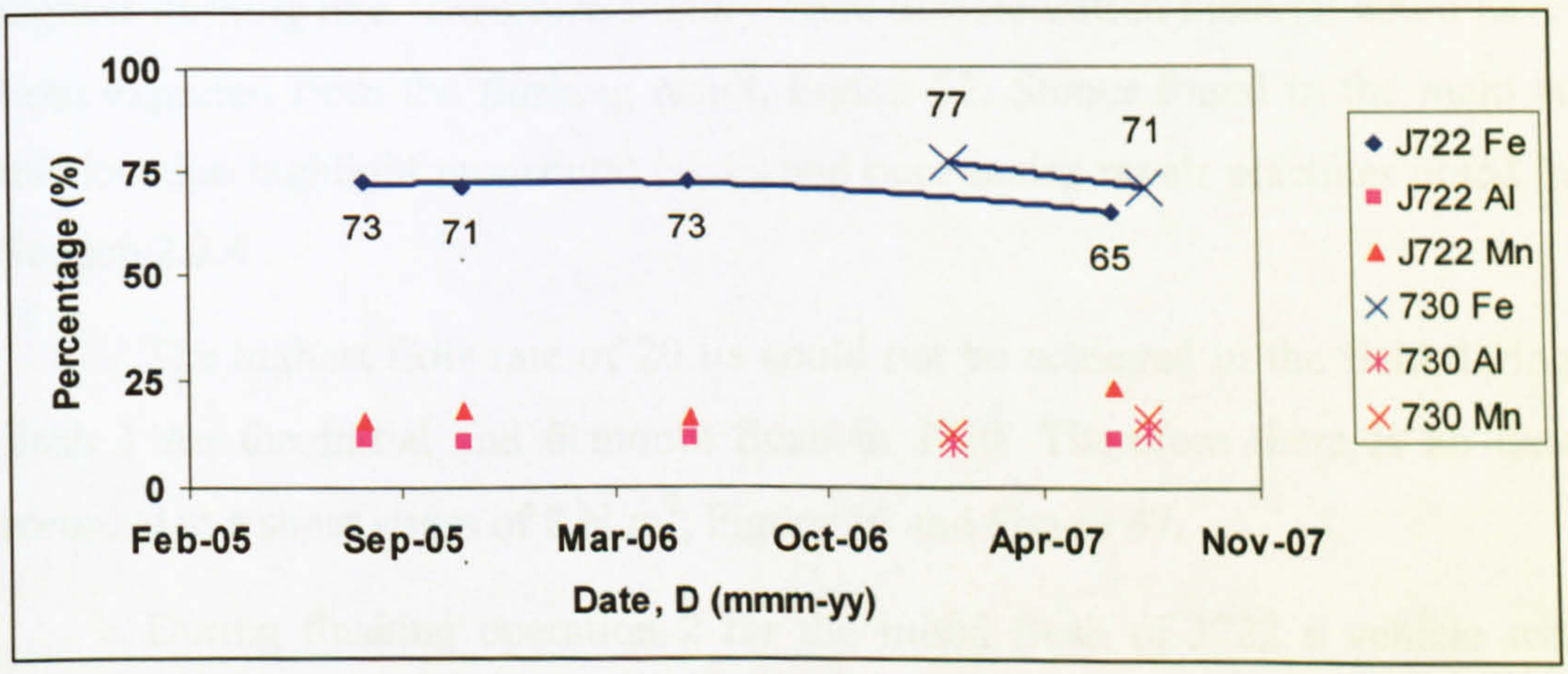

Figure 59 Percentage of metals at differing flush intervals

Figure 59 depicts the average percentage of iron, aluminium and manganese found in the grab samples for each flushing operation plotted with respect to time. Here it can be seen that in general the metal composition of the

discolouration material does not change over time. However in this data there is a reduction of 8% in the iron ratio between the 7month and 1 year flush in J722 and a 6% reduction in J730 between the initial and 6 month flushes.

5.5 Discussion

5.5.1 Field Constraints

Repeat flushing at different time intervals was used in this project with the intention a gaining insight into discoloured water regeneration rates. Accuracy of the data was partly determined by the ability to repeat subsequent flushing conditions as closely as possible for every flush, but by the nature of field work this was not always possible.

The flushing flow rates used in the field were sometimes inaccurate due to blocking of the flow gauge with small iron particles from the water main. In these cases flow rates in the field were often estimated, using expert judgment from Yorkshire Water field technicians. In post processing these flow rates could be more accurately confirmed by taking flow information from the DMA inlet meter and hydraulically modelling pressure data at the flushing hydrant.

In flush 9 of the initial flush carried out in J722 large stones became stuck in the gate valve on the flushing hydrant, and the flow became restricted for the highest flushing rate. Therefore slightly more discolouration material could have been expected from the flushing result, Figure 52. Stones found in the main at this location highlight procedural issues and poor mains repair practices noted in Section 2.2.4 .

The highest flow rate of 20 l/s could not be achieved in the field during flush 1 for the initial and 6 month flush in J730. Therefore there is no data recorded at a shear stress of 8 N/m^2, Figure 56 and Figure 57.

During flushing operation 2 for the initial flush of J722 a vehicle was parked over the valve necessary to isolate the loop (Figure 32), therefore the majority of the flow travelled along the pipe previously flushed in flush 1. Subsequent modelling of flush 2 however indicated that a maximum shear stress of 1.6 N/m^2 was achieved in this pipe. Thus less discolouration material is seen for initial flush 2, Figure 52 and slightly more than expected discolouration

material is present for the 3 month flush 2, Figure 53, as this had not previously been flushed at the middle and higher flushing forces.

Due to available time constraints for flushing operations, when J722 was initially flushed, only up to flush 9 was completed. During the 3 month flushing, operations progressed as far as the initial flushing step of flush 11. Since flush 10 and the initial step of flush 11 was not previously flushed, these results were assigned to the initial flush, Figure 52 and do not appear in the 3 month flush results, Figure 53. Flush 11 was not completely flushed until the 7 month flushing interval, therefore the 2.3 and 8 N/m^2 flushing results do not appear on the 7 month flush graph, Figure 54 but were assigned to the initial flush, Figure 52.

Pressure in J730 was very high (12 Bar). This proved problematic with connections in the flushing equipment in the initial flush. During the highest flushing rate of flush 2, the pressure was sufficient to blow the bagging from the fittings, causing water to be expelled onto a block paving driveway with sufficient force to lift the bricks, and the flush was aborted.

High pressure also blew the bagging off after 5 minutes of the middle flow rate of flush 10. The expelled water was then in danger of flooding the cellars of near by properties, and flushing at this location was abandoned. Thus less material than could be expected was recorded during this initial flush

Events such as highlighted above are to be expected when carrying out fieldwork of this nature, and have to be taken in to consideration when analysing the results.

5.5.2 Discolouration material layer characteristics.

Previous work by Boxall et al. (2001) suggested that discolouration material is held in cohesive layers, and the volume of material mobilised by flushing could be proportional to the shear stress applied. The three flushing steps carried out in this work were designed to explore this principal, and give an insight as to how these layers develop over time. This work on discolouration material generation rates is new and could prove effective in planning rehabilitation schemes. Figure 60 and Figure 61 depict the percentage of the

total thickness of discolouration material released at each flushing step for J722 and J730 respectively.

In flushes 1, 2, 7, and 9 performed in J722, Figure 60, and flush 11 in J730, Figure 61, it can be seen that successively more discolouration material is mobilised as the flushing force applied increases, indicating a linear relationship between the volume of turbidity remobilised and the applied shear stress. However the other flushes do not display this linear relationship and in some instances the greatest proportion of material was generally released during the middle flushing velocity, the lowest flushing, or was even between the flow rates. This supports the PODDS theory shown in Figure 9 Section 2.6.2 where the linear trend is the gradient, (k) and the non linearity is expressed as the power term, (b).

It was not possible to determine which factors influenced how much discolouration material was released at which flushing force. It would have been useful from an operational perspective to determine which flushing force was optimal for removing the most discolouration material. However, in all flushes, it can be seen that discolouration material was mobilised at the 8 N/m^2 flushing force. This is an important consideration when planning flushing operations. If a pipe was flushed at $4N/m^2$ and experienced a burst the next day which generated a force of $8N/m^2$ a discolouration event is likely to occur. Therefore flushing ideally should be carried out at a force that it is equal to or greater than possible burst generated shear stress.

In Figure 52 to Figure 57 it can be seen that for each individual flushing location a different total thickness of discolouration material was released at each flushing rate. From Figure 60 and Figure 61 it can be seen that although the total amount of material mobilised at a particular location at differing time intervals was different, the percentages of material released at each time interval was very similar. Any slight differences can be attributed to field work limitations described in 5.5.1. From this data it can be elucidated that the different layer strengths of discolouration material accumulate at the same rate. Therefore total thicknesses of discolouration material are considered further in this section.

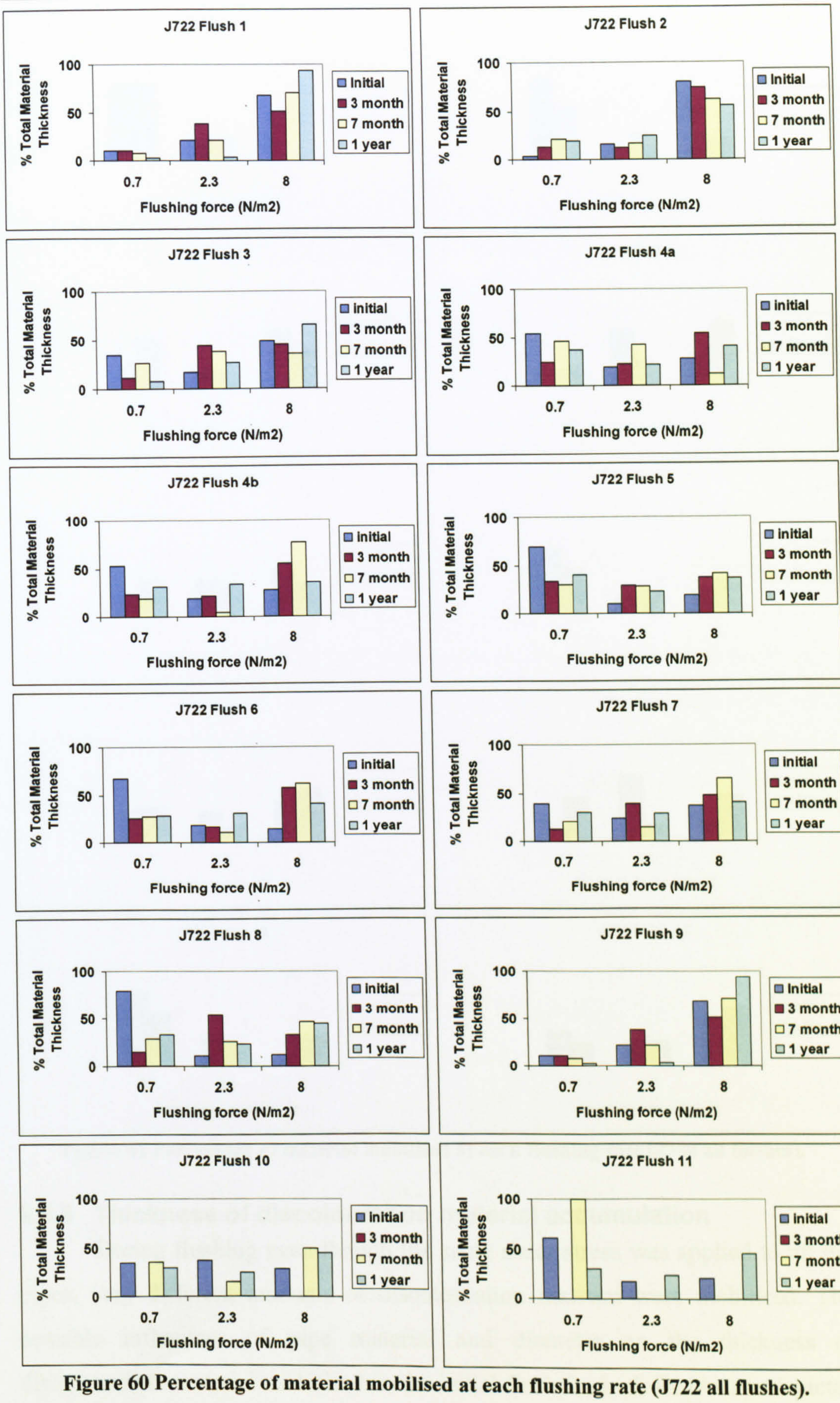

Figure 60 Percentage of material mobilised at each flushing rate (J722 all flushes).

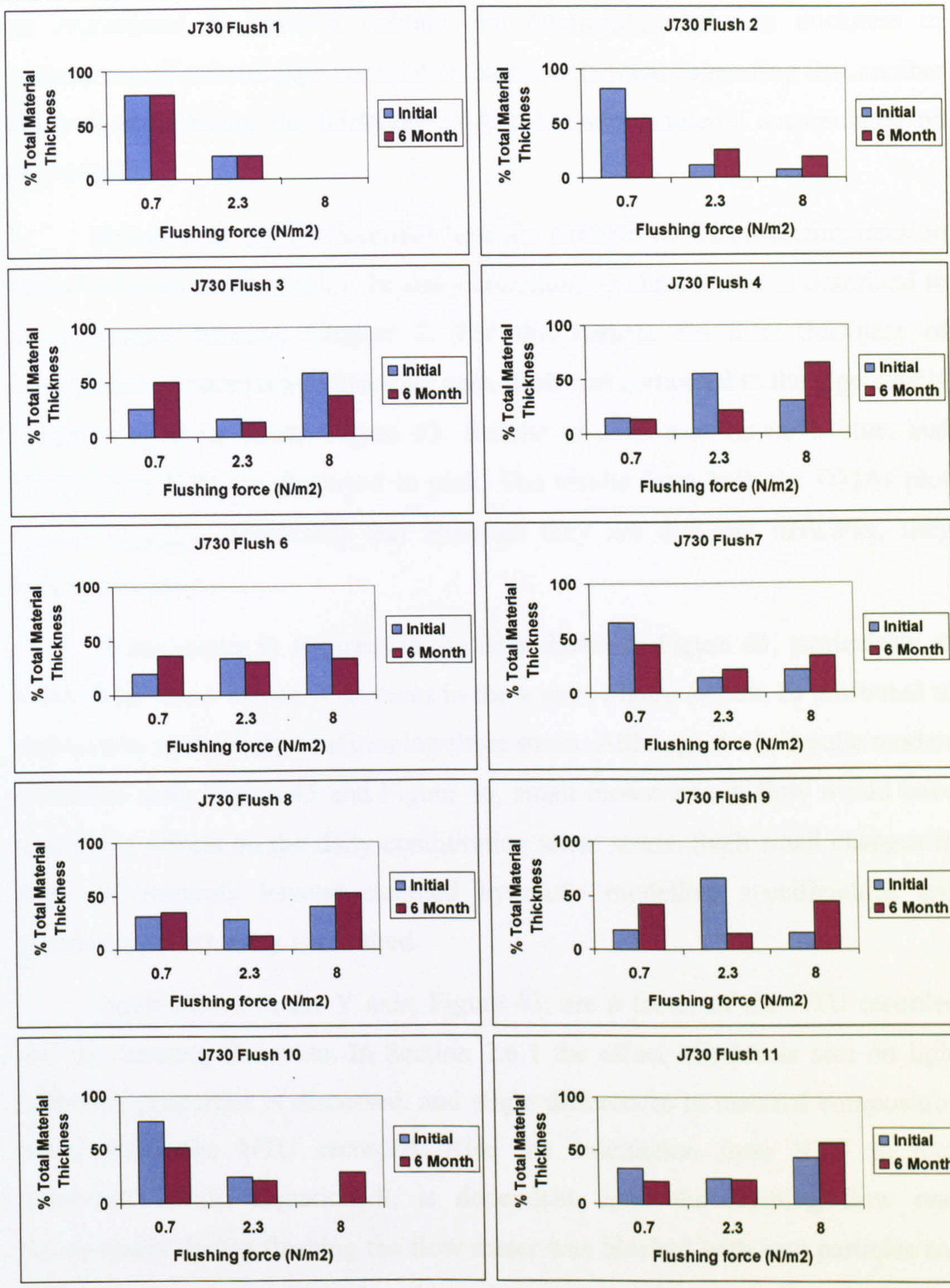

Figure 61 Percentage of material mobilised at each flushing rate (J730 all flushes).

5.5.3 Thickness of discolouration material accumulation

During flushing even though the same shear stress was applied to all the pipes, very different amounts of discolouration material were mobilised. The possible influences of pipe material and diameter on the thickness of discolouration material mobilised in the initial flush for both DMAs are depicted in Figure 62. Pipe diameter is shown on the x axis and different pipe materials

are represented in different colours. No relationship between thickness of material mobilised and pipe material or diameter is seen, suggesting that another factor must influence the thickness of discolouration material accumulated on pipe walls.

Boxall et al. (2003) describes how the strength of discolouration causing cohesive layers is affected by the daily conditioning shear stress as described in the Literature Review, Chapter 2. For this reason, the total thickness of discolouration material mobilised for each flush was compared to the pipe's daily conditioning shear stress, Figure 63. Results of J722 are shown in blue, and results from J730 are displayed in pink. The results from both the DMAs plot closely together, concurring that although they are different networks, they behave similarly.

Some scatter is apparent in the data shown in Figure 63, particularly at lower shear stress values. Variations in the x axis, Figure 63, can be attributed to ambiguities in the daily conditioning shear stress. Although the hydraulic models calibrated well, Figure 45 and Figure 46, small increments in flow would have significant affects on the daily conditioning shear stress. Such small changes in flow are currently beyond standard hydraulic modelling specifications and greater model accuracy is required.

Ambiguities in the Y axis, Figure 63, are a factor of the NTU recorded and the flushing flow rate. In Section 2.6.1 the effect of particle size on light scattering properties is discussed, and slight differences in material composition could affect the NTU recorded. Also the calculation from NTU to total suspended solids, Equation 9, is dependant upon the flushing flow rate. Occasionally during flushing the flow meter was blocked with iron particles and flows had to be estimated. Although pressures recorded during flushing calibrated well with the modelled pressures model accuracy is reduced at higher flow rates.

The thickness of discolouration material mobilised during flushing is also dependant on the pipe being undisturbed for a long period of time prior to flushing. Any increased flow events in the network such as bursts, increases in demand and fire fighting activity could have removed some of the accumulated

discolouration material prior to the initial flush. This is likely to be most apparent in the pipes subjected to low daily conditioning shear stress, hence the scatter in Figure 63 at low conditioning shear stress values.

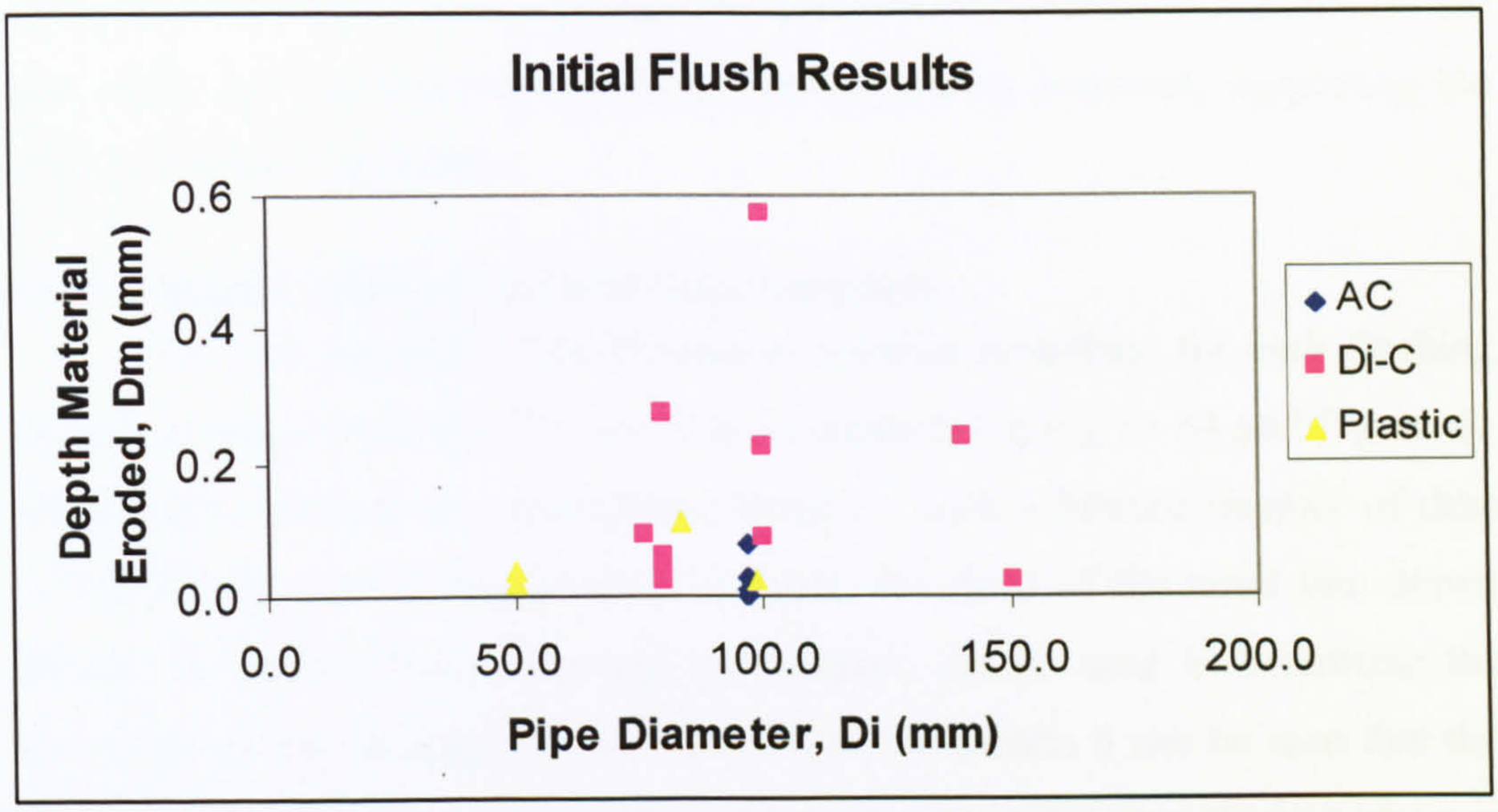

Figure 62 Comparison of pipe material and diameter with depth of discolouration material mobilised.

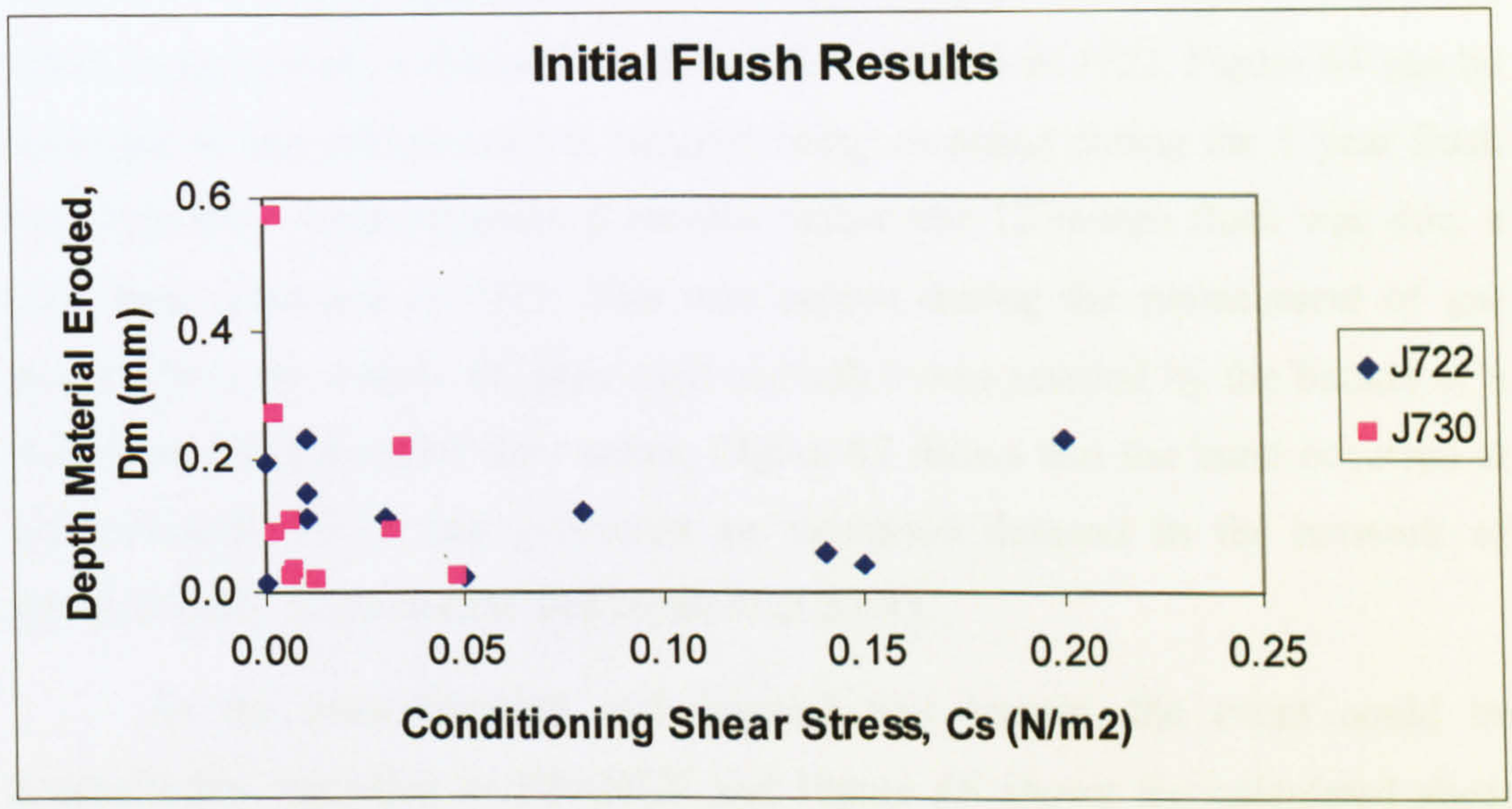

Figure 63 Comparison between daily conditioning shear stress and depth of discolouration material mobilised.

Taking into account the above possible inaccuracies and the scatter at low daily conditioning shear stress values, it can be seen that at higher daily conditioning shear stress, the thickness of discolouration material mobilised during flushing decreases, Figure 63. Assuming that these two networks have

been left undisturbed for a long period of time, the thickness of material mobilised during the initial flush can signify the maximum thickness of material it is possible to accumulate in the pipe. Therefore pipes which experience low daily hydraulic forces have a greater thickness of discolouration material on the pipe walls and therefore have a higher discolouration potential, supporting the work of Boxall et al (2003).

5.5.4 Discolouration material regeneration

The total amount of discolouration material mobilised for each flushing interval of every flush in J722 and J730 is displayed in Figure 64 and Figure 65 respectively. Making the assumption, based on such a limited number of data points, that the rate of regeneration is linear, the slope of the trend line drawn through the points (forced through the origin), can be used to determine the accumulation rate of material over time. From the graphs it can be seen that the accumulation rates are generally similar between the individual flushed pipes in both J722 and J730 DMAs. The mean value of the slope, or accumulation rate, is 0.0057 mm/month with a confidence level (95%) of 0.0015. The frequency distribution of the accumulation rate is shown in Figure 66. Variance in the data, which is particularly evident in flushes 1, 6, 7, and 10 in J722, Figure 64 can be attributed to less discolouration material being recorded during the 1 year flush than expected. Approximately 6 months before the 12 month flush was due, a large burst occurred in J722. This was caused during the replacement of gas mains where the 4 inch AC pipe used in flush 9 was severed by the bucket of a JCB. Data from the inlet flow meter, Figure 67 shows that the burst occurred at approximately 10:15 and generated an increased demand in the network of approximately 11 l/s until it was repaired at 23:45.

As the burst location and demand was known, the event could be hydraulically modelled in EPANET and Figure 68 shows the calculated shear stress in J722 generated by the burst. Analysis shows that the pipes depicted in light blue were subjected to a shear stress 0.7 N/m^2, which is equivalent to the lowest flushing rate. Pipes in green were subjected to the same force as the middle flushing rate (0.23N/m^2), and the pipe in yellow was subjected to the highest flushing force of 8 N/m^2. The pipe at the burst location is shown in red

and was subjected to a shear stress of over 10 N/m^2, much greater than the shear stress generated by the flushing operations used in this study.

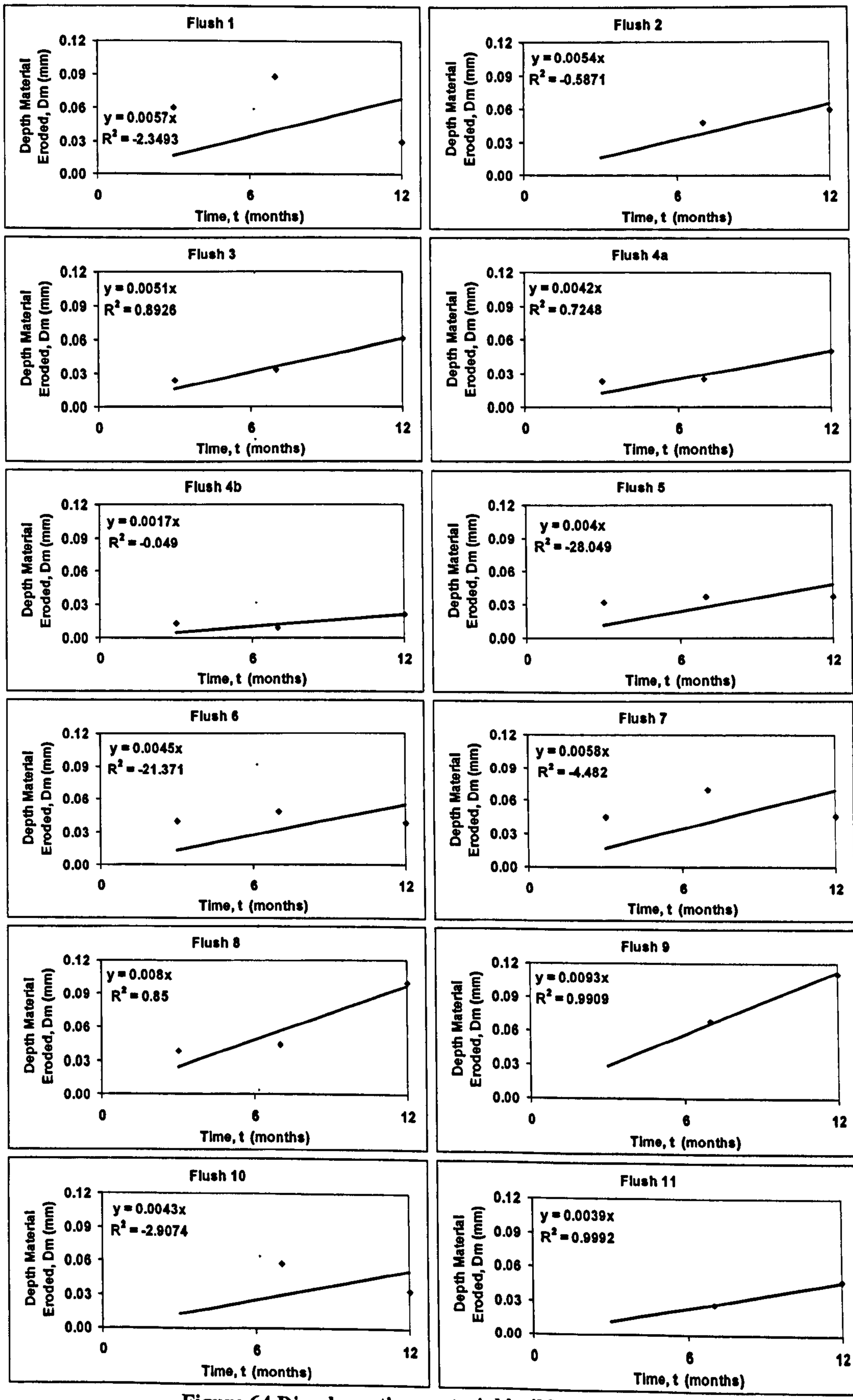

Figure 64 Discolouration material build up rate, J722.

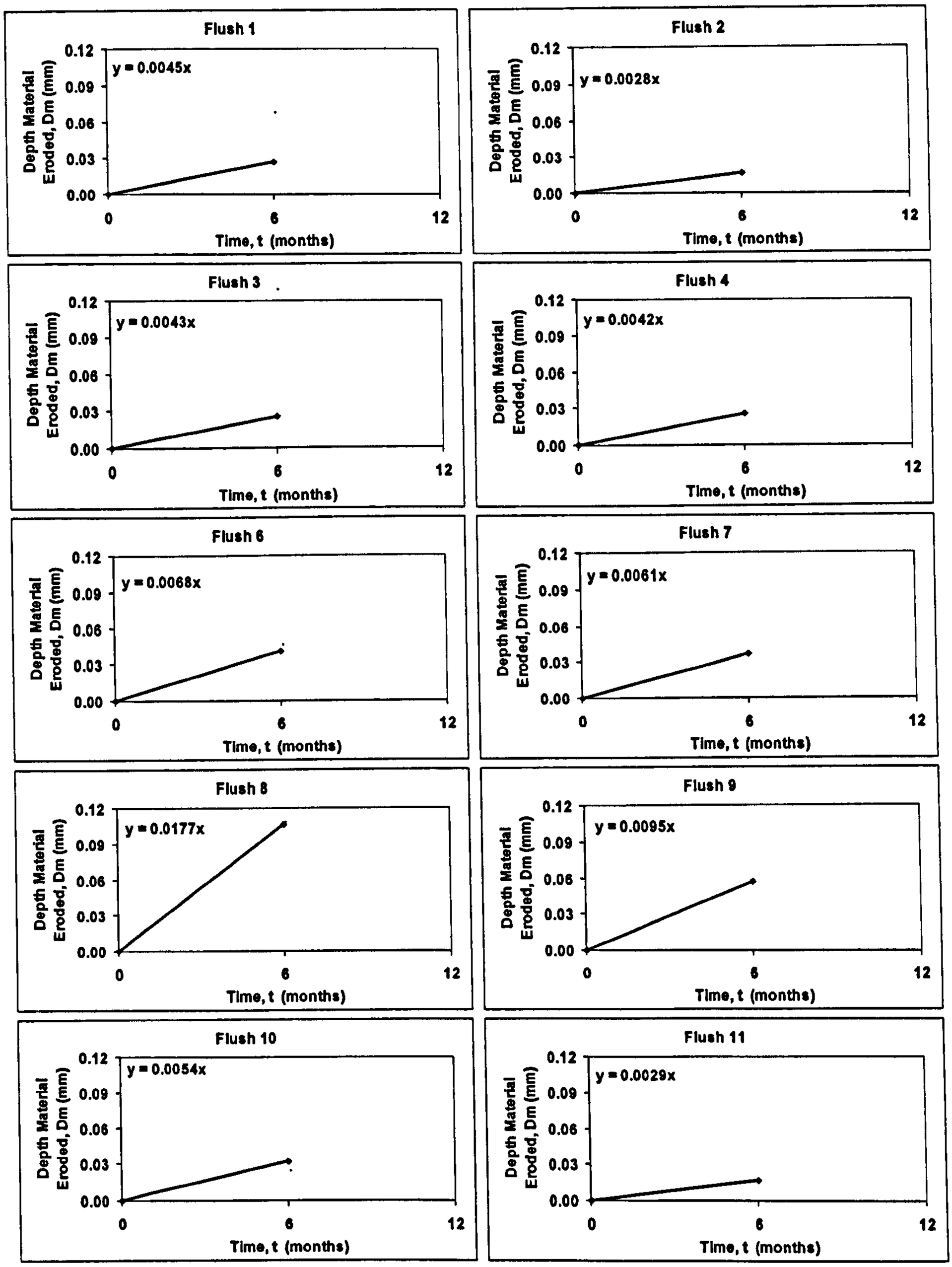

Figure 65 Discolouration material build up rate, J730.

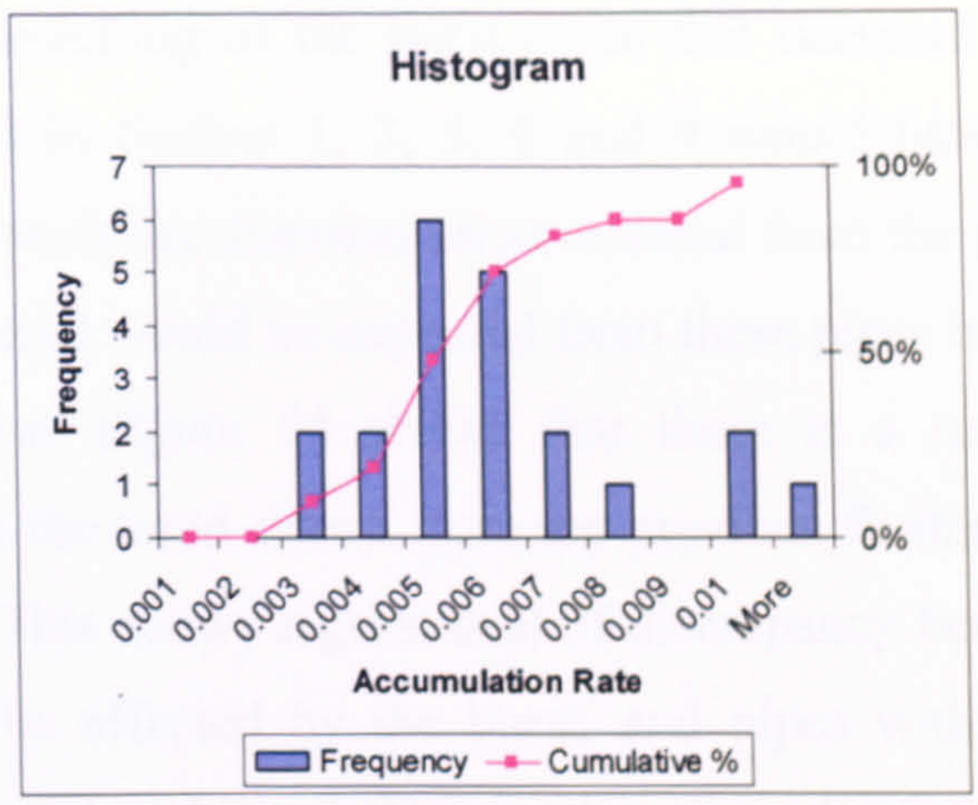

Figure 66 Frequency distribution of accumulation rates

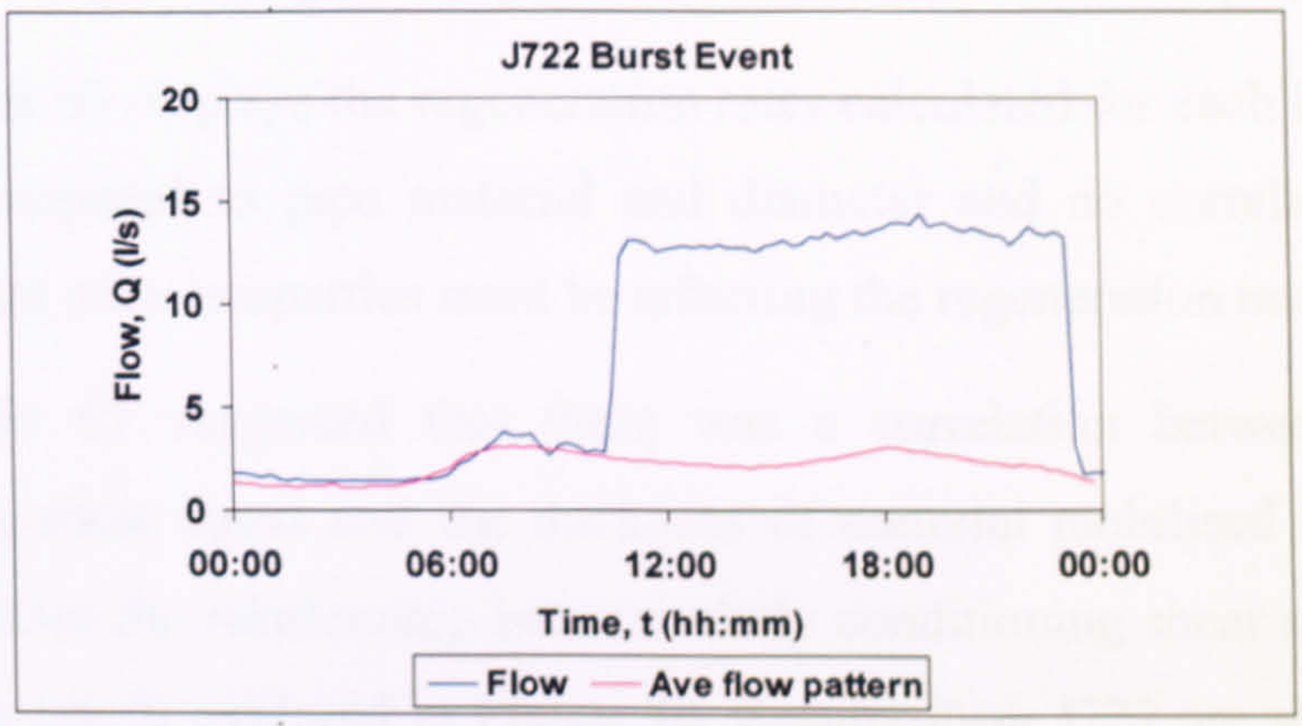

Figure 67 J722 inlet flow during burst event

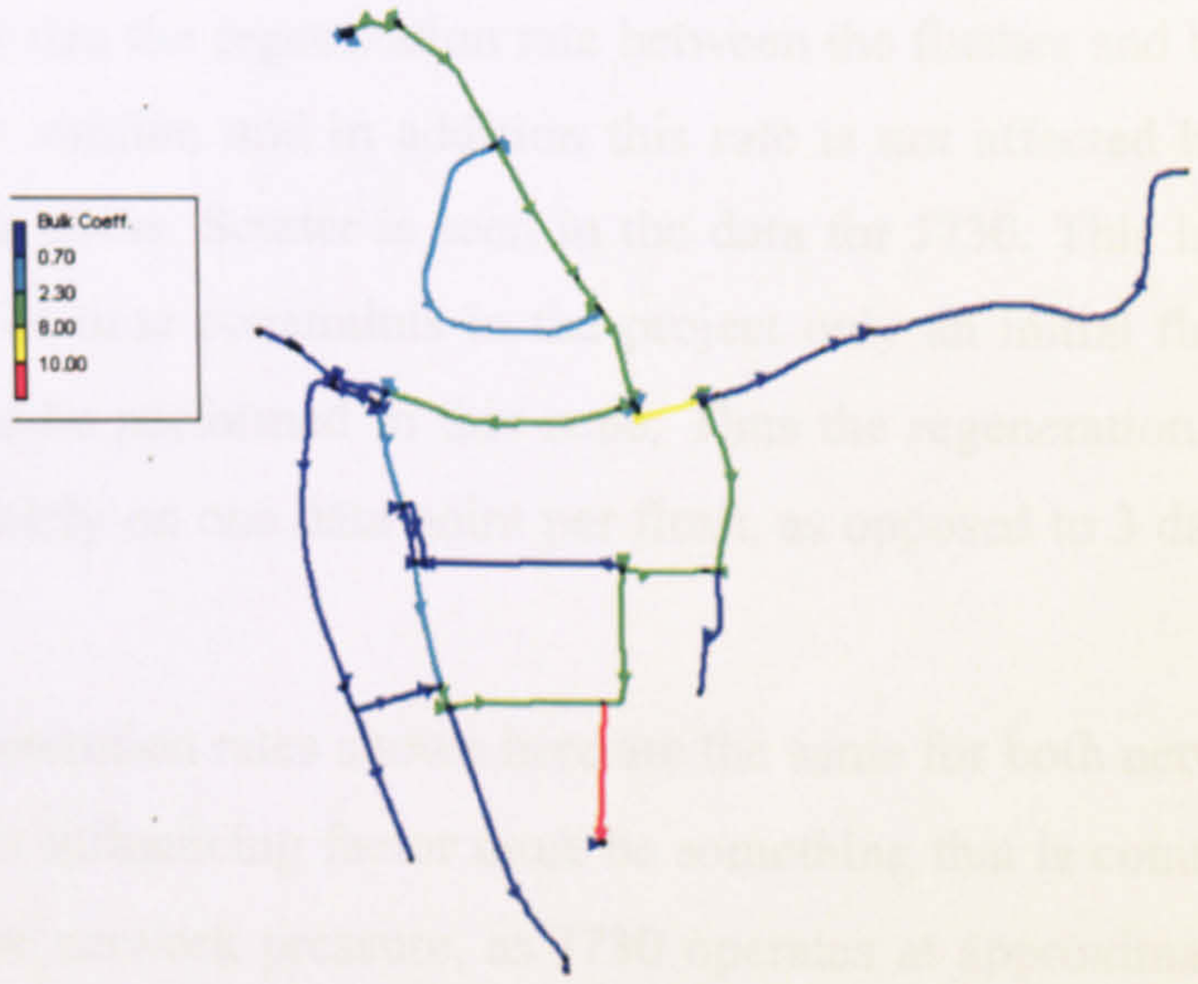

Figure 68 Maximum shear stress produced during burst event in J722.

From the modelling of the burst event that occurred in J722 it appears that the pipes used in flushes 1, 3, 5, 8 and 9 would have been affected by sufficient forces to mobilise discolouration material from the pipe walls, thus less discolouration material would be expected from these pipes in the results of the 1 year flush. However Figure 64 shows that there is a reduced thickness of discolouration than the trend drawn from the previous flushing events in flushes 1, 5, 6, 7, and 10. This shows a great deal of discrepancy between the pipes that were expected to be affected by the burst, and pipes with less than expected discolouration material mobilised. This implies that other influencing factors and events must have taken place in this network during the 12 month period, which could come to light during the long term monitoring phase of the project.

Figure 69 displays the regeneration rates calculated for each flush in J722 and J730 compared to pipe material and diameter and no correlation is seen indicating that other properties must be affecting the regeneration rate.

Figure 63 suggested that there was a correlation between the daily conditioning shear stress and the thickness of material mobilised in the initial flush. Therefore the relationship between daily conditioning shear stress and the regeneration rate is explored in Figure 70. Results form J722 are shown in blue and J730 is displayed in pink. Here it can be seen, particularly in J722, which was a better data set with more flushes, that there is a horizontal trend in the data reiterating the fact that the regeneration rate between the flushes and between the two zones is very similar, and in addition this rate is not affected by the daily conditioning shear stress. Scatter is seen in the data for J730. This is due to the fact that because of time constraints in the project only an initial flush and a 6 month flush could be performed in this zone. Thus the regeneration rate in this zone was based solely on one data point per flush, as opposed to 3 data points in J722.

Since regeneration rates shown here are the same for both networks it can be inferred that its influencing factor must be something that is common to both areas. It cannot be network pressure, as J730 operates at approximately 12 bar, three times more pressure than J722. It cannot be network age as J722, having the majority of its pipes being laid between 1920 and 1960, is much older than J730 which saw significant network expansion in the 1990s. Pipe properties and

daily conditioning shear stresses have already been discounted; therefore the only influence on discoloured water accumulation rates must be bulk water quality, as both DMAs are supplied from the same water treatment works and trunk main.

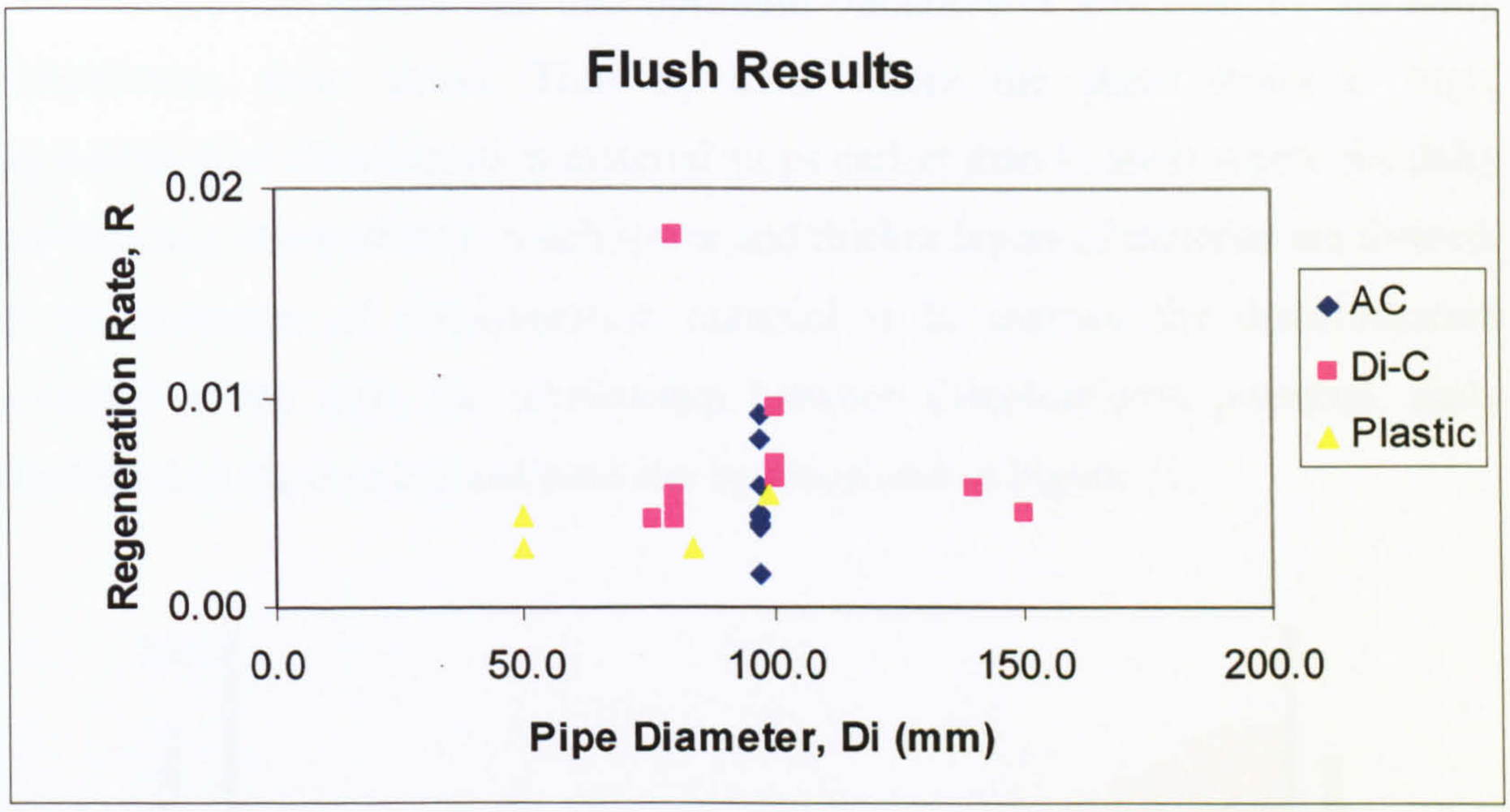

Figure 69 Regeneration rate of discolouration material compared to pipe material and diameter.

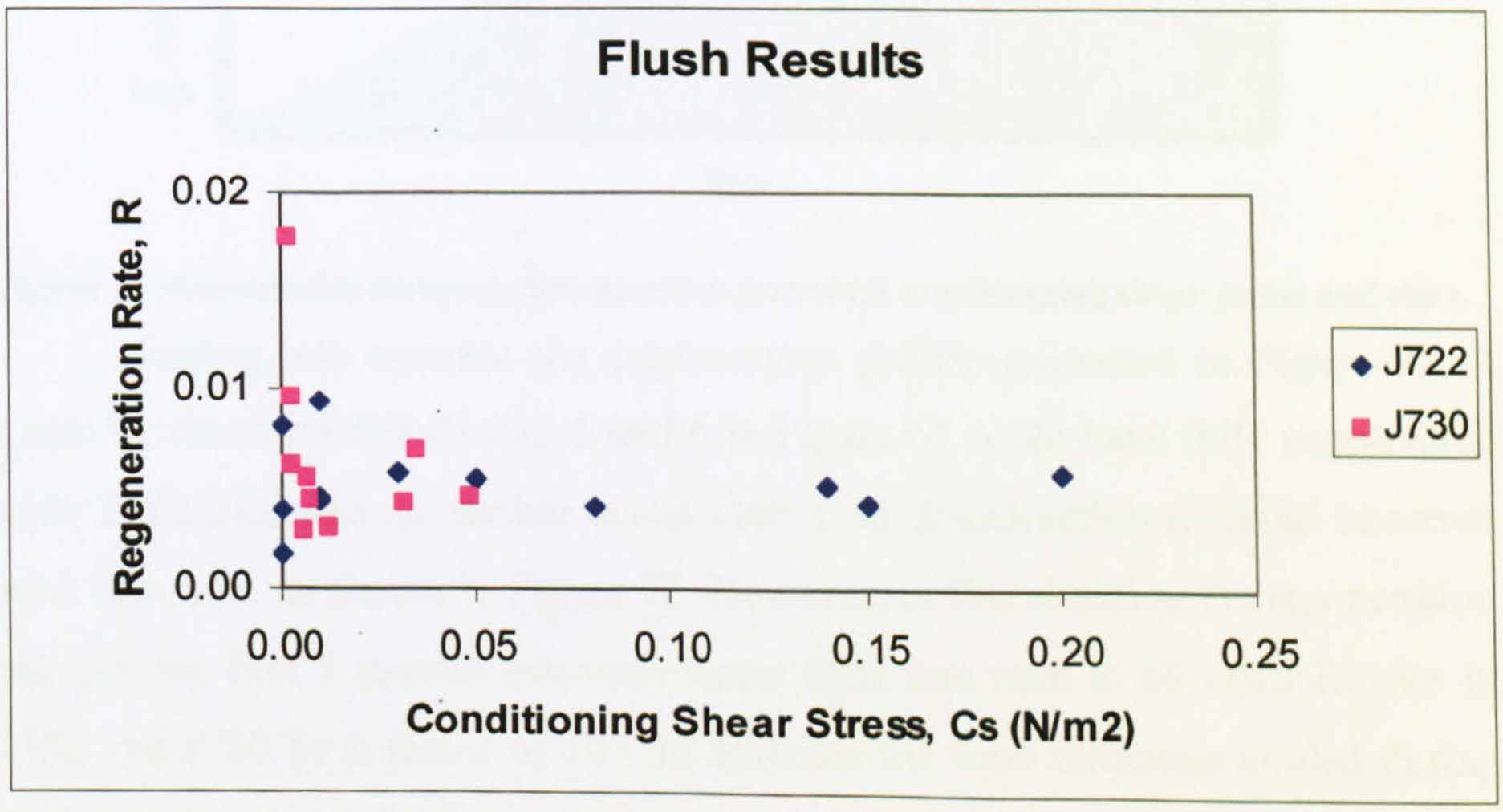

Figure 70 Regeneration rate of discolouration material compared to daily conditioning shear stress.

Thus it can be theorised that in both DMAs in this study, discolouration material regenerates at a similar linear rate in all parts of the network, governed by the source water quality. This regeneration continues until a maximum of material thickness is reached.

Figure 63 shows that this optimum thickness is governed by the daily conditioning shear stress. Thus in areas where the shear stress is high, regeneration of discolouration material stops earlier than in areas where the daily conditioning shear stress is much lower and thicker layers of material are formed. If the thickness of discolouration material is in essence the discolouration potential of the pipe, the relationship between discolouration potential, daily conditioning shear stress and time can be visualised in Figure 71.

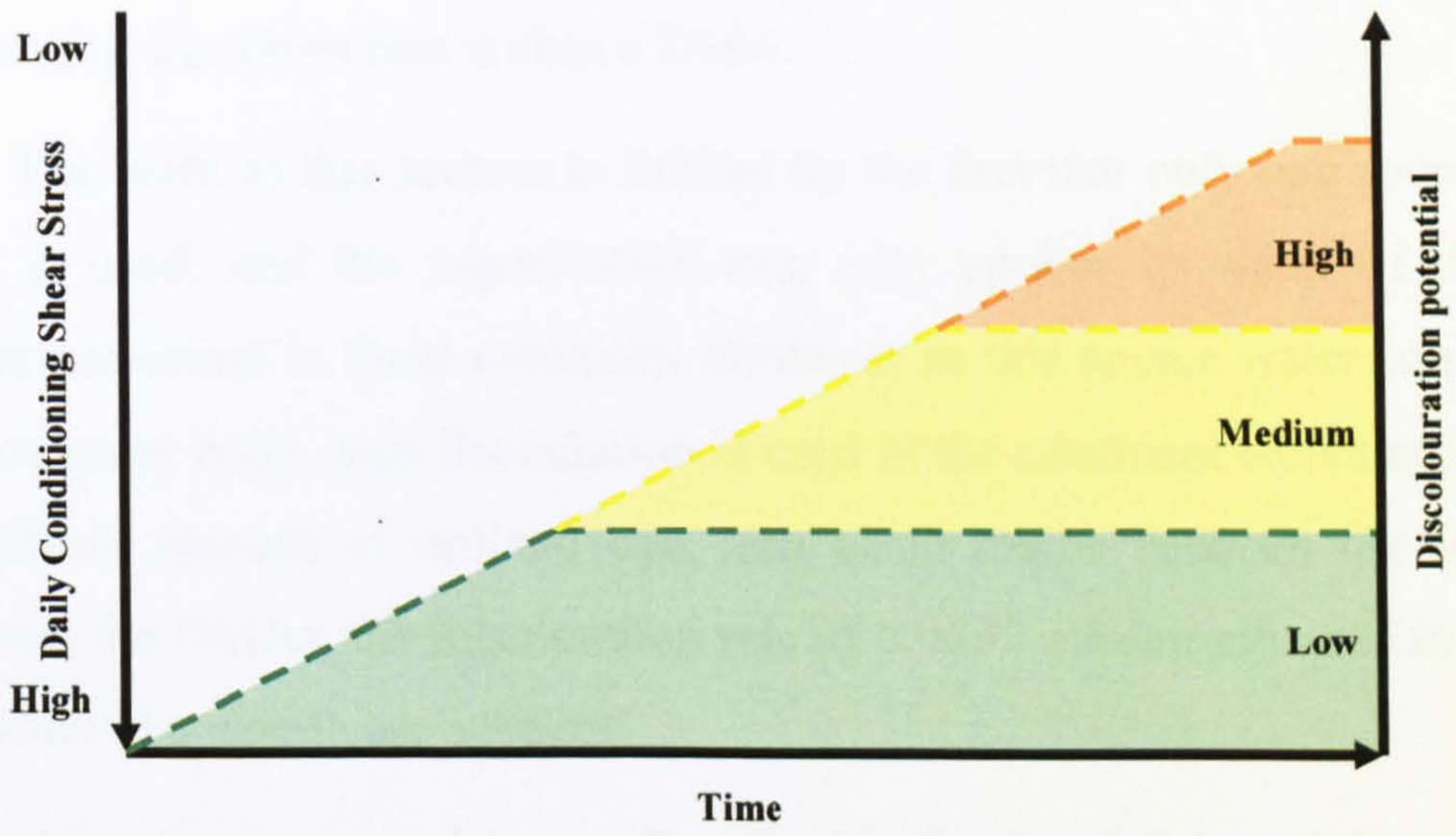

Figure 71 Relationship between discoloration potential, conditioning shear stress and time.

Taking into account the regeneration profile presented in Figure 71, it could be theorised that flushes 5 and 6 in Figure 61 could have fully regenerated after 3 months, and no further accumulation of discoloration material occurred after this time, as shown in Figure 72. However, in this situation the regeneration rate for the first 3 months becomes faster than was seen in all other flushes in J722 and J730 by a factor of 10. In addition the total thickness eroded during initial flushes 5 and 6, Figure 52, is never reached during the subsequent flushes, Figure 53, Figure 54 and Figure 55. Therefore 100% regeneration cannot have occurred in these pipes and the original regeneration profile shown in Figure 64 remains valid.

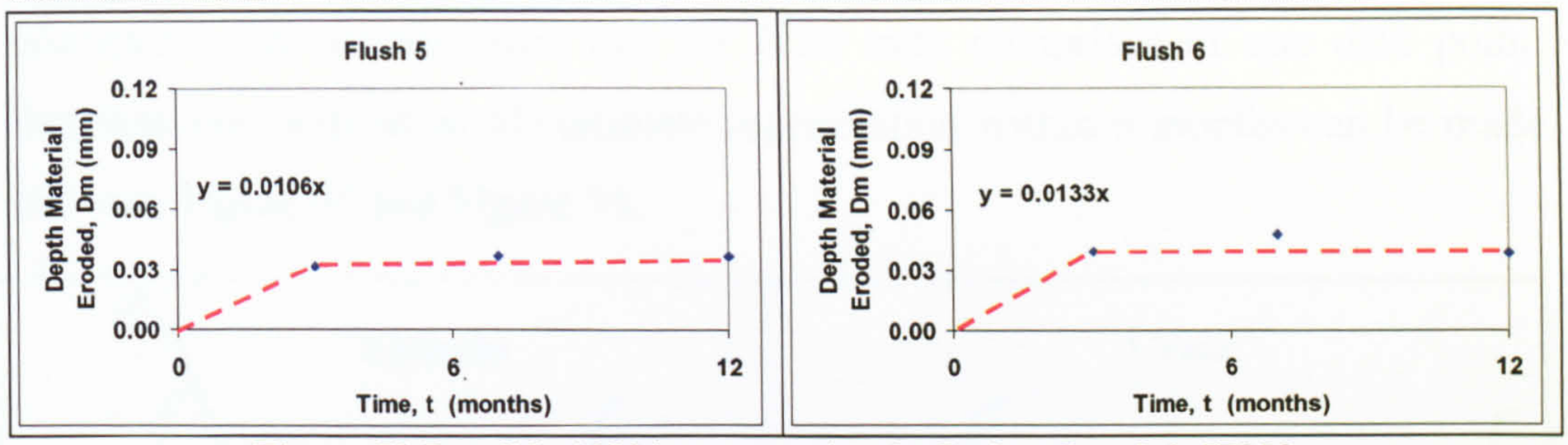

Figure 72 Possible 100%regeneration in flushes 5 and 6, J722?

5.5.5 Application of the regeneration theory

If the theory that all pipes regenerate discolouration material within a network at the same rate, until a maximum value is reached, governed by a conditioning shear stress, then the increasing discolouration potential or deterioration of a network after cleaning can be predicted. This information would be highly useful to water companies in targeting specific flushing areas and planning the return rate within a DMA.

The work in this section is limited by the fact that only one source water quality is used, and the regeneration rate only applies to water of the same chemistry as found in these networks. However as this source water comes from a surface water body, iron flocculation is used in the treatment works and there is a significant amount of unlined cast iron trunk mains between the treatment works and the DMAs, the regeneration rate of 0.0057 mm/month used here could be considered a worst case scenario.

Using the regeneration rate described in Section 5.5.4 and the maximum possible layer thickness, as a function of daily conditioning shear stress, in section 5.5.3 the change in discolouration potential of J277 and J730 are plotted in Figure 73 and Figure 74. These figures assume that no hydraulic events such as bursts occur during this time. Here it can be seen that pipes in flushes 2 and 4b in J722, Figure 73, and flushes 1, 10 and 11 in J730, Figure 74, regenerate completely within 6 months but remain stable after this time. Data for J722 flushes 2 and 4b shown in Figure 64 support this theory; however it could appear that flushes 5 and 6 in J722, Figure 64, have also regenerated in the 6 month period. These flushes could have been affected by the previously described events that affected the accumulation rate for the 12 month flush which is particularly apparent in flushes 1, 7 and 10, Figure 64. Due to the project time

constraints the accumulation rate for J730 only comprises of one data point, therefore no verification of complete regeneration within 6 months can be made between Figure 65 and Figure 74.

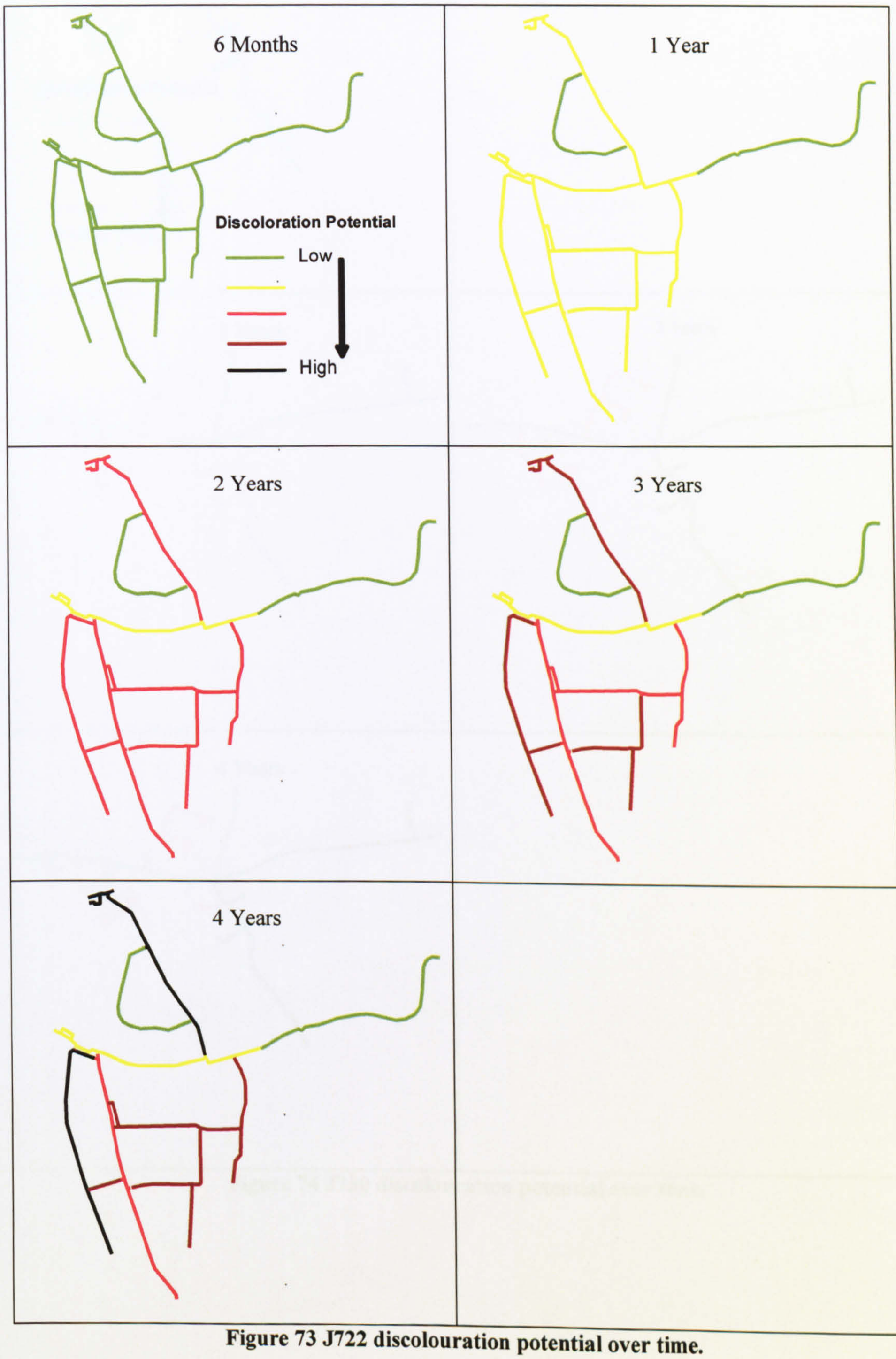

Figure 73 J722 discolouration potential over time.

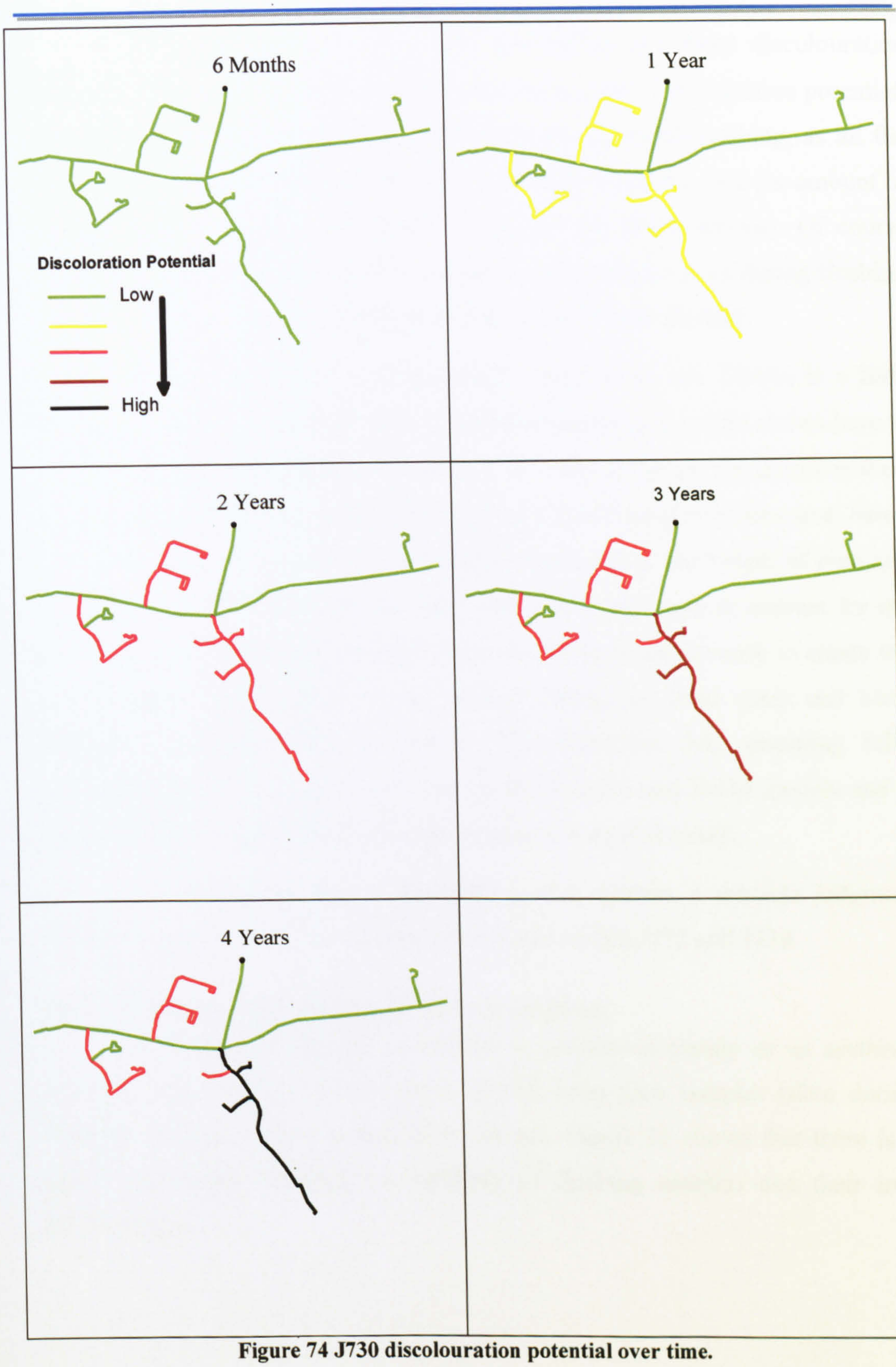

Figure 74 J730 discolouration potential over time.

The pipes that are seen to not accumulate any more discolouration material after 6 months can be considered to have a low discolouration potential. It could therefore be argued that these pipes are not worth flushing, as all the discolouration material would have returned within 6 months, and the amount of discolouration material in these pipes is never very much anyway. Of course practicality dictates that in order to maintain a clean water front during flushing operations, flush 1 in J730 DMA would always have to be flushed.

Deciding the return rate frequency within these two DMAs is a little harder as one has to relate the discolouration potential of the pipes shown here to a discolouration risk which is not shown. In order to assess the discolouration risk, the magnitude of the discolouration event would have to be assessed, based on the thickness of accumulated discolouration material, the length of pipe and the number of customers affected. The risk would also have to account for the likelihood of a sufficient hydraulic forces occurring in the network to create the discolouration event, based on the relative change in shear stress and burst frequency or other hydraulic 'event'. Discolouration risk, assuming fully developed layers is already dealt with in the PODDS and DRM models and it would be ideal to incorporate this regeneration conceptual model.

Considering the factors discussed in this section, a sensible judgment could be made of a two year flushing return rate within J722 and J730.

5.5.6 Further implications of discolouration.

Although currently discolouration is considered mainly as an aesthetic problem or a nuisance to customers, results from grab samples taken during flushing operations show a high iron content. Figure 75 shows that there is a linear relationship between the turbidity of flushing samples and their iron concentration.

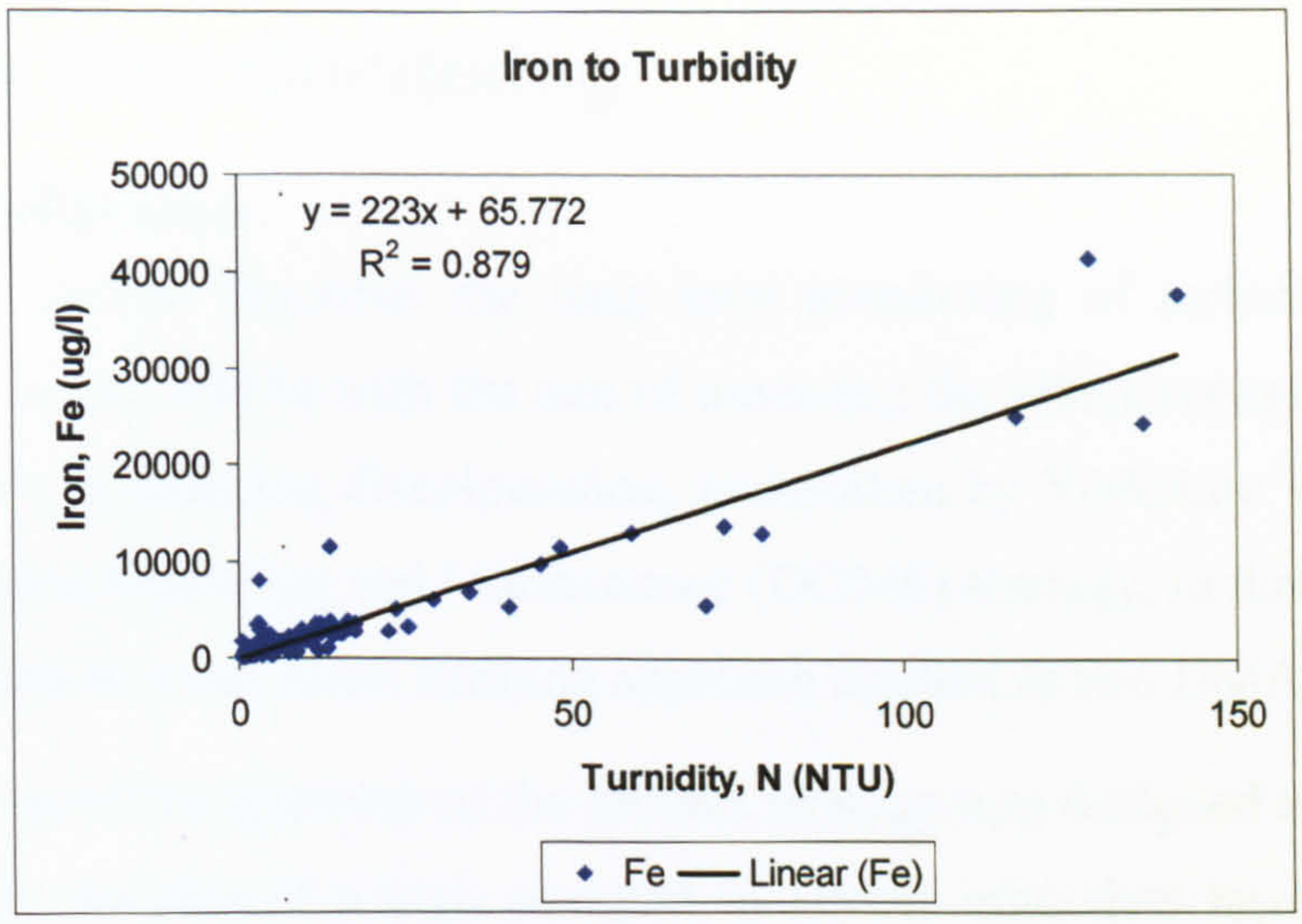

Figure 75 Relationship between turbidity and iron concentrations.

The UK drinking water standard set for Iron is 200 µg/l. Using the results shown in Figure 75 it can be calculated that in these two DMAs the drinking water standard for Iron is exceeded when the turbidity of the water reaches only 0.6 NTU. Therefore to maintain drinking water standards and minimise the cost imposed by regulatory penalties, managing discolouration risk should be a high priority for water companies.

6 Long Term Monitoring

6.1 Introduction

This section describes the long term monitoring of turbidity that was undertaken in five DMAs with the aim of assessing the effectiveness of selective rehabilitation, in reducing discolouration, undertaken by Yorkshire Water, under the Distribution Operation and Maintenance (DOMS) strategy, in three zones and comparing this to a full zonal flushing approach applied in two DMAs.

The selective approach of the DOMS strategy was designed to ensure that water quality remains of a high standard in DMAs after they have progressed through the Section 19 program. Section 19 was essentially a metre driven blanket wide approach to mains rehabilitation.

It is hypothesised that by deploying turbidity loggers in a DMA pre and post rehabilitation, a reduction in background turbidity levels and frequency of turbidity spikes post rehabilitation would measure the success of the intervention in reducing discolouration potential. Secondly by analysing the turbidity response by loggers deployed at the inlet and around the DMA to a discolouration incident, in conjunction with flow information from the DMA inlet, the origin of the event can be identified, be it internal to the DMA, or as a result of external influences.

6.2 Method

CT-Cense colour and turbidity loggers as described in Chapter 5 were used to monitor turbidity in the three DOMS DMAs and the two flushing trial zones. Before field deployment, loggers were calibrated in the lab by the process previously described in Section 5.3.3.2.

6.2.1 Monitoring location planning and installation

Three or four loggers were deployed in each DMA depending upon its size. Ideally logger locations were chosen based on areas where there was a history of discolouration customer contacts and where DOMS rehabilitation work was planned by the contractor, however actual field deployment of the loggers was often very different to that planned due to difficulties in finding suitable locations. Turbidity loggers are installed on the service pipe in Manifold

Small Meter (MSM) chambers. Not every property in the trial zones had a water meter fitted, and it is quite common for meters to be fitted under the kitchen sink so the number of available locations for logger deployment was limited. This number was further reduced by turbidity loggers not being able to fit in the MSM chambers because the service pipe was not deep enough in the ground, or the stop tap and manifold orifice was not central or square within the meter chamber to accommodate the bulky logger and manifold assembly (Figure 76).

Turbidity loggers were installed in suitable locations (Figure 77), in accordance with Yorkshire water's standard procedures (M. Powell 2004). Great care was taken to ensure that stop taps were fully closed before removing water meters as a mistake usually involved getting very wet!

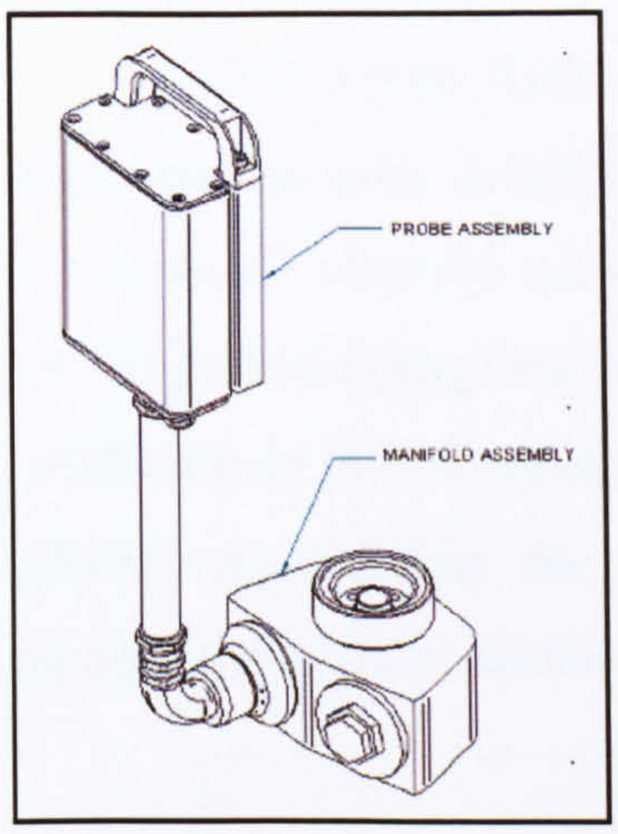

Figure 76 logger and manifold assembly.

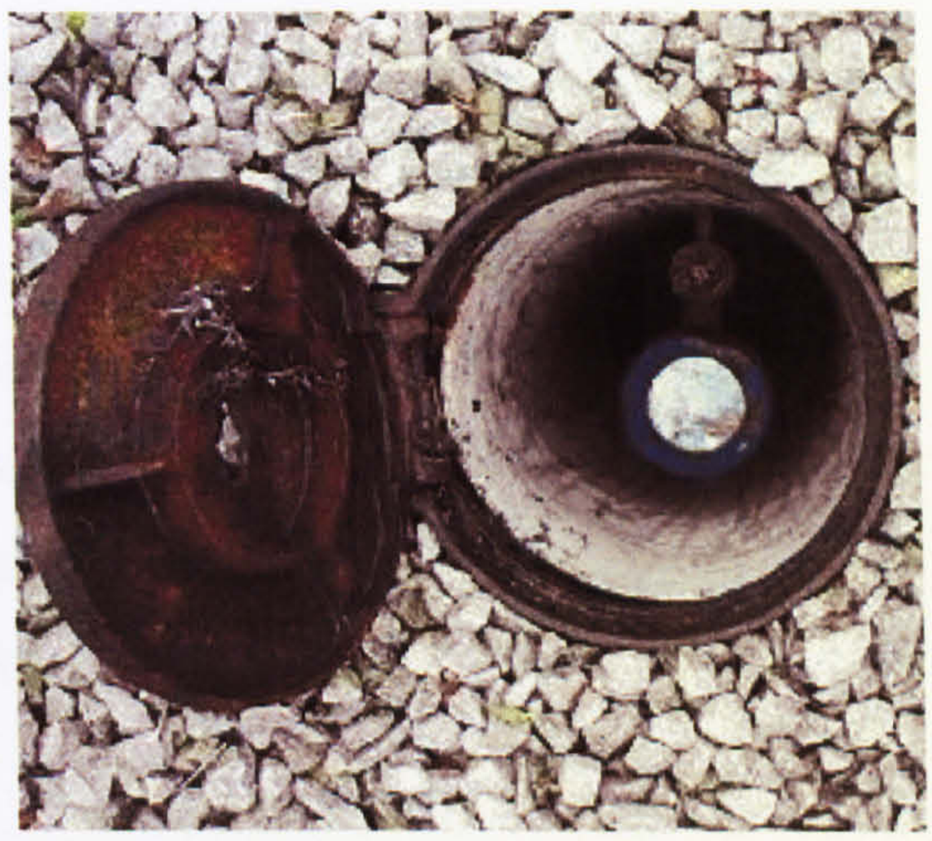

Figure 77 Suitable MSM Chamber.

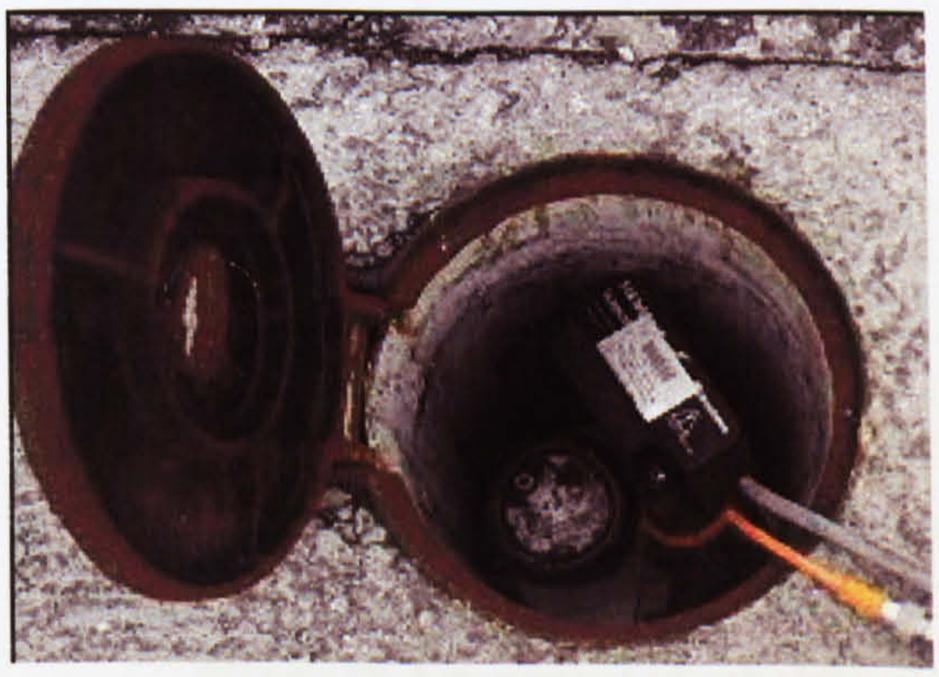

Figure 78 Probe and meter installed.

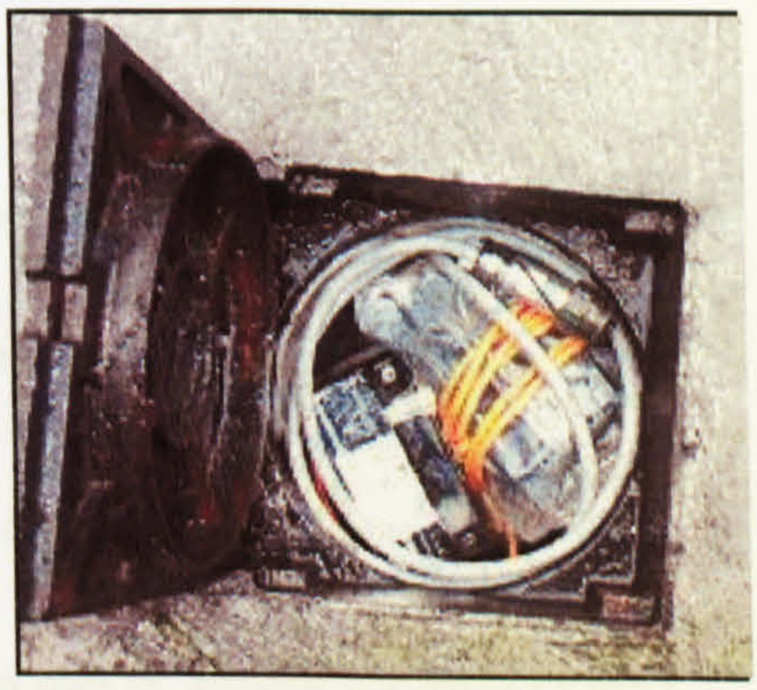

Figure 79 Battery and cables inside chamber.

Figure 78 depicts a turbidity logger installed with the water meter fitted on top of the manifold assembly, and highlights the closeness of fit of the equipment in the chamber, which is even tighter when the battery and cables are fitted (Figure 79).

Final locations of the turbidity loggers and the areas of rehabilitation being carried out in the DOMS Trial zones are shown in Figure 81 to Figure 83. Red dots depict the history of discolouration customer contacts from the period of 1999 to 2005.

The planned rehabilitation in the DOMS trial Zones was decided by Yorkshire Water personnel using Discolouration Risk Modelling software. The discolouration risk in the network is calculated by simulating bursts, by applying an additional demand to every node in a hydraulic model and noting the pipes with resulting increase in velocity. The likelihood of each burst occurring is then applied, as described in Section 2.6.2, and every pipe is then assigned a discolouration performance score.

The Capital Risk Analysis tool in DRM was used by Yorkshire Water personnel to plan rehabilitation scenarios. A maximum improvement scenario was created whereby all non-preferred materials are renovated (by replacement or scrape and lining) and all pipes of preferred materials are cleaned (by flushing, swabbing or Air scouring). This scenario termed the 'Full Monty' can then be plotted representing the greatest change in discolouration performance score against the highest solution cost (Figure 80).

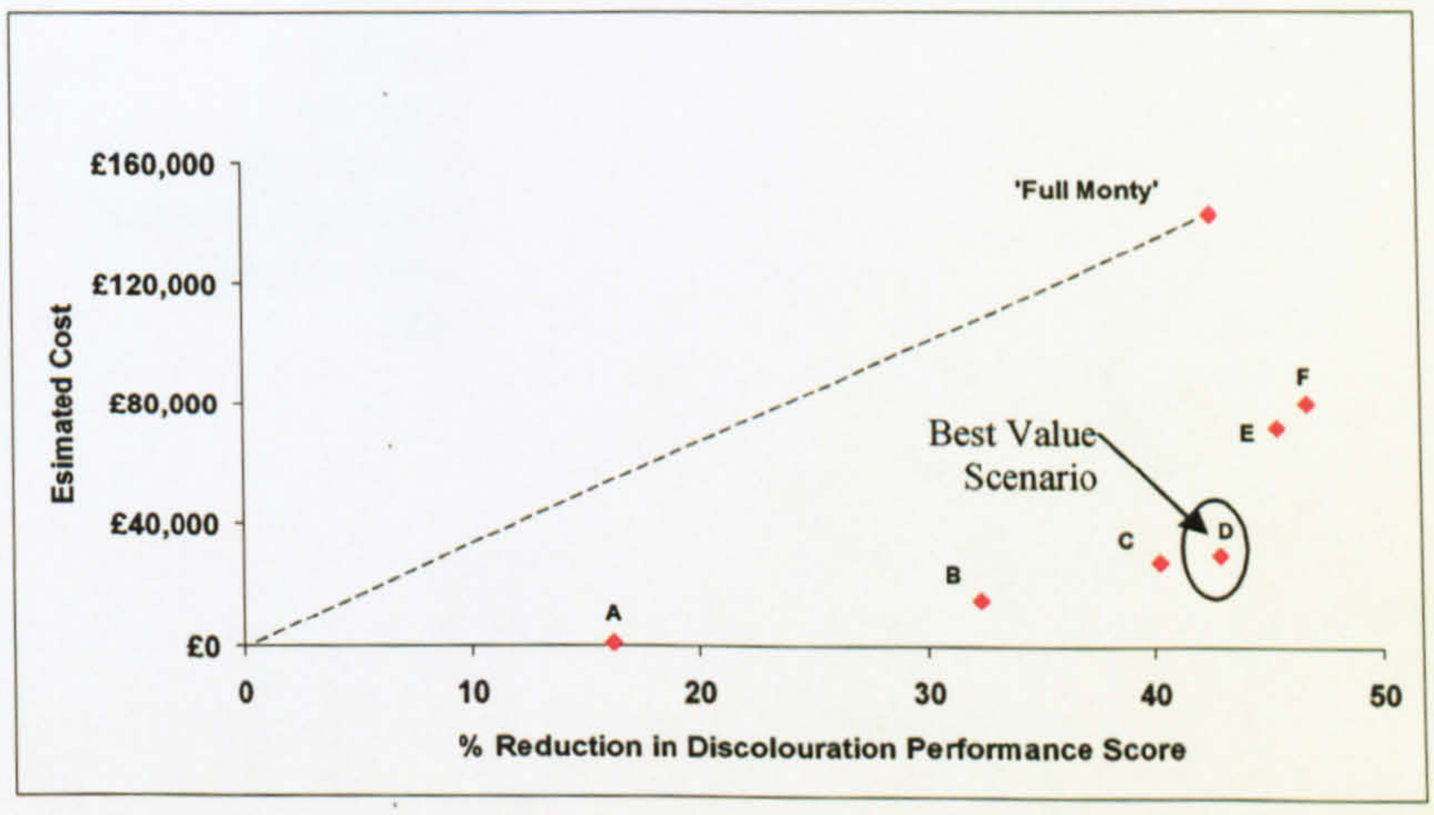

Figure 80 Assessment of rehabilitation scenario cost vs. benefit for B614 (YWS).

Different rehabilitation scenarios were then created and a new discolouration performance score was created. Rehabilitation work was then planned based on the scenario which gives the greatest value in terms of discolouration risk reduction per pound invested.

In Figure 80 it can be seen that scenarios E and F appear to have a higher percentage reduction in discolouration performance score than the 'Full Monty' which is intended to be the best solution. Personal communications with Yorkshire Water personnel indicate that this is a feature of DRM where some scenarios generate hydraulic improvements in the network. This changes the velocities calculated in the model which can in tern change the discolouration performance score.

The rehabilitation planned in C050 was essentially a cleaning program (Figure 81) and cost in the region of £11.5 thousand. The inlet to the DMA was swabbed, 4 lengths of pipe were air scored and 2 very short lengths of pipe were flushed. In B614, a mixture of renewal and cleaning was planned in only 3 pipes, (Figure 82) and cost approximately £46 thousand. A slightly different approach was undertaken in A285 where a cross connection was installed in the system to remove a bottleneck and increase the robustness of the network.

Figure 84 and Figure 85 show the final turbidity monitoring locations in the flushing trial zones. Historical discolouration customer contacts from 1999 until 2005 are shown in red.

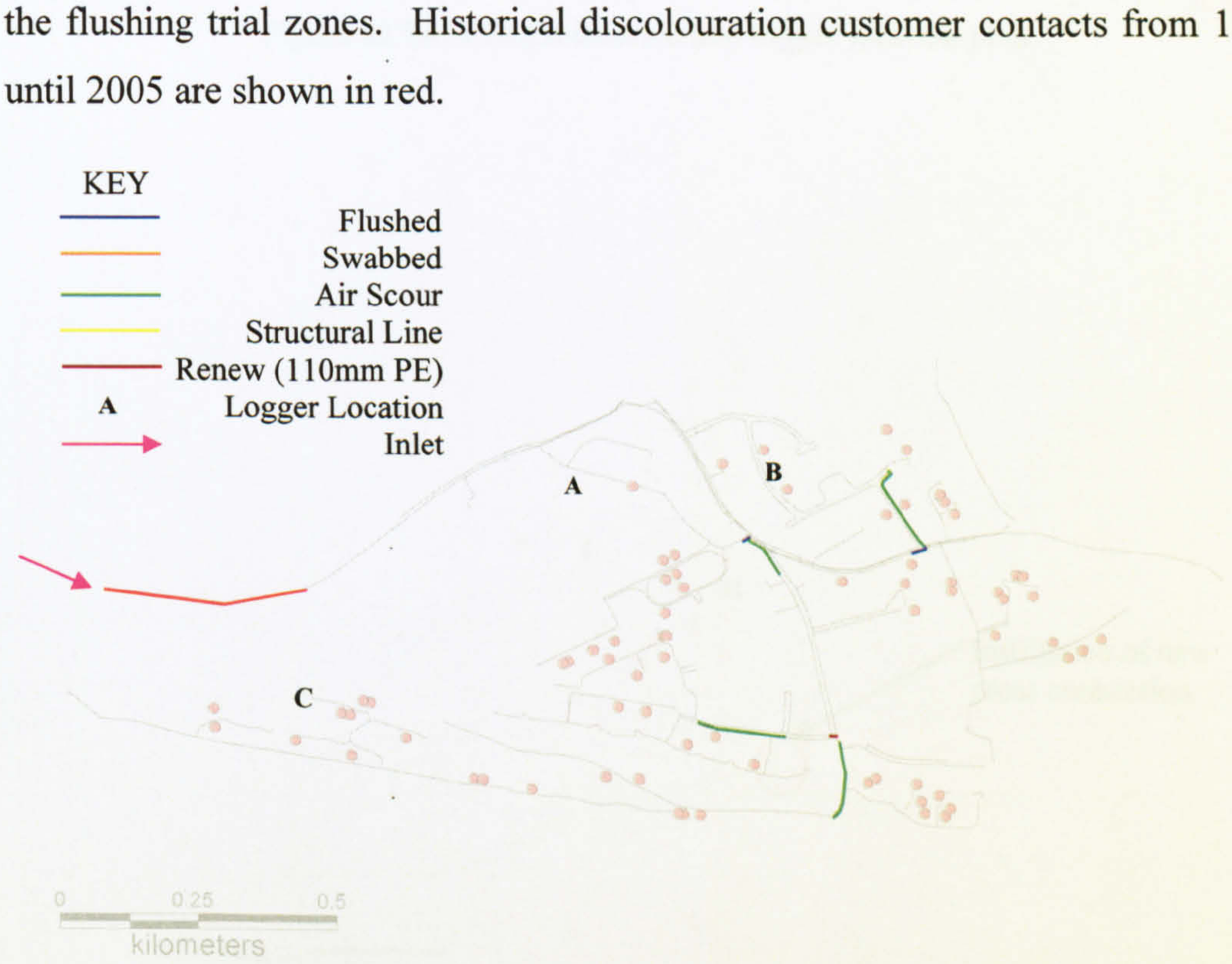

Figure 81 C050 Rehabilitation and logger location plan.

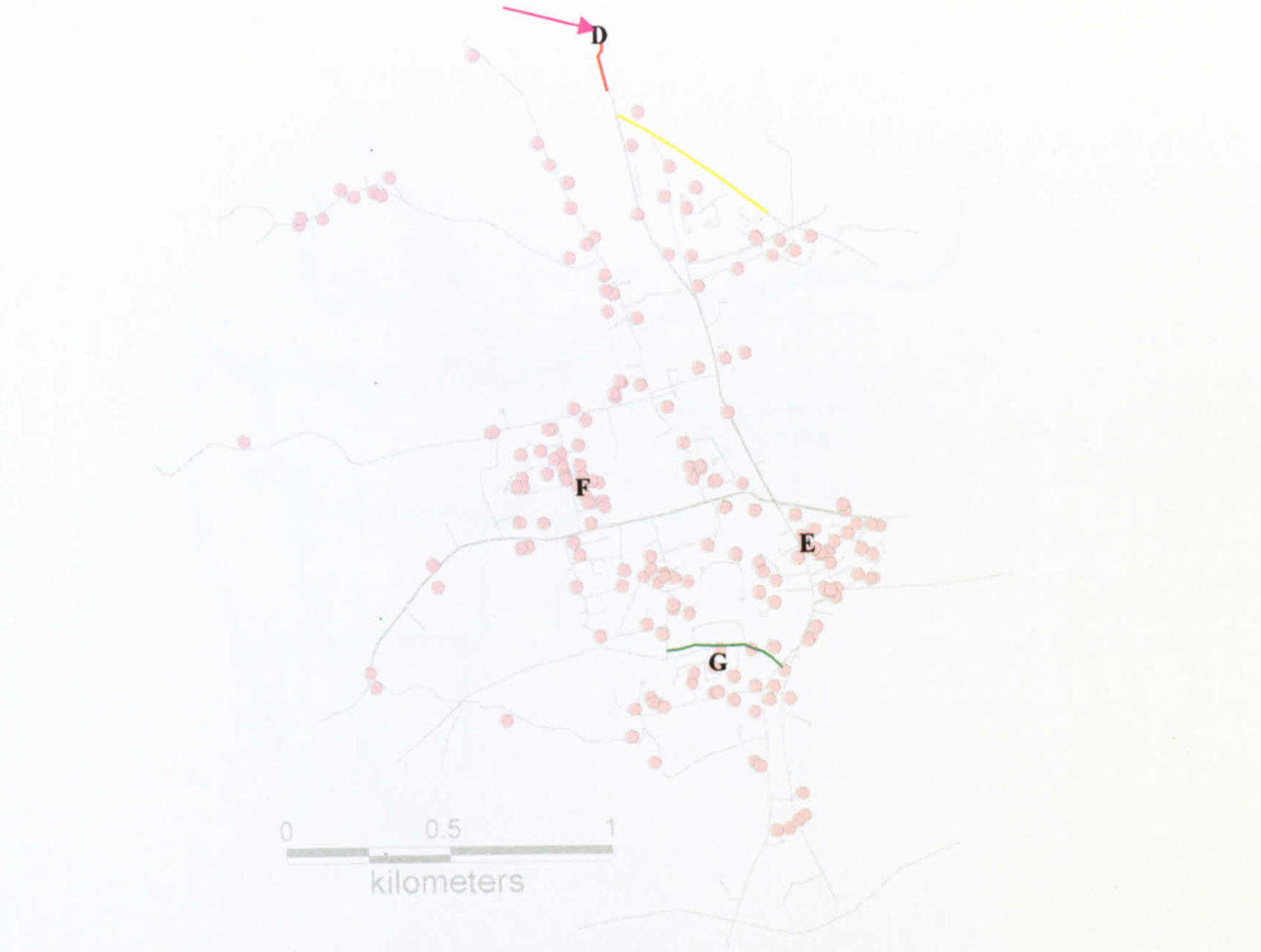

Figure 82 B614 Rehabilitation and logger location plan.

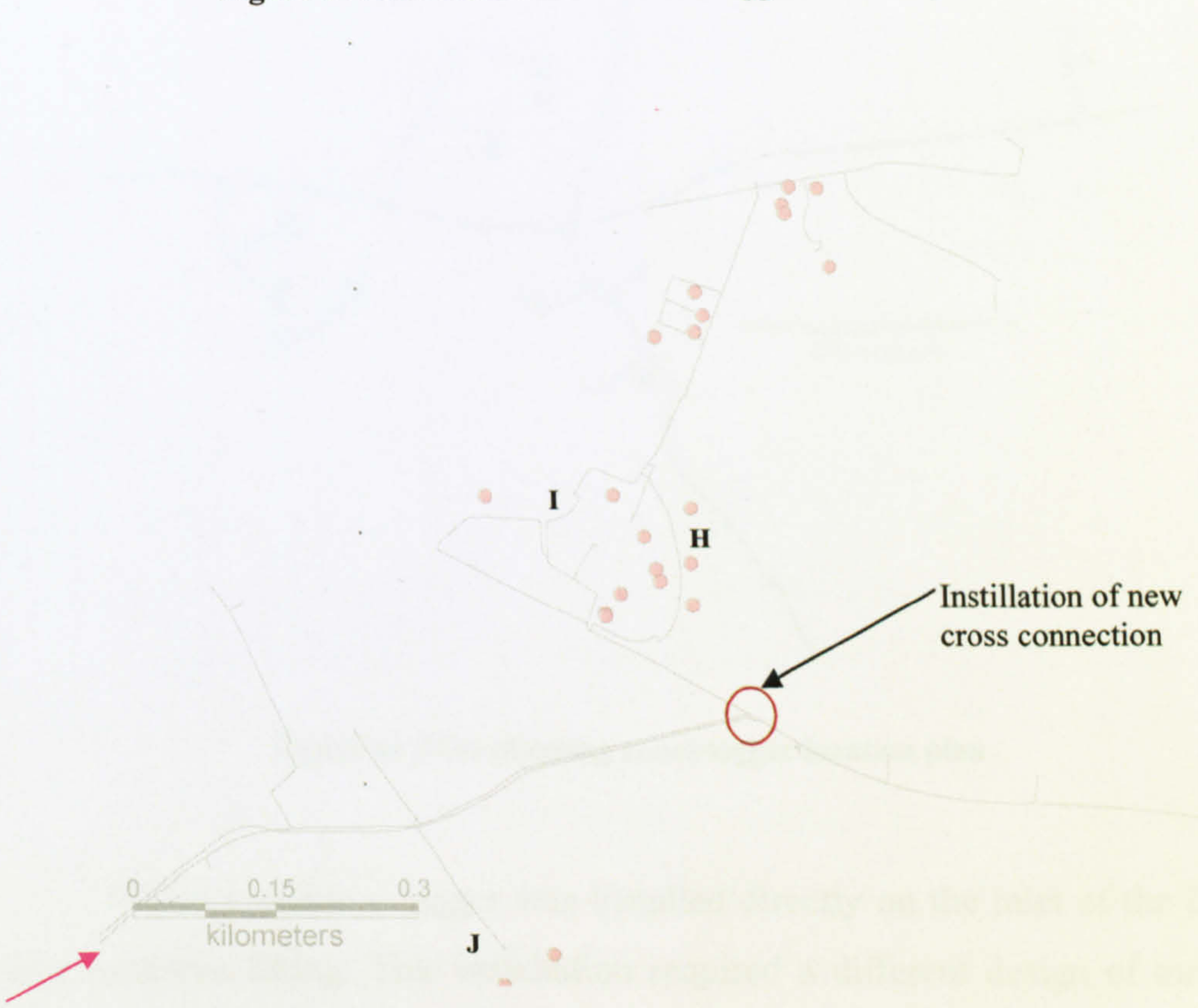

Figure 83 A285 Rehabilitation and logger location plan.

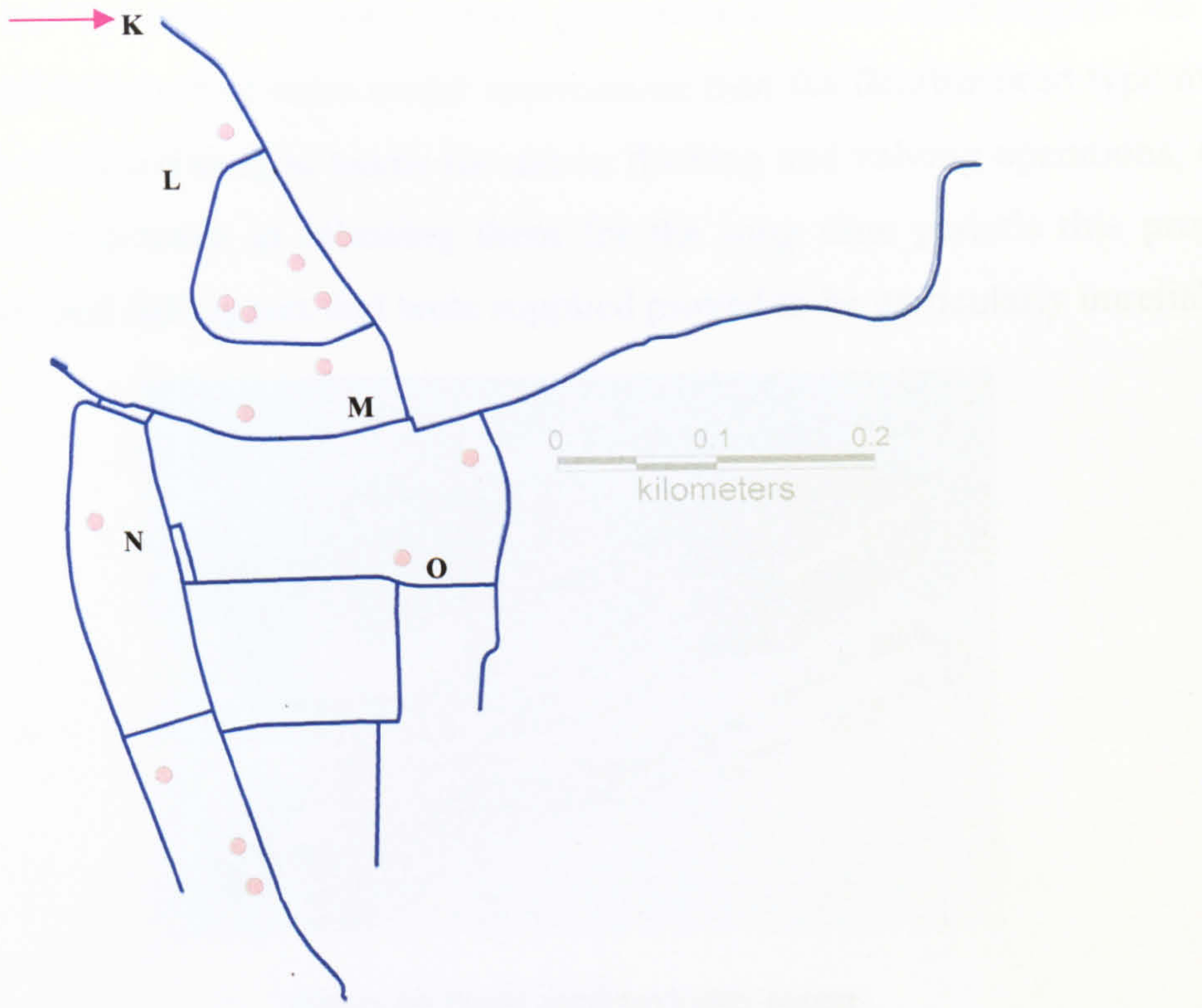

Figure 84 J722 (flushing zone) logger location plan.

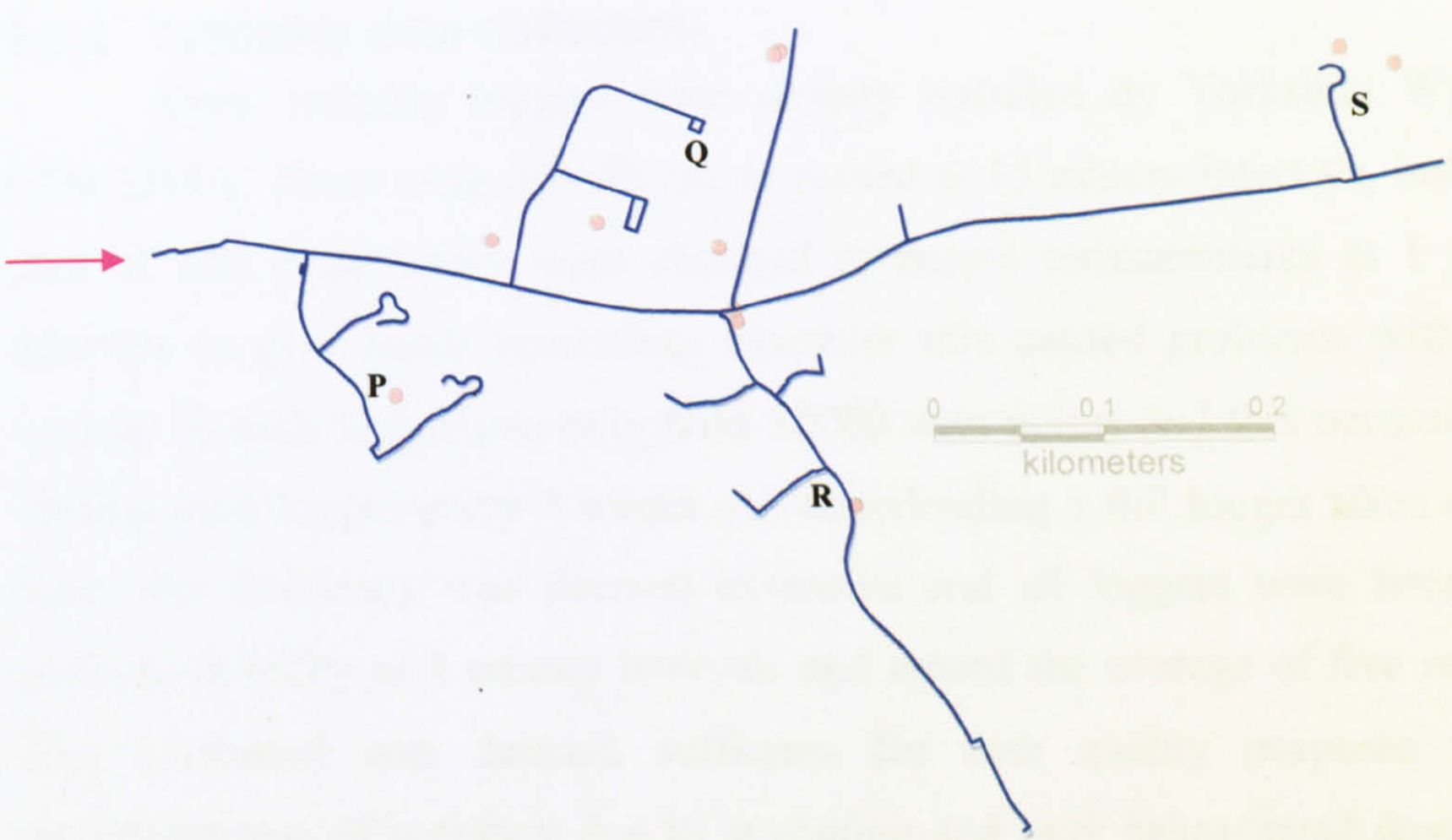

Figure 85 J730 (flushing zone) logger location plan.

Where possible a logger was installed directly on the inlet of the DMA, via a quadrena fitting. This installation required a different design of turbidity logger which was fitted on a steel shaft instead of a flexible head, Figure 86. However Yorkshire water had heavily invested in the flexible head type turbidity

loggers and had only purchased a small proportion of fixed shaft loggers. As the fixed shaft loggers had more useful applications than the flexible head type most had been assigned to field teams for use in flushing and valving operations, and there was reluctance in releasing them for the long time periods this project demanded and the loggers that were supplied proved to be particularly unreliable.

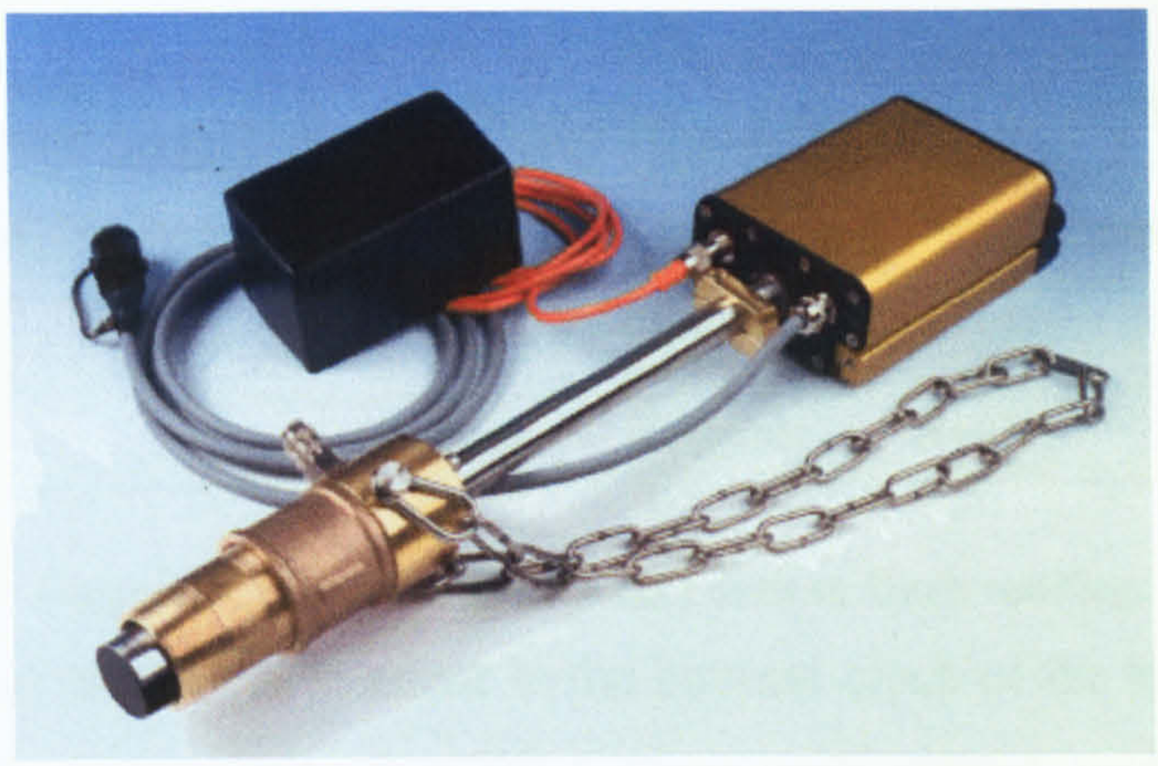

Figure 86 Fixed shaft turbidity logger.

6.2.2 Turbidity data collection

Some turbidity loggers were already installed by Yorkshire Water in C050 DMA. These were initially set to record at 15 minute intervals, but at the start of this project they were changed to record measurements at 1 minute intervals to give better resolution. However this caused problems with down loading as each logger can only hold 32000 data points and this necessitated a visiting each logger every 3 weeks. As downloading a full logger takes over an hour, this frequency was deemed excessive and all loggers were later set to measure turbidity at 1 minute intervals and record the average of five readings. This resolution was deemed sufficient for data quality purposes without significant loss of accuracy due to averaging and only necessitated down loads every three months.

Over periods of time turbidity loggers tend to drift as described in Section 5.3.3.3. To compensate for this at installation and every site visit thereafter independent Hach readings were taken from the customers tap, or nearest possible location on the same pipe, if the customer was out. Figure 87 is an example of how a bulk-shift of -0.2 NTU was applied to the entire data set of a

download period to align the instrument data to an independent Hach reading taken at the customer's tap.

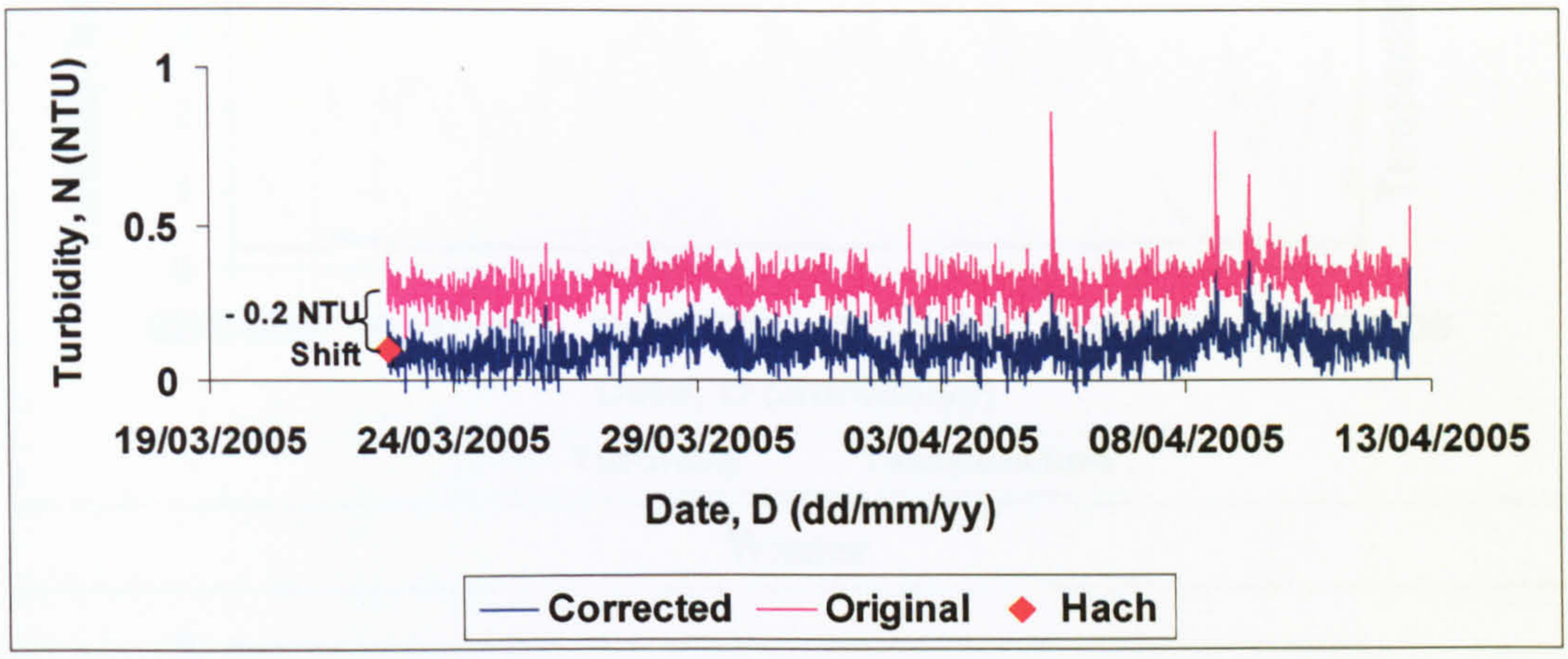

Figure 87 Alignment of turbidity data to Hach reading.

Drift was also noted to occur in the internal clock of the loggers to correct for this, timings were noted when the loggers were started, and each time they were downloaded. The internal logger's clock was also reset on every site visit.

6.2.3 Further Limitations in logger data analysis-stagnation.

By their design turbidity loggers installed in MSM chambers only record true turbidity of the network when the customer is drawing water and at other periods suffer from stagnation. This can cause a delay in the recording of a turbidity event, or miss the event entirely, as the turbid water travels along the main without being drawn up the service pipe. Also the turbidity event can appear to have a longer duration than reality, if turbid water is trapped in the manifold and not cleared until water is next drawn from the property. Lastly a greater effect can be seen where a property is vacant and water is not drawn for a long period of time and recorded turbidity appears to rise quite considerably.

These limitations can be identified by analysing the temperature data also recorded by the loggers. Stagnant water in the manifold is affected by the air/ ground temperature and as the customer draws water a temperature inflection is seen in the data. An increase in water temperature is seen in the winter periods, where the distributed water is warmer than the air temperature and a decrease in temperature is seen in the summer periods, where the distributed water temperature is much colder than the air temperature (Figure 88).

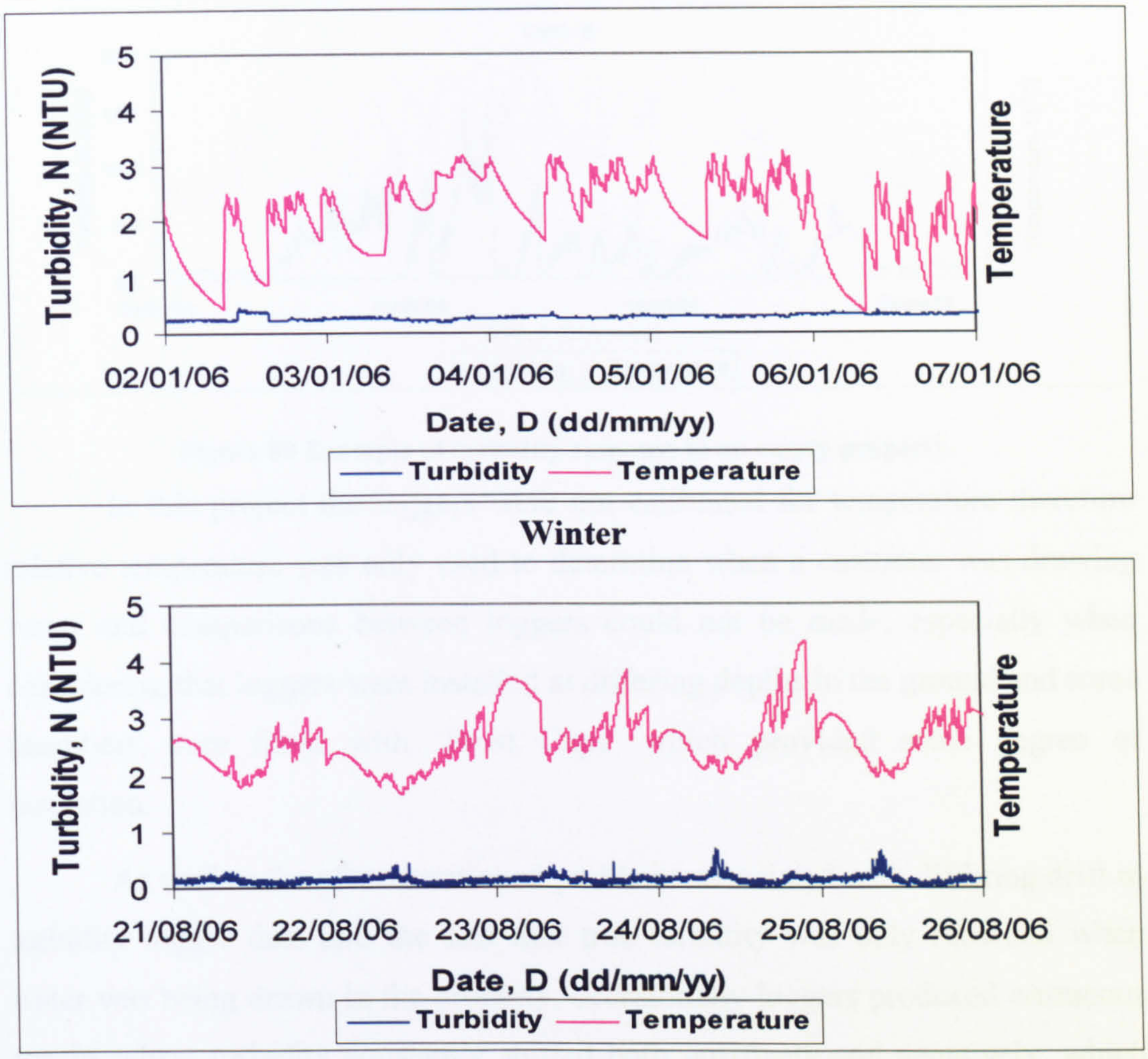

Figure 88 Example of temperature data recorded in the winter and summer

An example of turbidity and temperature data recorded when the occupants of a property were on holiday is shown in Figure 89. Normal occupation is shown in the beginning of the data up until 7/9/06 with a low turbidity and a saw tooth temperature profile as fresh water is constantly drawn. During the period where the house is unoccupied, the temperature profile displays wave like characteristics reflecting the daily air temperature and turbidity values become more pronounced. Sudden falls in the temperature profile can be explained by occasional visits to the house where some water was drawn for example to feed a cat. Turbidity data of this nature was identified manually and deleted from the data.

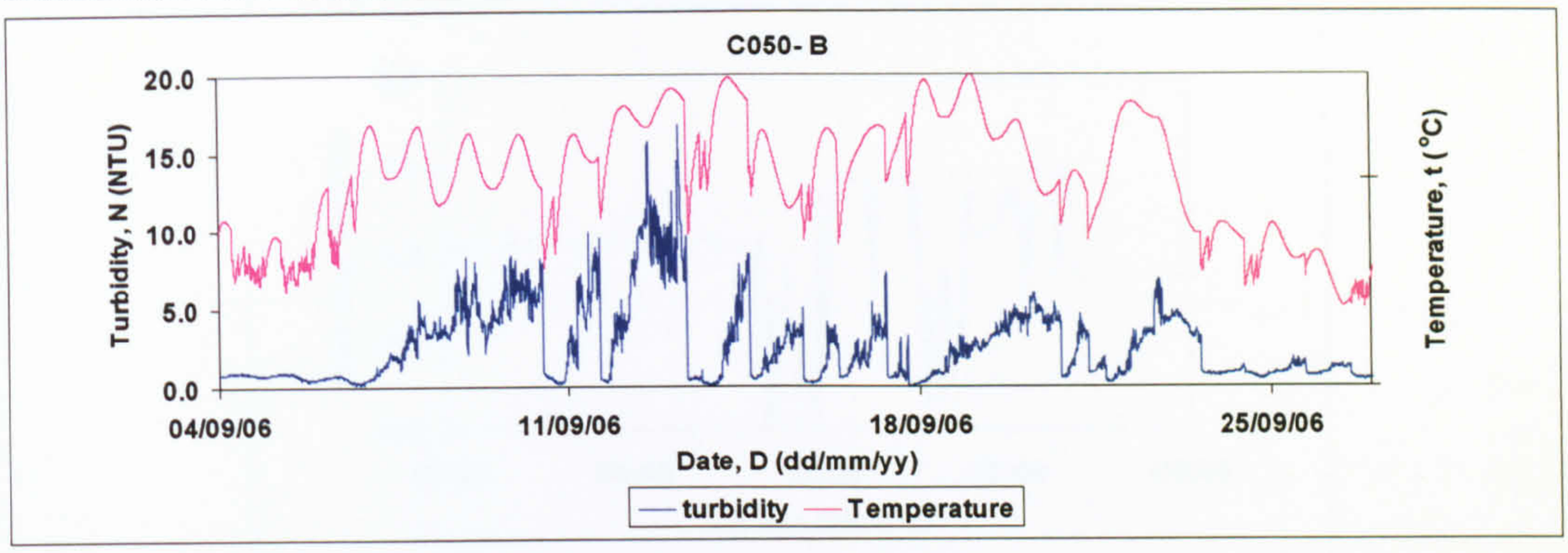

Figure 89 Example of turbidity response in an empty property.

In this project the loggers were not calibrated for temperature therefore relative temperature was only used to determine when a customer was drawing water and comparisons between loggers could not be made, especially when considering that loggers were installed at differing depths in the ground and some chambers were fitted with 'Frost Caps' which provided some degree of insulation.

As well as the afore mentioned problems associated with differing drift in turbidity logger data and the fact that true turbidity was only recorded when water was being drawn in the property, occasionally loggers produced erroneous results where turbidity constantly shifted both positively and negatively, which was uncharacteristic of proximal loggers recording at the same time. Similar results had occasionally been seen in the laboratory during the calibration process which had been attributed to air bubbles near the lens scattering light. Water companies do receive customer contacts regarding air in water, and air has been heard at the hydrant during the flushing operations in this project. It is therefore likely that air could occasionally become transported within a distribution system. Air is also present dissolved in water. Secondary pressure losses could occur inside the manifold at the logging location. This reduction in pressure could cause air to come out of solution, similarly to carbon dioxide bubbles being released when the cap is removed form a fizzy drink, and could cause air bubbles to become trapped near the lens of the instrument. An example of results possible affected by an air bubble is show in Figure 90 and was usually removed from the data.

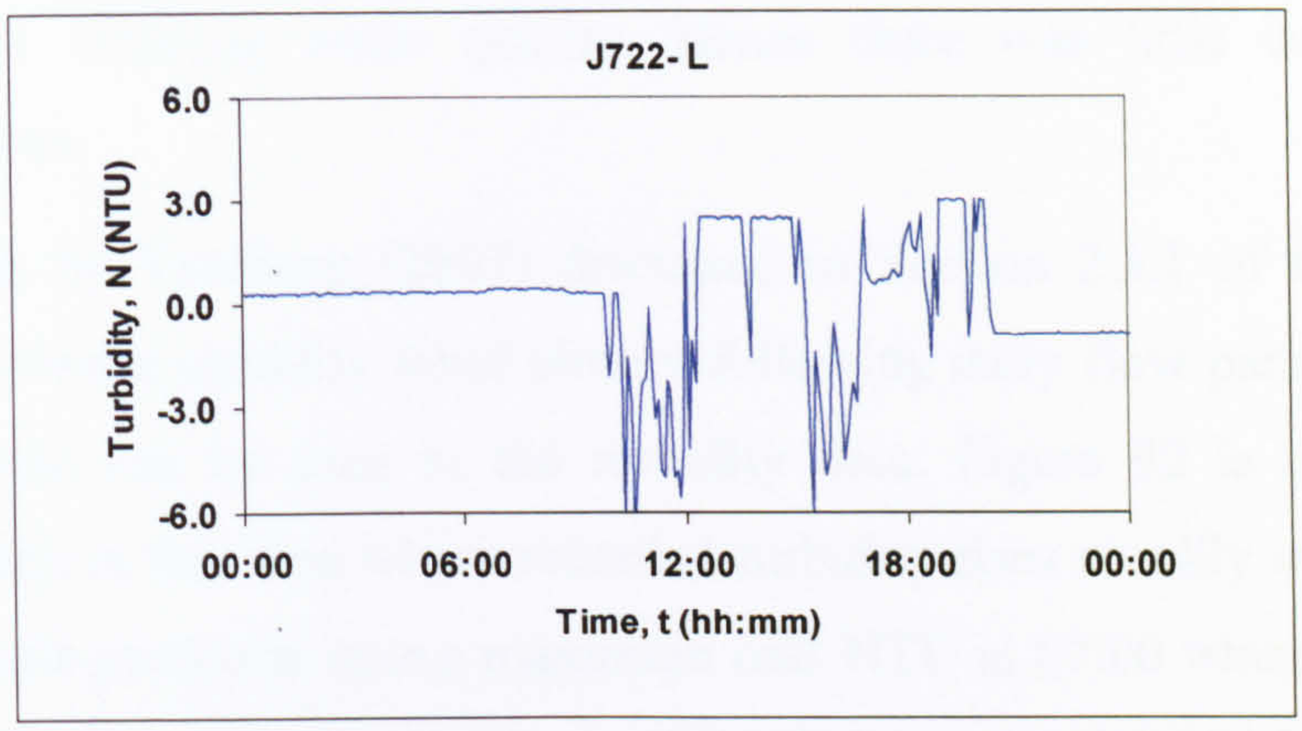

Figure 90 Example of turbidity response possibly caused by an air bubble.

6.2.4 Data analysis

Turbidity logger data was first corrected for gain and offset using calibration data as described in Section 5.3.3.2 and a secondary offset correction was applied to the data to align with the independent Hach reading, taken at logger installation and at every download as described in Section 6.2.2.

Over time loggers are affected by 'drift' where the turbidity recorded steadily increases over time. Figure 91 depicts an example of turbidity data where the logger was drifting at a rate of approximately 0.02 NTU/day. This drift could be due to material depositing (or fouling) on the lens.

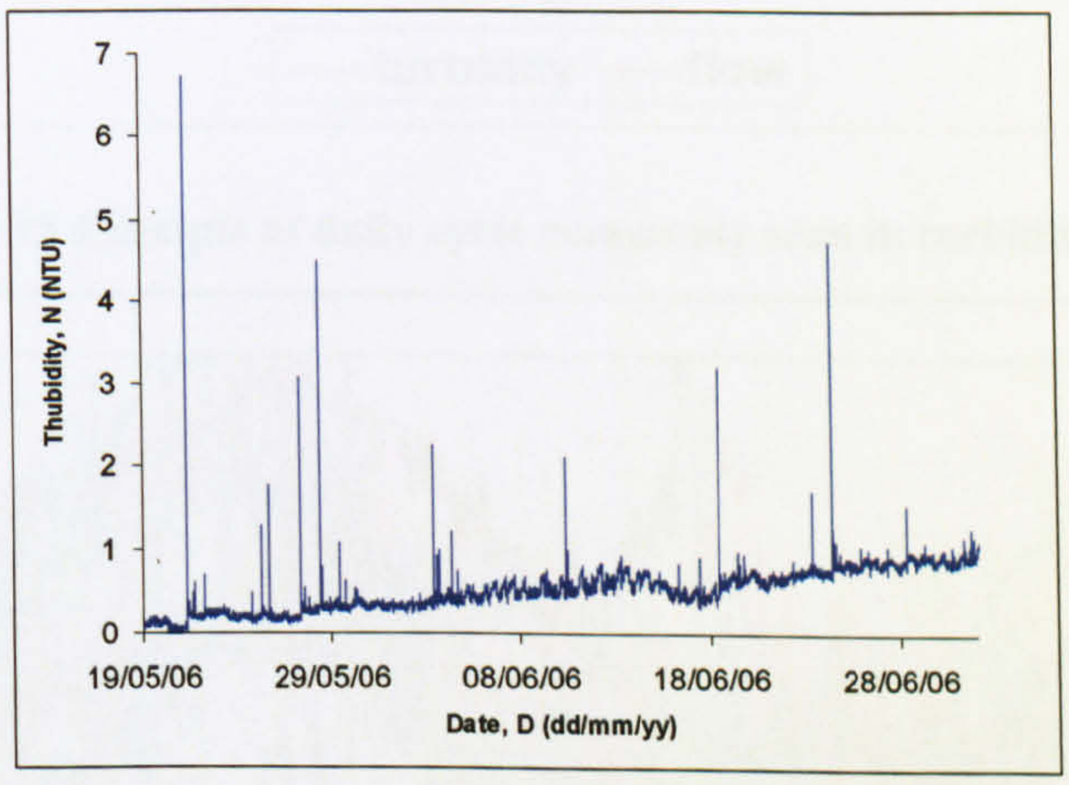

Figure 91 Example of 'Drift ' recorded in turbidity data

This drift effect and offset instability caused problems comparing information between different loggers, because over longer time periods, loggers tended to drift at differing rates and amounts. A logger measuring 2 NTU higher than another logger installed on the same network was not necessarily a valid

indication of differing water quality. Hence there was little confidence in absolute values.

Work by Vreeburg (2007) discussed in Section 2.3.1 of the literature review describes a turbidity trend closely following daily flow patterns. A daily turbidity cycle can be seen in the turbidity data. Figure 92 is one of many examples seen in this data where recorded turbidity rises steadily over the night to reach in this particular case a maximum of 3 NTU at 07:00 where it then falls during the day to reach its minimum of 0 NTU at around 16:00 before it then starts to rise again.

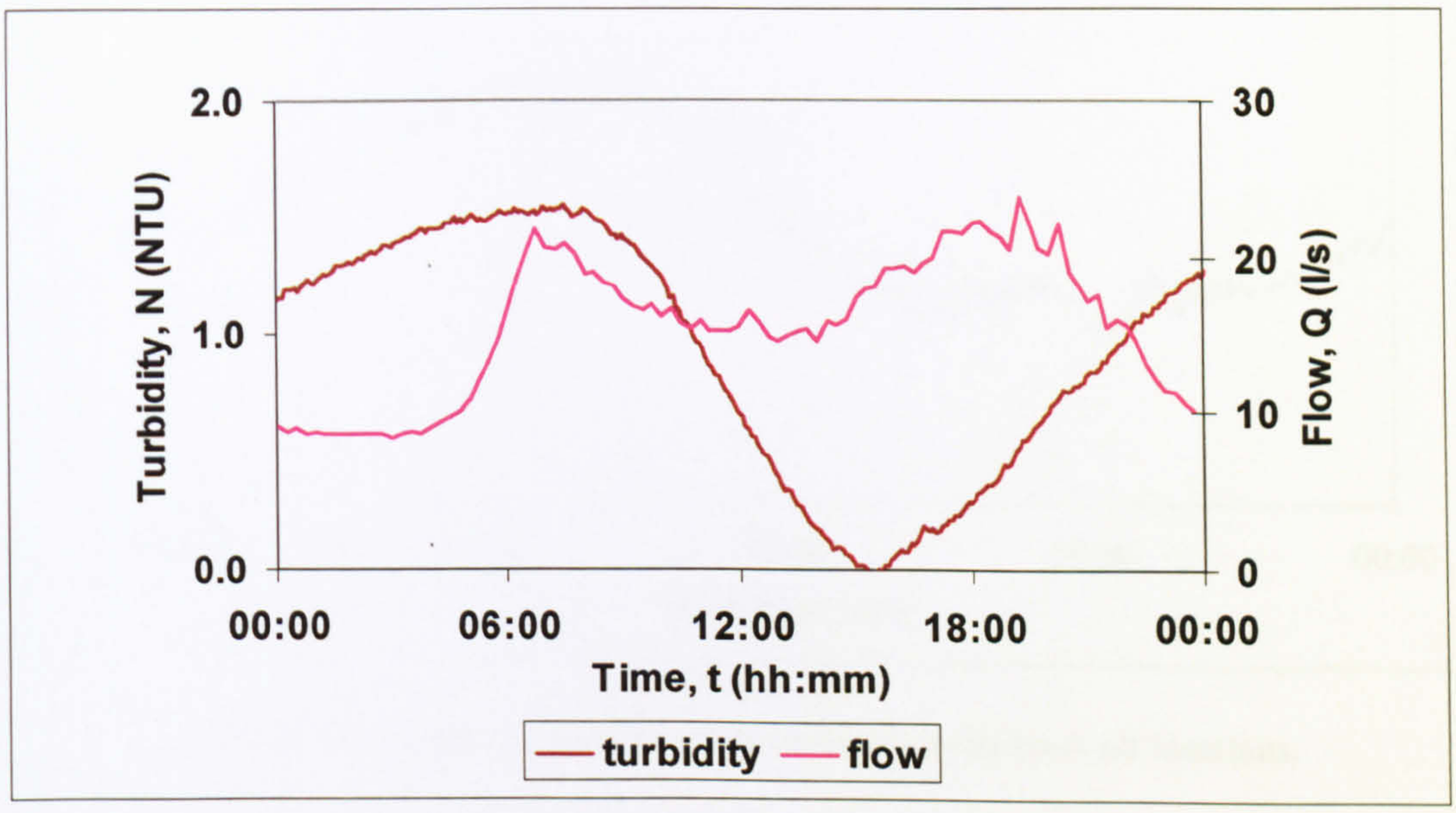

Figure 92 Example of daily cycle commonly seen in turbidity data.

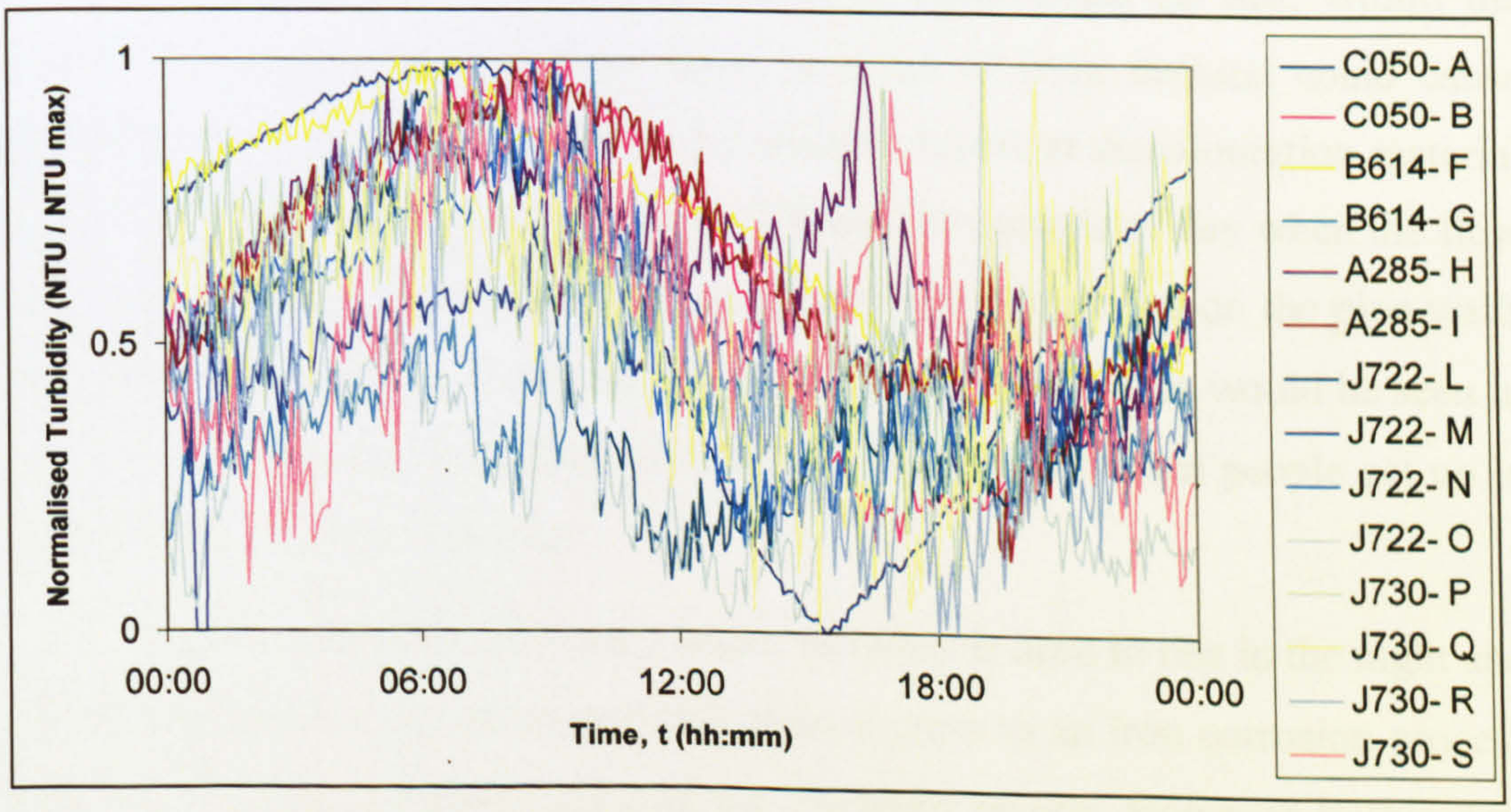

Figure 93 Examples of normalised daily turbidity cycle from different areas.

Since the amplitude of the daily turbidity cycle varies between locations and season, in order to compare typical daily turbidity cycles from different locations, data was normalised by dividing each value by the maximum turbidity during the 24 hour period. Results in Figure 93 show some degree of scatter, but this can be attributed to the frequency the customer draws water throughout the day. However, when the average daily turbidity cycle for all locations is plotted (Figure 94) a similar trend to Figure 92 is seen. This confirms that the trend seen is similar at all locations.

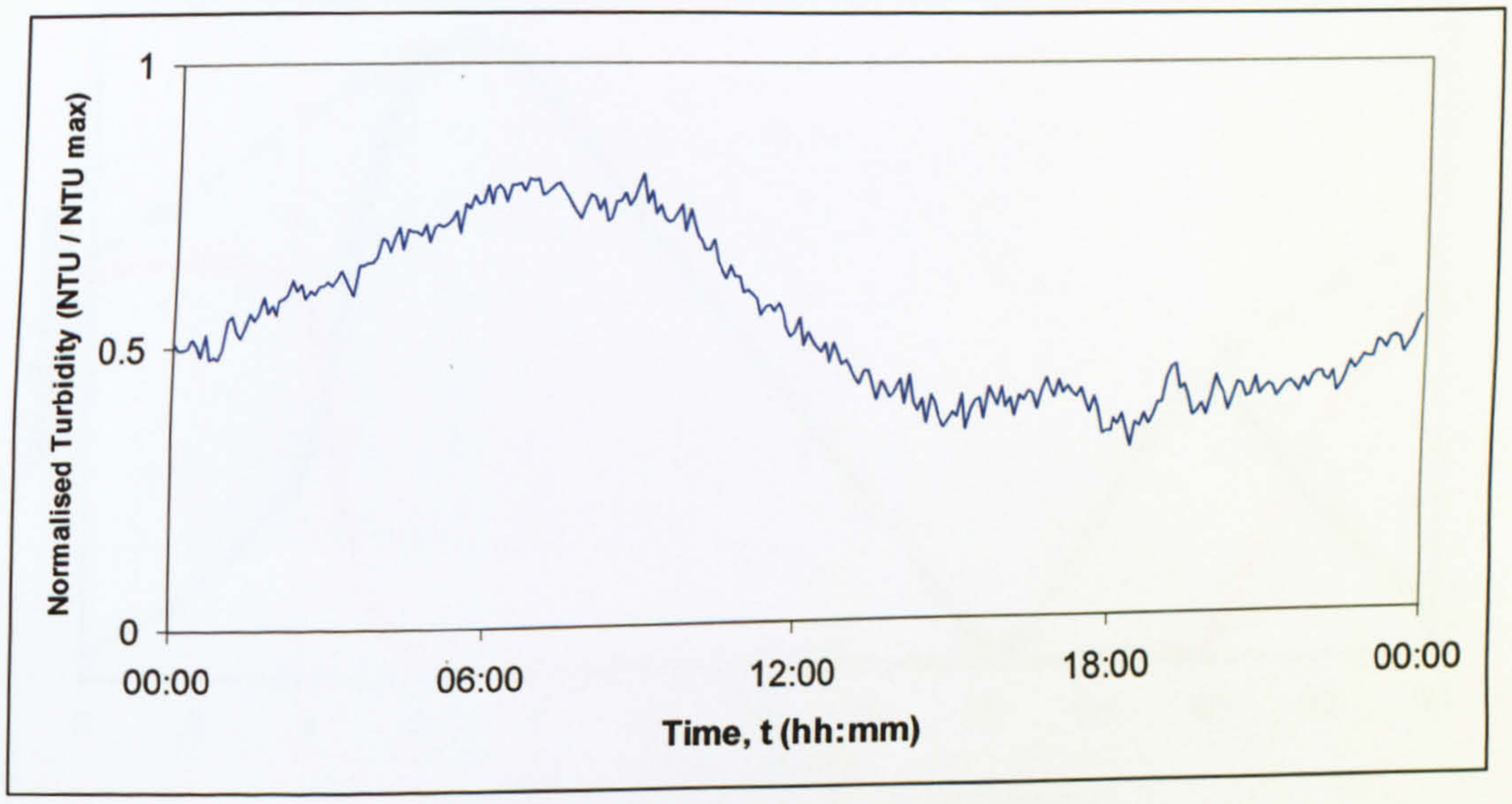

Figure 94 Average normalised daily turbidity cycle from all locations.

An explanation of this daily turbidity cycle could be that, within the distribution system the increased flows at times of peak demand could cause sufficient shear stresses to mobilise the weakest layers of discolouration material and create a slight increase in turbidity. During the periods of day when the flow rates and therefore shear stresses decrease material re-deposits on the pipe walls and the turbidity decreases. If this was the case here, two peaks would be seen in the turbidity data corresponding with the increase in flow when people get up in the morning and return to work.

McNeil describes examples where turbidity is seen to rise in the night and fall during the day, and attributed this phenomenon to an iron corrosion process and as discussed in Section 2.2.2 of the literature review. However In this data turbidity is commonly seen to rise in the mid afternoon (Figure 92). If this was

purely corrosion process turbidity would start to rise in the late evening, as flow decreases.

This could indicate that the common example of the daily turbidity cycle show in Figure 92 is the product of both corrosion processes occurring in the night and re-suspension processes occurring during periods of increased flow during the day. This dual process can be explained in Figure 95 which is a theoretical representation of the processes which could be occurring.

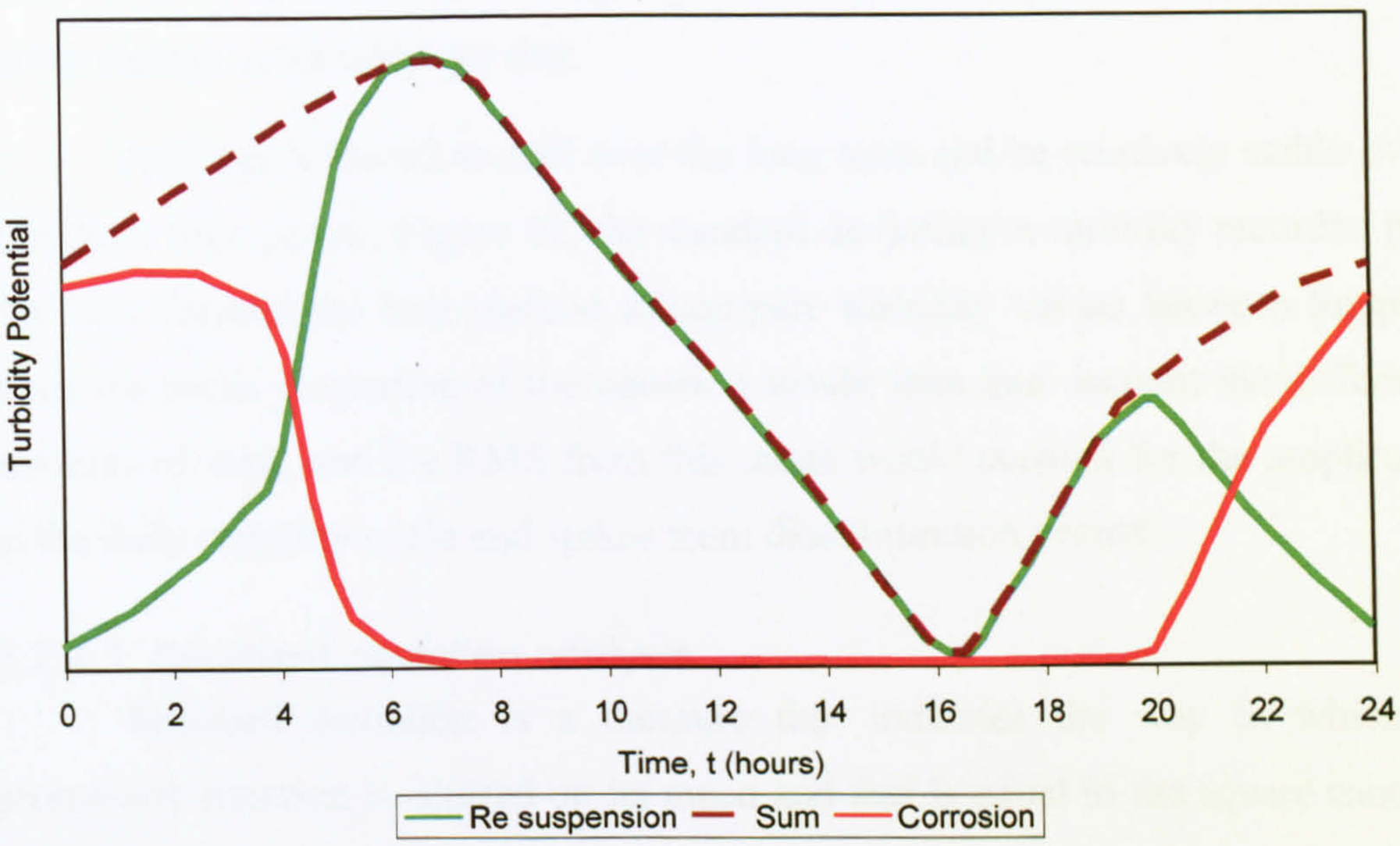

Figure 95 Stylisation of daily turbidity cycle.

Turbidity likely to be produced by re-suspension is shown in green and peaks at times of maximum flow in the network where the most weakly adhered layers of material are brought into suspension. The turbidity peak occurring at 8:00pm is smaller than that occurring at 7:00am. This is because there is a larger increase in flow (and therefore change in shear stress) from night until the morning peak than there is from afternoon until the evening peak (Figure 92).

The turbidity likely to be produced by corrosion processes is represented by the red line and peaks during the night at times of minimum flow. The brown dotted line is the summation of the green and red lines representing the combined effects of re-suspension and corrosion on turbidity. This summed line is very similar to the turbidity cycle shown in Figure 92, indicating that the turbidity

cycle commonly observed in this project is indeed a combination of both iron corrosion and re-suspension effects.

This daily turbidity cycle seen in the data, as a product of both corrosion and re-suspension processes, has the potential to be useful in indicating how 'clean' the network is. 'Clean' could refer to the amount and mobility of discolouration material within the network and could be numerically represented by the amplitude of the daily turbidity cycle. Networks with a higher change in turbidity per day could have a higher discolouration risk than networks with a lower change in turbidity per day.

As loggers tended to drift over the long term and be relatively stable over a 24 hour time period, Figure 92, the standard deviation in turbidity recorded per day was deemed the best method to compare turbidity values between loggers since the mean proportion of the equation would take into account the differing amounts of drift, and the RMS from this mean would account for the amplitude in the daily turbidity cycle and spikes from discolouration events.

6.2.4.1 Standard deviation analysis

Standard deviation is a measure that indicates the way in which a probability function is centred on its mean and that is equal to the square root of the moment in which the deviation from the mean is squared. It is used to describe sets of values to determine how far the value varies from the arithmetic mean or average. Here the standard deviation is calculated using the "unbiased" or "n-1" method (Equation 12):

Equation 12

$$\sqrt{\frac{\Sigma\left(x-\bar{x}\right)^2}{n-1}}$$

Where x = the sample mean

n = sample size

Microsoft Access was used to automatically calculate a standard deviation for every 24 hour period. Since turbidity here is recorded at 5 minute intervals 288 data points are used in each calculation.

Figure 96 shows the example of drifting logger data seen in Figure 91 which has had the standard deviation method applied. Here it can be seen that drift has been eliminated from the data and the turbidity spikes present in the original data are still apparent in the standard deviation data set. As well as eliminating drift, this method is ideal for summarising long term data into a more manageable format.

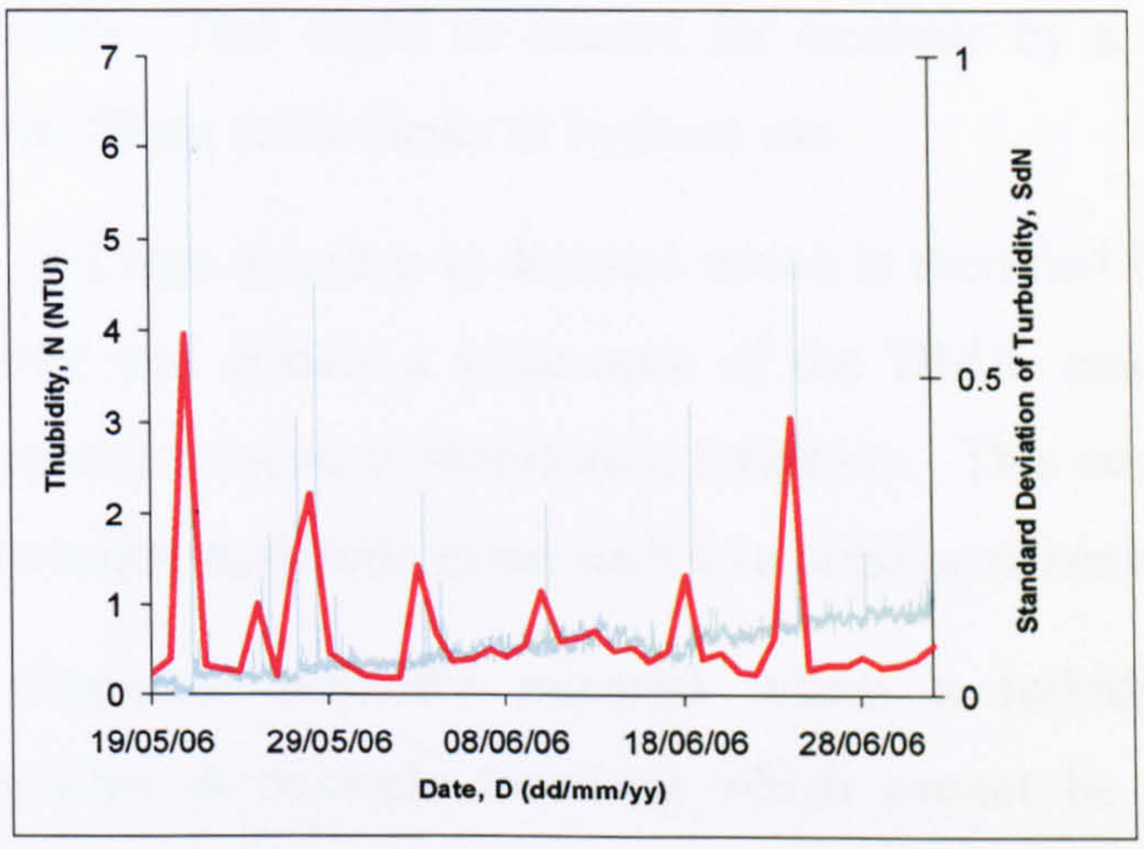

Figure 96 Example of turbidity data analysis.

6.2.5 Other data collected

In conjunction with turbidity data, flow data at the inlet meter for each of the monitored DMAs was collected to indicate changing hydraulic conditions in the network such as changing flows due to burst events or demand increases. Flow data was recorded at 15 minute intervals but for ease of presentation over the long time periods presented here; the minimum, maximum and average flow was plotted for 24 hour intervals.

Discolouration customer contacts were also collated for the monitoring DMAs.

In order to account for any changes in the source water chemistry affecting the DMA performance, water quality data from the output of the appropriate water treatment works supplying the respective DMAs was collected from January 1999 until September 2007.

6.3 Results

Investigation of the turbidity data recorded during the long term monitoring phase of this project indicate that turbidity events can be attributed to a limited number of factors:

- A small localised increase in demand which is not large enough to affect the inlet flow meter but causes a turbidity response at one location. This could be caused for example by a small factory, a farm filling water tanks or hydrant use.
- A Large increase in demand which is recorded by the inlet flow meter and affects a wide area of the DMA, causing a turbidity response at several monitoring locations. This could be attributed to a major hydraulic event such as a burst or re zoning of a DMA.
- Imported turbidity material where a turbidity response is recorded at multiple locations which cannot be attributed to an increase in flow. A turbidity response is also seen at the inlet to the DMA (if equipment is installed and working), verifying that this material was imported into the DMA from an event occurring elsewhere in the Water Supply Zone (WSZ).

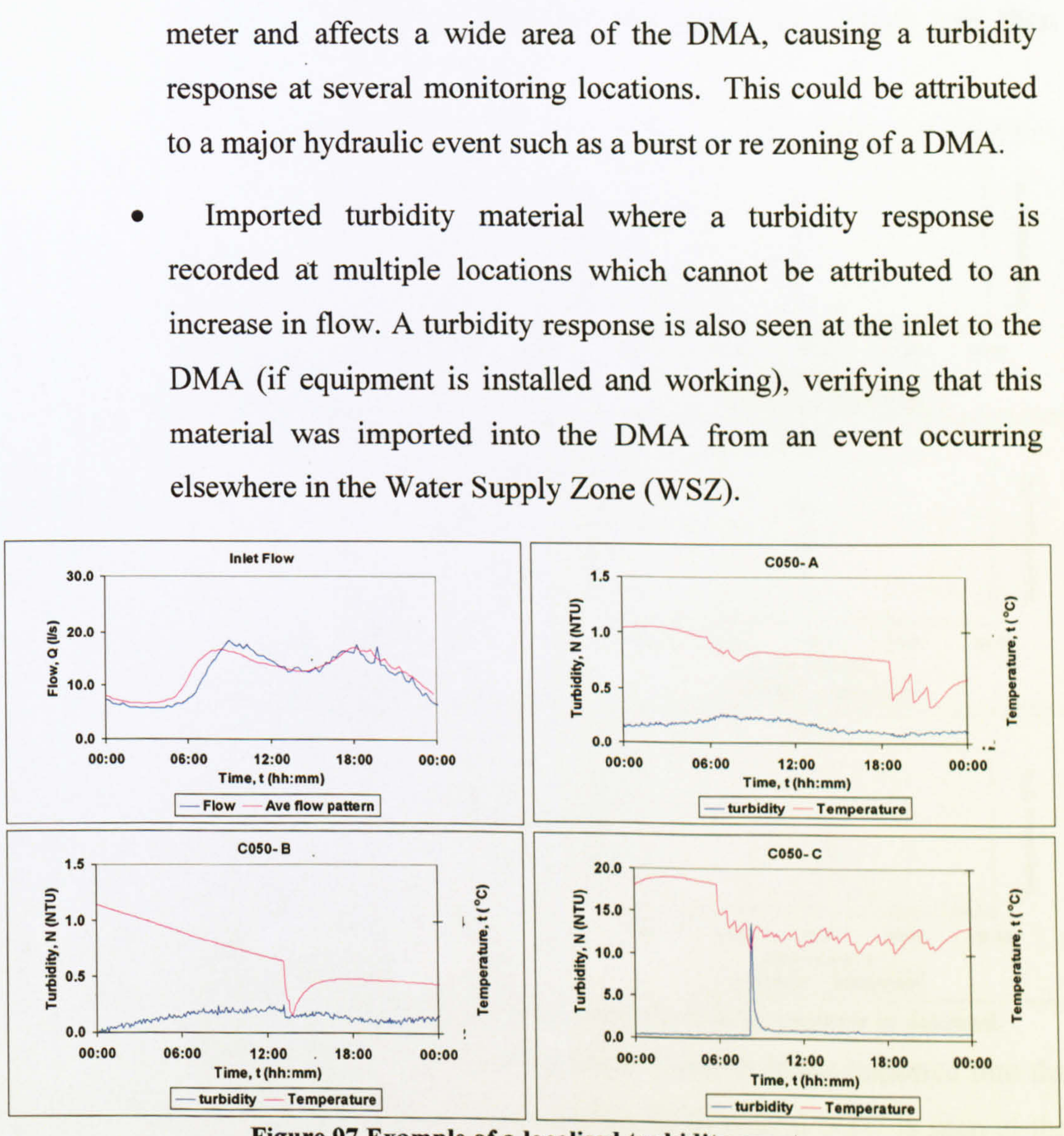

Figure 97 Example of a localised turbidity event.

Figure 97 depicts an example of a localised turbidity response. A turbidity spike of 15 NTU is seen at location C050- C which is not apparent at

any of the other locations, (although in this example temperature data suggests that C050- B was not drawing water) and no increase in flow is seen at the inlet flow meter.

A turbidity event caused by a large increase in demand is shown in Figure 98. An increase of approximately 10 l/s is recorded by the inlet flow meter as the result of a burst. This caused a turbidity response which was seen at all locations, except J722-L which was not drawing water at the time. The turbidity response at location J722-K is of particular note, as this is situated at the DMA inlet and indicates that the increased demand on the trunk main caused sufficient shear stresses to mobilise turbidity material from the trunk main which was then imported into the DMA.

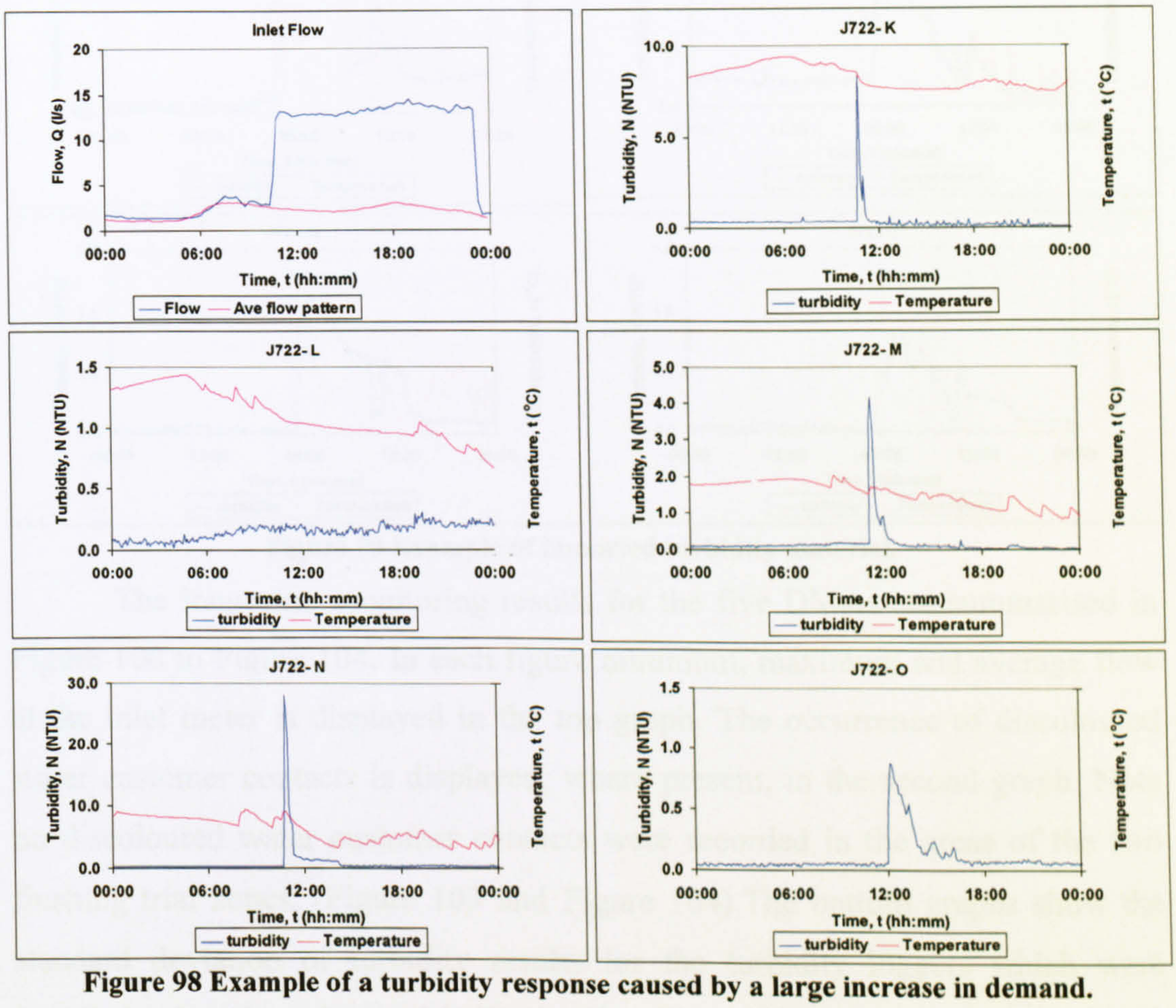

Figure 98 Example of a turbidity response caused by a large increase in demand.

Figure 99 shows an example of turbidity material being imported into the DMA. Here a turbidity response with a maximum of only 2 NTU is seen at the turbidity logger installed on the DMA inlet (J722-K) which has a duration of approximately 14 hours. The same turbidity pattern is seen at all other monitoring locations and decreasing amplitude is seen with increasing distance

from the DMA inlet (J722- O) as the event progresses through the DMA. No increase in flow is seen at the inlet flow meter. This loss of material indicates that discolouration material must be being brought out of suspension and accumulating on the pipe walls as it travels through the system.

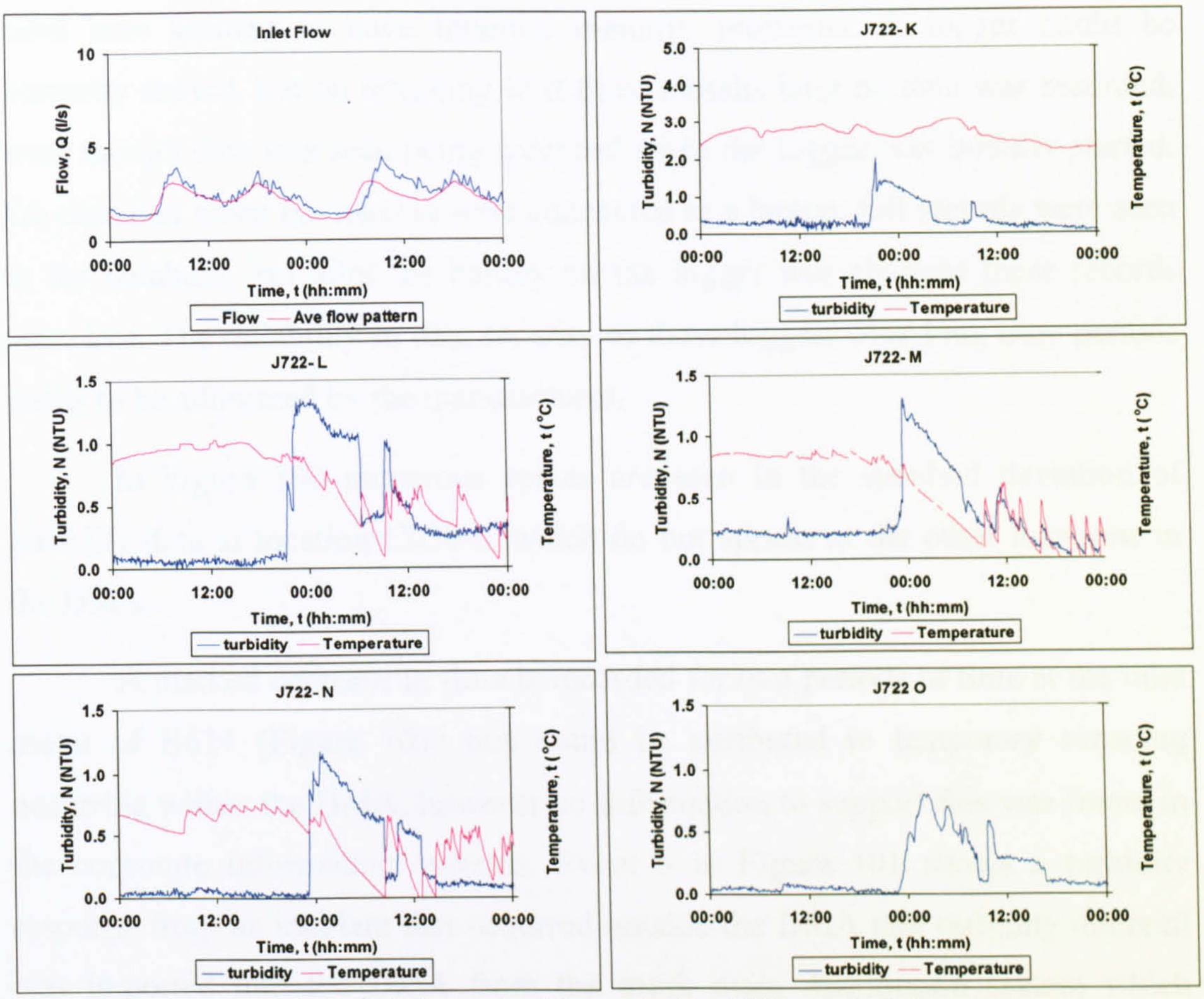

Figure 99 Example of imported turbidity material.

The long term monitoring results for the five DMAs are summarised in Figure 100 to Figure 104. In each figure minimum, maximum and average flow at the inlet meter is displayed in the top graph. The occurrence of discoloured water customer contacts is displayed, where present, in the second graph. Note no discoloured water customer contacts were recorded in the areas of the two flushing trial zones, (Figure 103 and Figure 104).The bottom graphs show the standard deviation of turbidity results for the turbidity loggers which were installed at locations depicted in Figure 81 to Figure 85.

Events which occurred in the DMA are highlighted by the numbered dotted lines which correspond to inlet flow and turbidity response graphs displayed in detail in Appendix 1. A time line depicting the period when rehabilitation was completed is shown by the red dotted line. Turbidity spikes

recorded at different locations often align indicating that a single event travelled throughout the DMA.

Blank periods in the turbidity data represent periods of time when the turbidity logger was faulty and not functioning properly. The turbidity loggers used here seemed to have inherent memory problems. A logger could be correctly started, but on returning to it three months later no data was recorded, even though data was seen being recorded when the logger was initially started. On occasion when the loggers were connected to a laptop, full records were seen in the database, but after the battery on the logger was changed these records were lost. The reliability in data security of these loggers over long time periods needs to be addressed by the manufactures.

In Figure 100 numerous spikes are seen in the standard deviation of turbidity data at location C050-C which do not appear at the other locations in the DMA.

A marked decrease in flow is recorded for two periods of time at the inlet meter of B614 (Figure 101) this could be attributed to temporary rezoning occurring within the DMA, however no information to support this was found in the corporate information systems. Event 5 in Figure 101 shows a turbidity response from an incident that occurred outside the DMA and turbidity material was imported into the DMA from the trunk main distribution system which generated nearly 50 discoloured water customer contacts within the DMA.

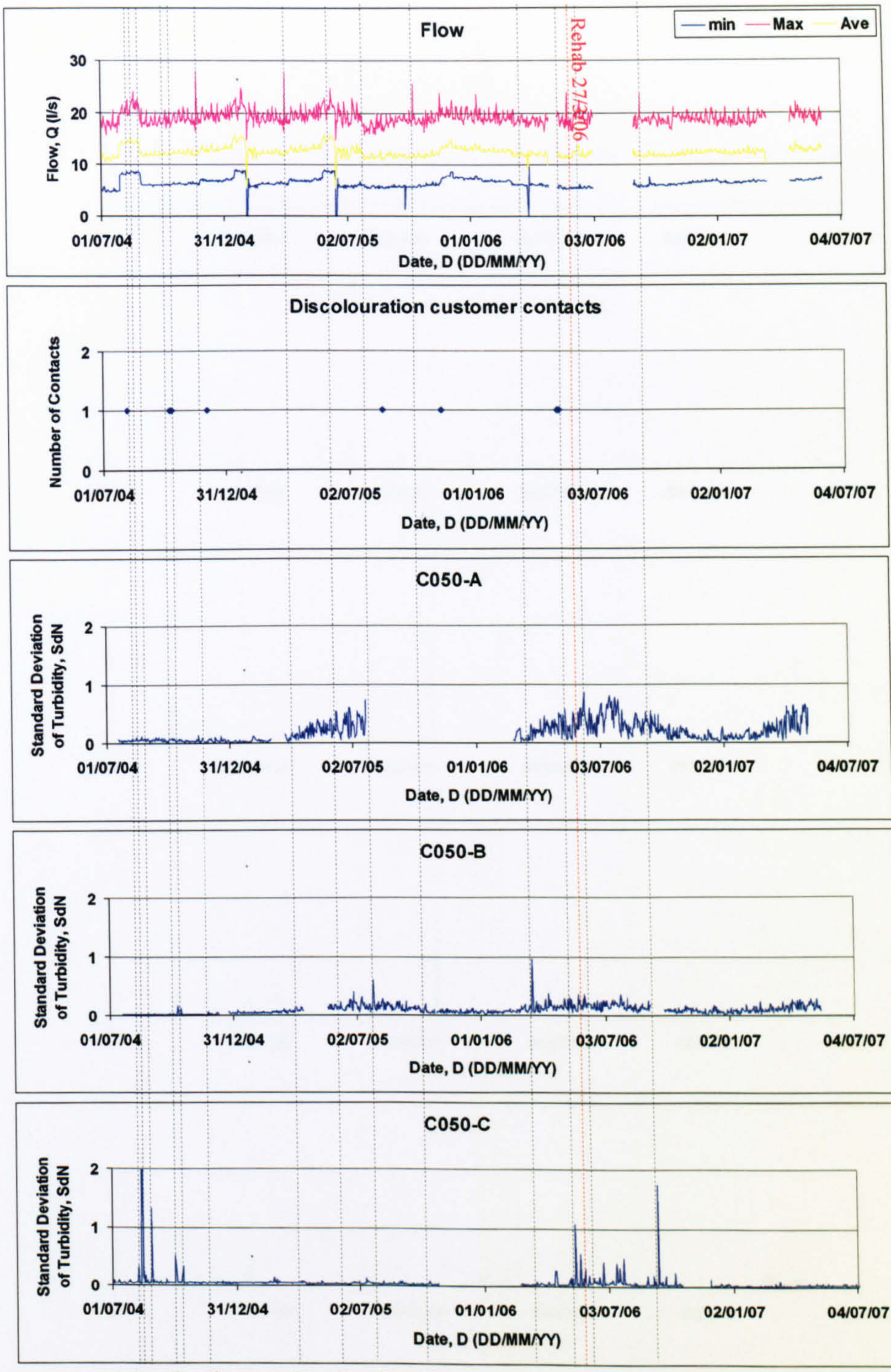

Figure 100 C050 DMA Standard deviation of turbidity plots.

A significant number of spikes can been seen in the turbidity data at all monitoring locations in Figure 102 which correspond to increased flow at the inlet flow meter.

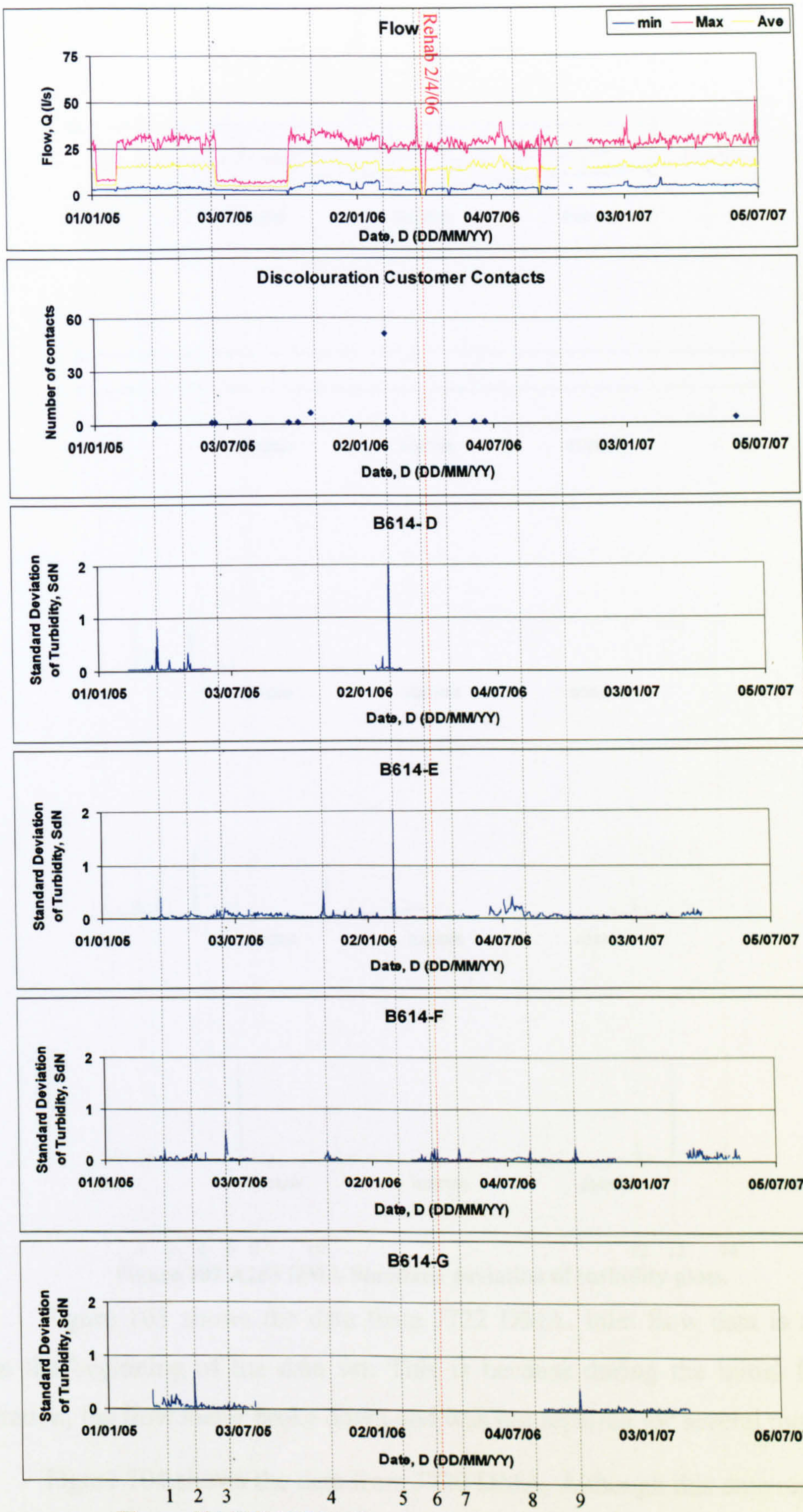

Figure 101 B614 DMA Standard deviation of turbidity plots.

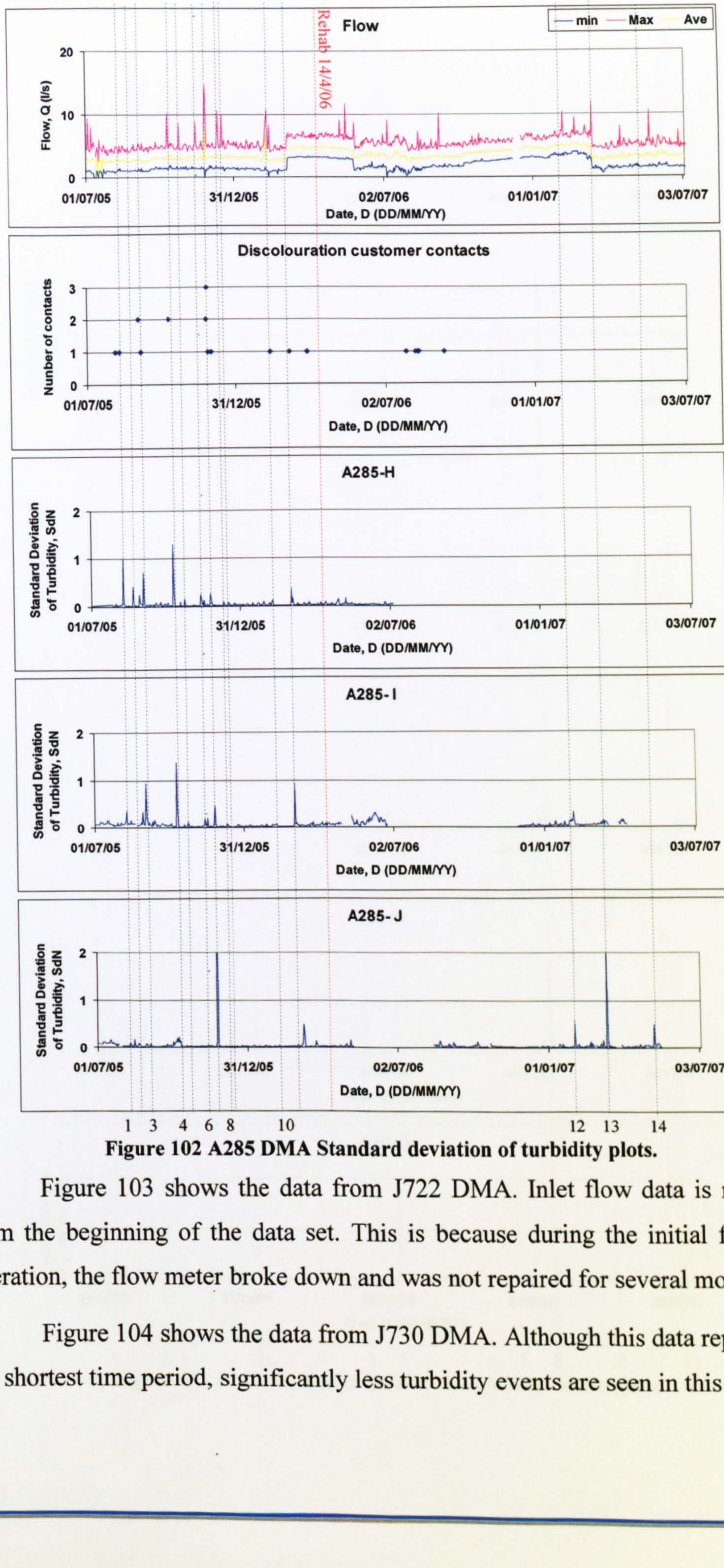

Figure 102 A285 DMA Standard deviation of turbidity plots.

Figure 103 shows the data from J722 DMA. Inlet flow data is missing from the beginning of the data set. This is because during the initial flushing operation, the flow meter broke down and was not repaired for several months.

Figure 104 shows the data from J730 DMA. Although this data represents the shortest time period, significantly less turbidity events are seen in this DMA.

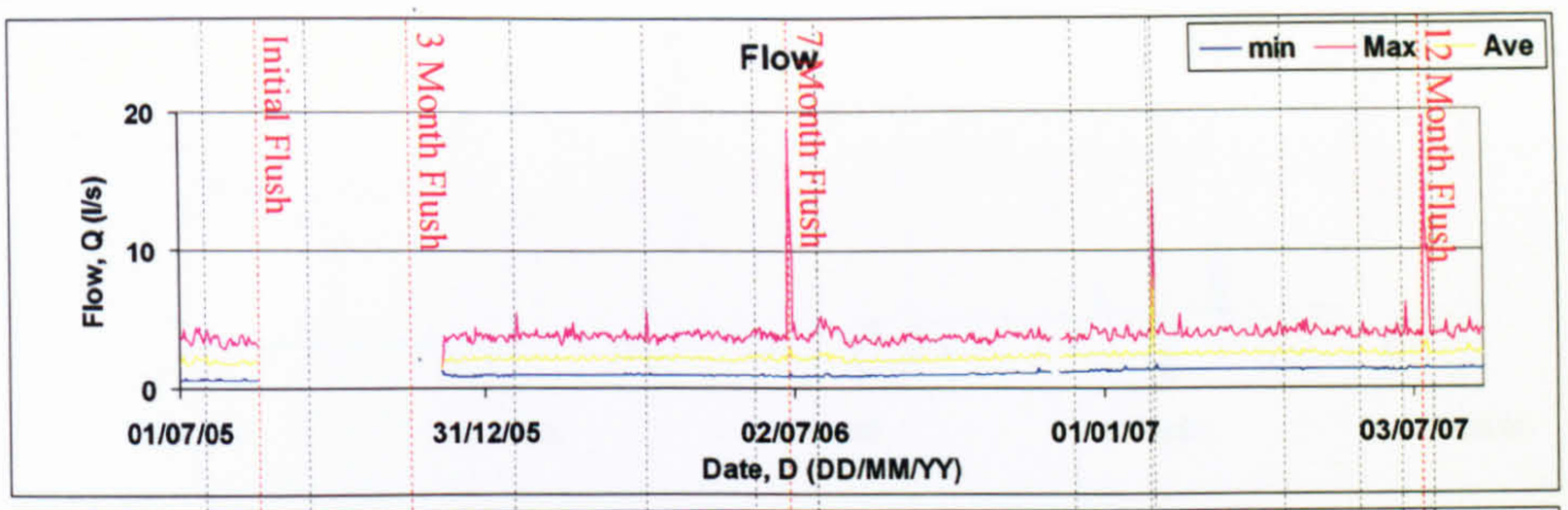

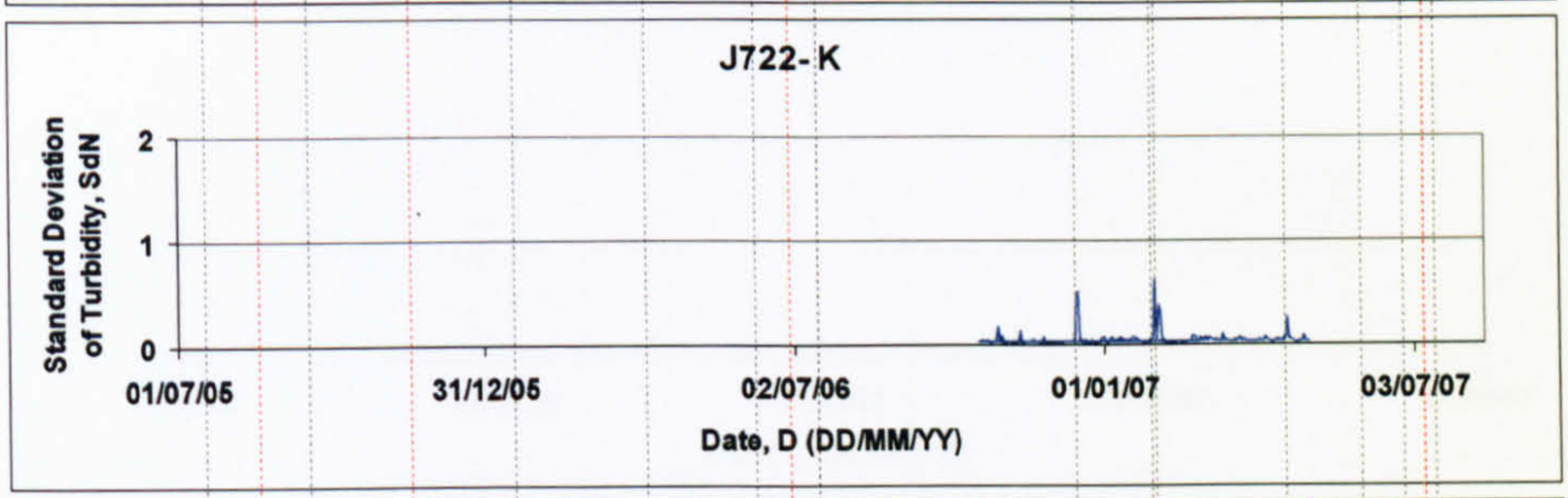

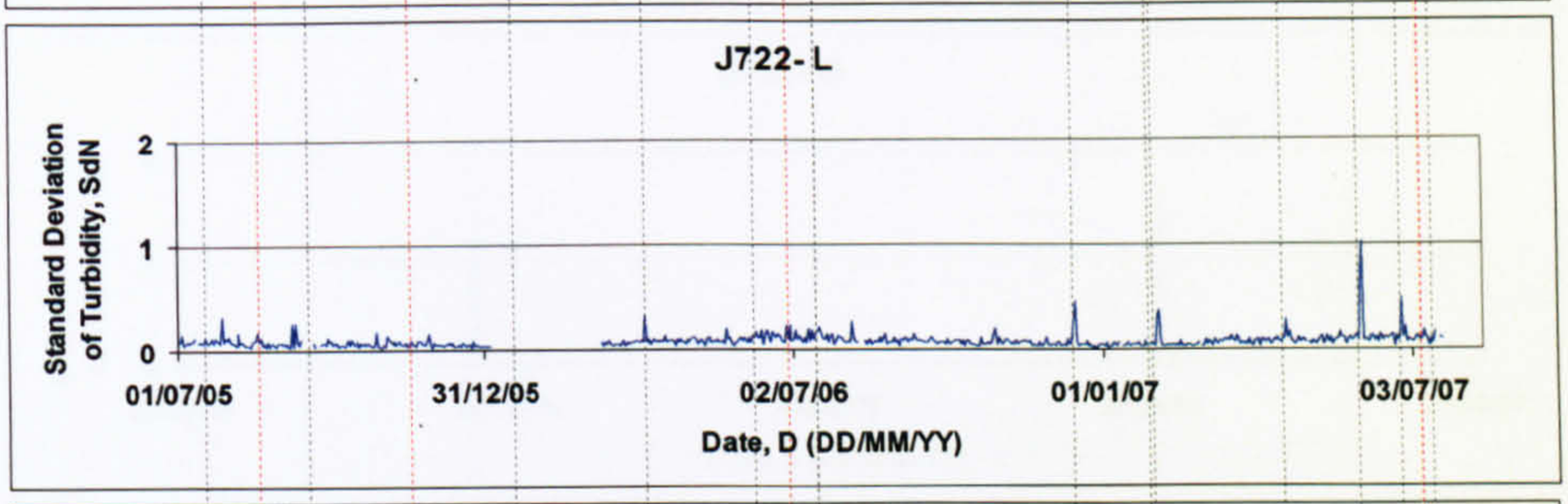

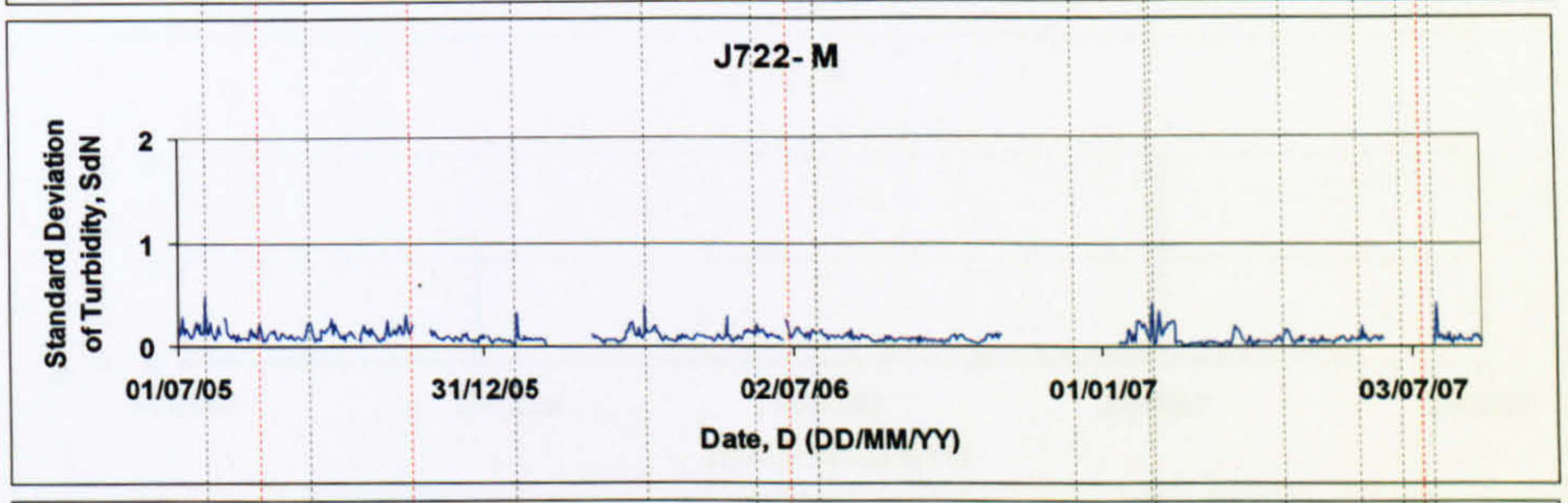

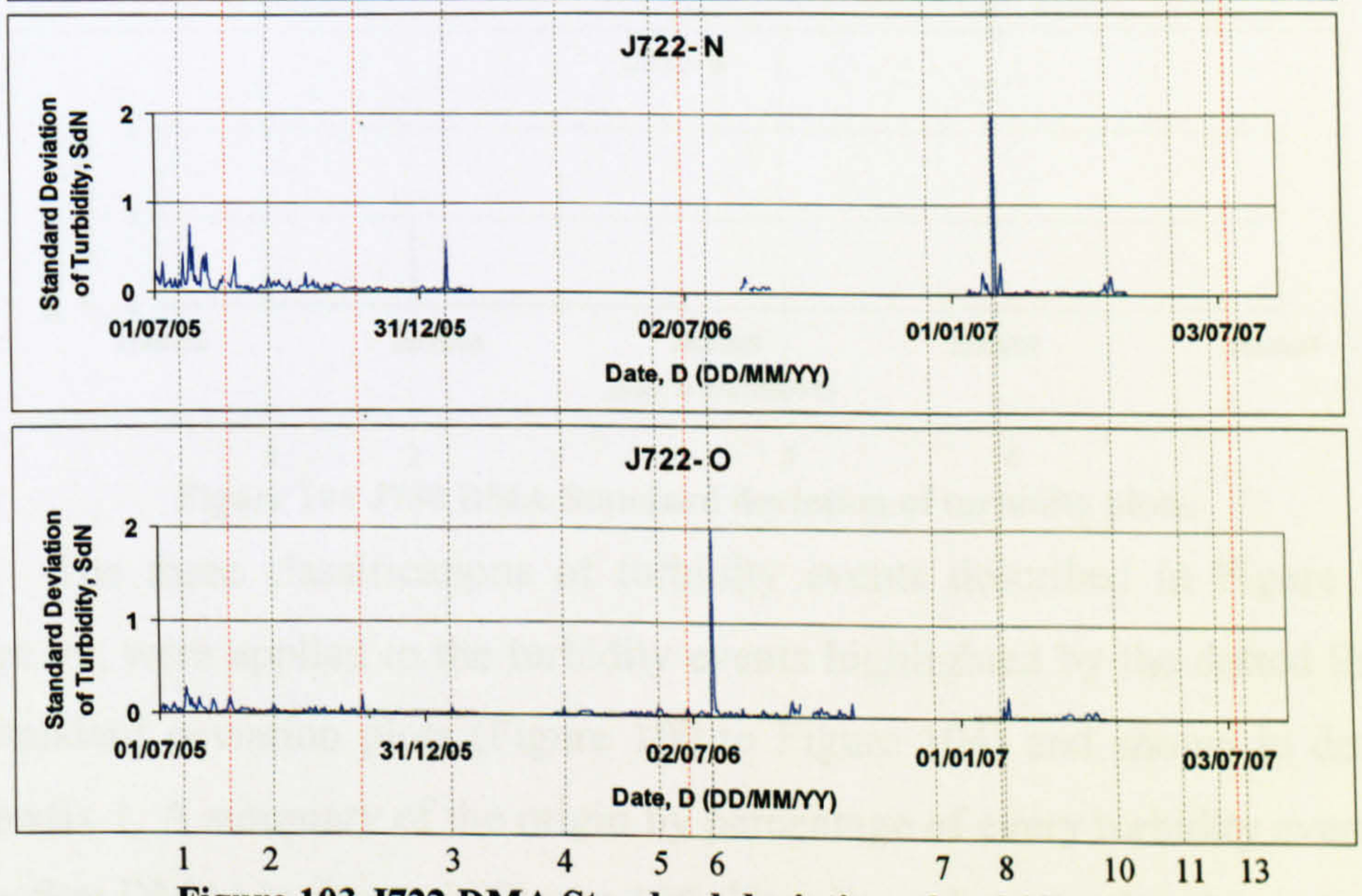

Figure 103 J722 DMA Standard deviation of turbidity plots.

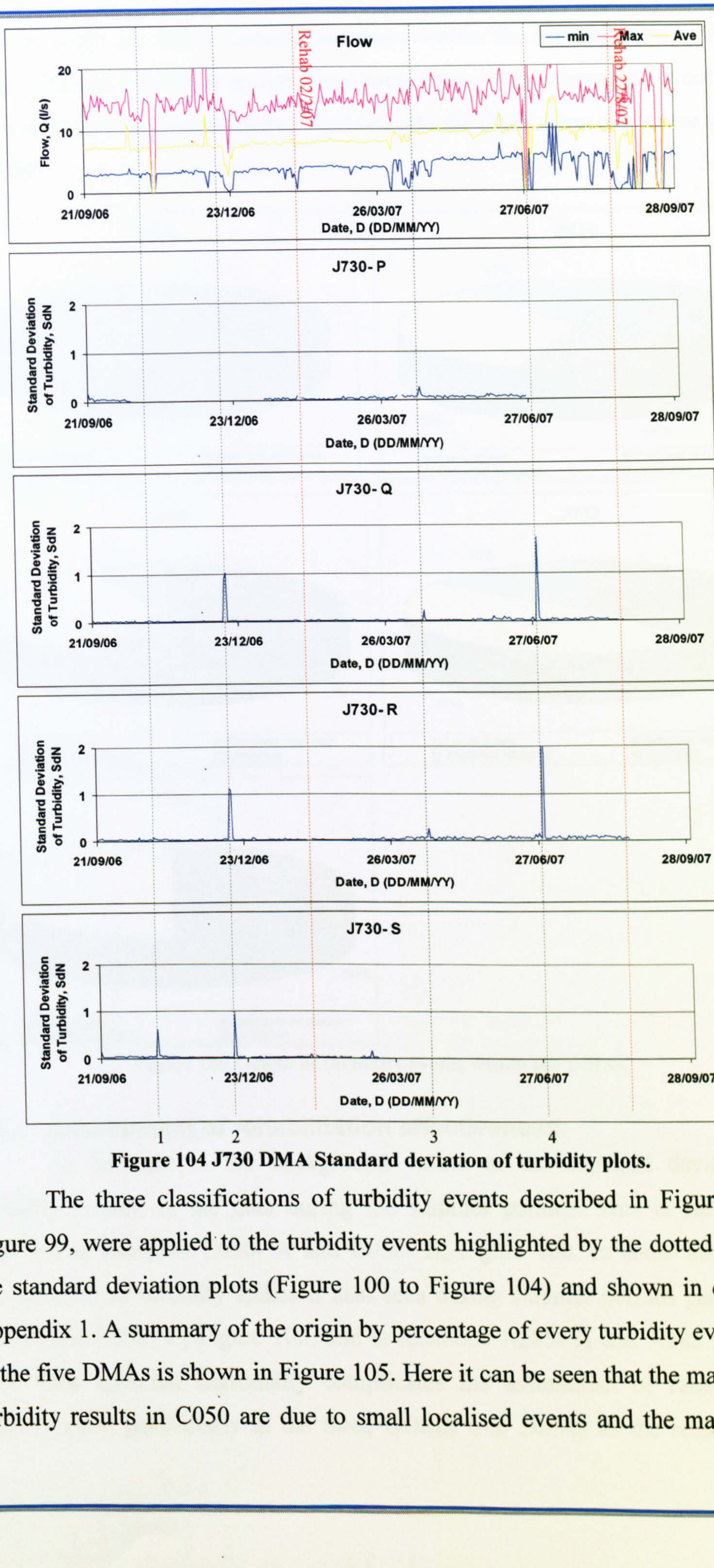

Figure 104 J730 DMA Standard deviation of turbidity plots.

The three classifications of turbidity events described in Figure 97 to Figure 99, were applied to the turbidity events highlighted by the dotted lines in the standard deviation plots (Figure 100 to Figure 104) and shown in detail in Appendix 1. A summary of the origin by percentage of every turbidity event seen in the five DMAs is shown in Figure 105. Here it can be seen that the majority of turbidity results in C050 are due to small localised events and the majority of

events in A285 are due to demand increases within the network. DMAs B614, A285, J722 and J730 have a significant proportion of discolouration events that can be attributed to material being imported into the DMA from elsewhere within the WSZ.

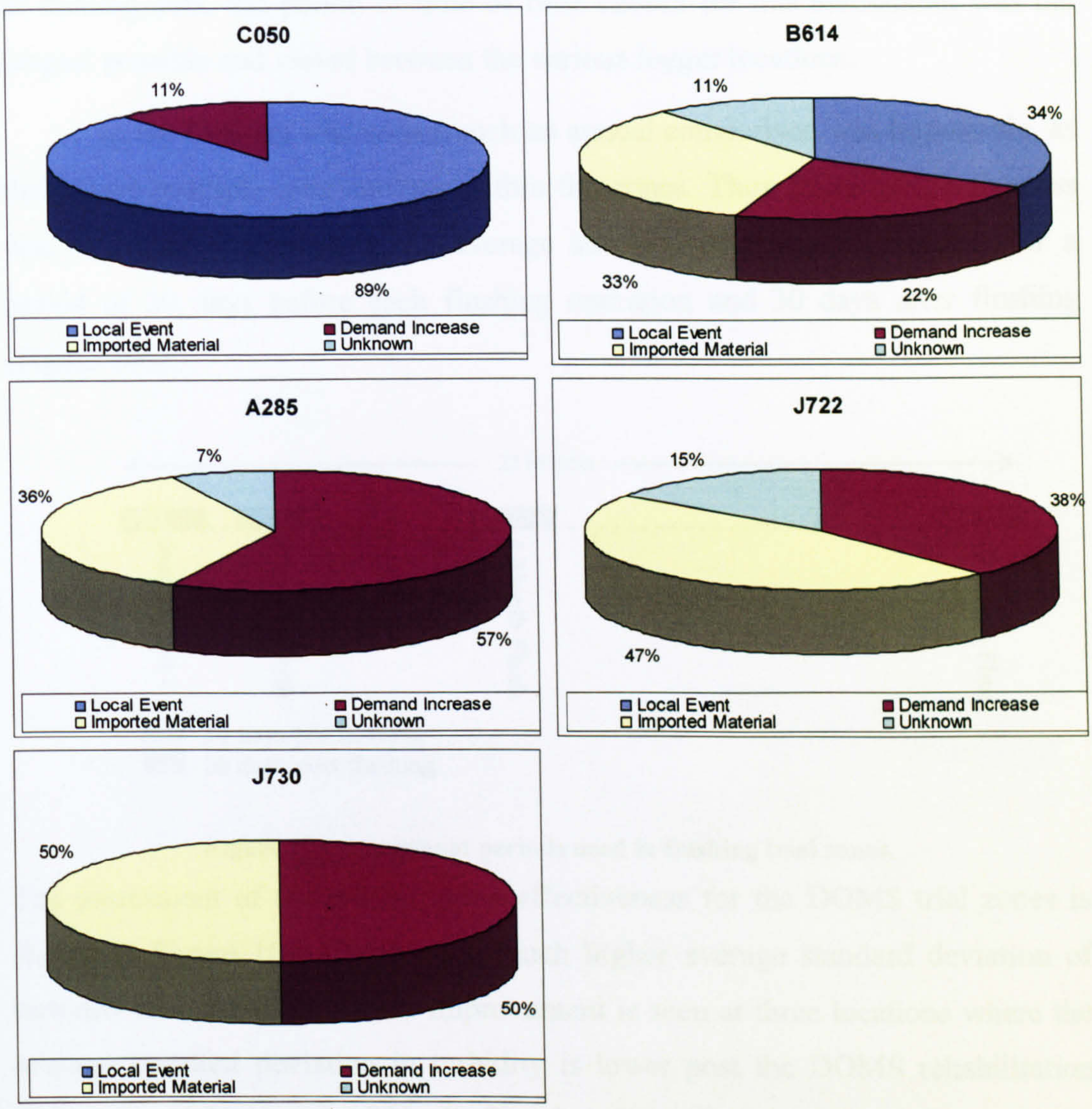

Figure 105 Origin of turbidity events within the DMAs.

6.3.1 Assessment of rehabilitation effectiveness.

An increase in the background values of the standard deviation of turbidity is seen in the data during the summer periods. This is particularly apparent at locations C050- A and C050- B, Figure 100. In some instances a proliferation of turbidity spikes is also seen during summer periods particularly at location C050- C, Figure 100, and at locations A285- H and A285 I, Figure 102. This apparent seasonality complicates the assessment of rehabilitation effectiveness, particularly in the three DOMS trial DMAs as the rehabilitation

occurred in late spring. For this reason the average of all the standard deviation data for a period of time after rehabilitation was compared to the average standard deviation for the same time period of the year preceding the rehabilitation. Due to reliability problems of the equipment resulting in sections of missing data, the period of time of time chosen for this assessment was the longest possible and varied between the various logger locations.

In the flushing trial zones, such an annual comparison was impossible, as there were multiple interventions within the zones. Thus flushing effectiveness was based upon comparing the average standard deviation of turbidity for a period of 30 days before each flushing operation and 30 days after flushing (Figure 106).

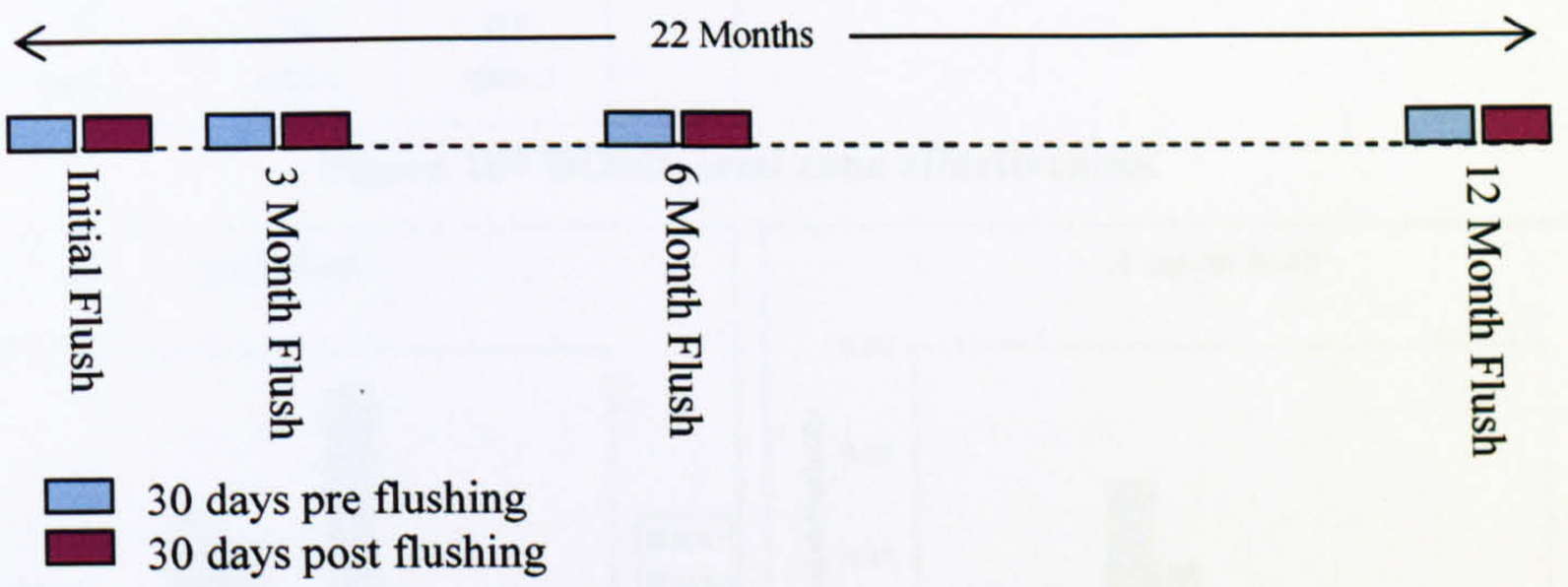

Figure 106 Assessment periods used in flushing trial zones.

The assessment of the rehabilitation effectiveness for the DOMS trial zones is shown in Figure 107. C050 has a much higher average standard deviation of turbidity than the other zones. Improvement is seen at three locations where the average standard deviation in turbidity is lower post the DOMS rehabilitation (B614- G, A285-H and A285- J). Five locations show a worsening in turbidity levels after the DOMS interventions (All locations in C050, B614- F and A285-I). Insufficient data was available to make an assessment for location B614- E. Taking each zone as a whole, there is a 21% improvement in A285, roughly no change in B614 and a 72% worsening in C050.

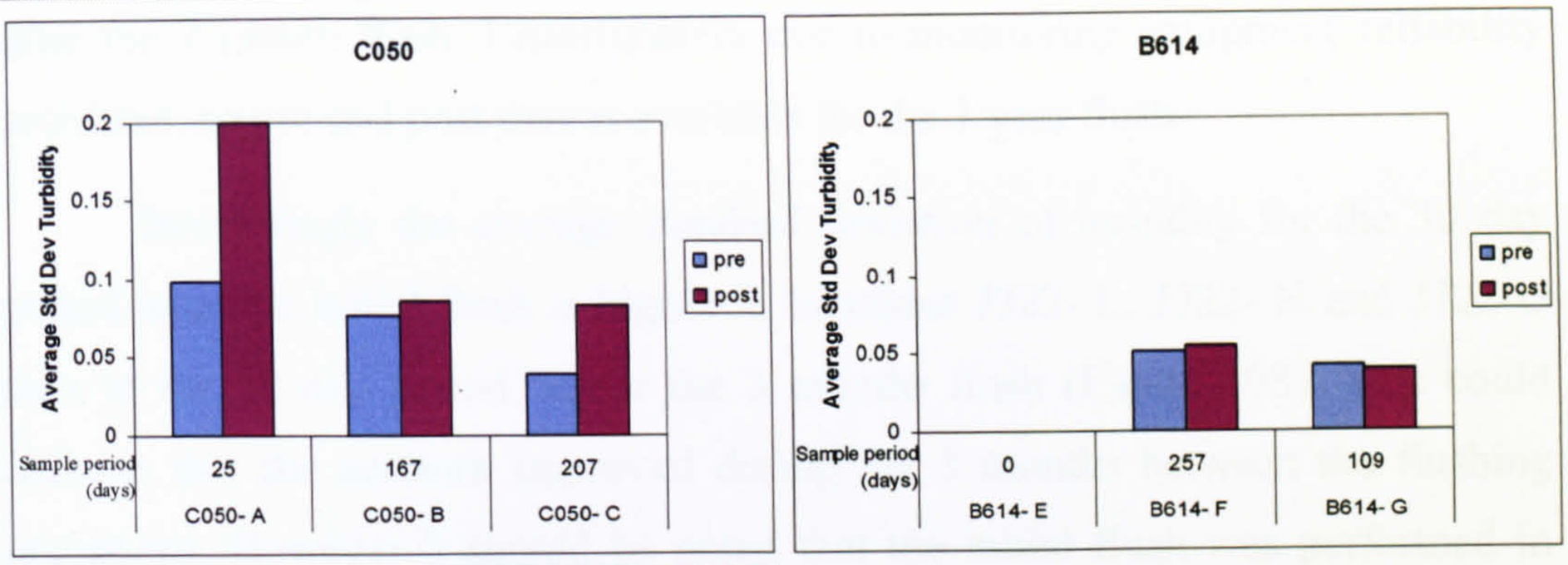

Figure 107 DOMS trial zone effectiveness.

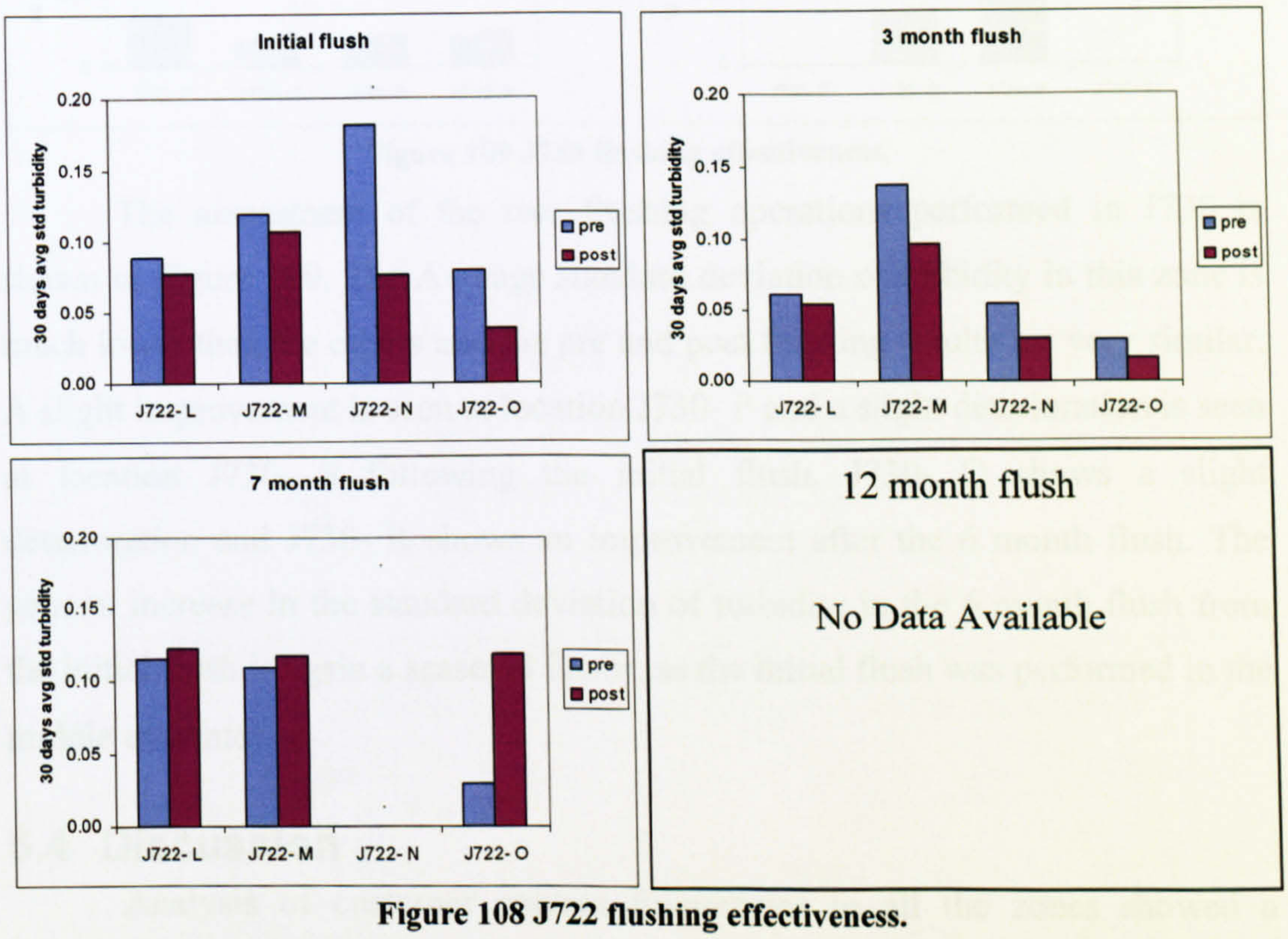

Figure 108 J722 flushing effectiveness.

The assessment of each flushing operation for J722 is show in Figure 108. It can be seen that there is a decrease in the average standard deviation of turbidity in the 30 day period after flushing from the 30 day period proceeding flushing. This indicates an improvement for the initial and three month flush. However deterioration in the discolouration performance is seen in the network

after the 7 month flush. Unfortunately due to monitoring equipment reliability problems, no pre and post data is available for the 1 year flush.

Interestingly the average standard deviation of turbidity for the 30 day period after the initial flush is higher in locations J722- L, J722- N and J722-O than in the 30 day period before the 3 months flush (Figure 108). This could indicate that the network improved during the 3 months between the flushing operations. However it should be noted that the initial flush was performed in mid summer, and the 3 month flush was performed in the beginning of winter and this apparent improvement could actually be a seasonal effect.

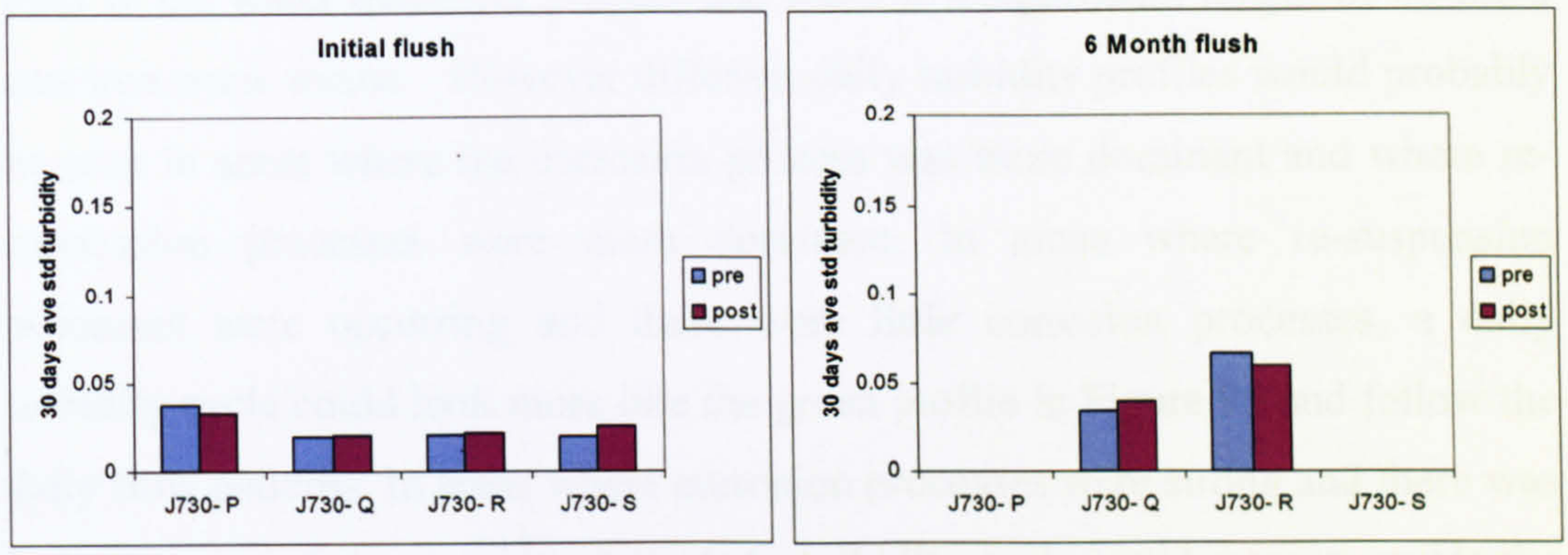

Figure 109 J730 flushing effectiveness.

The assessment of the two flushing operations performed in J730 is shown in Figure 109. The Average standard deviation of turbidity in this zone is much lower than the others and the pre and post flushing results are very similar. A slight improvement is seen at location J730- P and a slight deterioration is seen at location J730- S following the initial flush. J730- Q shows a slight deterioration and J730- R shows an improvement after the 6 month flush. The general increase in the standard deviation of turbidity in the 6 month flush from the initial flush is again a seasonal factor, as the initial flush was performed in the middle of winter.

6.4 Discussion

Analysis of customer contact frequencies in all the zones showed a reduction in frequency. However the reliability of customer contacts as a performance indicator is questionable as discussed in Section 2.1.

6.4.1 The daily turbidity cycle

The amplitude of the daily turbidity cycle (Figure 92) has been used in this study as an indicator of the discolouration potential within a network. Areas with higher amplitudes surest that there is more discolouration material within a network, which is more easily mobilised, than in areas where lower amplitudes are seen.

In this project the daily turbidity cycle has been shown to be a product of both corrosion and re-suspension processes, Figure 95. This is because all the DMAs in the study are fed from a surface water source where iron flocculation is used in the water treatment process and there is a significant length of un-lined cast iron trunk mains. However different daily turbidity profiles would probably be seen in areas where the corrosion process was more dominant and where re-suspension processes were more dominant. In areas where re-suspension processes were occurring and there were little corrosion processes, a daily turbidity cycle could look more like the green profile in Figure 95 and follow the daily flow patterns. In areas where corrosion processes were strong and there was little re-suspension occurring, there daily turbidity cycle could more resemble the red profile in Figure 95 with a single peak occurring at night during the lowest flow periods.

This daily turbidity cycle has great potential in not only gauging the size of the discolouration potential within a network (amplitude of cycle) but also aid in the rehabilitation decision process as the shape of the cycle could indicate the primary cause of the problem, either re-suspension or corrosion.

Further study is recommended in networks of differing characteristics in pipe materials and source water quality to investigate this theory further.

6.4.2 Seasonality in the data

Seasonality is seen in the Standard Deviation of Turbidity data. Figure 110 shows the average standard deviation of turbidity (SdN) recorded per month at each of the monitoring locations. Here it can be seen that in all locations a greater SdN is recorded during the summer periods than in the winter. This seasonality is seen more clearly in Figure 111 where the average of all monitoring locations per month is plotted. This average is however somewhat

biased by locations C050-A and C050-B which have the strongest seasonality trend. The peak occurring in November 2005 (Figure 111) is uncharacteristic of the trend, but can be attributed to a burst which occurred in A285 and (Appendix 1, A285- 7).

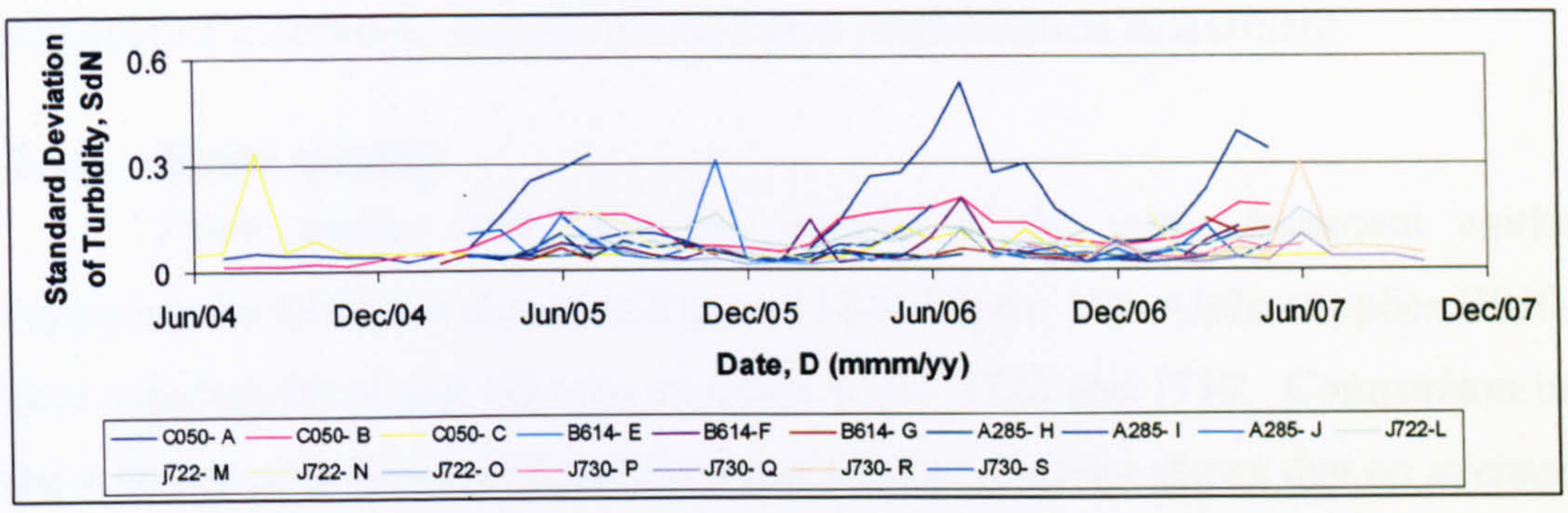

Figure 110Average standard deviation of turbidity per month

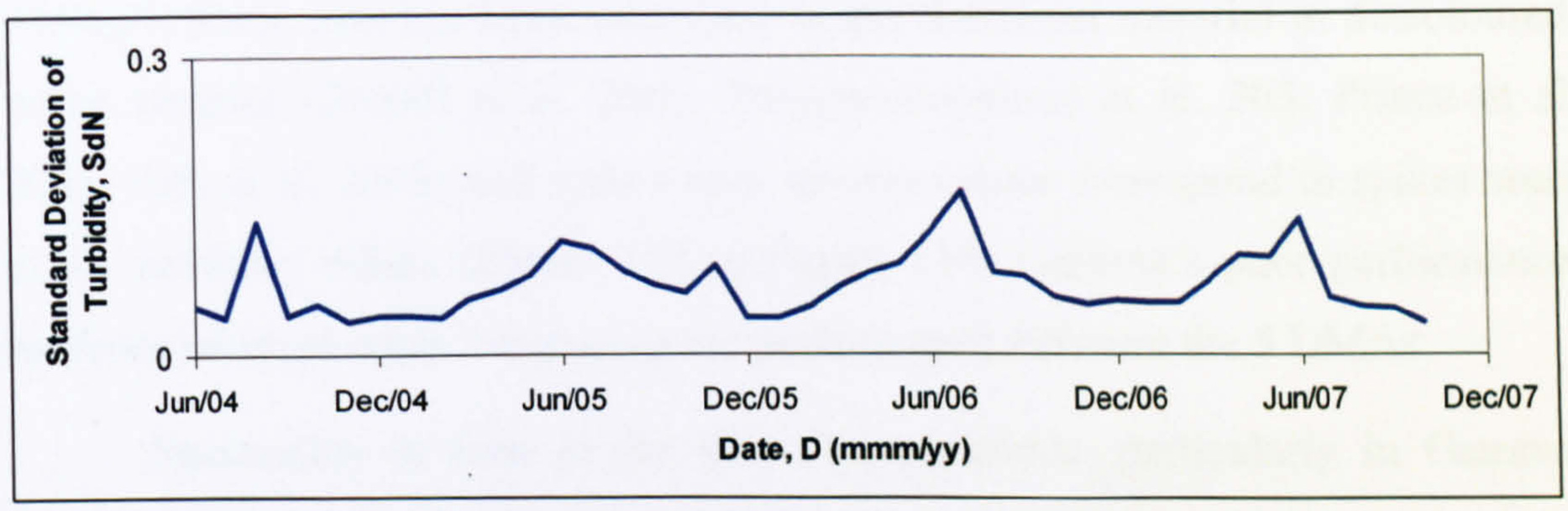

Figure 111 Average standard deviation of turbidity of all locations per month

Typical examples of the summer daily turbidity cycle are shown in Appendix 1 C050 8 and 13. In Figure 95 it is suggested that the daily turbidity cycle is a product of both corrosion and re-suspension processes. Temperature has been shown to increase corrosion and biofilm development rates (Holden et al. 1995). Increased demand during the summer can create increased shear stresses and therefore increased re-suspension in the network.

Further evidence that this seasonality is a factor of a corrosion process is that C050-B displays some of the strongest seasonality effects and is the only location on a bitumen lined cast iron pipe in this project. Personal communications with Yorkshire Water personnel indicate that bitumen linings are of such poor quality that for all intense and purpose they can be treated as unlined cast iron pipe. Conversely to this theory, C050-A displays the strongest seasonality effect but is situated on a HPPE pipe installed in 1999. However, both C050-A and C050- B are located fairly close to the DMA inlet and

corrosion occurring in the trunk mains outside the DMA could be responsible for the seasonality shown here.

Since temperature clearly affects the amplitude of the daily turbidity cycle seasonality must be taken in to account when assessing the discolouration potential of a network, and any pre and post rehabilitation assessment.

6.4.3 Water quality

Water quality data from the outputs of the water treatment works supplying the DMAs is shown in Figure 112 to Figure 114. Alpha supplies C050, Beta supplies B614 and Gamma supplies A285, J722 and J730. Comparison of the volumes of iron output from the water treatment works shows that on average Gamma outputs 64.6 ug/l, much higher than that of Alpha, 48.5ug/l and Beta, 31.9ug/l. Since iron has been identified as the dominant material in discoloured water samples (Boxall et al. 2003; Polychronopolous et al. 203; Prince et al 2003; Seth at al. 2003) and spikes seen in iron values correspond to spikes seen in the turbidity values (Figure 112 to Figure 114) Gamma's poor performance becomes relevant when comparing the performance between the 5 DMAs

Seasonality is seen in the iron concentrations, particularly in Gamma (Figure 114) where approximately three times the concentration of iron was output during the winter months than during the summer. In the winter period Gamma water treatment works has problems with increased colour in the source water, due to an increase in runoff over peat in the catchment area. To account for this operators increase the dosing of iron used during the flocculation process. Gamma was fitted with a relatively course filtration system which did not effectively retain all the iron. However in October 2006 a new second phase filtration system was installed and a reduction in iron and turbidity leaving the treatment works reduces sharply to an average of 13.4 μg/l.

This new filtration system came on line between the 6 month flush in J722 and the initial flush in J730, and could explain the reduction in the percentage of iron seen in flushing grab samples between the 6 and 12 month flushes in J722 and the initial and 6 month flush in J730, Figure 59.

The poor historical performance of Gamma water treatment works could explain why the three DMAs which are fed from its water experience the highest

proportion of turbidity events attributed to imported material, (Figure 105). However, as B614 also has a relatively high proportion of imported turbidity events (33%) and is supplied by a treatment works with a much lower iron output, the water treatment works cannot be held singularly responsible for imported turbidity material. This is further supported by the fact that increases in iron concentrations are seen at the treatment works during winter periods whereas higher turbidity values are recorded in the DMAs in the summer. This suggests that other in-system processes must be occurring within the trunk mains.

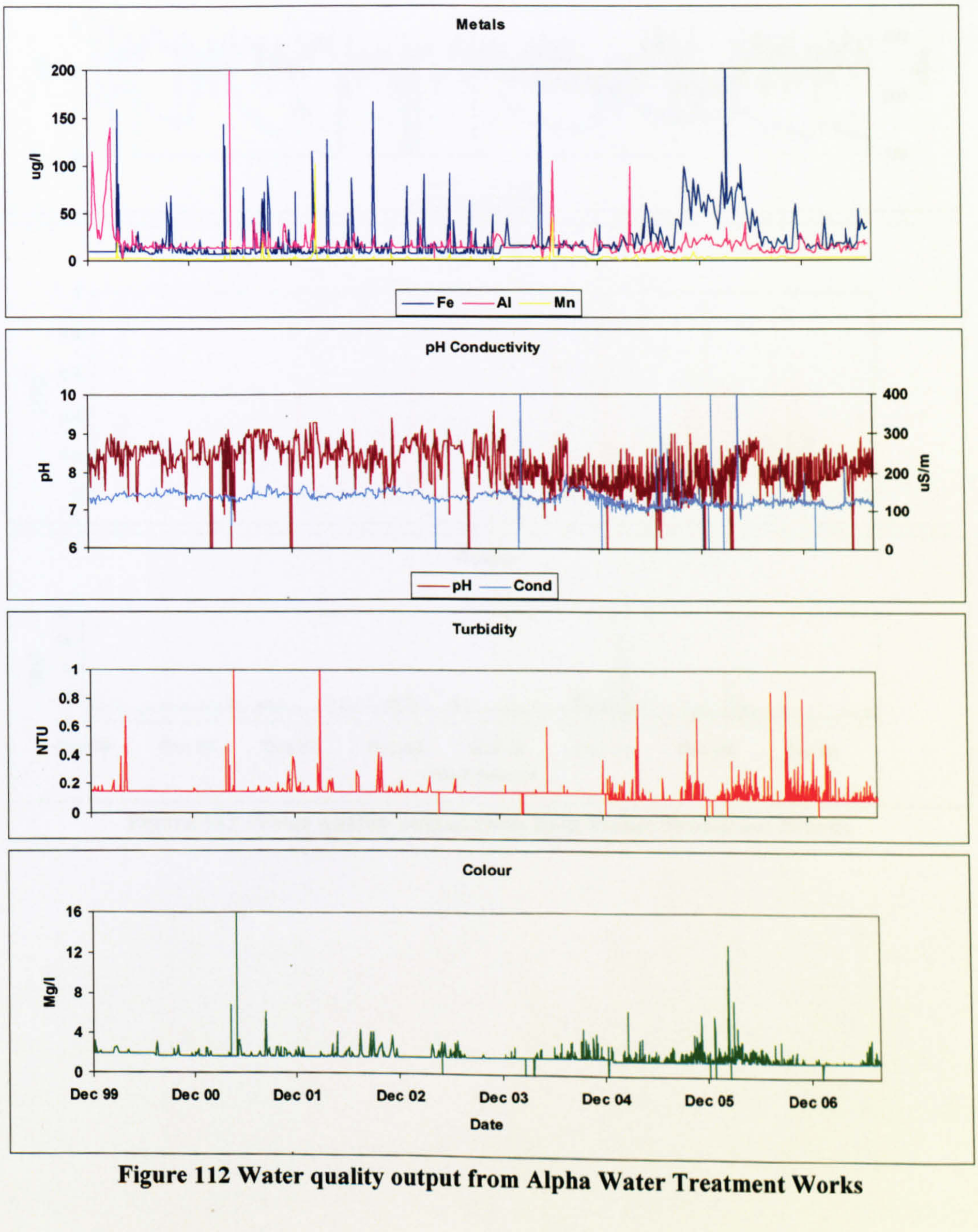

Figure 112 Water quality output from Alpha Water Treatment Works

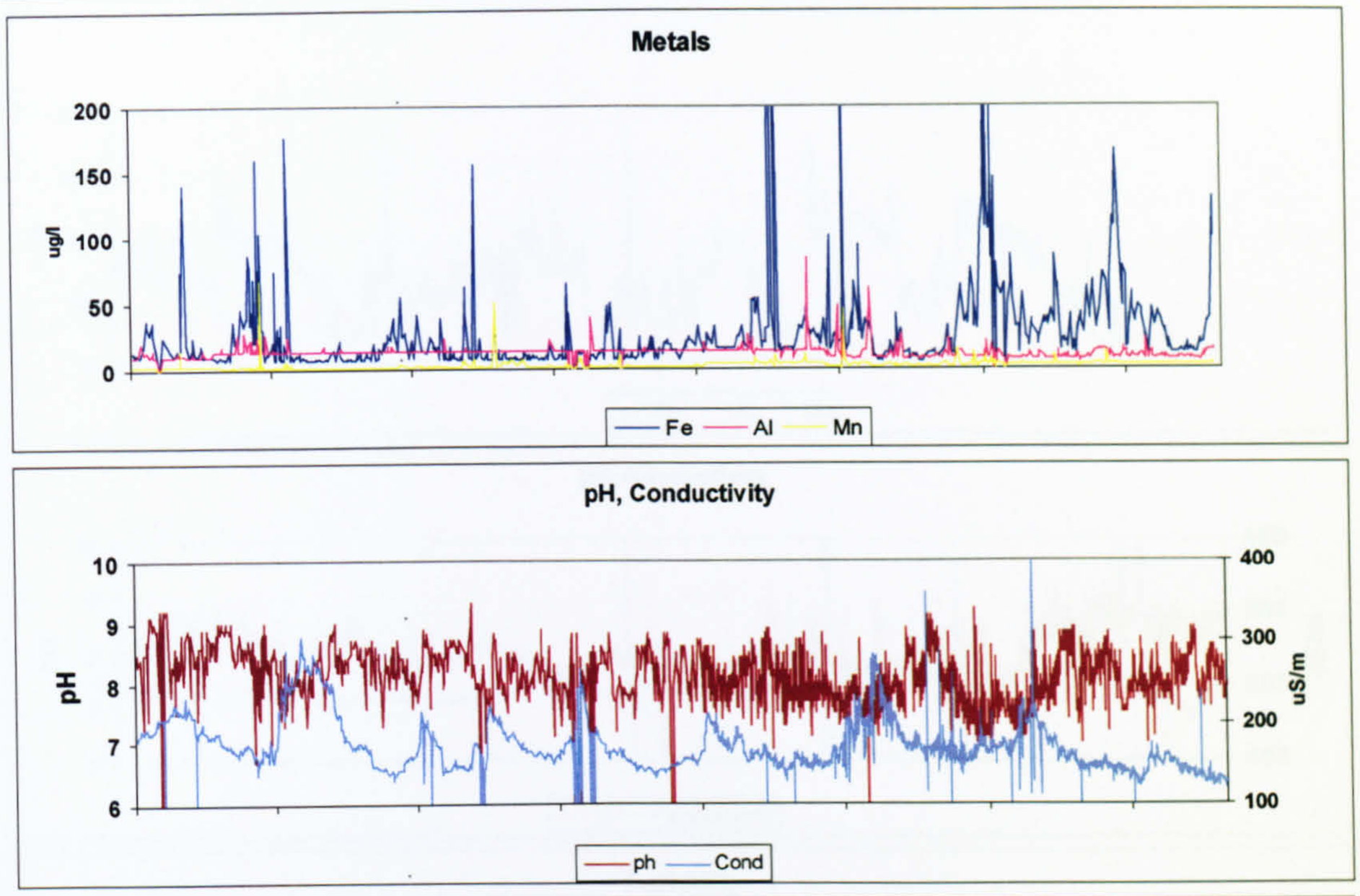

Figure 113 Water quality output from Beta Water Treatment Works

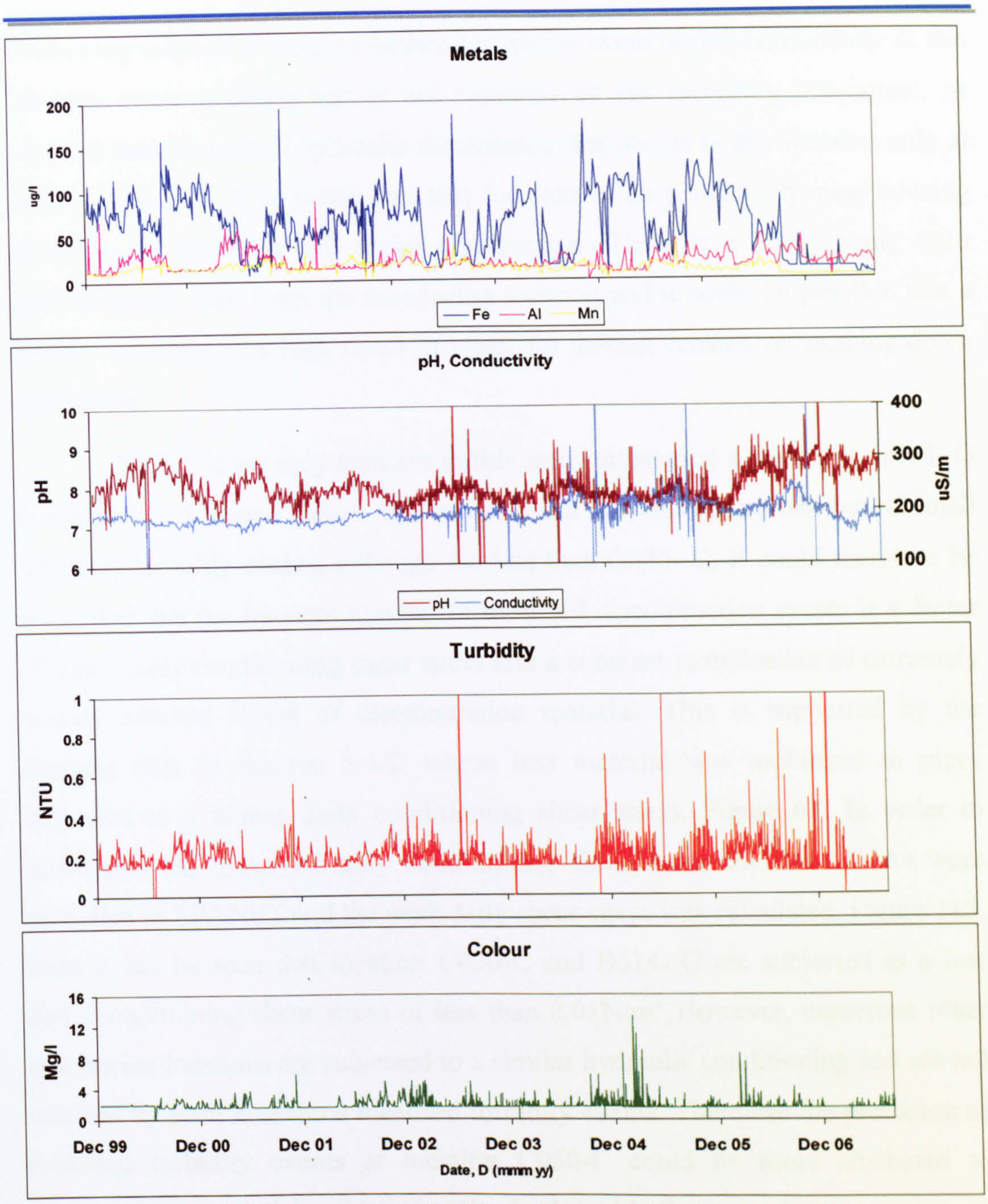

Figure 114 Water quality output from Gamma Water Treatment Works

6.4.4 Network hydraulics

The highest proportion of turbidity events in C050 (Figure 105) are attributed to local events occurring within the DMA. These particularly occur at location C050- C where turbidity spikes occur consistently at 8:00 am which are not seen elsewhere within the network. These events have only been recorded during the weekend, highlighted in Appendix 1. At this location, analysis of the water temperature data shows that the house holder does not draw water after 6:00am indicating that they leave for work early in the morning. Since turbidity loggers installed in MSM chambers only record true turbidity when the customer

is drawing water it is unsure whether a turbidity event occurs consistently at this location every morning and is not captured by the recording instrument, or whether there is a small hydraulic disturbance that occurs in this location only at weekend periods. It is noted that this location is on a relatively new housing development which is still under construction. There is a house being built approximately 50m from the monitoring location and it could be possible that a builder regularly uses high flows of water for mixing cement, or washing down equipment.

C050-C is the only location in this study situated at a dead end. B614- G is situated in a looped part of the network, and has also seen a number of small localised turbidity events, although far less than C050- C. It could therefore be suggested that the frequent number of localised discolouration events is a factor of a low daily conditioning shear stress and a constant mobilisation of extremely weakly adhered layers of discolouration material. This is supported by the flushing data in Section 5.4.2, where less material was mobilised in pipes subjected to a higher daily conditioning shear stress, Figure 63. In order to investigate the effect of daily conditioning shear stress the five DMAs were modelled in EPANET and the peak daily shear stress was calculated, Figure 115. Here it can be seen that location C050-C and B614- G are subjected to a low daily conditioning shear stress of less than $0.01N/m^2$. However, numerous other monitoring locations are subjected to a similar hydraulic conditioning and are not affected by such numerous localised turbidity events. Therefore the profusion of localised turbidity events at location C050-C could be more attributed to discolouration material collecting at the dead- end in the network.

High daily conditioning shear stress are found at locations C050-B, B614-E, A285- H and J722-M where less discolouration material could be expected, but turbidity spikes are still recorded at these locations. This highlights difficulties of comparing the results of turbidity loggers installed at different locations around a network which record the turbidity of the water passing through them, but cannot give an indication of this material's origin, as it could have been mobilised from anywhere upstream. It should be noted however that there is a correlation between clusters of discolouration customer contacts, shown in Figure 81 to Figure 85 and areas of lower daily conditioning shear

stress seen in Figure 115. However the average results form all monitoring locations in a DMA should be used to assess the effectiveness of the rehabilitation method rather than attempting to infer reasons why one particular location showed improvement over another.

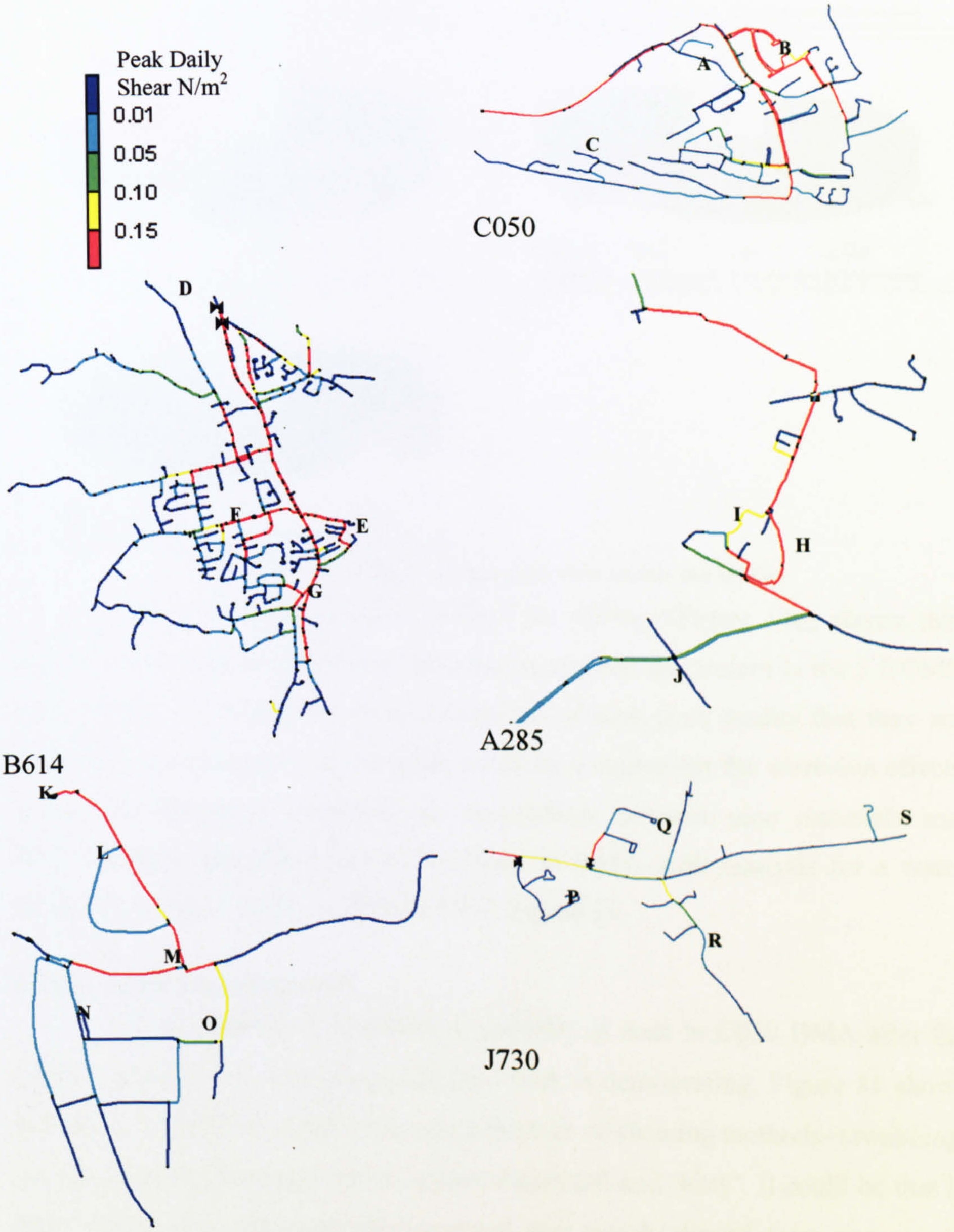

Figure 115 Analysis of peak daily conditioning shear stress.

6.4.5 DMA pipe materials

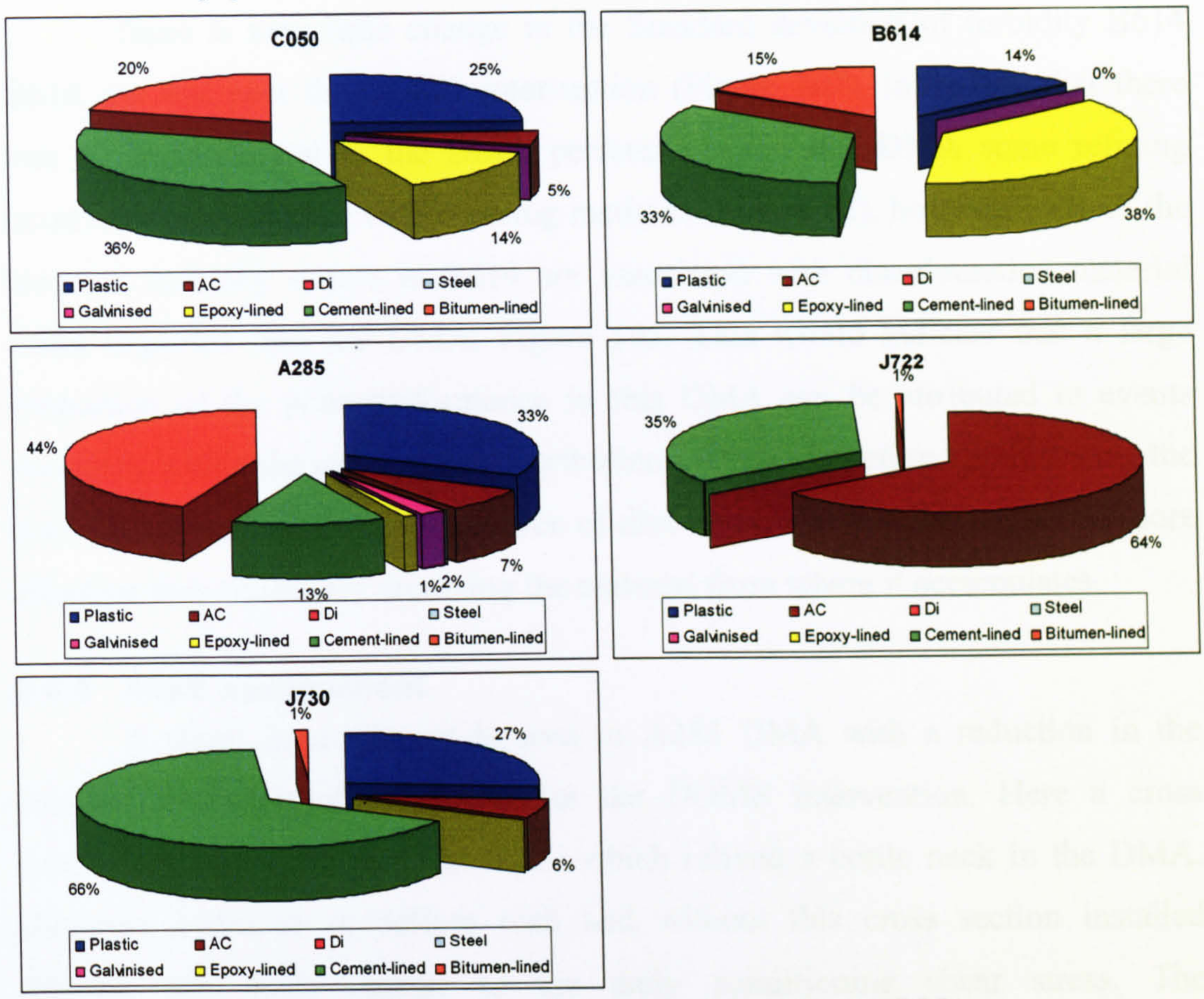

Figure 116 Percentage of pipe materials within the DMAs

Analysis of pipe materials within the DMAs (Figure 116) shows that significant quantities of bitumen lined cast iron pipes are present in the 3 DOMS trial DMAs (15- 44%) As these linings are of such poor quality that they are essentially unlined pipes, these pipes could be a source for the corrosion effects previously discussed. However no correlation between pipe materials and discolouration customer contacts was seen in DMA scale analysis for a water companies' entire region in Section 4.3.2, Figure 14.

6.4.6 C050 assessment

A higher standard deviation of turbidity is seen in C050 DMA after the DOMS intervention, indicating that the DMA is deteriorating. Figure 81 shows that the rehabilitation in this area was a mixture of cleaning methods- (swabbing, air scouring and flushing) which appear disjointed and 'bitty'. It could be that in this method some discolouration material was simply moved from one area to another. Especially if the works did not proceed at the inlet and then progress thought the DMA in order. Of particular concern is the short length of flushing in the middle of the DMA, where a clean water front cannot be guaranteed.

6.4.7 B614 assessment

There is very little change in the Standard deviation of turbidity B614 DMA pre and post the DOMS intervention (Figure 107), indicating that there was no improvement in the DMA performance. In this DMA some relining occurred in conjunction with cleaning methods (Figure 82), however 33% of the recorded turbidity events in B614 are associated with discolouration material being imported into the DMA, Figure 105. This would indicate that a large proportion of the poor performance in this DMA can be attributed to events occurring within the trunk mains distribution system. Therefore rehabilitating the trunk mains and removing the source of discolouration material would be more effective than constantly removing the material from where it accumulates.

6.4.8 A285 assessment

A slight improvement is seen in A285 DMA with a reduction in the standard deviation of turbidity after the DOMS intervention. Here a cross connection was installed (Figure 83) which relived a bottle neck in the DMA. However hydraulic modelling with and without this cross section installed showed very little change to the daily conditioning shear stress. The improvement in this DMA could have been due to the upgrading of water treatment works.

6.4.9 J722 assessment

Improvement was seen after all flushing operations in J722 except for the 7 month flush which showed a worsening. Only a few days after the 7 month flush a large fire occurred at Fletchers Bakery which is located within the same WSZ. The large number of fire appliances in attendance caused an increase in demand in the WSZ mobilising a large volume of discolouration material which was then imported into J722 and affected the post flushing results.

Figure 117 Smoke from Fletcher's Bakery fire.

The large proportion of discolouration events seen in J722 (47%, Figure 105) indicate that the majority of discolouration in this zone is

imported from outside the DMA. However in this situation the full zonal flushing kept ahead of the reseeding effect of poor water treatment and trunk main processes.

6.4.10 J730 assessment

Little change was seen in J730 DMA post the flushing operations. This DMA differs from the others in the study because the network is much newer with 96% of the network being laid after 1970. Standard deviation of turbidity plots (Figure 103) indicate that this DMA was much cleaner that the other DMAs in the study and probably did not require flushing in the first place.

6.4.11 Recommendations

No significant improvement was seen in the turbidity at the monitoring locations in the DOMS trial DMAs post the rehabilitation. This could be attributed to the disjointed 'bitty' approach to the rehabilitation and it is possible that discolouration material could have been moved from one area to another. This could be due to the decision tool used. DRM models the change in velocity in pipes due to an increase in demand; however it then applies a scaling to this value based on the propensity of the pipe bursting in the first place. It could be that this propensity to burst, which is based on expert judgments could be incorrectly weighting the discolouration potential score. This could also be a factor of the velocity criteria used in the DRM model as opposed to a shear stress criteria.

The flushing method used here, based on flushing the entire network, at the highest force consistently attainable, whilst maintaining a clean water front proved more effective in reducing the discolouration potential in the network than the approach applied in the DOMS trial zones. The attractiveness of the flushing program becomes more apparent when considering the economic factors. Although the flushing zones are smaller than the DOMS zones, it only cost in the region of £1000 to flush each of the flushing zones as opposed to the £11,500 that was spent on C050 and £45,000 that was spent in B614.

All of the five DMAs monitored in this project demonstrated that a significant amount of discolouration material was imported into the DMA from elsewhere in the distribution system suggesting that the trunk mains are

constantly reseeding DMAs with discolouration material. It is therefore recommended that addressing discolouration in the trunk main distribution system should be of a higher priority than the DMAs, as addressing the source of the reseeding effect would reduce the return rate in the DMAs themselves.

7 Valve Operations

7.1 Introduction

Within the water industry valve movements have long been thought to create discolouration events, but are frequently necessary for the operational management of distribution systems. Material is thought to be dislodged from the valve mechanism itself as it is moved and be mobilised elsewhere in the system due to changing hydraulics. Hence water companies have a need to be able to predict the discolouration risk of differing valving operations such that they can select the result with the lowest risk. The aim of this section is to model the change in shear in a pipe due to valve closures and to compare these modelled results with field data, by recording turbidity in a live DMA as the valves are closed, with the objective of verifying the method for a simple discolouration risk tool.

It is theorised that closing a valve in a looped network causes increased flows elsewhere within the network, Figure 118. This increased flow will create increased shear stresses on the pipe walls in excess of the daily conditioning shear stress, subject to the time of day the valve movement occurs. This increase in shear stress above conditioning forces could mobilise previously accumulated layers of discolouration material, creating a discolouration event. The risk of discolouration could be proportional to the increase from the daily maximum shear stress.

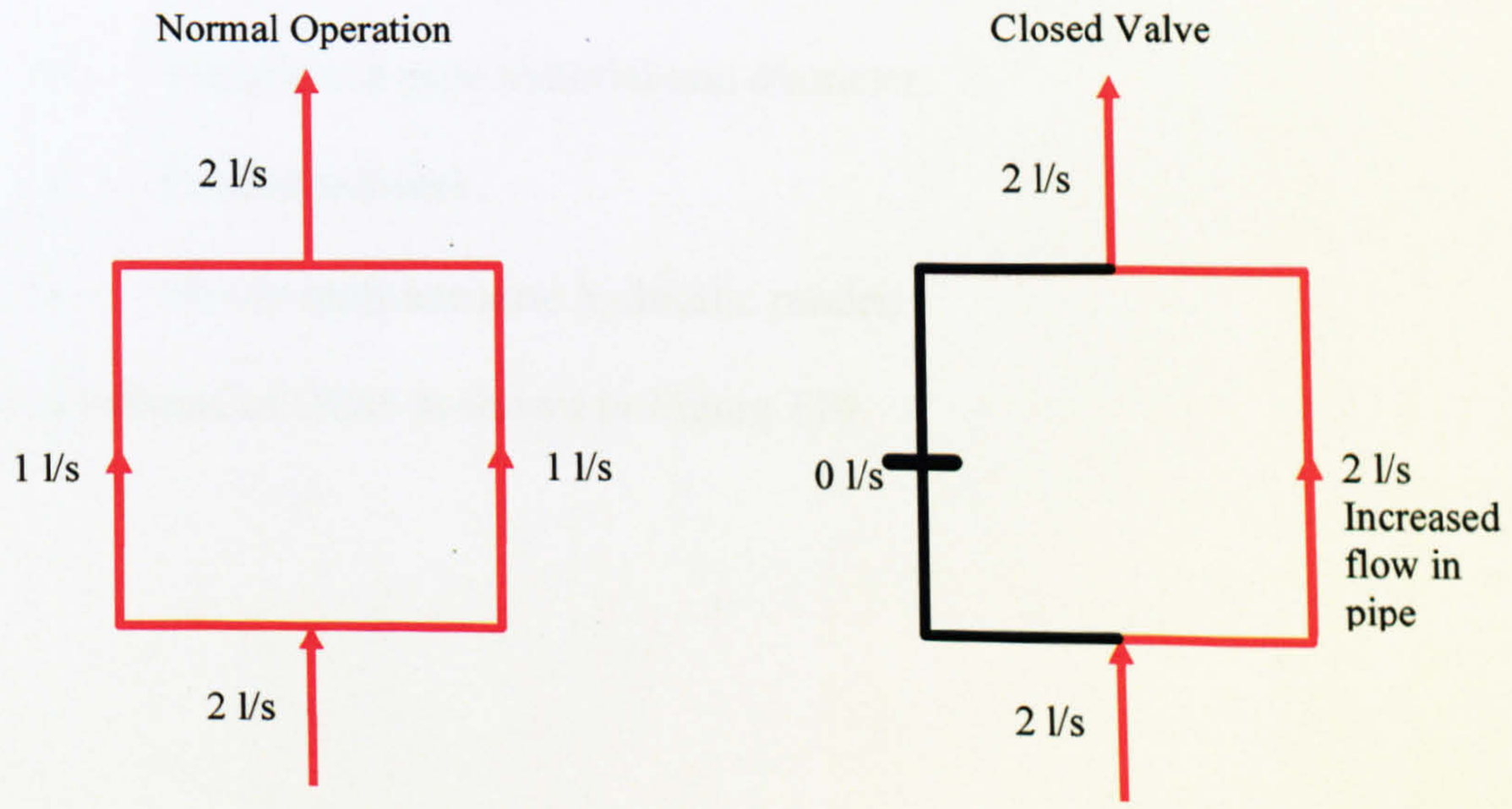

Figure 118 Idealised increased flow and therefore shear due to valve closure

7.2 Method

The method employed in monitoring valve movements followed a logical progression involving several key stages briefly outlined below:

- Planning and initial hydraulic modelling.
  - Site selection.
  - Modelling the hydraulic effect of valve closures to plan turbidity monitoring locations.
- Field work-
  - Collection of pressure data to validate the hydraulic model being used.
  - Turbidity monitoring during the valve movements.
- Post Processing:
  - Validation of the hydraulic model based on flow and pressure data.
  - Re – modelling valve closures at time of closure.
  - Modelling valve closures at different times of the day.

7.2.1 Planning and Hydraulic Modelling

Initial planning involved choosing an appropriate DMA for the study. G286 was chosen based upon:

- Manageable size (266 properties).
- Variation in pipe material and diameter.
- Looped network.
- Newly built accurate hydraulic model.

A schematic of G286 is shown in Figure 119.

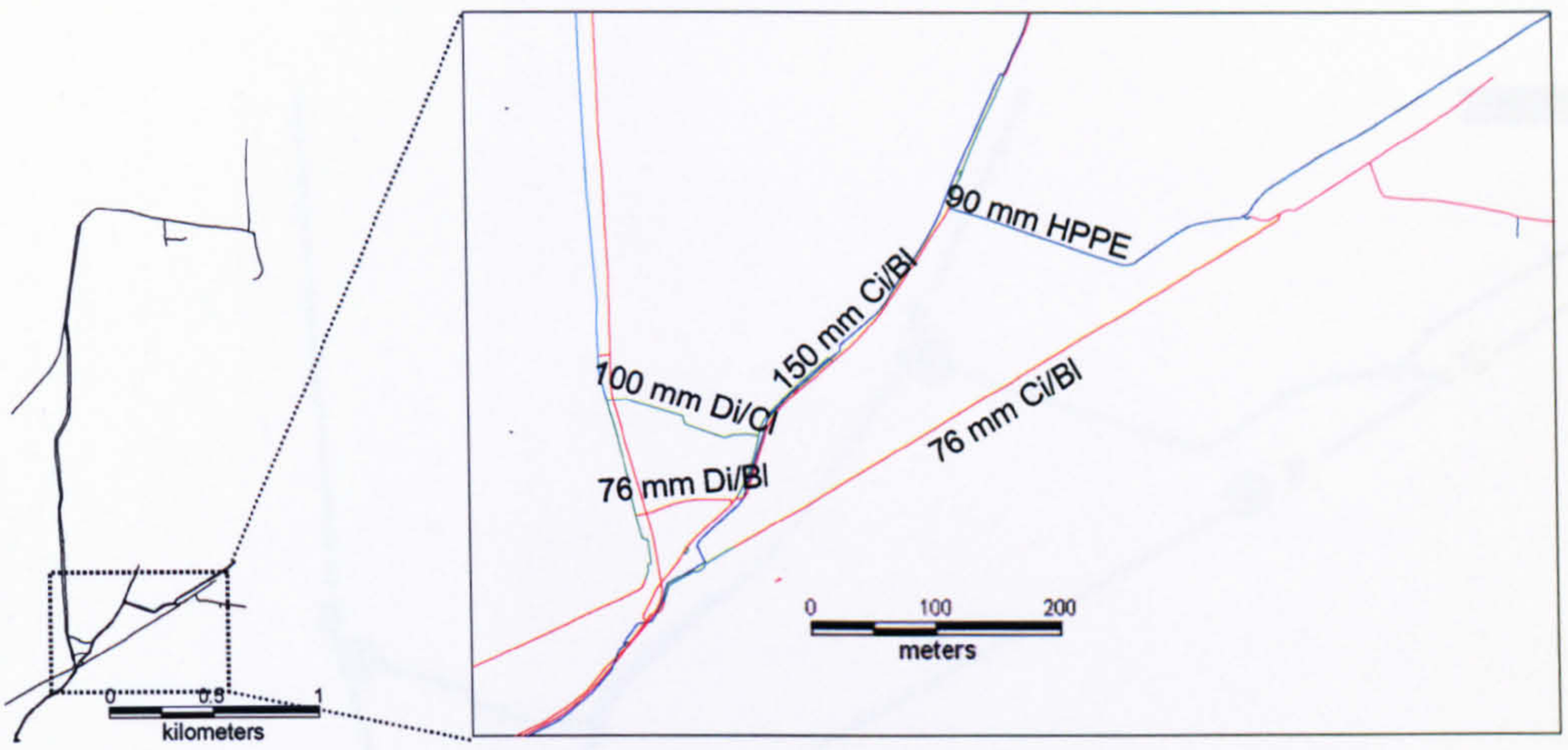

Figure 119 G286 DMA.

To assess the hypothesis it would be necessary to generate a modicum of discolouration. However, it must be stressed that these operations were performed on a 'live network' and water companies cannot intentionally cause discolouration or be seen to use their customers as 'guinea pigs'. Therefore G286 was chosen as it was considered of having a low discolouration risk based upon historical customer contact frequencies and regulatory sampling results. To further limit the impact on customers letter warnings were sent. In discussions with the water company it was decided that valves would have to be closed in a controlled stepped manner, whilst closely monitoring the turbidity in real time. Experienced water company personnel were on hand to stop operations if turbidity reached unacceptable levels, and a flushing plan was devised as a contingency measure.

It was deemed possible to close and monitor four valves operations in one day. These valves were located on the central looped part of the network to ensure that no customers would be cut off from supply during their operation, Figure 120.

A Hydraulic simulation was run and the modelled headloss in each pipe at peak flow was used to calculate the peak daily shear stress, and thus daily conditioning shear stress for each pipe, using Equation 6, Section 5.3.2.3. Peak daily flow conditions are seen in Figure 120.

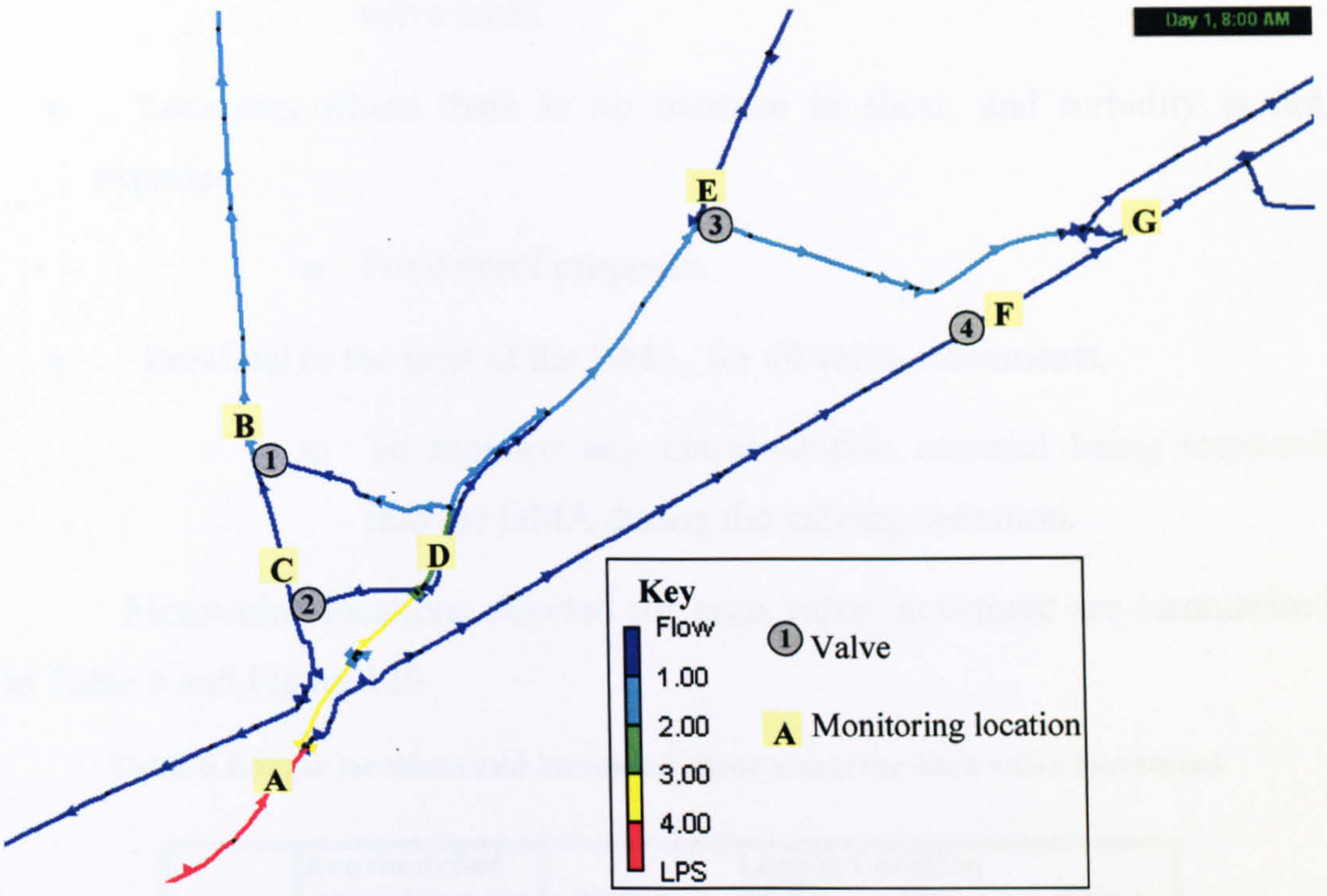

Figure 120 Peak daily flow conditions, valves and monitoring locations

Each of the four valves closures were simulated in the model by simply closing a pipe at peak daily flow, then shear stress for every pipe were calculated. The increase in shear stress above the peak daily value for each pipe was then investigated. Areas where the shear stress generated by the valve closure was less than the peak daily shear stress were given a value of zero. The higher the increase in shear for each pipe, the higher the probable discolouration risk.

Based on the areas of probable discolouration indicated by the model, monitoring locations for the field work stage of the project were chosen. Four sets of turbidity monitoring equipment were available for the project, and for each of the valve movements, locations were chosen on hydrants based on the following criteria:

- Downstream of where turbidity is expected,
    - Based on modelled shear increases.
- Immediately downstream of valve, where possible,

- To record discolouration material mobilised form the valve itself.

- Locations where there is no increase in shear, and turbidity is not expected,
  - For control purposes.
- Proximal to the inlet of the DMA, for all valve movements,
  - To monitor any discolouration material being imported into the DMA during the valving operation.

Monitoring locations selected for each valve movement are summarised in Table 6 and Figure 120.

Table 6 Logger locations and increased shear stress for each valve movement.

Valve	Ave modelled shear increase	Logger Location C&T 1	C&T 2	C&T 3	C&T 4
1	0.53	A	B	C	D
2	0.23	A	B	C	D
3	1.36	A	B	E	F
4	0.12	A	B	E	G

Primary turbidity monitoring location
Secondary turbidity monitoring location
(Where primary turbidity will travel based on flow/ transport paths)

7.2.2 Field work

Two days before field operations were scheduled pressure loggers were deployed at locations shown in figure 4. This would allow for one full days logging of the network running in normal conditions. The data collected would be used to verify the accuracy of the hydraulic model and facilitate model re-calibration if necessary in the post processing stage of the project. Pressure loggers were removed the day after the valving operation.

For each valve movement monitoring equipment, described in section 5.2, was set up on hydrants at locations depicted in Table 6 and Figure 120, using the method previously described in section 5.3.4.1. The appropriate valve was closed in a step manner. Monitoring continued for at least the duration of two pipe volumes of water from the start of the effected pipe to the primary monitoring locations, or until no more turbidity was observed.

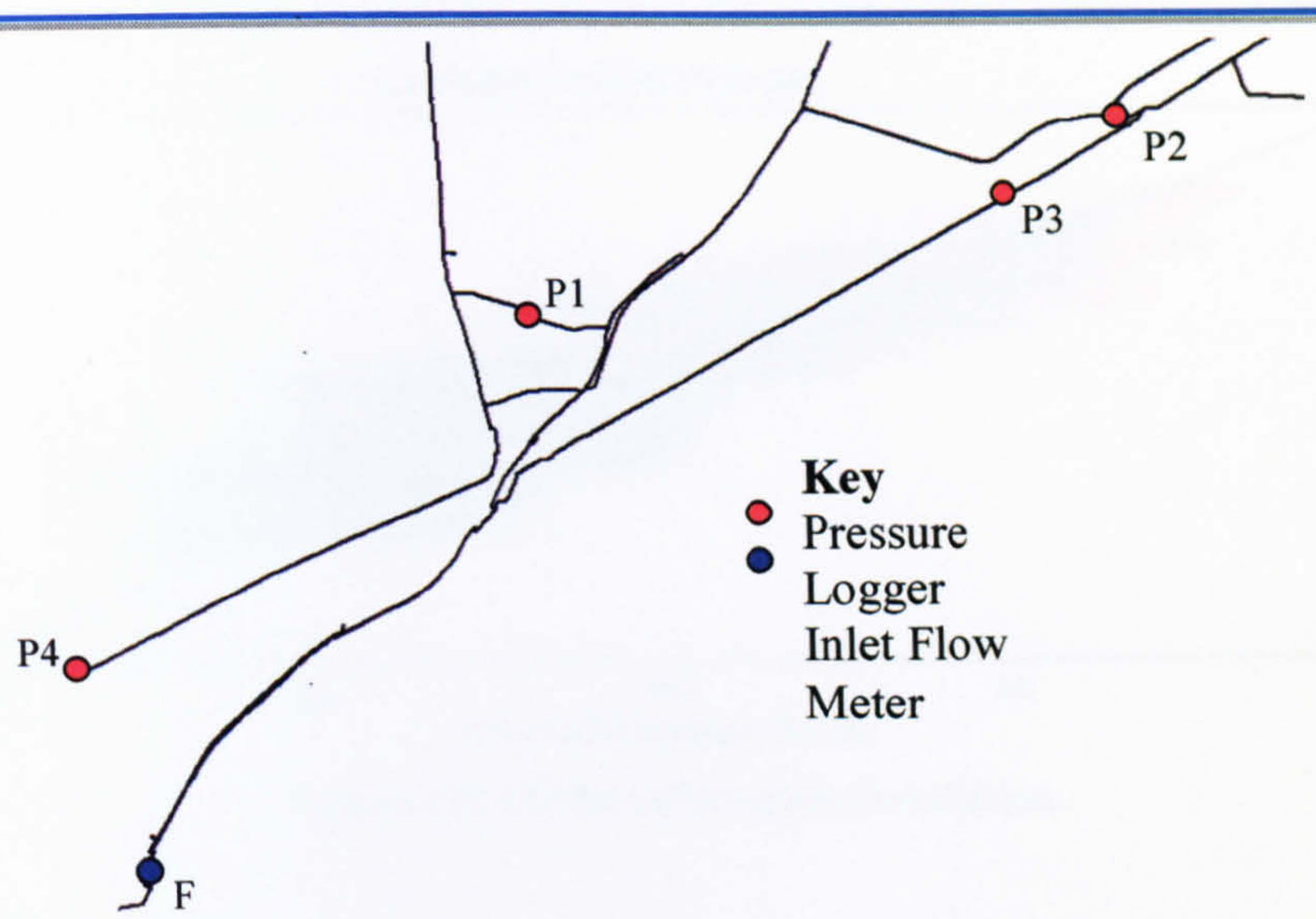

Figure 121 Pressure logger locations.

Hach readings were taken frequently during the operation (every couple of minutes during turbidity events) to provide an independent measure of turbidity to validate the equipment. All timings of the operation including when the valves were closed and by how many turns was carefully noted.

7.2.3 Model Calibration

Pressure data collected from the day before valving operations along with the flow profile at the inlet meter to the DMA was used to validate the hydraulic model. The model was recalibrated to reflect the flow and pressure conditions at the time of the valving operation. New demand and leakage profiles were calculated using the modelling contractor's software. Flow at the meter was used as the boundary condition and pressure at the inlet was adjusted so the profiles matched. The calibrated results are shown in Figure 122. The model calibrates well with an RMS error of 2.8. The apparent scatter in the x axis is because the hydraulic model runs on a 1 hour hydraulic time step, and the pressure data was at 1 minute intervals. The model time step in the model could not be reduced, as every node had a unique demand pattern assigned.

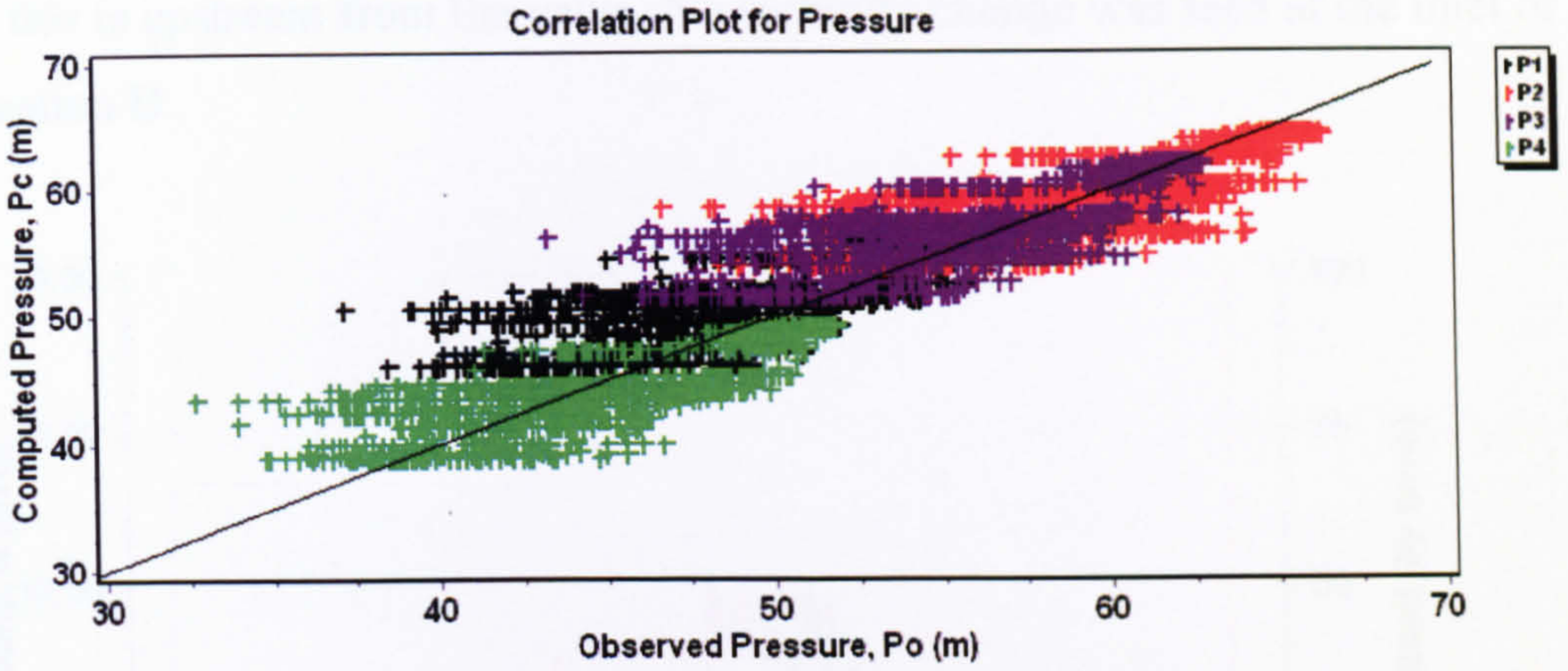

Figure 122 Model calibration correlation.

7.2.4 Post processing

Valve closures were remodelled at the time of closure and all figures of modelled shear stresses seen in the results section reflect recalibrated model data at time of valve closure.

For each stepped valve movement the diameter of open pipe was estimated using the percentage closed by number of turns of the valve. For example if a valve on a 100mm pipe takes 9 turns to close it, after 4.5 turns the valve would be 50% closed and the insertion of a short length of 50mm pipe in the model would reflect this condition.

The four valve closures were also modelled at the time of peak daily flow, and minimum night flow to assess the impact of flow conditions and valve scheduling on discolouration risk.

7.3 Results

7.3.1 Valve 1 closure

The turbidity response to valve closure 1 is seen in Figure 123. Turbidity is first seen, as expected, at location C as it is immediately downstream of pipe where an increase in shear was expected. The same turbidity profile is recorded with a slight delay at location B which is located further down the flow path. The two distinct turbidity traces are seen at both locations which have a broad profile and reach a maximum of approximately 10 NTU. The initial three turbidity spikes seen at 10:58, 11:00 and 11:07 at location B represents discolouration material dislodging from the valve mechanism itself, and is not seen at location C

as this is upstream from the valve. No turbidity change was seen at the inlet or at location D.

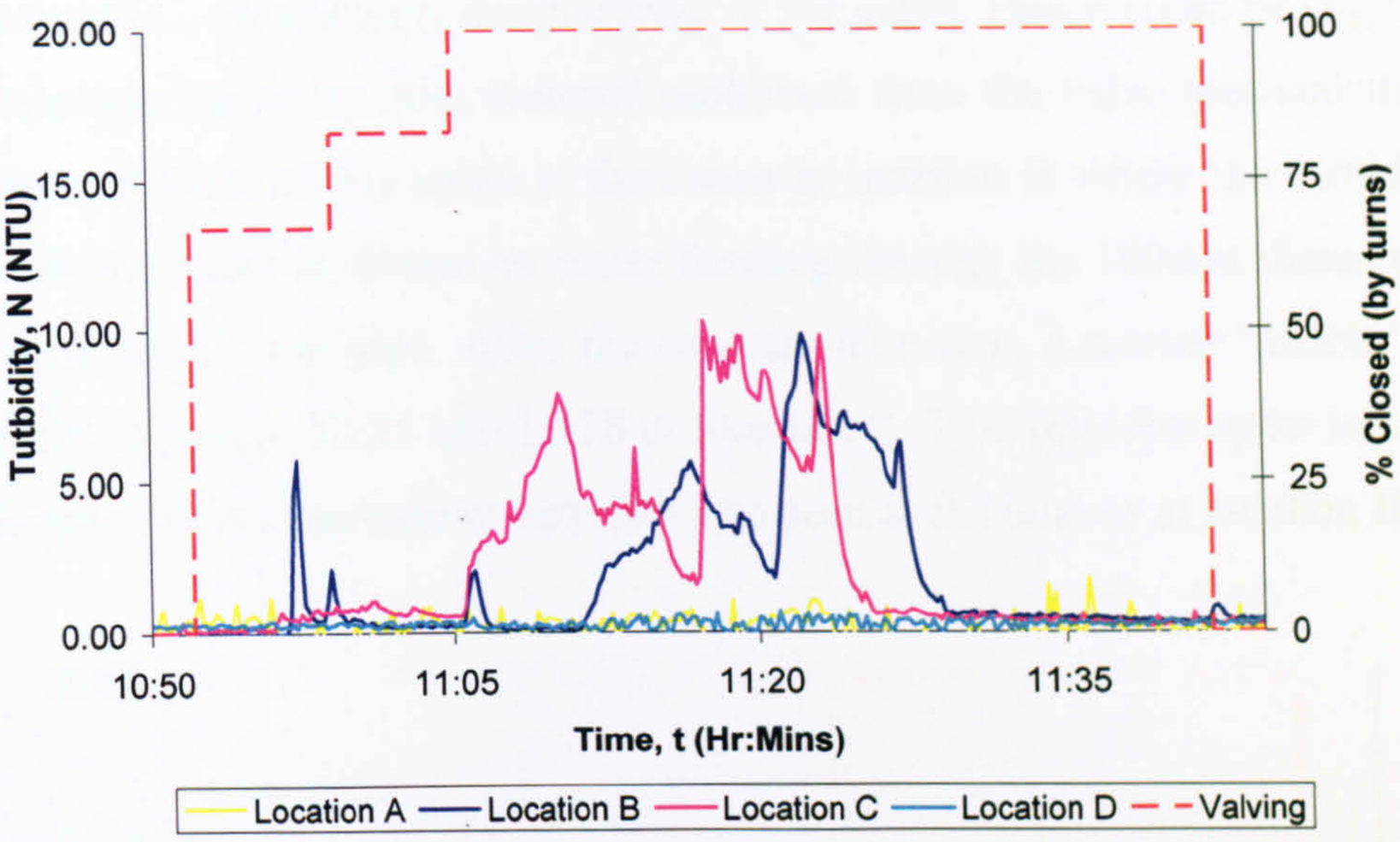

Figure 123 Turbidity recorded during valve operation 1.

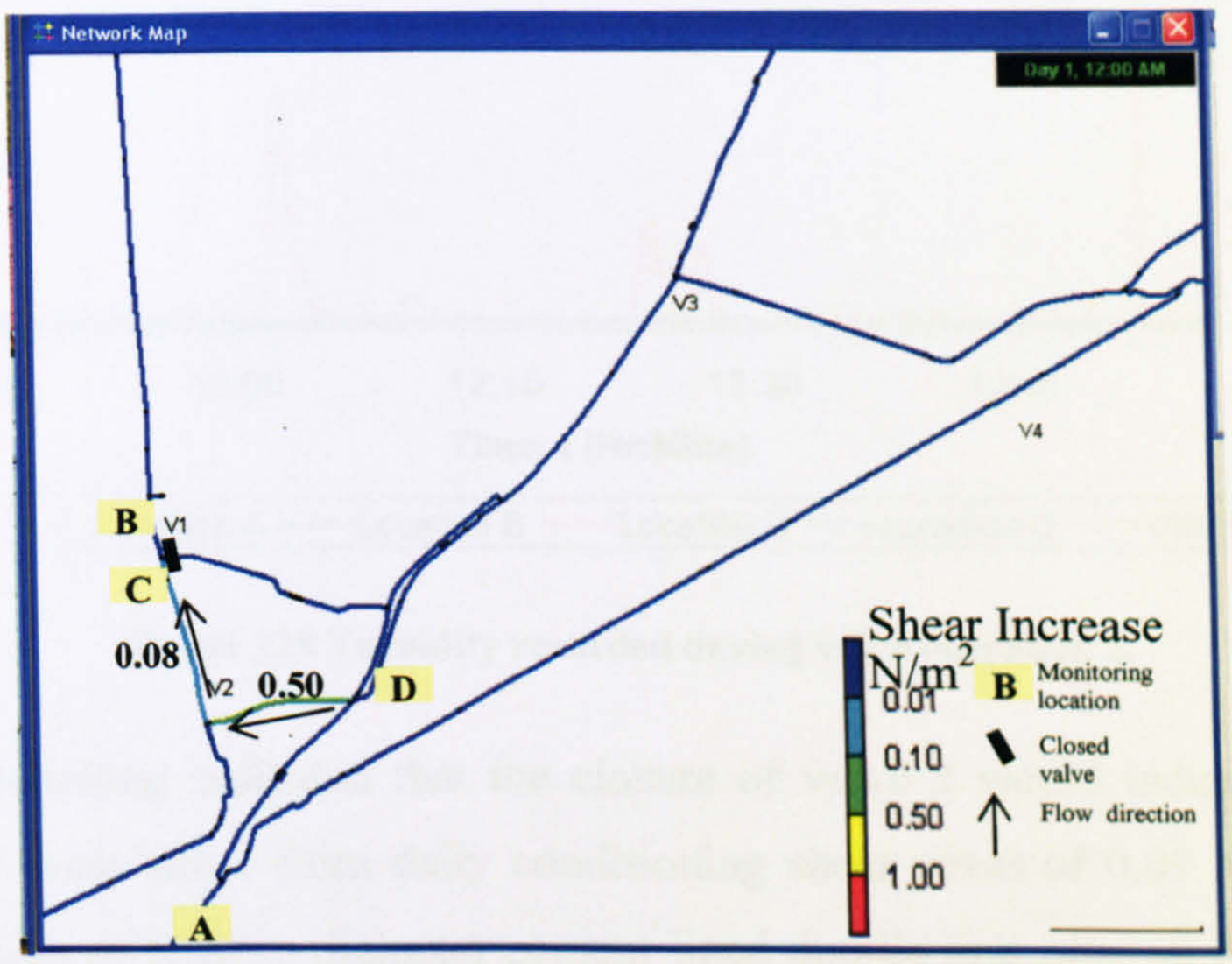

Figure 124 Valve operation 1 modelled closure.

Modelling of the valve movement at time of closure indicated that the closure of valve 1 induced an increased shear stress of 0.5 N/m^2 from the daily conditioning shear stress in the 78m long 76mm diameter bitumen lined ductile iron pipe on the opposite side of the loop from the valve indicated in green in Figure 124. A slight increase is also seen in the loop of 0.08 N/m^2 in the 100mm diameter epoxy lined cast iron pipe section.

7.3.2 Valve 2 closure

Field data depicted in Figure 125 displays the turbidity response seen during valve closure 2. An initial narrow spike of 7.5 NTU is seen at 12:03 at location C, immediately down stream of the valve. Hence it can be suggested that its origin has to be from material mobilised from the valve mechanism itself. A reduced form of this spike is then seen at location B where the turbid material from the valve is diluted by water flowing through the 100mm diameter cement lined ductile iron pipe. After the second valve step, a second 'double' turbidity spike is seen at 12:25 and 12:28 at location C. This turbidity spike is not seen at location B. No increase in turbidity was seen at the inlet or at location D.

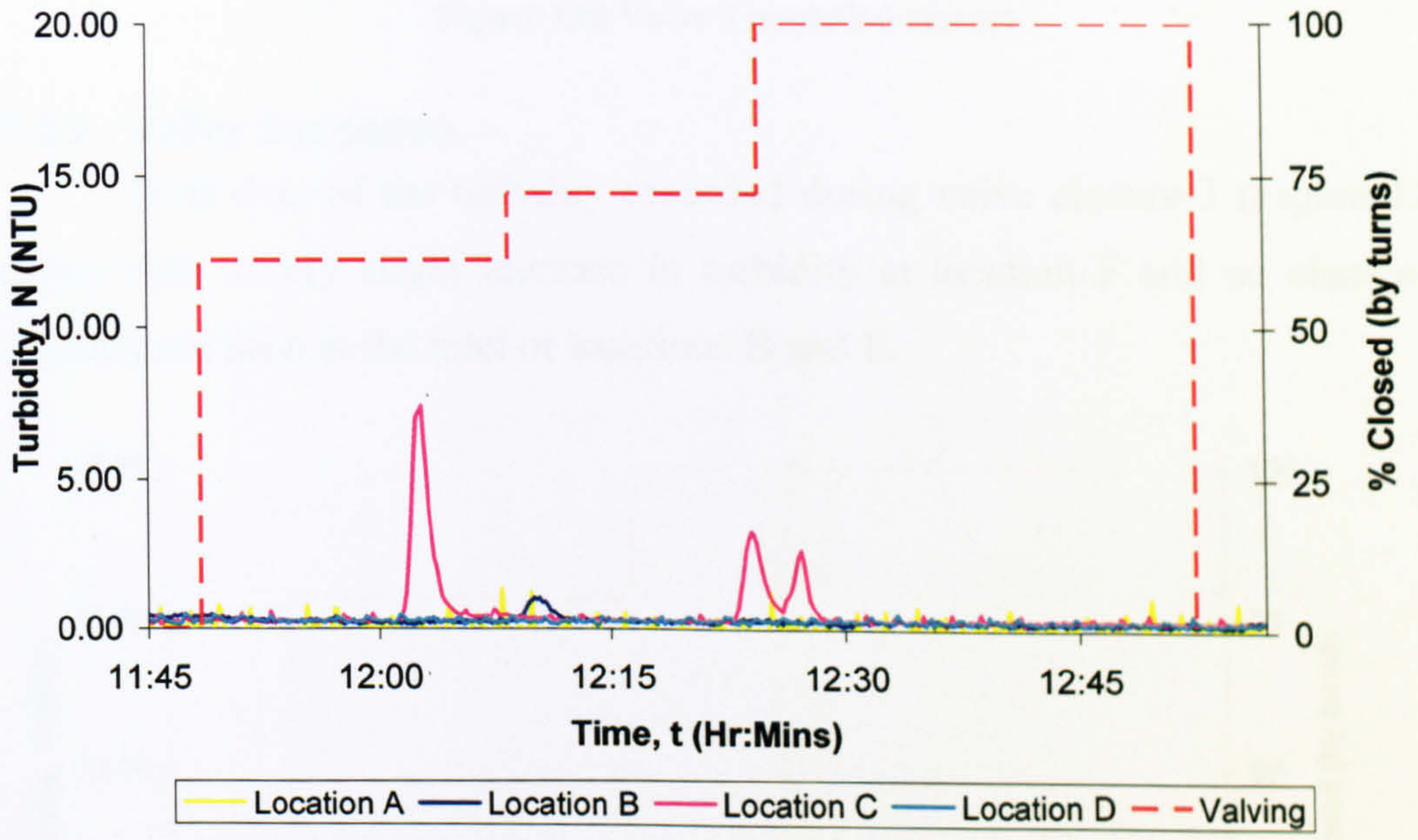

Figure 125 Turbidity recorded during valve operation 2.

Modelling indicated that the closure of valve 2 would induced a slight increased shear stress from daily conditioning shear stress of 0.09 N/m^2 in the 129m length of 100mm diameter cement lined ductile iron pipe on the opposite side of the loop from the valve, Figure 126. A very small increase of 0.02 N/m^2 is also seen in the 54m length of 100mm diameter cement lined ductile iron pipe section of the loop.

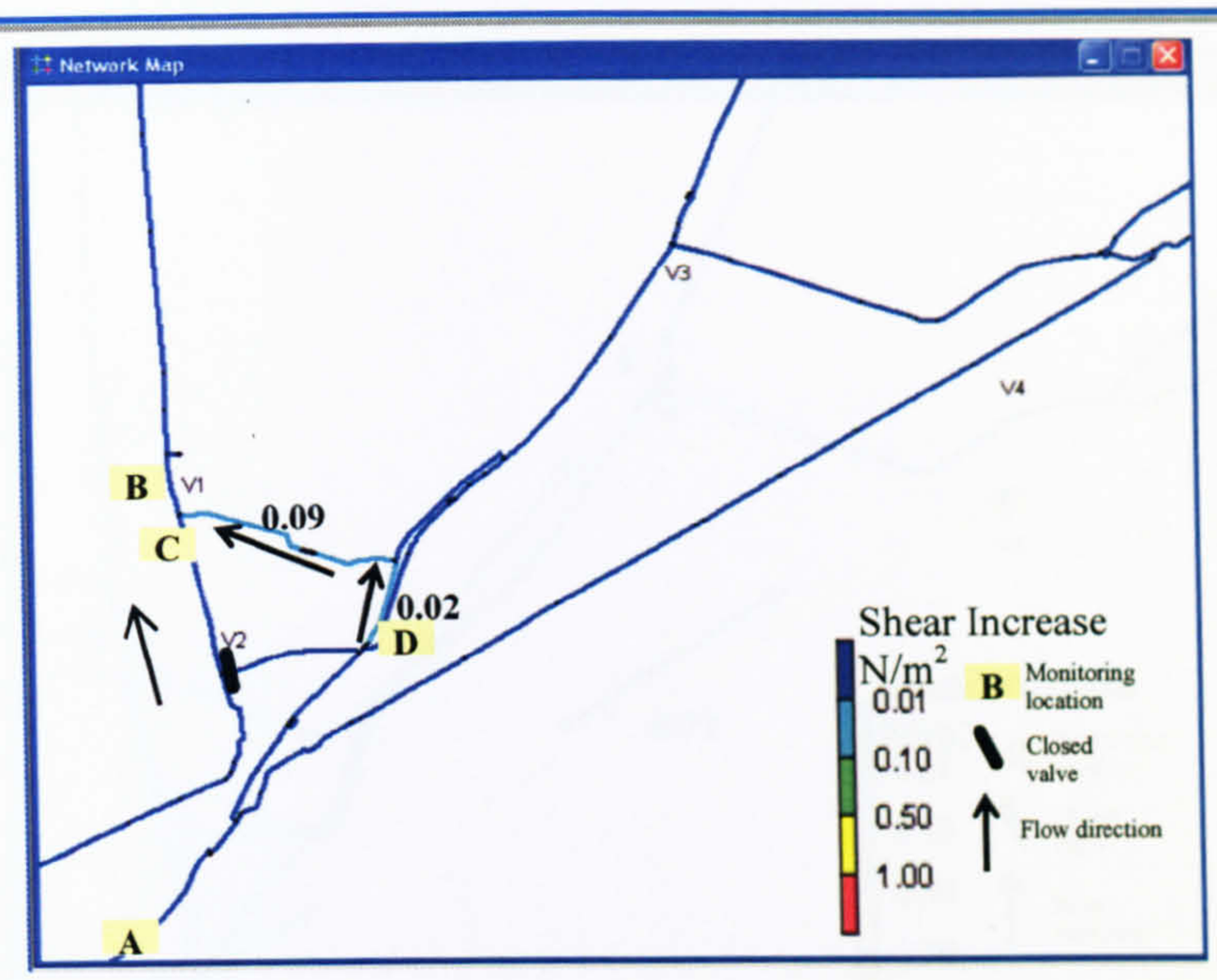

Figure 126 Valve 2 modelled closure

7.3.3 Valve 3 closure.

Field data of the turbidity recorded during valve closure 3 (Figure 127) shows only a very slight increase in turbidity at location F and no change in turbidity are seen at the inlet or locations B and E.

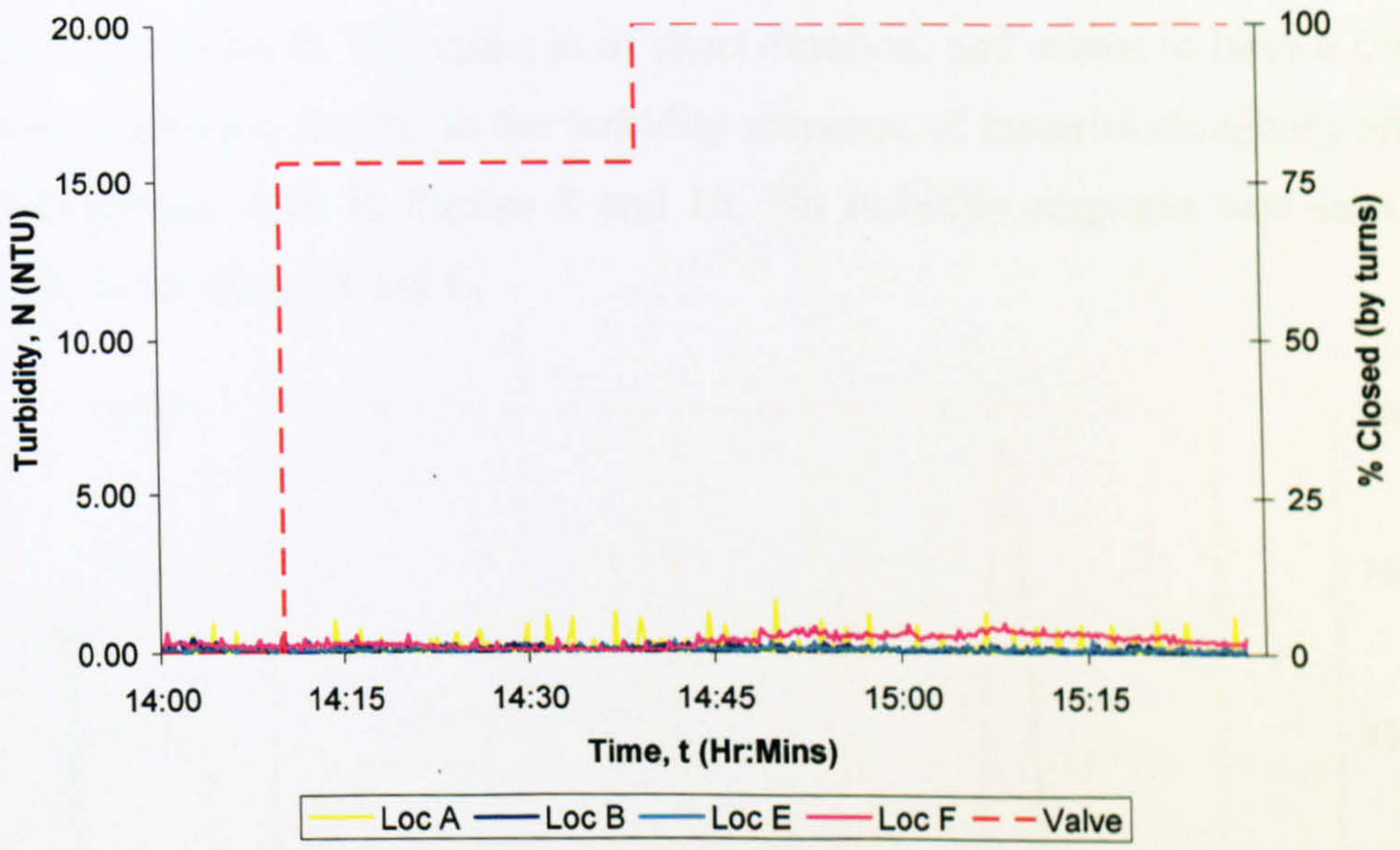

Figure 127 Turbidity response to valve closure 3.

Modelling indicated that the closure of valve 3 would induced the largest increase in shear stress from daily conditioning shear stress of an average of 0.72 N/m^2 in the 561m long 76mm diameter bitumen lined cast iron pipe on the opposite side of the loop from the valve, Figure 128.

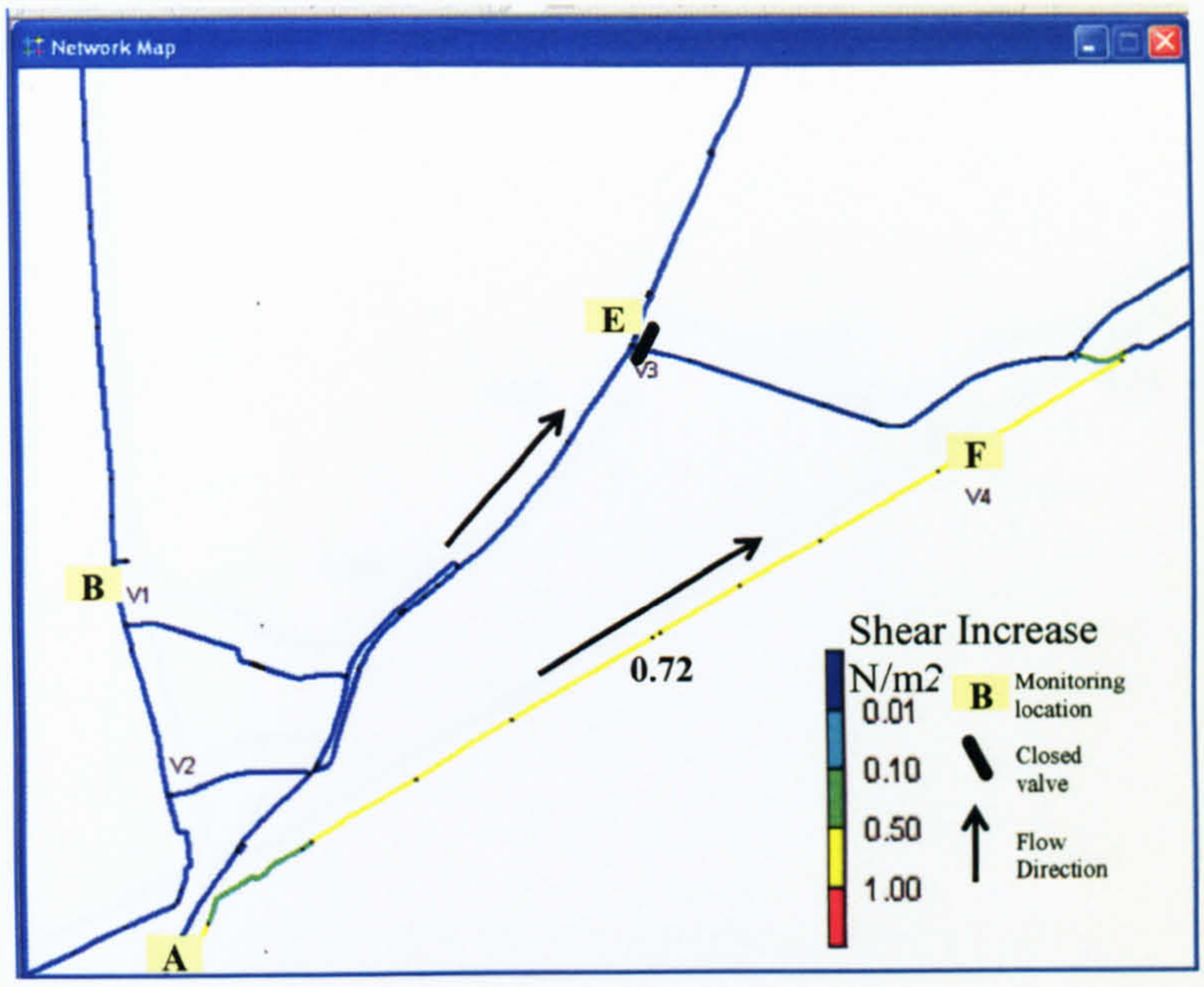

Figure 128 Valve 3 modelled closure

7.3.4 Valve 4 closure.

The turbidity response to the closure of valve 4 is shown in Figure 129. Several small spikes are seen at location G which can be attributed to material sloughing off valve 4, Figure 14. At 16:24 a large turbidity spike of 19 NTU is seen at location G. The spike is of short duration, and seems to have a Gaussian like distribution similar to the turbidity response of material sloughing off valve mechanisms, seen in figures 8 and 10. No turbidity response was seen at the inlet, or locations B and E.

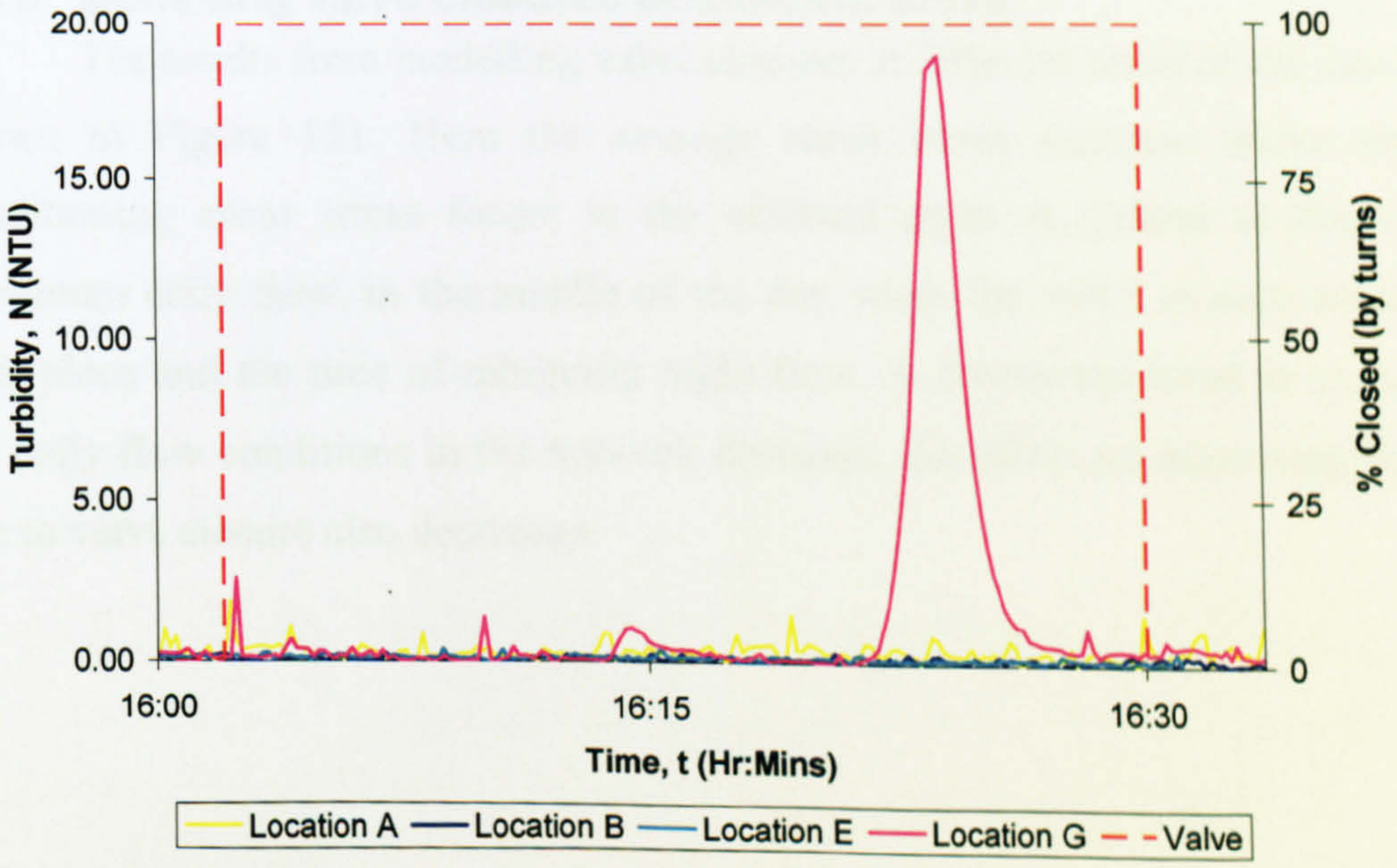

Figure 129 Turbidity recorded during closure of valve 4.

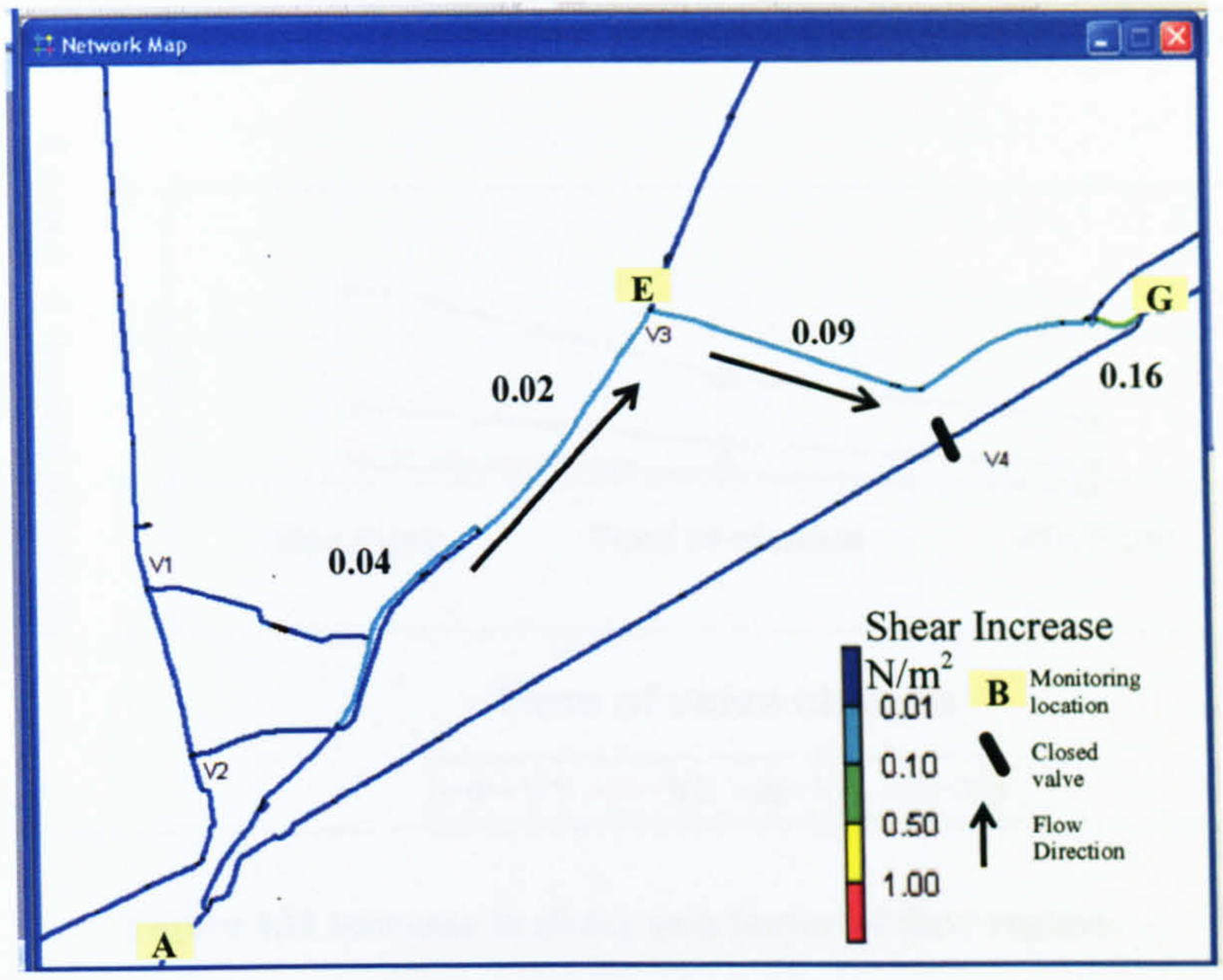

Figure 130 Valve 4 modelled closure

Modelling indicated that the closure of valve 4 induced a slight increase from daily conditioning shear stress of on average 0.09 N/m^2 in the 90mm diameter HPPE pipe on the opposite side of the loop from the valve, Figure 130. A shear stress of 0.02 N/m^2 affected the 150mm diameter bitumen lined cast iron pipe and 0.04 N/m^2 in the 100mm diameter cement lined ductile iron pipe. An increase of 0.16 N/m^2 is seen in the 76mm cement lined cast iron pipe, however this was not perceived as significant for this valve movement as this pipe was already subjected to 0.3 N/m^2 shear stress increase during valve operation 3.

7.3.5 Modelling valve closures at different times

The results from modelling valve closures at different times of the day are shown in Figure 131. Here the average shear stress increase above daily conditioning shear stress forces in the effected pipes is plotted at times of maximum daily flow, in the middle of the day when the valve closure actually took place and the time of minimum night flow. A downward trend is seen, as the daily flow conditions in the network decrease, the effect on increasing shear due to valve closure also decreases.

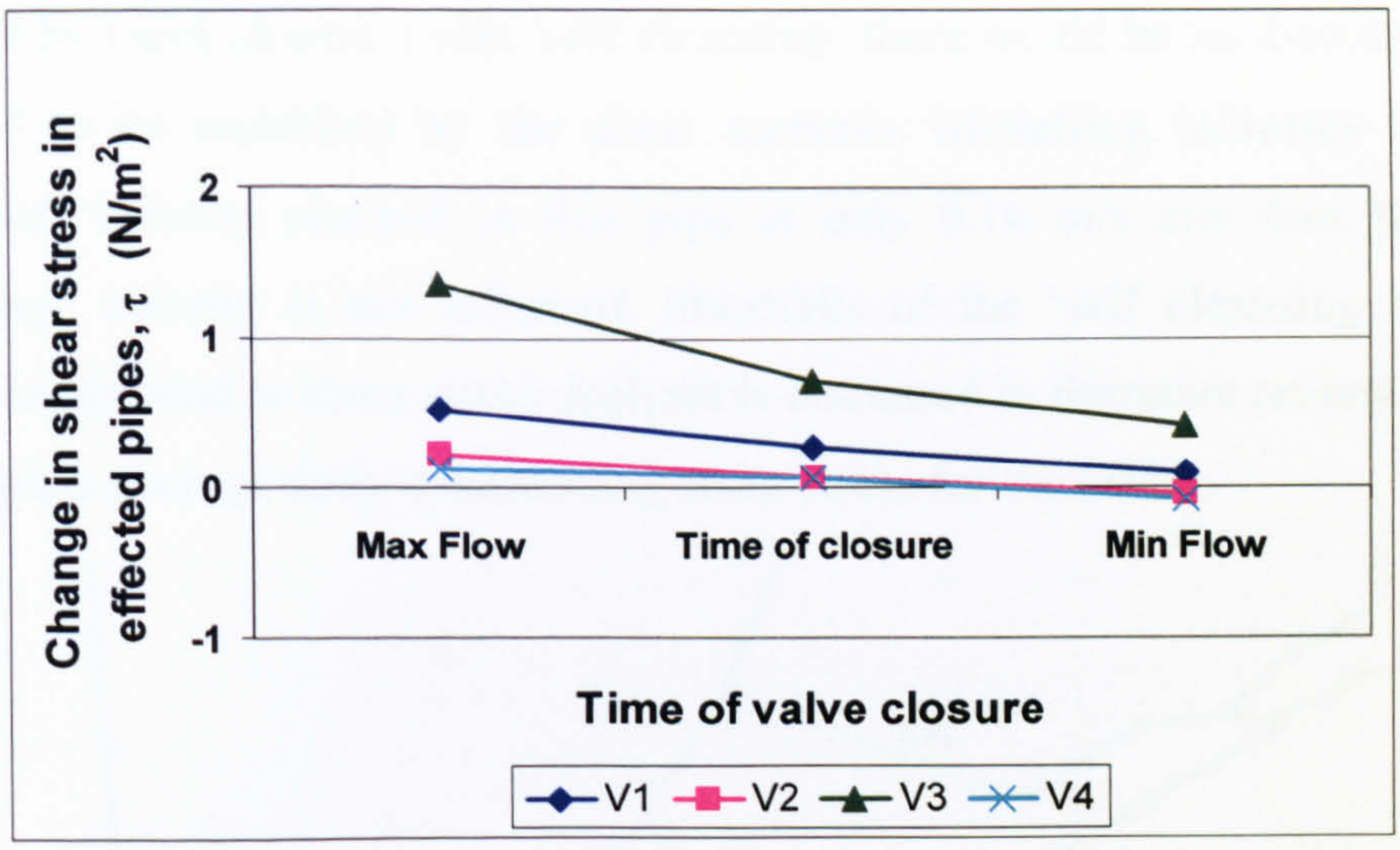

Figure 131 increase in shear as a factor of flow regime.

7.4 Discussion

During the field trials the greatest turbidity response was seen during the closure of valve 1. Closing valve 1 increased the shear stress in a 78m length of 76mm diameter pipe to 0.5 N/m^2 above the daily conditioning shear stress. This added force mobilised the previously accumulated cohesive layers of discolouration material within the pipe causing discolouration. Valve closures 2 and 4 only created a maximum shear stress increase of 0.09N/m^2 above the daily conditioning shear stress forces. From this data it would appear that this slight increase in shear stress was insufficient to mobilise any discolouration material and no turbidity response was seen from the effected pipes.

Modelling indicated that valve closure 3 created the largest increase in shear stress and thus the greatest discolouration risk. Hence it was surprising to find very little turbidity response to this valve closure. Especially considering that this pipe was over 7 times the length of the pipe which was responsible for the significant turbidity event, seen in valve operation 1. This could be due to a number of factors:

1- Self cleansing velocities. Slaats (2002) suggest that increasing velocities in pipes to above 0.4 m/s could create self cleansing networks and conditions where hydraulic forces prevent discolouration material from accumulating on the pipe wall and is discussed in Section 2.6.5. If the pipe

affected by valve closure 4 was 'self cleansing' there would be no discolouration material to be mobilised by the shear increase. Modelling indicates that the maximum velocity reached in this pipe is only 0.16 m/s and thus the 'self cleansing' velocity is not achieved. Shortfalls of the 'self cleansing velocity theory as opposed to shear stress analysis is discussed in literature review. Figure 132 depicts average daily conditioning shear stress for the DMA.

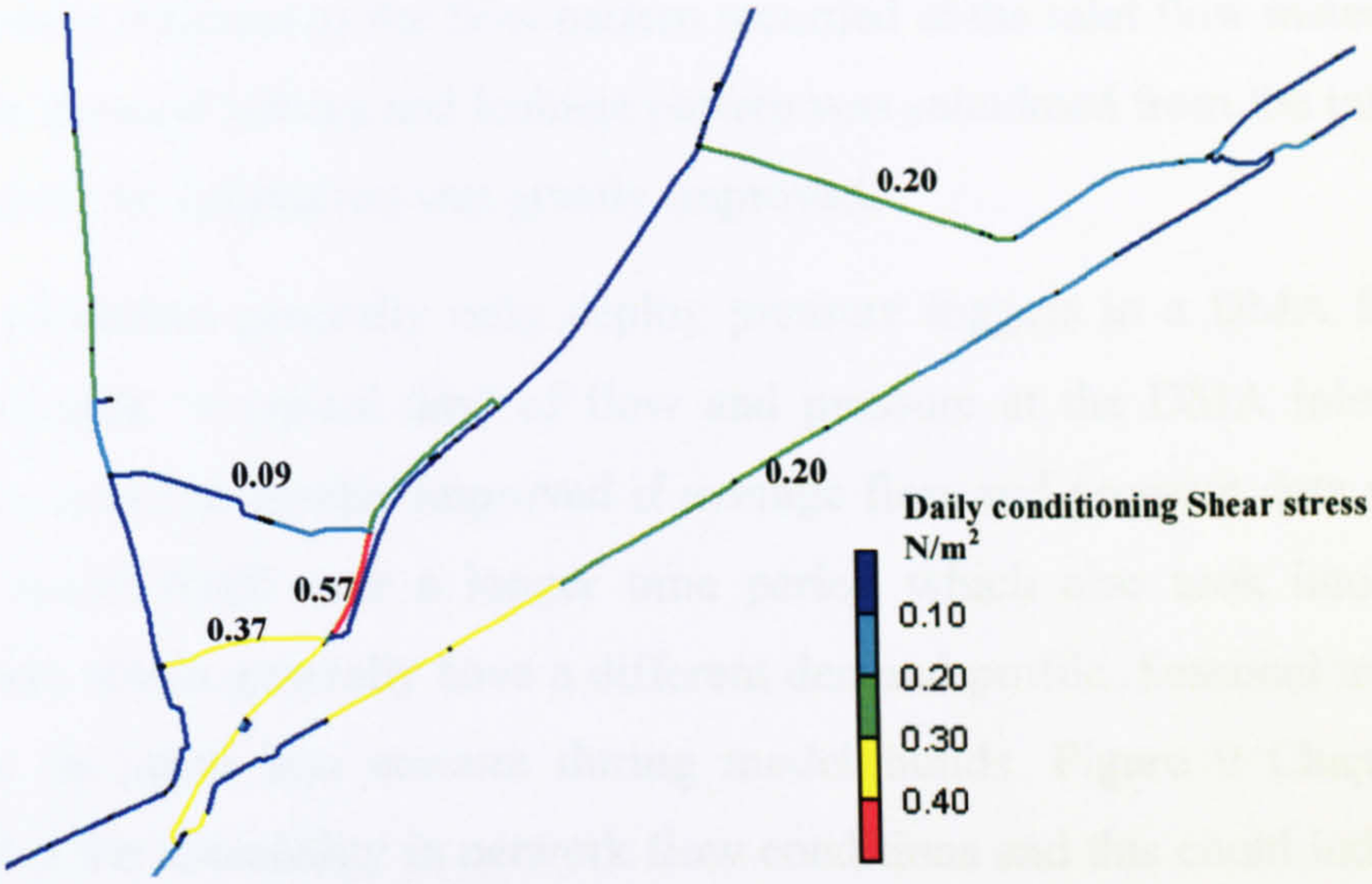

Figure 132 Daily conditioning shear stress.

As can be seen, the peak daily shear stress in the pipe affected by valve closure 1 (0.37N/m^2) is higher than that of the pipe affected by valve closure 3 (0.20 N/m^2). Since both pipes are quite similar, in diameter and material, and significant discolouration material was mobilised during valve closure 1, the pipe affected by valve closure 3 cannot be experiencing 'self cleansing' conditions.

2- Throttled Valve. Another explanation could be that the pipe affected by valve closure 3 was experiencing higher daily flow conditions and thus a higher daily conditioning shear stress than the hydraulic model indicated. This could be due to a restriction or throttled valve on the opposite side of the loop, forcing higher flow rates through the pipe in question. Or there was a significant error in roughness in the pipe creating a higher headloss than as modelled.

3- Leakage A leak along this section of pipe could also be causing elevated flow rates or the demand was allocated incorrectly in this section of pipe. This introduces further discussion on the accuracy of hydraulic models used in the water industry, especially when attempting to accurately to model small changes in shear stress.

4- Model precision. Model accuracy was questioned during the calibration phase of this work. The model used here was only built a few months before the valving project and reached the standard specifications of the water company. However, pressures and flows measured in the field the day before the valving operation were significantly different from the modelled results. The inaccuracy in the model was attributed to the domestic demand profile being significantly different to the flow pattern recorded at the inlet flow meter. A new domestic demand pattern and leakage pattern was calculated from the inlet meter data and model calibration was greatly improved.

Modellers generally only deploy pressure loggers in a DMA for a few days and pick 'a typical day' of flow and pressure at the DMA inlet. Model accuracy could be greatly improved if average flow and pressure data was used in the model build over a longer time period which also took into account weekends, which generally have a different demand profile. Seasonal trends also have to be taken into account during model builds. Figure 9 Chapter 4.2.1 highlights the seasonality in network flow conditions and this could indicate that different models should be built for the seasons of the year. Generally cost is the limiting factor in model accuracy in the water industry however as water companies strive to reduce discolouration customer contacts perhaps analysis at the level shown here should be the driver for greater accuracy in hydraulic models.

4-DMA Size. This was a small DMA with only 266 domestic properties. Higher consumption by a few numbers of properties would have a greater influence on the flow in a DMA of this size and would be less significant in a DMA of much greater size. This could be the cause of the inaccuracy both temporally and spatially in the demand profiles seen in the model which would have been resolved by averaging several days of data rather than just using a 'typical day'.

5- Burst History. This model assumes that the network has been running in a homogenous state with diurnal flow patterns described by the hydraulic model. However over time events can occur in the network which are not taken into account. It could be possible that a burst has occurred in this section of pipe which has not been recorded in the corporate data bases. There are records of

service pipes leading off this pipe being repaired, and it could be possible that this section of pipe has been flushed after reinstatement of the service pipe. Both a burst event and flushing could have removed previously accumulated discolouration material in this section of pipe thus there was no further material to be mobilised by the increased shear at valve closure. It could also be possible that this section of pipe had been affected by fire fighting operations or hydrant testing by the fire department which would not be reported to the water company.

7.4.1 Material from the valve mechanism

During valve closure 2 a turbidity spike is recorded at location C, immediately downstream of the valve, which can be attributed to material dislodged from the valve mechanism as it is moved. This spike is seen later in a diluted form at location B. As this valve is closed further another turbidity spike is created as material sloughs off the valve mechanism. This second turbidity event has a 'double spike' and is not seen at location B, this can be attributed to flow reversal. Material from the valve passes location C but as the valve shuts completely the flow in the pipe reverses (Figure 17), and the turbid water is drawn back towards location C before it gets the chance to reach location B creating the 'double spike'.

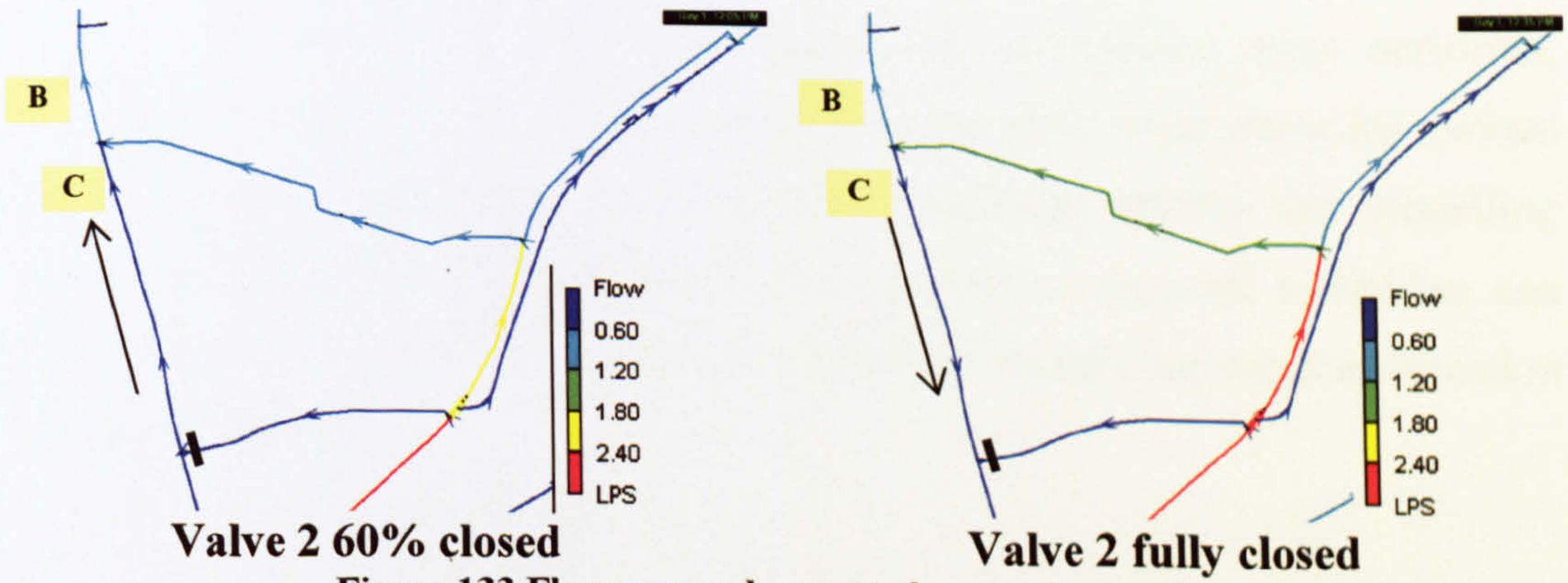

Figure 133 Flow reversal seen at closure of valve 2.

The turbidity spike that occurred during valve closure 4 was interesting. The turbidity spike of 19 NTU had a short time period (5 minutes) and appeared to have a Gaussian distribution suggesting it originated from a point source from the valve mechanism itself. Also the increase in shear stress ($0.09 N/m^2$) was the same as valve 2 closure which was deemed insufficient to mobilise discolouration material.

Travel time analysis from the time of closure of this valve to the arrival of the turbidity spike indicate that the material originated at the location of valve 3. This material could have been loosened as valve 3 was reopened and mobilised by the increased flows at the closure of valve 4.

7.4.2 Model Application

The model represented here could prove highly effective for water companies planning valving operations. From data shown here it can be concluded that an increase of 0.5 N/m^2 shear stress above the daily conditioning shear stress was sufficient to mobilise previously accumulated discolouration material, and an increase of 0.09 N/m^2 was insufficient to mobilise material. Thus based on this shear stress criterion valve operations can be selected with the lowest discolouration risk. Analysing areas of increased shear stress and accounting for the flow direction can indicate optimum locations for turbidity monitoring equipment so that valve operations can be successfully managed in the field to further reduce risk. Scheduling of valve closures to periods of minimum flow is also essential to minimise discolouration risk and impact on customers.

This study was carried out on one network using 4 valve closures. Further work is necessary to validate the model and incorporate more networks, especially to ascertain the minimum required increase in shear stress for various pipe properties, capable of generating discolouration. Ideally this modelling method could lead to a simplified field tool where a network technician can simulate a valve closure on a tough book and then visually see the discolouration potential generated.

8 Discussion

The build-up of discolouration material is a chronic problem in all drinking water distribution systems and a better understanding of the factors contributing to discolouration events is vital to enable water companies to proactively manage their distribution systems at least cost. Managing discolouration is vital to maintain customer satisfaction and to fulfil regulatory requirements.

In order to gain further insight into discolouration, this project has focused on 4 phases: Initially there was a data analysis operation; however the lack of defining contributory factors to discolouration events lead to the need for flushing operations to measure how discolouration material is building up in real networks. Long term monitoring of turbidity was carried out to assess the effectiveness of the flushing operations in reducing the discolouration potential in the networks, and these results were compared to long term monitoring that was performed in DMAs which had been rehabilitated under the DOMS program. Lastly information learned on the significance of shear stress on both the accumulation and mobilisation of discolouration material was applied in an operational scenario to reduce the discolouration risk due to valving operations.

Throughout this project common themes have been occurring in all the sections:

8.1 Pipe material and diameter

Results from the data analysis section (Chapter 4) showed that there was no clear correlation between pipe material (Figure 14) and diameter (Figure 16) with discolouration customer contact frequencies at the DMA level. During the flushing operations described in Chapter 5, no correlation was also found between pipe material and diameter and the thickness of discolouration material mobilised during the initial flush, Figure 62, or with the discolouration material accumulation rate, Figure 69. Lastly no correlation between pipe material and diameter and pre and post intervention turbidity levels was seen in Section 6.4.5. Thus it can be concluded that pipe material and diameter do not play a significant role in discolouration material processes and there must be other influencing

factors. However it must be noted that there was no unlined cast iron mains in this fieldwork.

8.2 Hydraulic influences

Shear stress is described as the force acting on an area of pipe wall perpendicular to the direction of flow and is product of the hydraulic radius and gradient (Equation 6). Flushing data in Figure 63 shows that the thickness of discolouration material mobilised during the initial flush in both flushing zones is inversely proportional to the daily conditioning shear stress. Therefore areas with a low daily conditioning shear stress have a higher discolouration potential.

Long-term turbidity monitoring in the DMAs showed a tentative link between the standard deviation of turbidity calculated from the daily turbidity cycle and conditioning shear stress in the network. The average SdN in J722 was higher than that in J730; as seen in the standard deviation turbidity plots (Figure 103 and Figure 104). This could be because J722 has a higher daily conditioning shear stress which was constantly re-suspending material which was subsequently recorded by the turbidity loggers. J730 had a much lower daily conditioning shear stress and a smaller average SdN. This could indicate that turbidity material was settling in the network, and not being recorded by the turbidity loggers.

Turbidity events occur as a result of an increase in shear stress mobilising previously accumulated layers of discolouration material. This principle was applied and demonstrated during flushing operations where a specific shear stress was applied to the pipe being flushed, allowing comparisons of material mobilised in different flushes to be made.

The principal that discolouration is caused by increased shear was also applied in an operational sense to valve movements, Chapter 7. Here it was seen that an increase in shear of only 0.5 N/m^2 above the daily conditioning shear stress was capable of causing discolouration events well above regulatory limits and easily observable by customers. An increase of only 0.09 N/m^2 was insufficient to mobilise discolouration material. These figures could however be specific to this site, and further work in differing areas is recommended.

Hydraulic events such as increases in consumer demand and bursts can also cause sufficient shear stresses to mobilise discolouration material. During the long term monitoring, numerous increases in demand with associated discolouration events were documented, Appendix 1. However during the long term monitoring, increases in demand were also seen in the long term monitoring data which were not necessarily associated with discolouration events. This was particularly evident in A285 (Figure 102) where in some instances, increases in demand immediately following a demand increase which had caused discolouration, did not necessarily cause discolouration themselves.

This could indicate that bursts could have a positive cleaning effect in networks. Indeed the data analysis performed in Chapter 4 supported this idea where DMAs with a higher burst frequency were shown to have fewer discolouration customer contacts (Figure 13), and the temporal analysis of Water Company A (Figure 11) showed that much higher discolouration customer contact frequency occurred in the summer immediately following a winter with a characteristically lower burst frequency. However demand increases recorded at the DMA flow meter give no indication as where the extra demand was located within the network. During the long term monitoring of J722 a large burst occurred and the associated turbidity response to the increased shear stresses, depicted in (Figure 68), is shown in Figure 98. Here it can be seen that the burst mobilised a significant volume of discolouration material from the trunk main which was imported into the DMA.

8.3 Water quality issues

During the flushing operations it was noted that given the constraints in the accuracy of low daily conditioning shear stress values, Section 5.5.3, the initial thickness of discolouration material removed was tentatively inversely proportional to the daily conditioning shear stress of the network . Assuming that there had been no significant events occurring in the network in the preceding years this was said to be the maximum thickness of material.

The repeat flushes in the zones showed that there was a linear trend in the in the regeneration rate of this material after flushing which essentially had the same gradient in both zones, Figure 64 and Figure 65. Further investigation

showed that this rate was not affected by pipe material or diameter (Figure 69) or daily conditioning shear stress (Figure 70). Therefore the regeneration rate had to be a factor of the water quality, as it was the only other dynamic that was common to both zones. Thus it was theorised that within a DMA discolouration material accumulates in all the pipes at the same rate until a maximum threshold value is reached governed by the daily conditioning shear stress. Hence pipes with a low daily conditioning shear stress continue to accumulate discolouration material long after pipes with a high daily conditioning shear stress have reached their threshold (Figure 71).

Data for the water quality output of the treatment works supplying the two flushing DMAs indicated that there was a significant reduction in the iron levels following the installation of a new second phase filtration system. As there has long been a correlation between the turbidity of water and its iron content, (Boxall et al. 2003; Polychronopolous et al. 2003; Prince et al. 2003; Seth et al. 2003) which was confirmed in Figure 75. This change in water quality could have affected the regeneration results in the flushing zones and indeed a reduction in the percentage of iron in flushing samples was seen in Figure 59 post the new filter installation. However the water quality entering DMAs is more likely to be more greatly affected by processes occurring in the trunk main system.

As the water treatment works has been demonstrated as a significant influence on discolouration material generation, it could be suggested that the historical build up of this material within the larger trunk mains is a function of the upstream treatment process. Even though treatment works do now operate to a very high standard, historical performance has to be accounted for. The small amounts of discolouration material output from treatment works, when allowed to accumulate over a long period of time can lead to a significant accumulation of discolouration material in the trunk mains.

Long term monitoring (Chapter 6) of the 5 DMAs showed that up to 50% of discolouration events were the result of material being imported into the DMA from the trunk main system. This indicates that there could be a constant 'seeding' of discolouration material from the trunk mains into the DMAs. Therefore it could be concluded that tackling the source of discolouration

material by rehabilitating the trunk mains would be more sagacious than constantly cleaning where it is accumulating. However water companies reluctance to rehabilitate trunk mains stem from the difficulties in taking a trunk main out of service for cleaning.

Calculations from the trend between turbidity and iron content shown in Figure 75 indicate that in J722 and J730, the regulatory limit for iron concentration (200 µg/l) is exceeded when the turbidity reaches only 0.6 NTU. If the water quality was similar in C050 DMA, and there was the same gradient to the relationship between iron and turbidity, this regulatory limit would be exceeded every day during the summer periods, due to increases in the daily turbidity cycle as demonstrated in Figure 92.

8.4 Seasonality

Seasonality was first seen in the data analysis phase, Chapter 4. Figure 11 showed that the majority of discolouration customer contacts occur in the summer period due to increased demands in the network causing a sufficient increase in shear to mobilise previously accumulated discolouration material. Seasonality is also seen throughout the long term monitoring data, Chapter 6. Here an increase in the standard deviation of turbidity is seen during the summer periods, Figure 111. It must also be noted that the flushing operations took place at different times of the year, therefore the thickness of discolouration material mobilised could be affected by the season, and thus the accuracy of the regeneration rate could be affected.

This seasonality is a factor of seasonal changes in demand where more water is consumed during the summer periods and can be seen in the 'water into supply' figures in Figure 11. This can affect the re-suspension potential in the distribution network as higher shear stresses are created. Higher temperatures during the summer periods can also increase the rate of the iron corrosion process and biological activity (Holden et al. 1995; Hallam et al. 2001).

Therefore seasonality in the data must be taken into account when using any metal analysis, bacteriological data, total suspended solids, turbidity or discolouration customer contacts in any assessment of network discolouration performance.

8.5 Hydraulic models

Hydraulic models were employed during: flushing, long term monitoring and valve moment phases of this project, to calculate shear stresses. Currently in the water industry hydraulic models have traditionally been used for 'simple' tasks such new demand analysis, redirecting flows during incidents and pressure management, for which their accuracy has been sufficient. However the valve operation section (Chapter 7), demonstrated that relatively small changes in flow can be quite significant in terms of the associated change in shear stress. Such small values could be considered beyond the capabilities of current model build accuracy which are restricted by available time and budget constraints. Shear stress analysis in discolouration management and other water quality applications will become the cost driver for greater hydraulic model accuracy.

9 Conclusions

Analysis of commonly maintained databases during the data analysis phase suggested that there was no identifiable relationship between discolouration customer contacts, and DMA properties. This finding was substantiated during flushing field trials, which were designed to measure and identify the influences on discolouration material regeneration rates. Long term monitoring of turbidity was performed throughout the duration of the project in the two flushing zones and an additional 3 DMAs which underwent rehabilitation in accordance with Yorkshire Waters DOMS rehabilitation scheme. The effectiveness of the various rehabilitation methods in reducing discolouration potential was measured and compared. Finally theories attained from the data analysis, flushing field trials and long-term monitoring were combined in a practical application to assess and measure the discolouration risk due to valve operations.

Combining together the facts gained from, all phases of this project, the following conclusions were made:

- Analysis of discolouration customer contacts, burst records and water into supply figures for two water companies' entire regions indicated that discolouration customer contacts were not necessarily related to burst incidents.
    - Peaks in discolouration customer contacts relating to increased water into supply are seen in summer periods.
    - Peaks in burst frequencies, and water into supply figures are seen in winter periods.
- Analysis of burst frequencies and discolouration customer contacts at the DMA level showed that those those DMAs higher burst frequencies generally had fewer discolouration customer contacts.
    - Bursts could have a positive cleaning effect on networks.

- No trend was seen in discolouration customer contacts and available pipe asset data at DMA level. But this could be due to subject nature of customer contacts.
- Variable layer strength was confirmed during flushing operations
    - This supports the cohesive layer theory, as opposed to a sedimentation process.
    - However, a consistent relationship between layer strength and discolouration characteristics was not necessarily seen.
- The maximum thickness of discolouration material accumulated on the pipe walls was governed by the daily conditioning shear stress.
- A liner discolouration material regeneration rate of 0.0057 mm/month was seen consistently in both flushing zones.
    - No relationship between available factors (pipe material, diameter, age, conditioning shear stress, and pressure) and discolouration material accumulation rate was seen.
    - Therefore the regeneration rate of discolouration material is a factor of the source water quality.
    - The discolouration material was homogeneous in respect to layer strength, metal concentrations and time.
- All pipes within a DMA will regenerate discolouration material at the same rate, until a maximum thickness is reached.
    - In pipes experiencing lower daily conditioning shear stresses discolouration material will continue to accumulate for longer, generating thicker layers, than pipes subjected to a higher daily conditioning shear stress.

- A daily cycle is seen in the turbidity data where turbidity is highest at peak daily flow in the morning and lowest in mid afternoon.
    - This is a factor of both re-suspension and iron corrosion processes.
    - Using Standard deviation, the amplitude of this cycle can be used to assess rehabilitation effectiveness as a decrease in the average standard deviation of turbidity is seen post flushing.
- Analysis of turbidity events occurring in DMAs indicated that DMAs receive a constant supply of discolouration material as a result of processes occurring within the distribution trunk mains.
    - Therefore in any rehabilitation strategy, trunk mains should be addressed before attempting anything in the DMAs.
- A full zonal flushing approach was seen to be more effective in terms of cost and reduction in discolouration potential than The DOMS approach.
- Throughout this work it has been confirmed that discolouration events occur due to an increase in shear stress mobilising previously accumulated discolouration material from the pipe walls.
    - This can be practically applied to evaluate the discolouration risk of valve operations.
    - An increase of only 0.5 N/m^2 shear stress was sufficient to mobilise discolouration material at a level that would be observed by customers.
- The full zonal flushing employed here was more effective in terms of both cost and reduction in discolouration potential than the rehabilitation performed in the DOMS trial DMAs.

- A homogeneous metal composition of discolouration material was found in flushing samples.
    - Regardless of pipe material or diameter, layer strength or age.
- Seasonality is seen in the data where there are higher recorded turbidity and discolouration customer contact rates in summer periods. As a result of:
    - Increased flows in the network increasing the re-suspension processes.
    - Higher temperatures increase the corrosion and biological activity rates.

10 Further Work

Due to time and budget constraints the repeat flushing operations in this project were only performed in two DMAs of limited pipe materials fed from the same surface water source. In order gain a greater understanding as to how differing source water qualities would effect the regeneration rate of discolouration material, more repeat flushing operations should be carried out in areas with both ground water and surface water sources where there is likely to be differing background iron and manganese concentrations.

In this project only 23 separate pipes were flushed, and further flushing operations would be ideal in areas of differing pipe material diameter and daily conditioning shear stresses to more accurately quantify the role of daily conditioning shear stress on limiting the thickness of discolouration material accumulation. Ideally these areas would have better hydraulic models or hydraulic data for calibration.

The amplitude of the daily turbidity profile discussed in the long term monitoring section has great potential in quickly assessing the scale of discolouration potential in distribution systems, and the shape of the profile would give an insight as to the route cause of discolouration such as re-suspension or corrosion processes. Additional wide deployment of turbidity loggers in as many different distribution networks is highly recommended in order to further explore these phenomena.

The increase in shear stress, from daily conditioning shear stresses, as a result of valve closure is investigated in this project in order to manage discolouration in valving operations. However in this project only 4 valve operations were modelled and monitored. More valving operations are recommended in order to more accurately predict how such small relative changes in shear affect the discolouration risk.

The long-term monitoring section highlighted that processes occurring in the trunk main distribution systems account for the resulting turbidity recorded in DMAs. However turbidity in the trunk mains was not monitored in this project and the long term deployment of water quality sensors in the trunk mains is

recommended in order to gain further insight to the discolouration processes that are occurring.

Historically water companies manage discolouration at the DMA level rather than tackling the trunk mains because of the logistical issues involved in taking a trunk main out of commission in order to renew, scrape and line, or clean it. More development is recommended into trunk main rehabilitation methods particularly regarding rehabilitation methods which do not require the trunk main to be taken out of service.

11 References

Ackers, J., Brandit, M. and Powell (2001) *Hydraulic characterisation of deposits and rewiew of sediment modelling.* Drinking Water Quality and Health - Distribution Systems DW-03. UKWIR, Thames Water Utilities Limited

Ackers P White W R (1973) Sediment transport : New approach and analysis; Proc. ASCE J Hyd Div.Vol. 99 (HY11) p2041-2060.

Barbeau, B., Julienne, K., Gaultier, V., Millette, R. and Prevost, M. (2005). *Dead-end flushing of a distribution system: Short and long-term impacts on water quality.* Journal of Water Supply: Reasurch and Technology – Aqua Vol: **54** (6): 371- 383.

Blokker, E. J. M., Vreeburg, J., Schaap, P. G. and Horst, P. (2007). *Self- cleaning networks put to the test.* World Environmental and Water Resources Congress 2007: Restoring Our Natural Habitat. American Society of Civil Engineers.

Bocock, C. (1997). *An underground movment.* Water Bulletin **735**.

Boxall, J. B. and Dewis, N. (2005*). Identification of discolouration risk through simplified modelling.* ASCE EWRI. World Water and Environmental Water Resources, 15- 19th May.

Boxall, J. B. and Saul, A. J. (2005). *Modelling Discolouration in Potable Water Distribution Systems*. Journal of Environmental Engineering ASCE **131**(5), 716-725.

Boxall, J. B., Saul, A. J., Gunstead, J. D. and Dewis, N. (2003). *Regeneration of discolouration in distribution systems.* ASCE, EWRI, World water and environmental resources conference, Philadelphia.

Boxall, J. B., Saul, A. J., Husband, S. and Edyvean, R. (2004). *Prediction of Discolouration in Distribution Systems- PODDS model.* UKIWR Preventing Discolouration Technology Transfer Seminar.

Boxall, J. B., Saul, A. J. and Skipworth, P. J. (2001). *A Novel Approach to modelling sediment movement in distribution mains based on particle characteristics.* Water Software Systems **1**: 263-273.

Boxall, J. B., Skipworth, P. J. and Saul, A. J. (2003). *Aggressive flushing for discolouration event mitigation in water distribution networks*. Water Science and Technology - Water Supply **3**(1/2): 179-186.

Brazos, B. J. and O'Connor, J. T. (1991). *Seasonal effects on the generation of particle associated bacteria during distribution.* Journal of Environmental Engineering **122**(12): 1050- 1057.

Cerrato, J. M., Reyes, L. P., Alvarado, C. M. and Dietrich, A. M. (2006). *Effect of PVC and iron materials on Mn(II) deposition in drinking water distribution systems.* Water Research **40**: 2720-2726.

Chandy, P. J. and Angles, M. L. (2001). *Determination of nutrients limiting biofilm formation and the subsequent impact on disinfectant decay.* Water Research **35**(11): 2677-2682.

Cook, D. M., Boxall, J. B., Hall, S. J. and Styan, E. (2005). *Structural integrity and water quality in water distribution networks.* Proceedings on the 8th International Conference on Computing and Control for the Water Industry. **2**: 205- 210

Dewis, N. and Randall - Smith, M. (2005). *Discolouration risk modelling.* Proceedings on the 8th International Conference on Computing and Control for the Water Industry. **2**: 223- 228.

Donlan, R., Pipes, W. and Jasper, S. (1994). *Biofilm formation on cast iron substrata in water distribution systems.* Water Resources. **28**(6): 1497-503.

DWI (2000). *The Water Supply (Water Quality) Regulations 2000.* 2000 No.3184, DWI: 74.

Gaultier, V., Barbeau, B., Millette, R., Block, J.-C. and Prevost, M. (2001). *Suspended particles in the drinking water of two distribution systems.* Water Science and Technology: Water Supply **1**(4): 237-245.

Gaultier, V., Rosin, C., Mathieu, L., Portal, J.-M., Block, J.-C., Chaix, P. and Gatel, D. (1996). *Characterization of the loose deposits in drinking water distribution systems.* In: Proceedings of the Water Quality Technology Conference of American Water Works Association, Boston, Ma, USA.

Gray, N. F. (1994). *Drinking water quality - problems and solutions*. Chichester, John Wiley and Sons.

Hallam, N. B., West, J. R., Forster, C. F. and Simms, J. (2001). *The potential for biofilm growth in water distribution systems.* Water Research **35**(17): 4063-4071.

Holden, B., Greetham, M., Croll, B. T. and Scutt, J. (1995). *The effect of changing inter process and final disinfection reagents on corrosion and biofilm growth in distribution pipes.* Water Science and Technology **32**(8): 213-220.

Kerneis, A., Nakache, F. and Deguin, A. (1995). *The effect of water residence time on the biological quality in a distribution network.* Water Research **29**(7): 1719-1727.

LeChevallier, M. W., Evans, T. M. and Seidler, R. J. (1981). *The effect of turbidity on chlorination efficiency and bacterial persistence in drinking water.* Applied and Environmental Microbiology **42**(1): 159-167.

Lee, S. H., O'Connor, J. T. and Banerji, S. K. (1980). *Biologically mediated corrosion and its effects on water quality in distribution systems.* Journal of the American Water Works Association **82**: 636-645.

Lin, J. and Collier, B. A. (1997). *Aluminium in a water supply, part 3: domestic tap waters.* Water, Journal of the Australian Water Works Association. Vol: 24: 11-13.

Marshall, G. P. (2001). *Understanding and Preventing Discoloured Water. Drinking Water Quality and Health* - Distribution Systems DW-03. UKWIR, Thames Water Utilities Limited: 75.

McCoy, W. F. and Olsen, B. H. (1986). *Relationship among turbidity, particle counts and bacteriological quality within water distribution lines.* Water Resources **20**(8): 1023-1029.

McNeill, L. S. and Edwards, M. (2001). *Iron pipe corrosion in distribution systems.* Journal of the American Waterworks Association **93**(7): 88-100.

Polychronopolous, M., Dudley, K., Ryan, G. and Hearn, J. (2003). *Investigation of factors contributing to dirty water events in reticulation systems and evaluation of flushing methods to remove accumulated particles*. Water Science and Technology: Water Supply **3**(1-2): 295-306.

Powell, J. (2004). *Identification of discolouration risks.* UKIWR Preventing Discolouration Technology Transfer Seminar.

Powell, M. (2004) *Turbidity Logger installation Procedure*. Yorkshire Water Services.

Prince, R., Goulter, I. and Ryan, G. (2003). *What causes customer complaints about discoloured water*. WATER, Journal of the Australian Water Association **30**(2): 62-68.

Prince, R., McManus, K. and Goulter, I. (2000). *Colour, turbidity levels and dirty water customer complaints - water system performance indicators?* 10th World Water Congress, "Sharing the Waters of the World", Melbourne, Australia.

Ryan, G. and Jayaratne, A. (2003). *Particles in Distribution systems and assessment of discoloured water*. Maintenance and Assessment of Distribution Systems to Improve Water Quality. C. G. Workshop. Sydney.

Sarin, P., Snoeyink, V. L., Bebee, J., Jim, K. K., Beckett, M. A., Kriven, W. M. and Clement, J. A. (2004). *Iron release from corroded iron pipes in drinking water distribution systems: effect of dissolved oxygen.* Water Research **38**: 1259-1269.

Sarin, P., Snoeyink, V. L., Lytle, D. A. and Kriven, W. M. (2004). *Iron Corrosion Scales: Model for Scale Growth, Iron Release, and Coloured Water Formation.* Journal of Environmental Engineering **130**(4): 364-373.

Servais, P., Laurent, P. and Randon, G. (1995). *Comparison of the bacterial dynamics in various French distribution systems*. Journal of Water Science Research and Technology **44**: 10-17.

Seth, A., Bachmann, R., Boxall, J., Saul, A. J. and Edyvean, R. (2003). *Characterisation of materials causing discolouration in potable water systems.* Water Science and Technology **49**(2): 27-32.

Slaats, N. (2002). *Processes involved in the generation of discoloured water.* Project no. 30.3974.011, Kiwa.

Sly, L. I., Hodgkinson, M. C. and Arunpairojana, V. (1990). *Deposition of manganese in a drinking water distribution system.* Applied and Environmental Microbiology **56**(3): 628-639.

Thurman, R., Smith, K., Ford, R., Sterry, S. J. and Grichting, W. (1999). *Telephone survey of water customers.* The Journal of the Australian Water Association **26**(6).

Twort, A. C., Ratnayaka, D. D. and Brandt, M. J. (2000). *Water Supply.* London, Arnold.

Unwin, D.M., Boxall, J.B. and Saul, A.J. (2003) *Data mining and relationship analysis of water distribution databases for improved understanding of operations performance.* Advances in Water Supply Management-Proceedings of the International Conference on Computing and Control for the Water Industry. 51- 58

Van der Wende, E. and Characklis, W. G. (1990). *Biofilms in portable water distribution systems,* Springer-Verlag, New York.

Vreeburg, J. (2007). *Discolouration in drinking water systems: a particular approach.*, Technical University Delft. **PhD:** 183.

Vreeburg, J., Schaap, P. G. and van Dijk, J. C. (2004). *Measuring discolouration risk: Re-suspension potential method.* IWA leading edge conference, Prague.

Water UK (2003). *Water customers focus on quality and reliability.* http://www.water.org.uk/home/news/press-releases/water-cust-171203-1

WHO (2006). *Guidelines for drinking water quality, 3rd Edition incorporation first addendum.* World Health Organisation.

WRc (1994). *'Water Industry Instrument Handbook- Book 4 Turbidity'* Water Research Council Wiltshire.

YWS (2005). Field Guide to Potable Water Sampling Issue 4.3, Yorkshire Water Services.

Appendix 1

Long term monitoring 'events'

C050

1 08/08/04
Localised demand increase

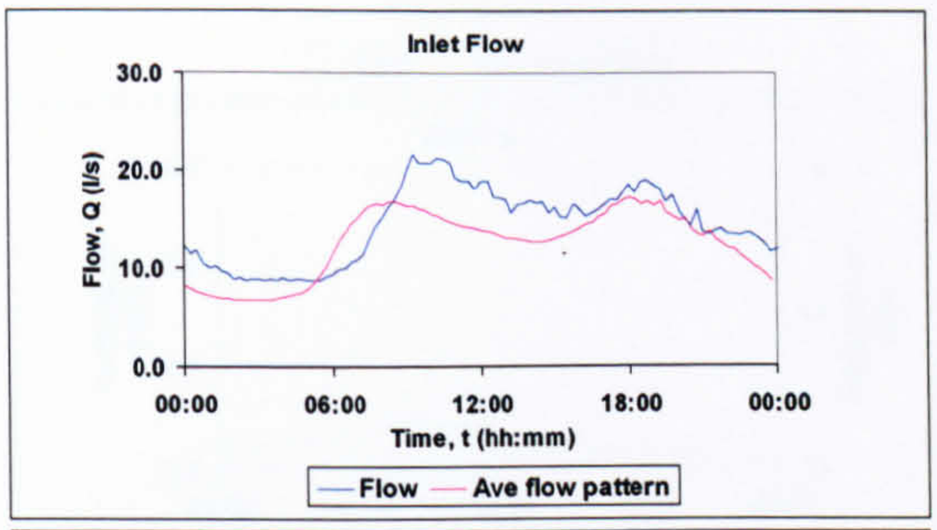

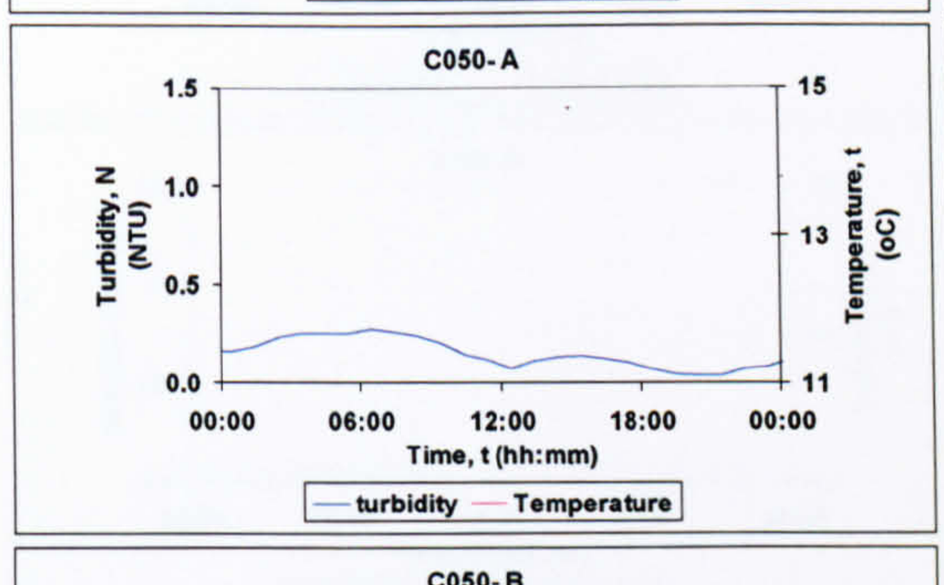

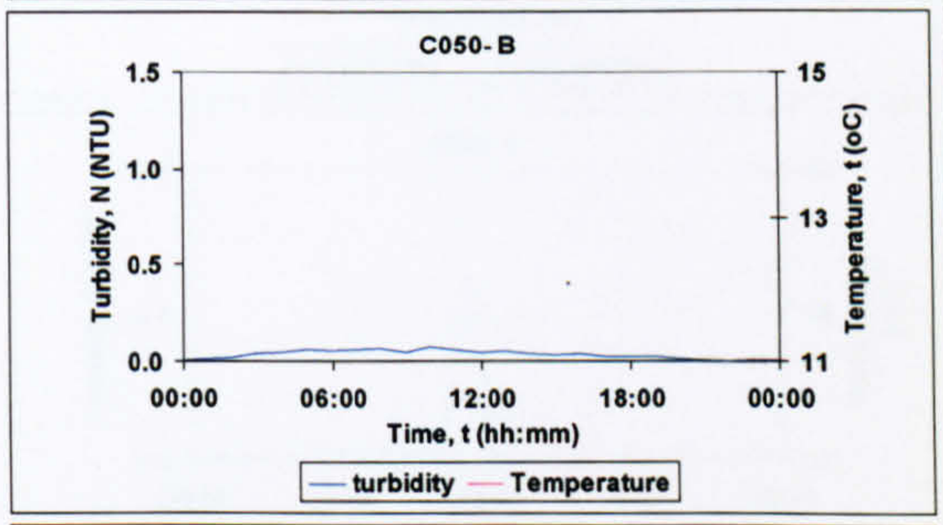

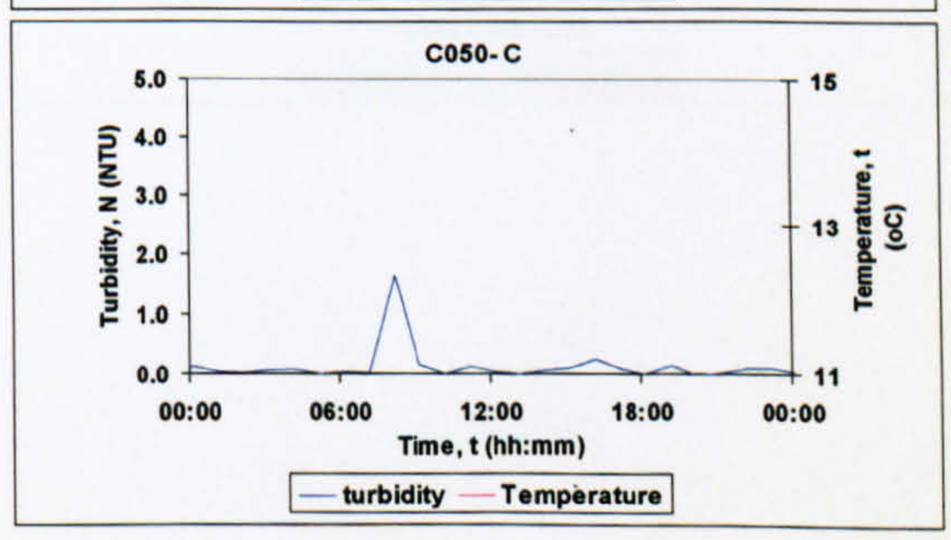

2 14/08/04
Localised demand increase

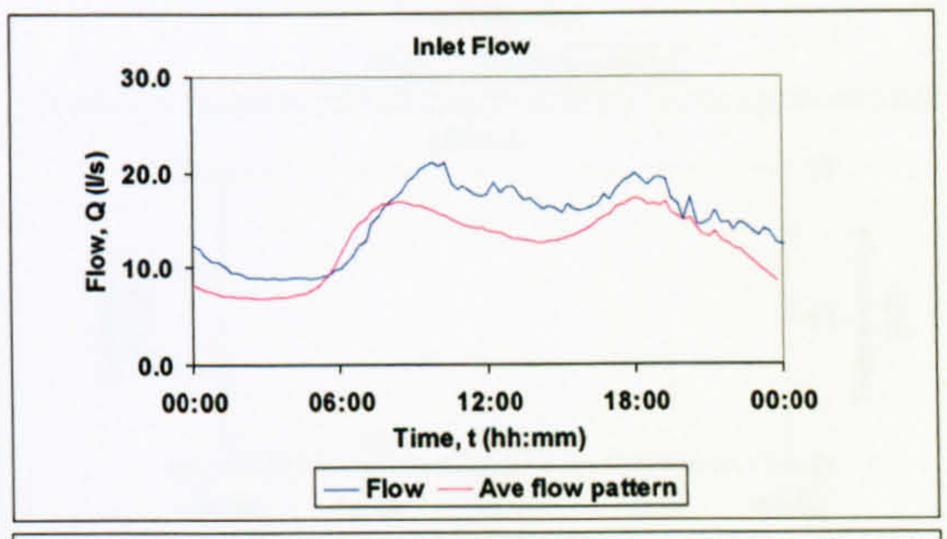

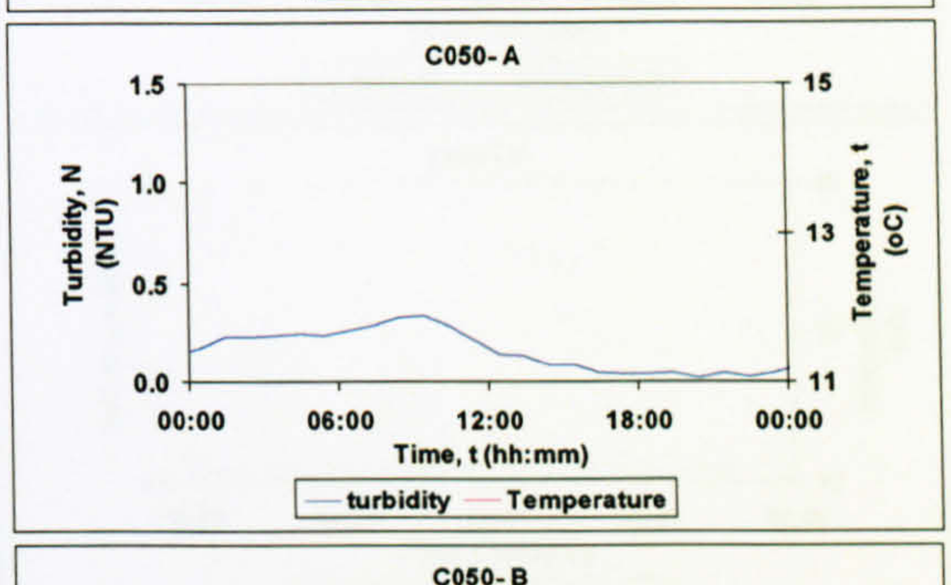

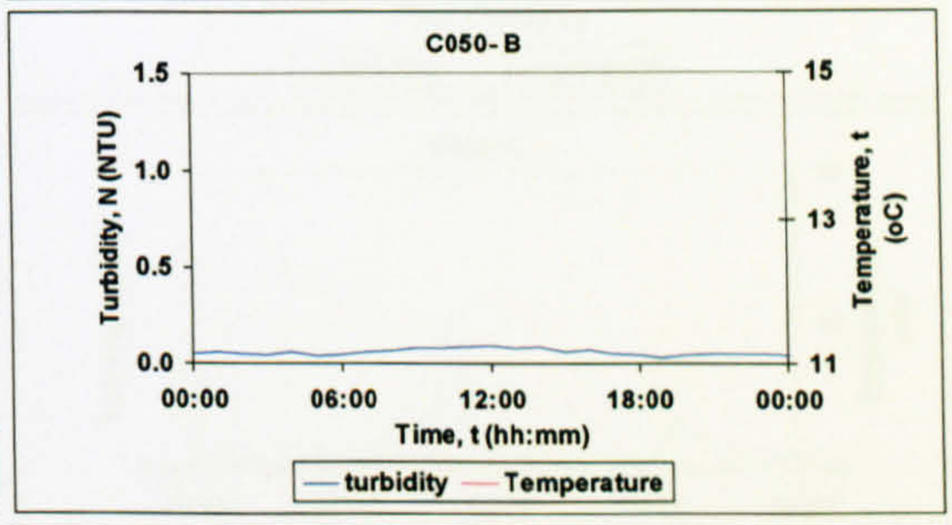

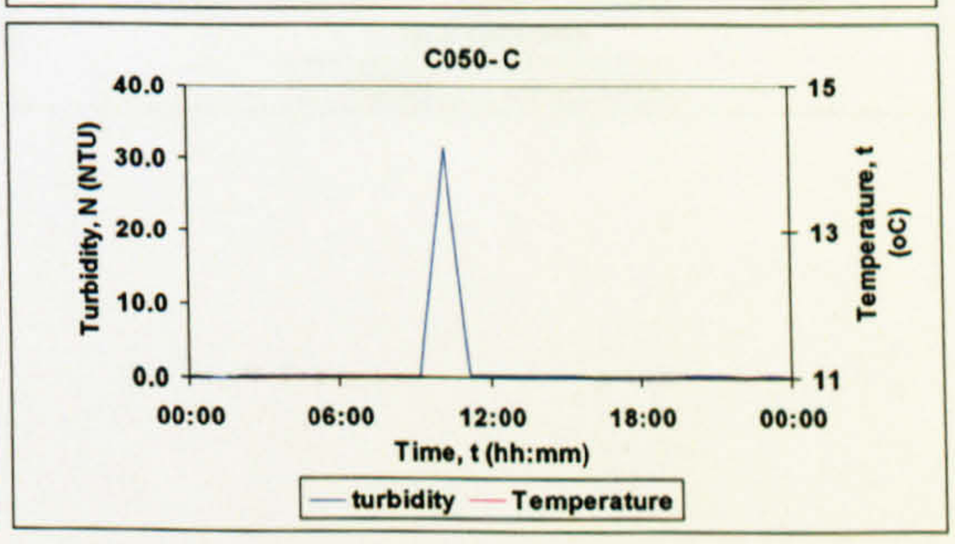

3 28/08/04

Localised demand increase

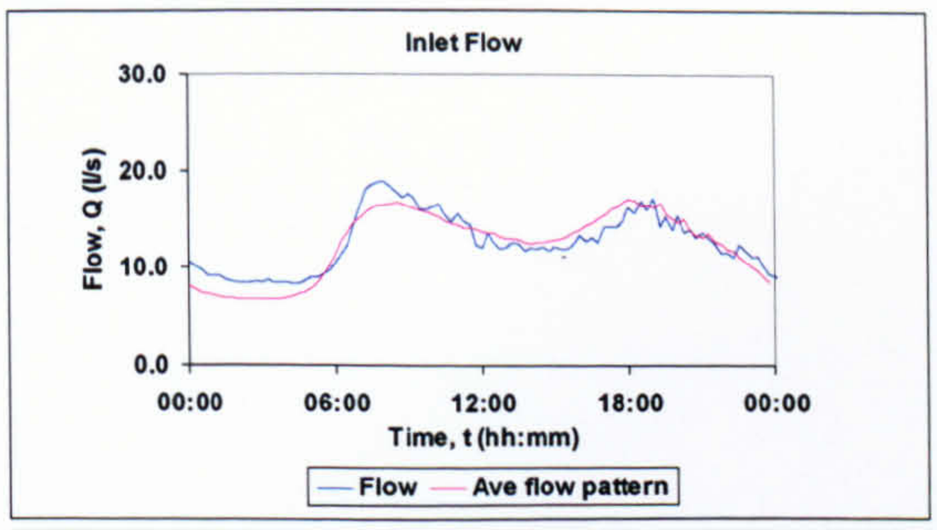

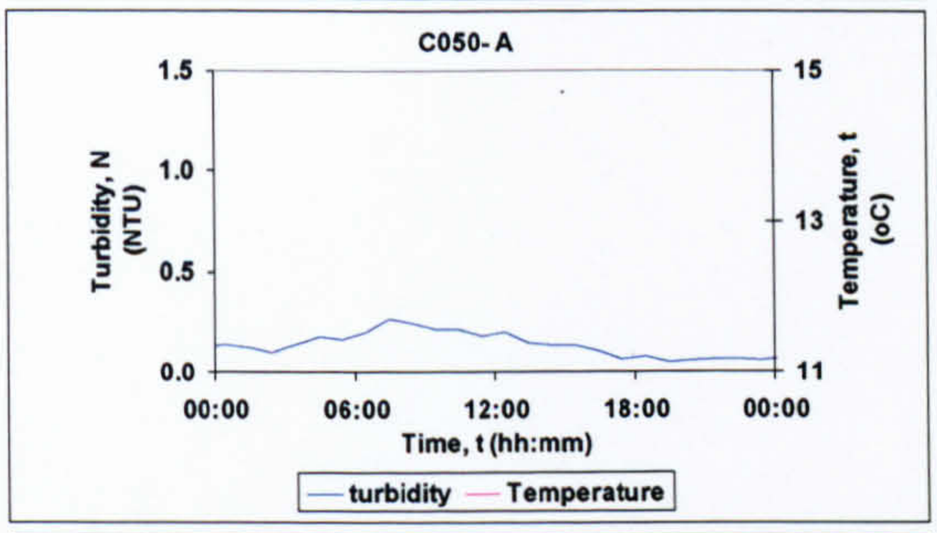

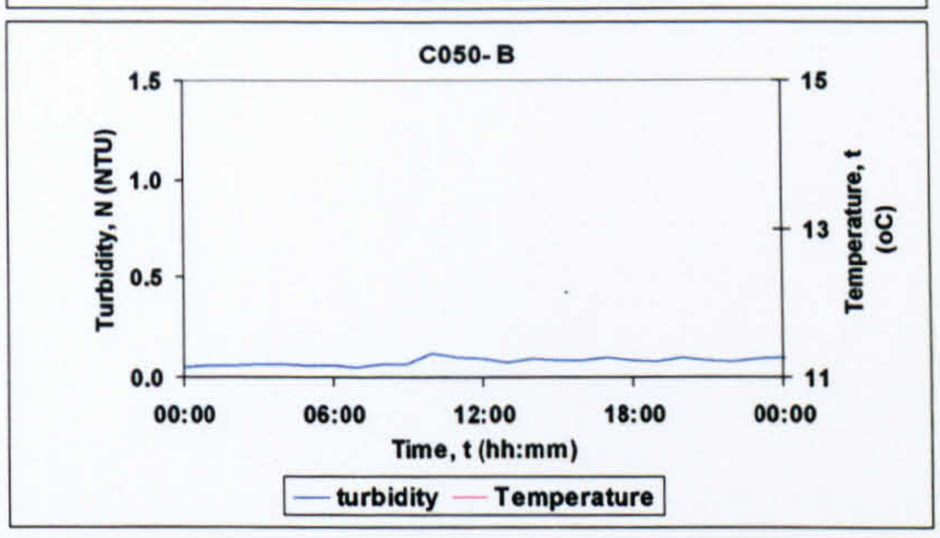

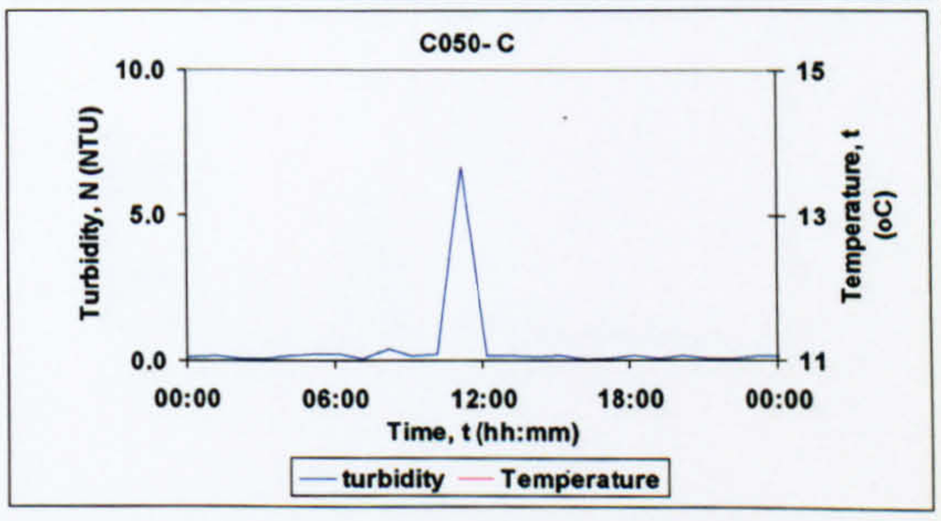

4 02/10/04

Localised demand increase

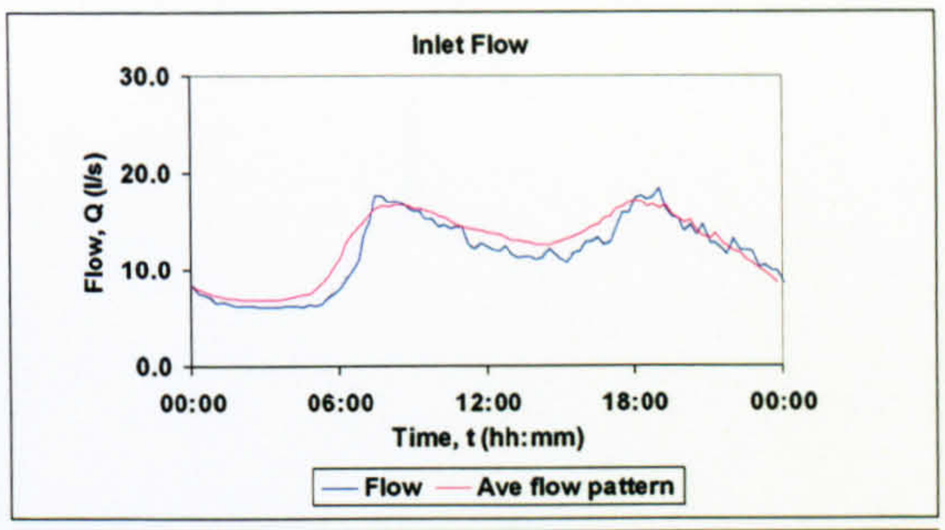

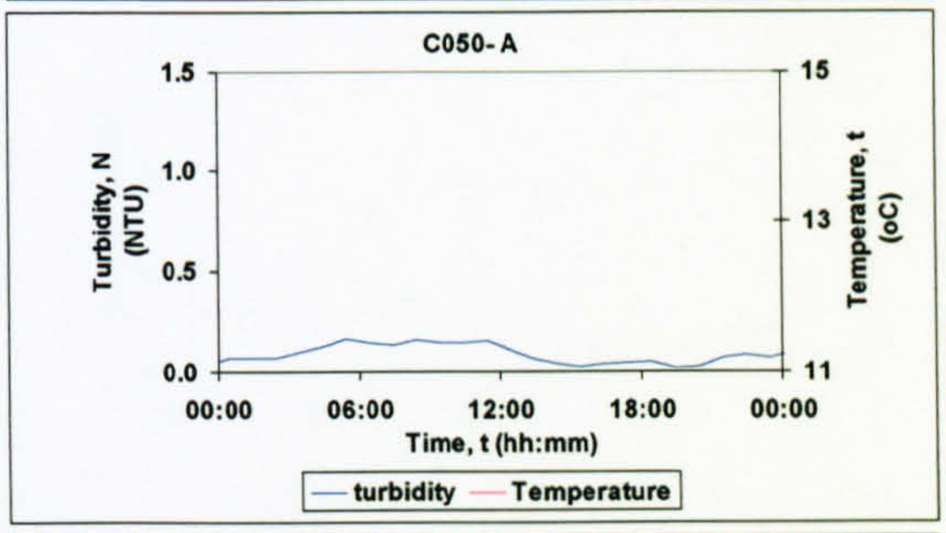

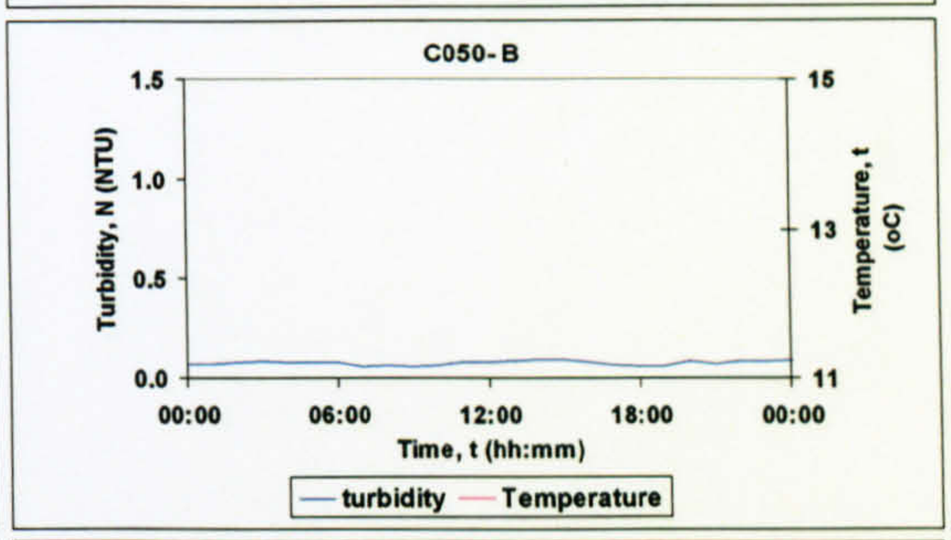

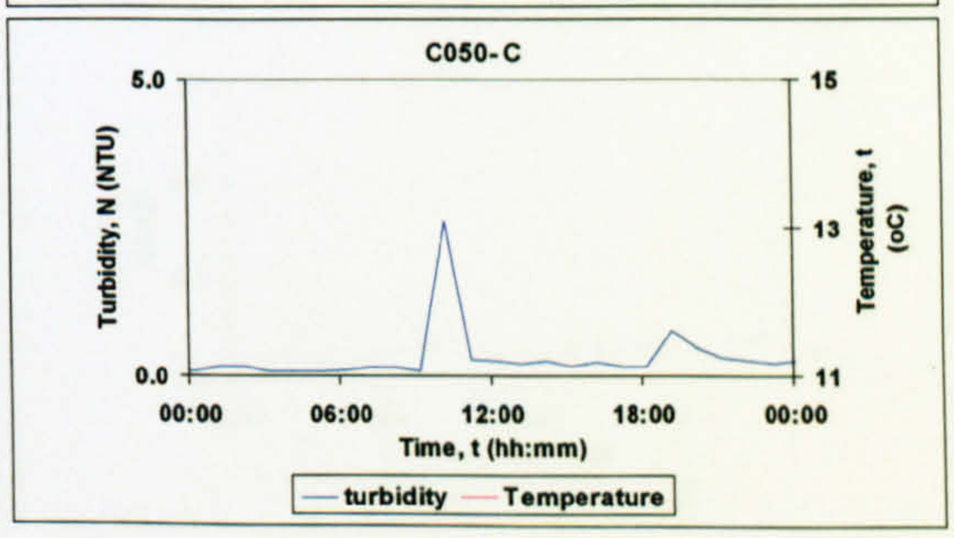

5 12/10/04
Localised demand increase

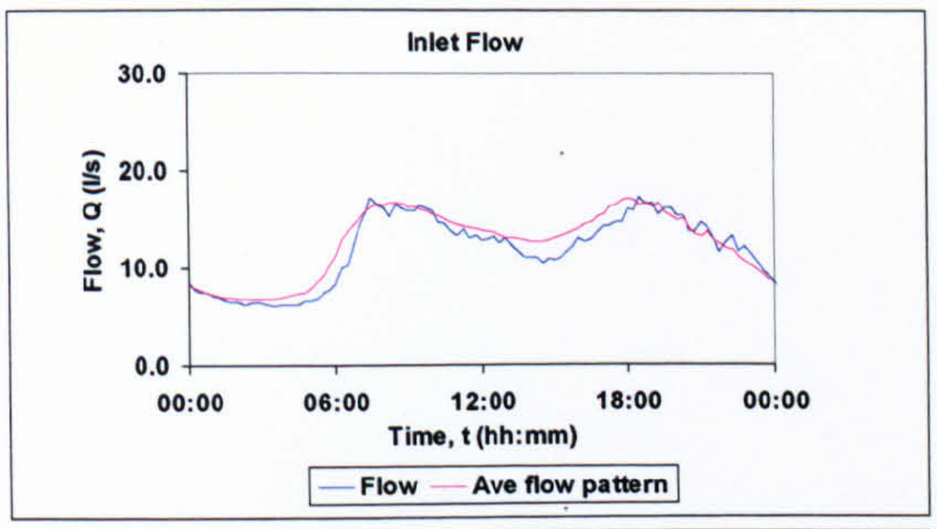

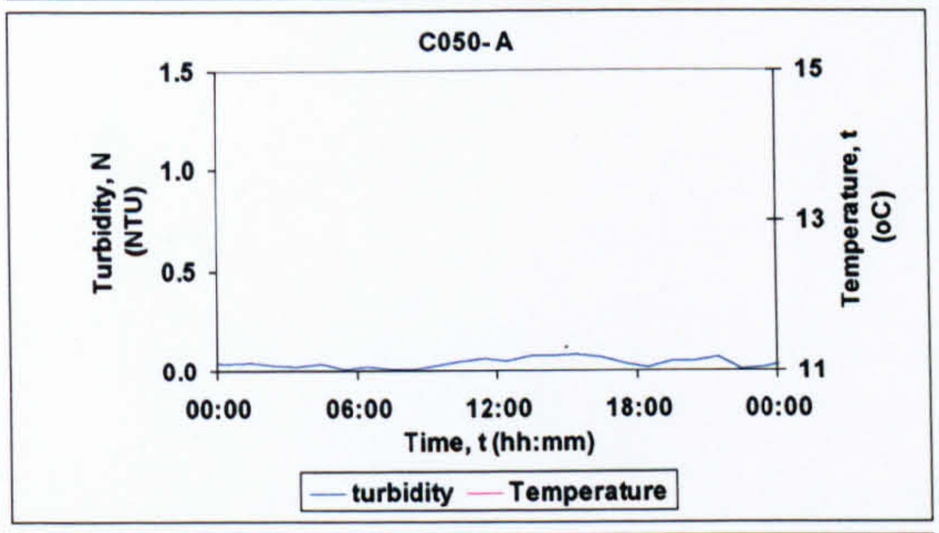

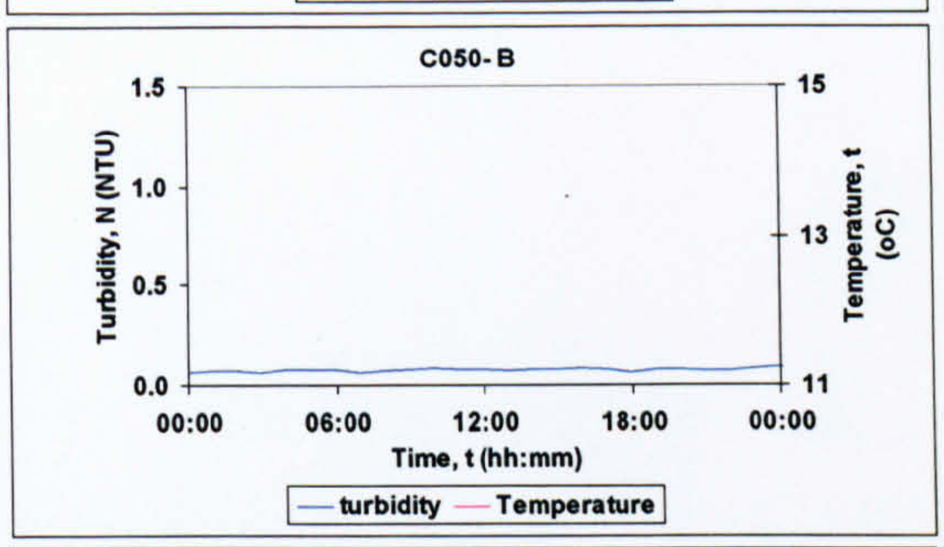

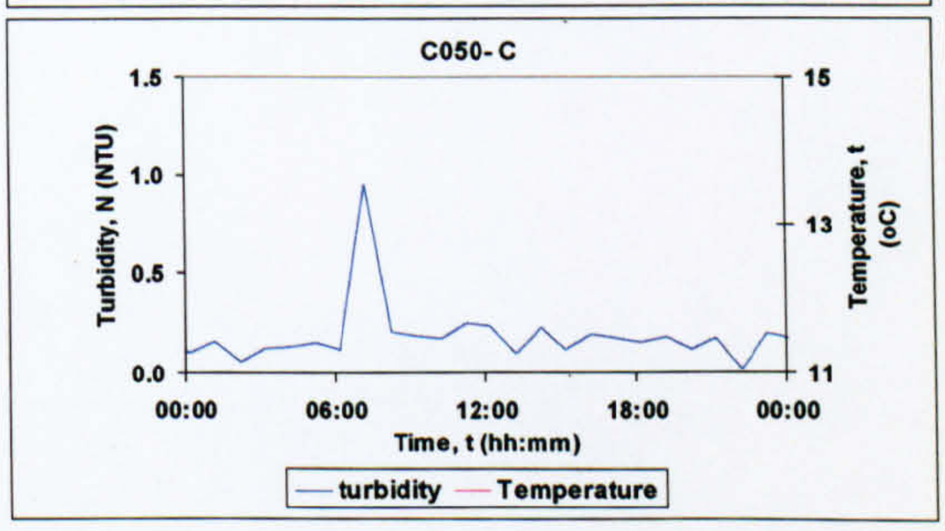

6 19/11/04
Demand increase with no turbidity

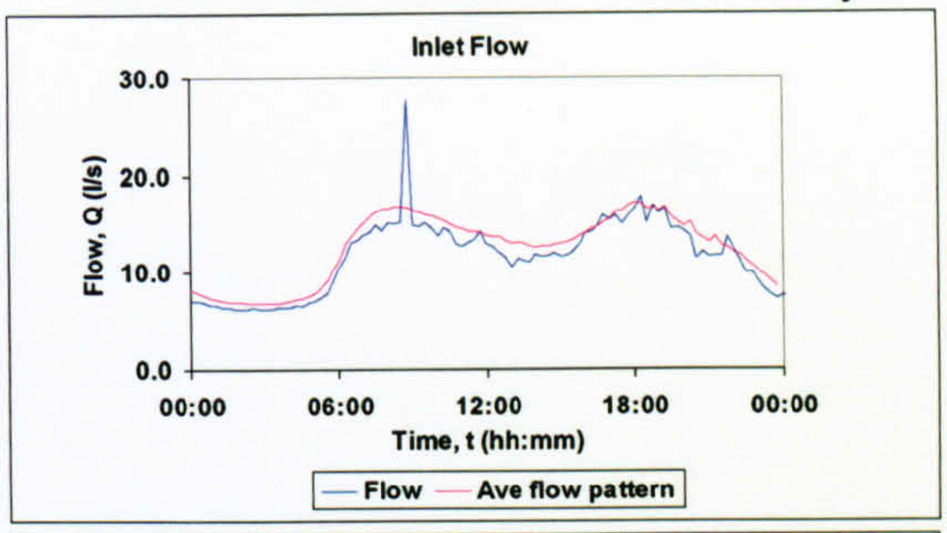

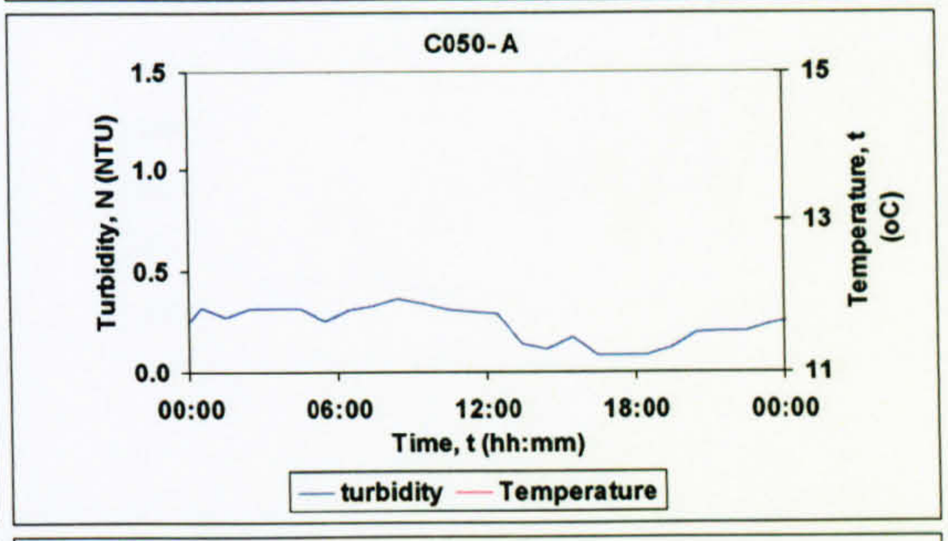

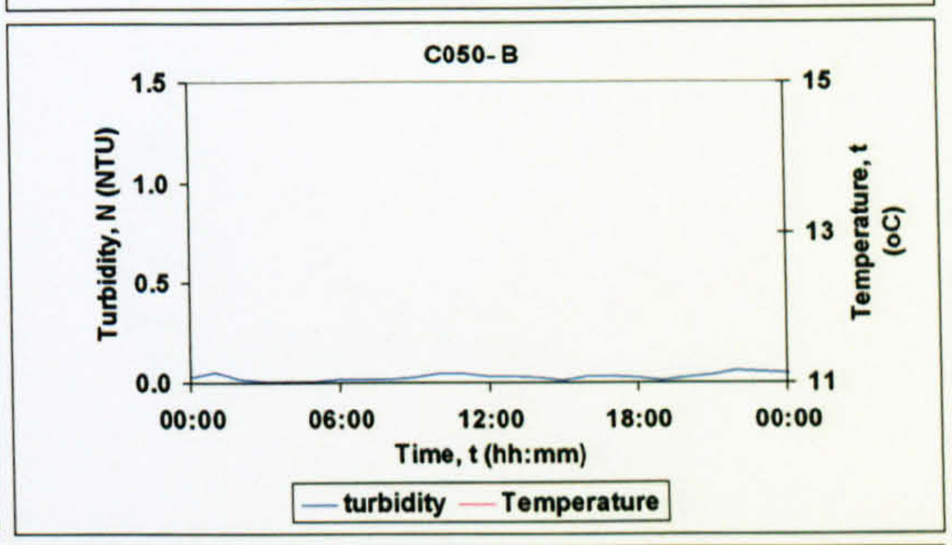

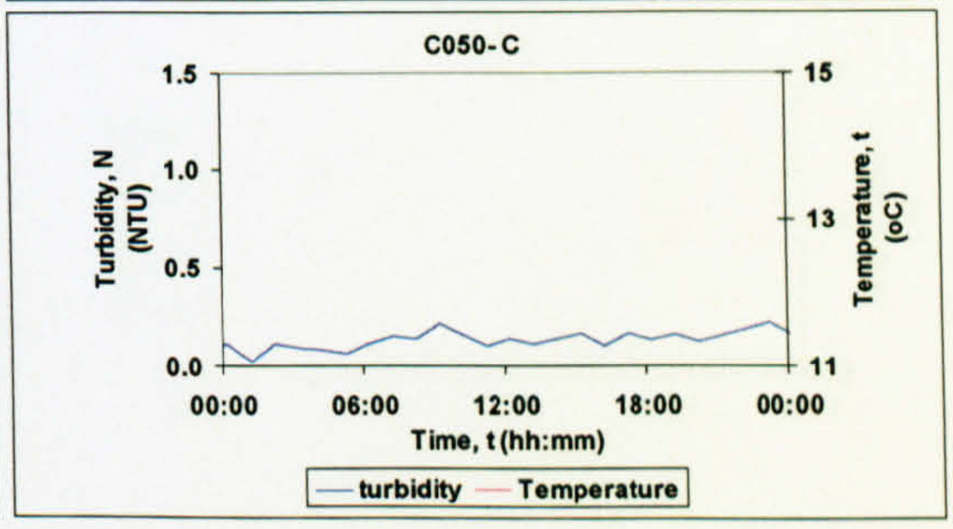

7 31/03/05

Demand increase with no turbidity

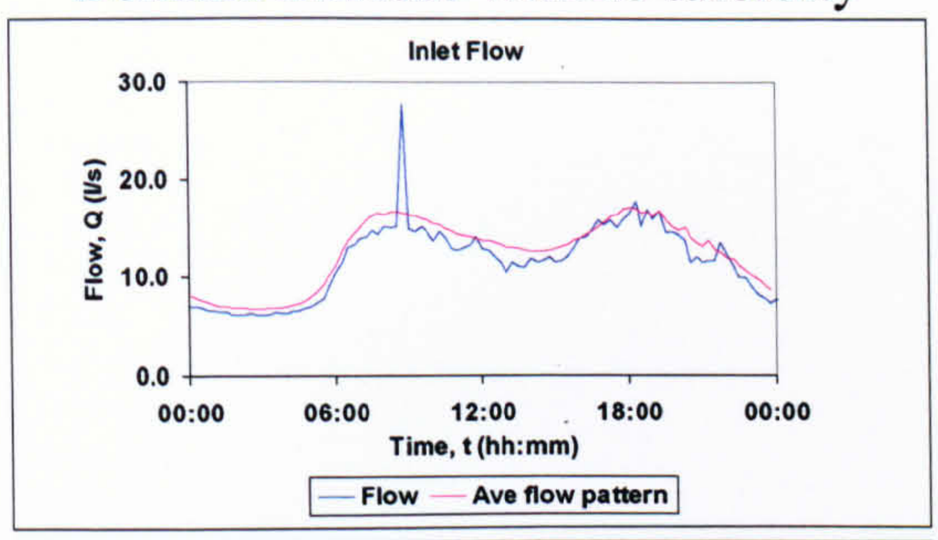

8 08/06/05

Example of daily turbidity cycle

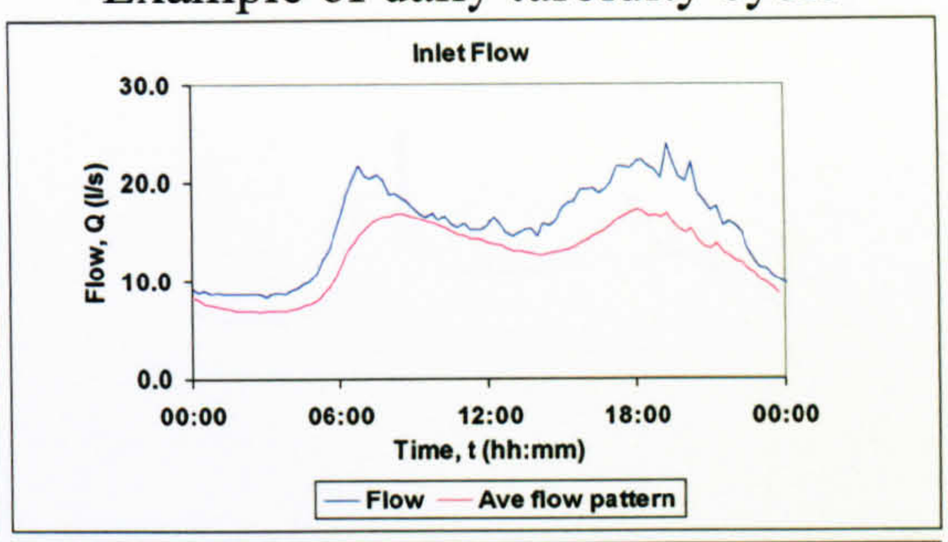

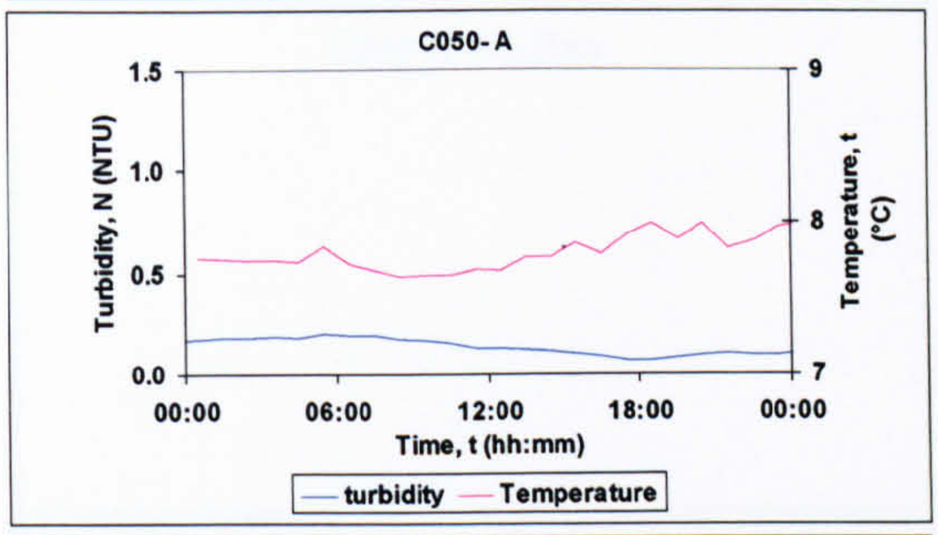

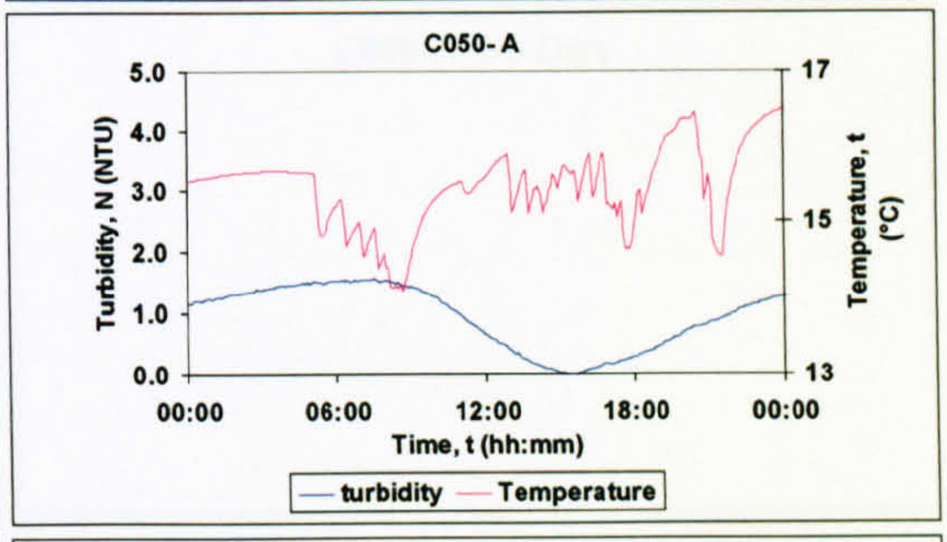

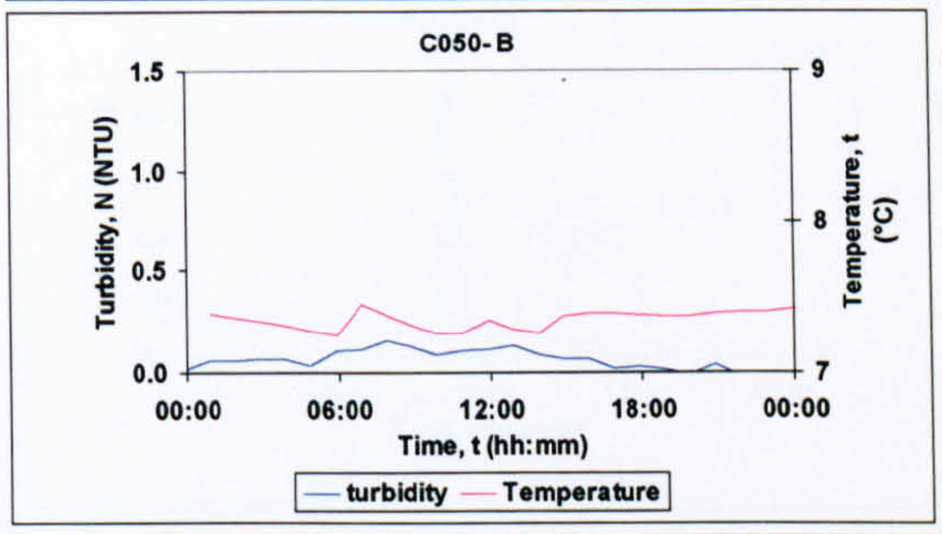

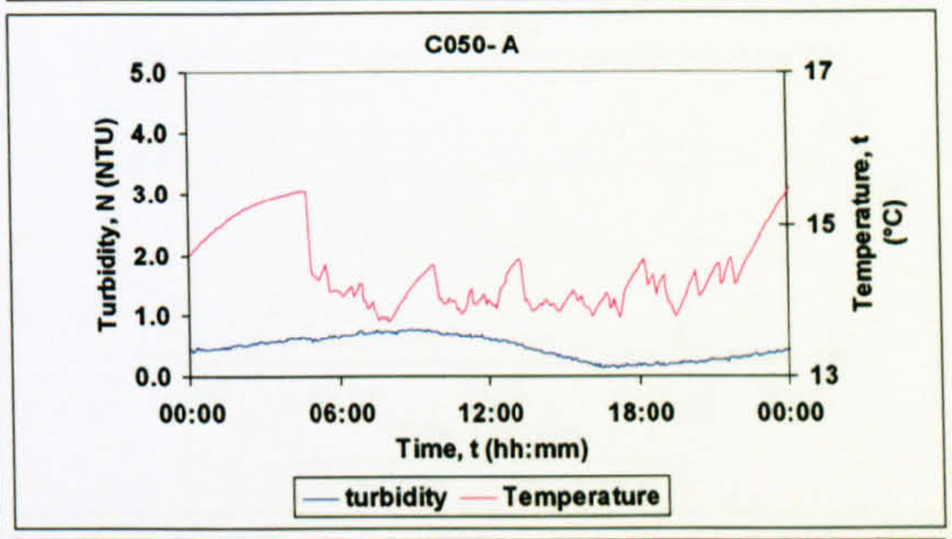

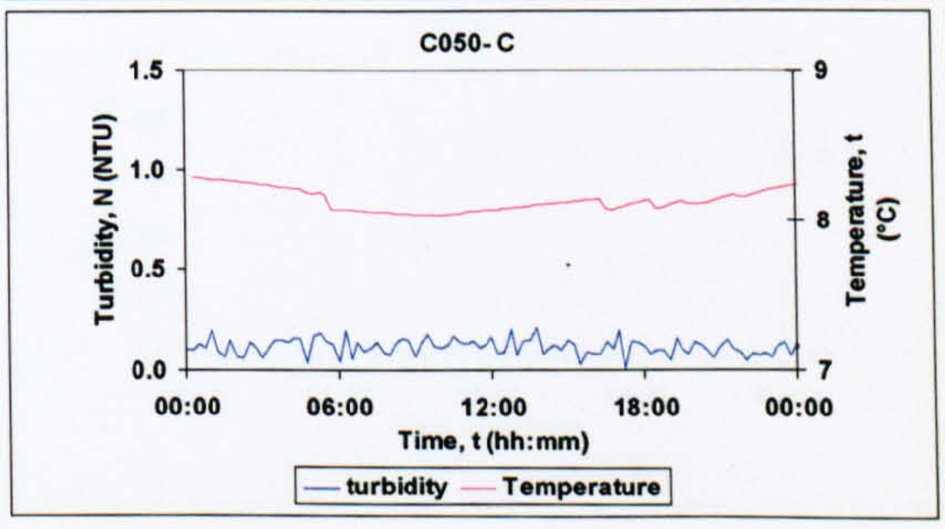

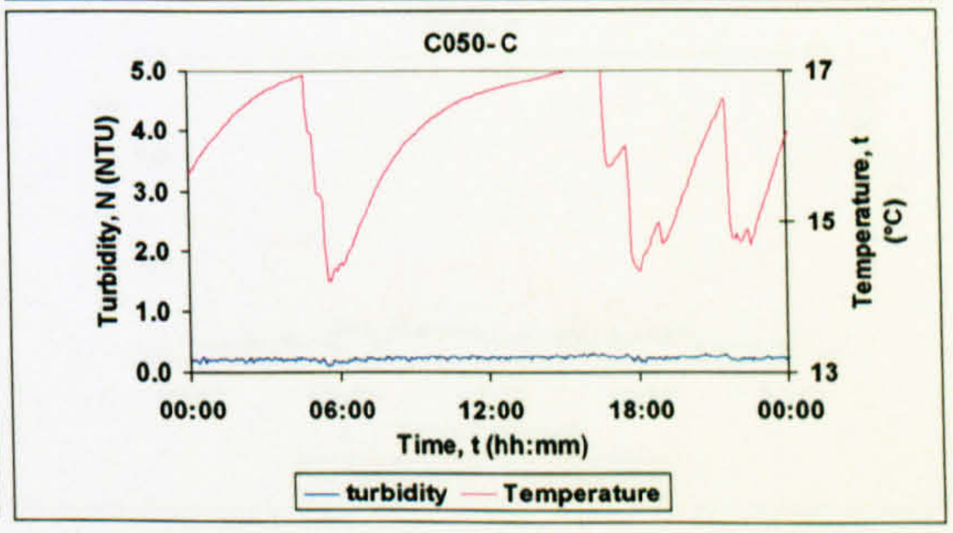

9 26/07/05

Large demand increase

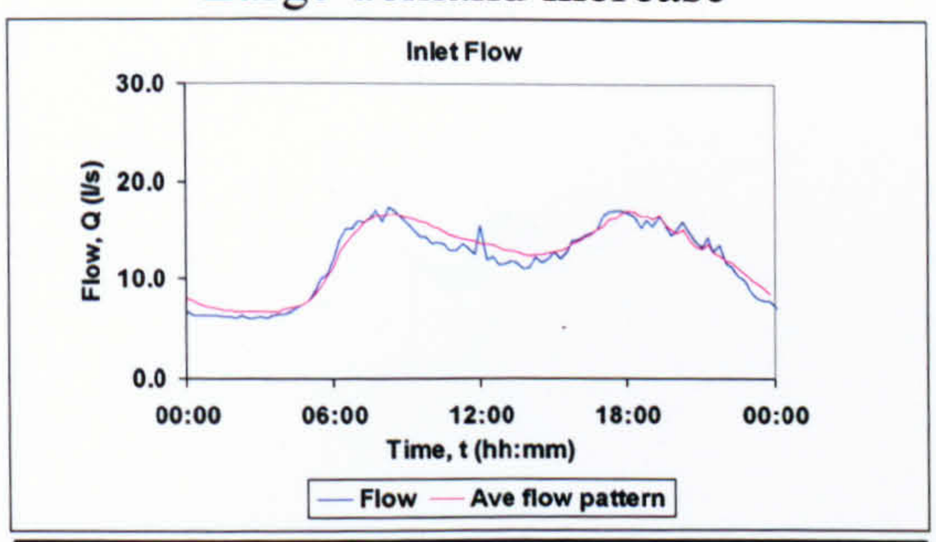

C050-A -No Data

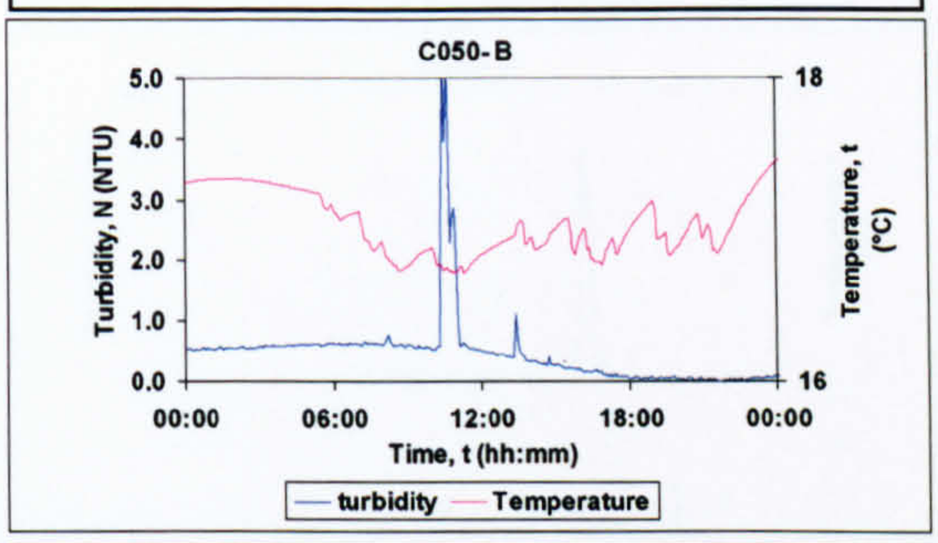

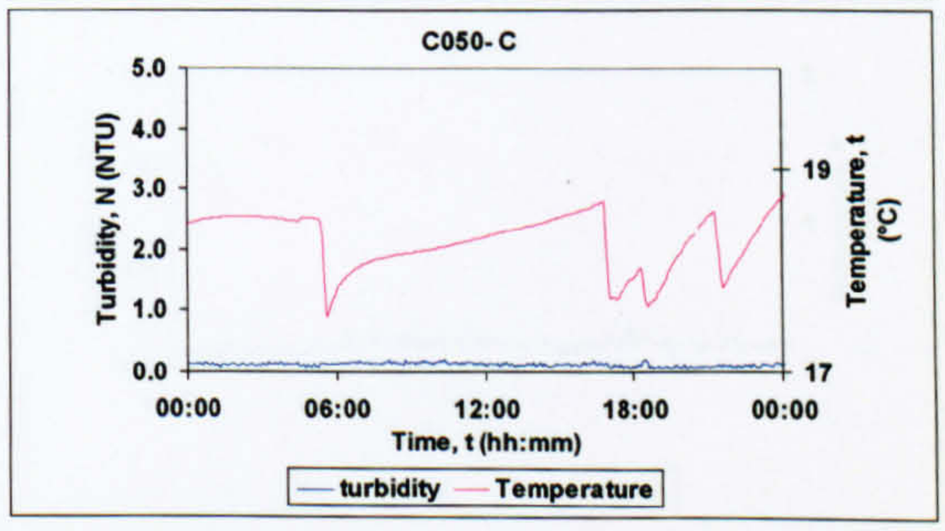

10 07/10/05

Demand increase with no turbidity

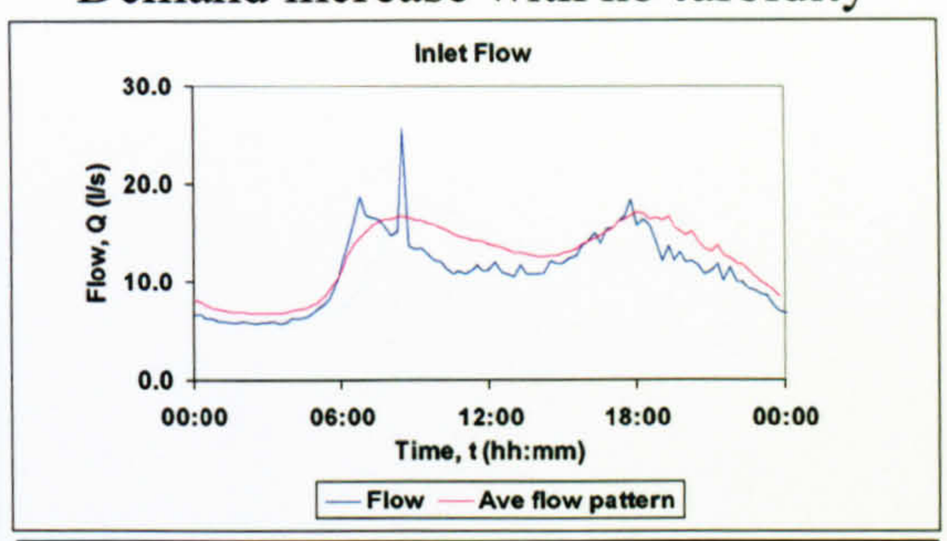

C050-A -No Data

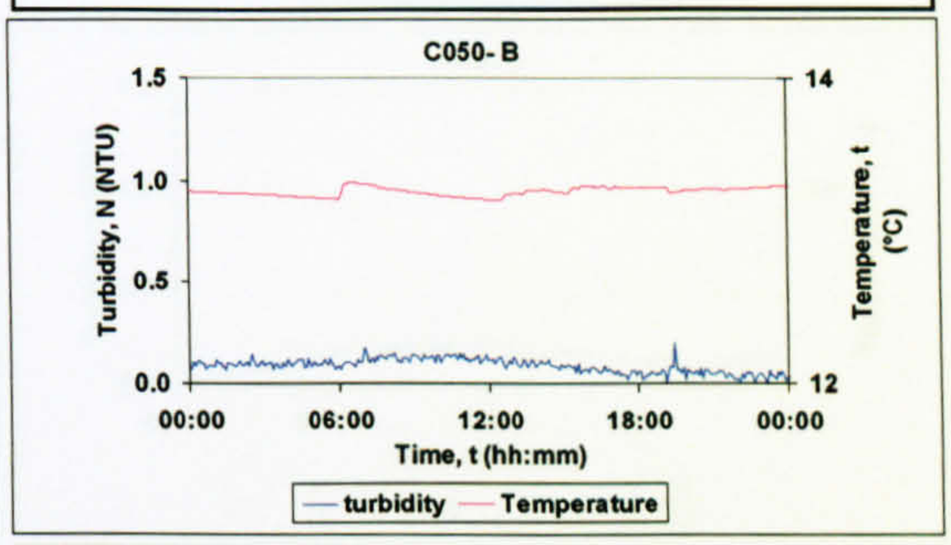

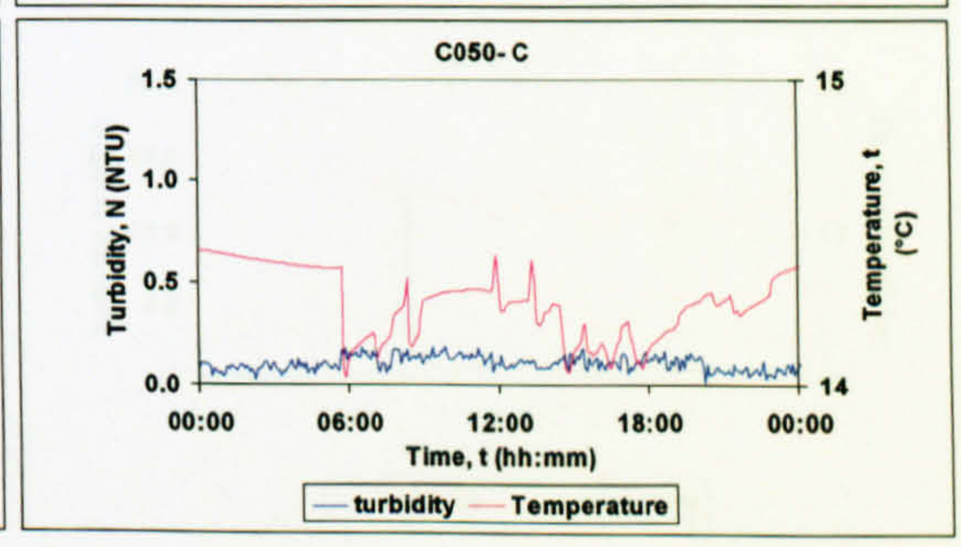

11 17/03/06
Large demand increase

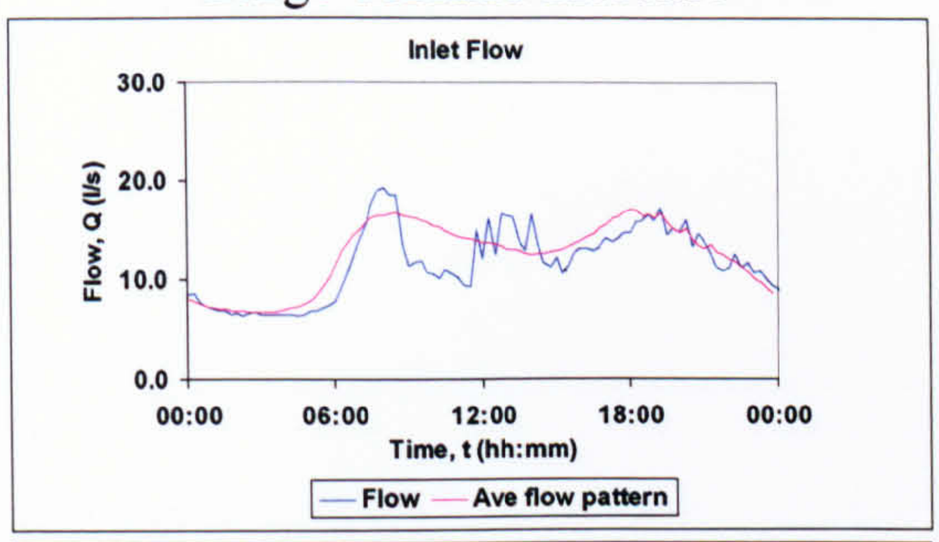

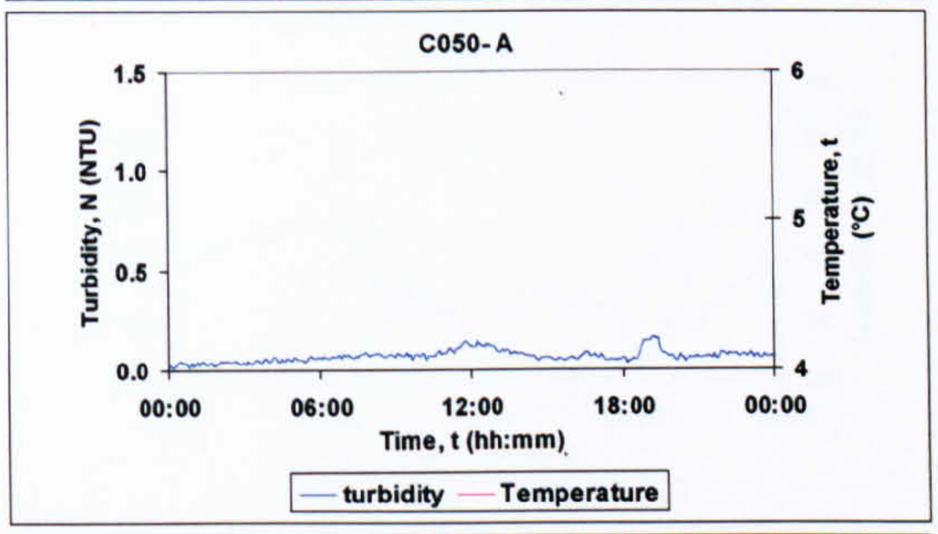

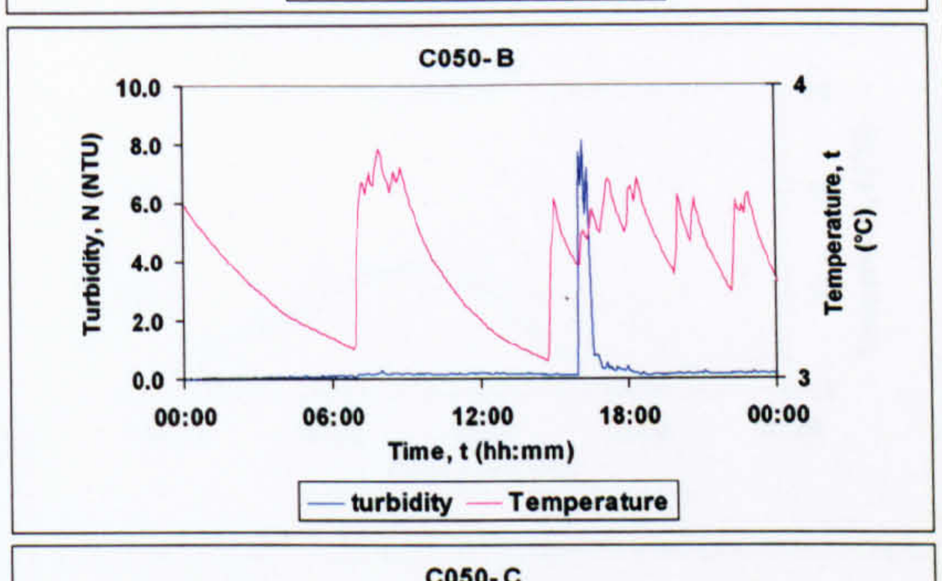

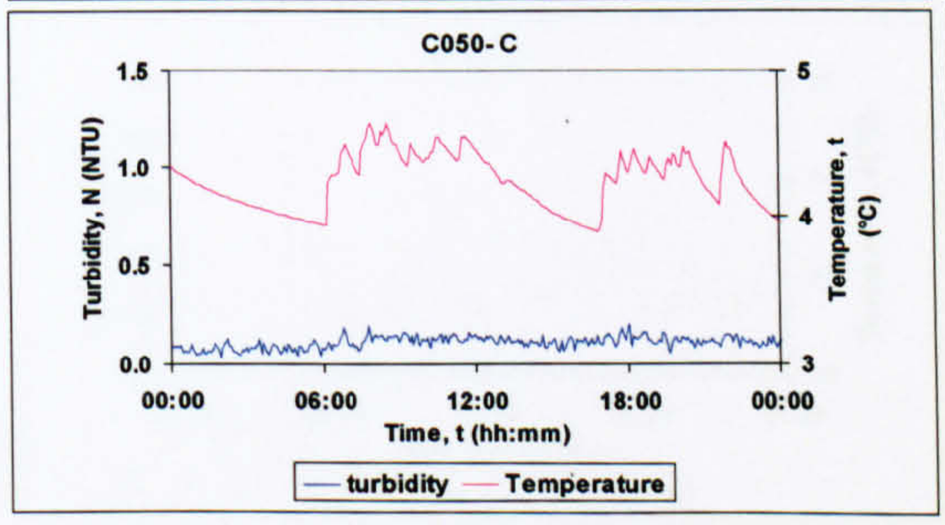

12 14/05/06
Localised demand increase

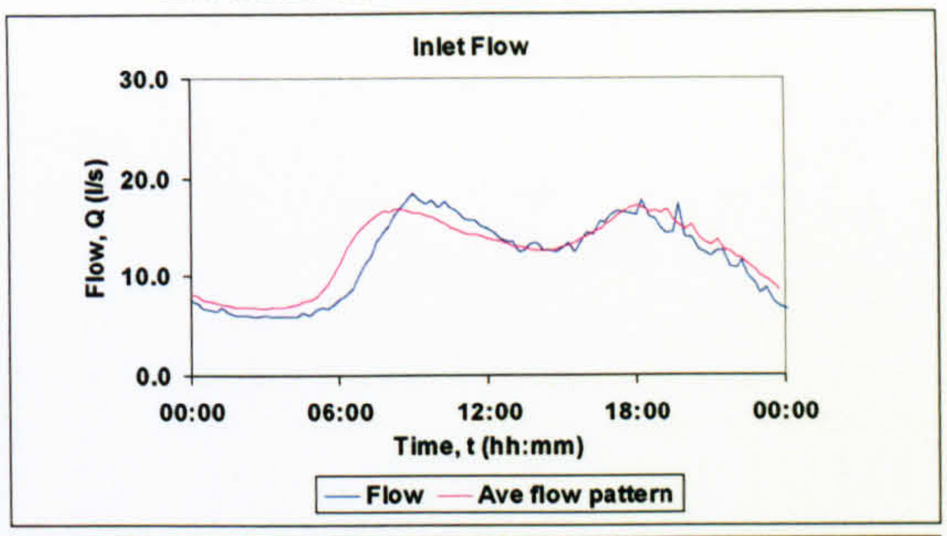

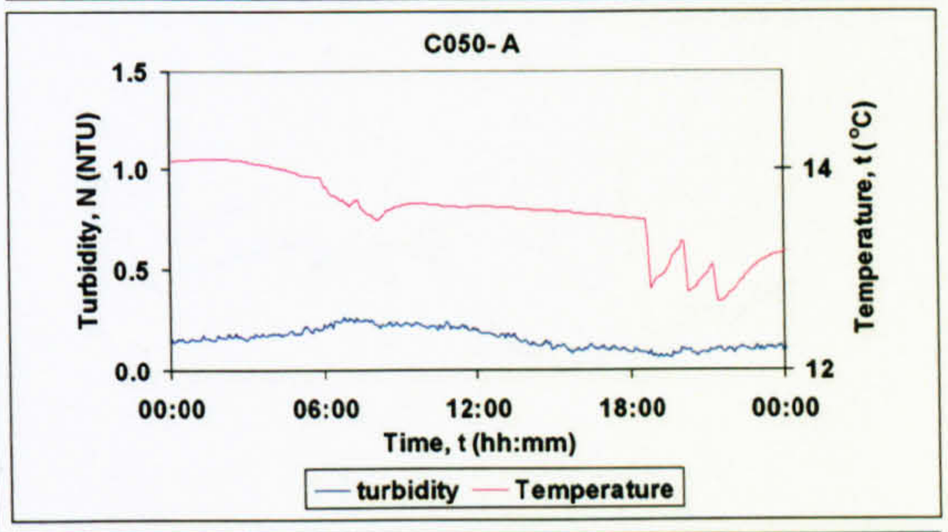

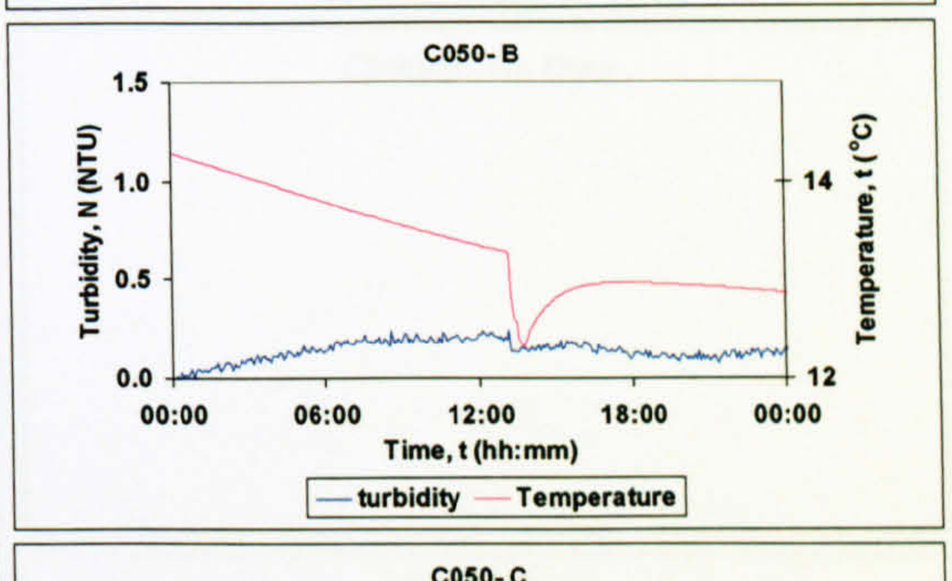

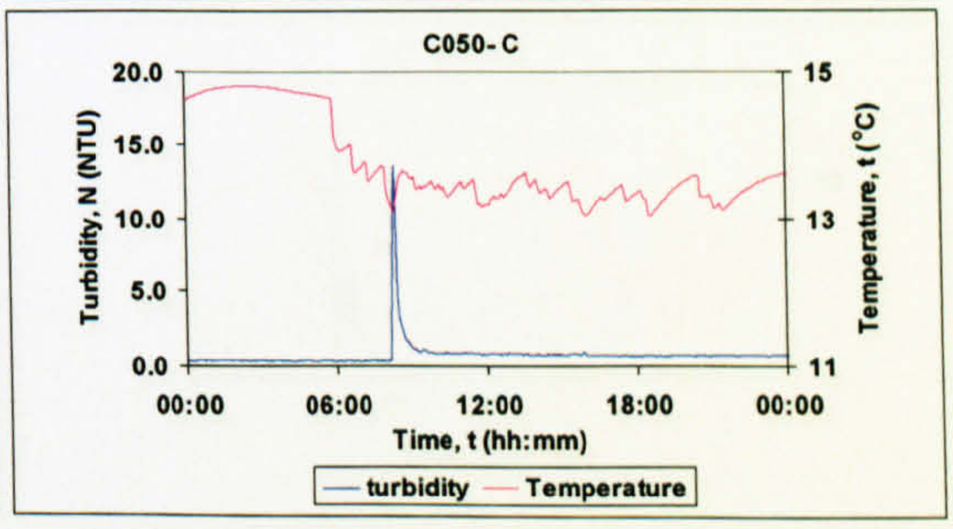

13 09/06/06

Example of daily turbidity cycle

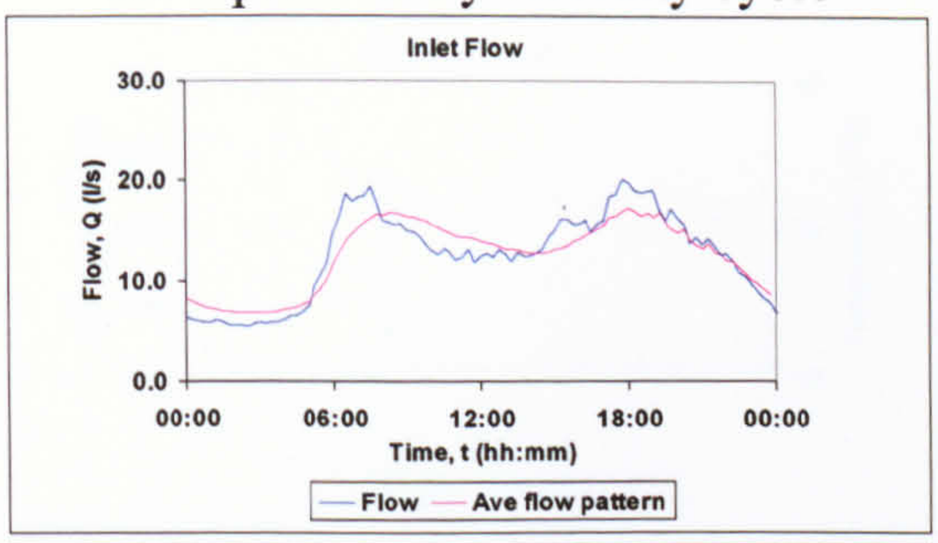

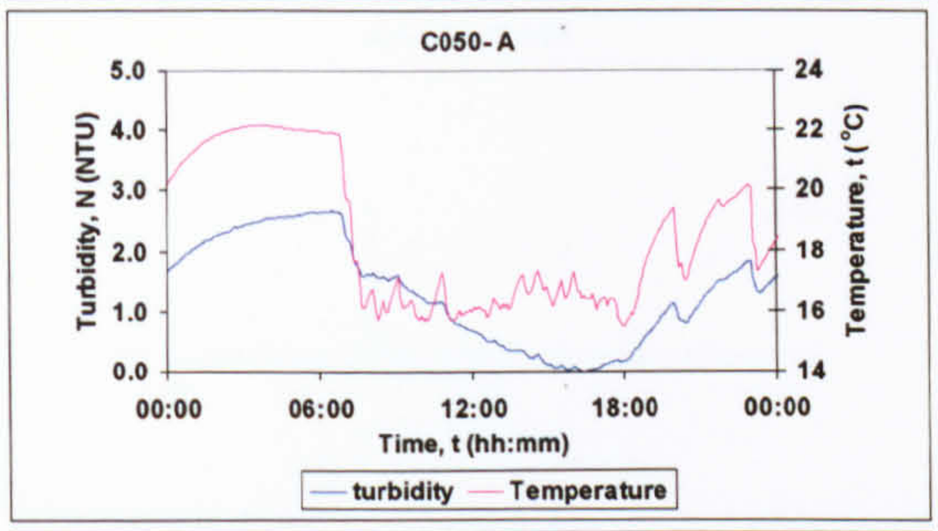

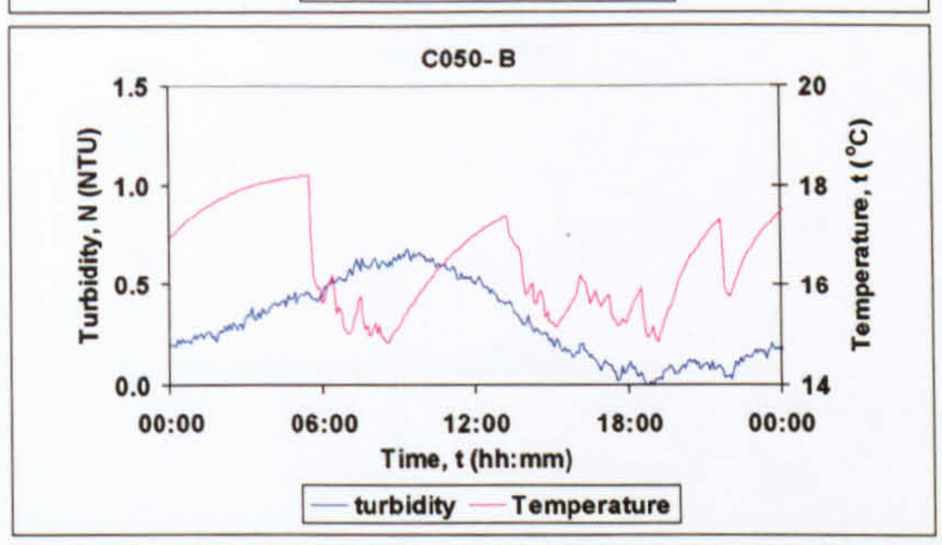

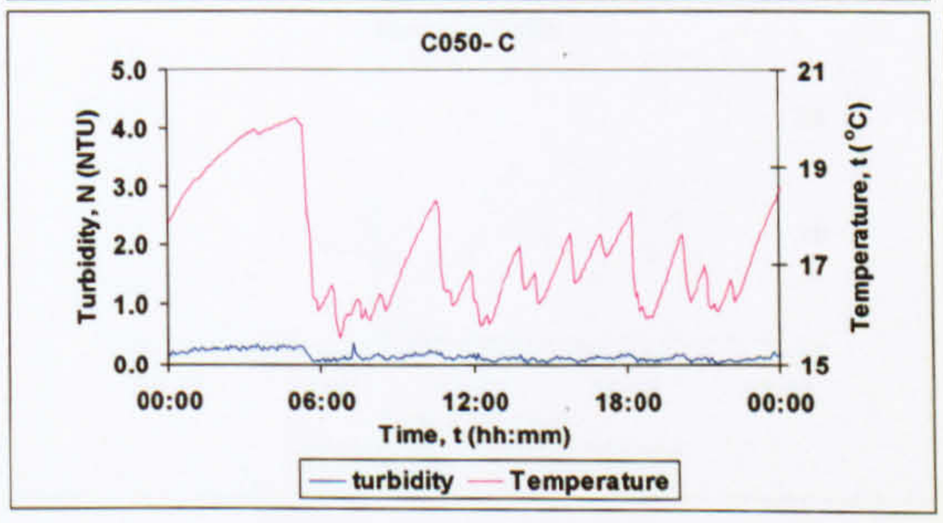

14 13/09/06

Localised demand increase

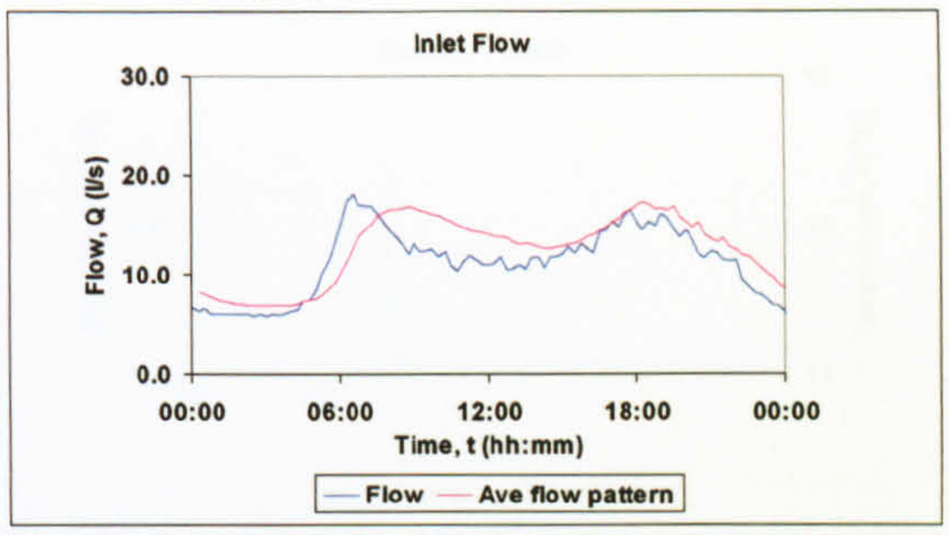

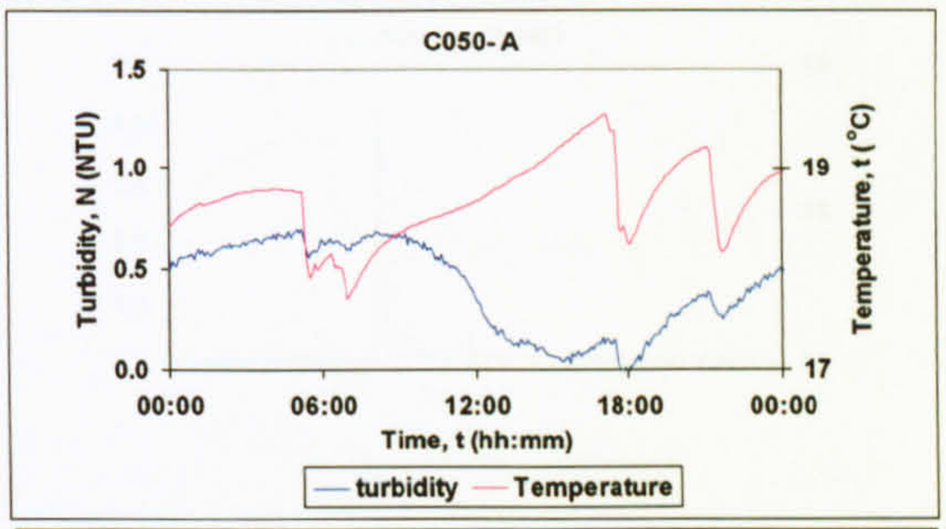

C050-B -No Data

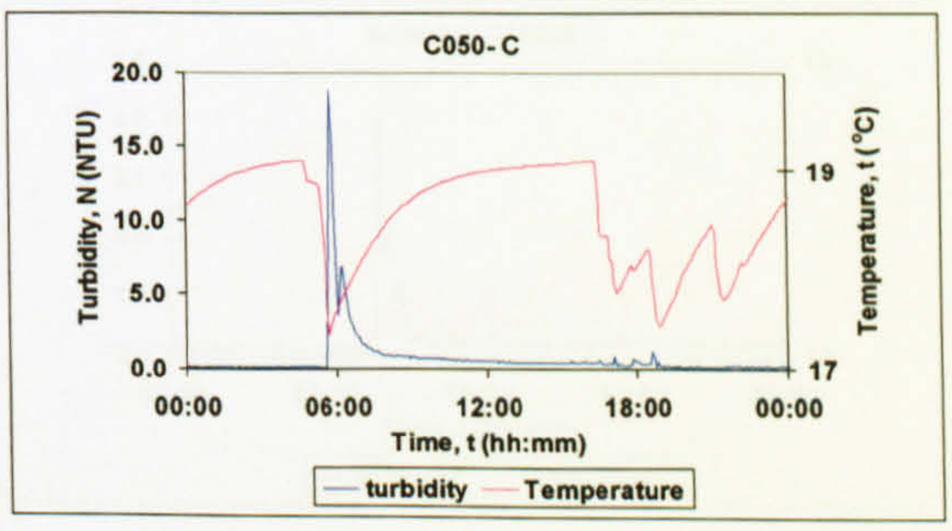

C050 C- Weekend Events

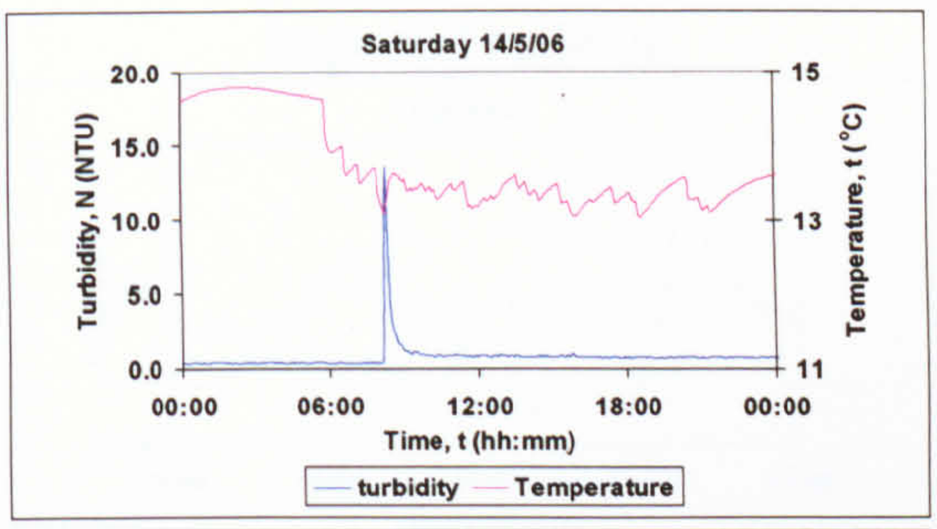

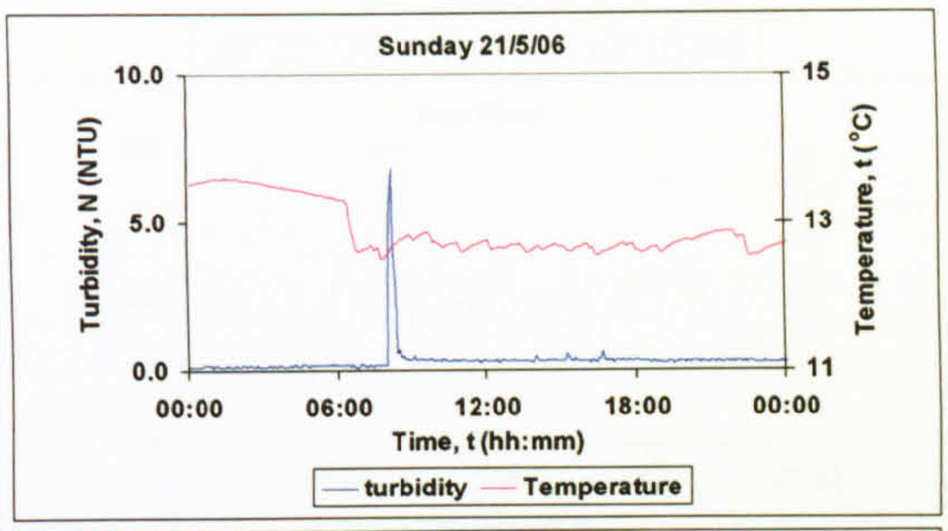

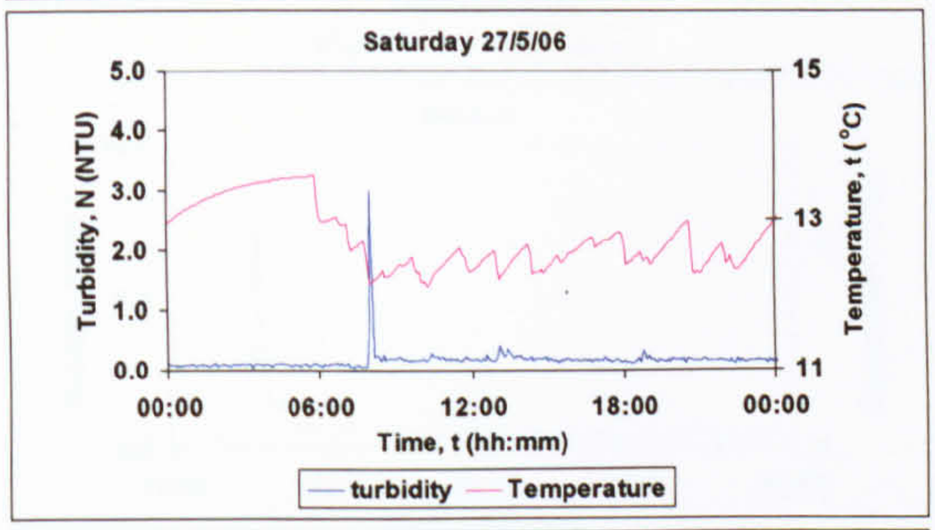

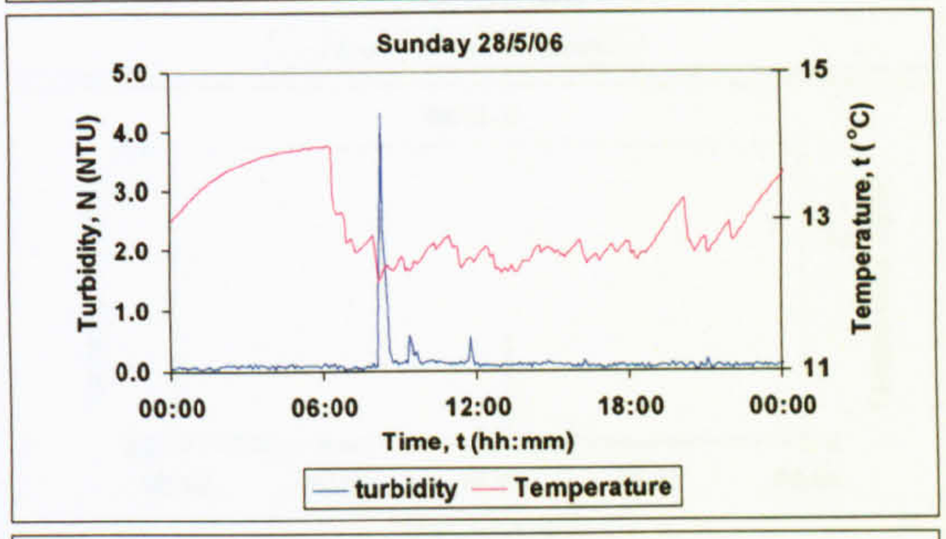

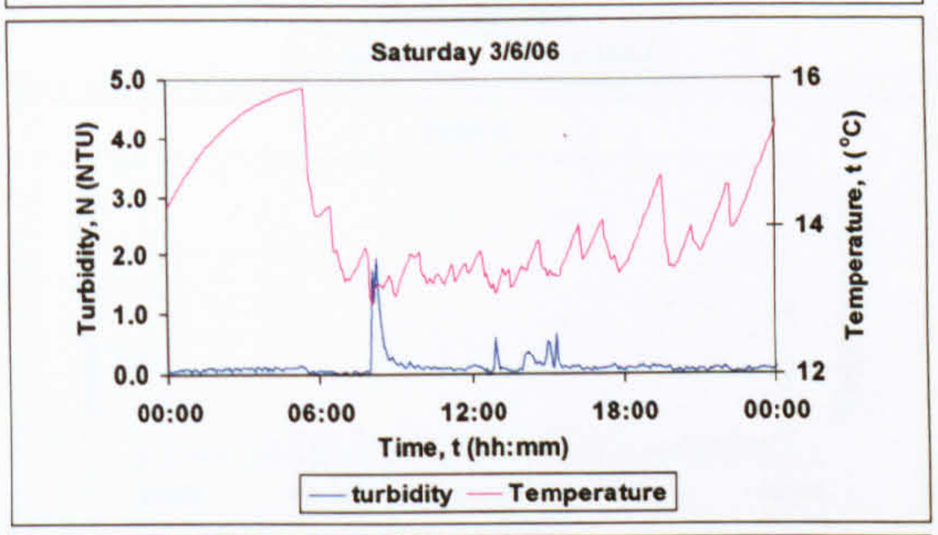

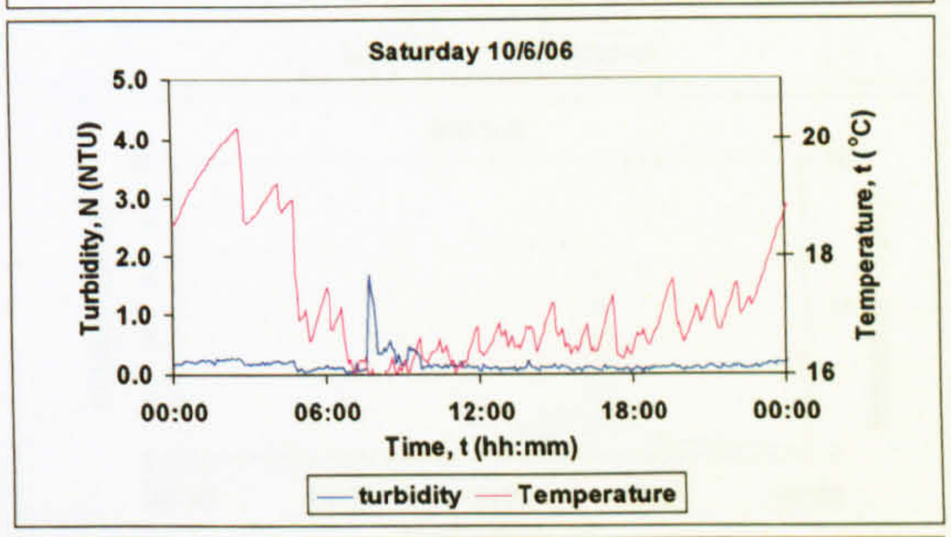

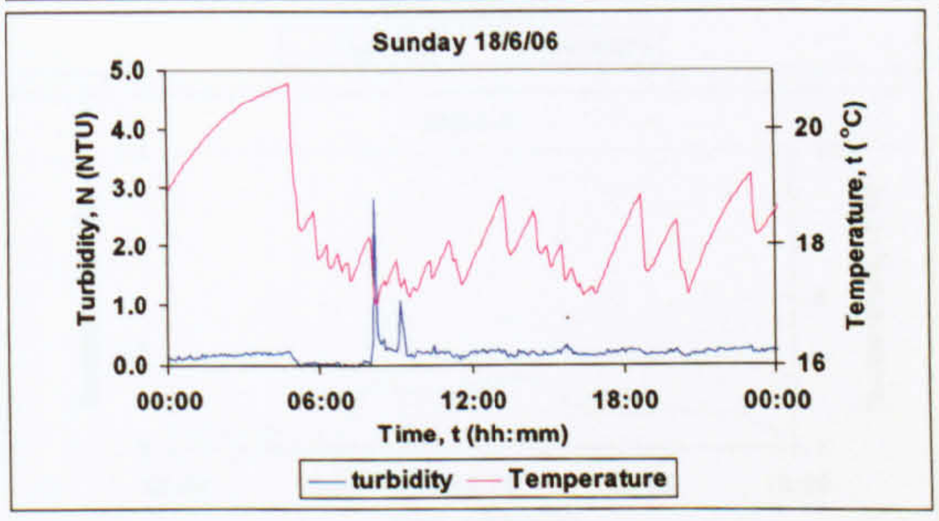

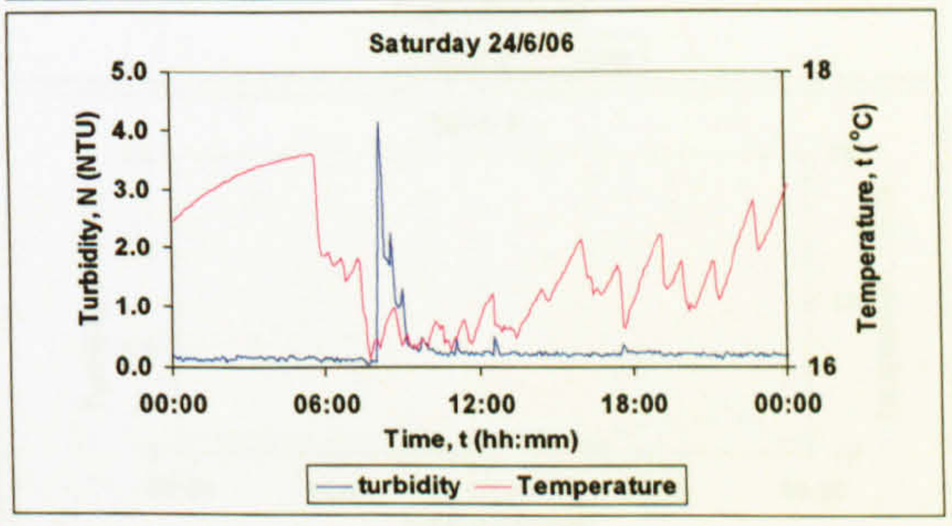

1 23/01/05
Imported material

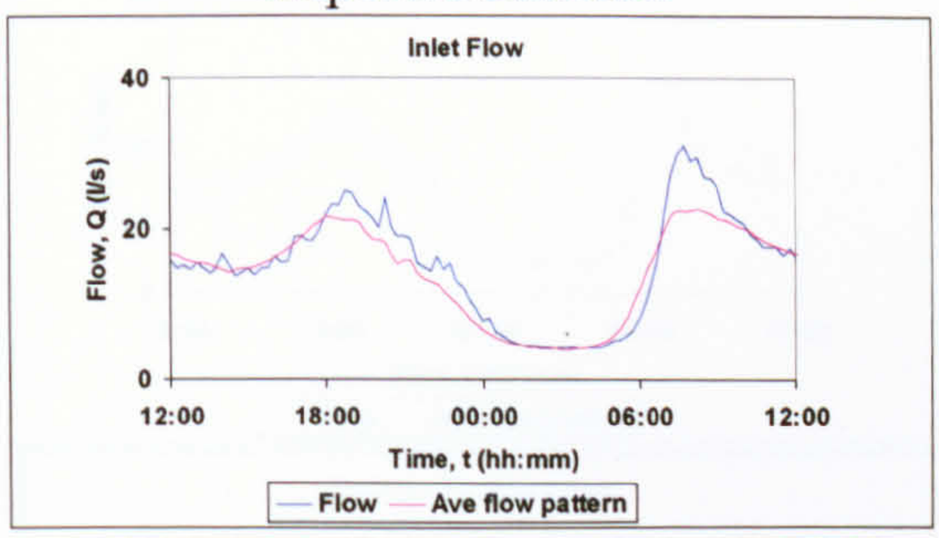

2 28/04/05
Large increase in demand

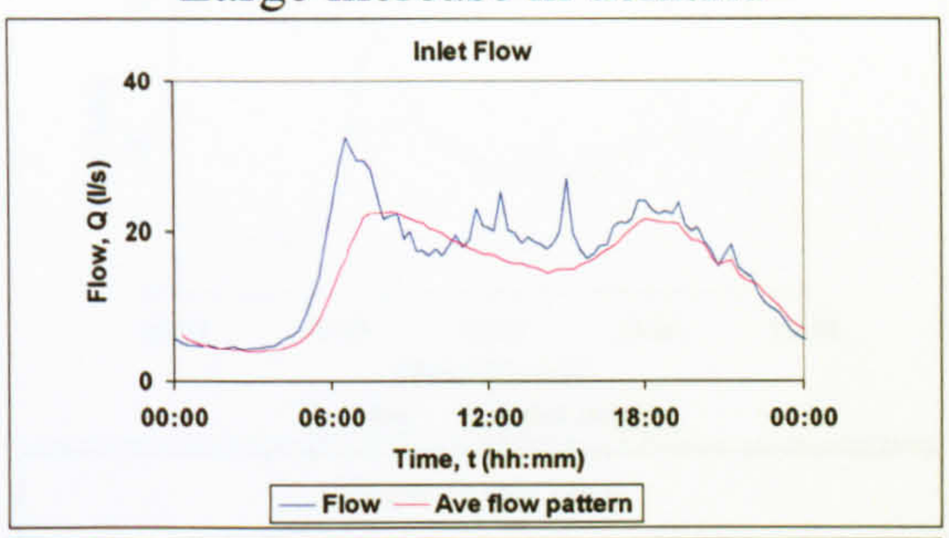

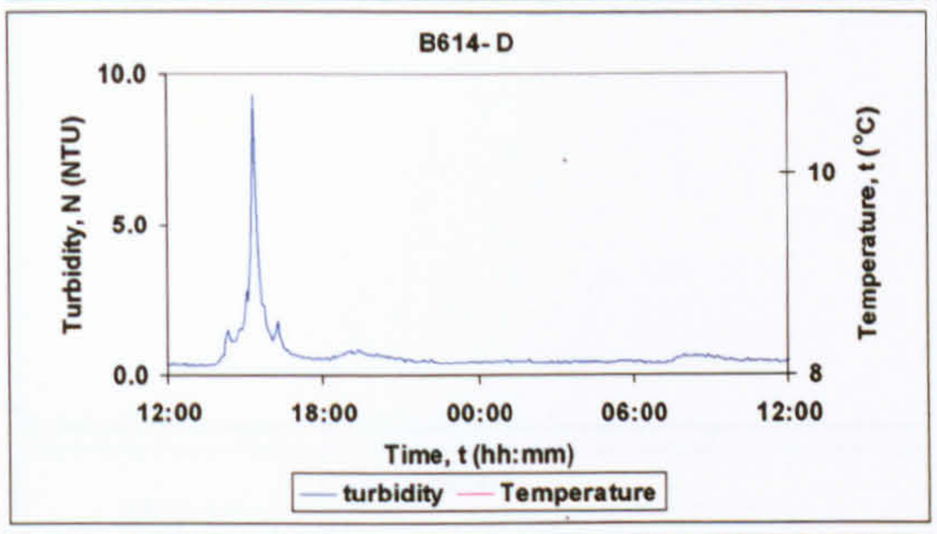

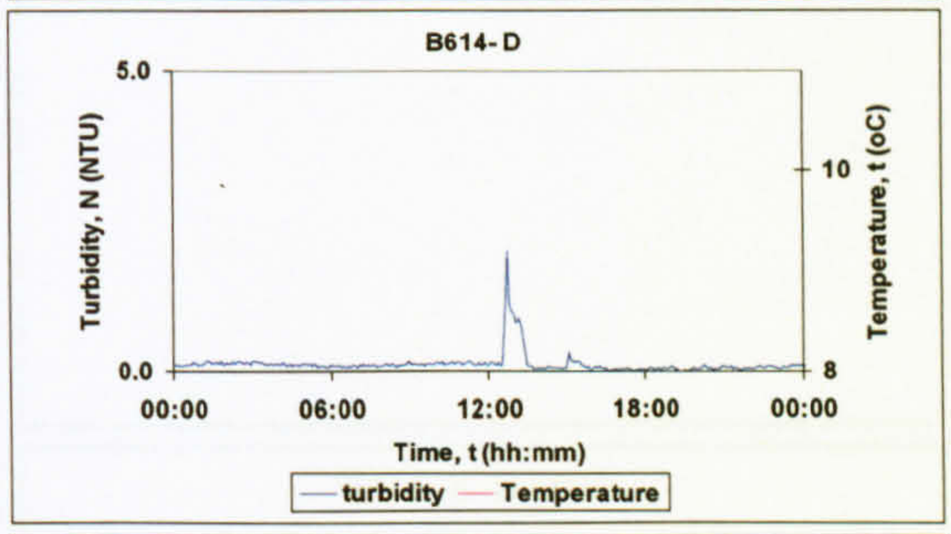

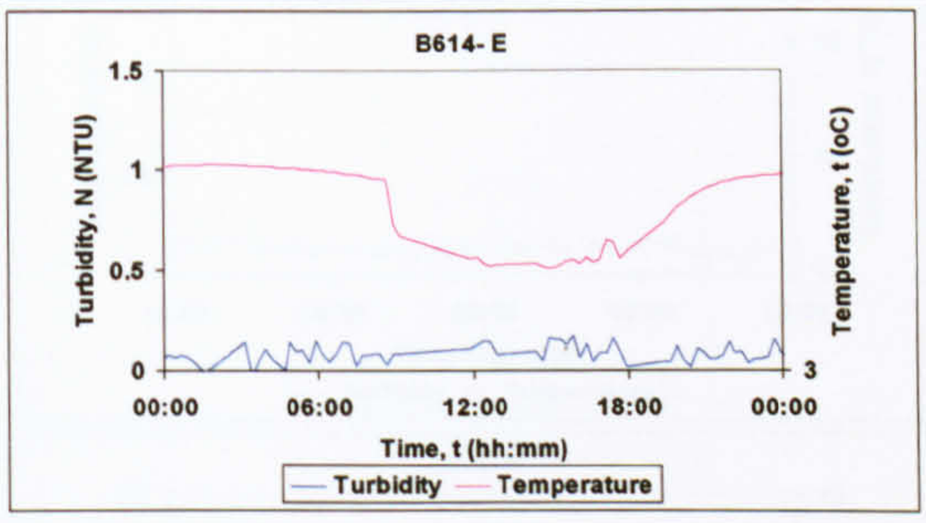

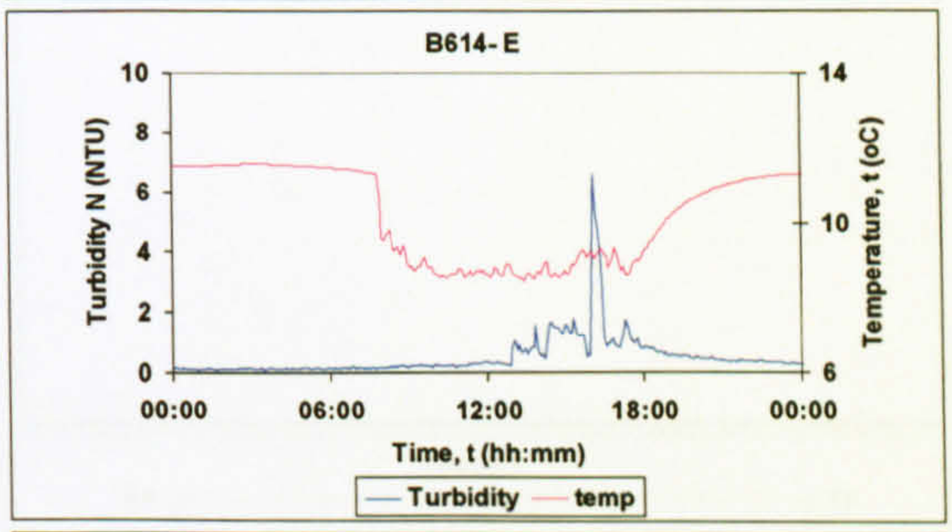

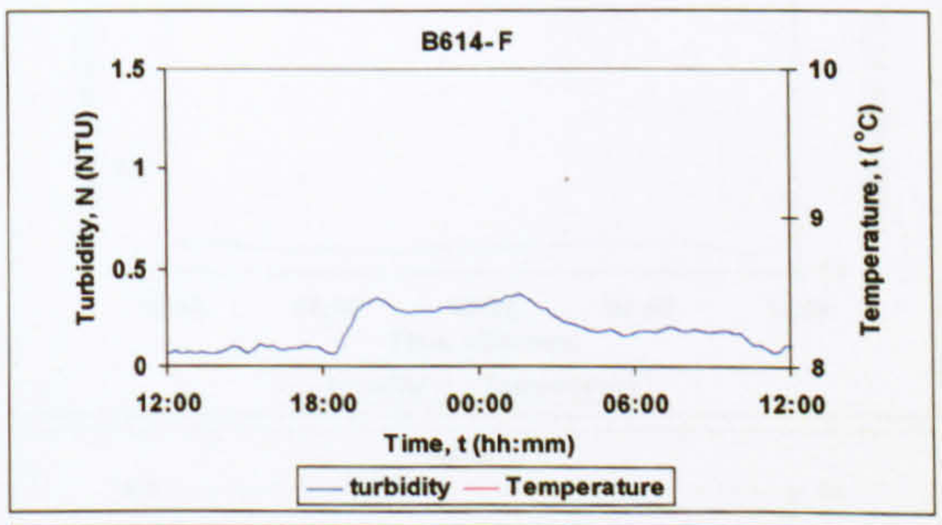

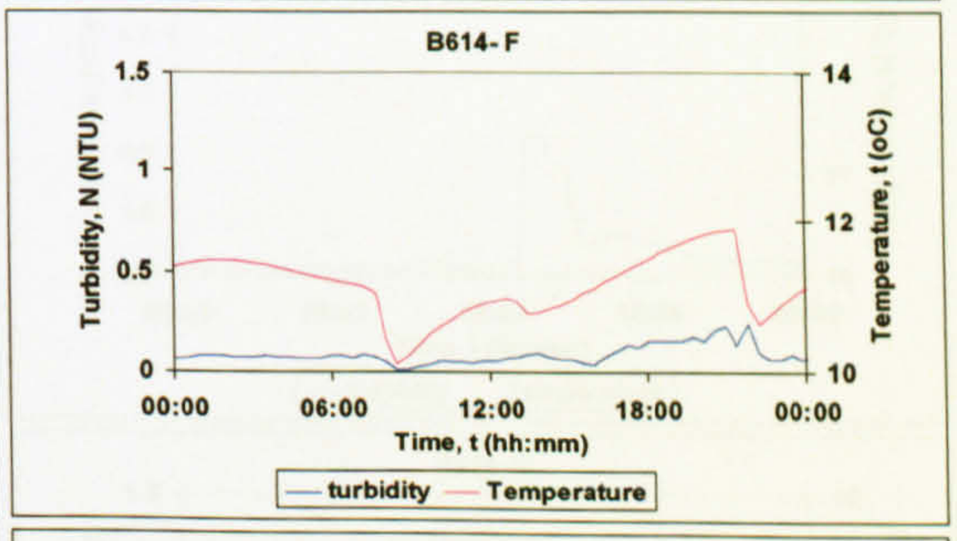

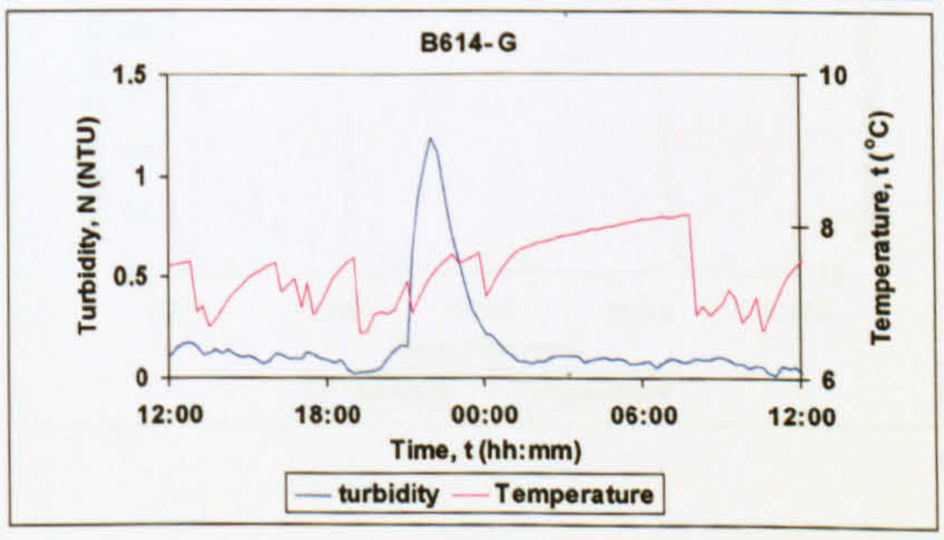

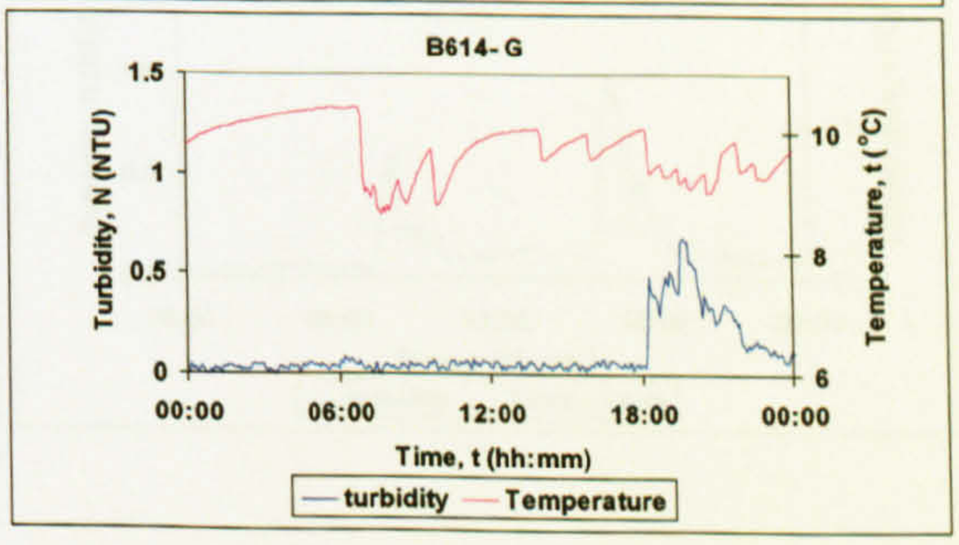

3 15/06/05
Localised demand increase

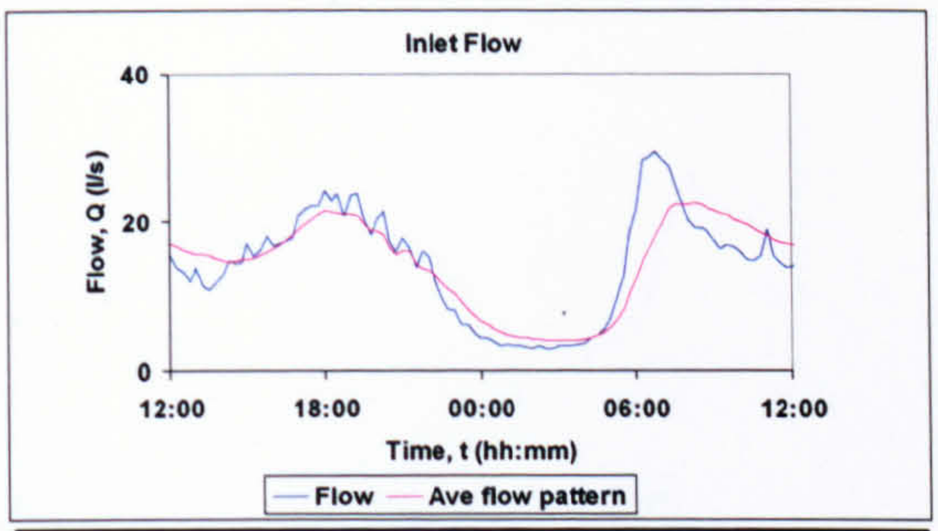

4 01/11/05
Imported material

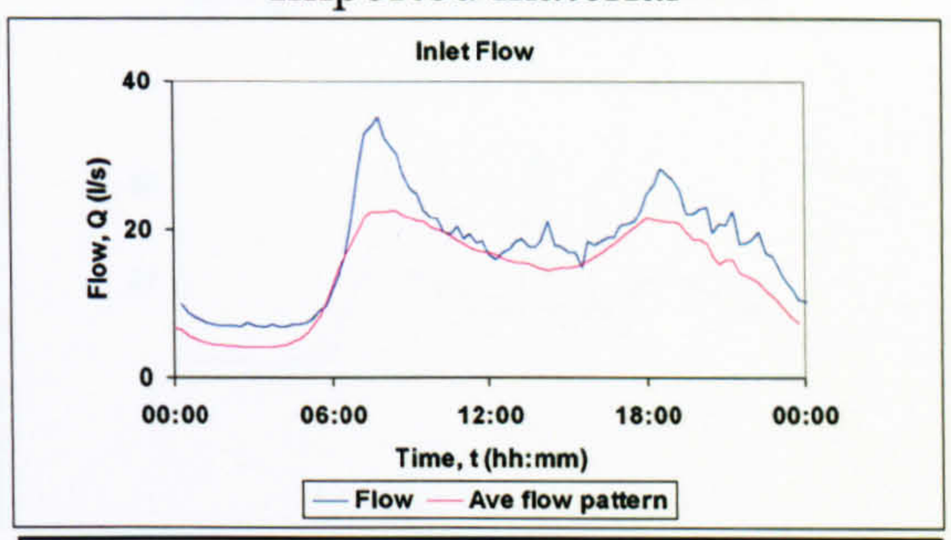

B614- D -No Data

B614- D -No Data

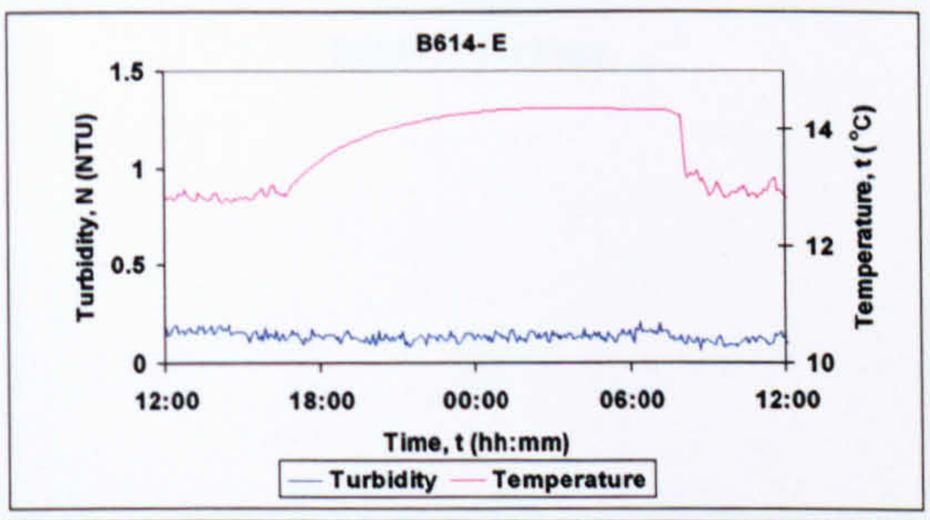

B614- E -No Data

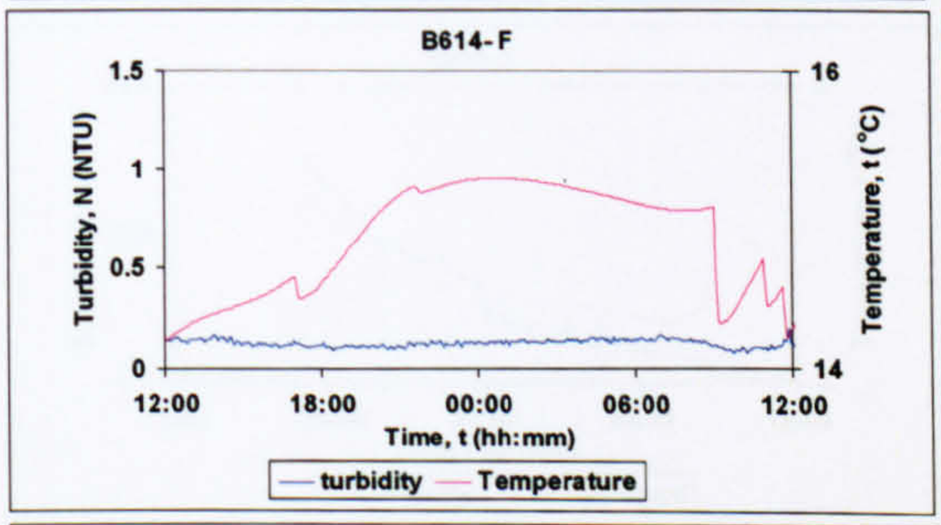

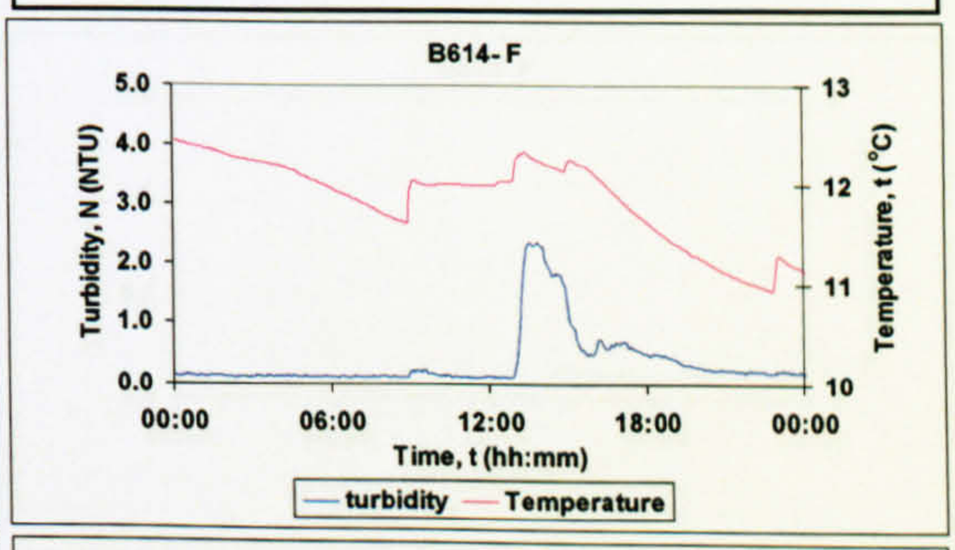

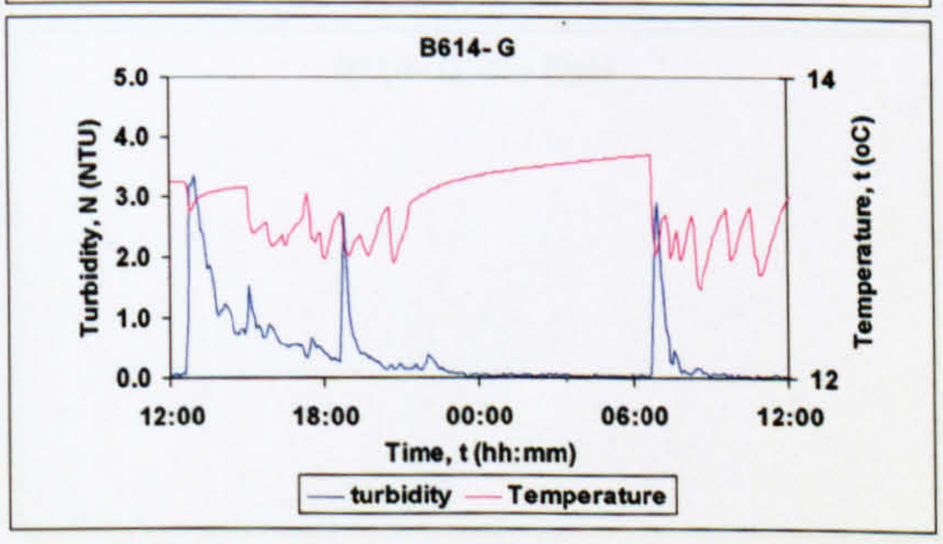

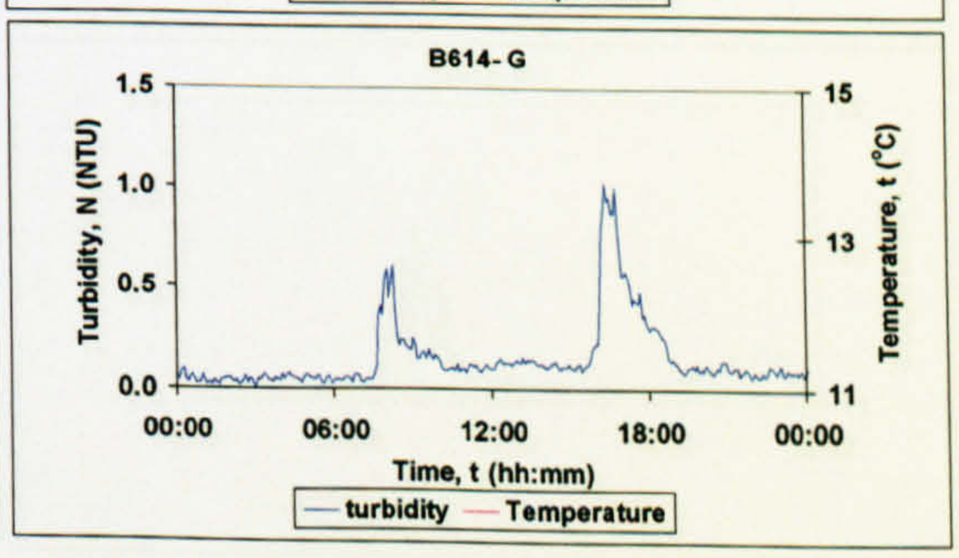

5 05/02/06

Imported material

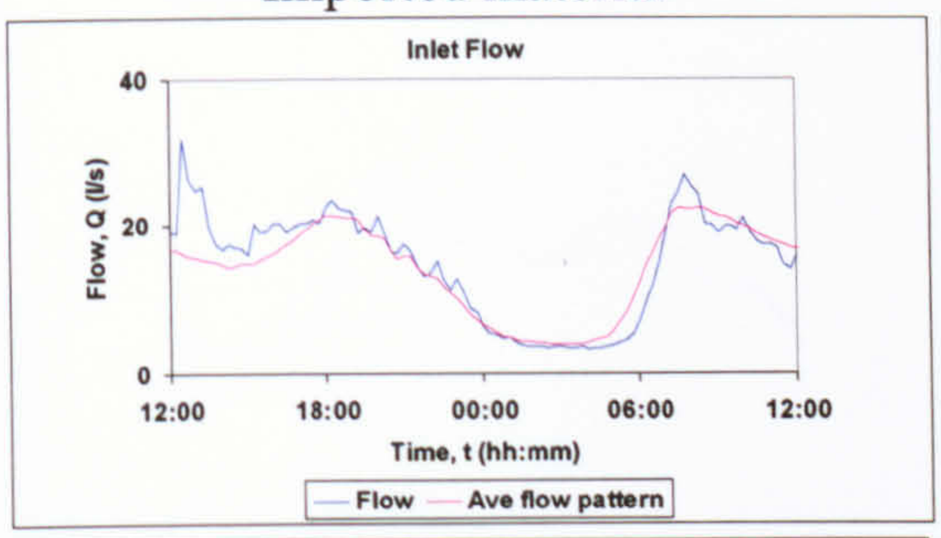

6 23/03/06

Large increase in demand

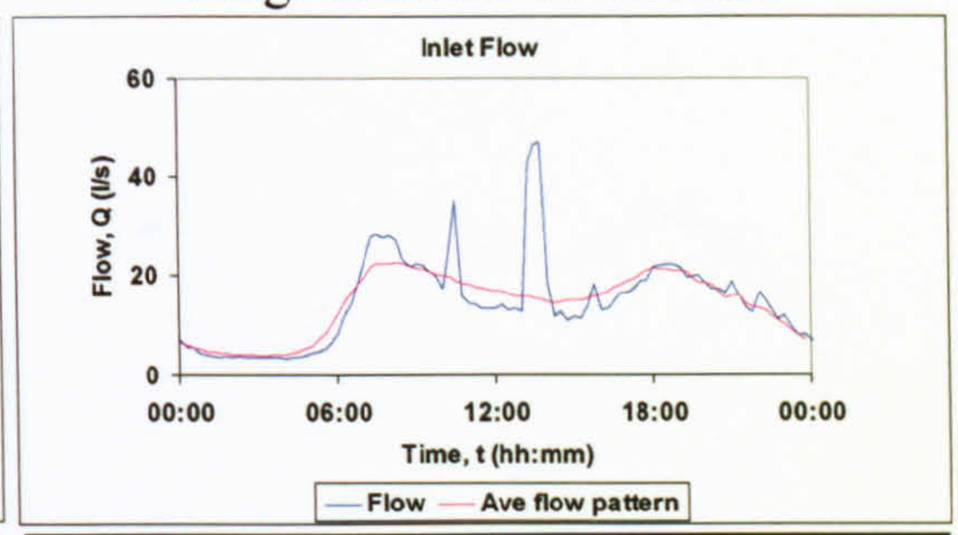

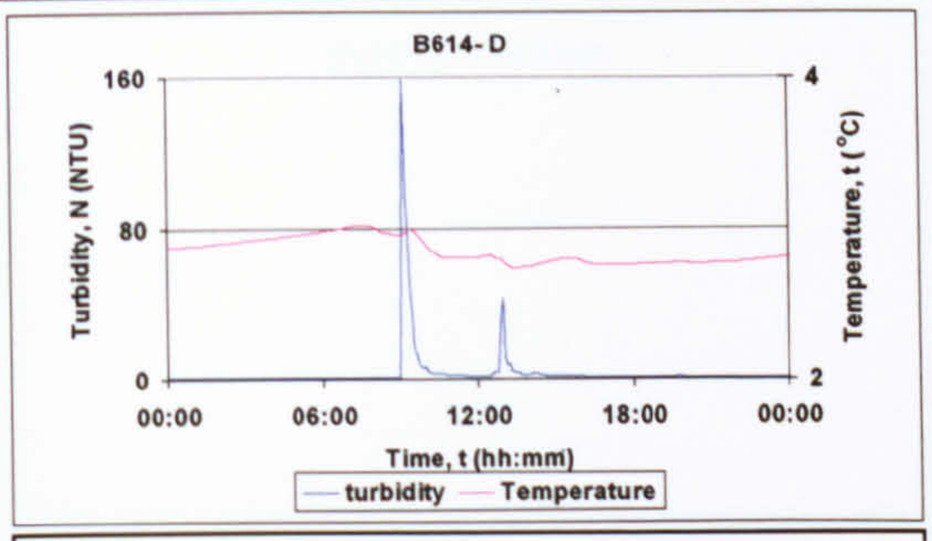

B614- D -No Data

B614- E -No Data

B614- E -No Data

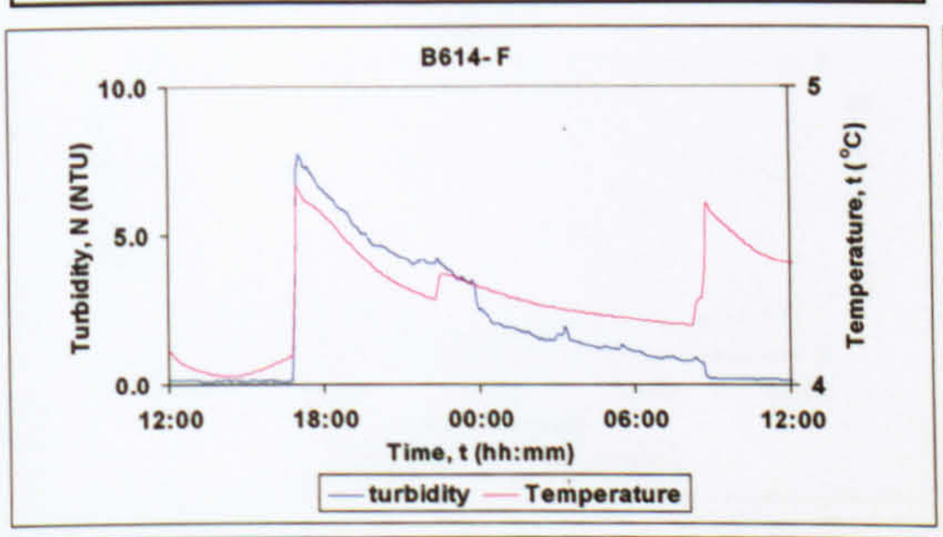

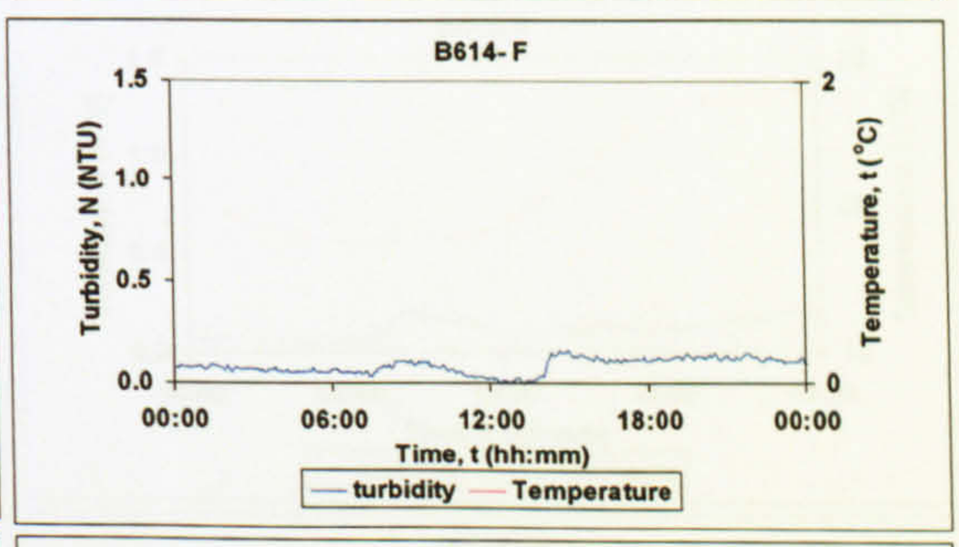

B614- G -No Data

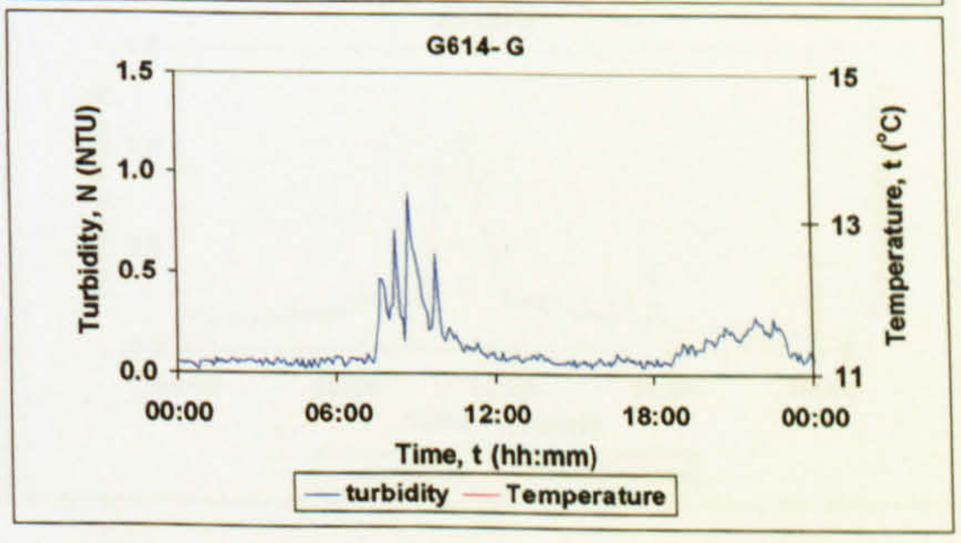

7 29/04/06
Localised demand increase

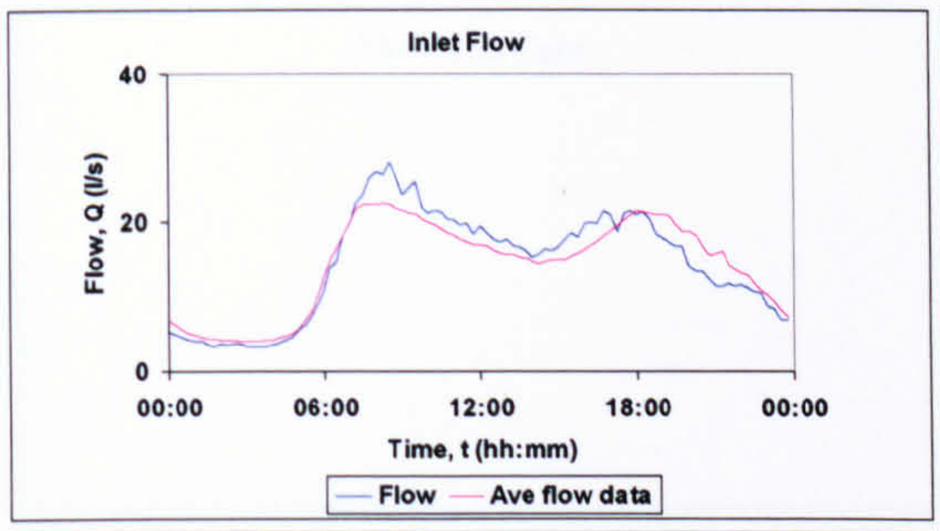

B614- D -No Data

B614- E -No Data

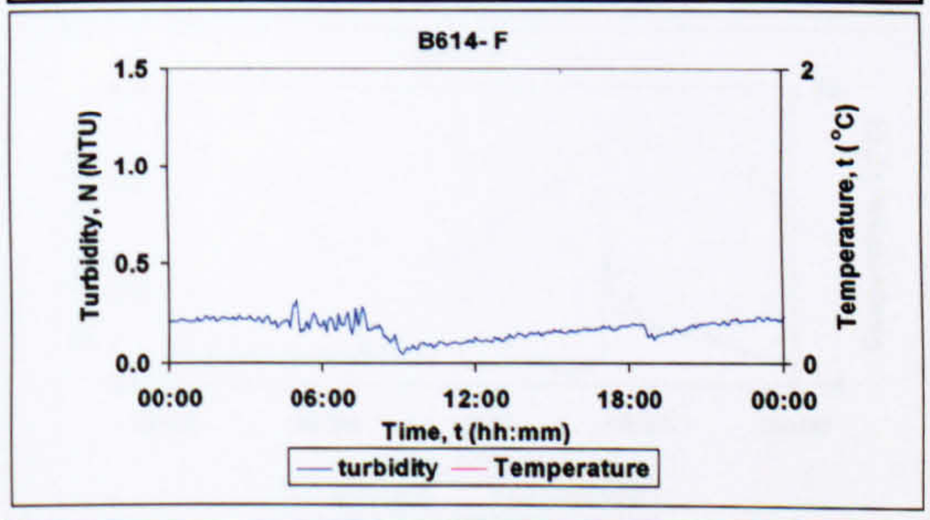

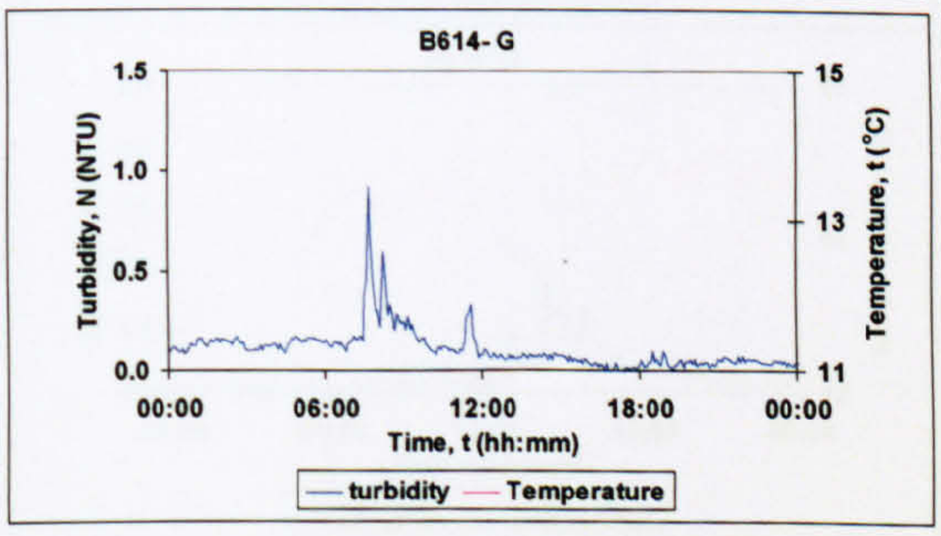

8 03/08/06
Imported material

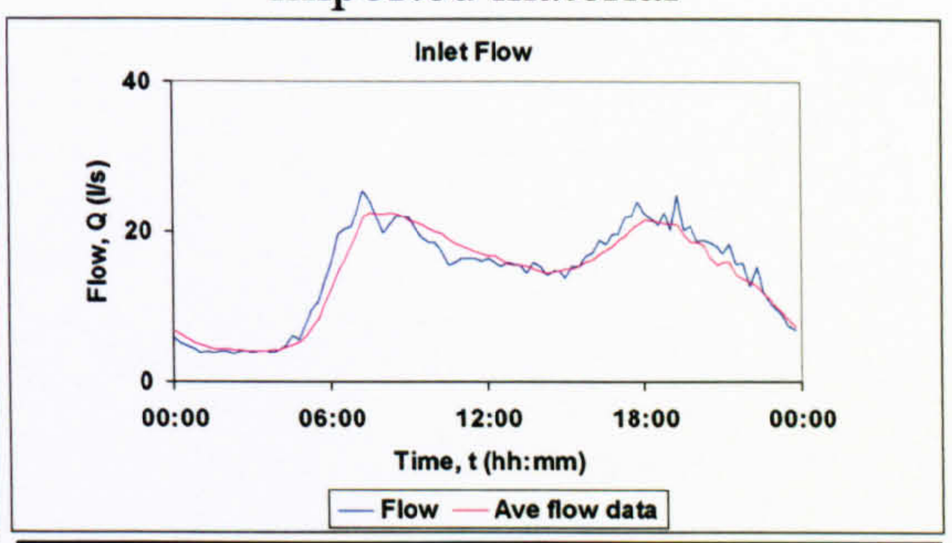

B614- D -No Data

B614- E -No Data

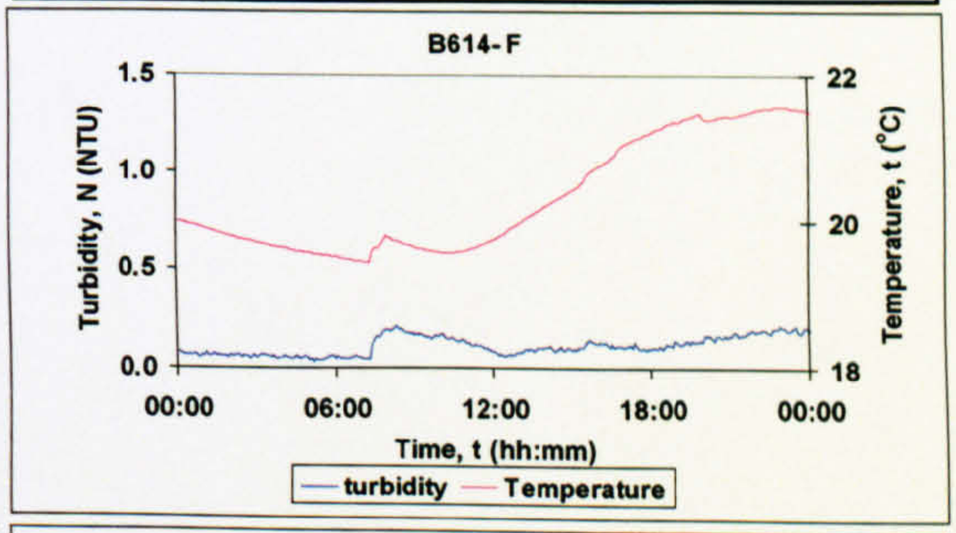

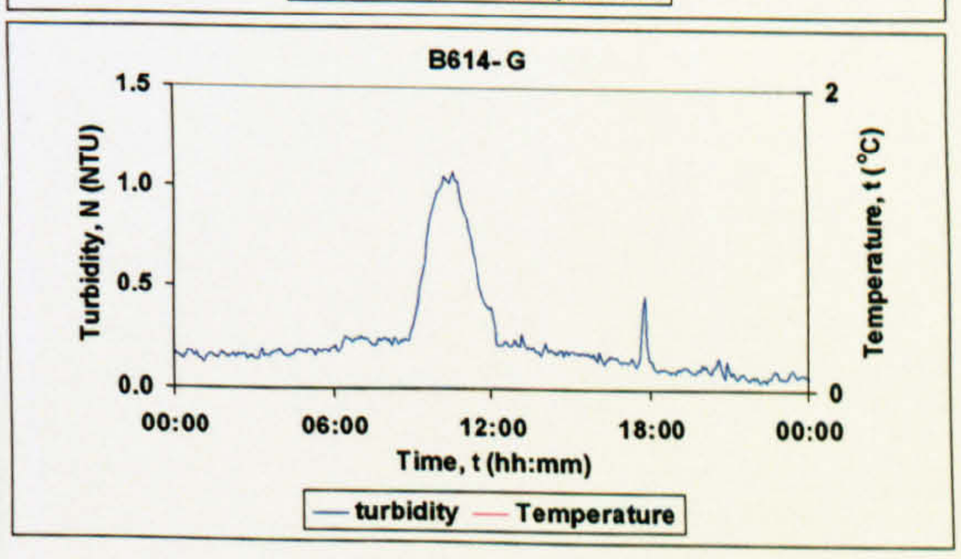

9 04/10/07

Unknown

Flow -No Data

B614-D -No Data

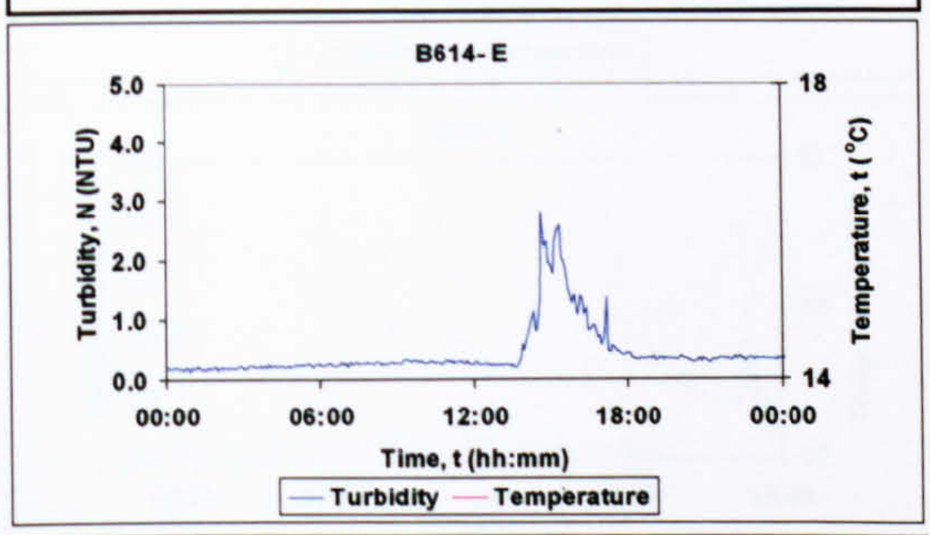

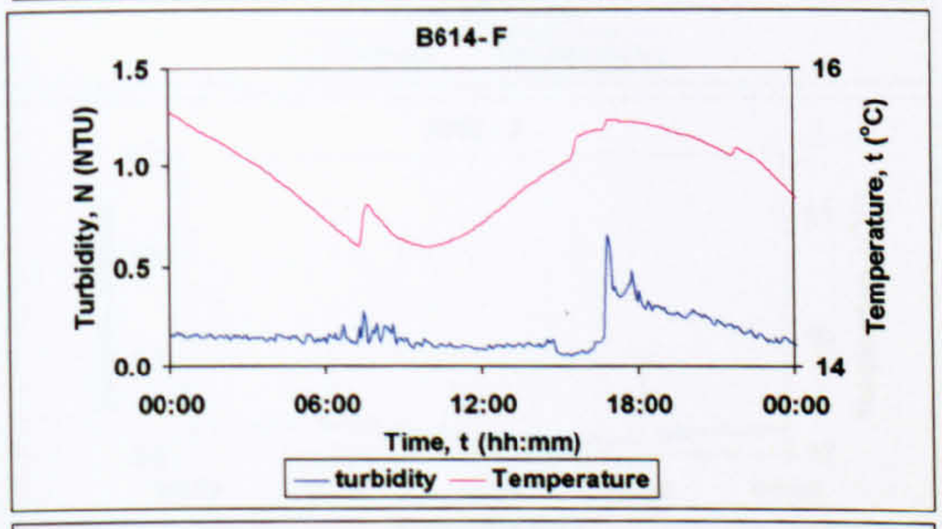

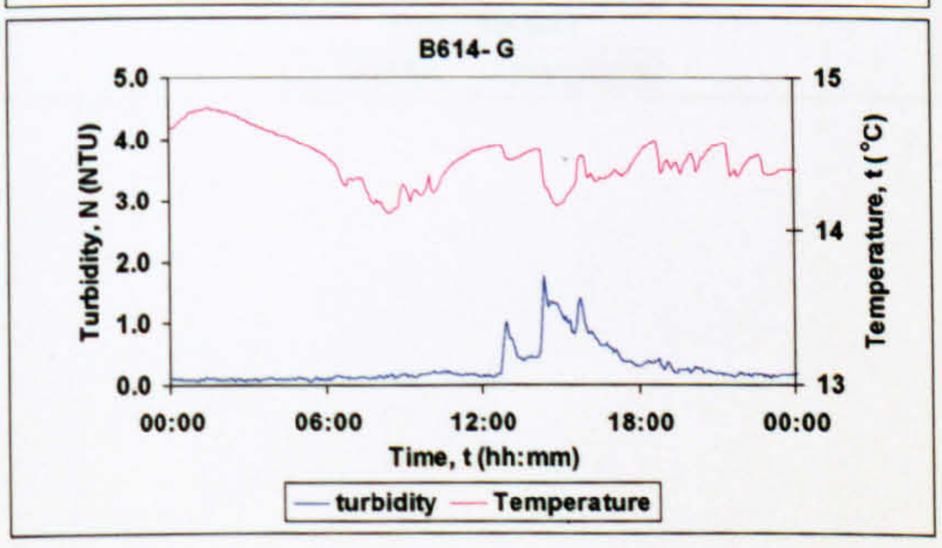

A285

1 09/08/05
Imported material

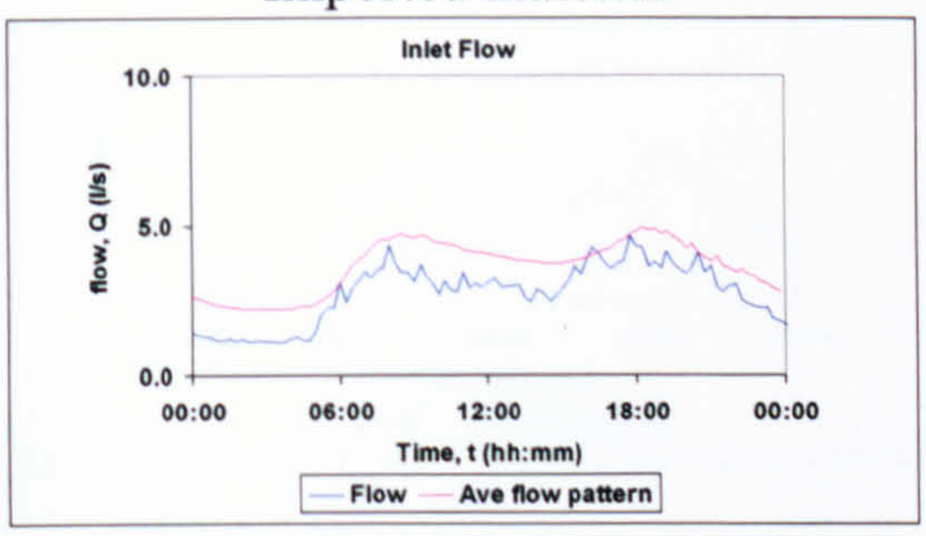

2 21/08/05
Imported material

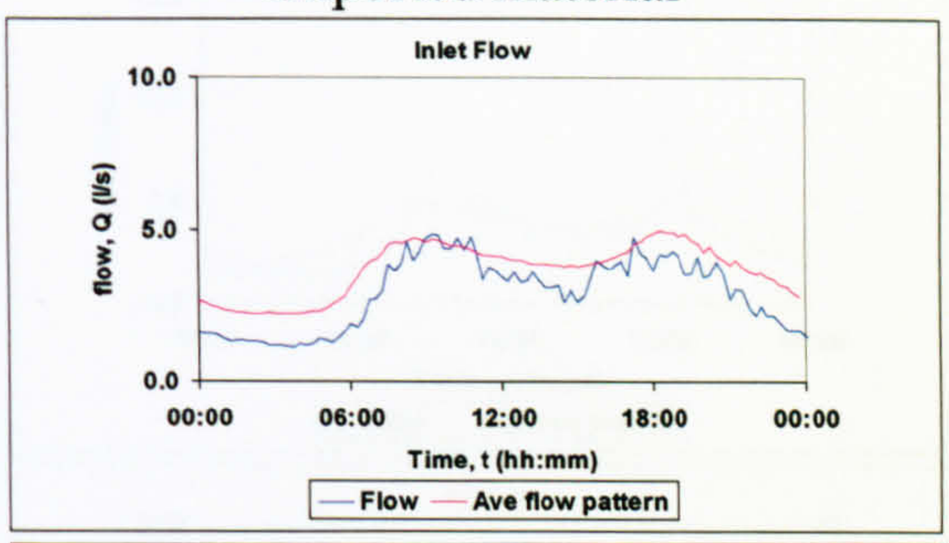

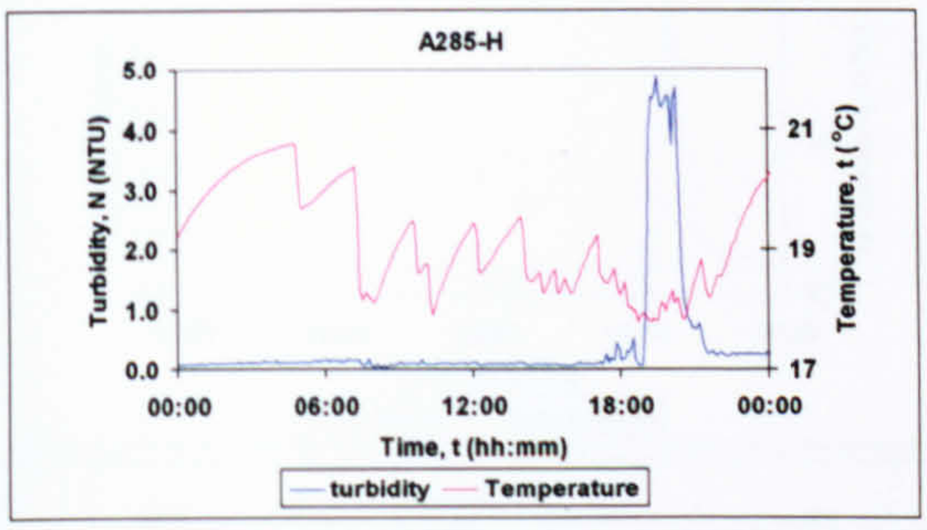

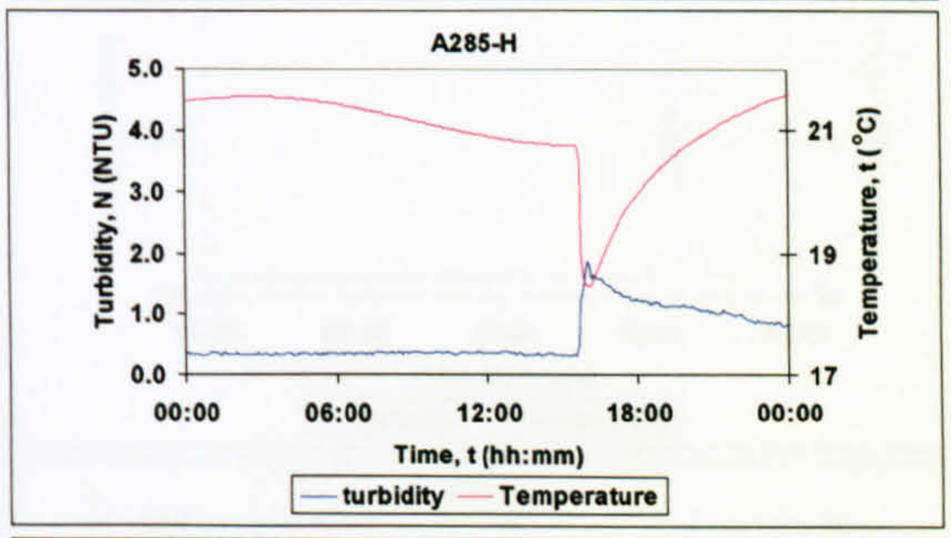

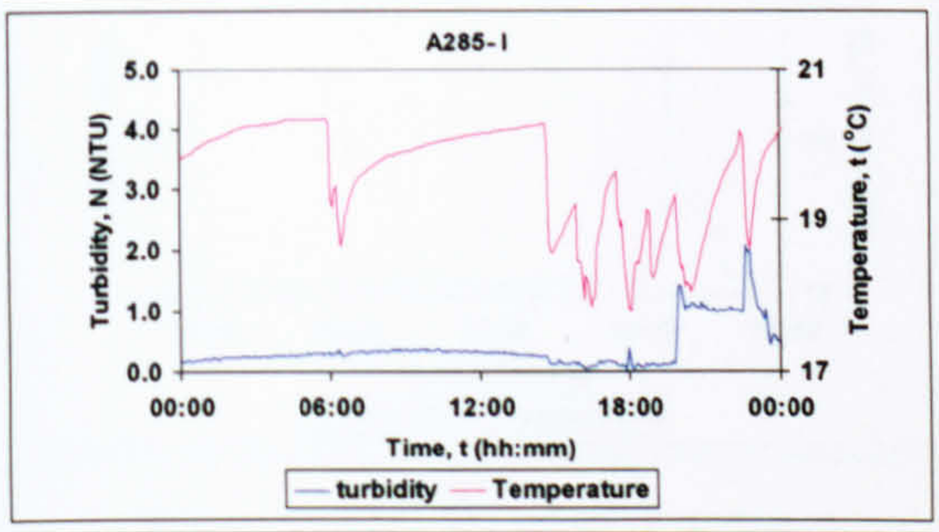

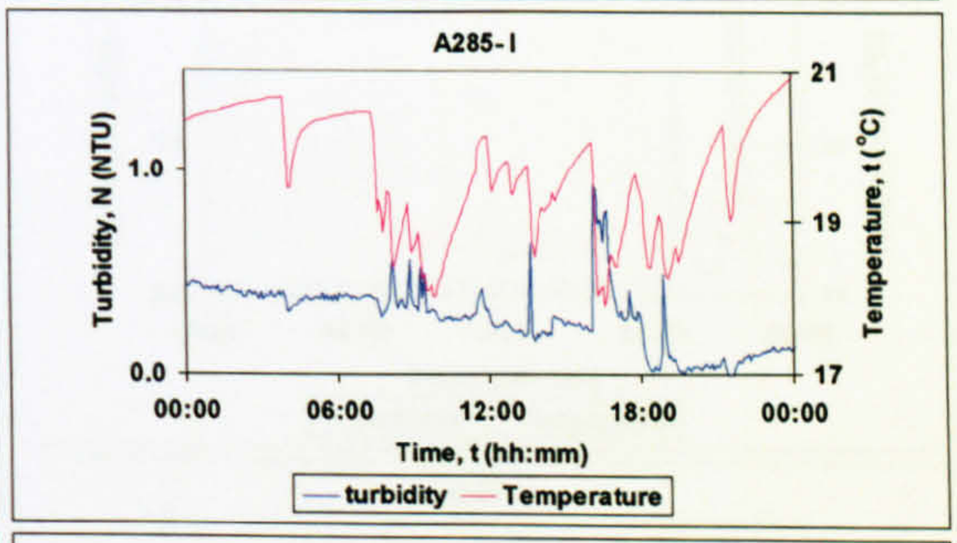

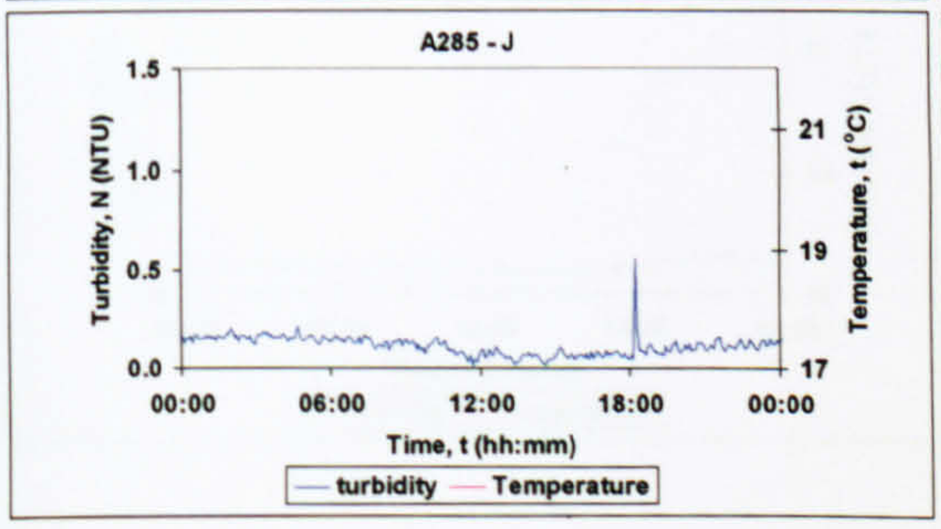

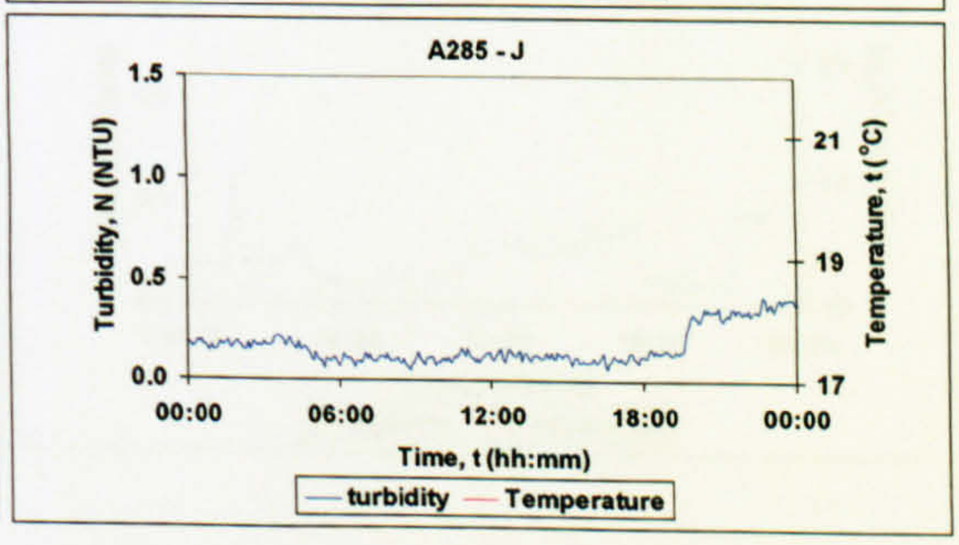

3 02/09/05

Imported material

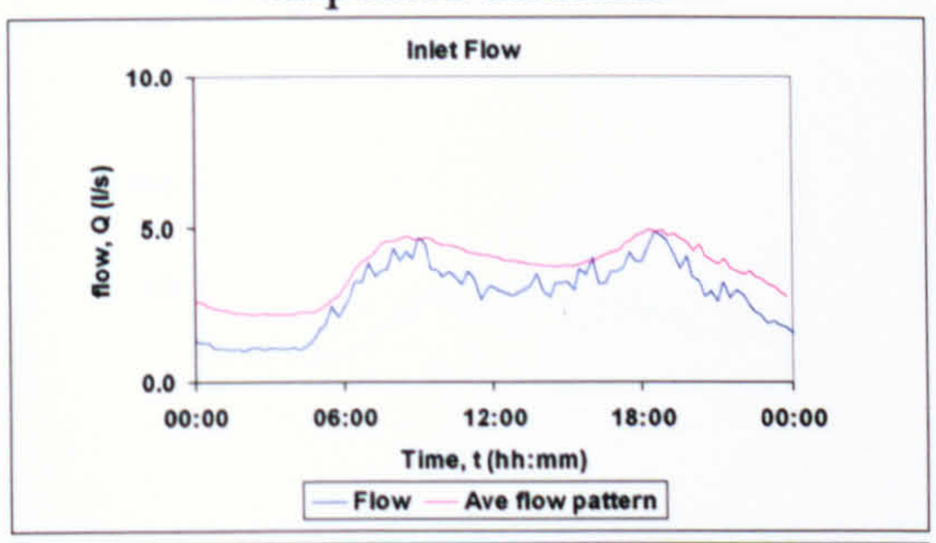

4 9/10/05

Large increase in demand

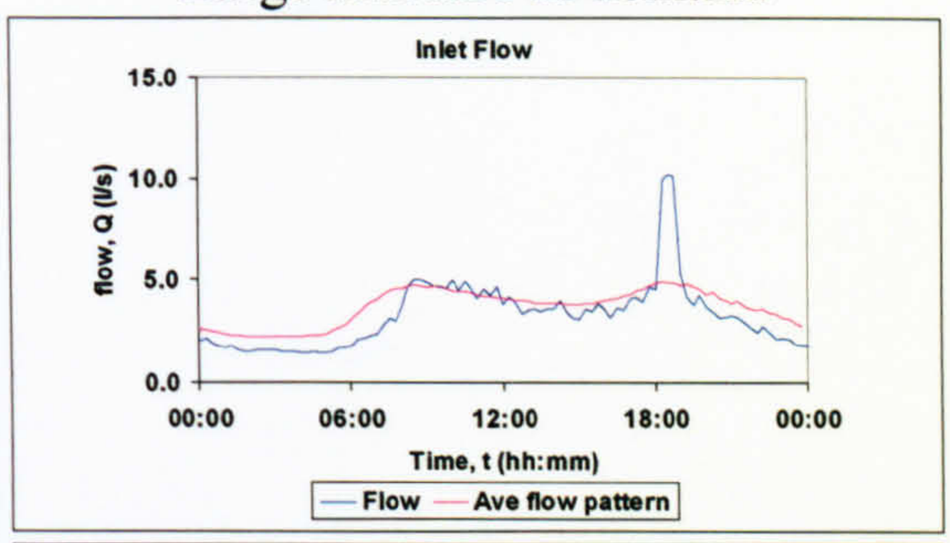

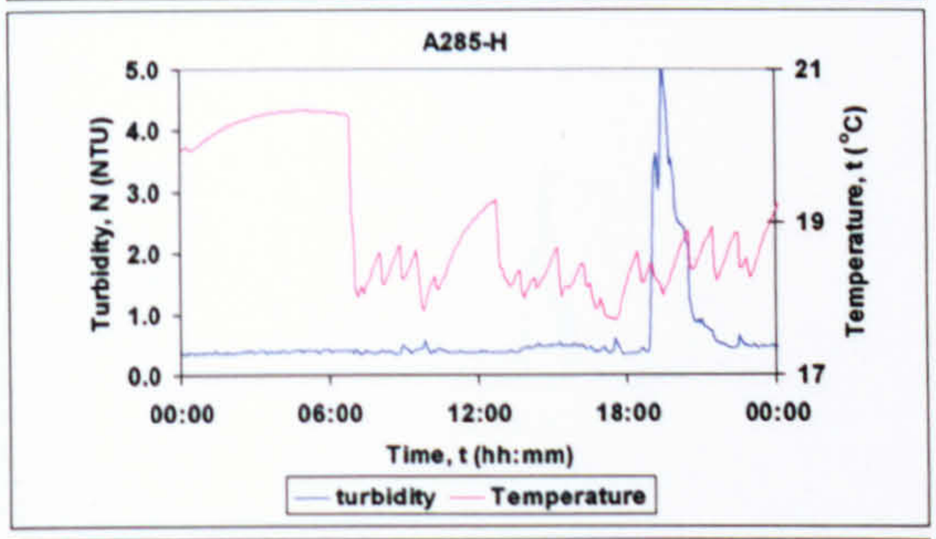

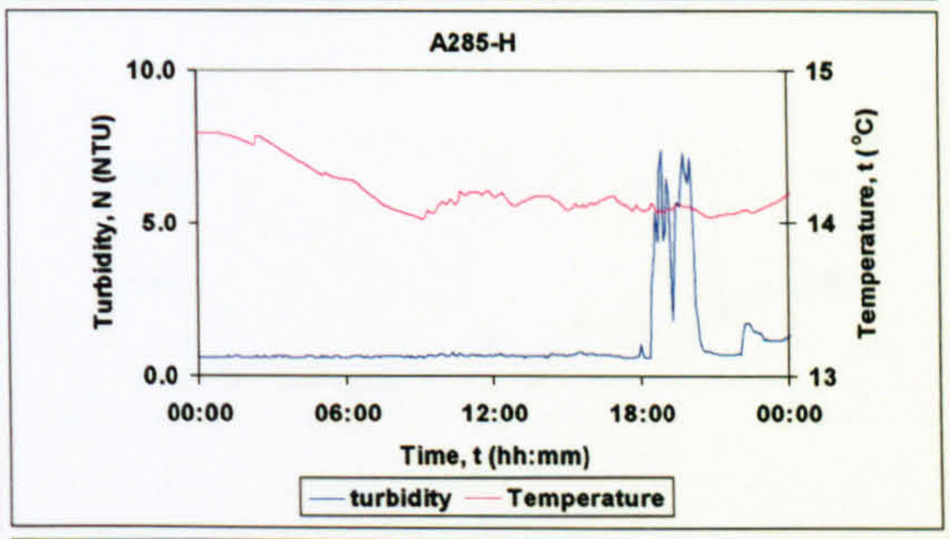

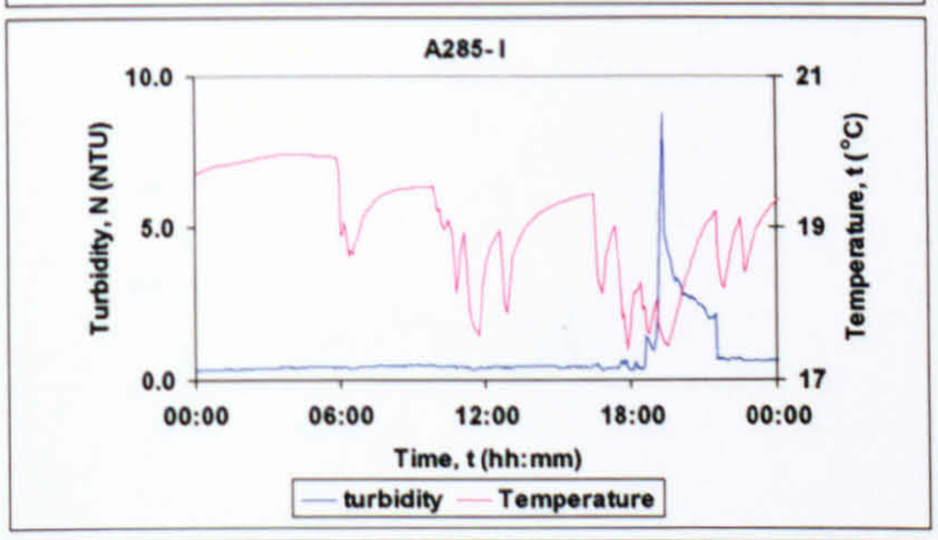

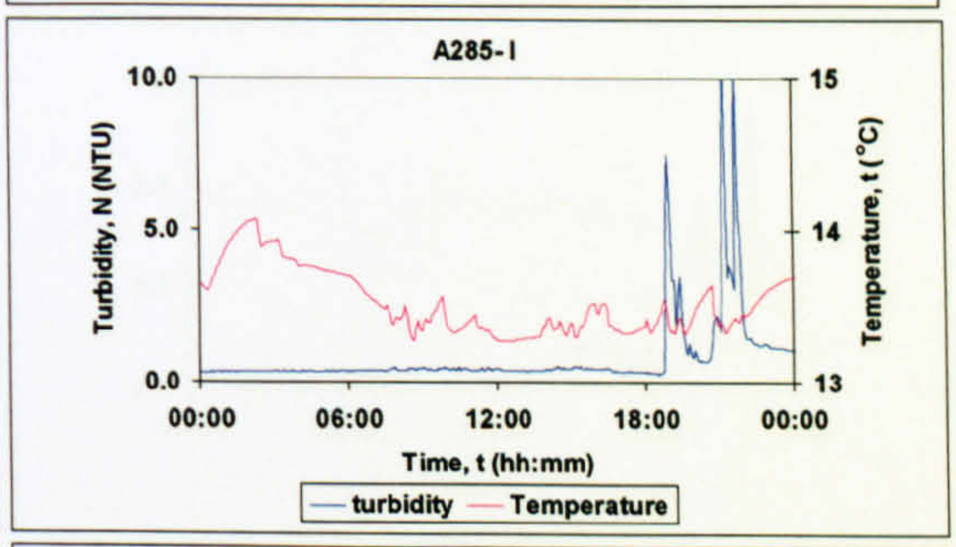

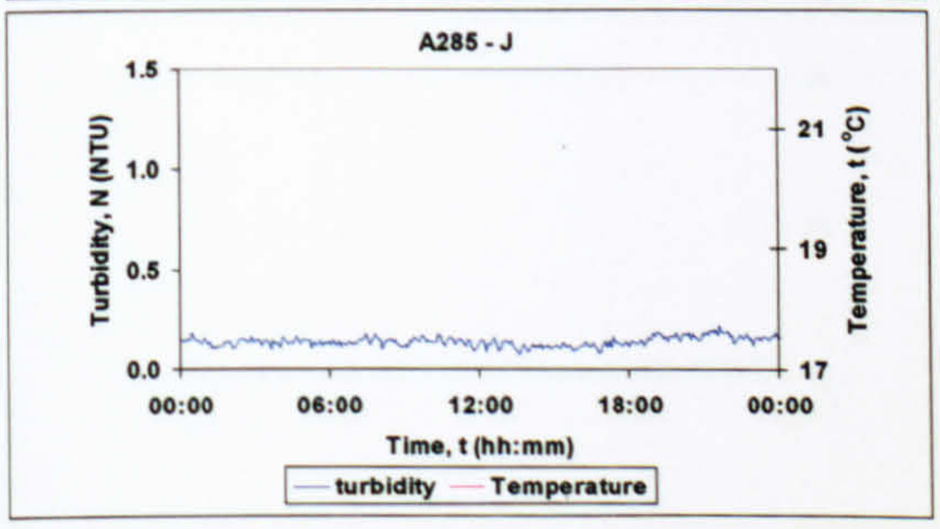

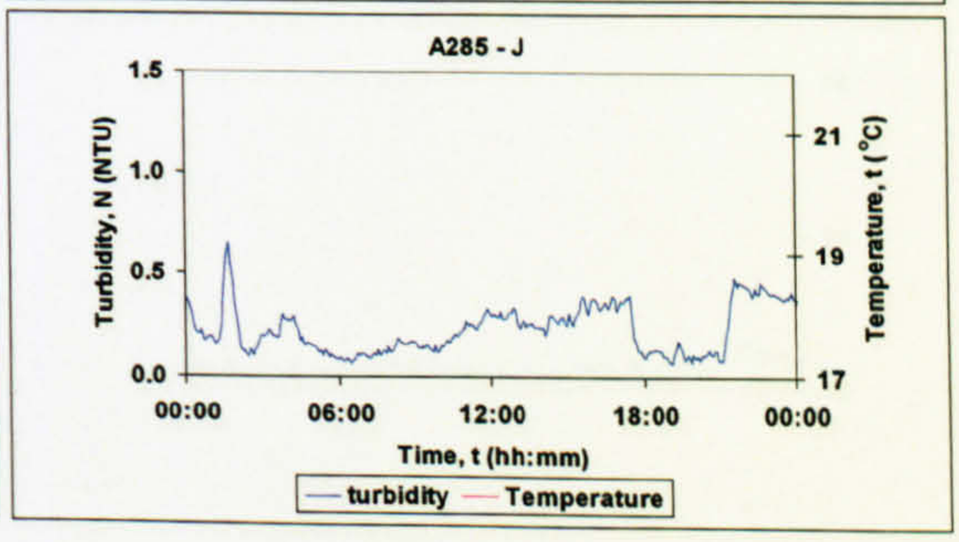

5 23/10/05

Large demand increase

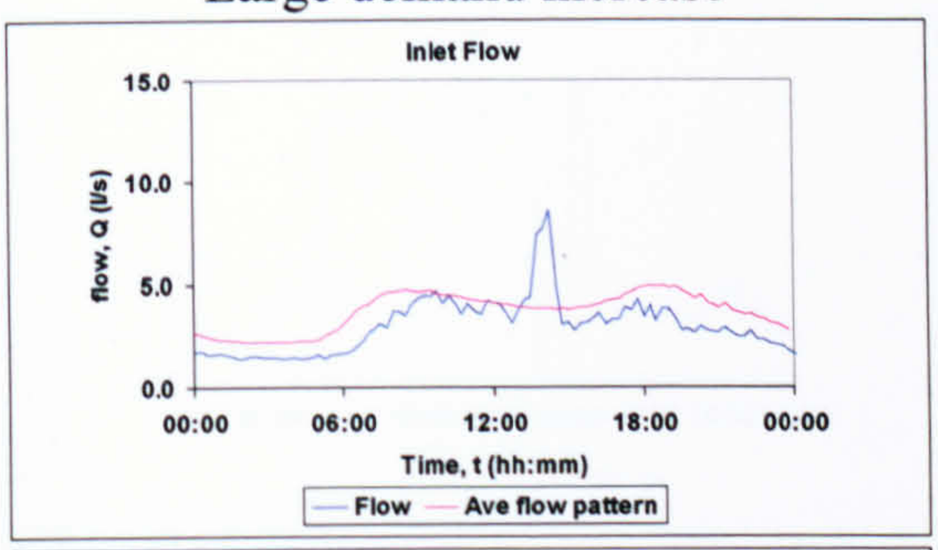

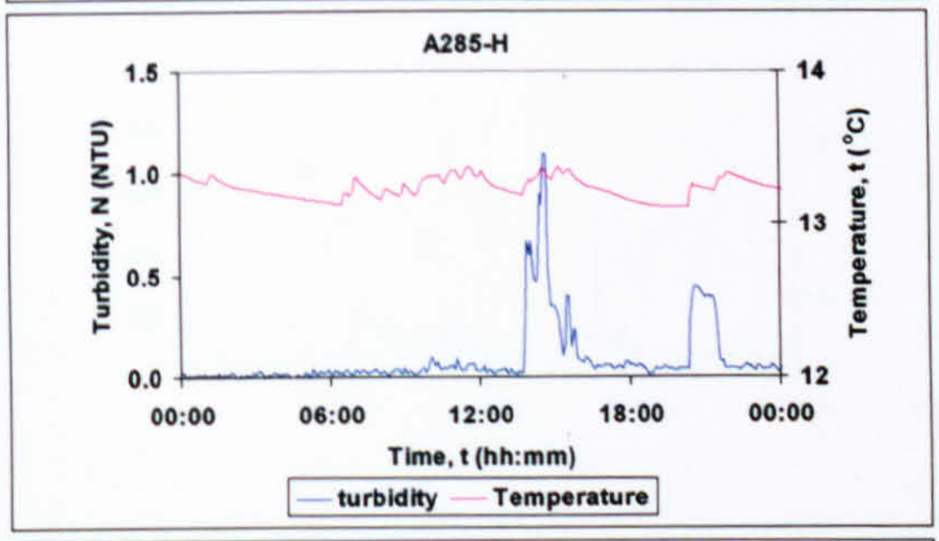

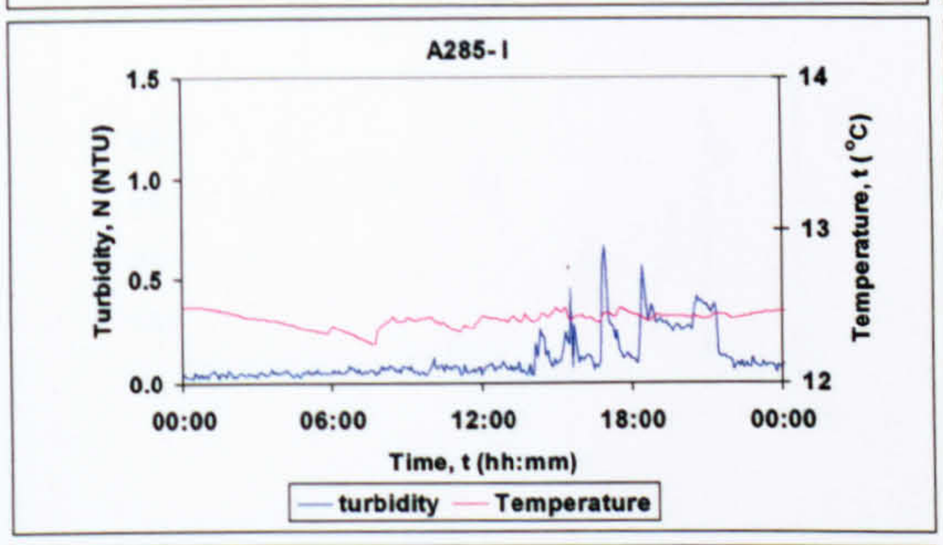

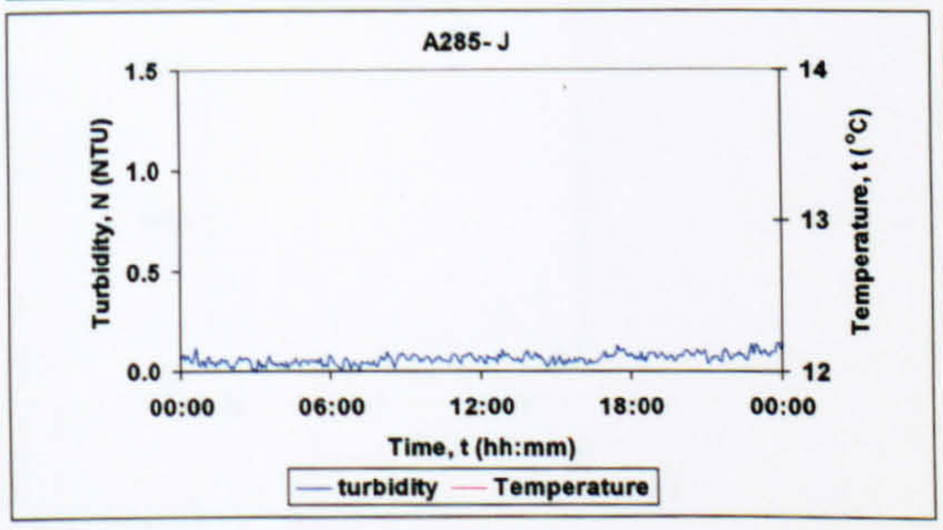

6 13/11/05

Large demand increase

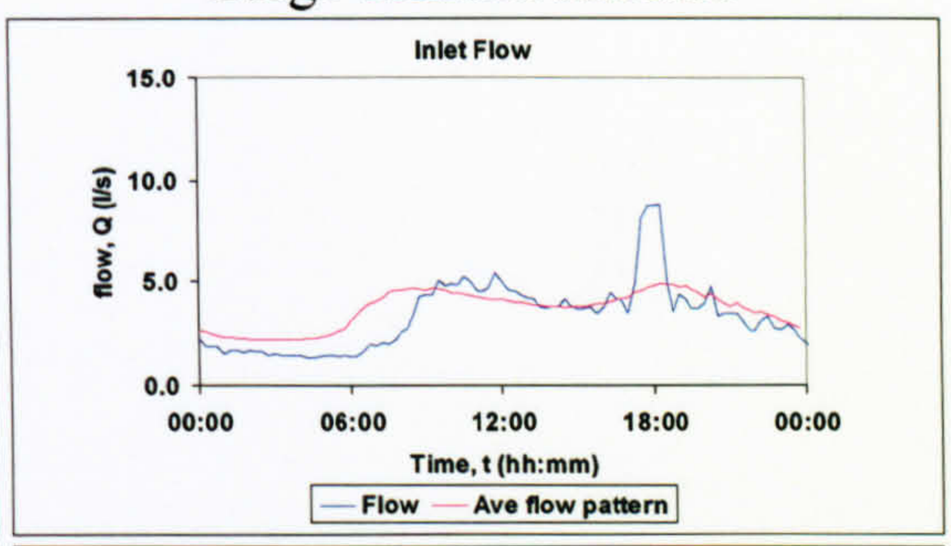

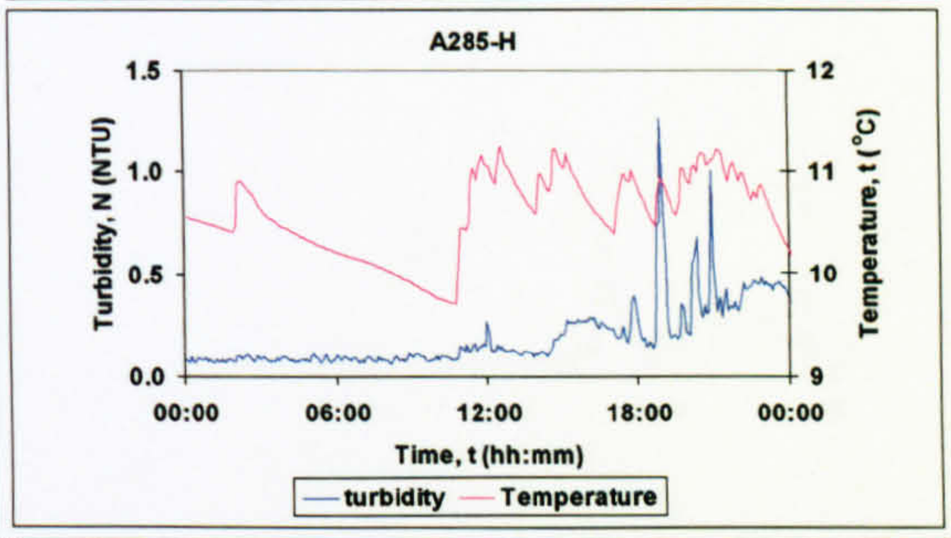

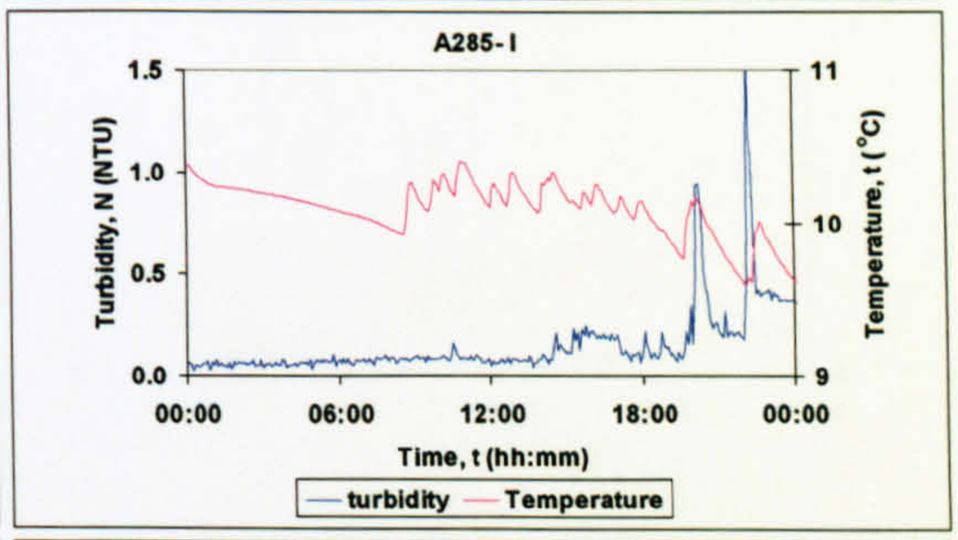

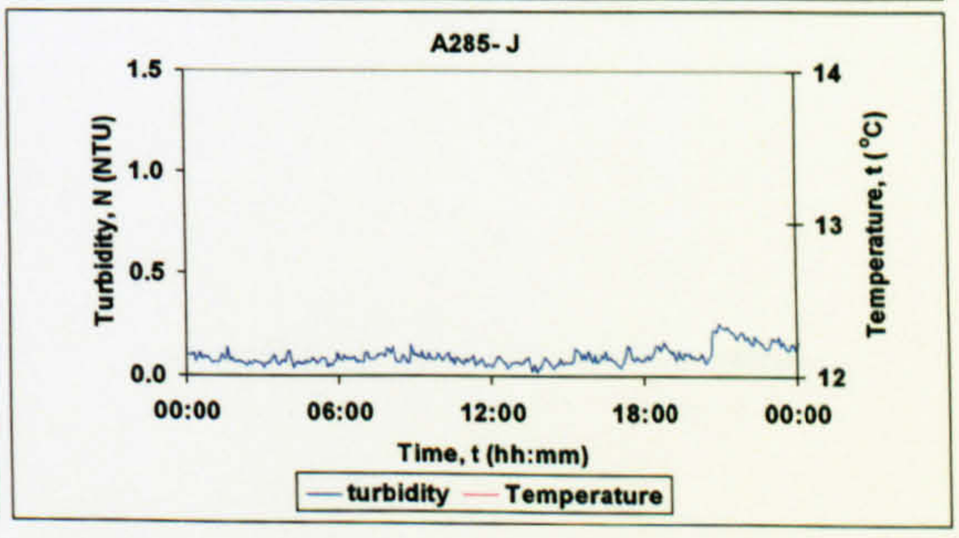

7 24-25/11/05
Large demand increase

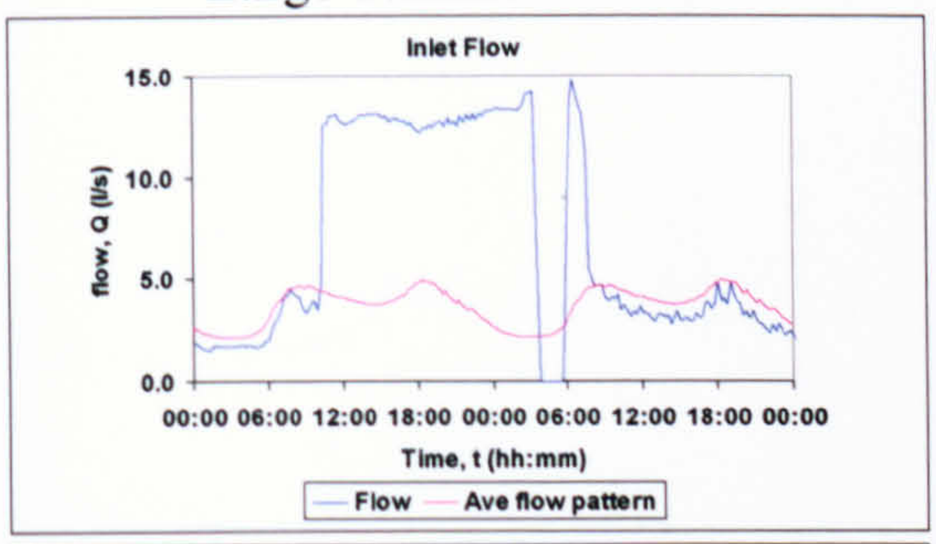

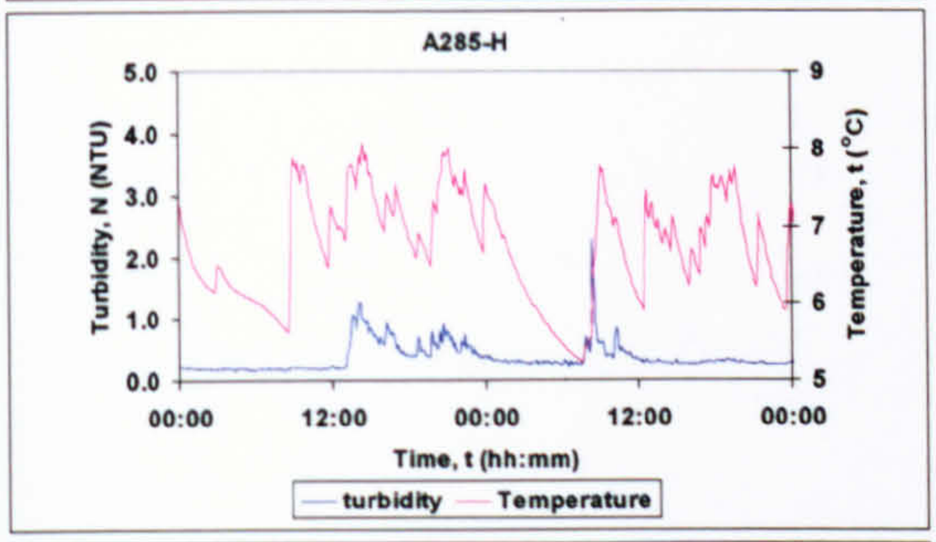

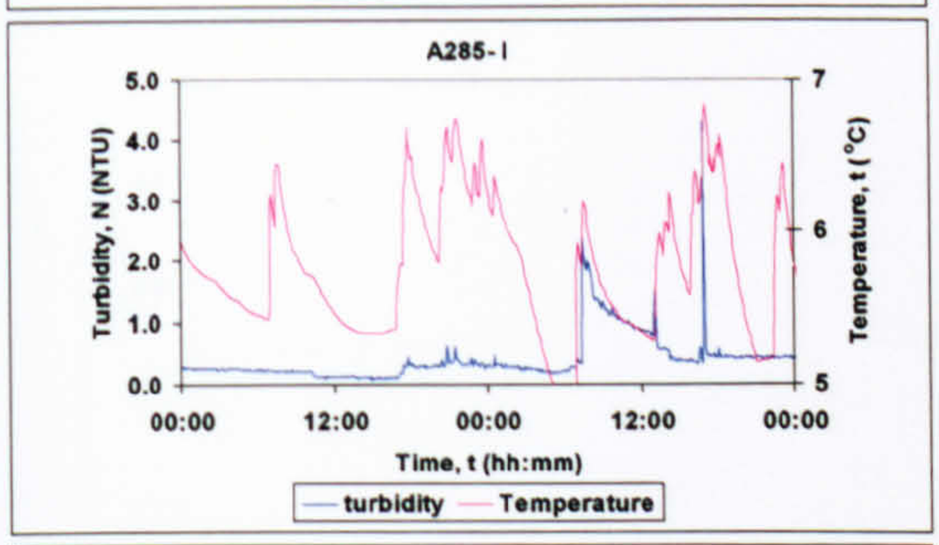

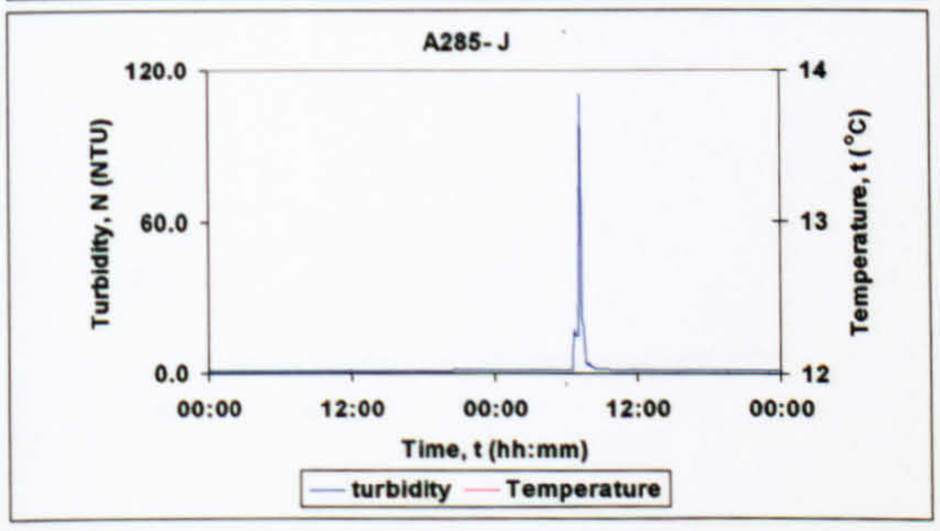

8 10/12/05
Large demand increase

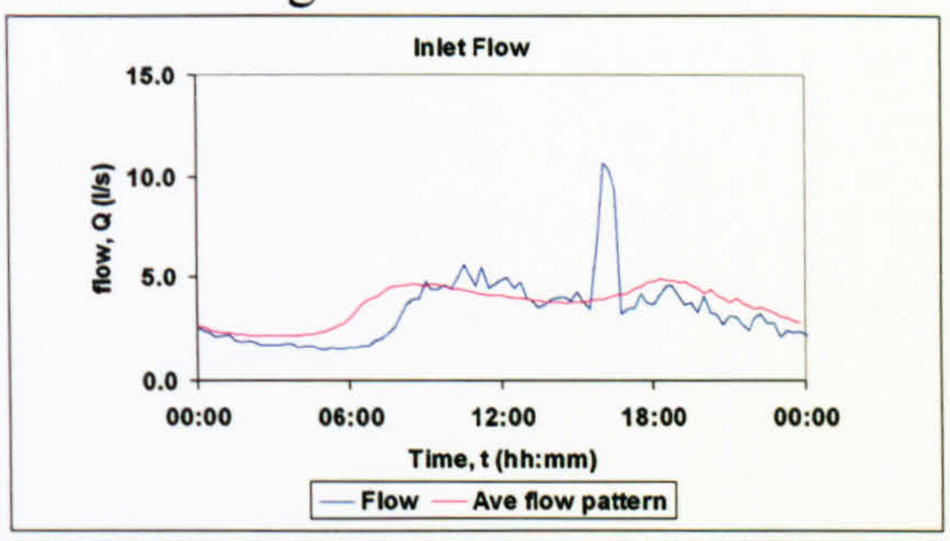

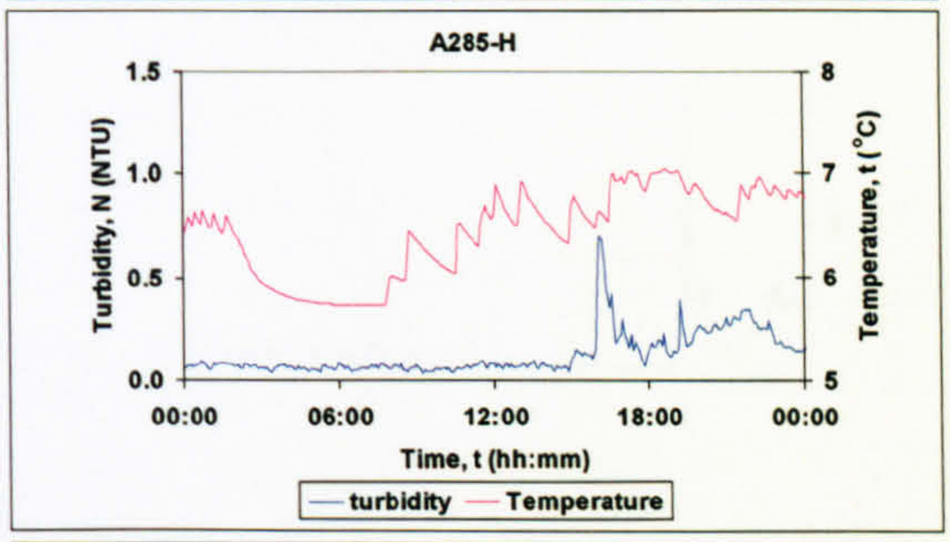

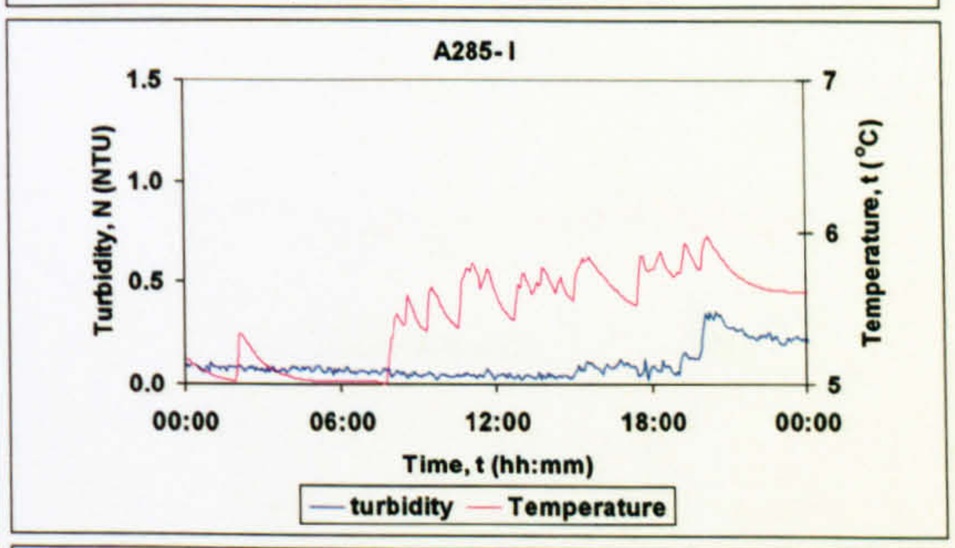

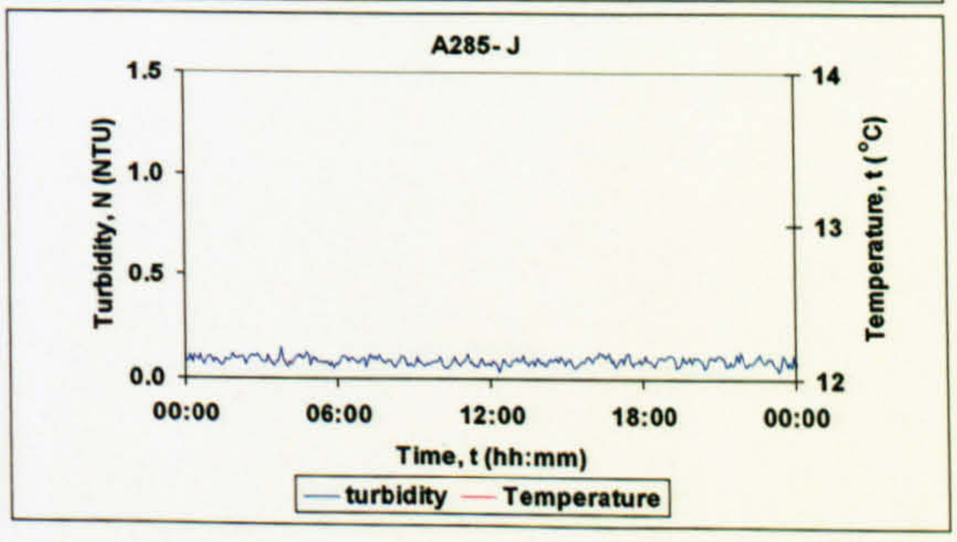

9 15/12/05

Large demand increase

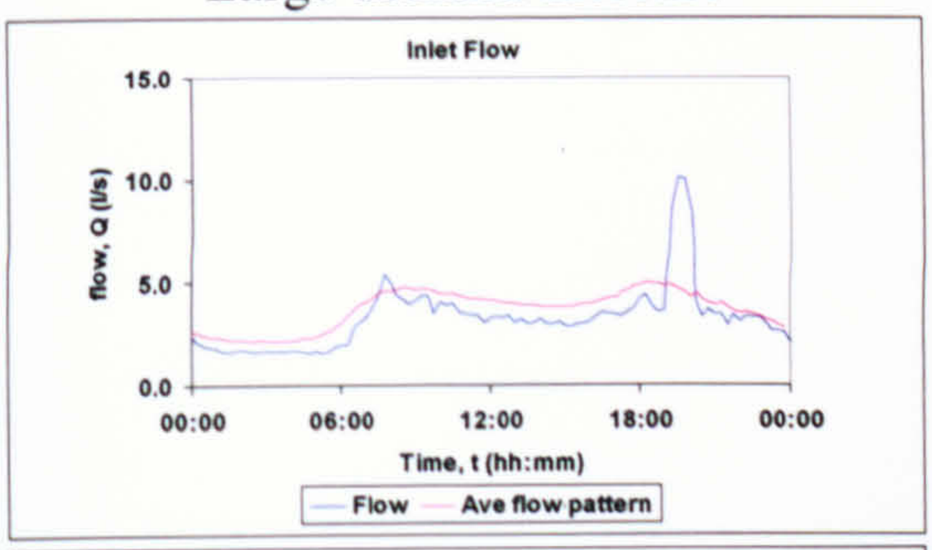

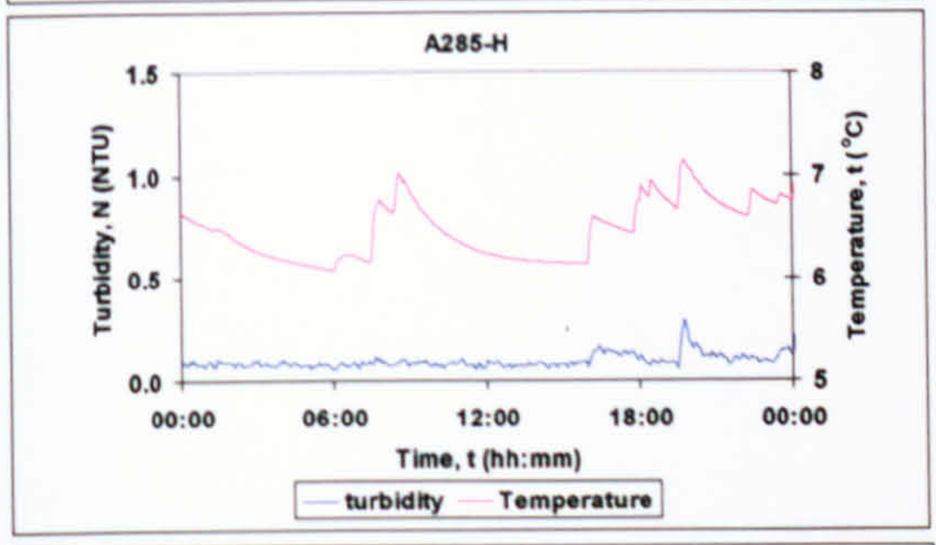

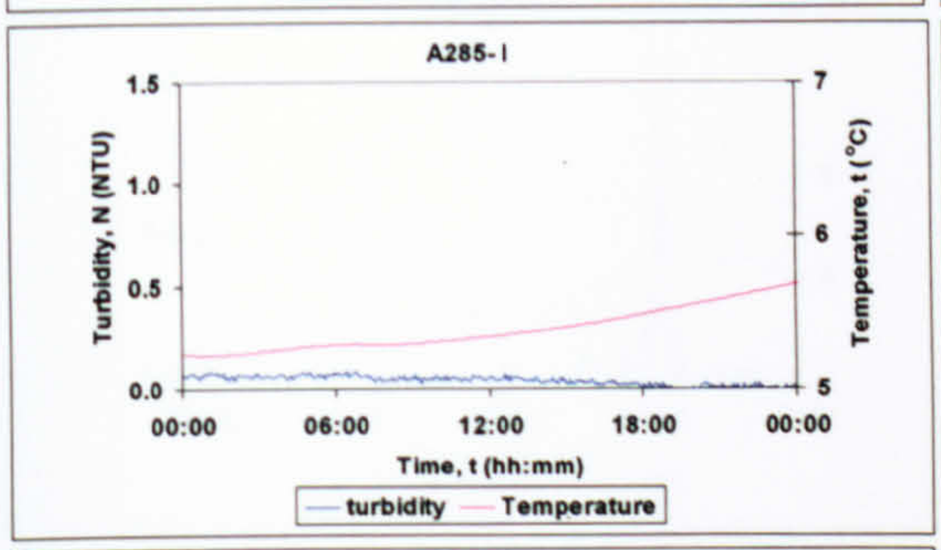

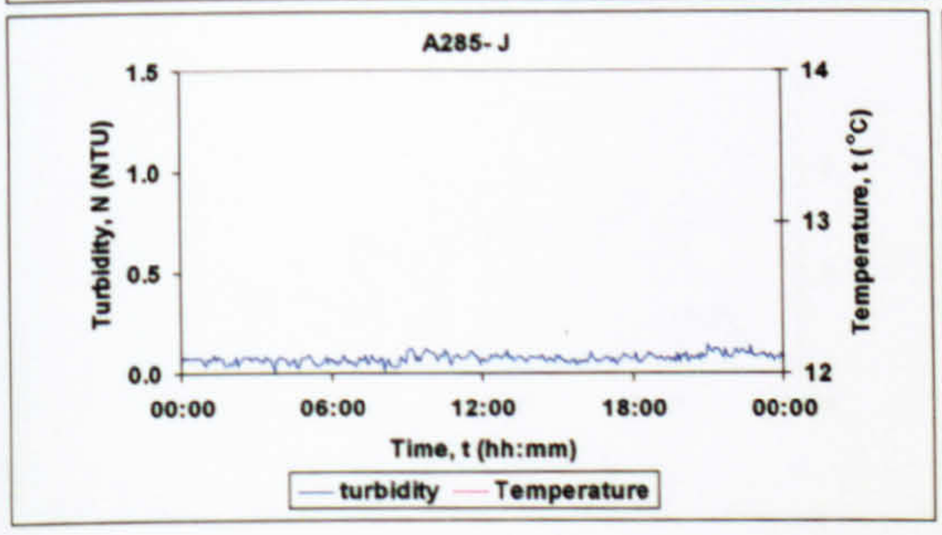

10 8/02/06

Large demand increase

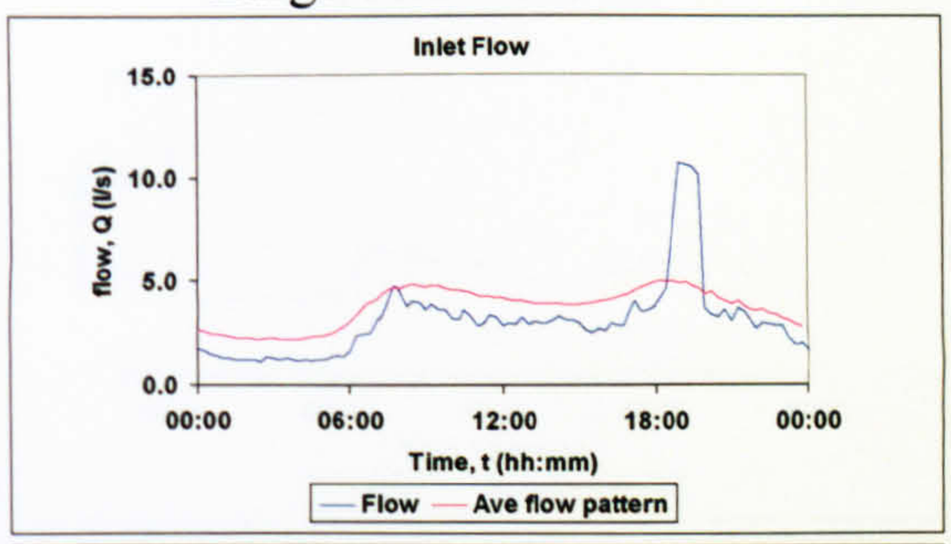

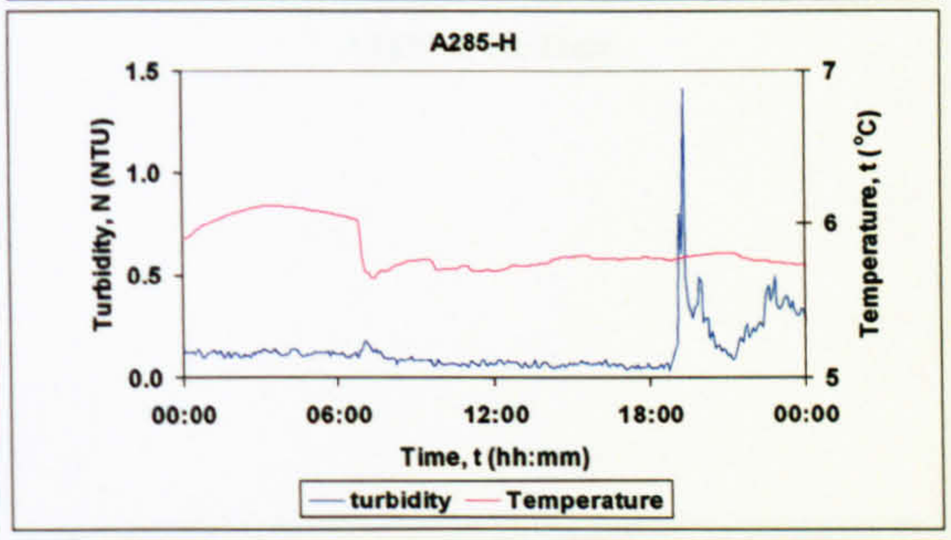

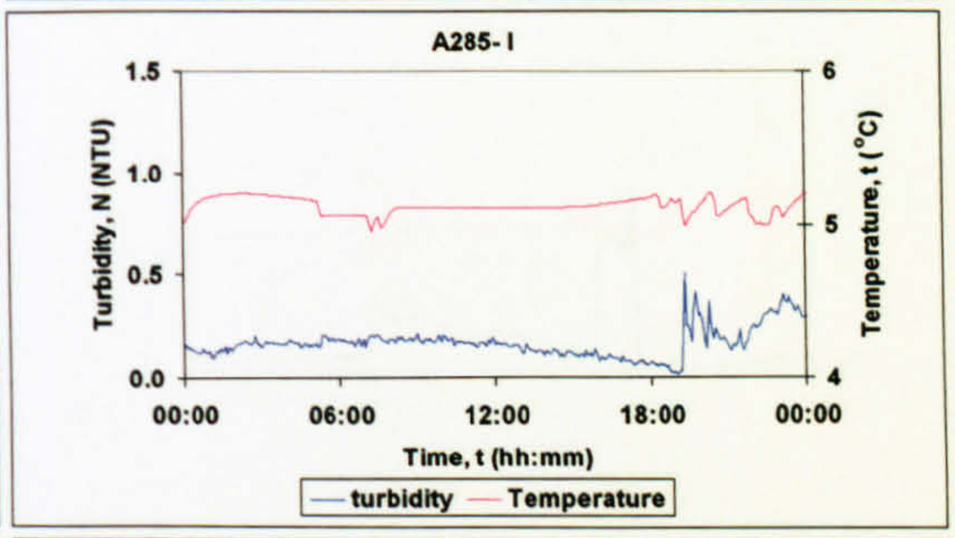

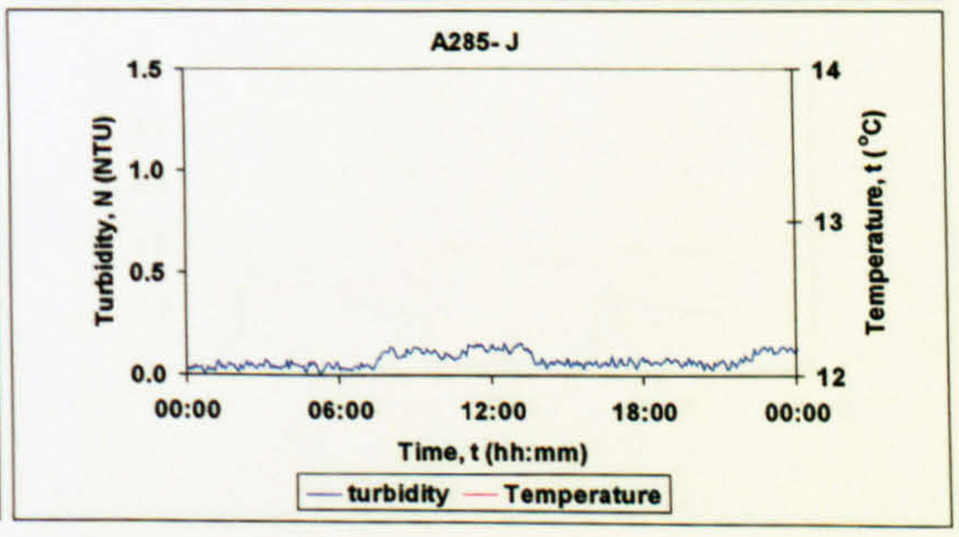

11 03/03/06
Imported material

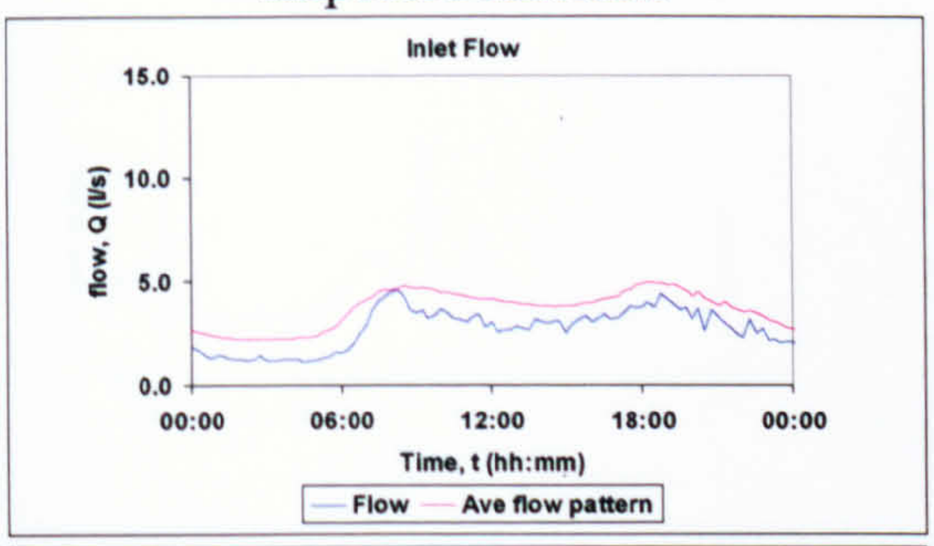

12 01/02/07
Imported material

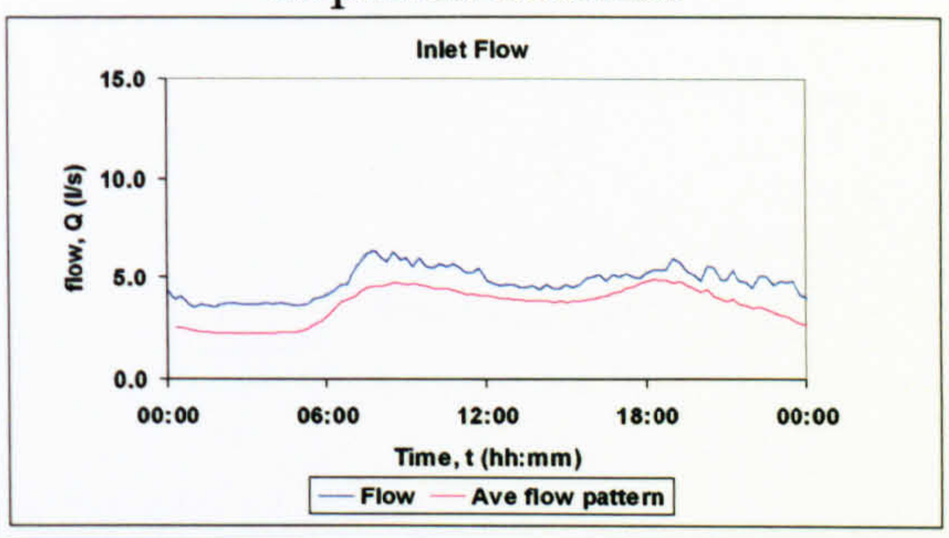

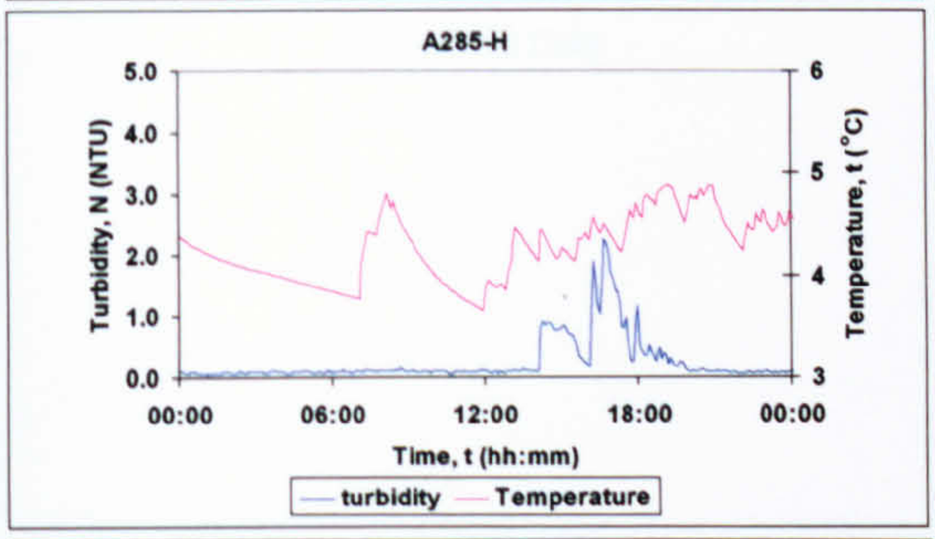

A285- H No Data

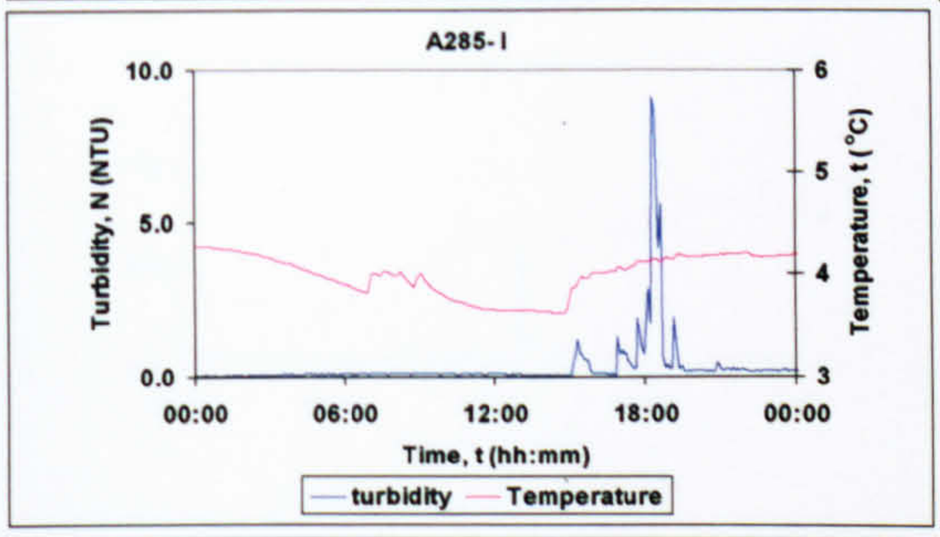

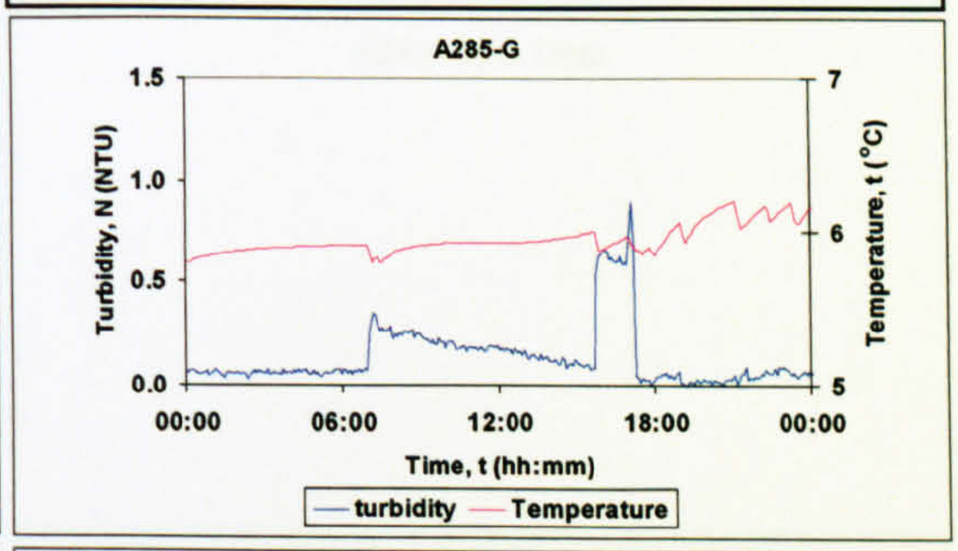

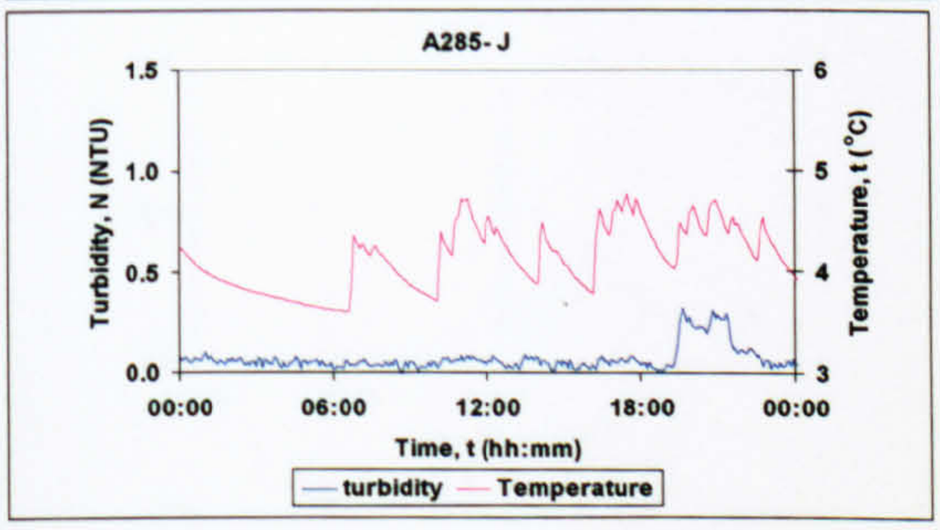

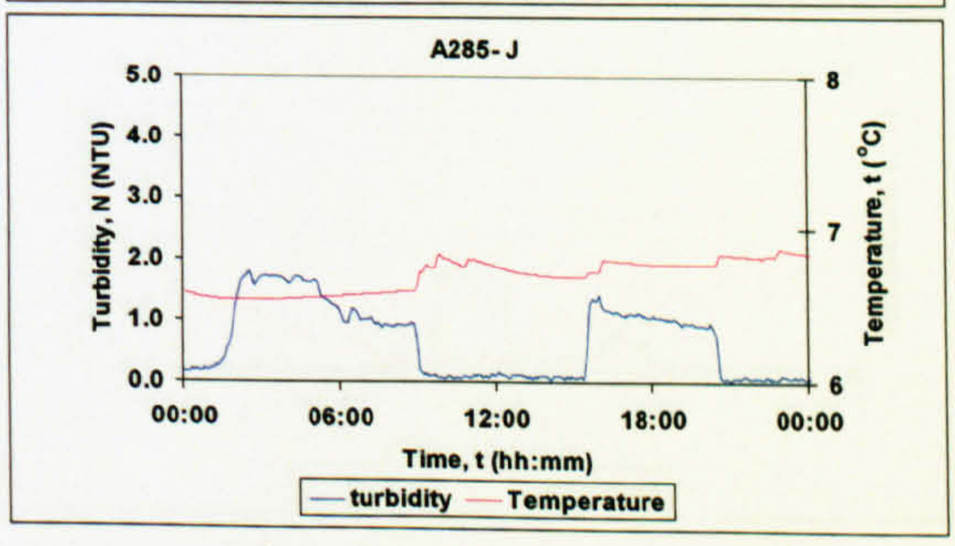

13 13/03/07

Large demand increase

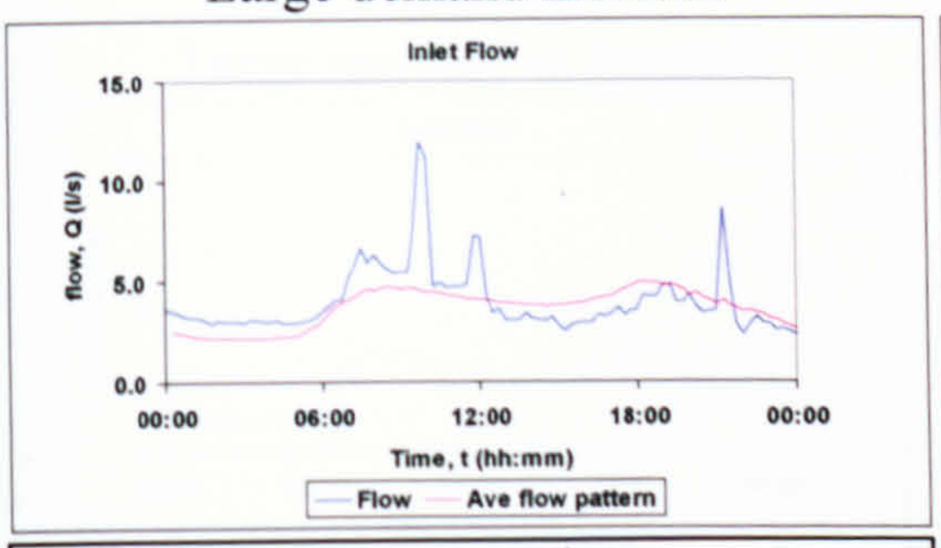

14 09/05/07

Unknown

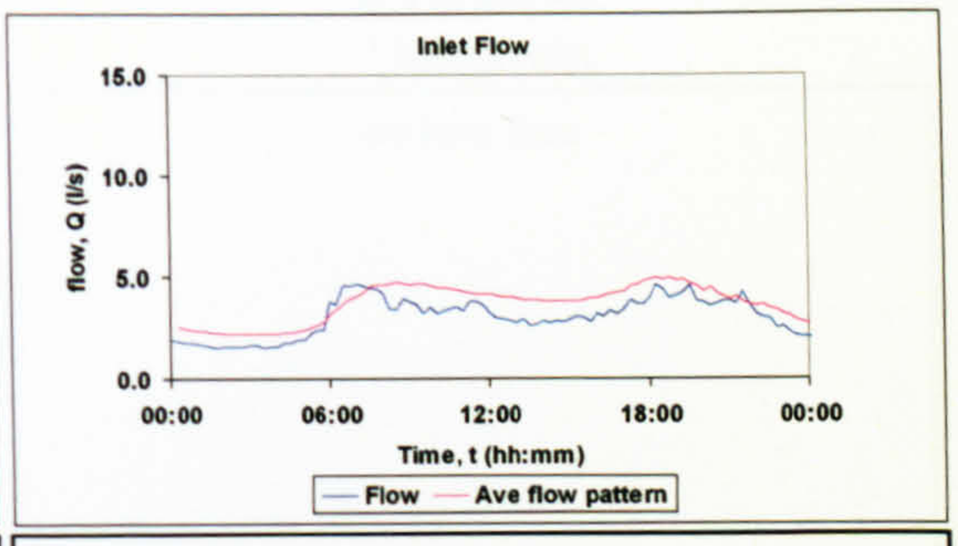

A285- H No Data

A285- H No Data

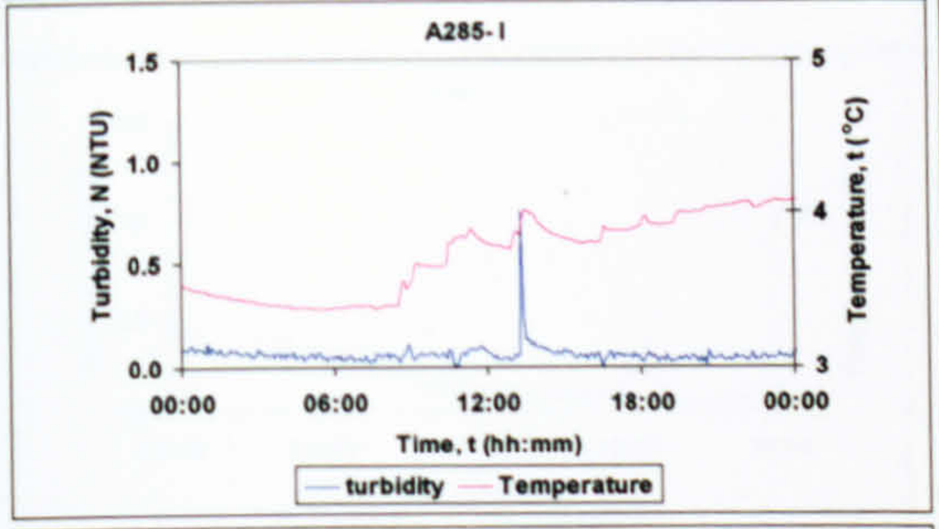

A285- I No Data

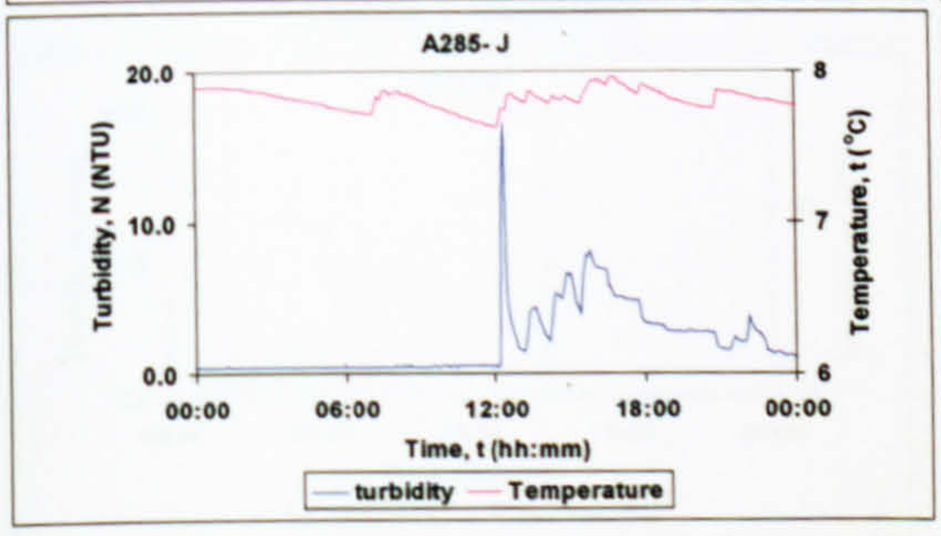

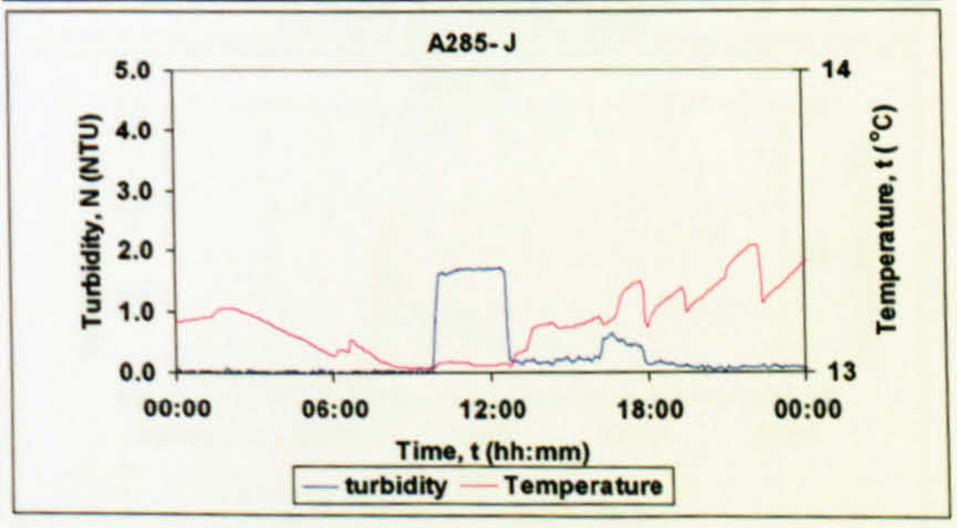

J722

1 17/07/05
Large increase in demand

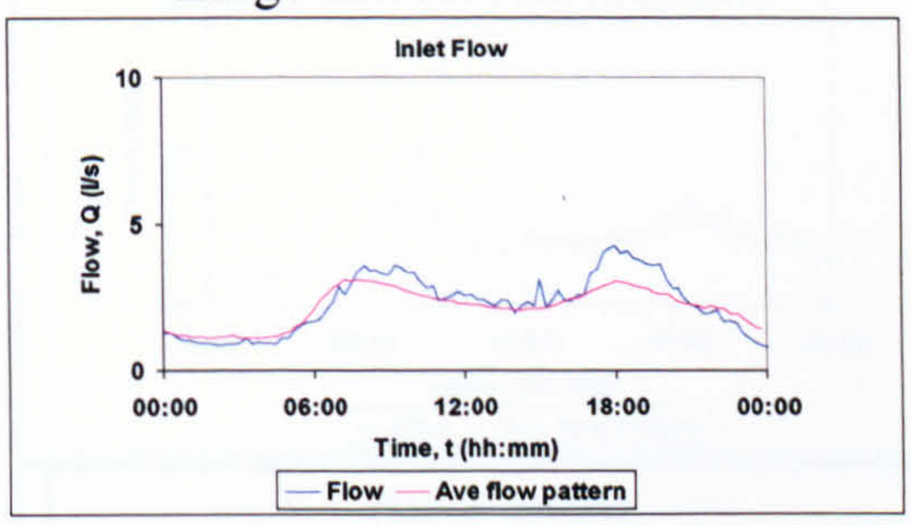

2 18/09/05
Unknown

No Flow Data

J722- K -No Data

J722- K -No Data

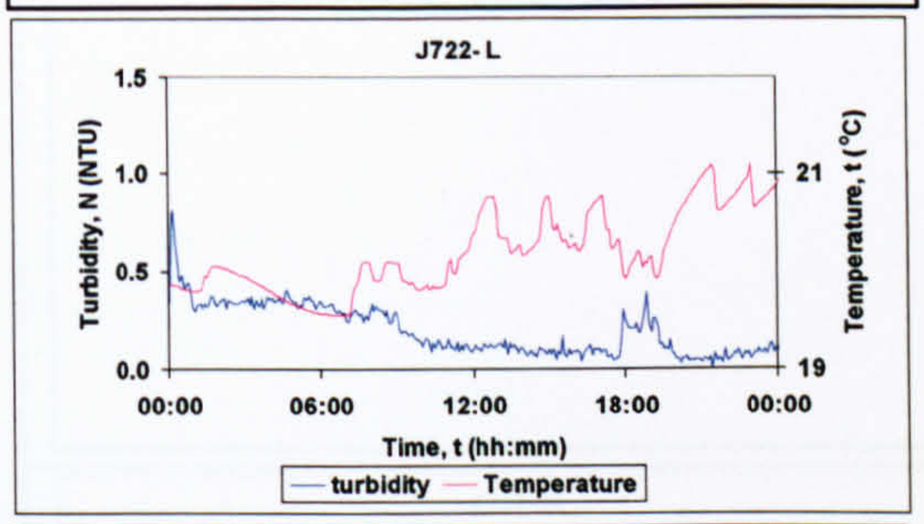

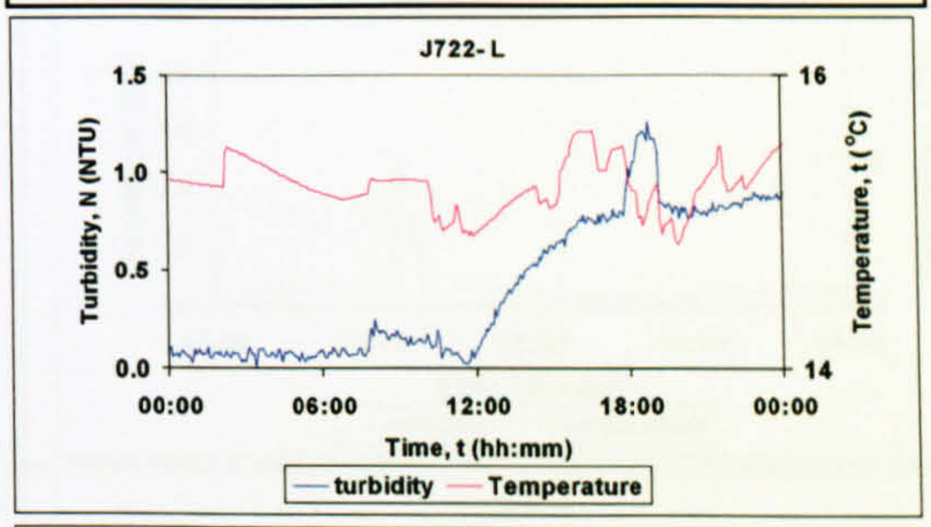

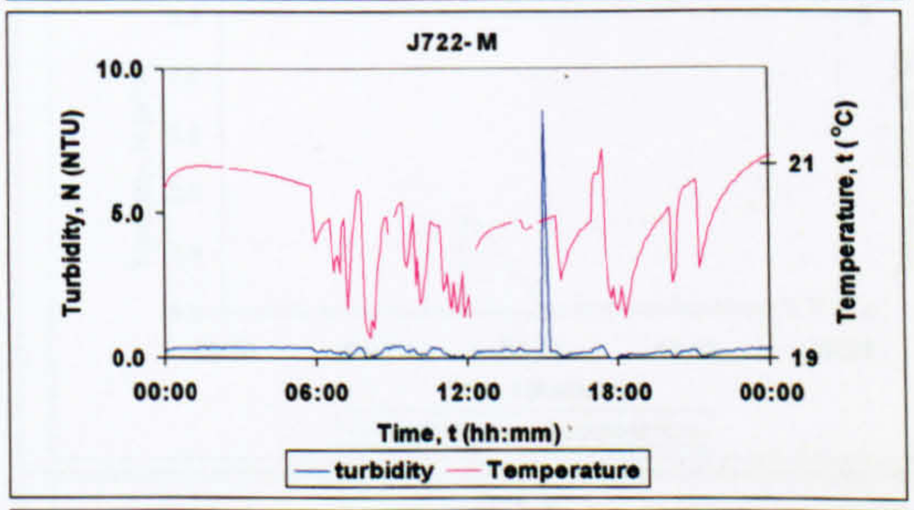

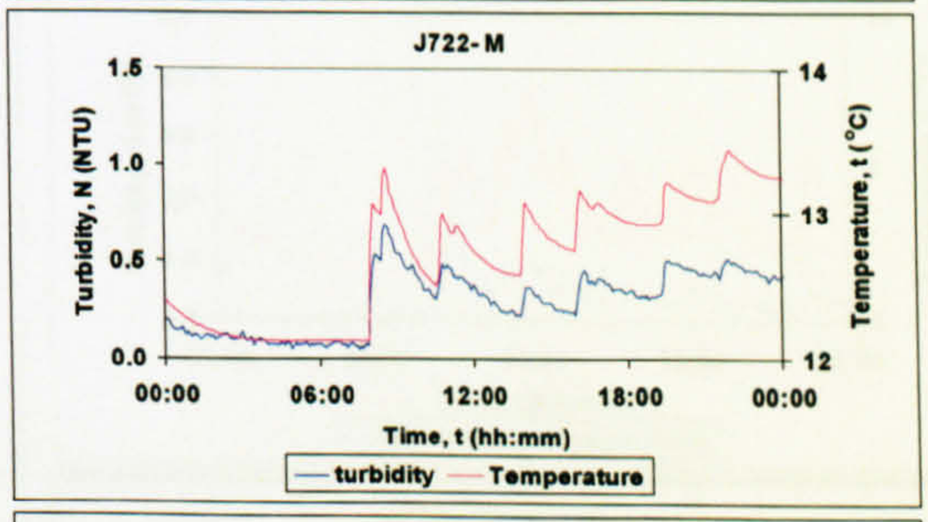

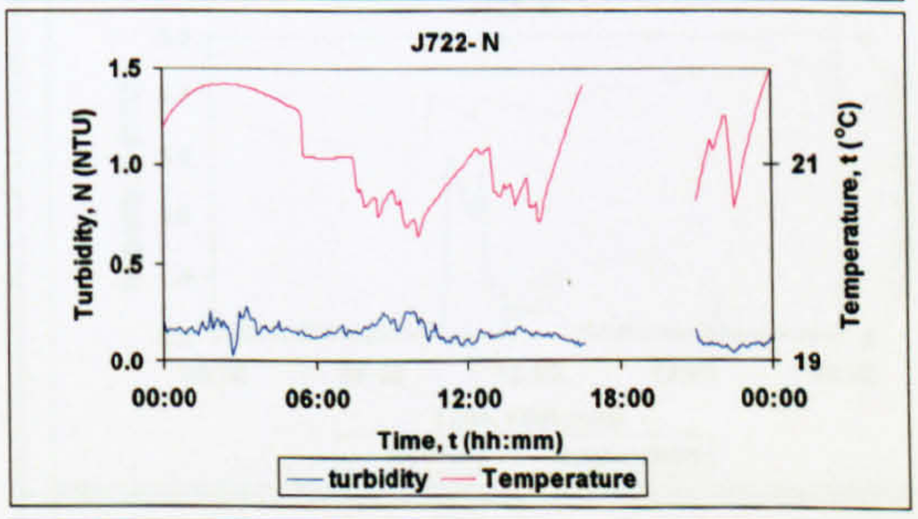

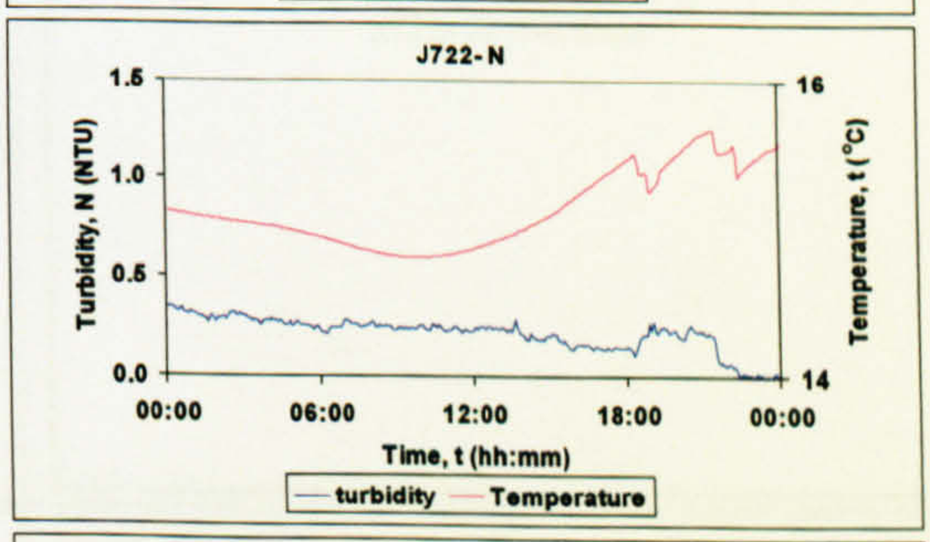

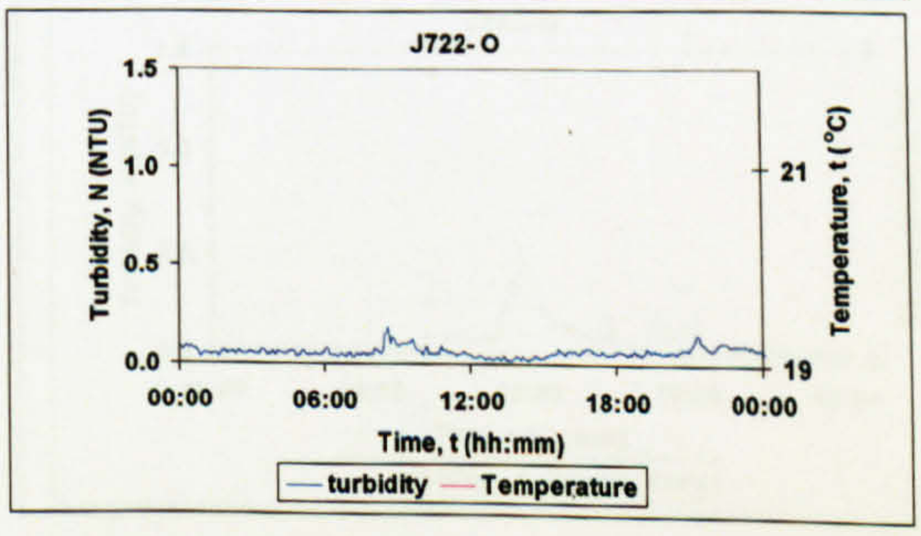

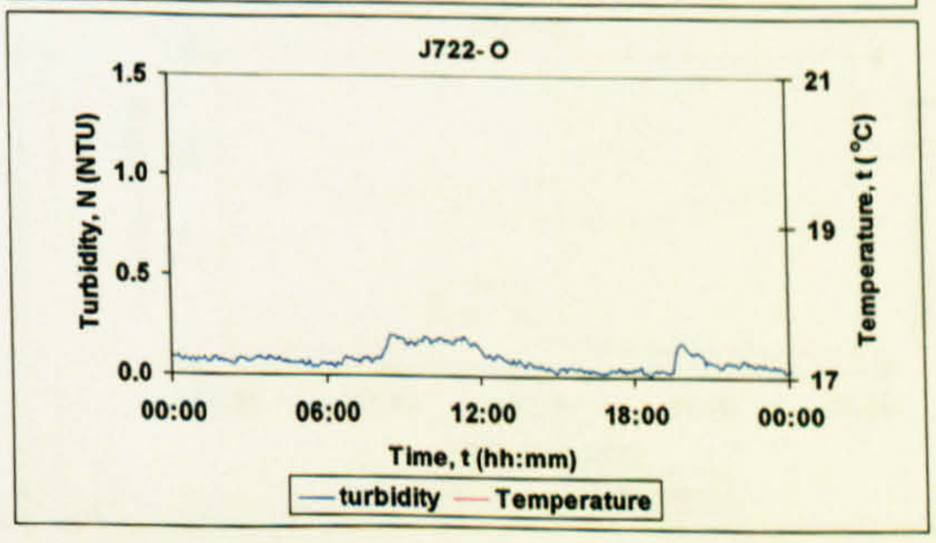

3 18/1/06

Large increase in demand

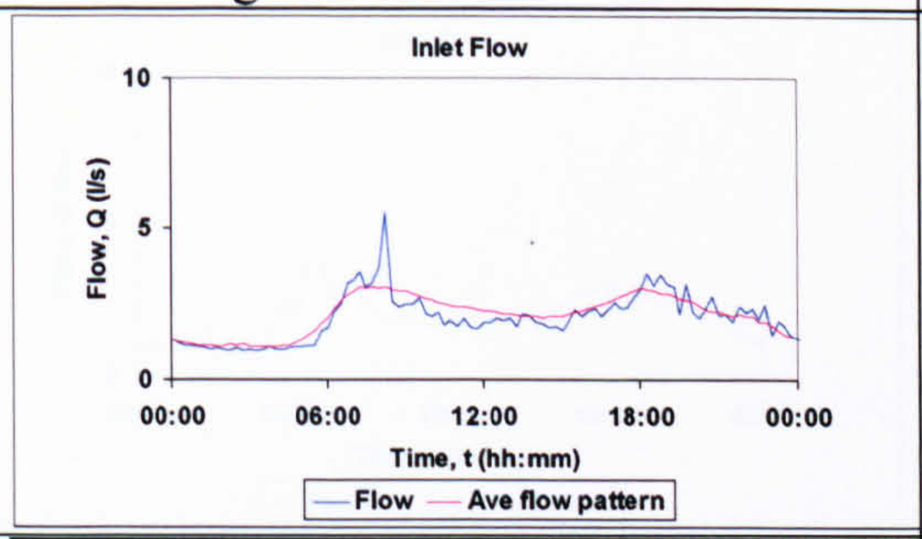

4 05/04/06

Large increase in demand

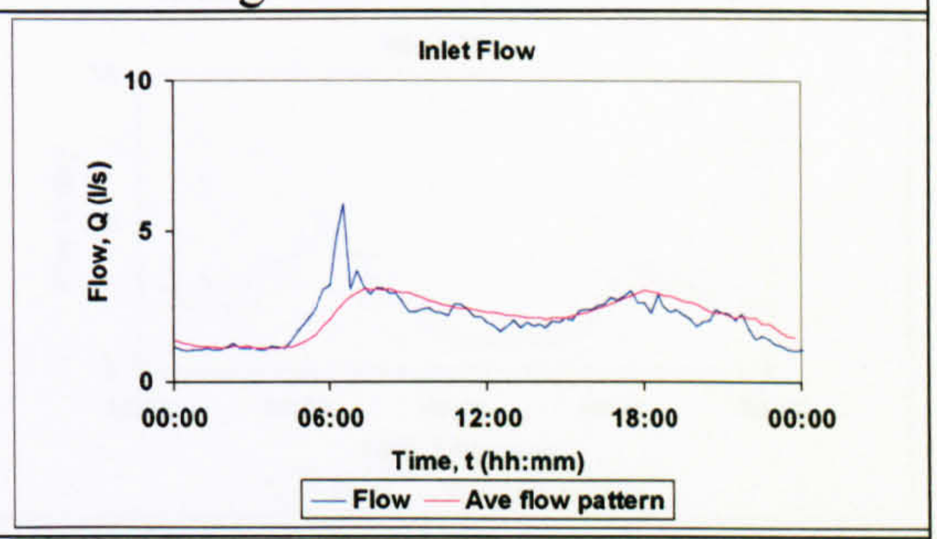

J722- K -No Data

J722- K -No Data

J722-L No Data

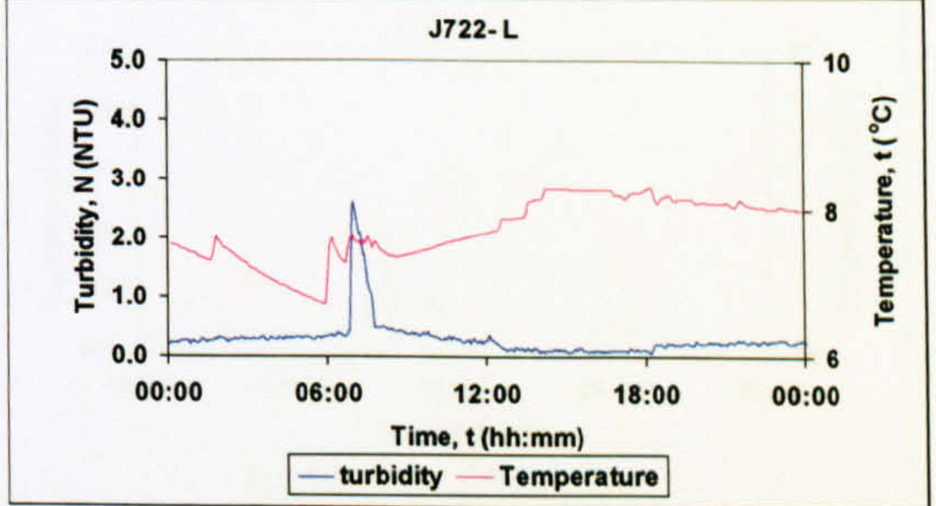

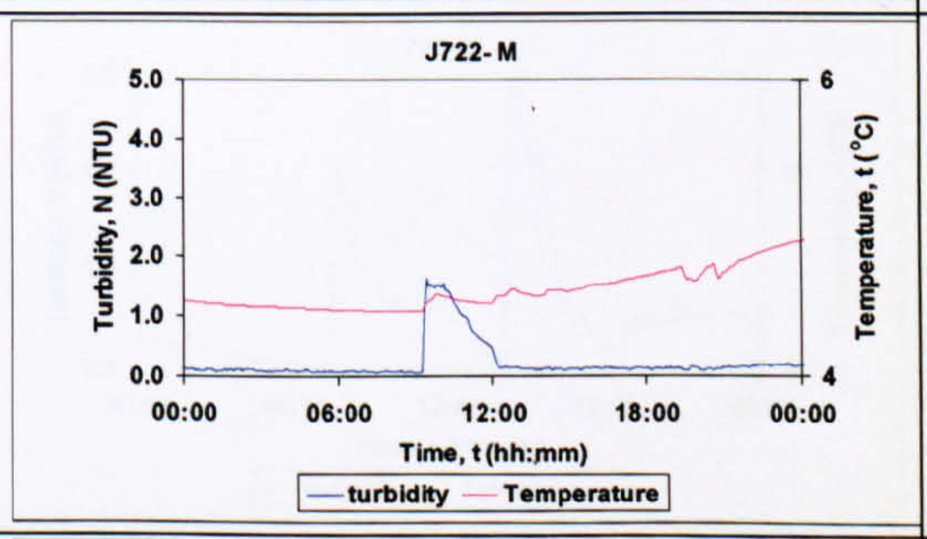

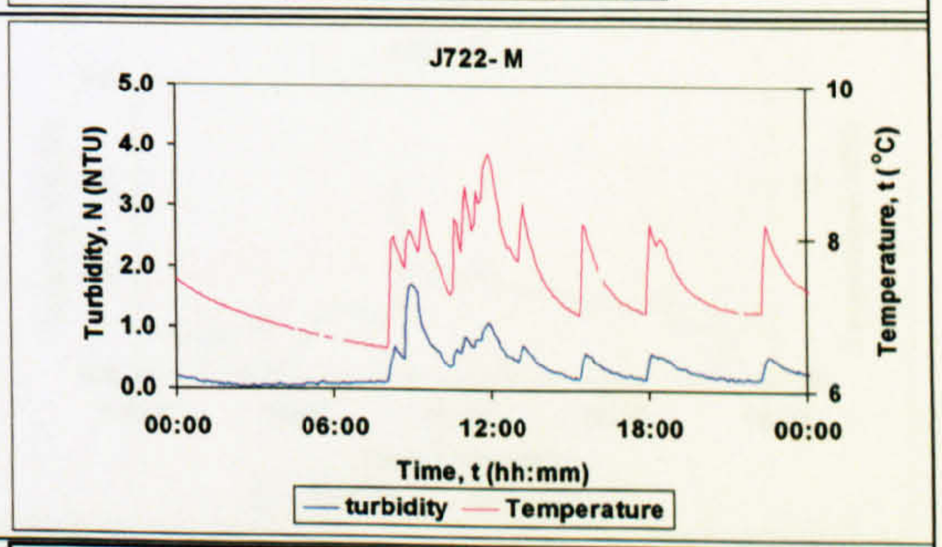

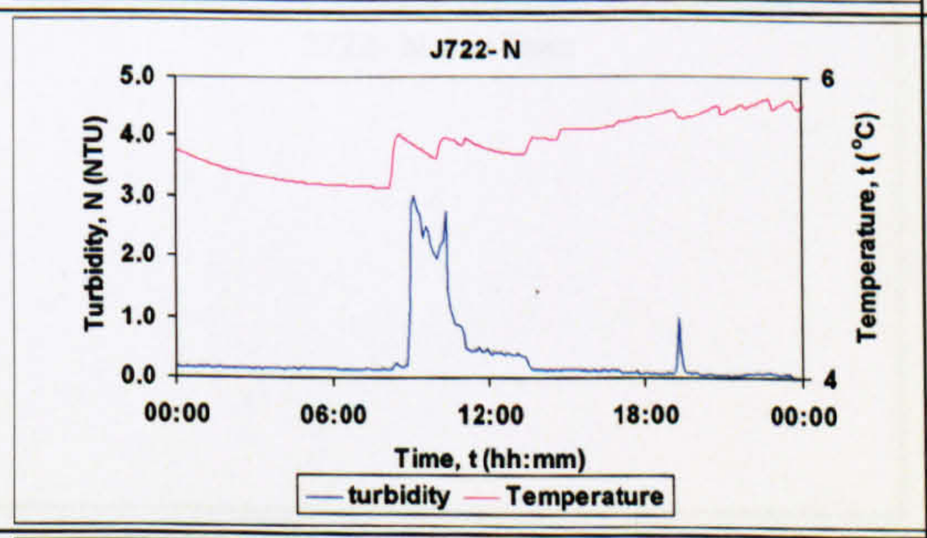

J722- N -No Data

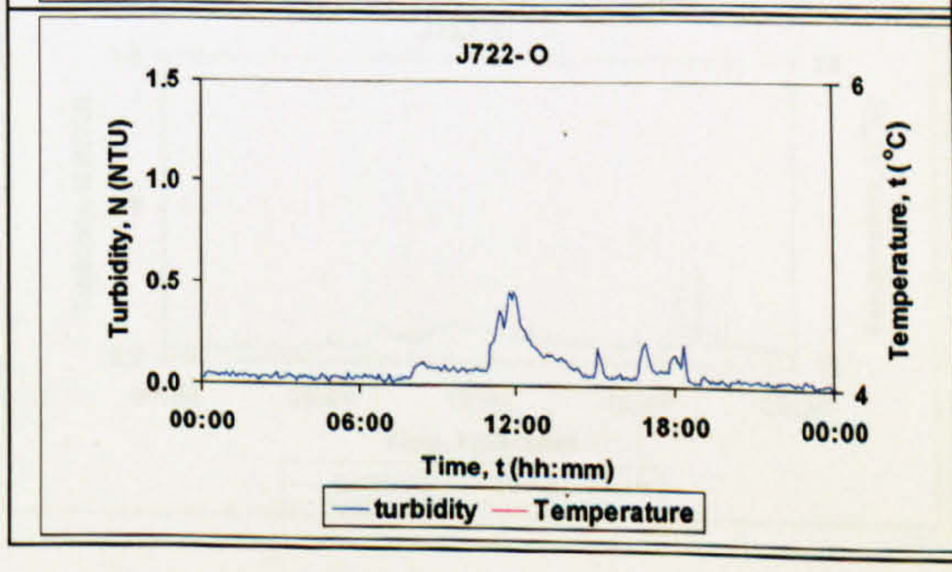

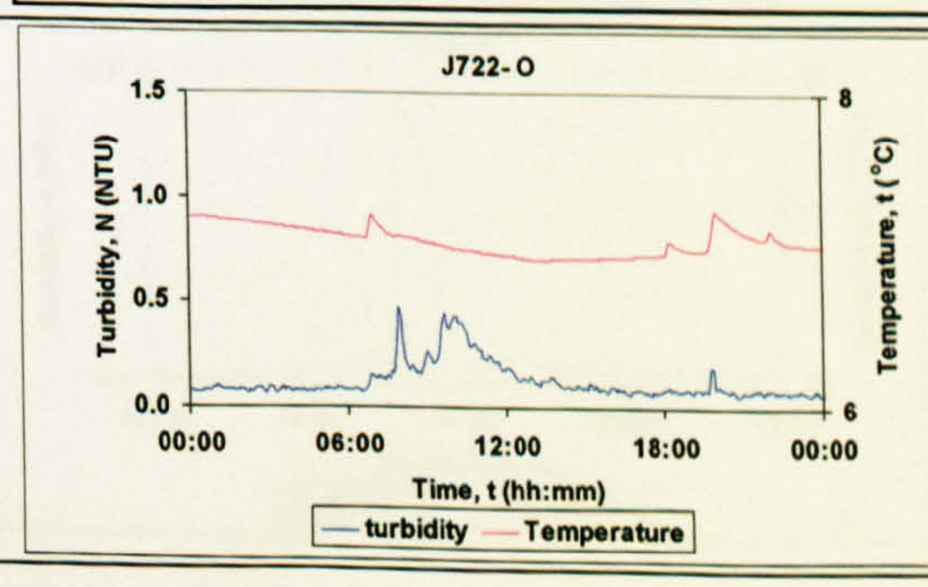

5 23/05/06
Imported material

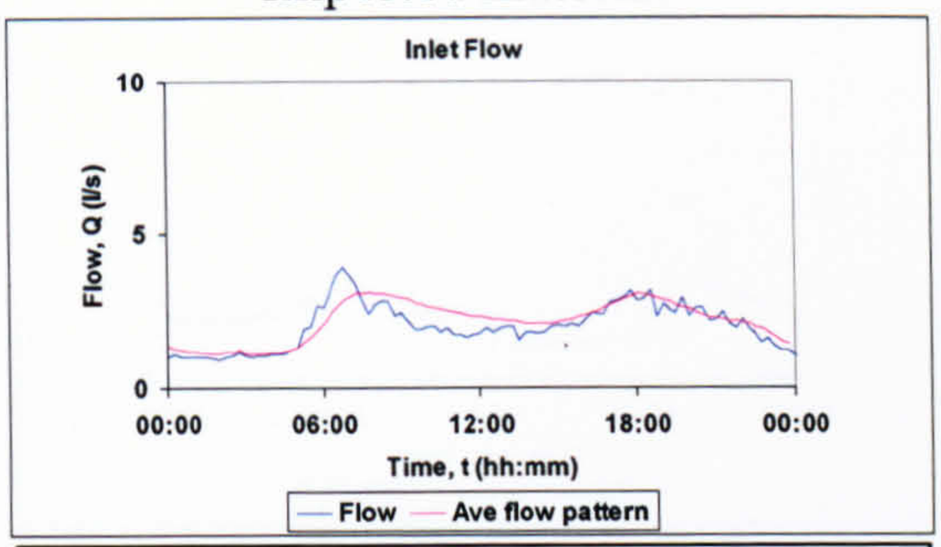

J722- K -No Data

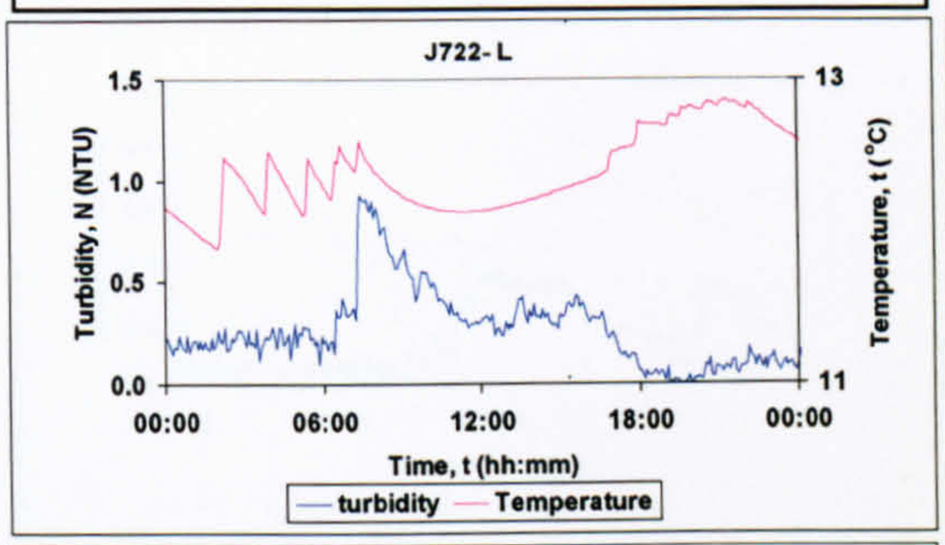

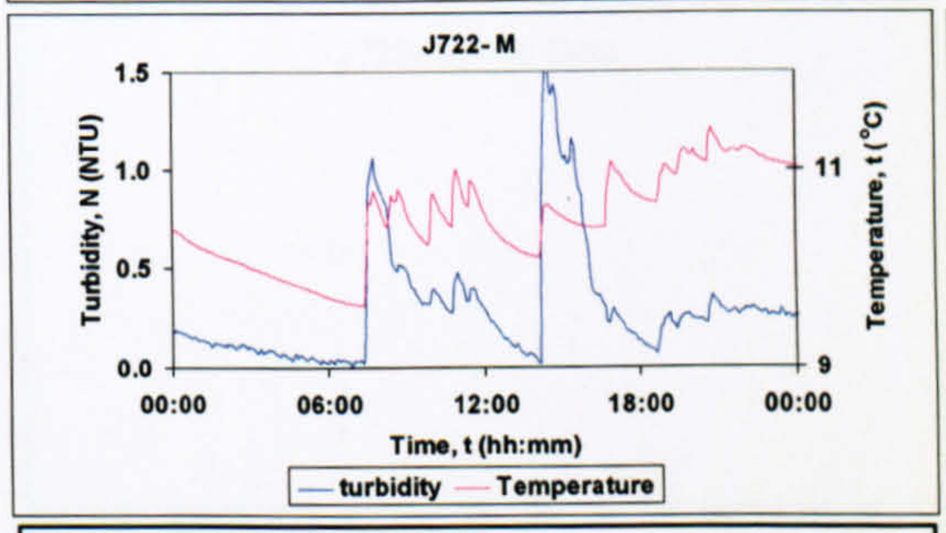

J722- N -No Data

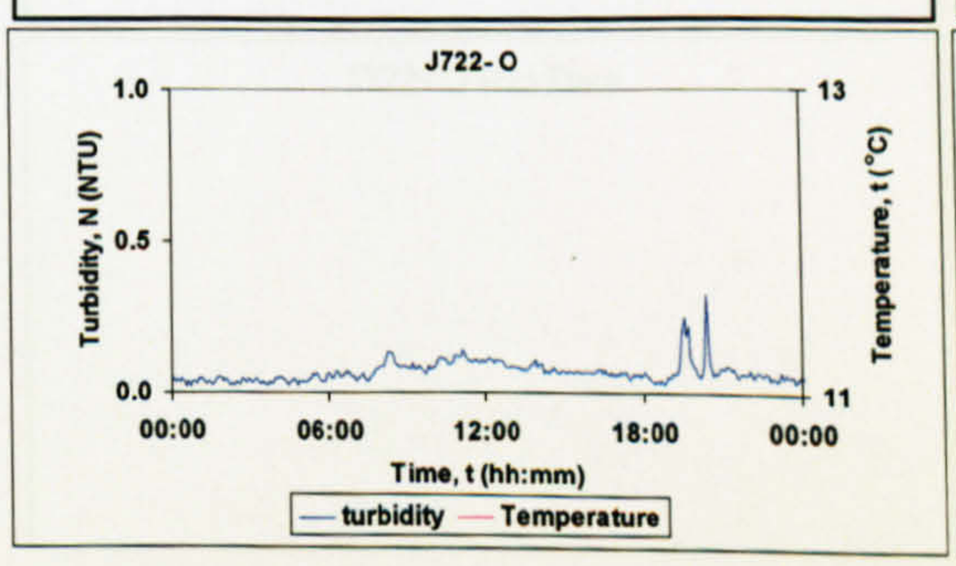

6 16/07/06
Imported Material

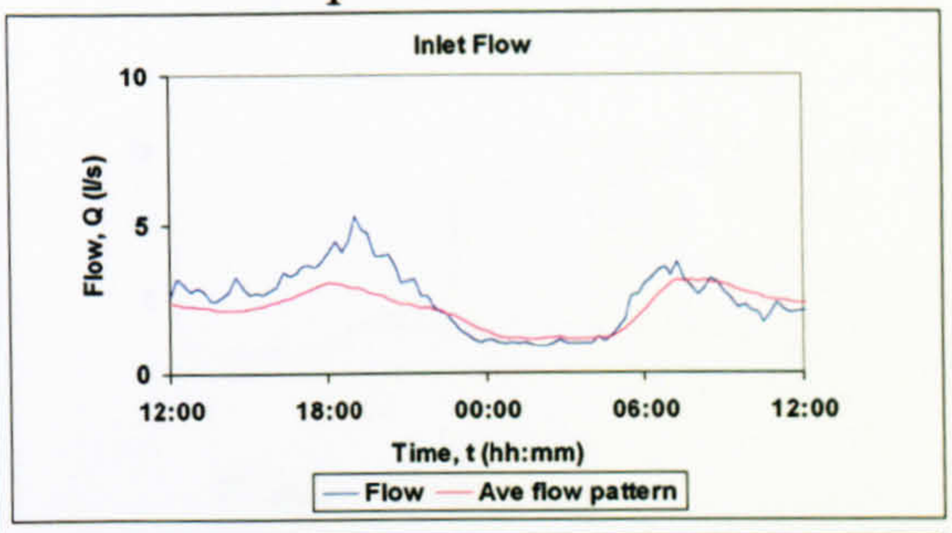

J722- K -No Data

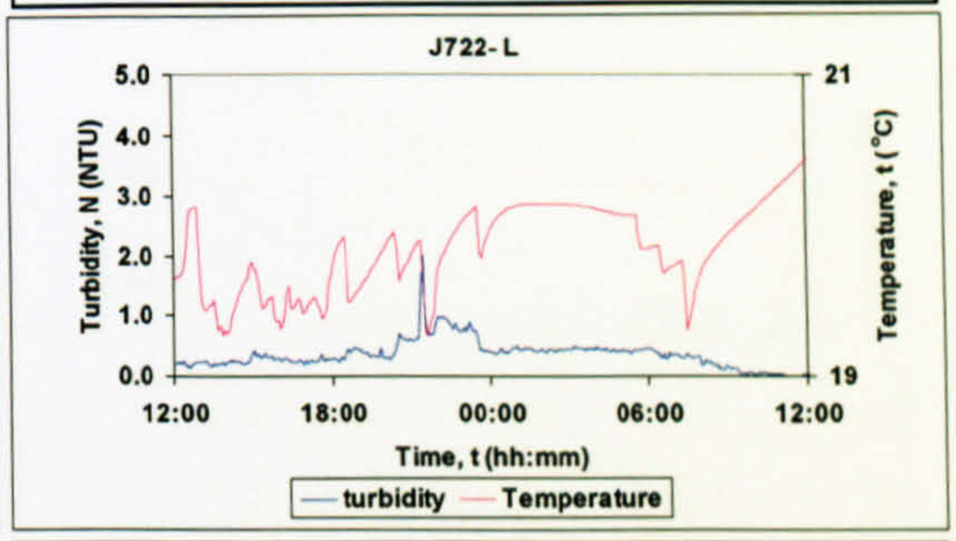

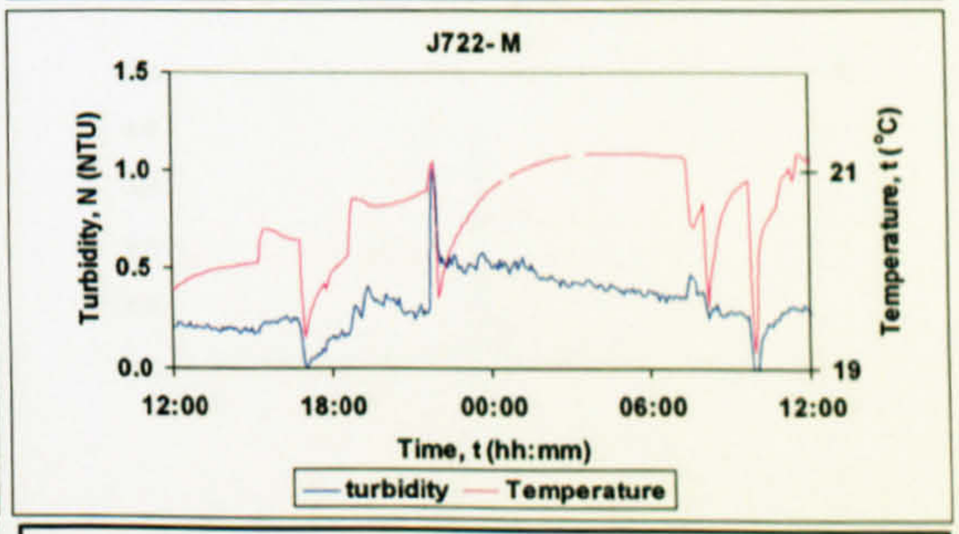

J722- N -No Data

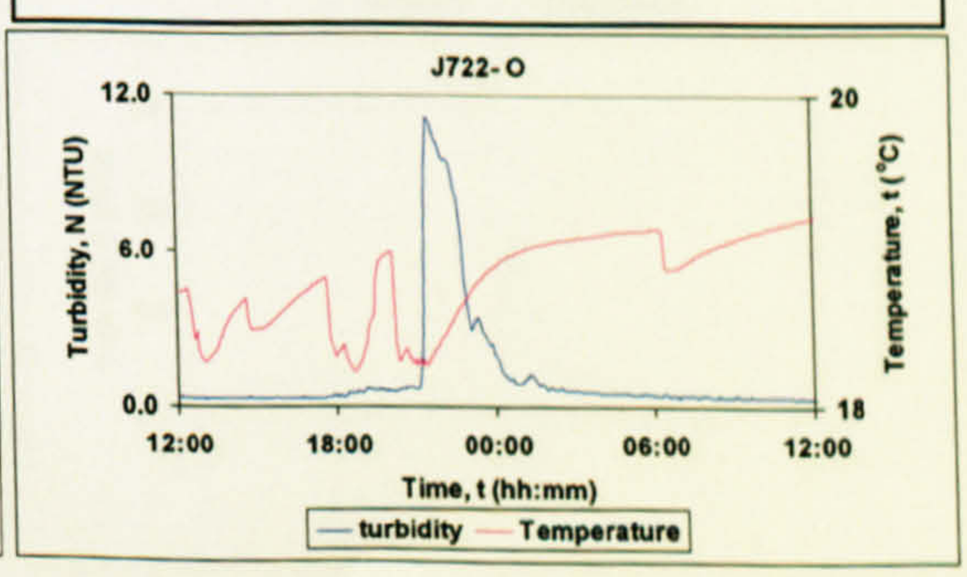

7 14/12/06
Imported material

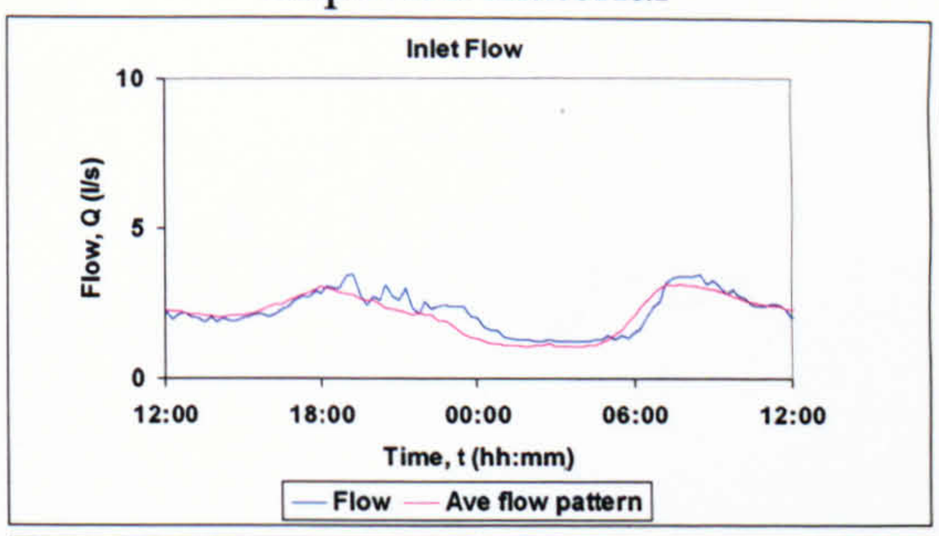

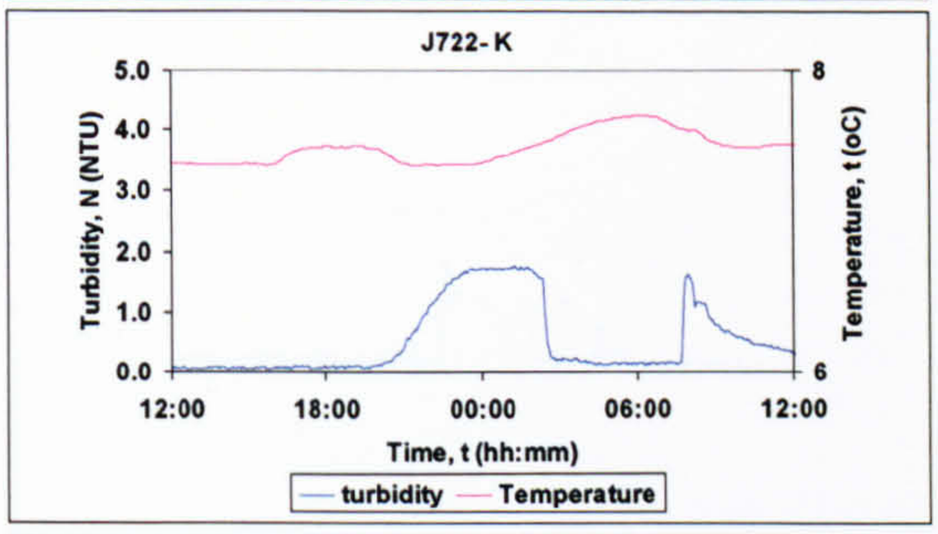

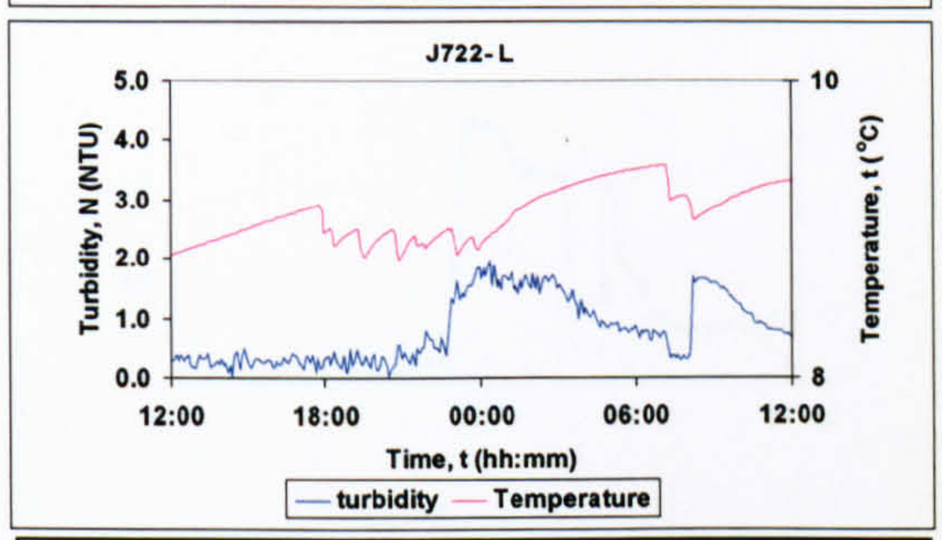

J722- M -No Data

J722- N -No Data

J722- O -No Data

8 30/01/07
Large increase in demand

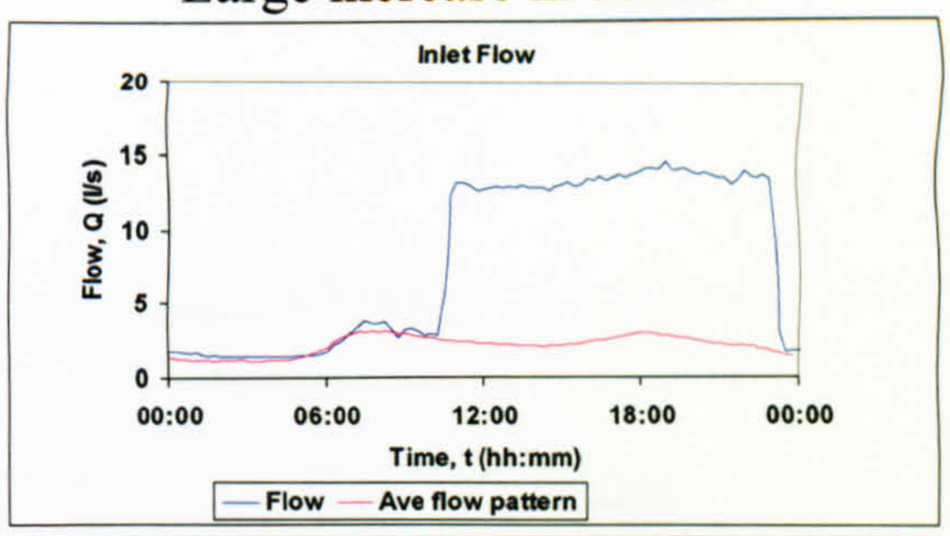

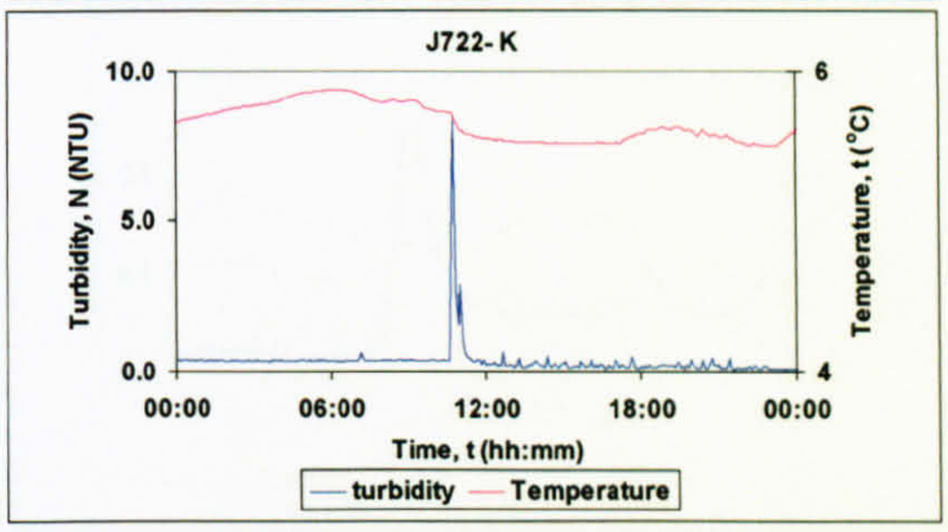

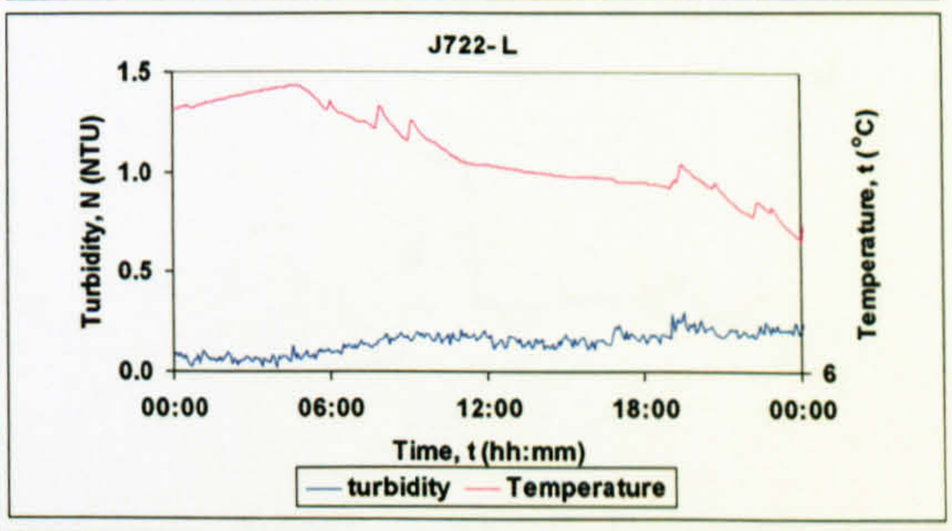

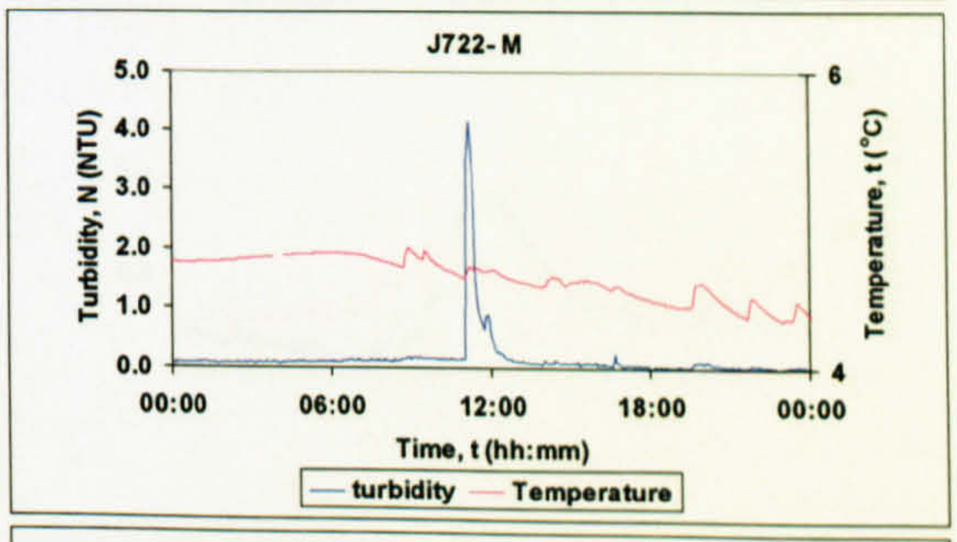

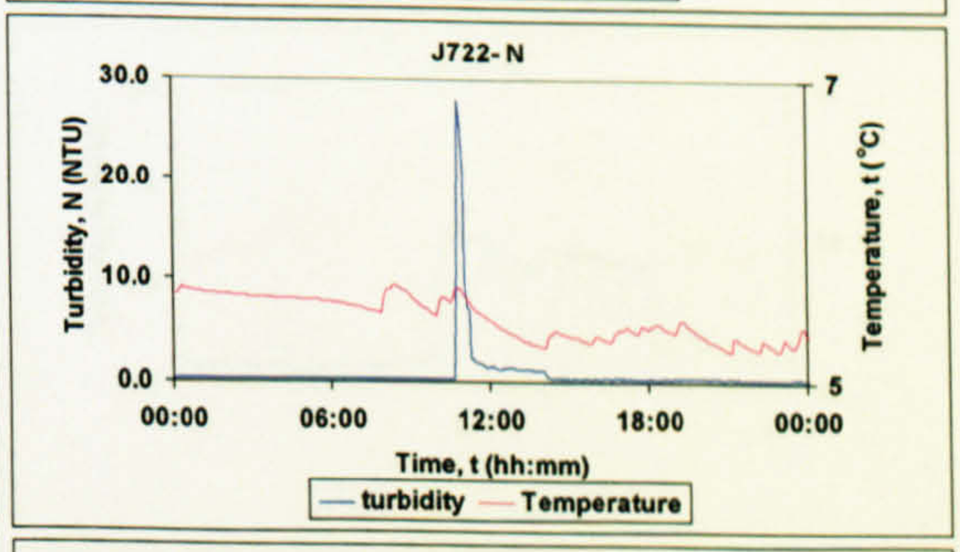

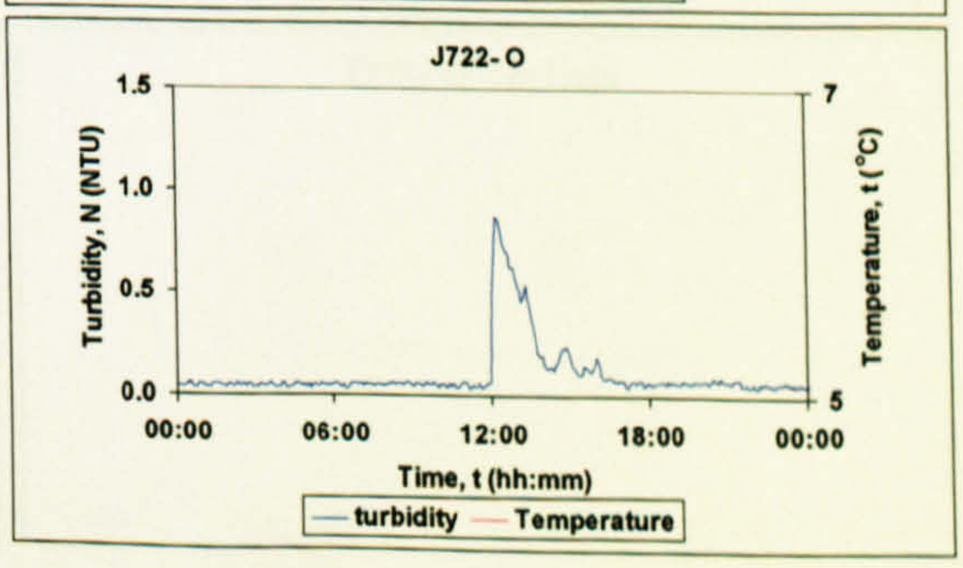

9 02/02/07 to 03/02/07
Imported material

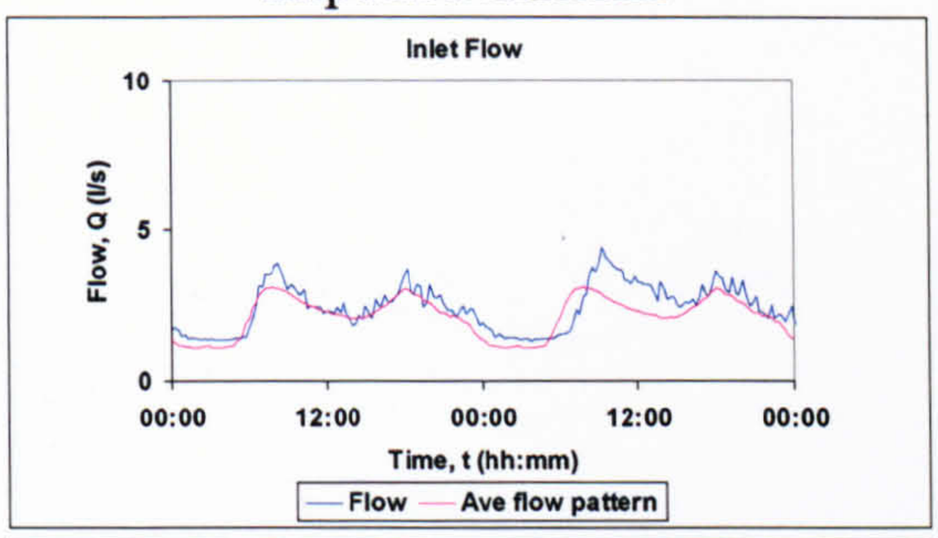

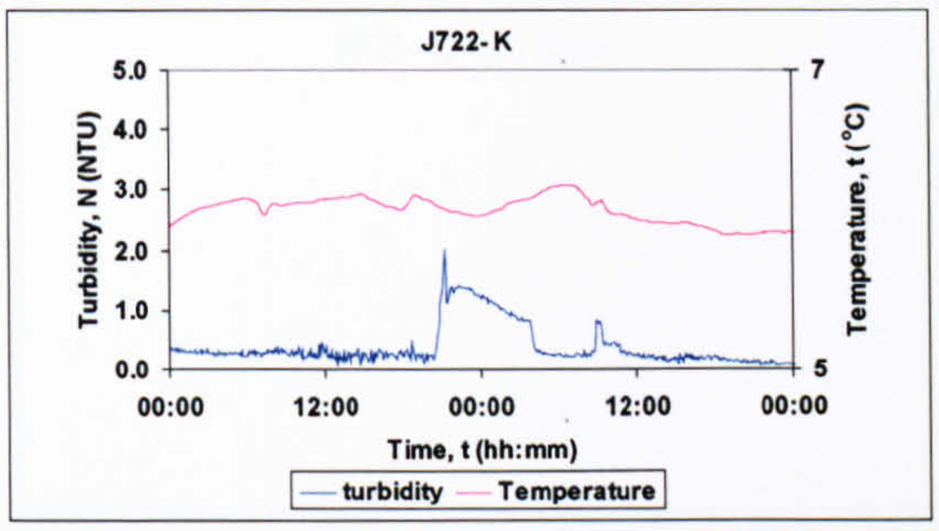

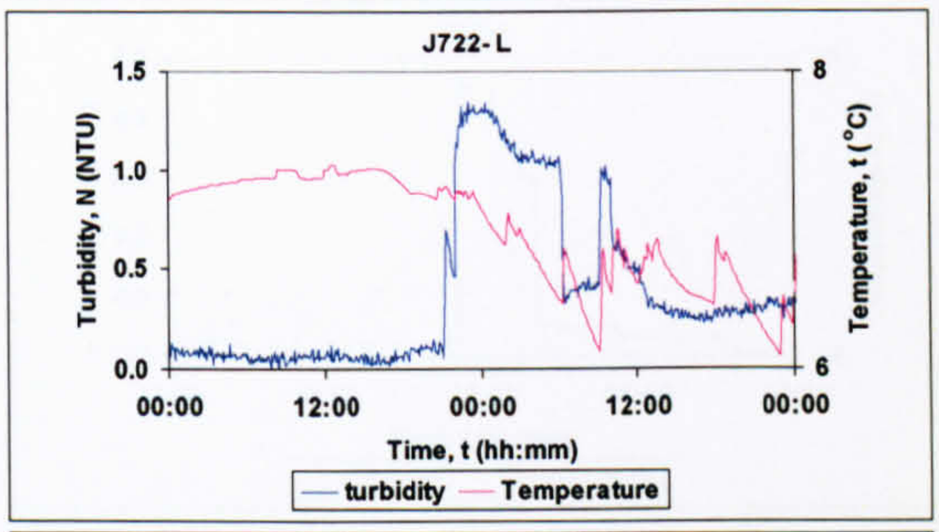

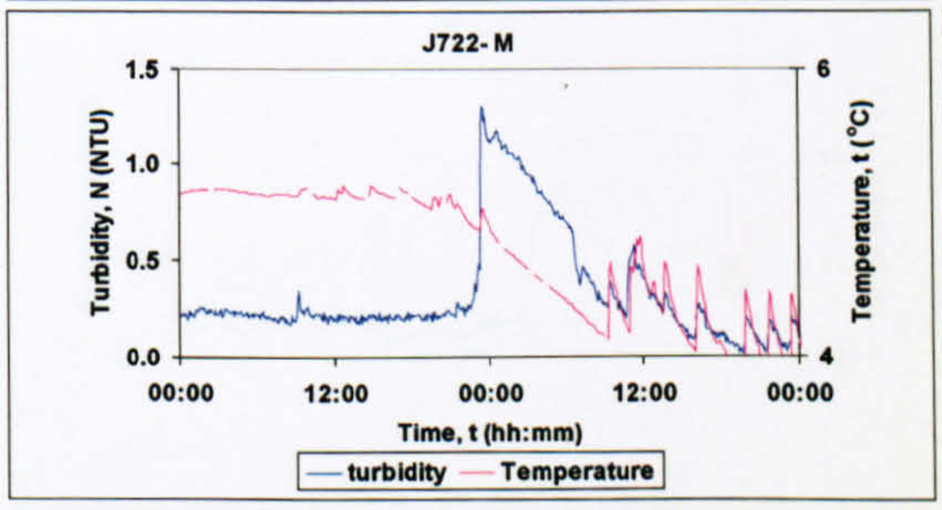

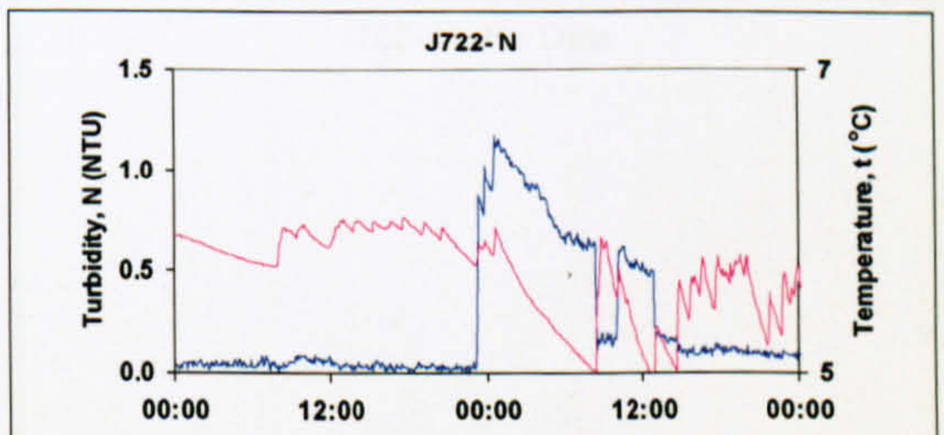

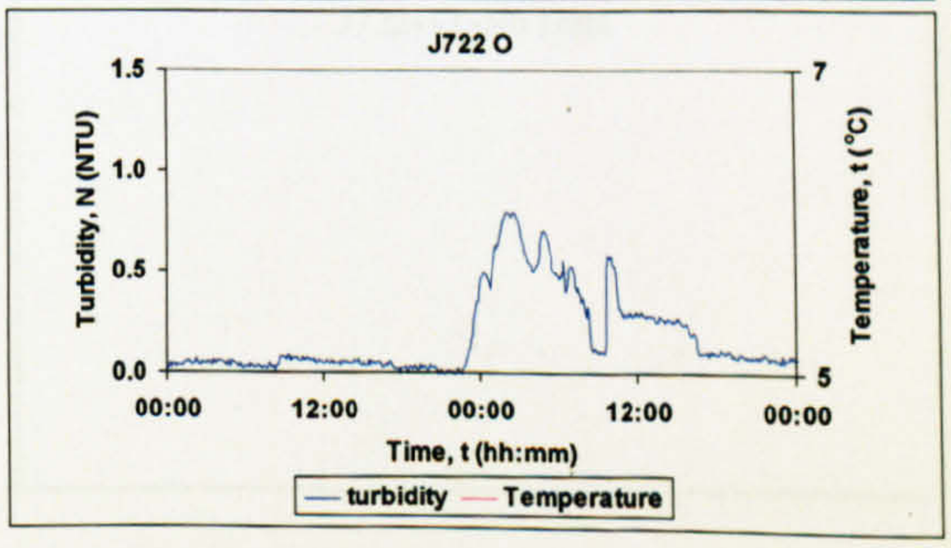

10 19/04/07
Imported material

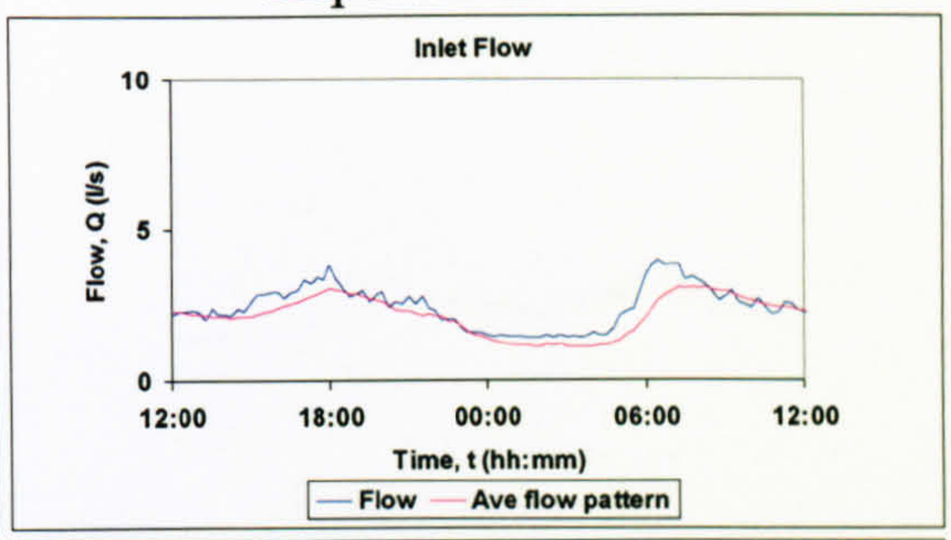

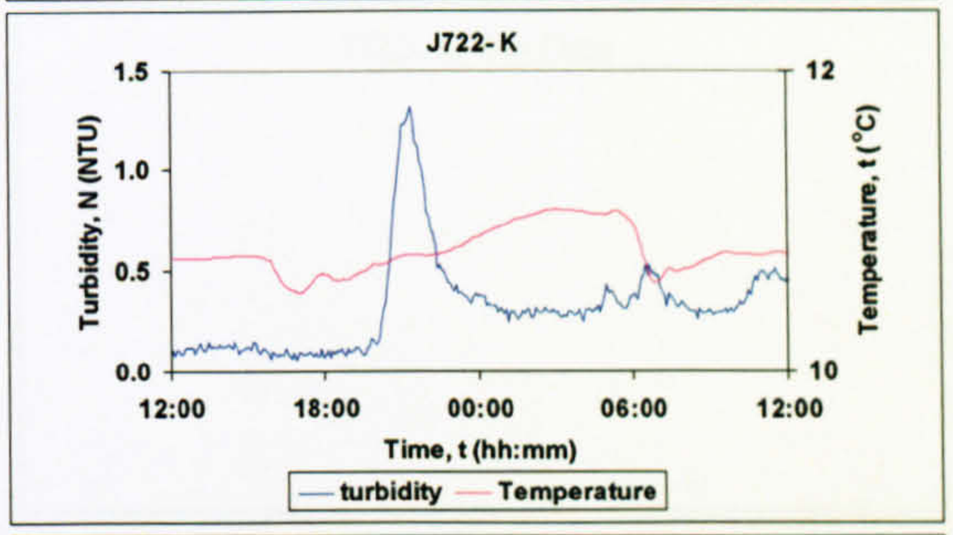

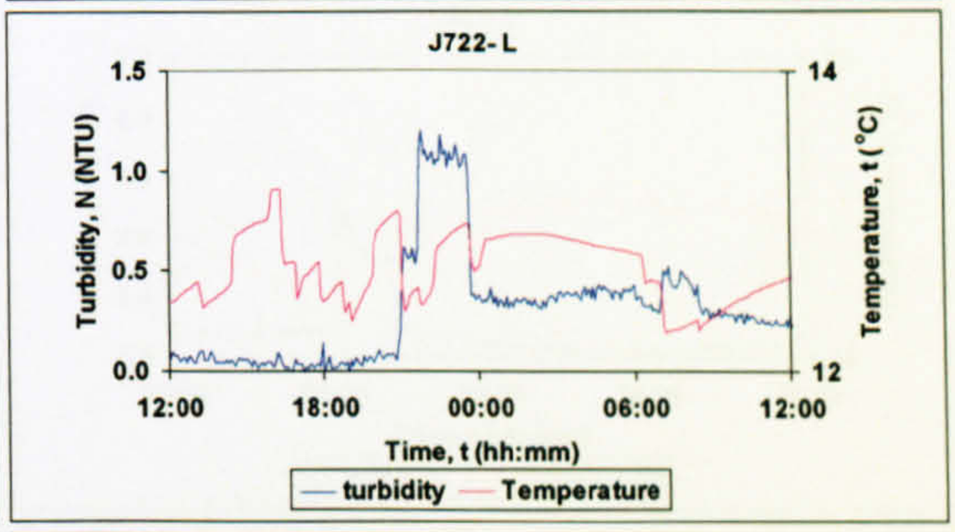

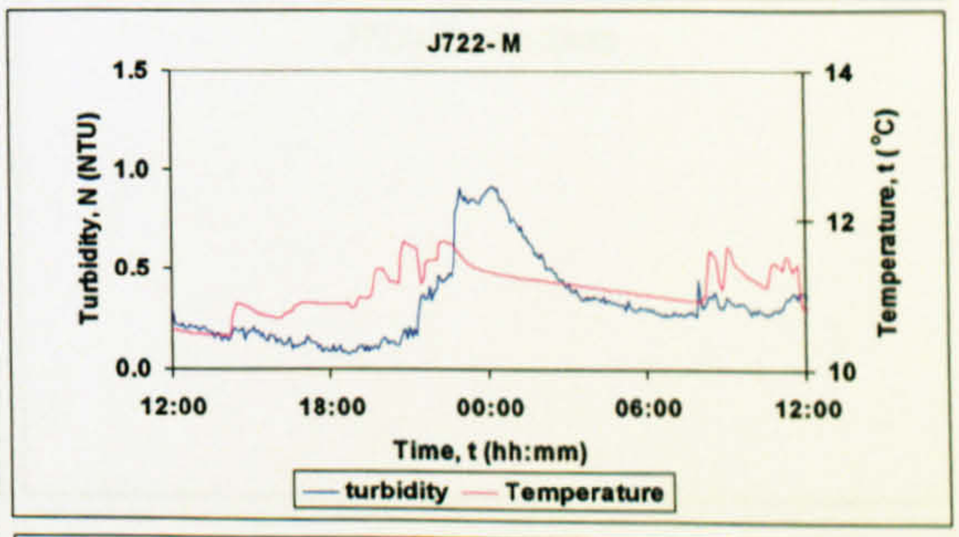

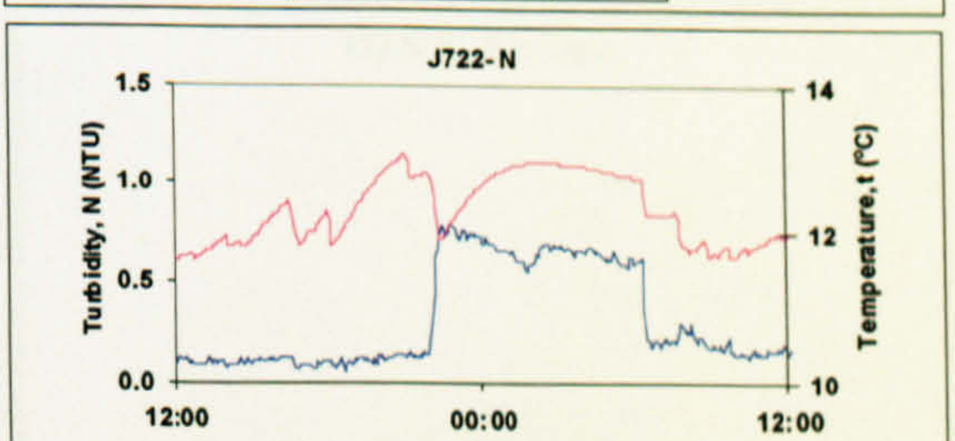

J722- O -No Data

11 03/06/07
Large increase in demand

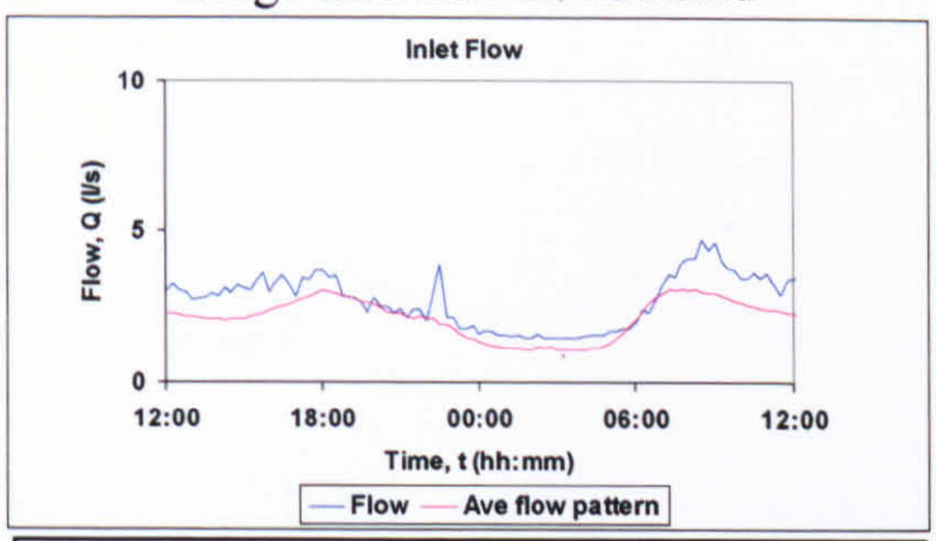

J722- K -No Data

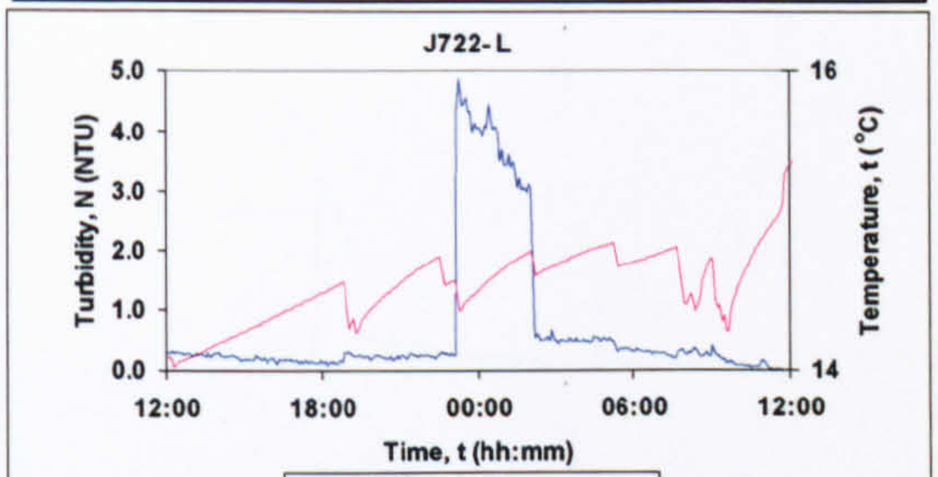

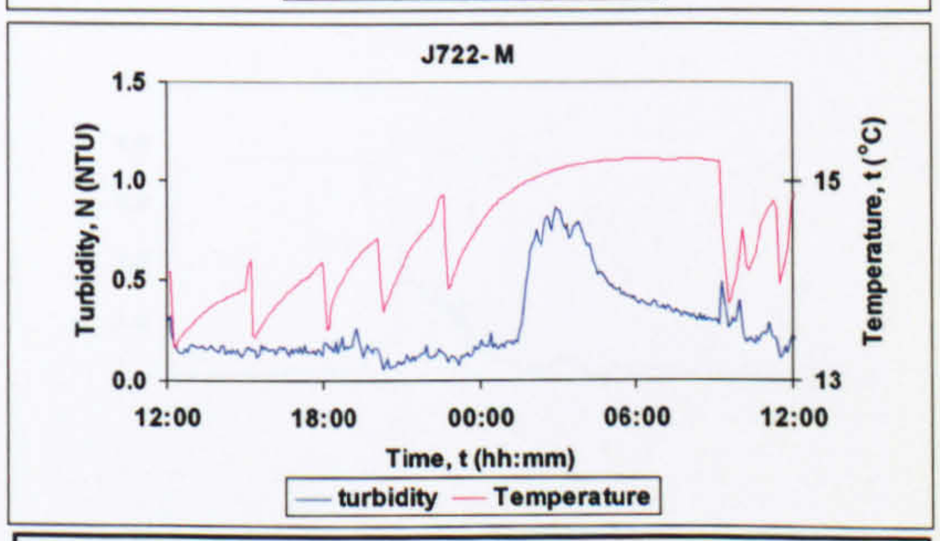

J722- N -No Data

J722- O -No Data

12 26/06/07
Unknown

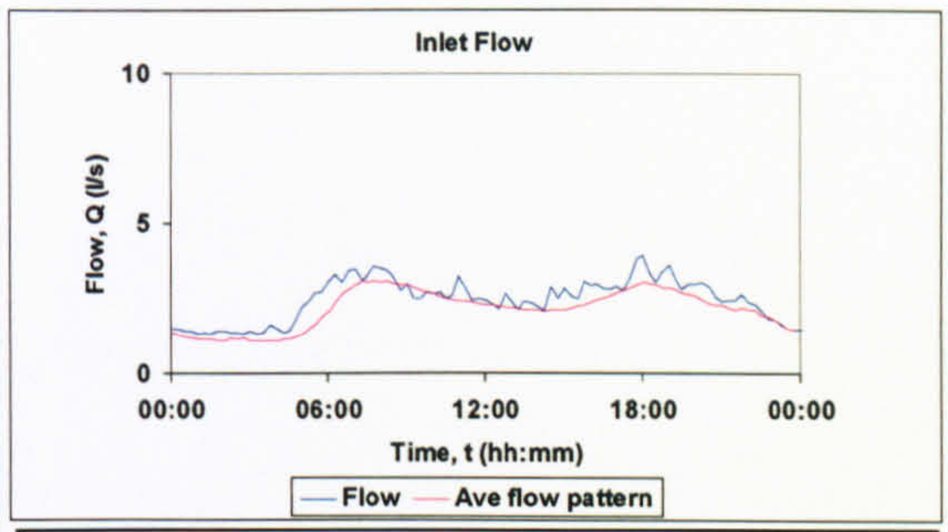

J722- K -No Data

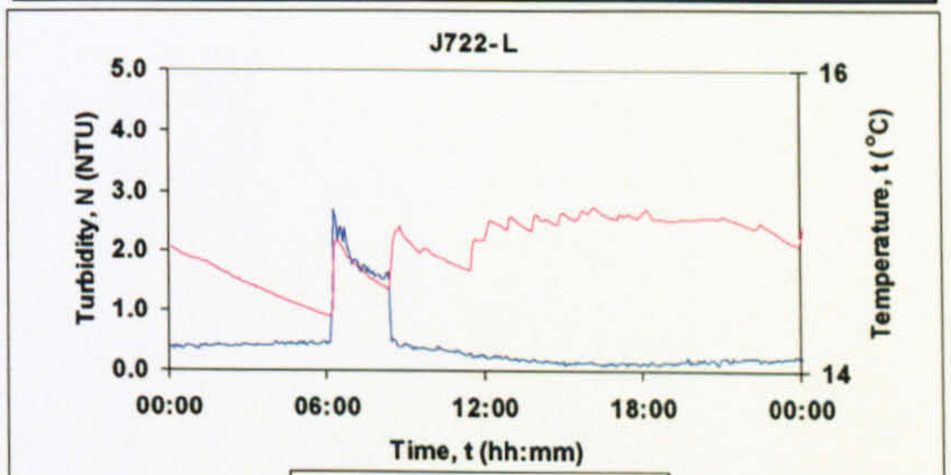

J722- K -No Data

J722- K -No Data

13 17/07/07

Imported material

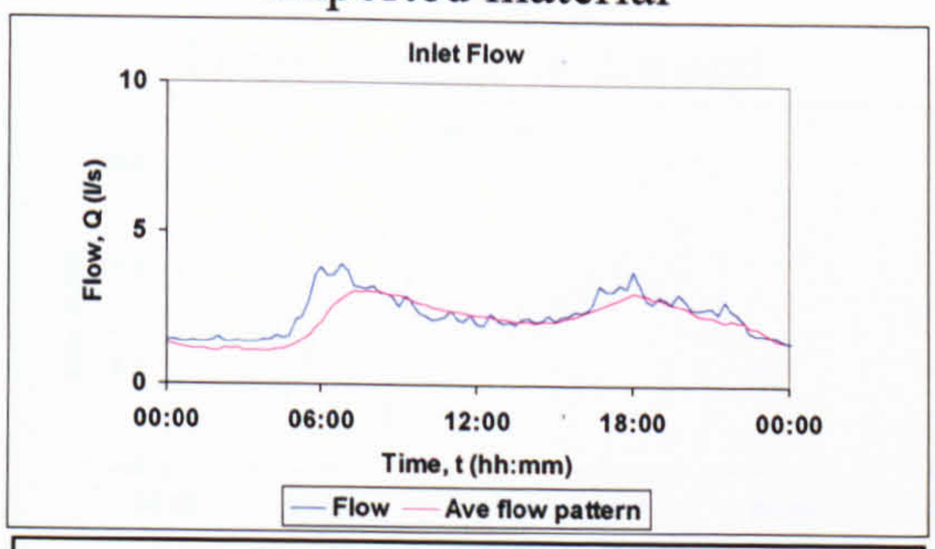

J722- K -No Data

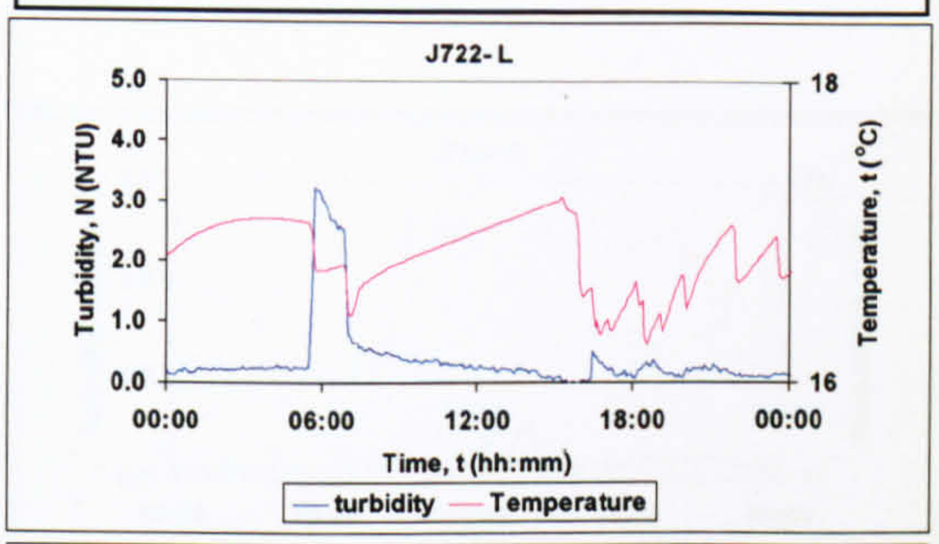

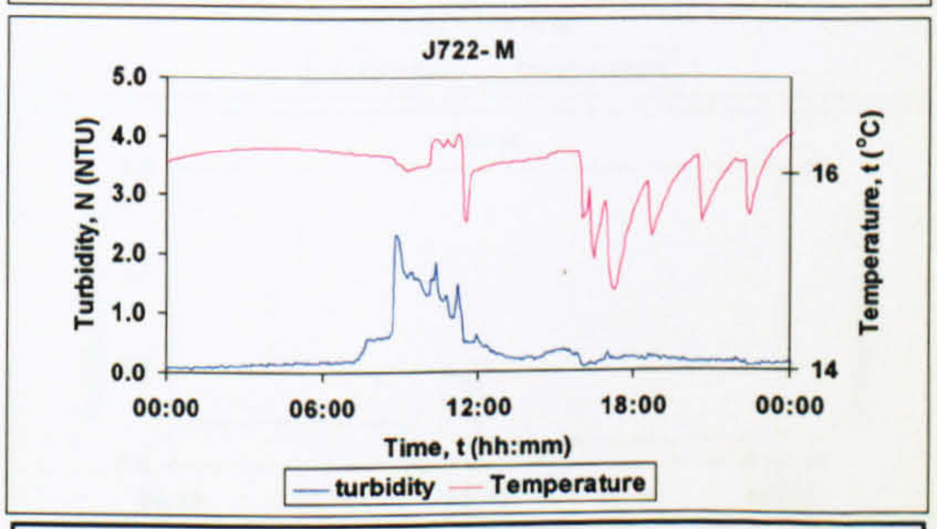

J722- N -No Data

J722- O -No Data

J730

1 27/10/06
Large increase in demand

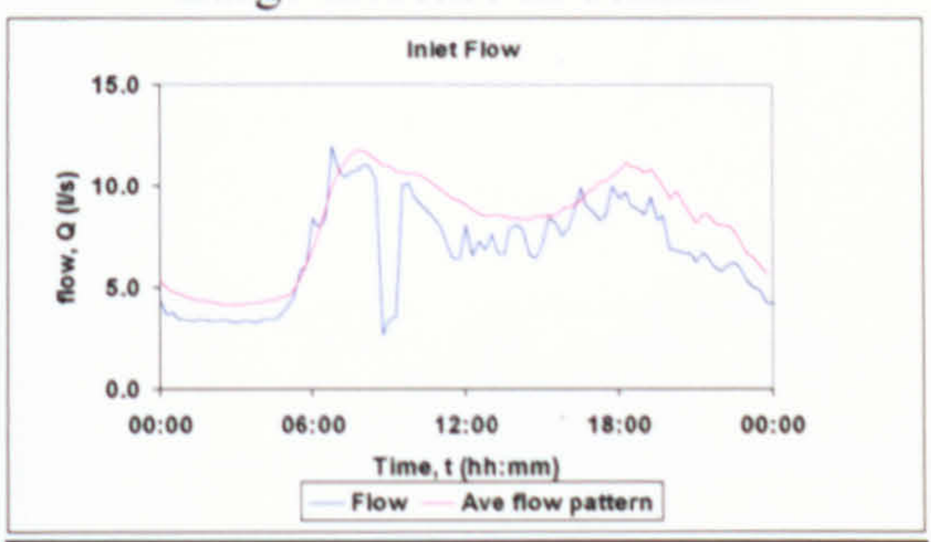

2 15/12/06
Imported material

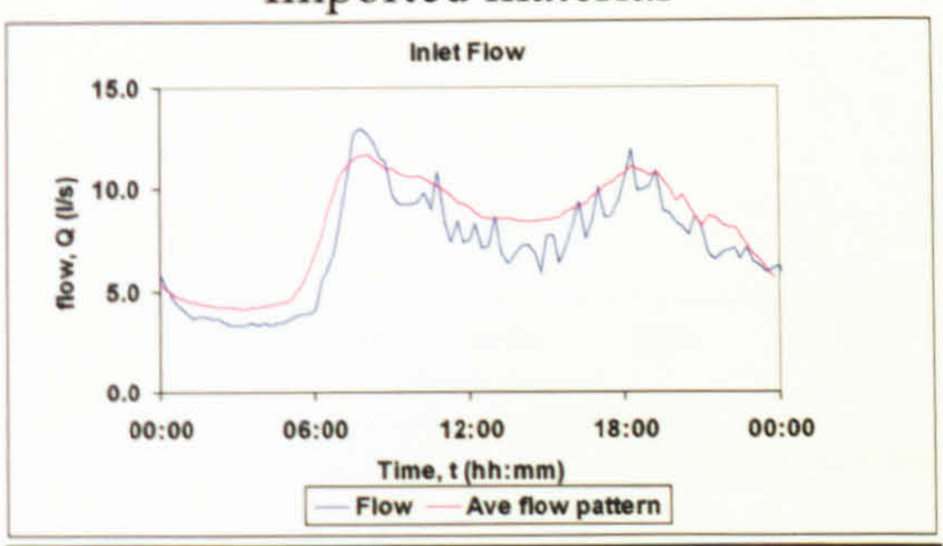

J730-P - No Data

J730-P -No Data

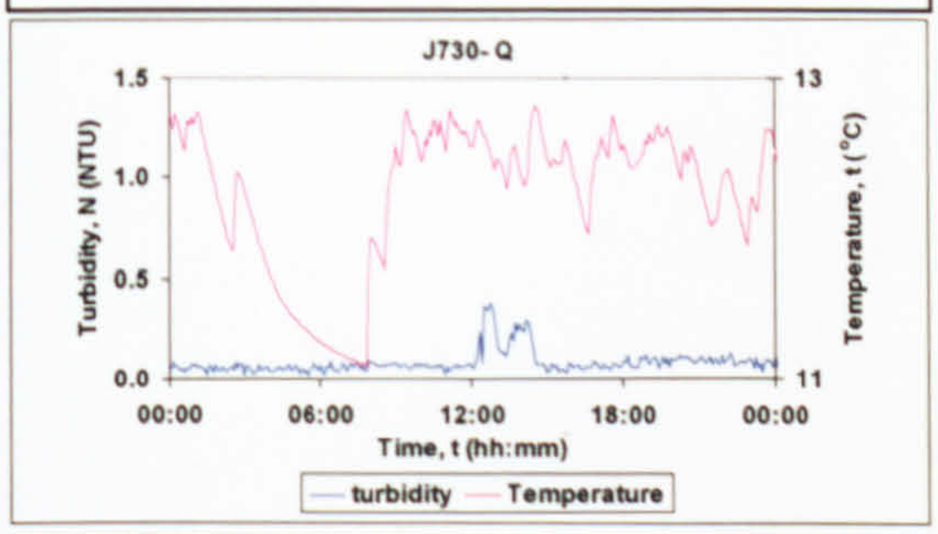

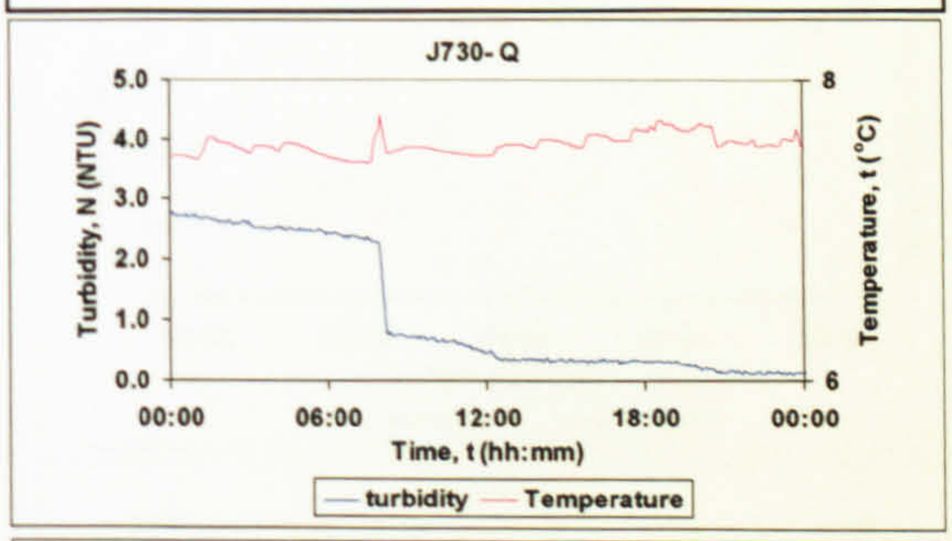

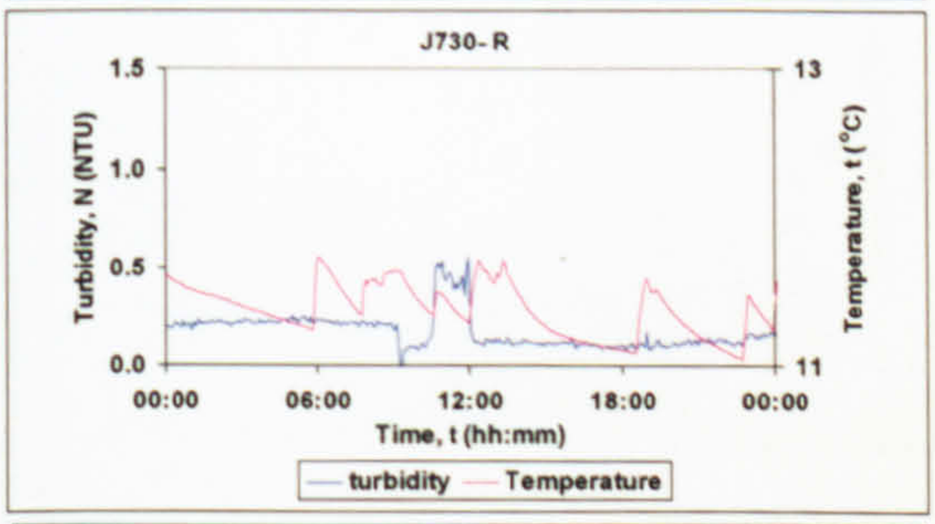

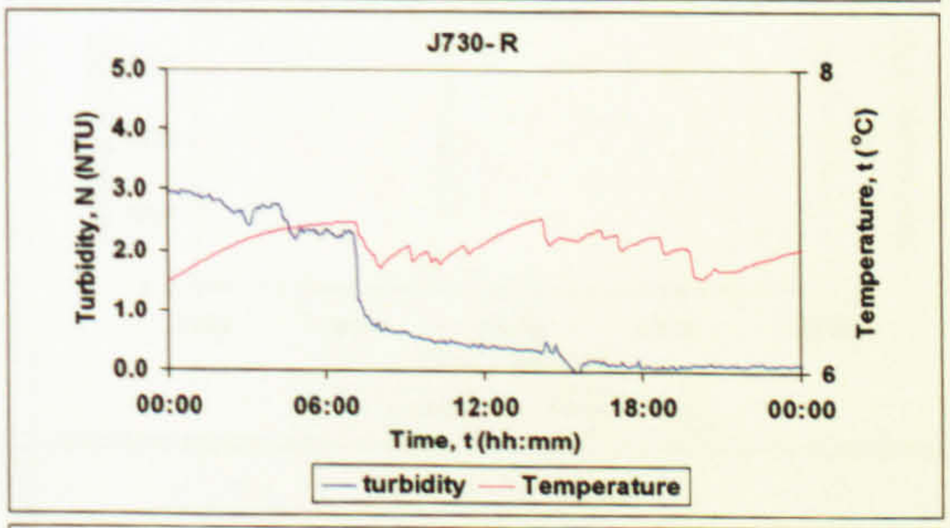

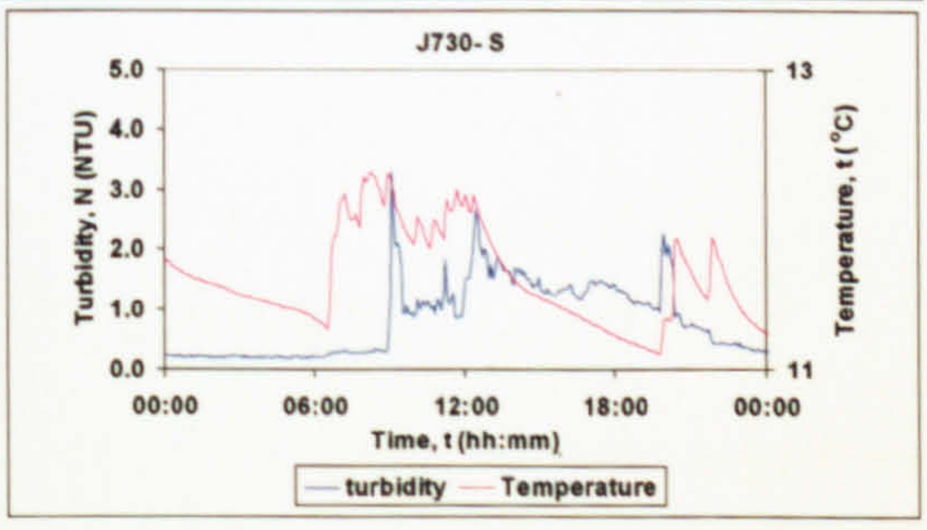

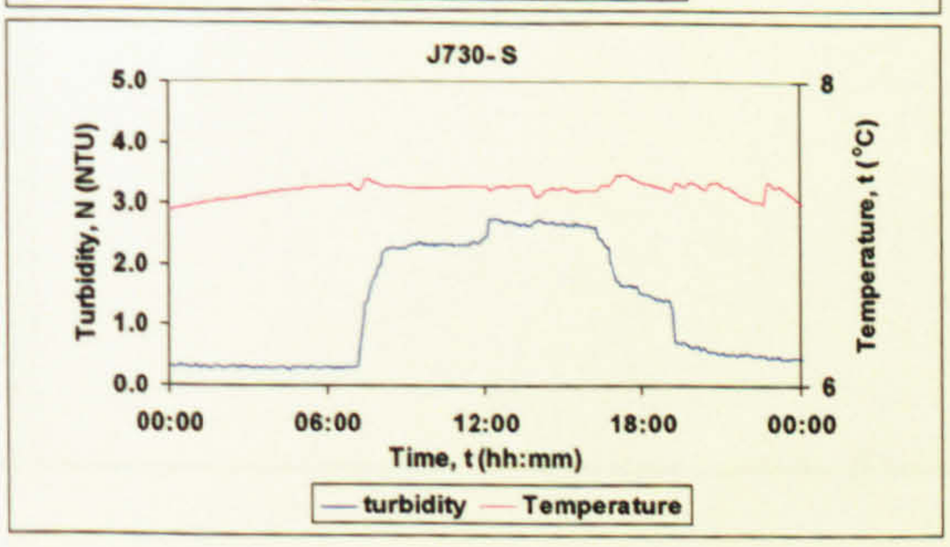

3 19/04/07
Imported material

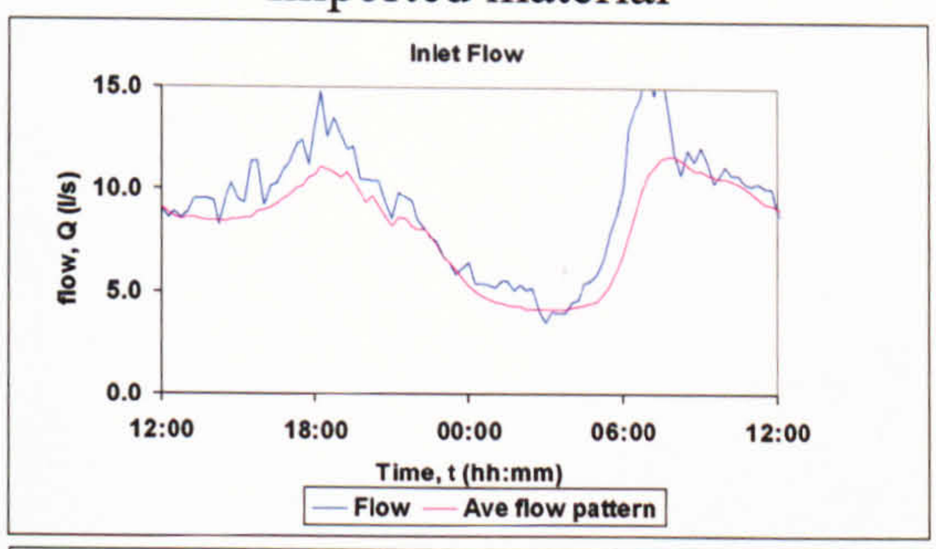

4 30/06/07
Large increase in demand

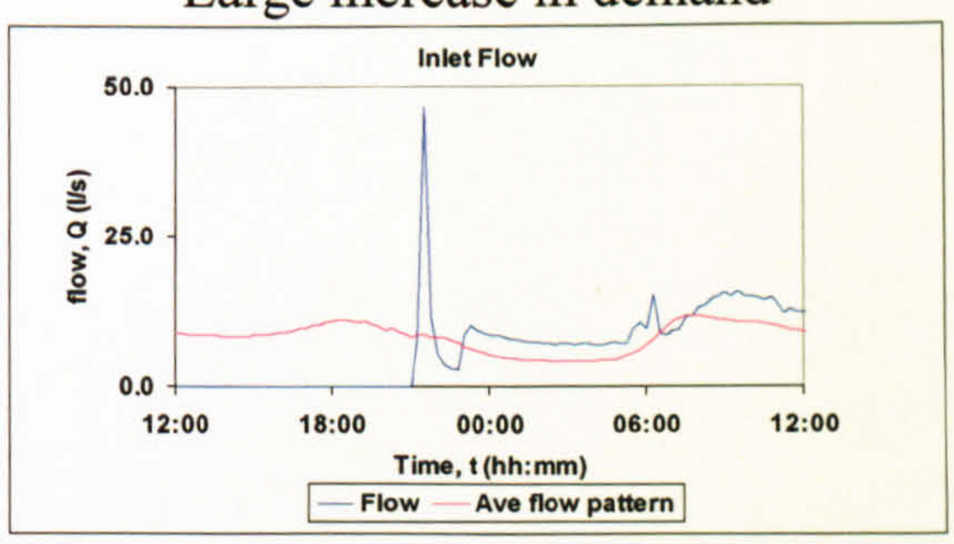

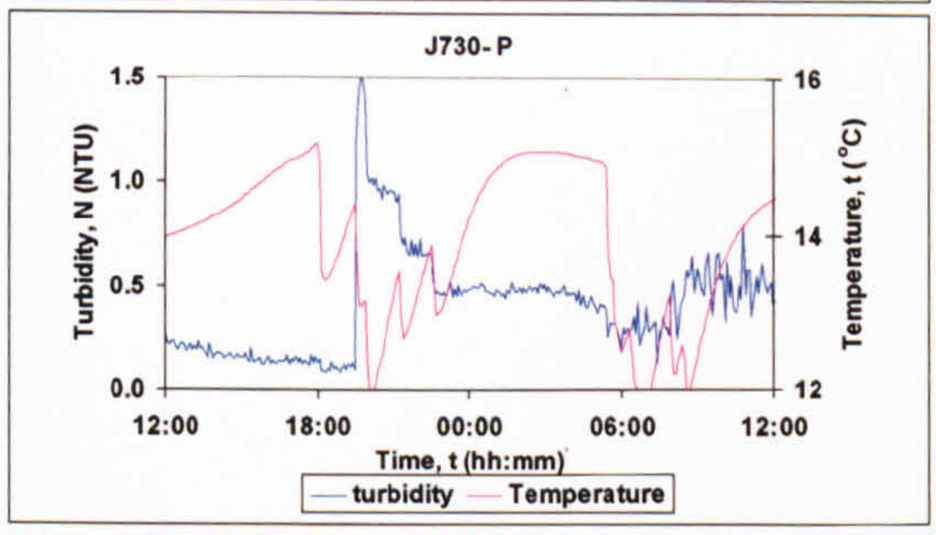

J730-P -No Data

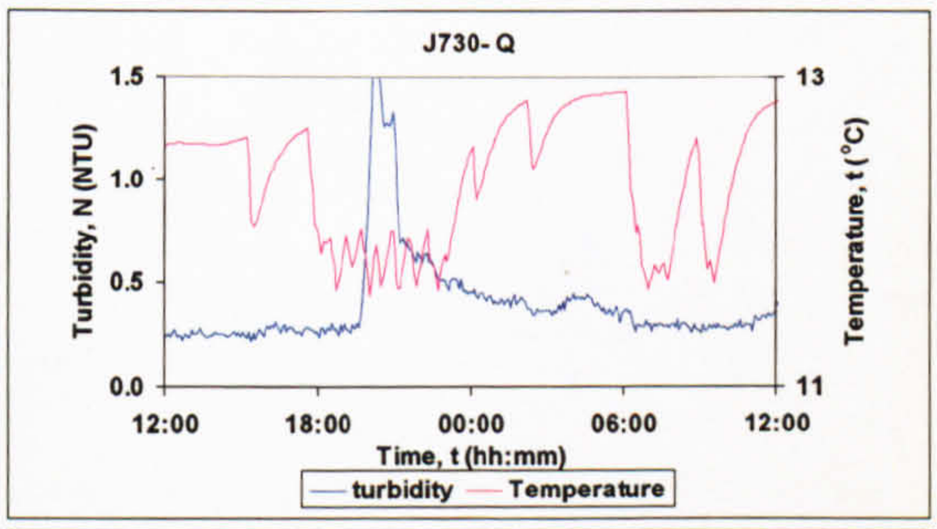

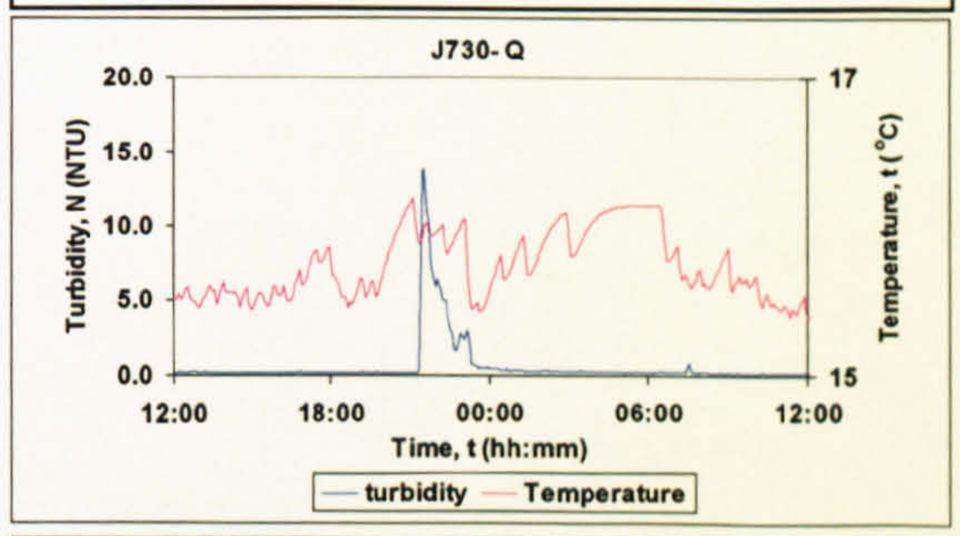

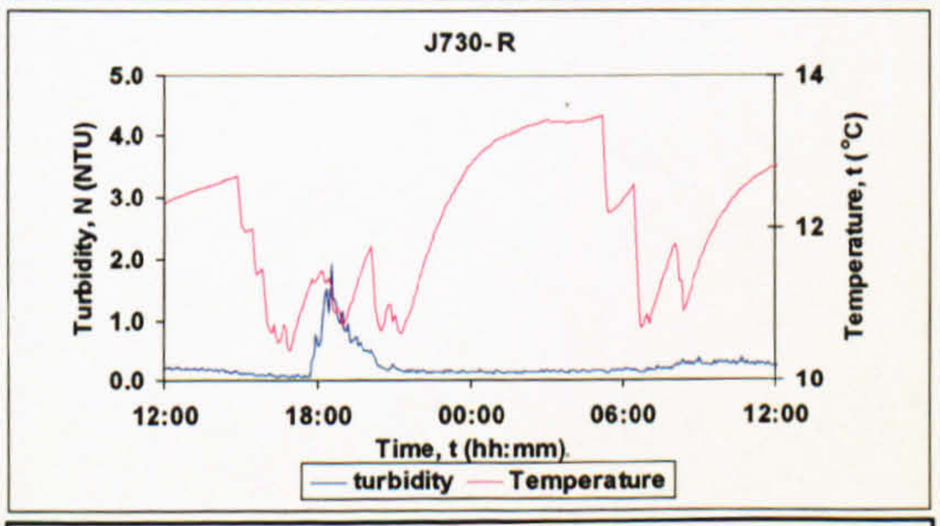

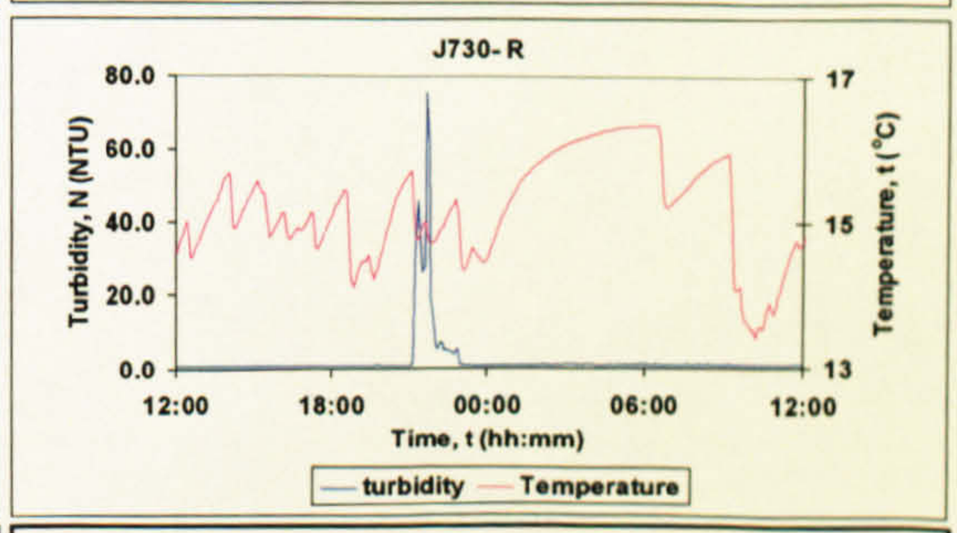

J730-S -No Data

J730-S -No Data